frontiers | Research Topics

GABAergic circuits in health and disease

Edited by
Lisa Topolnik, Graziella DiCristo
and Elsa Rossignol

Published in
Frontiers in Neural Circuits

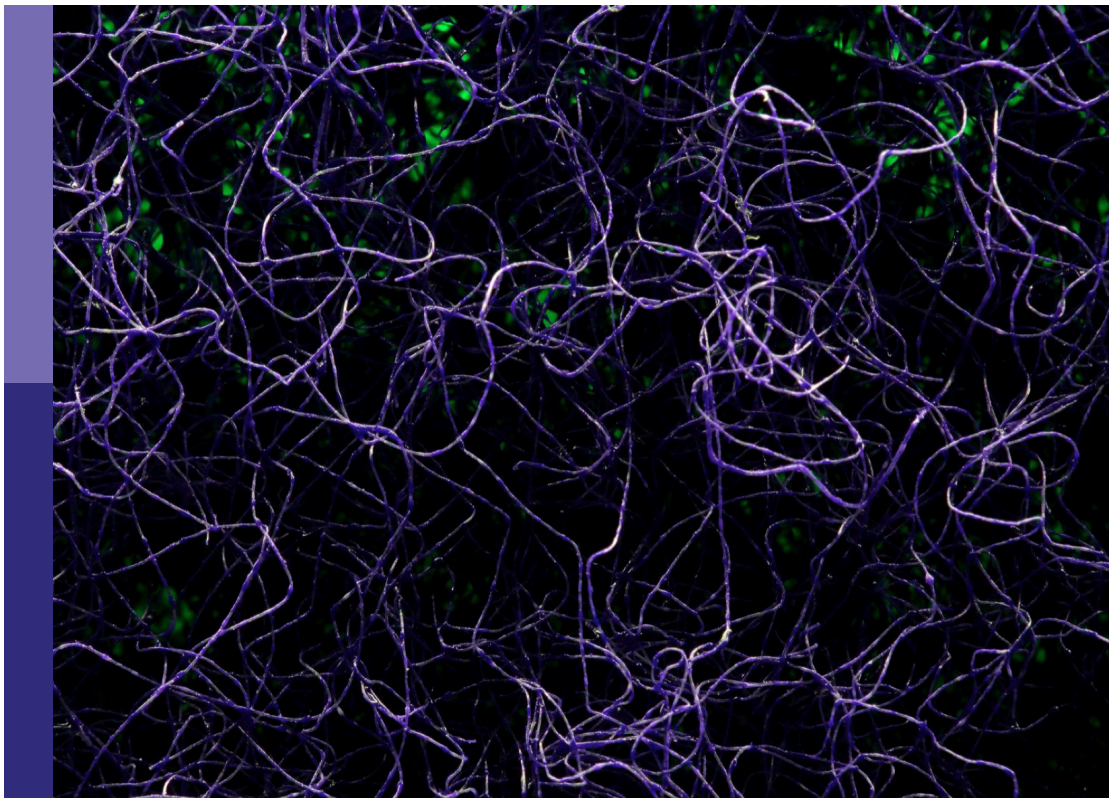

ISSN 1664-8714
ISBN 978-2-8325-3919-4
DOI 10.3389/978-2-8325-3919-4

About Frontiers

Frontiers is more than just an open access publisher of scholarly articles: it is a pioneering approach to the world of academia, radically improving the way scholarly research is managed. The grand vision of Frontiers is a world where all people have an equal opportunity to seek, share and generate knowledge. Frontiers provides immediate and permanent online open access to all its publications, but this alone is not enough to realize our grand goals.

Frontiers journal series

The Frontiers journal series is a multi-tier and interdisciplinary set of open-access, online journals, promising a paradigm shift from the current review, selection and dissemination processes in academic publishing. All Frontiers journals are driven by researchers for researchers; therefore, they constitute a service to the scholarly community. At the same time, the *Frontiers journal series* operates on a revolutionary invention, the tiered publishing system, initially addressing specific communities of scholars, and gradually climbing up to broader public understanding, thus serving the interests of the lay society, too.

Dedication to quality

Each Frontiers article is a landmark of the highest quality, thanks to genuinely collaborative interactions between authors and review editors, who include some of the world's best academicians. Research must be certified by peers before entering a stream of knowledge that may eventually reach the public - and shape society; therefore, Frontiers only applies the most rigorous and unbiased reviews. Frontiers revolutionizes research publishing by freely delivering the most outstanding research, evaluated with no bias from both the academic and social point of view. By applying the most advanced information technologies, Frontiers is catapulting scholarly publishing into a new generation.

What are Frontiers Research Topics?

Frontiers Research Topics are very popular trademarks of the *Frontiers journals series*: they are collections of at least ten articles, all centered on a particular subject. With their unique mix of varied contributions from Original Research to Review Articles, Frontiers Research Topics unify the most influential researchers, the latest key findings and historical advances in a hot research area.

Find out more on how to host your own Frontiers Research Topic or contribute to one as an author by contacting the Frontiers editorial office: frontiersin.org/about/contact

GABAergic circuits in health and disease

Topic editors
Lisa Topolnik — Laval University, Canada
Graziella DiCristo — Montreal University, Canada
Elsa Rossignol — CHU Sainte-Justine, Canada

Citation
Topolnik, L., DiCristo, G., Rossignol, E., eds. (2023). *GABAergic circuits in health and disease*. Lausanne: Frontiers Media SA. doi: 10.3389/978-2-8325-3919-4

Table of contents

frontiers | Frontiers in Neural Circuits

TYPE Editorial
PUBLISHED 31 October 2023
DOI 10.3389/fncir.2023.1322193

OPEN ACCESS

EDITED AND REVIEWED BY
Edward S. Ruthazer,
McGill University, Canada

*CORRESPONDENCE
Lisa Topolnik
lisa.topolnik@bcm.ulaval.ca

RECEIVED 15 October 2023
ACCEPTED 19 October 2023
PUBLISHED 31 October 2023

CITATION
Topolnik L, Di Cristo G and Rossignol E (2023) Editorial: GABAergic circuits in health and disease. *Front. Neural Circuits* 17:1322193. doi: 10.3389/fncir.2023.1322193

Editorial: GABAergic circuits in health and disease

Lisa Topolnik[1]*, Graziella Di Cristo[2] and Elsa Rossignol[2]

[1]Department of Biochemistry, Microbiology and Bioinformatics, Laval University, Québec, QC, Canada, [2]Neurosciences Department, CHU Sainte Justine Research Center, University of Montreal, Montreal, QC, Canada

KEYWORDS

GABA, inhibition, interneuron, learning, disorder, epilepsy, PTSD, autism

Editorial on the Research Topic
GABAergic circuits in health and disease

The intricate web of GABAergic circuits in the brain has long captivated neuroscientists, serving as the backbone of inhibitory control that delicately balances neural excitation. In this Research Topic of articles, we delve into the multifaceted contributions of GABAergic circuits to both the maintenance of cognitive health and the genesis of neurological disorders. A consortium of research teams has explored various aspects of GABAergic inhibition, unraveling novel insights that collectively broaden our understanding of the inhibitory interneuron function and dysfunction. Their groundbreaking work sheds light on how inhibitory circuits impact diverse aspects of cortical information processing, spanning circuit assembly, motor learning, episodic memory formation, epileptiform activities, and fear-related disorders.

Toudji et al. provide a comprehensive overview of the molecular and cellular mechanisms governing the migration of GABAergic interneurons from the ventral telencephalon to their integration within cortical circuits. They delve into the various extrinsic guidance cues, critical interactions with blood vessels, and intrinsic cellular mechanisms that remodel the cytoskeleton to facilitate cellular locomotion in response to these cues. They emphasize how disorders of interneuron migration underlie a subset of genetically determined neurodevelopmental disorders and how cell-based therapies may be envisioned as future therapeutic strategies.

Lee et al. turn their focus to the primary motor cortex, dissecting the role of vasoactive intestinal peptide-expressing (VIP) inhibitory interneurons in motor learning. They reveal how VIP interneurons process diverse inputs, including reward-related information, to orchestrate local circuit plasticity and facilitate reward-based motor learning.

Fossati et al. delve deep into the anterior cingulate cortex, elucidating the response dynamics of cortical layer 1 (L1) interneurons during fear memory processing. Their findings suggest that different subpopulations of L1 interneurons may exert distinct functions in regulating fear learning and memory, offering critical insights into microcircuit organization. This concept is further expanded by Singh and Topolnik, who zoom in on the interplay between excitatory and inhibitory neurons in fear processing circuits across the prefrontal cortex, amygdala, and hippocampus. They highlight the region-specific roles of parvalbumin-, somatostatin-, and VIP-expressing interneurons in fear memory acquisition and related disorders.

Hernández-Frausto et al. provide a comprehensive overview of the multifaceted roles of hippocampal CA1 GABAergic circuits, from shaping neural computations to orchestrating network activity and memory formation. They emphasize the relevance of interneuron dysfunction in the early stages of Alzheimer's disease.

Sun et al. provide novel insights on the biophysical mechanisms by which hippocampal oriens-lacunosum/moleculare (OLM) cells exhibit theta frequency spiking resonance, a feature critical to their ability to modulate hippocampal theta rhythms. By creating a simplified single compartment computational model that preserves the biophysical fidelity of hippocampal rhythm generation, Sun et al. reveal that the combination of hyperpolarization-activated cation and muscarinic type potassium currents specifically enable OLM cells to exhibit theta frequency spiking resonance. They also demonstrate the utility of their novel model in estimating various conductance parameters in real-time from *in vitro* data, providing novel avenues to explore hippocampal rhythm generation.

Piskorowski and Chevaleyre provide an overview of the unique properties of inhibitory transmission and synaptic plasticity in the CA2 region of the hippocampus. They discuss how inhibitory circuit dysfunctions in this region may contribute to deficits in social recognition memory in different neurological and psychiatric disorders, including multiple sclerosis, autism spectrum disorders, Alzheimer's disease, epilepsy, schizophrenia, and 22q11.2 deletion syndrome.

Avoli et al. discuss the paradoxical role of GABAergic signaling in epileptogenesis, uncovering its unexpected involvement in generating interictal discharges and initiating focal seizures. They offer hope for novel pharmacological treatments in focal epileptic disorders like mesial temporal lobe epilepsy.

Dharavath et al. explore how GABAergic signaling is disrupted in alcohol use disorder, including during withdrawal, and provide insights into novel therapeutic avenues aimed at reversing these circuit deficits.

Finally, Gosgnach provides an extensive overview of the roles of different types of GABAErgic interneurons in the regulation of locomotion at the level of the spinal cord central pattern generators, with a focus on the mechanisms regulating left-right and flexor-extensor alternation. These mechanistic insights inform the development of novel strategies to enhance the recovery of motor function following spinal cord injuries.

As we navigate this collective journey through the labyrinth of GABAergic circuits, we gain valuable insights into their pivotal roles in health and disease, painting a rich portrait of the brain's intricate balance between excitation and inhibition. These novel insights not only expand our theoretical understanding but also hold promise for the development of innovative therapeutic interventions in the realm of neurology and psychiatry.

Author contributions

LT: Writing – original draft, Writing – review & editing. GD: Writing – original draft, Writing – review & editing. ER: Writing – original draft, Writing – review & editing.

Funding

The author(s) declare that no financial support was received for the research, authorship, and/or publication of this article.

Conflict of interest

The authors declare that the research was conducted in the absence of any commercial or financial relationships that could be construed as a potential conflict of interest.

The author(s) declared that they were an editorial board member of Frontiers, at the time of submission. This had no impact on the peer review process and the final decision.

Publisher's note

frontiers | Frontiers in Neural Circuits

TYPE Systematic Review
PUBLISHED 05 October 2022
DOI 10.3389/fncir.2022.984802

OPEN ACCESS

EDITED BY
Lisa Topolnik,
Laval University, Canada

REVIEWED BY
Sabato Santaniello,
University of Connecticut, United States
Carlos Cepeda,
University of California, Los Angeles, United States

*CORRESPONDENCE
Massimo Avoli
massimo.avoli@mcgill.ca

RECEIVED 02 July 2022
ACCEPTED 13 September 2022
PUBLISHED 05 October 2022

CITATION
Avoli M, de Curtis M, Lévesque M, Librizzi L, Uva L and Wang S (2022) $GABA_A$ signaling, focal epileptiform synchronization and epileptogenesis. *Front. Neural Circuits* 16:984802. doi: 10.3389/fncir.2022.984802

$GABA_A$ signaling, focal epileptiform synchronization and epileptogenesis

Massimo Avoli[1,2,3]*, Marco de Curtis[4], Maxime Lévesque[1,2], Laura Librizzi[4], Laura Uva[4] and Siyan Wang[1,2]

[1]Montreal Neurological Institute-Hospital, Montreal, QC, Canada, [2]Departments of Neurology and Neurosurgery, Montreal, QC, Canada, [3]Department of Physiology, McGill University, Montreal, QC, Canada, [4]Epilepsy Unit, Fondazione Istituto di Ricovero e Cura a Carattere Scientifico (IRCCS), Istituto Neurologico Carlo Besta, Milan, Italy

Under physiological conditions, neuronal network synchronization leads to different oscillatory EEG patterns that are associated with specific behavioral and cognitive functions. Excessive synchronization can, however, lead to focal or generalized epileptiform activities. It is indeed well established that in both epileptic patients and animal models, focal epileptiform EEG patterns are characterized by interictal and ictal (seizure) discharges. Over the last three decades, employing *in vitro* and *in vivo* recording techniques, several experimental studies have firmly identified a paradoxical role of $GABA_A$ signaling in generating interictal discharges, and in initiating—and perhaps sustaining—focal seizures. Here, we will review these experiments and we will extend our appraisal to evidence suggesting that $GABA_A$ signaling may also contribute to epileptogenesis, i.e., the development of plastic changes in brain excitability that leads to the chronic epileptic condition. Overall, we anticipate that this information should provide the rationale for developing new specific pharmacological treatments for patients presenting with focal epileptic disorders such as mesial temporal lobe epilepsy (MTLE).

KEYWORDS

epileptiform synchronization, excitatory transmission, $GABA_A$ receptor, inhibitory transmission, interictal spikes, mesial temporal lobe epilepsy, seizures

Background

Neuronal synchronization reflects the integrated activity occurring over time among neuronal networks that are located in the brain (Niedermeyer and da Silva, 2005). Under physiological conditions, neuronal synchronization results in different EEG oscillations that are associated with specific behavioral states, which include cognitive functions and sleep (Steriade et al., 1990; Buzsáki, 2015). However, neuronal synchronization can become abnormally excessive thus leading to focal (Jefferys et al., 2012; Avoli et al., 2016) and/or generalized epileptic discharges (Timofeev and Steriade, 2004;

Crunelli et al., 2012). In this review, we will address the cellular and pharmacological mechanisms that cause the generation of epileptiform discharges in *in vivo* and *in vitro* animal models of focal epilepsy as well as in epileptic patients who were investigated with invasive electrophysiological recordings (including single unit activity) before undergoing brain surgery. These studies were performed in limbic brain structures—including the hippocampus, the rhinal cortices and the amygdala—since these areas are known to play a role in mesial temporal lobe epilepsy (MTLE) (Gloor, 1997; Engel et al., 2012).

Interictal discharges or spikes (i.e., short-lasting events with duration less than 1 s and unaccompanied by any detectable clinical symptom) (**Figure 1A**) as well as ictal discharges (i.e., periods of abnormal, hypersynchronous activity lasting up to several minutes and thus disrupting normal brain function) (**Figure 1B**) are recorded in the EEG obtained from animals or patients presenting with a focal epileptic condition such as MTLE (Gloor, 1997; de Curtis and Avanzini, 2001; Jefferys et al., 2012; Avoli et al., 2016). More recently, it has been shown that focal epileptiform activity is accompanied by the occurrence of high frequency oscillations (HFOs) in the EEG (field potential) recordings (**Figure 1C**); HFOs are not visible in standard EEG recordings but can be extracted by amplifying the appropriately filtered signals. Based on their frequency content, they have been categorized in two groups: (i) ripples, which include oscillatory events between 80 and 200 Hz and (ii) fast ripples, i.e., oscillatory events occurring between 250 and 500 Hz (Bragin et al., 1999a,b; Staba et al., 2004; Jirsch et al., 2006; Urrestarazu et al., 2006; Foffani et al., 2007; Ibarz et al., 2010; Lévesque et al., 2011, 2012; Zijlmans et al., 2011). It has been proposed that ripples may represent, mainly, summated IPSPs while fast ripples should mirror synchronized action potential firing generated by principal (glutamatergic) cells (Jefferys et al., 2012; Jiruska et al., 2017), although fast-spiking GABAergic interneurons could also contribute to the generation of fast ripples (Cepeda et al., 2020). To note how interictal and ictal discharges along with HFOs share some common synchronizing mechanisms.

The topic of our review is the surprisingly active role played by $GABA_A$ receptor signaling, in focal epileptiform synchronization. $GABA_A$ receptors, once activated, open ionotropic anionic channels that are permeable to Cl^- and HCO_3^- (Kaila, 1994). Early clinical evidence indicated that interfering with GABA synthesis leads to convulsions (Coursin, 1954). In addition, experimental studies, which were mainly published in the 1980s, revealed that: (i) several convulsive drugs are $GABA_A$ receptor antagonists (Dingledine and Gjerstad, 1980; Schwartzkroin and Prince, 1980; Hablitz, 1984); (ii) inhibition is markedly reduced at the onset of electrographic hippocampal and neocortical seizures (Ben-Ari et al., 1979; Kostopoulos et al., 1983); (iii) functional disconnection of interneurons from excitatory inputs causes a decrease in inhibition in epileptic brains (Sloviter, 1987); (iv) inhibition in human MTLE may be reduced due to deficits in GABA transporter functions or alterations in $GABA_A$ receptor subunit composition (McDonald et al., 1991; Johnson et al., 1992; Olsen et al., 1992; Williamson et al., 1995). Therefore, in the early 1990s, weakening of inhibition was considered by the majority of epilepsy researchers as the main mechanism leading to focal interictal and ictal discharges and thus to epileptic disorders. This view has been, however, challenged by several successive studies that will be summarized here. To note, however, that we will limit the focus of our review to experimental studies involving electrophysiology methods as it is not meant to cover studies involving other investigative approaches.

$GABA_A$ signaling and epileptiform synchronization

Voskuyl and Albus (1985) were the first investigators to report that a pharmacological procedure that does not decrease $GABA_A$ receptor function—i.e., bath application of the K^+ blocker 4-aminopyridine (4AP)—can induce epileptiform activity in isolated rat hippocampal slices. By employing field potential recordings, they identified the spontaneous occurrence of two types of interictal spikes, with distinct shapes and rates of occurrence (Voskuyl and Albus, 1985). These two types of interictal patterns were confirmed to occur in successive studies in which field and intracellular potentials were simultaneously recorded from hippocampal slices (Perreault and Avoli, 1991, 1992). As shown in **Figure 2A**, field potential recordings obtained during 4AP application revealed: (i) "slow" interictal spikes occurring simultaneously in CA1, CA3, and dentate gyrus (DG), and (ii) "fast" interictal spikes that originate in CA3 and spread to CA1. Moreover, intracellular recordings from CA3 pyramidal cells demonstrated that "slow" interictal spikes were mirrored by slow depolarizations (which were abolished by $GABA_A$ receptor antagonists), while "fast" interictal spikes were associated to intracellular bursts of action potentials riding on depolarizations that were caused by ionotropic glutamatergic currents (**Figure 2B**; Perreault and Avoli, 1991, 1992). It was also confirmed in these experiments (*cf.*, Buckle and Haas, 1982; Rutecki et al., 1987) that the postsynaptic responses caused by the activation of both $GABA_A$ and, presumably, $GABA_B$ receptors were not only preserved but greatly increased in amplitude and duration by 4AP (**Figure 2C**; Perreault and Avoli, 1991); to note as this complex, augmented response was characterized by a pronounced depolarizing component (asterisk in **Figure 2C**) that may be contributed by HCO_3^-—an anion that goes through the open $GABA_A$ receptor and has an equilibrium potential more positive than Cl^- (Grover et al., 1993; Kaila, 1994)—as well as by the transient increase in extracellular $[K^+]$ caused by $GABA_A$ receptor postsynaptic activation (*cf.* Kaila et al., 1997). Presumptive ectopic, fractionated action potentials (arrow in **Figure 2C**)

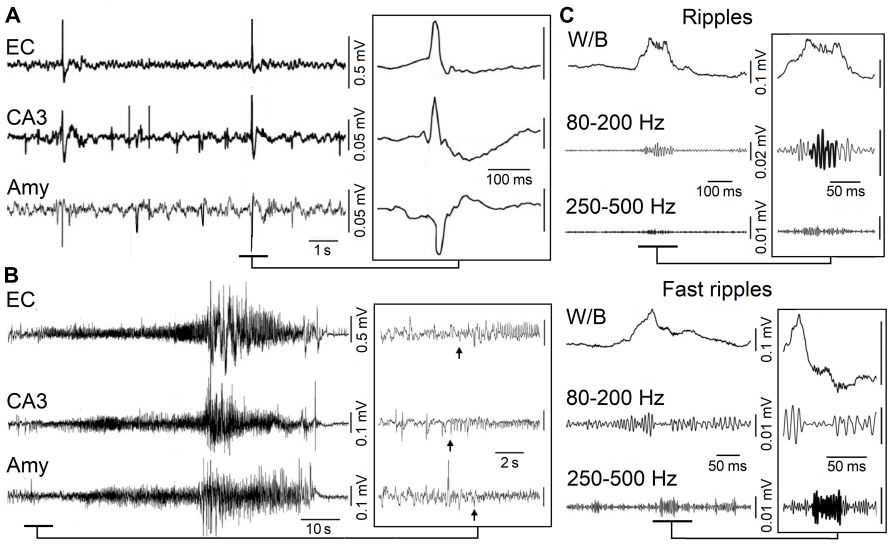

FIGURE 1
(A) Spontaneous interictal discharges recorded from the entorhinal cortex (EC), the hippocampal CA3 region and the amygdala (Amy) in a pilocarpine-treated epileptic rat. Note that only two interictal spikes are present in all regions. **(B)** Spontaneous ictal (seizure) discharge recorded in a pilocarpine-treated epileptic animal from the same areas as in **(A)**; low-voltage fast activity (arrows) marks the onset of this seizure. **(C)** High-frequency oscillations (HFOs, 80–500 Hz) recorded in association with interictal spikes in a pilocarpine-treated epileptic animal. Interictal spikes are visible on the wideband signal (W/B) whereas high-frequency activity is detectable only after filtering the signals between 80 and 200 Hz (Ripples) and between 250 and 500 Hz (Fast ripples).

could consistently be recorded during these "slow" stimulus-induced or spontaneous events (Avoli et al., 1998), and this evidence has been confirmed in neocortical interneurons as well (Keros and Hablitz, 2005).

The two types of 4AP-induced interictal spikes were later recorded in extended brain slices—which included the hippocampus proper and other limbic or para-limbic areas such as the entorhinal/perirhinal cortices, the amygdala and the insular cortex (**Figure 2D**; Avoli et al., 1996a,b; Sudbury and Avoli, 2007)—as well as in the *in vitro* guinea pig isolated brain (**Figure 2F**; Uva et al., 2009). These studies (see also Morris et al., 1996; Lamsa and Kaila, 1997) have demonstrated that "fast" interictal spikes are abolished by ionotropic glutamatergic antagonists, a pharmacological procedure that does not appear to influence the recurrence of "slow" interictal spikes (**Figures 2D,F**), which are, however, eliminated by application of the $GABA_A$; receptor antagonists picrotoxin (**Figure 2E**) or bicuculline (**Figure 2F**) as well as by activating μ-opioid receptors (Avoli et al., 1996a,b); this pharmacological procedure abolishes the presynaptic release of GABA (Capogna et al., 1993).

As shown in **Figures 2D,F**, slow, glutamatergic independent, interictal events continued to propagate through the extended brain slice and in the guinea pig isolated brain. As further discussed below, such propagation may depend on the increases in extracellular $[K^+]$ that accompany the slow interictal spikes induced by 4AP. To note as two types of interictal spikes have been identified in *in vivo* EEG recordings obtained from epileptic animals, and have been thereafter termed "type 1" and "type 2" (Bortel et al., 2010; Chauvière et al., 2012; Salami et al., 2014; Lévesque et al., 2021b). It should also be emphasized that preservation of inhibition is present in several *in vitro* models of epileptiform interictal synchronization such as those induced by application of Mg^{2+} free-medium (Mody et al., 1987; Tancredi et al., 1990), high K^+ medium (Rutecki et al., 1985) or tetraethylammonium (Rutecki et al., 1990).

The likely role played by elevations in extracellular $[K^+]$ in the spread of the "slow," mainly GABAergic, interictal spikes recorded during application of 4AP and ionotropic glutamatergic antagonists was originally proposed by Perreault and Avoli (1992). Shortly before, Barolet and Morris (1991) had discovered that $GABA_A$ receptor activation, resulting from the application of exogenous GABA or the $GABA_A$ receptor agonist THIP, led to increases in extracellular $[K^+]$ even when voltage-gated Na^+ channels were blocked by tetrodotoxin, thus excluding any relevant contribution of action potential firing to such elevations in extracellular $[K^+]$. As illustrated in **Figure 3A**, a few years later, Morris et al. (1996) reported that the "slow," 4AP-induced spikes recorded from different regions of the isolated, adult rat hippocampal slice are mirrored by increases in extracellular $[K^+]$ that continue to occur in the presence of the ionotropic glutamate receptor antagonists 6- cyano-7-nitroquinoxalone-2,3-dione (CNQX) and DL-2- amino-5-phosphonovaleric acid (APV); however, these field events—along with their associated increases in extracellular $[K^+]$—were reversibly blocked by the $GABA_A$ receptor antagonist

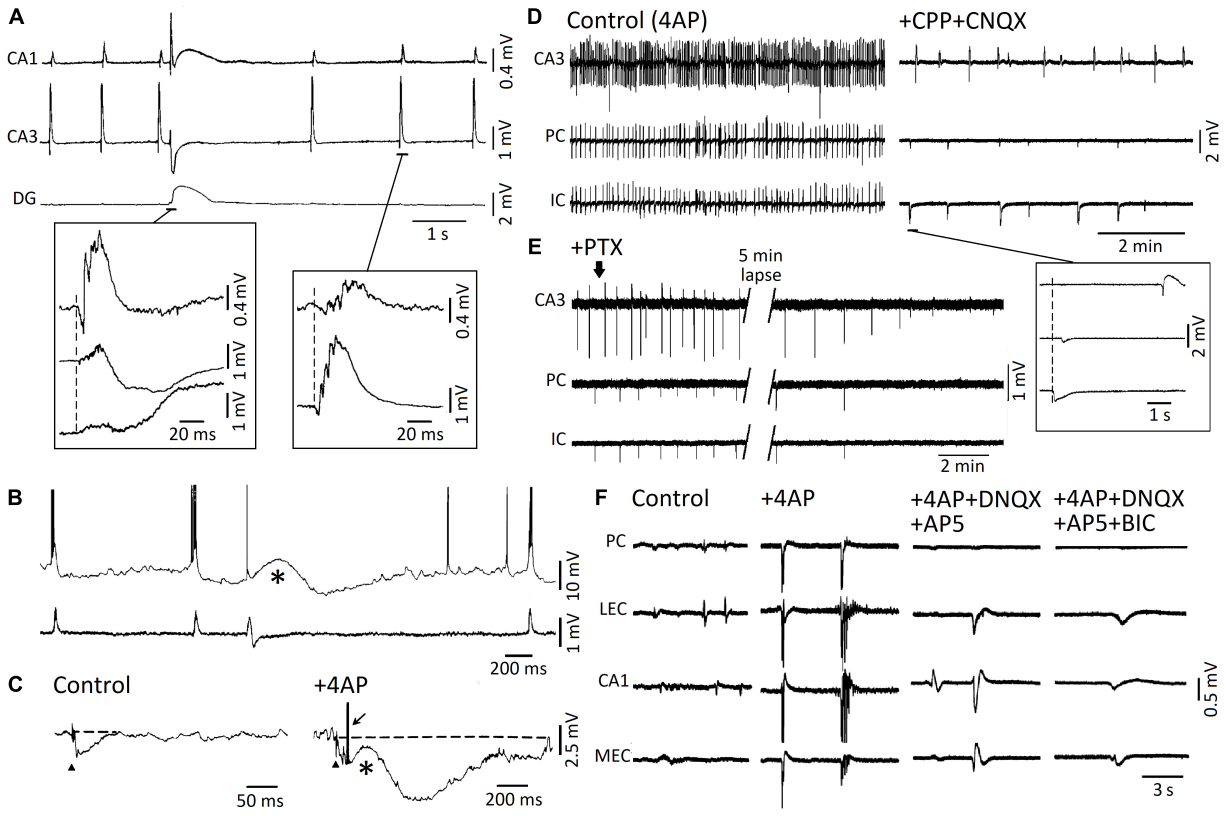

FIGURE 2

(A) Simultaneous field recordings obtained from CAI, CA3, and dentate gyrus in an adult rat hippocampal slice during 4AP application. Note that two types of spontaneous interictal spikes are spontaneously generated. The first type is long-lasting and less frequent, it is recorded in all three regions, and it is characterized by a late, "slow" wave; the second type is recorded in CA3 and CA1 only, it is characterized by a short burst of population spikes, and it occurs at a "fast" rate. **(B)** Simultaneous intracellular (top trace) and field potential (bottom trace) recordings obtained from the CA3 subfield during 4AP application. Note that intracellular bursts of action potentials correlated with the "fast" interictal field events, whereas a long-lasting depolarization corresponded to the "slow" interictal field event. **(C)** Responses to Schaffer collateral electrical stimulation (triangle) recorded intracellularly from a CA3 pyramidal cell under control conditions and in the presence of 4AP. Note that in control the presumptive recurrent hyperpolarizing IPSP lasts approx. 60 ms while, in the presence of 4AP, the same stimulation induces an initial hyperpolarizing IPSP followed by a slow depolarization (asterisk) and a long-lasting (almost 1 s long) hyperpolarization; the arrow indicates a fractionated, presumably ectopic, action potential that arises from the peak of the early hyperpolarizing IPSP. **(D)** Simultaneous field potential recordings obtained in an extended brain slice from the hippocampal CA3 area, the perirhinal cortex and the insular cortex under control (4AP) conditions and during application of NMDA and non-NMDA ionotropic glutamatergic receptor antagonists (+ CPP + CNQX). Note in the inset that during ionotropic glutamatergic receptor antagonism, "slow" field potentials continue to occur independently in CA3 from those seen *quasi* synchronously in PC and IC. **(E)** Under experimental conditions similar to those described for **(D)** (+ CPP + CNQX), addition of the $GABA_A$ receptor antagonist picrotoxin abolishes the presumptive, "slow" GABAergic field potentials in all areas of the brain slice. **(F)** Epileptiform activity induced by 4AP arterial application in the piriform cortex (PC), lateral entorhinal cortex (l-EC), hippocampal CA1 subfield, and medial entorhinal cortex (m-EC) of the isolated brain preparation is greatly reduced by ionotropic glutamatergic receptor antagonists (+ DNQX + AP5). The residual field potential events are then abolished by further administration of the $GABA_A$ receptor antagonist bicuculline (BIC). **(A,B)** Are modified from Perreault and Avoli (1992); **(C)** is modified from Perreault and Avoli (1991); **(D,E)** are modified from Sudbury and Avoli (2007); **(F)** is modified from Uva et al. (2009).

bicuculline methiodide (BMI). Similar data have been obtained in successive studies that were aimed at analyzing the elevations in extracellular $[K^+]$ associated to the "slow" interictal spikes induced by 4AP in slices of the rat hippocampus (Avoli et al., 1996b; Lamsa and Kaila, 1997), the rat or mouse entorhinal cortex (Avoli et al., 1996a; Librizzi et al., 2017) and the human neocortex (Louvel et al., 2001; D'Antuono et al., 2004). Extracellular $[K^+]$ elevations associated to $GABA_A$ receptor-mediated spikes were also shown to occur in the entorhinal cortex of the *in vitro* isolated whole guinea pig brain (Librizzi et al., 2017). Overall, these data indicate that slow interictal spikes induced by 4AP mainly result from synchronous firing of interneurons that causes massive release of GABA, subsequent activation of post-synaptic $GABA_A$ receptors and thus sizeable increases in extracellular $[K^+]$ through the activation of the KCC2 cotransporter (Viitanen et al., 2010).

A turning point on the role played by $GABA_A$ receptor signaling in epileptiform synchronization coincided with the discovery that the onset of ictal discharges recorded

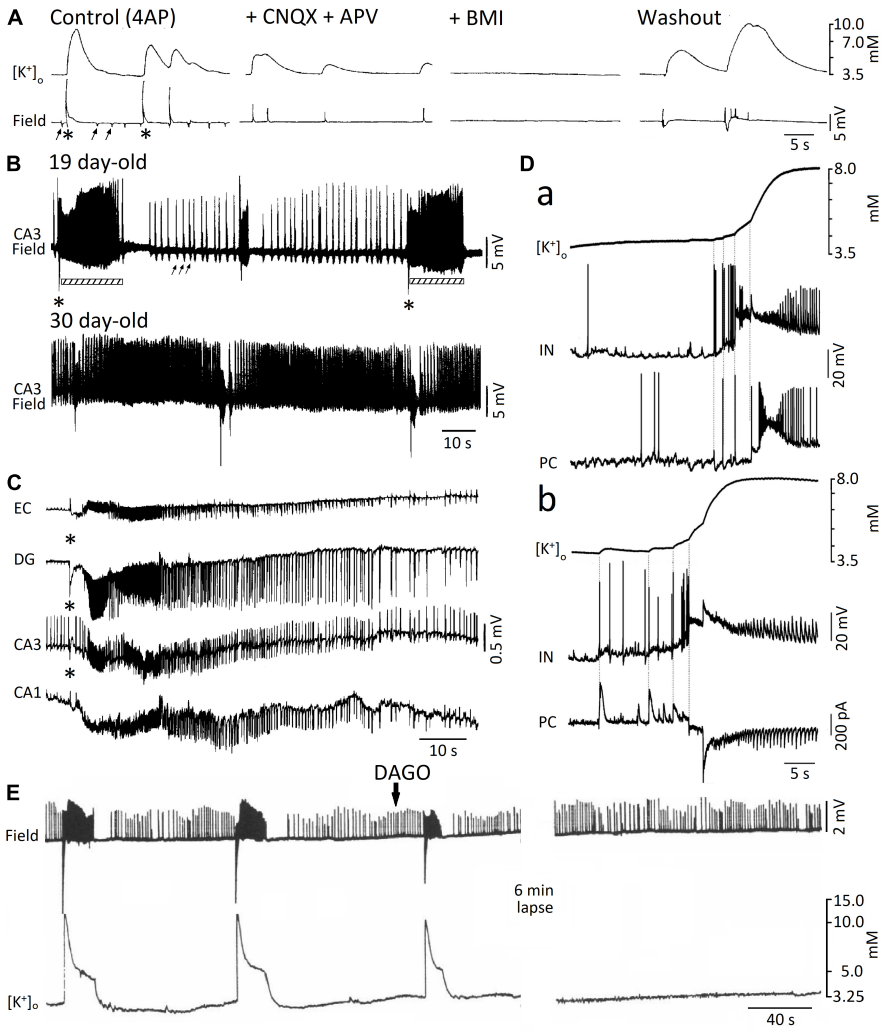

FIGURE 3
(A) Simultaneous extracellular [K^+] and field potential recordings obtained from the CA1 subfield of an adult rat hippocampal slice during 4AP (Control) and successive application of ionotropic glutamatergic receptor antagonists (+ CNQX + CPP), $GABA_A$ receptor antagonist (BMI), and washout (i.e., return to 4AP application for over 3 h); note in control the occurrence of both "slow" (asterisks) and "fast" (arrows) interictal spikes as well as that only the "slow" spikes are associated with sizable increases in extracellular [K^+]. Note also that these "slow" spikes continue to occur during CNQX + CPP but are abolished by (BMI). **(B)** Field potential recordings from the CA3 *stratum radiatum* of two hippocampal slices obtained from 19 and 30 day-old rats during application of 4AP; note that at day 19, "fast" (arrows) and "slow" (asterisks) interictal spikes occur along with ictal discharges (bars) that are shortly preceded by a low interictal; ictal discharges are, however, not recorded in the experiment performed at postnatal day 30. **(C)** Simultaneous field potential recordings obtained from the entorhinal cortex (EC) and from the hippocampal the dentate gyrus (DG) and CA1 and CA3 subfields during application of 4AP in an extended brain slice; note that the "slow" (asterisk), along with the subsequent ictal discharge, are recorded from all areas while the "fast" interictal spikes are clearly detected in CA3 only. **(D)** Simultaneous extracellular [K^+] and intracellular recordings from fast-spiking interneurons (IN) and principal cells (PC) in the medial entorhinal cortex at the onset of two ictal discharges occurring during 4AP application. Current-clamp recordings from both IN and PC are shown in **(a)**, while current -clamp and voltage-clamp recordings from and IN and a PC, respectively, are illustrated in **(b)**. Note that in both examples the IN fires action potentials earlier than the PC and that these firings correspond to time-locked elevations in extracellular [K^+]; note also in **(b)** that interneuron firing is mirrored by outward currents in the PC. **(E)** Effects induced by the μ-opioid receptor agonist DAGO on the epileptiform activity recorded from the CA3 of a 15-day-old rat brain slice during 4AP application; note that the negative-going, "slow" spikes and the subsequent ictal activity along with the associated increases in extracellular [K^+] are abolished by DAGO, and are replaced by continuous "fast" interictal events. **(A)** Is modified from Morris et al. (1996); **(B)** is modified from Avoli (1990); **(C)** is modified from Avoli et al. (1996a); **(D)** is modified from Librizzi et al. (2017); **(E)** is modified from Avoli et al. (1996b).

from juvenile (15–22 day-old) rat hippocampal slices during 4AP application, is shortly preceded, and thus presumably caused by a field event that resemble the "slow" GABAergic spike (asterisk in **Figure 3B**, 19 day-old field recording) (Avoli, 1990; Avoli et al., 1993, 1996b); to note how this interictal-ictal pattern disappeared with brain maturation to be replaced by a continuous pattern of "fast" and "slow" interictal spikes (**Figure 3B**, 30 day-old field recording)

(*cf.* also Psarropoulou and Avoli, 1996). However, successive *in vitro* studies, which were performed in extended brain slices and in the isolated guinea pig brain revealed that ictal (seizure-like) discharges can occur in adult brain tissue during 4AP application as well as that they are initiated and presumably maintained by $GABA_A$ receptor signaling (**Figure 3C**; Avoli et al., 1996a, 2004; Sudbury and Avoli, 2007; Carriero et al., 2010; Uva et al., 2013, 2015; Librizzi et al., 2017). The role of $GABA_A$ receptor signaling in the initiation of seizure-like activity has been confirmed by computational studies; Kurbatova et al. (2016) have indeed reported that before seizure onset, high frequency firing of GABAergic interneurons generates an increase of the depolarizing $GABA_A$ onto pyramidal cells, which induces a massive drop of inhibition that may allow seizure initiation. Interestingly, it has been also shown that the fast activity that occurs at seizure onset and characterizes low-voltage fast onset seizures is associated with interneuron firing, while pyramidal cells remain silent. Employing a biophysically network model (González et al., 2018), have also reported, that seizure-like activity triggered by interneuron firing would not depend on depolarizing $GABA_A$ signaling, but would instead rely on an increase of intracellular $[Cl^-]$, which is sufficient for KCC2 activation, the subsequent accumulation of extracellular $[K^+]$ and the development of epileptiform activity (González et al., 2018).

In line with the mechanism discussed above (i.e., that interneuron firing leading to $GABA_A$ receptor activation does, in turn, cause sizeable elevations in extracellular $[K^+]$), several studies have reported that the initial (sentinel) spikes preceding the ictal events induced by 4AP is associated with interneuron action potential firing along with a large increase in extracellular $[K^+]$ (Avoli et al., 1996a,b; Ziburkus et al., 2006; Lévesque et al., 2016; Librizzi et al., 2017). This aspect is further illustrated in **Figure 3D**. First, double patch-clamp recordings of an interneuron and a principal cell in mouse entorhinal cortex slices demonstrated that interneuron burst discharges coupled with IPSPs (**Figure 3Da**) or IPSCs (**Figure 3Db**) in principal neurons occur at the onset of 4AP-induced ictal activity; second, such "pre-ictal" patterns were associated with rises in extracellular $[K^+]$ that were closely related to interneuron firing and further enhanced by the ensuing recruitment of neuronal networks into the seizure activity. These results firmly support the view that elevations in extracellular $[K^+]$ are caused by interneuron firing, which consistently precedes the initiation of ictal events as well as that these extracellular $[K^+]$ elevations contribute to seizure precipitation. Interestingly, the emergence of seizure-like activity during extracellular $[K^+]$ perturbations has been demonstrated by a realistic computational model of cortical networks (Fröhlich et al., 2010).

It is well known that elevating extracellular $[K^+]$ induces neuronal hyperexcitability along with seizure activity (Zuckermann and Glaser, 1968). Successive studies have demonstrated that increased extracellular $[K^+]$ causes a positive shift of the membrane reversal of the $GABA_A$ receptor-mediated currents thus weakening inhibition (Jensen et al., 1993); it has also been shown that neuronal network resonance, which leads to oscillatory patterns in the beta-gamma range, emerges during increased extracellular $[K^+]$ (Bartos et al., 2007). These data are therefore in line with the role played by $GABA_A$ receptor activation in promoting epileptiform synchronization and thus seizure-like activity. To be emphasized as pharmacological procedures that interfere with $GABA_A$ signaling (e.g., $GABA_A$ receptor antagonists or μ-opioid receptor agonists) halt ictal discharges induced *in vitro* by 4AP and replace them with a pattern of recurring, short-lasting interictal spikes (**Figure 3E**; Avoli et al., 1996a,b, 2004; Sudbury and Avoli, 2007). In human epileptic tissue, blockade of $GABA_A$ receptors also halts interictal discharges (Cohen et al., 2002; Blauwblomme et al., 2019) or modifies their spatial propagation (Sabolek et al., 2012). Suppression of interictal discharges can also be obtained with the application of the NKCC1 blocker bumetanide, in brain slices obtained from pediatric patients with focal cortical dysplasia (Blauwblomme et al., 2019) or in slices obtained from patients with temporal lobe epilepsy and hippocampal sclerosis (Huberfeld et al., 2007), therefore suggesting that the depolarizing responses to GABA in a subset of pyramidal cells during interictal spikes results from excessively high intracellular $[Cl^-]$. A depolarizing action of GABA due to altered intracellular $[Cl^-]$ homeostasis has also been demonstrated in tissue obtained from pediatric patients with cortical dysplasia (Abdijadid et al., 2015).

The paradoxical role played by $GABA_A$ receptors in initiating 4AP-induced ictal (seizure-like) events (*cf.*, de Curtis and Avoli, 2016) has been confirmed by studies in which optogenetic activation of parvalbumin- or somatostatin-positive interneurons was found capable of triggering ictal events with electrographic features similar to those occurring spontaneously (Shiri et al., 2015, 2016; Yekhlef et al., 2015; Lado et al., 2022). As illustrated in **Figure 4A**, optogenetic activation of parvalbumin-positive interneurons in the entorhinal cortex (panel b) initiates local ictal discharges that are characterized by an onset that is superimposable to what recorded during spontaneous events (panel a); in fact; the onset of both spontaneous and optogenetic-induced ictal events is typified by one-two interictal-like spikes that lead to fast, beta-gamma oscillations, which characterize the initial component of the seizure activity; these electrographic characteristics represent the hallmark of low-voltage fast onset ictal discharges recorded in patients presenting with focal epileptic disorders (Perucca et al., 2014) and in animal models *in vivo* (Lévesque et al., 2012). Moreover, it was found in these experiments that optogenetic activation of parvalbumin-positive interneurons could evoke

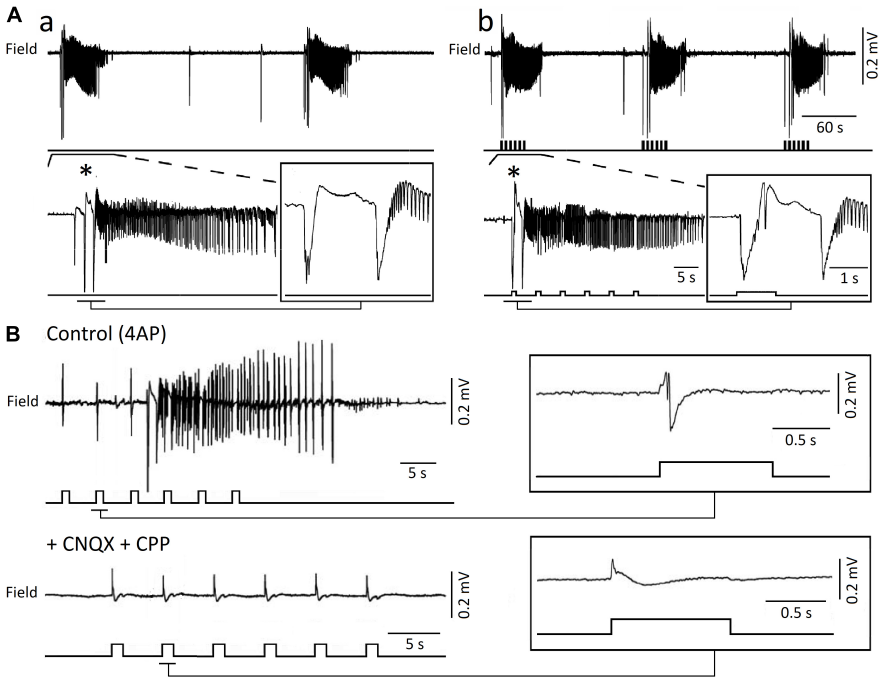

FIGURE 4
(A) Ictal discharges recorded extracellularly from the mouse entorhinal cortex during application of 4AP can occur spontaneously **(a)** or be triggered by optogenetic activation of parvalbumin interneurons **(b)**. One ictal event for each experimental condition is further expanded to show the onset patterns that are in both cases characterized by 1 or 2 negative-going interictal-like spikes. **(B)** Blockade of ionotropic glutamatergic receptors (+ CNQX + CPP) abolishes ictal discharges induced by the optogenetic activation of parvalbumin-positive interneurons in the presence of 4AP; however, under these experimental conditions optogenetic stimuli continue to evoke slow interictal spike. **(A,B)** Are modified from Shiri et al. (2016). The onset of the ictal discharge (*) is shown on an expanded time scale in the inset.

slow interictal spikes both during application of 4AP and after blockade of ionotropic excitatory transmission (**Figure 4B**; Shiri et al., 2016).

The surprisingly active role played by $GABA_A$ signaling in initiating and, perhaps, sustaining seizure activity *in vitro* has been identified under different experimental conditions, including perfusion of low doses of bicuculline in the isolated guinea pig brain (Gnatkovsky et al., 2008), perfusion of brain slices with Mg^{2+} free medium (Köhling et al., 2000), or high frequency electrical stimuli (Velazquez and Carlen, 1999; Fujiwara-Tsukamoto et al., 2010). The contribution of $GABA_A$ receptors to epileptiform synchronization is also supported by the ability of CA1 hippocampal networks *in vitro* to generate prolonged discharges following pharmacological blockade of both $GABA_B$ and ionotropic glutamatergic receptors (Uusisaari et al., 2002). Evidence obtained from *in vivo* models of MTLE have also shown that increased activity of GABA releasing interneurons (which in turns silences principal neurons) coincides with the onset of focal seizures (Grasse et al., 2013; Fujita et al., 2014; Toyoda et al., 2015; Karunakaran et al., 2016). Last but not least, seizure onsets recorded from epileptic patients undergoing presurgical depth electrode investigations, is associated with increased interneuron firing and marked reduction of principal cell excitability (Truccolo et al., 2011; Schevon et al., 2012; Elahian et al., 2018).

$GABA_A$ signaling and epileptiform discharges *in vivo*

The kainic acid (KA) (Lévesque and Avoli, 2013) and the pilocarpine models of MTLE (Lévesque et al., 2021a) have been widely used to study how epileptic discharges are generated from mesial temporal lobe structures *in vivo*. Both models rely on the chemical induction of an initial brain insult (i.e., a *status epilepticus,* SE), that is followed a few days later by the development of a chronic epileptic condition. $GABA_A$ signaling could play a role in ictogenesis in these animal models, since alterations in $GABA_A$ receptor function and in GABA releasing interneurons have been reported (Friedman et al., 1994; Schwarzer et al., 1997; Tsunashima et al., 1997; Laurén et al., 2005; Fritsch et al., 2009; Drexel et al., 2013; Dubanet et al., 2021).

In the KA model, spontaneous seizures occurring in epileptic mice can be stopped, and the frequency of seizures with severe behavioral symptoms reduced, when optogenetic

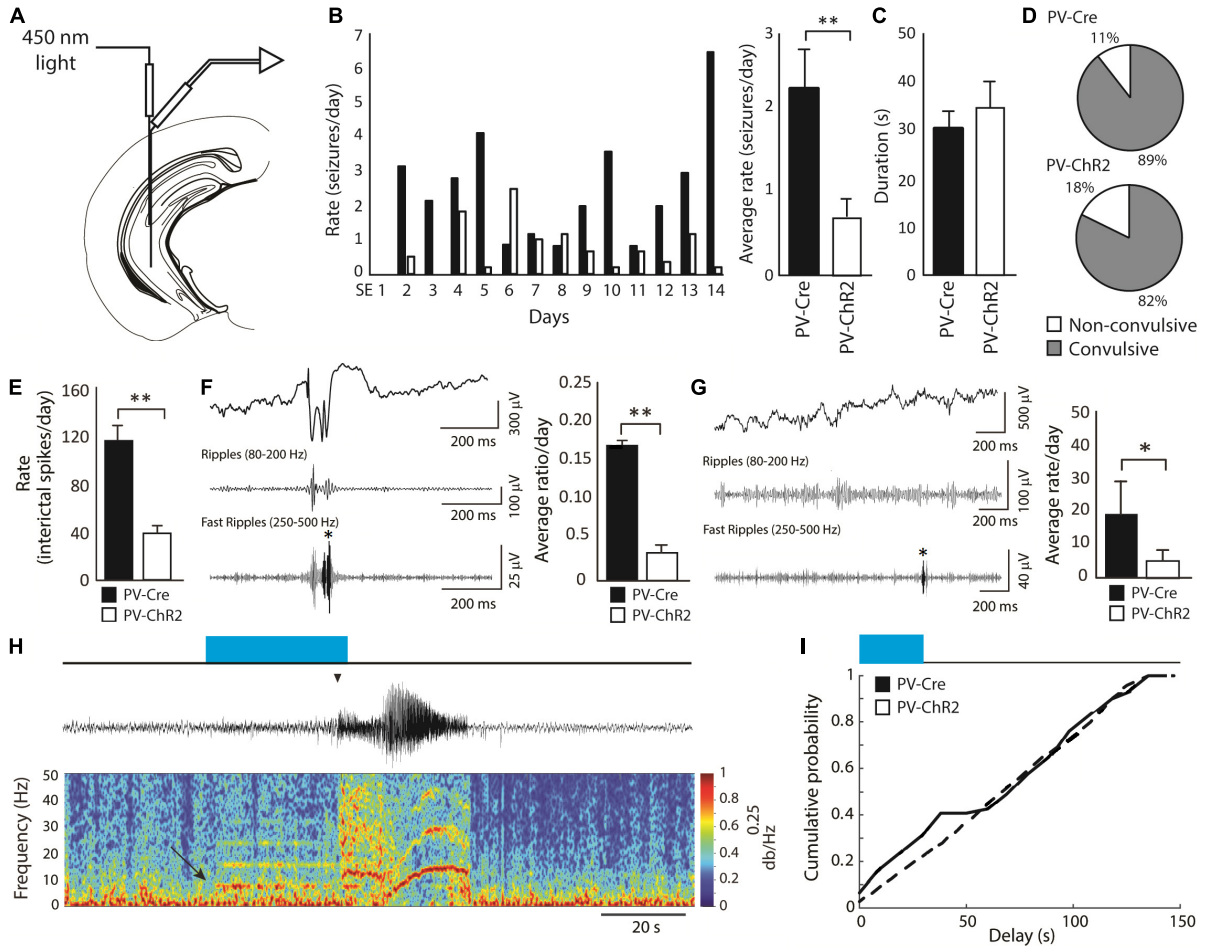

FIGURE 5
(A) Schematic diagram showing the location of the optic fiber and electrode in the CA3 region of the hippocampus. The tip of the optic fiber was glued less than 1 mm above the tip of the electrode. Optogenetic stimulation of PV-positive interneurons (8 Hz for 30 s every 2 min) was performed for 14 continuous days, starting 3 days after SE. **(B)** Average daily rates of spontaneous seizures in PV-ChR2 and PV-Cre animals. PV-ChR2 animals showed significantly less seizures compared to PV-Cre animals (**$p < 0.005$). **(C)** Bar graph showing the average duration of seizures in both groups. No significant differences were observed. **(D)** Proportion of non-convulsive and convulsive seizures in both groups. No significant differences were observed. **(E)** Bar graph showing rates of interictal spikes in both groups. PV-Cre animals showed significantly higher rates of interictal spikes compared to PV-ChR2 animals (**$p < 0.001$). **(F)** Bar graph showing the average ratio of interictal spikes with fast ripples on the total number of interictal spikes for each group. PV-Cre animals showed a higher ratio compared to the PV-ChR2 group (**$p < 0.001$). A representative example of an interictal spike with a fast ripple is shown on the right. **(G)** Bar graph showing the average rate of isolated fast ripples in both groups. PV-ChR2 animals showed significantly lower rates of isolated fast ripples compared to PV-Cre animals (*$p < 0.01$). **(H)** Example of a spontaneous seizure that was triggered by optogenetic stimulation of PV-positive interneurons (blue rectangle) in a PV-ChR2 animal. Note that oscillations around 8 Hz in the field (arrow) were triggered by light stimulation and that the seizure occurred approximately 25 s after (arrowhead). **(I)** Cumulative probability curves showing that PV-ChR2 animals are more likely to show seizures between 0 and 30 s after the onset of optogenetic stimulation compared to PV-Cre animals. Modified from Lévesque et al. (2019).

activation of ChR2-expressing PV-positive interneurons is performed in the hippocampus ipsilateral or contralateral to the hippocampus that was injected with KA (Krook-Magnuson et al., 2013). Similar findings were obtained by Chen et al. (2021), who used optogenetics in KA-treated epileptic animals to activate hippocampal PV-interneurons expressing ChRmine; this is a red-shifted opsin that exhibits high sensitivity to light stimulation (Marshel et al., 2019), thus making neurons expressing these opsins sensitive to transcranial optogenetic stimulation. The application of on-demand transcranial optogenetic stimulation to these ChRmine-expressing PV-positive interneurons during the chronic period induced a 51% decrease in seizure duration compared to sham treatment. Interestingly, optogenetic activation of PV-positive interneurons in the hippocampus of KA-treated animals also improves performance in cognitive tasks (Kim et al., 2020).

Such anti-ictogenic effect is not restricted to the hippocampus but it is also observed when optogenetic stimulation is applied to PV-expressing Purkinje cells of the cerebellum, a brain structure that is anatomically and

functionally connected to the hippocampus (Watson et al., 2018) and that is known to modulate hippocampal function during cognitive tasks (Zeidler et al., 2020). Krook-Magnuson et al. (2014) found that optogenetic excitation or inhibition of PV-expressing Purkinje cells in the lateral or midline cerebellum of KA-treated animals during the chronic period shortens seizure duration. However, it remains unclear through which mechanisms cerebellar optogenetic stimulation controls hippocampal seizures, since both excitation and inhibition of cerebellar Purkinje cells could decrease seizure duration (Krook-Magnuson et al., 2014). Similar anti-ictogenic effects in the KA model resulting from the activation of GABAergic neuronal populations in remote regions were also reported recently by Hristova et al. (2021), who performed optogenetic stimulation of GABAergic populations in the medial septum, a region that sends GABAergic projections to hippocampal GABAergic interneurons (Unal et al., 2015).

In the pilocarpine model, Lévesque et al. (2019) investigated whether continuous, unilateral, optogenetic stimulation of ChR2-expressing PV-positive interneurons in the CA3 subfield of the hippocampus (**Figure 5A**) could decrease seizure rates in pilocarpine-treated epileptic mice. These results have revealed that activation of PV-ChR2 interneurons at 8 Hz for 30 s every 2 min for 14 continuous days induce a decrease in rates of spontaneous seizures compared to what was observed in PV-Cre (opsin-negative) animals (**Figure 5B**). Seizure duration (**Figure 5C**) and proportion of convulsive seizures (**Figure 5D**) were not decreased by PV optogenetic stimulation; however, rates of interictal spikes (**Figure 5E**), of interictal spikes with fast ripples (**Figure 5F**) and of isolated fast ripples (**Figure 5G**)—which are considered as markers of epileptogenesis (Jefferys et al., 2012)–were significantly lower in the PV-ChR2 group compared to the PV-Cre group.

These findings are in line with the evidence obtained by Krook-Magnuson et al. (2013), who reported a decrease in seizure rates in the KA model by using closed-loop activation of PV-positive interneurons. However, Lévesque et al. (2019) also found that the "residual" seizures that continued to occur, could be triggered by optogenetic stimuli (**Figures 5H,I**). These data are in line with what was reported *in vitro* (Shiri et al., 2015, 2016; Yekhlef et al., 2015; Chang et al., 2018; Botterill et al., 2019).

Concluding remarks

The studies reviewed here disclose an unexpected role played by $GABA_A$ receptors in epileptiform synchronization including the generation of interictal and ictal (seizure) events. Such paradoxical role depends on the large increases in extracellular $[K^+]$ that are caused by KCC2 activation due to massive release of GABA consequent to synchronous firing of inhibitory interneurons (Di Cristo et al., 2018). We have also summarized recent findings suggesting that activation of inhibitory interneurons can exert unexpected effects on the processes associated to epileptogenesis. These results reveal a complex pattern of participating mechanisms. Thus, while synaptic excitation and voltage-gated Na^+ channels remain the key components of synchronous epileptiform discharges, $GABA_A$ receptors have emerged as surprising, paradoxical players in the generation of interictal spikes and in the initiation and maintenance of prolonged epileptiform phenomena (i.e., to ictogenesis).

The evidence that enhanced $GABA_A$ receptor function supports epileptiform synchronization and thus focal seizure generation may explain the disappointingly limited clinical efficacy of some antiepileptic compounds that were "mechanistically" developed to potentiate $GABA_A$ signaling during the 1980s and were introduced into clinical practice at the start of the 1990s. These compounds include γ-vinyl-GABA (which inhibits the breakdown of GABA by the enzyme GABA transaminase) (Rogawski and Löscher, 2004), tiagabine (which increases GABA levels by inhibiting GABA reuptake) (Brodie, 1995; Pollack et al., 2005), and progabide (Lloyd et al., 1983; Loiseau et al., 1983). It should also be emphasized that benzodiazepines, which can halt seizure activity and stop *status epilepticus* (Pang and Hirsch, 2005), increase $GABA_A$ receptor function by acting on an allosteric "benzodiazepine site" that is located in most of the α subunit-containing $GABA_A$ receptors (Costa et al., 1975; Choi et al., 1977; Olsen, 2015). However, and in line with a synchronizing action of GABA, benzodiazepines have been reported to precipitate seizures, when given intravenously in patients with Lennox-Gastaut syndrome (Perucca et al., 1998).

Data availability statement

The original contributions presented in this study are included in the article/supplementary material, further inquiries can be directed to the corresponding author.

Author contributions

MA wrote the early draft of this review. All authors contributed to the manuscript revision, read, and approved the submitted version.

Funding

This review was based on experiments that were supported by the Canadian Institutes of Health Research (Grants

PJT153310, PJT166178, and MOP130328), CURE and the Savoy Foundation to MA, and the Italian Ministry of Health (Current Research 2021 and Grant RF 2018-12365681), and the Paolo Zorzi Association for Neuroscience (Grant 2021-24 EPICARE project) to MC.

Conflict of interest

The authors declare that the research was conducted in the absence of any commercial or financial relationships that could be construed as a potential conflict of interest.

Publisher's note

All claims expressed in this article are solely those of the authors and do not necessarily represent those of their affiliated organizations, or those of the publisher, the editors and the reviewers. Any product that may be evaluated in this article, or claim that may be made by its manufacturer, is not guaranteed or endorsed by the publisher.

References

Abdijadid, S., Mathern, G. W., Levine, M. S., and Cepeda, C. (2015). Basic mechanisms of epileptogenesis in pediatric cortical dysplasia. *CNS Neurosci. Ther.* 21, 92–103. doi: 10.1111/cns.12345

Avoli, M. (1990). Epileptiform discharges and a synchronous GABAergic potential induced by 4-aminopyridine in the rat immature hippocampus. *Neurosci. Lett.* 117, 93–98. doi: 10.1016/0304-3940(90)90125-s

Avoli, M., Benini, R., de Guzman, P., and Omar, A. (2004). GABA(B) receptor activation and limbic network ictogenesis. *Neuropharmacology* 46, 43–51. doi: 10.1016/s0028-3908(03)00307-1

Avoli, M., de Curtis, M., Gnatkovsky, V., Gotman, J., Köhling, R., Lévesque, M., et al. (2016). Specific imbalance of excitatory/inhibitory signaling establishes seizure onset pattern in temporal lobe epilepsy. *J. Neurophysiol.* 115, 3229–3237. doi: 10.1152/jn.01128.2015

Avoli, M., Barbarosie, M., Lücke, A., Nagao, T., Lopantsev, V., and Köhling, R. (1996a). Synchronous GABA-mediated potentials and epileptiform discharges in the rat limbic system in vitro. *J. Neurosci.* 16, 3912–3924.

Avoli, M., Louvel, J., Kurcewicz, I., Pumain, R., and Barbarosie, M. (1996b). Extracellular free potassium and calcium during synchronous activity induced by 4-aminopyridine in the juvenile rat hippocampus. *J. Physiol.* 493(Pt 3), 707–717. doi: 10.1113/jphysiol.1996.sp021416

Avoli, M., Methot, M., and Kawasaki, H. (1998). GABA-dependent generation of ectopic action potentials in the rat hippocampus. *Eur. J. Neurosci.* 10, 2714–2722. doi: 10.1046/j.1460-9568.1998.00275.x

Avoli, M., Psarropoulou, C., Tancredi, V., and Fueta, Y. (1993). On the synchronous activity induced by 4-aminopyridine in the CA3 subfield of juvenile rat hippocampus. *J. Neurophysiol.* 70, 1018–1029.

Barolet, A. W., and Morris, M. E. (1991). Changes in extracellular K^+ evoked by GABA, THIP and baclofen in the guinea-pig hippocampal slice. *Exp. Brain Res.* 84, 591–598. doi: 10.1007/BF00230971

Bartos, M., Vida, I., and Jonas, P. (2007). Synaptic mechanisms of synchronized gamma oscillations in inhibitory interneuron networks. *Nat. Rev. Neurosci.* 8, 45–56. doi: 10.1038/nrn2044

Ben-Ari, Y., Krnjević, K., and Reinhardt, W. (1979). Hippocampal seizures and failure of inhibition. *Can. J. Physiol. Pharmacol.* 57, 1462–1466. doi: 10.1139/y79-218

Blauwblomme, T., Dossi, E., Pellegrino, C., Goubert, E., Iglesias, B. G., Sainte-Rose, C., et al. (2019). Gamma-aminobutyric acidergic transmission underlies interictal epileptogenicity in pediatric focal cortical dysplasia. *Ann. Neurol.* 85, 204–217. doi: 10.1002/ana.25403

Bortel, A., Lévesque, M., Biagini, G., Gotman, J., and Avoli, M. (2010). Convulsive status epilepticus duration as determinant for epileptogenesis and interictal discharge generation in the rat limbic system. *Neurobiol. Dis.* 40, 478–489. doi: 10.1016/j.nbd.2010.07.015

Botterill, J. J., Lu, Y.-L., LaFrancois, J. J., Bernstein, H. L., Alcantara-Gonzalez, D., Jain, S., et al. (2019). An excitatory and epileptogenic effect of dentate gyrus mossy cells in a mouse model of epilepsy. *Cell Rep.* 29, 2875–2889.e6. doi: 10.1016/j.celrep.2019.10.100

Bragin, A., Engel, J. Jr., Wilson, C. L., Fried, I., and Mathern, G. W. (1999a). Hippocampal and entorhinal cortex high-frequency oscillations (100–500 Hz) in human epileptic brain and in kainic acid–treated rats with chronic seizures. *Epilepsia* 40, 127–137. doi: 10.1111/j.1528-1157.1999.tb02065.x

Bragin, A., Engel, J., Wilson, C. L., Fried, I., and Buzsáki, G. (1999b). High-frequency oscillations in human brain. *Hippocampus* 9, 137–142. doi: 10.1002/(SICI)1098-106319999:2<137::AID-HIPO5<3.0.CO;2-0

Brodie, M. J. (1995). Tiagabine pharmacology in profile. *Epilepsia* 36(Suppl. 6), S7–S9.

Buckle, P. J., and Haas, H. L. (1982). Enhancement of synaptic transmission by 4-aminopyridine in hippocampal slices of the rat. *J. Physiol.* 326, 109–122.

Buzsáki, G. (2015). Hippocampal sharp wave-ripple: A cognitive biomarker for episodic memory and planning. *Hippocampus* 25, 1073–1188. doi: 10.1002/hipo.22488

Capogna, M., Gähwiler, B. H., and Thompson, S. M. (1993). Mechanism of mu-opioid receptor-mediated presynaptic inhibition in the rat hippocampus in vitro. *J. Physiol.* 470, 539–558. doi: 10.1113/jphysiol.1993.sp019874

Carriero, G., Uva, L., Gnatkovsky, V., Avoli, M., and de Curtis, M. (2010). Independent epileptiform discharge patterns in the olfactory and limbic areas of the in vitro isolated Guinea pig brain during 4-aminopyridine treatment. *J. Neurophysiol.* 103, 2728–2736. doi: 10.1152/jn.00862.2009

Cepeda, C., Levinson, S., Nariai, H., Yazon, V.-W., Tran, C., Barry, J., et al. (2020). Pathological high frequency oscillations associate with increased GABA synaptic activity in pediatric epilepsy surgery patients. *Neurobiol. Dis.* 134:104618. doi: 10.1016/j.nbd.2019.104618

Chang, M., Dian, J. A., Dufour, S., Wang, L., Moradi Chameh, H., Ramani, M., et al. (2018). Brief activation of GABAergic interneurons initiates the transition to ictal events through post-inhibitory rebound excitation. *Neurobiol. Dis.* 109, 102–116. doi: 10.1016/j.nbd.2017.10.007

Chauvière, L., Doublet, T., Ghestem, A., Siyoucef, S. S., Wendling, F., Huys, R., et al. (2012). Changes in interictal spike features precede the onset of temporal lobe epilepsy. *Ann. Neurol.* 71, 805–814. doi: 10.1002/ana.23549

Chen, R., Gore, F., Nguyen, Q.-A., Ramakrishnan, C., Patel, S., Kim, S. H., et al. (2021). Deep brain optogenetics without intracranial surgery. *Nat. Biotechnol.* 39, 161–164. doi: 10.1038/s41587-020-0679-9

Choi, D. W., Farb, D. H., and Fischbach, G. D. (1977). Chlordiazepoxide selectively augments GABA action in spinal cord cell cultures. *Nature* 269, 342–344. doi: 10.1038/269342a0

Cohen, I., Navarro, V., Clemenceau, S., Baulac, M., and Miles, R. (2002). On the origin of interictal activity in human temporal lobe epilepsy in vitro. *Science* 298, 1418–1421. doi: 10.1126/science.1076510

Costa, E., Guidotti, A., and Mao, C. C. (1975). "Evidence for involvement of GABA in the action of benzodiazepines: Studies on rat cerebellum," in *Advances in biochemical psychopharmacology*, Vol. 14, eds E. Costa and P. Greengard (New York, NY: Raven), 113–130.

Coursin, D. B. (1954). Convulsive seizures in infants with pyridoxine-deficient diet. *J. Am. Med. Assoc.* 154, 406–408. doi: 10.1001/jama.1954.02940390030009

Crunelli, V., Leresche, N., and Cope, D. W. (2012). "GABA-A receptor function in typical absence seizures," in *Jasper's basic mechanisms of the epilepsies*, eds J. L. Noebels, M. Avoli, M. A. Rogawski, R. W. Olsen, and A. V. Delgado-Escueta (Bethesda, MD: National Center for Biotechnology Information (US)).

D'Antuono, M., Louvel, J., Köhling, R., Mattia, D., Bernasconi, A., Olivier, A., et al. (2004). GABAA receptor-dependent synchronization leads to ictogenesis in the human dysplastic cortex. *Brain* 127, 1626–1640. doi: 10.1093/brain/awh181

de Curtis, M., and Avanzini, G. (2001). Interictal spikes in focal epileptogenesis. *Prog. Neurobiol.* 63, 541–567.

de Curtis, M., and Avoli, M. (2016). GABAergic networks jump-start focal seizures. *Epilepsia* 57, 679–687. doi: 10.1111/epi.13370

Di Cristo, G., Awad, P. N., Hamidi, S., and Avoli, M. (2018). KCC2, epileptiform synchronization, and epileptic disorders. *Prog. Neurobiol.* 162, 1–16. doi: 10.1016/j.pneurobio.2017.11.002

Dingledine, R., and Gjerstad, L. (1980). Reduced inhibition during epileptiform activity in the in vitro hippocampal slice. *J. Physiol.* 305, 297–313.

Drexel, M., Kirchmair, E., and Sperk, G. (2013). Changes in the expression of GABAA receptor subunit mRNAs in parahippocampal areas after kainic acid induced seizures. *Front. Neural Circuits* 7:142. doi: 10.3389/fncir.2013.00142

Dubanet, O., Ferreira Gomes Da Silva, A., Frick, A., Hirase, H., Beyeler, A., and Leinekugel, X. (2021). Probing the polarity of spontaneous perisomatic GABAergic synaptic transmission in the mouse CA3 circuit in vivo. *Cell Rep.* 36:109381. doi: 10.1016/j.celrep.2021.109381

Elahian, B., Lado, N. E., Mankin, E., Vangala, S., Misra, A., Moxon, K., et al. (2018). Low-voltage fast seizures in humans begin with increased interneuron firing. *Ann. Neurol.* 84, 588–600. doi: 10.1002/ana.25325

Engel, J. Jr., McDermott, M. P., Wiebe, S., Langfitt, J. T., Stern, J. M., Dewar, S., et al. (2012). Early surgical therapy for drug-resistant temporal lobe epilepsy: A randomized trial. *J. Am. Med. Assoc.* 307, 922–930. doi: 10.1001/jama.2012.220

Foffani, G., Uzcategui, Y. G., Gal, B., and Menendez de la Prida, L. (2007). Reduced spike-timing reliability correlates with the emergence of fast ripples in the rat epileptic hippocampus. *Neuron* 55, 930–941. doi: 10.1016/j.neuron.2007.07.040

Friedman, L. K., Pellegrini-Giampietro, D. E., Sperber, E. F., Bennett, M. V., Moshé, S. L., and Zukin, R. S. (1994). Kainate-induced status epilepticus alters glutamate and GABAA receptor gene expression in adult rat hippocampus: An in situ hybridization study. *J. Neurosci.* 14, 2697–2707. doi: 10.1523/JNEUROSCI.14-05-02697.1994

Fritsch, B., Qashu, F., Figueiredo, T. H., Aroniadou-Anderjaska, V., Rogawski, M. A., and Braga, M. F. M. (2009). Pathological alterations in GABAergic interneurons and reduced tonic inhibition in the basolateral amygdala during epileptogenesis. *Neuroscience* 163, 415–429. doi: 10.1016/j.neuroscience.2009.06.034

Fröhlich, F., Sejnowski, T. J., and Bazhenov, M. (2010). Network bistability mediates spontaneous transitions between normal and pathological brain states. *J. Neurosci.* 30, 10734–10743. doi: 10.1523/JNEUROSCI.1239-10.2010

Fujita, S., Toyoda, I., Thamattoor, A. K., and Buckmaster, P. S. (2014). Preictal activity of subicular, CA1, and dentate gyrus principal neurons in the dorsal hippocampus before spontaneous seizures in a rat model of temporal lobe epilepsy. *J. Neurosci.* 34, 16671–16687. doi: 10.1523/JNEUROSCI.0584-14.2014

Fujiwara-Tsukamoto, Y., Isomura, Y., Imanishi, M., Ninomiya, T., Tsukada, M., Yanagawa, Y., et al. (2010). Prototypic seizure activity driven by mature hippocampal fast-spiking interneurons. *J. Neurosci.* 30, 13679–13689. doi: 10.1523/JNEUROSCI.1523-10.2010

Gloor, P. (1997). *The temporal lobe and limbic system*. New York, NY: Oxford University Press.

Gnatkovsky, V., Librizzi, L., Trombin, F., and de Curtis, M. (2008). Fast activity at seizure onset is mediated by inhibitory circuits in the entorhinal cortex in vitro. *Ann. Neurol.* 64, 674–686. doi: 10.1002/ana.21519

González, O. C., Shiri, Z., Krishnan, G. P., Myers, T. L., Williams, S., Avoli, M., et al. (2018). Role of KCC2-dependent potassium efflux in 4-aminopyridine-induced epileptiform synchronization. *Neurobiol. Dis.* 109, 137–147. doi: 10.1016/j.nbd.2017.10.011

Grasse, D. W., Karunakaran, S., and Moxon, K. A. (2013). Neuronal synchrony and the transition to spontaneous seizures. *Exp. Neurol.* 248, 72–84. doi: 10.1016/j.expneurol.2013.05.004

Grover, L. M., Lambert, N. A., Schwartzkroin, P. A., and Teyler, T. J. (1993). Role of HCO3- ions in depolarizing GABAA receptor-mediated responses in pyramidal cells of rat hippocampus. *J. Neurophysiol.* 69, 1541–1555. doi: 10.1152/jn.1993.69.5.1541

Hablitz, J. J. (1984). Picrotoxin-induced epileptiform activity in hippocampus: Role of endogenous versus synaptic factors. *J. Neurophysiol.* 51, 1011–1027. doi: 10.1152/jn.1984.51.5.1011

Hristova, K., Martinez-Gonzalez, C., Watson, T. C., Codadu, N. K., Hashemi, K., Kind, P. C., et al. (2021). Medial septal GABAergic neurons reduce seizure duration upon optogenetic closed-loop stimulation. *Brain J. Neurol.* 144, 1576–1589. doi: 10.1093/brain/awab042

Huberfeld, G., Wittner, L., Clemenceau, S., Baulac, M., Kaila, K., Miles, R., et al. (2007). Perturbed chloride homeostasis and GABAergic signaling in human temporal lobe epilepsy. *J. Neurosci.* 27, 9866–9873. doi: 10.1523/JNEUROSCI.2761-07.2007

Ibarz, J. M., Foffani, G., Cid, E., Inostroza, M., and de la Prida, L. M. (2010). Emergent dynamics of fast ripples in the epileptic hippocampus. *J. Neurosci.* 30, 16249–16261. doi: 10.1523/JNEUROSCI.3357-10.2010

Jefferys, J. G. R., Menendez de la Prida, L., Wendling, F., Bragin, A., Avoli, M., Timofeev, I., et al. (2012). Mechanisms of physiological and epileptic HFO generation. *Prog. Neurobiol.* 98, 250–264. doi: 10.1016/j.pneurobio.2012.02.005

Jensen, M. S., Cherubini, E., and Yaari, Y. (1993). Opponent effects of potassium on GABAA-mediated postsynaptic inhibition in the rat hippocampus. *J. Neurophysiol.* 69, 764–771. doi: 10.1152/jn.1993.69.3.764

Jirsch, J. D., Urrestarazu, E., LeVan, P., Olivier, A., Dubeau, F., and Gotman, J. (2006). High-frequency oscillations during human focal seizures. *Brain J. Neurol.* 129, 1593–1608. doi: 10.1093/brain/awl085

Jiruska, P., Alvarado-Rojas, C., Schevon, C. A., Staba, R., Stacey, W., Wendling, F., et al. (2017). Update on the mechanisms and roles of high-frequency oscillations in seizures and epileptic disorders. *Epilepsia* 58, 1330–1339. doi: 10.1111/epi.13830

Johnson, E. W., de Lanerolle, N. C., Kim, J. H., Sundaresan, S., Spencer, D. D., Mattson, R. H., et al. (1992). "Central" and "peripheral" benzodiazepine receptors: Opposite changes in human epileptogenic tissue. *Neurology* 42, 811–815. doi: 10.1212/wnl.42.4.811

Kaila, K. (1994). Ionic basis of GABAA receptor channel function in the nervous system. *Prog. Neurobiol.* 42, 489–537.

Kaila, K., Lamsa, K., Smirnov, S., Taira, T., and Voipio, J. (1997). Long-lasting GABA-mediated depolarization evoked by high-frequency stimulation in pyramidal neurons of rat hippocampal slice is attributable to a network-driven, bicarbonate-dependent K^+ transient. *J. Neurosci.* 17, 7662–7672. doi: 10.1523/JNEUROSCI.17-20-07662.1997

Karunakaran, S., Grasse, D. W., and Moxon, K. A. (2016). Role of CA3 theta-modulated interneurons during the transition to spontaneous seizures. *Exp. Neurol.* 283, 341–352. doi: 10.1016/j.expneurol.2016.06.027

Keros, S., and Hablitz, J. J. (2005). Ectopic action potential generation in cortical interneurons during synchronized GABA responses. *Neuroscience* 131, 833–842. doi: 10.1016/j.neuroscience.2004.12.010

Kim, H. K., Gschwind, T., Nguyen, T. M., Bui, A. D., Felong, S., Ampig, K., et al. (2020). Optogenetic intervention of seizures improves spatial memory in a mouse model of chronic temporal lobe epilepsy. *Epilepsia* 61, 561–571. doi: 10.1111/epi.16445

Köhling, R., Vreugdenhil, M., Bracci, E., and Jefferys, J. G. (2000). Ictal epileptiform activity is facilitated by hippocampal GABAA receptor-mediated oscillations. *J. Neurosci.* 20, 6820–6829. doi: 10.1523/JNEUROSCI.20-18-06820.2000

Kostopoulos, G., Avoli, M., and Gloor, P. (1983). Participation of cortical recurrent inhibition in the genesis of spike and wave discharges in feline generalized penicillin epilepsy. *Brain Res.* 267, 101–112. doi: 10.1016/0006-8993(83)91043-0

Krook-Magnuson, E., Armstrong, C., Oijala, M., and Soltesz, I. (2013). On-demand optogenetic control of spontaneous seizures in temporal lobe epilepsy. *Nat. Commun.* 4:1376. doi: 10.1038/ncomms2376

Krook-Magnuson, E., Szabo, G. G., Armstrong, C., Oijala, M., and Soltesz, I. (2014). Cerebellar directed optogenetic intervention inhibits spontaneous hippocampal seizures in a mouse model of temporal lobe epilepsy. *eNeuro* 1:ENEURO.0005-14.2014. doi: 10.1523/ENEURO.0005-14.2014

Kurbatova, P., Wendling, F., Kaminska, A., Rosati, A., Nabbout, R., Guerrini, R., et al. (2016). Dynamic changes of depolarizing GABA in a computational model of epileptogenic brain: Insight for Dravet syndrome. *Exp. Neurol.* 283, 57–72. doi: 10.1016/j.expneurol.2016.05.037

Lado, W. E., Xu, X., and Hablitz, J. J. (2022). Modulation of epileptiform activity by three subgroups of GABAergic interneurons in mouse somatosensory cortex. *Epilepsy Res.* 183:106937. doi: 10.1016/j.eplepsyres.2022.106937

Lamsa, K., and Kaila, K. (1997). Ionic mechanisms of spontaneous GABAergic events in rat hippocampal slices exposed to 4-aminopyridine. *J. Neurophysiol.* 78, 2582–2591. doi: 10.1152/jn.1997.78.5.2582

Laurén, H. B., Lopez-Picon, F. R., Korpi, E. R., and Holopainen, I. E. (2005). Kainic acid-induced status epilepticus alters GABA receptor subunit mRNA and

protein expression in the developing rat hippocampus. *J. Neurochem.* 94, 1384–1394. doi: 10.1111/j.1471-4159.2005.03274.x

Lévesque, M., and Avoli, M. (2013). The kainic acid model of temporal lobe epilepsy. *Neurosci. Biobehav. Rev.* 37, 2887–2899. doi: 10.1016/j.neubiorev.2013.10.011

Lévesque, M., Bortel, A., Gotman, J., and Avoli, M. (2011). High-frequency (80–500 Hz) oscillations and epileptogenesis in temporal lobe epilepsy. *Neurobiol. Dis.* 42, 231–241. doi: 10.1016/j.nbd.2011.01.007

Lévesque, M., Chen, L.-Y., Etter, G., Shiri, Z., Wang, S., Williams, S., et al. (2019). Paradoxical effects of optogenetic stimulation in mesial temporal lobe epilepsy. *Ann. Neurol.* 86, 714–728. doi: 10.1002/ana.25572

Lévesque, M., Herrington, R., Hamidi, S., and Avoli, M. (2016). Interneurons spark seizure-like activity in the entorhinal cortex. *Neurobiol. Dis.* 87, 91–101. doi: 10.1016/j.nbd.2015.12.011

Lévesque, M., Macey-Dare, A. D. B., Wang, S., and Avoli, M. (2021b). Evolution of interictal spiking during the latent period in a mouse model of mesial temporal lobe epilepsy. *Curr. Res. Neurobiol.* 2:100008. doi: 10.1016/j.crneur.2021.100008

Lévesque, M., Biagini, G., de Curtis, M., Gnatkovsky, V., Pitsch, J., Wang, S., et al. (2021a). The pilocarpine model of mesial temporal lobe epilepsy: Over one decade later, with more rodent species and new investigative approaches. *Neurosci. Biobehav. Rev.* 130, 274–291. doi: 10.1016/j.neubiorev.2021.08.020

Lévesque, M., Salami, P., Gotman, J., and Avoli, M. (2012). Two seizure-onset types reveal specific patterns of high-frequency oscillations in a model of temporal lobe epilepsy. *J. Neurosci.* 32, 13264–13272. doi: 10.1523/JNEUROSCI.5086-11.2012

Librizzi, L., Losi, G., Marcon, I., Sessolo, M., Scalmani, P., Carmignoto, G., et al. (2017). Interneuronal network activity at the onset of seizure-like events in entorhinal cortex slices. *J. Neurosci.* 37, 10398–10407. doi: 10.1523/JNEUROSCI.3906-16.2017

Lloyd, K. G., Morselli, P. L., Depoortere, H., Fournier, V., Zivkovic, B., Scatton, B., et al. (1983). The potential use of GABA agonists in psychiatric disorders: Evidence from studies with progabide in animal models and clinical trials. *Pharmacol. Biochem. Behav.* 18, 957–966. doi: 10.1016/s0091-3057(83)80021-5

Loiseau, P., Bossi, L., Guyot, M., Orofiamma, B., and Morselli, P. L. (1983). Double-blind crossover trial of progabide versus placebo in severe epilepsies. *Epilepsia* 24, 703–715.

Louvel, J., Papatheodoropoulos, C., Siniscalchi, A., Kurcewicz, I., Pumain, R., Devaux, B., et al. (2001). GABA-mediated synchronization in the human neocortex: Elevations in extracellular potassium and presynaptic mechanisms. *Neuroscience* 105, 803–813. doi: 10.1016/s0306-4522(01)00247-0

Marshel, J. H., Kim, Y. S., Machado, T. A., Quirin, S., Benson, B., Kadmon, J., et al. (2019). Cortical layer-specific critical dynamics triggering perception. *Science* 365:eaaw5202. doi: 10.1126/science.aaw5202

McDonald, J. W., Garofalo, E. A., Hood, T., Sackellares, J. C., Gilman, S., McKeever, P. E., et al. (1991). Altered excitatory and inhibitory amino acid receptor binding in hippocampus of patients with temporal lobe epilepsy. *Ann. Neurol.* 29, 529–541. doi: 10.1002/ana.410290513

Mody, I., Lambert, J. D., and Heinemann, U. (1987). Low extracellular magnesium induces epileptiform activity and spreading depression in rat hippocampal slices. *J. Neurophysiol.* 57, 869–888. doi: 10.1152/jn.1987.57.3.869

Morris, M. E., Obrocea, G. V., and Avoli, M. (1996). Extracellular K^+ accumulations and synchronous GABA-mediated potentials evoked by 4-aminopyridine in the adult rat hippocampus. *Exp. Brain Res.* 109, 71–82. doi: 10.1007/BF00228628

Niedermeyer, E., and da Silva, F. H. L. (2005). *Electroencephalography: Basic principles, clinical applications, and related fields*. Philadelphia, PA: Lippincott Williams & Wilkins.

Olsen, R. W. (2015). Allosteric ligands and their binding sites define γ-aminobutyric acid (GABA) type A receptor subtypes. *Adv. Pharmacol.* 73, 167–202. doi: 10.1016/bs.apha.2014.11.005

Olsen, R. W., Bureau, M., Houser, C. R., Delgado-Escueta, A. V., Richards, J. G., and Möhler, H. (1992). GABA/benzodiazepine receptors in human focal epilepsy. *Epilepsy Res. Suppl.* 8, 383–391.

Pang, T., and Hirsch, L. J. (2005). Treatment of convulsive and nonconvulsive status epilepticus. *Curr. Treat. Options Neurol.* 7, 247–259. doi: 10.1007/s11940-005-0035-x

Perreault, P., and Avoli, M. (1991). Physiology and pharmacology of epileptiform activity induced by 4-aminopyridine in rat hippocampal slices. *J. Neurophysiol.* 65, 771–785.

Perreault, P., and Avoli, M. (1992). 4-aminopyridine-induced epileptiform activity and a GABA-mediated long- lasting depolarization in the rat hippocampus. *J. Neurosci.* 12, 104–115. doi: 10.1523/JNEUROSCI.12-01-00104.1992

Perucca, E., Gram, L., Avanzini, G., and Dulac, O. (1998). Antiepileptic drugs as a cause of worsening seizures. *Epilepsia* 39, 5–17. doi: 10.1111/j.1528-1157.1998.tb01268.x

Perucca, P., Dubeau, F., and Gotman, J. (2014). Intracranial electroencephalographic seizure-onset patterns: Effect of underlying pathology. *Brain J. Neurol.* 137, 183–196. doi: 10.1093/brain/awt299

Pollack, M. H., Roy-Byrne, P. P., Van Ameringen, M., Snyder, H., Brown, C., Ondrasik, J., et al. (2005). The selective GABA reuptake inhibitor tiagabine for the treatment of generalized anxiety disorder: Results of a placebo-controlled study. *J. Clin. Psychiatry* 66, 1401–1408.

Psarropoulou, C., and Avoli, M. (1996). Developmental features of 4-aminopyridine induced epileptogenesis. *Brain Res. Dev. Brain Res.* 94, 52–59.

Rogawski, M. A., and Löscher, W. (2004). The neurobiology of antiepileptic drugs. *Nat. Rev. Neurosci.* 5, 553–564. doi: 10.1038/nrn1430

Rutecki, P. A., Lebeda, F. J., and Johnston, D. (1985). Epileptiform activity induced by changes in extracellular potassium in hippocampus. *J. Neurophysiol.* 54, 1363–1374.

Rutecki, P. A., Lebeda, F. J., and Johnston, D. (1987). 4-Aminopyridine produces epileptiform activity in hippocampus and enhances synaptic excitation and inhibition. *J. Neurophysiol.* 57, 1911–1924. doi: 10.1152/jn.1987.57.6.1911

Rutecki, P. A., Lebeda, F. J., and Johnston, D. (1990). Epileptiform activity in the hippocampus produced by tetraethylammonium. *J. Neurophysiol.* 64, 1077–1088.

Sabolek, H. R., Swiercz, W. B., Lillis, K. P., Cash, S. S., Huberfeld, G., Zhao, G., et al. (2012). A candidate mechanism underlying the variance of interictal spike propagation. *J. Neurosci.* 32, 3009–3021. doi: 10.1523/JNEUROSCI.5853-11.2012

Salami, P., Lévesque, M., Benini, R., Behr, C., Gotman, J., and Avoli, M. (2014). Dynamics of interictal spikes and high-frequency oscillations during epileptogenesis in temporal lobe epilepsy. *Neurobiol. Dis.* 67C, 97–106. doi: 10.1016/j.nbd.2014.03.012

Schevon, C. A., Weiss, S. A., McKhann, G., Goodman, R. R., Yuste, R., Emerson, R. G., et al. (2012). Evidence of an inhibitory restraint of seizure activity in humans. *Nat. Commun.* 3:1060. doi: 10.1038/ncomms2056

Schwartzkroin, P. A., and Prince, D. A. (1980). Changes in excitatory and inhibitory synaptic potentials leading to epileptogenic activity. *Brain Res.* 183, 61–76.

Schwarzer, C., Tsunashima, K., Wanzenböck, C., Fuchs, K., Sieghart, W., and Sperk, G. (1997). GABA(A) receptor subunits in the rat hippocampus II: Altered distribution in kainic acid-induced temporal lobe epilepsy. *Neuroscience* 80, 1001–1017. doi: 10.1016/s0306-4522(97)00145-0

Shiri, Z., Manseau, F., Lévesque, M., Williams, S., and Avoli, M. (2015). Interneuron activity leads to initiation of low-voltage fast-onset seizures. *Ann. Neurol.* 77, 541–546. doi: 10.1002/ana.24342

Shiri, Z., Manseau, F., Lévesque, M., Williams, S., and Avoli, M. (2016). Activation of specific neuronal networks leads to different seizure onset types. *Ann. Neurol.* 79, 354–365. doi: 10.1002/ana.24570

Sloviter, R. S. (1987). Decreased hippocampal inhibition and a selective loss of interneurons in experimental epilepsy. *Science* 235, 73–76. doi: 10.1126/science.2879352

Staba, R. J., Wilson, C. L., Bragin, A., Jhung, D., Fried, I., and Engel, J. Jr. (2004). High-frequency oscillations recorded in human medial temporal lobe during sleep. *Ann. Neurol.* 56, 108–115. doi: 10.1002/ana.20164

Steriade, M., Gloor, P., Llinás, R. R., Lopes de Silva, F. H., and Mesulam, M. M. (1990). Report of IFCN committee on basic mechanisms. Basic mechanisms of cerebral rhythmic activities. *Electroencephalogr. Clin. Neurophysiol.* 76, 481–508. doi: 10.1016/0013-4694(90)90001-z

Sudbury, J. R., and Avoli, M. (2007). Epileptiform synchronization in the rat insular and perirhinal cortices in vitro. *Eur. J. Neurosci.* 26, 3571–3582. doi: 10.1111/j.1460-9568.2007.05962.x

Tancredi, V., Hwa, G. G., Zona, C., Brancati, A., and Avoli, M. (1990). Low magnesium epileptogenesis in the rat hippocampal slice: Electrophysiological and pharmacological features. *Brain Res.* 511, 280–290. doi: 10.1016/0006-8993(90)90173-9

Timofeev, I., and Steriade, M. (2004). Neocortical seizures: Initiation, development and cessation. *Neuroscience* 123, 299–336. doi: 10.1016/j.neuroscience.2003.08.051

Toyoda, I., Fujita, S., Thamattoor, A. K., and Buckmaster, P. S. (2015). Unit activity of hippocampal interneurons before spontaneous seizures in an animal model of temporal lobe epilepsy. *J. Neurosci.* 35, 6600–6618. doi: 10.1523/JNEUROSCI.4786-14.2015

Truccolo, W., Donoghue, J. A., Hochberg, L. R., Eskandar, E. N., Madsen, J. R., Anderson, W. S., et al. (2011). Single-neuron dynamics in human focal epilepsy. *Nat. Neurosci.* 14, 635–641. doi: 10.1038/nn.2782

Tsunashima, K., Schwarzer, C., Kirchmair, E., Sieghart, W., and Sperk, G. (1997). GABA(A) receptor subunits in the rat hippocampus III: Altered messenger RNA expression in kainic acid-induced epilepsy. *Neuroscience* 80, 1019–1032. doi: 10.1016/s0306-4522(97)00144-9

Unal, G., Joshi, A., Viney, T. J., Kis, V., and Somogyi, P. (2015). Synaptic targets of medial septal projections in the hippocampus and extrahippocampal cortices of the mouse. *J. Neurosci.* 35, 15812–15826. doi: 10.1523/JNEUROSCI.2639-15.2015

Urrestarazu, E., Jirsch, J. D., LeVan, P., Hall, J., Avoli, M., Dubeau, F., et al. (2006). High-frequency intracerebral EEG activity (100-500 Hz) following interictal spikes. *Epilepsia* 47, 1465–1476. doi: 10.1111/j.1528-1167.2006.00618.x

Uusisaari, M., Smirnov, S., Voipio, J., and Kaila, K. (2002). Spontaneous epileptiform activity mediated by GABA(A) receptors and gap junctions in the rat hippocampal slice following long-term exposure to GABA(B) antagonists. *Neuropharmacology* 43, 563–572. doi: 10.1016/s0028-3908(02)00156-9

Uva, L., Avoli, M., and de Curtis, M. (2009). Synchronous GABA-receptor-dependent potentials in limbic areas of the in-vitro isolated adult guinea pig brain. *Eur. J. Neurosci.* 29, 911–920. doi: 10.1111/j.1460-9568.2009.06672.x

Uva, L., Breschi, G. L., Gnatkovsky, V., Taverna, S., and de Curtis, M. (2015). Synchronous inhibitory potentials precede seizure-like events in acute models of focal limbic seizures. *J. Neurosci.* 35, 3048–3055. doi: 10.1523/JNEUROSCI.3692-14.2015

Uva, L., Trombin, F., Carriero, G., Avoli, M., and de Curtis, M. (2013). Seizure-like discharges induced by 4-aminopyridine in the olfactory system of the in vitro isolated guinea pig brain. *Epilepsia* 54, 605–615. doi: 10.1111/epi.12133

Velazquez, J. L., and Carlen, P. L. (1999). Synchronization of GABAergic interneuronal networks during seizure-like activity in the rat horizontal hippocampal slice. *Eur. J. Neurosci.* 11, 4110–4118. doi: 10.1046/j.1460-9568.1999.00837.x

Viitanen, T., Ruusuvuori, E., Kaila, K., and Voipio, J. (2010). The K^+–Cl^- cotransporter KCC2 promotes GABAergic excitation in the mature rat hippocampus. *J. Physiol.* 588, 1527–1540. doi: 10.1113/jphysiol.2009.181826

Voskuyl, R. A., and Albus, H. (1985). Spontaneous epileptiform discharges in hippocampal slices induced by 4-aminopyridine. *Brain Res.* 342, 54–66.

Watson, T. C., Obiang, P., Torres-Herraez, A., Watilliaux, A., Coulon, P., Rochefort, C., et al. (2018). Anatomical and physiological foundations of cerebello-hippocampal interaction. *eLife* 8:e41896. doi: 10.7554/eLife.41896

Williamson, A., Telfeian, A. E., and Spencer, D. D. (1995). Prolonged GABA responses in dentate granule cells in slices isolated from patients with temporal lobe sclerosis. *J. Neurophysiol.* 74, 378–387. doi: 10.1152/jn.1995.74.1.378

Yekhlef, L., Breschi, G. L., Lagostena, L., Russo, G., and Taverna, S. (2015). Selective activation of parvalbumin- or somatostatin-expressing interneurons triggers epileptic seizurelike activity in mouse medial entorhinal cortex. *J. Neurophysiol.* 113, 1616–1630. doi: 10.1152/jn.00841.2014

Zeidler, Z., Hoffmann, K., and Krook-Magnuson, E. (2020). HippoBellum: Acute cerebellar modulation alters hippocampal dynamics and function. *J. Neurosci.* 40, 6910–6926. doi: 10.1523/JNEUROSCI.0763-20.2020

Ziburkus, J., Cressman, J. R., Barreto, E., and Schiff, S. J. (2006). Interneuron and pyramidal cell interplay during in vitro seizure-like events. *J. Neurophysiol.* 95, 3948–3954. doi: 10.1152/jn.01378.2005

Zijlmans, M., Jacobs, J., Kahn, Y. U., Zelmann, R., Dubeau, F., and Gotman, J. (2011). Ictal and interictal high frequency oscillations in patients with focal epilepsy. *Clin. Neurophysiol.* 122, 664–671. doi: 10.1016/j.clinph.2010.09.021

Zuckermann, E. C., and Glaser, G. H. (1968). Hippocampal epileptic activity induced by localized ventricular perfusion with high-potassium cerebrospinal fluid. *Exp. Neurol.* 20, 87–110. doi: 10.1016/0014-4886(68)90126-x

frontiers | Frontiers in Neural Circuits

TYPE Original Research
PUBLISHED 03 February 2023
DOI 10.3389/fncir.2023.1076761

OPEN ACCESS

EDITED BY
Elsa Rossignol,
CHU Sainte-Justine, Canada

REVIEWED BY
Fernando Roman Fernandez,
Boston University, United States
Michal Zochowski,
University of Michigan, United States

*CORRESPONDENCE
Frances K. Skinner
✉ frances.skinner@utoronto.ca

RECEIVED 21 October 2022
ACCEPTED 16 January 2023
PUBLISHED 03 February 2023

CITATION
Sun Z, Crompton D, Lankarany M and Skinner FK (2023) Reduced oriens-lacunosum/moleculare cell model identifies biophysical current balances for *in vivo* theta frequency spiking resonance. *Front. Neural Circuits* 17:1076761. doi: 10.3389/fncir.2023.1076761

Reduced oriens-lacunosum/moleculare cell model identifies biophysical current balances for *in vivo* theta frequency spiking resonance

Zhenyang Sun[1], David Crompton[1,2], Milad Lankarany[1,2,3,4] and Frances K. Skinner[1,5]*

[1]Krembil Brain Institute, University Health Network, Toronto, ON, Canada, [2]Institute of Biomedical Engineering, University of Toronto, Toronto, ON, Canada, [3]Department of Physiology, University of Toronto, Toronto, ON, Canada, [4]KITE, Toronto Rehabilitation Institute, University Health Network, Toronto, ON, Canada, [5]Departments of Medicine (Neurology) and Physiology, University of Toronto, Toronto, ON, Canada

Conductance-based models have played an important role in the development of modern neuroscience. These mathematical models are powerful "tools" that enable theoretical explorations in experimentally untenable situations, and can lead to the development of novel hypotheses and predictions. With advances in cell imaging and computational power, multi-compartment models with morphological accuracy are becoming common practice. However, as more biological details are added, they make extensive explorations and analyses more challenging largely due to their huge computational expense. Here, we focus on oriens-lacunosum/moleculare (OLM) cell models. OLM cells can contribute to functionally relevant theta rhythms in the hippocampus by virtue of their ability to express spiking resonance at theta frequencies, but what characteristics underlie this is far from clear. We converted a previously developed detailed multi-compartment OLM cell model into a reduced single compartment model that retained biophysical fidelity with its underlying ion currents. We showed that the reduced OLM cell model can capture complex output that includes spiking resonance in *in vivo*-like scenarios as previously obtained with the multi-compartment model. Using the reduced model, we were able to greatly expand our *in vivo*-like scenarios. Applying spike-triggered average analyses, we were able to to determine that it is a combination of hyperpolarization-activated cation and muscarinic type potassium currents that specifically allow OLM cells to exhibit spiking resonance at theta frequencies. Further, we developed a robust Kalman Filtering (KF) method to estimate parameters of the reduced model in real-time. We showed that it may be possible to directly estimate conductance parameters from experiments since this KF method can reliably extract parameter values from model voltage recordings. Overall, our work showcases how the contribution of cellular biophysical current details could be determined and assessed for spiking resonance. As well, our work shows that it may be possible to directly extract these parameters from current clamp voltage recordings.

KEYWORDS

hippocampus, interneuron, theta rhythm, h-current, M-current, Kalman Filter, parameter estimation, spiking resonance

1. Introduction

It is challenging not only to classify the multitude of different cell types, but also to understand their contributions in brain circuits under normal and pathological states (Zeng and Sanes, 2017; Fishell and Kepecs, 2020). While it is currently possible to record from different cell types *in vivo*, this is technically difficult and laborious to achieve for identified cell types in large numbers. Moreover, a cell's biophysical characteristics necessarily have to be obtained from *in vitro* studies. Neuronal modeling can bring *in vitro* and *in vivo* studies together by computationally creating artificial *in vivo* states with mathematical models of a given cell type (Destexhe et al., 2003). These models can be viewed as virtual *in vivo* brain circuits. Taking advantage of this approach, we have previously used our computational models to show specialized contributions of interneuron-specific inhibitory cell types in the creation of temporally precise coordination of modulatory pathways (Guet-McCreight and Skinner, 2021). In this way, computational models can help us to gain insight into how specific cell types contribute in different brain states *in vivo*.

Oriens-lacunosum/moleculare (OLM) cells are inhibitory cell types in the hippocampus that function to gate sensory and contextual information in the CA1 (Leão et al., 2012) and support fear memory acquisition (Lovett-Barron et al., 2014). Their firing is phase-locked to the prominent theta rhythms of behaving animals (Klausberger et al., 2003; Varga et al., 2012; Katona et al., 2014). OLM cells have the ability to spike at theta frequencies (Maccaferri and McBain, 1996) and to have a spiking preference to theta frequency sinusoidal inputs (Pike et al., 2000) *in vitro*, although they exhibit little if any subthreshold resonance at theta frequencies (Zemankovics et al., 2010; Kispersky et al., 2012). It is unlikely that OLM cells play a theta pacemaking role since experiments by Kispersky et al. (2012) have shown that OLM cells do not fire preferentially at theta frequencies when injected with artificial synaptic inputs to mimic *in vivo* states. However, if frequency-modulated inputs are presented instead, then there is a theta frequency firing preference. This suggests that OLM cells could contribute to theta rhythms by amplifying theta-modulated activity from presynaptic sources due to their ability to phase-lock with theta-modulated inputs—i.e., they exhibit theta frequency spiking resonance. What biophysical characteristics possessed by OLM cells might be essential to allow them to exhibit spiking resonance at theta frequencies?

A long-known prominent feature of OLM cells is their "sag" which is due to the presence of hyperpolarization-activated cation channels or h-channels (Maccaferri and McBain, 1996). However, in their experimental work, Kispersky et al. (2012) found that theta frequency spiking resonance did not depend on h-channel currents, but it did depend on an after-hyperpolarization (AHP)-like current. OLM cells have a distinct cholinergic fingerprint (Lawrence, 2008; Pancotti and Topolnik, 2022), possessing muscarinic (M-) potassium channel currents that can contribute to AHP behaviors (Lawrence et al., 2006b). Interestingly, muscarinic acetylcholine receptor (mAChR) activation (which inhibits M-channels) of OLM cells has been shown to enhance firing reliablility and precision to theta frequency input (Lawrence et al., 2006a).

Kispersky et al. (2012) generated *in vivo*-like scenarios in their slice preparations using dynamic clamp technology which limited the artificial synaptic inputs to somatic locations. However, synaptic input mostly occurs in dendritic regions. Given this, Sekulić and Skinner (2017) used a developed database of detailed multi-compartment OLM model cells which either had h-channels in their dendrites or not, and created *in vivo*-like scenarios but with artificial synapses that included dendritic regions. They found that OLM cells could be recruited by high or low theta frequency inputs that was dependent on whether h-channels were present in the OLM model cell dendrites or not, respectively (Sekulić and Skinner, 2017). Following this, tightly integrated experimental and modeling work demonstrated that h-channels must necessarily be present on OLM cell dendrites to be able to match experiments (Sekulić et al., 2020). Moving forward, these OLM cell models were used to produce *in vivo*-like (IVL) states, but with consideration of actual presynaptic cell populations (Guet-McCreight and Skinner, 2020). That is, actual synapses were modeled with determined characteristics based on known presynaptic input to OLM cells. Using these IVL states, we showed that spiking resonance at theta frequencies is possible in OLM cells (Guet-McCreight and Skinner, 2021). However, we were limited in the IVL frequencies that our models could express and the detailed multi-compartment nature of the model with thousands of presynaptic inputs prevented a full exploration of what OLM cell biophysical characteristics during IVL states might be critical in bringing about theta frequency spiking resonances.

To tackle this, we here develop a reduced biophysically faithful single compartment OLM cell model and consider this model embedded in a virtual network as represented by IVL states. We use these IVL virtual networks to determine what biophysical details of OLM cells matter for them to exhibit theta frequency spiking resonance. We first "validate" that our reduced model is capable of capturing complex behaviors by showing that it can match results expressed by the full multi-compartment models (Guet-McCreight and Skinner, 2021), and we then examine spiking resonance in IVL states. From an extensive exploration, we are able to show that a combination of h- and M-channels produce the controlling currents for theta frequency spiking resonance. Inspired by Azzalini et al. (2022), we then move on to adjust a robust Kalman Filter (KF) algorithm and use it to estimate parameters of the reduced OLM cell model from membrane potential recordings of the model cells. This indicates that it should be possible to extract parameter values directly from experimental recordings in a real-time fashion. Overall, our work shows that linking *in vitro, in vivo* experimental, computational, and engineering techniques can bring about novel ways to obtain biophysical, cellular understandings of brain circuits.

2. Methods

We used two models in this work. The first model is of our previously published full multi-compartment OLM cell model (Sekulić et al., 2020), but with some minor modifications described below. We refer to this slightly modified model as "FULL." The second model is a reduced single compartment model that is derived from FULL, and is described in detail below. We refer to it as "SINGLE."

2.1. Multi-compartment OLM cell model

All of the details of our previously developed multi-compartment model can be found in Sekulić et al. (2020). This detailed model was

developed in direct and tight correspondence with experimental data and we have referred to it as a "neuron-to-model matched" (NMM) model in our previous work (Guet-McCreight and Skinner, 2021). Here, we use *Cell 1* of the previously developed NMM models. There are nine different currents in this model and we refer to them by their bracketed acronyms: hyperpolarization-activated cation current (Ih), transient sodium (INa), fast delayed rectifier (IKdrf), slow delayed rectifier (IKdrs), A-type potassium (IKa), M-type (IM), T-type calcium (ICaT), L-type calcium (ICaL), and calcium-dependent potassium (IKCa).

In examining the multi-compartment model for subsequent reduction, we first simplified the representation of the calcium dynamics to obtain a slightly modified multi-compartment model that we refer to as FULL. The specifics of this modification are provided in Supplementary material. We note that there is minimal difference (on average <1.5 ms difference in spike timing, and <0.6% in the resulting voltage and <0.12% for any of the biophysical currents in comparing 30, 60, and −120 pA current steps) between FULL and the previously published *Cell 1 NMM model*. The set of equations for all the biophysical currents of FULL are provided in Supplementary material.

2.2. Single compartment OLM cell model development

Starting from FULL, we created a single compartment OLM cell model in which biophysical fidelity was maintained as best as possible. In examining all the currents in FULL, we noticed that IKdrs could be removed without much effect. Specifically, we found that there is <0.35% difference when comparing voltage peaks (30 and 60 pA current steps) and <0.15% for any of the other currents when the IKdrs conductance was set to zero, and <0.0015% for voltage or current differences at -120 pA step. Also, we note that in order to be able to capture any of the calcium dynamics in FULL, at least a two-compartment model would be required since calcium channels are only present in the dendrites of FULL—see Supplementary material for further details.

For practical reasons of: (i) Computational efficiency in doing extensive spiking resonance explorations, and (ii) Evaluating parameter estimation techniques for direct use with experimental OLM cells, we aimed to have a single compartment mathematical model to use. We thus made the decision to remove consideration of calcium at this stage to enable these practicalities. Therefore, ICaT, ICaL and IKCa were not included in the single compartment model. There are five remaining currents (IKa, IKdrf, IM, Ih, and INa) and we proceeded with them to create a single compartment model with biophysical fidelity as follows.

As this *Cell 1 NMM model* was directly matched with experimental data in which both Ih characteristics and passive properties were obtained in the same cell, we created a single compartment model in which these aspects were maintained. Specifically, the surface area, passive properties (leak current, I_L) and Ih, as directly obtained in *Cell 1* (model and experiment) (Sekulić et al., 2020), were minimally changed. The resulting input resistance, time constant and total Ih are comparable to FULL. Further details are provided in Supplementary material. The conductances of the other four currents, IKa, IKdrf, IM and INa were optimized using BluePyOpt (Van Geit et al., 2016) based on comparison with FULL. Optimization details are provided in Supplementary material. We refer to this single compartment model with optimized values as SINGLE, and it constitutes our developed single compartment model that is used in this work.

The contribution of the different currents to cell firing is shown in Figure 1 for a 60 pA current step for FULL and SINGLE. As easily seen using the currentscape visualization tool (Alonso and Marder, 2019), the relative contribution of the various currents are similar. Although similar, one can observe that there is some compensation for the missing IKCa and calcium currents via IM and IKdrs. These similar balances are apparent at other step currents as shown in Supplementary Figure S4. We reasonably claim that SINGLE is a single compartment OLM cell model that maintains biophysical fidelity.

2.3. SINGLE analyses

2.3.1. Synaptic perturbation model

Previously, Guet-McCreight and Skinner (2021) applied synaptic perturbations to their detailed multi-compartment model, which as noted above is essentially the same as FULL and so we will not distinguish them moving forward. These perturbations were mostly done using 30 (inhibitory or excitatory) synapses randomly distributed across the dendritic tree as a reasonable capturing of experimental observations. Synaptic weights had been optimized based on experiment (Guet-McCreight and Skinner, 2020). Since SINGLE only has one compartment, perturbation was set to be 30 times the individual synaptic weight to maintain an approximately equivalent response in SINGLE relative to FULL. Synaptic equations, implementation and parameter values are identical to *Equation 1* in Guet-McCreight and Skinner (2020) except for the synaptic weight values that are 0.006 (excitatory) and 0.0054 (inhibitory) μS here.

2.3.2. Direct comparisons with FULL

2.3.2.1. *In vitro* setup and phase response curve (PRC) analyses

2.3.2.1.1. Firing rates

As done for FULL in Guet-McCreight and Skinner (2021), different firing frequencies in *in vitro* states were obtained by injecting constant currents into the cell to produce stable firing rates and inter-spike intervals (ISIs). Firing rates were determined by counting spikes over a 10 s interval.

2.3.2.1.2. Phase response curves (PRCs)

This analysis was conducted using inhibitory synaptic perturbations with the same setup as in Guet-McCreight and Skinner (2021). That is, we calculated percent phase change in spiking behavior ($\Delta\phi$) from the length of the ISI before the perturbation (T0) and with the perturbation (T1):

$$\Delta\phi = \frac{T1 - T0}{T0} \times 100 \quad (1)$$

A positive value indicates shortening of the ISI while a negative value indicates a prolonging of the ISI. That is, a phase advance or phase delay respectively. The PRC is generated using perturbations at the full range of phases. To quantify the contribution of the

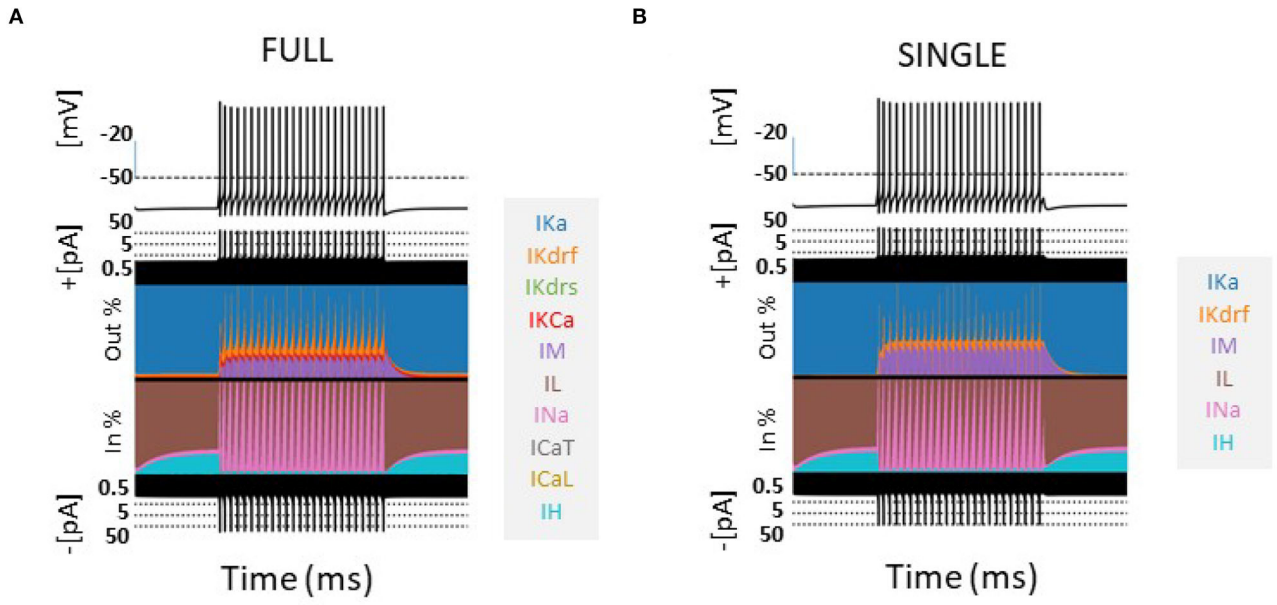

FIGURE 1
Comparison of models-FULL and SINGLE. Currentscapes (Alonso and Marder, 2019) are shown for models of FULL (somatic location) **(A)** and SINGLE **(B)**. Their firings are similar and corresponding biophysical currents have similar balances. Simulations were conducted for 4,000 ms, with a holding current of 4 pA throughout. A step current of 60 pA was injected at 1,000 ms for 2,000 ms. Comparisons at other step currents are provided in Supplementary material.

various currents to the PRCs, we also calculated percent change in currents (ΔI) as done in Guet-McCreight and Skinner (2021). For each current, we obtained its maximum amplitude between the 2nd last spike preceding the perturbation (I0), and its maximum amplitude between the perturbation and the second spike following the perturbation (I1). The percent change in maximum amplitude due to perturbation (ΔI) was calculated as:

$$\Delta I = \frac{I1 - I0}{I0} \times 100 \quad (2)$$

A positive value indicates an increase in maximum current amplitude while a negative value indicates a decrease.

2.3.2.2. Spiking resonance calculations

In Guet-McCreight and Skinner (2021), we computed spiking resonances for *in vitro* and *in vivo*-like (IVL) states. We computed spiking resonances for SINGLE using the same measure as described below.

Each voltage trace obtained was converted to a spike train (1 at spike onset and 0 elsewhere), and the power spectral density (PSD) of each spike train was calculated using the welch function from the Scipy signal module: signal.welch (signal, fs = 1/dt, scaling = "density," nperseg = 20,000). We defined a measure called the 'baseline ratio' to quantify how much a perturbation changes the PSD value from its baseline state. The baseline ratio (δPSD) was calculated as:

$$\delta PSD = \frac{PSD_{f_i\ perturbed}}{PSD_{f_i\ baseline}} \quad (3)$$

Where f_i is the frequency of the input perturbation. That is, $PSD_{f_i\ perturbed}$ is the spectral density value of the f_i perturbed state spike train, while $PSD_{f_i\ baseline}$ is the spectral density value of the baseline state spike train when there is no perturbation (or a perturbation of "0"). Thus, δPSD measures the effectiveness of an f_i perturbation frequency entraining the cell to fire at that frequency. A value of 1 indicates no effect, while higher values suggest more effective entrainment. The resonant frequency (f_r) is defined as the perturbation frequency that produces the largest δPSD value.

2.3.2.2.1. *In vitro state*

With holding currents between 25.4 and 156.8 pA, we generated 50 baseline firing rates from 1 to 36 Hz. For each of the firing rates, we perturbed the voltage using either excitatory or inhibitory synaptic input. As we were doing a direct comparison, we used the same 15 perturbation frequencies as Guet-McCreight and Skinner (2021) that ranged from 0.5 to 30 Hz.

2.3.2.2.2. *In vivo*-like (IVL) state

A much wider range of baseline firing rates in IVL states can be obtained with SINGLE relative to FULL. For direct comparison with spiking resonances obtained using the multi-compartment model, we restricted the baseline frequencies of SINGLE as such and used the same 15 perturbation frequencies that ranged from 0.5 to 30 Hz.

2.3.3. Expanded explorations with SINGLE

2.3.3.1. *In vivo*-like (IVL) states with SINGLE

To define an IVL state, we used the same metric as in Guet-McCreight and Skinner (2020) which was previously developed to reflect literature statistics of the OLM cell type in an IVL state. That is:

$$IVLMetric = (\overline{V_m} > -70.588mV) + (\sigma_{V_m} > 2.2mV) + (ISICV > 0.8) + (3Hz < f < 25Hz) \quad (4)$$

in which the average sub-threshold voltage or membrane potential, $\overline{V_m}$, the standard deviation of the sub-threshold membrane potential, σ_{V_m}, the coefficient of variation for inter-spike intervals, *ISICV*, and the firing rate, f, are computed.

In Guet-McCreight and Skinner (2021), several IVL states were obtained with the multi-compartment model by randomizing the synaptic locations on the dendrites. This is of course not possible with SINGLE as it is a single compartment model. Instead, we followed the approach of Destexhe et al. (2001) that implements stochastic synapses via an Ornstein-Uhlenbeck process (Uhlenbeck and Ornstein, 1930). It is formulated as:

$$I_{syn} = g_e(t)(V - E_e) + g_i(t)(V - E_i) \tag{5}$$

where $g_e(t)$ and $g_i(t)$ are excitatory and inhibitory conductance values as functions of time. E_e and E_i are excitatory and inhibitory reversal potentials, and $g_e(t)$ and $g_i(t)$ are given by:

$$\frac{dg_e(t)}{dt} = \frac{-1}{\tau_e}(g_e(t) - g_{e0}) + \sqrt{D_e}N_1(t) \tag{6}$$

$$\frac{dg_i(t)}{dt} = \frac{-1}{\tau_i}(g_i(t) - g_{i0}) + \sqrt{D_i}N_2(t) \tag{7}$$

where τ_e and τ_i are decay time constants; g_{e0} and g_{i0} are steady state, or average conductances; $N_1(t)$ and $N_2(t)$ are Gaussian white noise following a standard normal distribution; $\sqrt{D_e}$and $\sqrt{D_i}$ are standard deviations of the noise generated.

2.3.3.1.1. IVL state parameter search

We note that while this stochastic synaptic model would allow several IVL states to be generated with SINGLE, most of its parameters are not directly comparable to IVL states generated with FULL, and as such, we cannot use pre-existing parameter values obtained for IVL states and instead must search for them. We used a brute force approach with nested for loops to search for sets of parameter values for $g_{e0}, g_{i0}, \sqrt{D_e}$, and $\sqrt{D_i}$ that would generate IVL states. For each set of parameter values, a 10 s long simulation was performed and the resulting voltage trace was evaluated by the IVL metric.

2.3.3.1.2. Constrained search

After experimenting with several parameter range values, we were able to narrow values down to smaller ranges that would mostly output IVL states. The smaller range exploration had g_{e0} varying from 0.003 to 0.006 with a resolution of 0.0002 μS, g_{i0} varying from 0.008 to 0.012 μS with resolution of 0.00027 μS, $\sqrt{D_e}$ varying from 0 to 0.0016 μS with resolution of 0.000107 μS, and $\sqrt{D_i}$ varying from 0 to 0.01 μS with resolution of 0.00067 μS. In addition, we further constrained our IVL states to be comparable with those obtained with FULL. From an analysis of voltage traces of IVL states with FULL from Guet-McCreight and Skinner (2020), we obtained further constraints of: $8 < \sigma^2_{V_m} < 10\ mV^2$ and $-70 < \overline{V_m} < -67.5\ mV$. This additional constraint was applied only once to every parameter set to allow output that was close enough to that obtained with FULL.

2.3.3.1.3. Selecting representative IVL states

For each IVL parameter set, fifty 10 s long simulations were run with 50 distinct seeds (the same seeds were used for each set). From these 50 simulations for each IVL parameter set, the minimum and maximum firing rates were recorded, and each set would be clustered as a two-dimensional (2D) system when plotted using its minimum vs. maximum firing rate. From this 2D system, 10 IVL parameter sets that span the firing rate space were selected as representative IVL states encompassing the range of firing rate frequencies observed *in vivo* for OLM cells. Since 50 distinct seeds were used, we would have 500 IVL states. For each of these 500 states, we computed firing rates (f's) and resonant frequencies (f_r's). f's were computed as the number of spikes occurring in the 10 s simulation divided by 10, and f_r's were computed as described above. We removed timepoints occurring at 7 ms on either side of the peak of each spike, and the mean and standard deviation of the remaining (independent) timepoints after spike removal were used to obtain $\overline{V_m}$ and σ_{V_m}. It is possible that some of these 500 states may not fully be IVL states (as defined by the metric) since due to stochasticity the same parameter set might not always generate a (further constrained) IVL state for each random seed used. Based on plots of σ_{V_m}, $\overline{V_m}$ and *ISICV* when using thousands of seeds, the majority of the resulting states remain as IVL states (see Supplementary Figure S7).

2.3.3.2. Spike Triggering Average (STA) analyses

To extract biophysical contributions of resonant frequencies in IVL states, we used STA analyses (Schwartz et al., 2006; Ito, 2015). Oftentimes, a STA analysis (or reverse correlation) is applied using mean input currents that precede spikes, and in a comparative fashion with different cells types in experiments to gain insight (e.g., see Moradi Chameh et al., 2021). Here, because we are using mathematical models, we are able to consider relative contributions of the underlying active and passive currents preceding spikes in a comparative fashion. This is in an analogous vein to when we considered how the different currents responded with phase-dependent perturbations in addition to the 'standard' PRC obtained when one considers how much the subsequent spike is advanced or delayed given phase-dependent perturbations as done in Guet-McCreight and Skinner (2021).

For spiking resonances, we used 27 different perturbation frequencies. For direct comparisons of spiking resonances in IVL states between FULL and SINGLE we had used the same set of perturbation frequencies (15) as used in Guet-McCreight and Skinner (2021). However, with a much wider range of baseline firing rates in IVL states with SINGLE, we could obtain a larger set of spike resonant frequencies using the larger number of different perturbation frequencies.

2.3.3.2.1. Generating STA plots

We define a set of frequencies $F = \{0.5\} \cup \{1 \leq i \leq 25, i \in \mathbb{Z}\} \cup \{30\}$ Hz. To obtain a spiking resonant frequency, f_r, in F, we ran 10 s long simulations using the 10 representative parameter sets to find IVL states where the model was resonant to that frequency. For each representative set, each of the 10 s long simulations were produced with a different seed. Histogram distributions of the different f_r's naturally depend on how many random seeds one uses. See OSF figure https://osf.io/6twdb/ that show these distributions. With enough seeds, we were able to obtain f_r for all of the different frequencies in F for each representative parameter set.

We generated STA plots in which we considered up to 200 ms preceding a spike. To do this, we found as many 200+ ms long ISIs as possible within each 10 s long simulation. We used new seeds to run our simulations until there were 50 (200+ ms ISIs) for each

representative set of f_r's for all of the 27 frequencies in F. The actual number of seeds required ranged from 40,000 to 120,000 differing across the 10 representative sets. For the 200 ms ISIs we obtained, we preserved sections from 195 to 10 ms before each spike so as to remove the influence from the last and the next spike on the underlying currents. As there is 'curving up' before a spike in the STA plots (see Supplementary Figure S8) that could drastically affect the slope analysis (see below), we chose a timepoint range of 195 ms to 25 ms before a spike. One hundred and ninety-five milliseconds is justified to be approximately the furthest back one can push to avoid the previous spike, and 25 ms is approximately the furthest forward one can push to not include the curving portion before slope computation. For computational ease, we used this same range in doing both the slope and spread analyses described below. With these ISIs, we generated STA plots to consider the contribution of the different biophysical currents.

The biophysical currents in the STA plots were produced from a f_r and representative set (*set#*) perspective. That is, for each current type I_x, there were 270 different average (of 50) I_x's for each timepoint from –195 to –25 ms, each corresponding to a permutation of f_r value (27) and *set#* (10). The biophysical current value itself represents the proportion of the total (absolute) current at the given timepoint where it is assigned as negative (inward current) or positive (outward current) accordingly.

Referring to these currents as $\overline{I_x}^{(f_r,set\#)}$, the average current (of 50), $f_r \in F$, and $0 \leq set\# \leq 9$, we took the absolute values of the averages, and normalized them across the representative sets to keep the values of each current between 0 and 1. We refer to normalized $\overline{I_x}^{(f_r,set\#)}$ as $\tilde{I}_x^{(f_r,set\#)}$. That is, we now have:

$$\tilde{I}_x^{(f_r,set\#)} = \frac{|\overline{I_x}^{(f_r,set\#)}| - min(|\overline{I_x}^{(f_r,set\#)}|)}{max(|\overline{I_x}^{(f_r,set\#)}|)} \tag{8}$$

In Figure 7A, a selection of $\tilde{I}_x^{(f_r,set\#)}$'s are shown.

2.3.3.2.2. Slope analysis

For each timepoint of $\tilde{I}_x^{(f_r,set\#)}$, we calculated the mean across the 10 representative sets. These means can be seen in Figure 7B with the standard deviations.

For each f_r, we did a least squares linear fit line of the mean, and obtained the slope of the linear fit line. We also considered a combined slope of IM and Ih where the two currents were first summed before obtaining the mean and subsequent slope from the linear fit.

2.3.3.2.3. Spread analysis

For each timepoint of $\tilde{I}_x^{(f_r,set\#)}$, we calculated the standard deviation across the representative sets. We defined the function $Spread(\tilde{I}_x^{(f_r)})$ as twice the standard deviation summed over all the timepoints from 195 to 25 ms before a spike. In Figure 7B, the precursor to $Spread(\tilde{I}_x^{f_r})$, the mean and standard deviations of $\tilde{I}_x^{(f_r,set\#)}(t)$ are shown for a selected set of f_r's.

We also considered a combined spread of two currents IM and Ih, $Spread(\tilde{I_M}^{(f_r)} + \tilde{I}_h^{(f_r)})$, where the two currents were first summed, and then twice the standard deviation of the resulting summation was summed over all the timepoints. Note that with given current type(s), the spread is a function of f_r only as we sum over the timepoints.

2.4. Direct parameter estimation

2.4.1. Robust adaptive unscented Kalman Filter (RAUKF)

The mathematical model structure of SINGLE may also be used in data assimilation methods to estimate parameters based on an "observation". Application of the RAUKF method (Azzalini et al., 2022) here was developed based on the reduced OLM model cell, and the model parameters were estimated from simulated noisy observations of SINGLE or FULL. The RAUKF method was adapted so that the conductance based model used for state prediction was the same as that used in SINGLE (see details in Supplementary material). The general formulation of the Kalman Filter (KF) is:

$$\mathbf{x}_k = \mathbf{f}(\mathbf{x}_{k-1}, \mathbf{u}_{k-1}) + \mathbf{m}_{\mathbf{x},k-1} \tag{9}$$

Where the state at k, $\mathbf{x}_k$ depends upon the previous state $\mathbf{x}_{k-1}$ and some control input $\mathbf{u}_{k-1}$, i.e., injected current, and $\mathbf{m}_\mathbf{x} \sim \mathcal{N}(0, \mathbf{Q}_\mathbf{x})$. The function $\mathbf{f}$ is the system's state model, which in this case are the set of equations governing model SINGLE. In order to estimate parameters of the system, additional trivial dynamics were added to the system for each given parameter $\boldsymbol{\theta}$ via a random walk:

$$\boldsymbol{\theta}_k = \boldsymbol{\theta}_{k-1} + \mathbf{m}_{\boldsymbol{\theta},k-1} \tag{10}$$

With $\mathbf{m}_{\boldsymbol{\theta}} \sim \mathcal{N}(0, \mathbf{Q}_{\boldsymbol{\theta}})$. Combining $\mathbf{x}$ and $\boldsymbol{\theta}$ we may produce a new state $\mathbf{X}$ with the dynamics represented by $\mathbf{F}$ and noise $\mathbf{M}$, where $\mathbf{I}$ is the identity function:

$$\mathbf{X} = \begin{bmatrix} \begin{pmatrix} \mathbf{x}, \mathbf{u} \end{pmatrix} \\ \boldsymbol{\theta} \end{bmatrix}, \mathbf{F} = \begin{bmatrix} \mathbf{f} \\ \mathbf{I} \end{bmatrix}, \mathbf{M} = \begin{bmatrix} \mathbf{m}_\mathbf{x} \\ \mathbf{m}_{\boldsymbol{\theta}} \end{bmatrix} \tag{11}$$

$$\mathbf{X}_k = \mathbf{F}(\mathbf{X}_{k-1}) + \mathbf{M}_{k-1} \tag{12}$$

The observation model used to characterize noisy membrane voltage measurements is described by

$$\mathbf{y}_k = \mathbf{V}_k + \mathbf{n}_{V,k} \tag{13}$$

Where $n_{V,k}$ denotes measurement noise (in the general case, $\mathbf{y}_k = \mathbf{g}(\mathbf{X}_k) + \mathbf{n}_k$, $\mathbf{n}_k \sim \mathcal{N}(\mathbf{0}, \mathbf{R})$). Here, the direct observation of the membrane voltage y_k mimics experimental recording techniques (e.g., current-clamp methods). With only a subset of $\mathbf{X}_k$ being measurable, the method presented in this study allows hidden states to be estimated.

The system's dynamics model $\mathbf{F}$, an initial estimate of the state $\mathbf{X}_0$, as well as the control input $\mathbf{u}$ were used to maximize the probability of an observation $\mathbf{y}$ afforded by the noise profiles of each.

$$p(\mathbf{X}_{k-1} \mid \mathbf{X}_0, \mathbf{u}_{1:k-1}, \mathbf{y}_{0:k-1}) = \mathcal{N}(\hat{\mathbf{X}}_{k-1|k-1}, \hat{\mathbf{P}}^{xx}_{k-1|k-1}) \tag{14}$$

$$p(\mathbf{X}_k \mid \mathbf{X}_0, \mathbf{u}_{1:k}, \mathbf{y}_{0:k-1}) = \mathcal{N}(\hat{\mathbf{X}}_{k|k-1}, \hat{\mathbf{P}}^{xx}_{k|k-1}) \tag{15}$$

To estimate the next state (15) a set of points (sigmapoints) were sampled according to (14), described in more detail in Azzalini et al. (2022). This process also updates the current covariance $\mathbf{P}$ of the process.

Since the precise noise profile $\mathbf{Q}$ of the state vector $\mathbf{X}$ is not well known for a given neuronal model, and its respective discrepancies to

the observation, we employed an adaptive method used in previous work in order to update **Q** as well as the estimate of the observation noise **R** over time (Azzalini et al., 2022). See Supplementary material for further details.

The adaptation of **Q** and **R** can be tuned by user defined variables a, b, λ_0, and δ_0, Where λ_0 and δ_0 are the minimum weights used when updating **Q** and **R**, the percent shift from the current to the new estimated value. To ease computational load these updates to **Q** and **R** were not applied after every sample, instead they were applied when a fault was detected (see Supplementary material). The values of λ_0 and δ_0 were both set to a value of 0.2. The variables a and b are weights of how much **Q** and **R** will be updated proportional to the magnitude of fault detected. The values of a and b were set according to explorations done in previous work when RAUKF was applied to a conductance based model (Azzalini et al., 2022). $a >> b$ was found to be effective and here we use $a = 10$ and $b = 1$.

2.4.2. Application of RAUKF to OLM cell models

When applying the RAUKF to an observation of either SINGLE or FULL, $\boldsymbol{\theta}$ was set to estimate the same conductance values that were optimized in the reduced model SINGLE. That is,

$$\boldsymbol{\theta} = \begin{bmatrix} g_M \\ g_{Kdrf} \\ g_{Ka} \\ g_{Na} \end{bmatrix} \tag{16}$$

To generate an observation, an input train of step currents was injected into either SINGLE or FULL models. The input train consisted of 500 ms of zero current, then a step to 30, 60, 90, 0, –30, –60, and –90 pA, repeating 4 times. The current was also mixed with a Gaussian white noise $\sim \mathcal{N}(4, 5)$ pA. The mean of the noisy stimulation was chosen to match the characterized bias current in FULL and SINGLE. This input train of multiple positive and negative pulses is designed to be able to expose a full dynamic range of spiking, resting and subthreshold activities due to the underlying biophysical currents, and can be used in real-time to estimate parameter values.

The initialization of **P** and **Q** was derived from the order of magnitude $\boldsymbol{\theta}$, while **x** was made constant to 1×10^{-4} and 1×10^{-8}, respectively. For the **P** of $\boldsymbol{\theta}$ the value was set to 2× the magnitude of the value of $\boldsymbol{\theta}$ used in SINGLE, e.g., $340 \longrightarrow 1 \times 10^2 \longrightarrow 1 \times 10^4$, and 4× the order of magnitude was used to initialize **Q**. Two initial states were used for $\boldsymbol{\theta}_0$, one where $\boldsymbol{\theta}_0 = \boldsymbol{\theta}_{SINGLE}$, known as the optimized initial estimate, and another where $\boldsymbol{\theta}_0 = 10^{\lfloor \log_{10}(\boldsymbol{\theta}_{SINGLE}) \rfloor}$, known as the poor initial estimate.

2.5. Computing

The extensive SINGLE simulations with spiking resonance and STA analyses were done using the Neuroscience Gateway (NSG) for high-performance computing (Sivagnanam et al., 2013). Code pertaining to FULL, SINGLE and analyses is available at: https://github.com/FKSkinnerLab/Reduced_OLM_example_code. Code pertaining to RAUKF and the respective figures is available at: https://github.com/nsbspl/RAUKF_OLM.

3. Results

3.1. Reduced model can capture complex outputs obtained with full, detailed multi-compartment model

From our detailed multi-compartment OLM cell model (FULL), we derived a reduced, single compartment model (SINGLE) as described in the Methods. While SINGLE can reproduce features of FULL (e.g., see Figure 1), it is not obvious that SINGLE would produce similar results to those obtained using the full, detailed multi-compartment model regarding more complex phenomena such as spiking resonance (Guet-McCreight and Skinner, 2021).

Considering this, we used SINGLE to examine previously explored phenomena so as to directly compare with observations obtained using the detailed multi-compartment model. In Figure 2, we show that SINGLE and FULL have similar frequency-current (f–I) curves, with the required injected current to obtain about a 1 Hz firing frequency differing by about 4 pA. As described in the Methods, the detailed multi-compartment model used in Guet-McCreight and Skinner (2021) is essentially the same as FULL. Thus, moving forward we will not specifically distinguish these multi-compartment models in comparing our results.

We examined phase response curves (PRCs) and the phase-dependent contribution of the different biophysical currents at four different frequencies when inhibitory perturbations were applied, as previously done in Guet-McCreight and Skinner (2021). We show the results in Figures 3A–C for the PRCs, Ih and IM which illustrates that similar results are obtained. That is, inhibitory perturbations mostly delay spiking and drive up the responses of Ih and IM. Further, the percent change in maximum Ih increases in magnitude as the firing rate increases, and its peak initially shifts rightward followed by a gradual leftward shift. For IM, the magnitude increases and the negative peak shifts leftward as the firing rate increases. Phase-dependent changes for all the other currents are shown in an OSF figure https://osf.io/6twdb/.

We also undertook a full examination of spiking resonance in an *in vitro*-like scenario, using the same range of firing frequencies as used in Guet-McCreight and Skinner (2021). A side-by-side comparison of spiking resonance results using SINGLE and the previously published data using a detailed multi-compartment model is shown in Figure 4. Again, the results are similar. That is, with inhibitory perturbations, the resonant frequency of both models increases as the baseline firing rate increases (Figure 4A). However, with excitatory perturbations, the resonant frequencies mostly lie within the theta frequency range regardless of the baseline firing rate (Figure 4B).

As described in the Methods, we can generate *in vivo*-like (IVL) states in our reduced model. Restricting the baseline frequencies to those used in Guet-McCreight and Skinner (2021), similar spiking resonance results in IVL scenarios are also obtained as shown in Supplementary Figure S6. That is, excitatory perturbations mostly do not evoke spiking resonance at theta frequencies whereas inhibitory perturbations do. Thus, our reduced model, SINGLE, is not diminished in being able to reproduce complex results found in FULL.

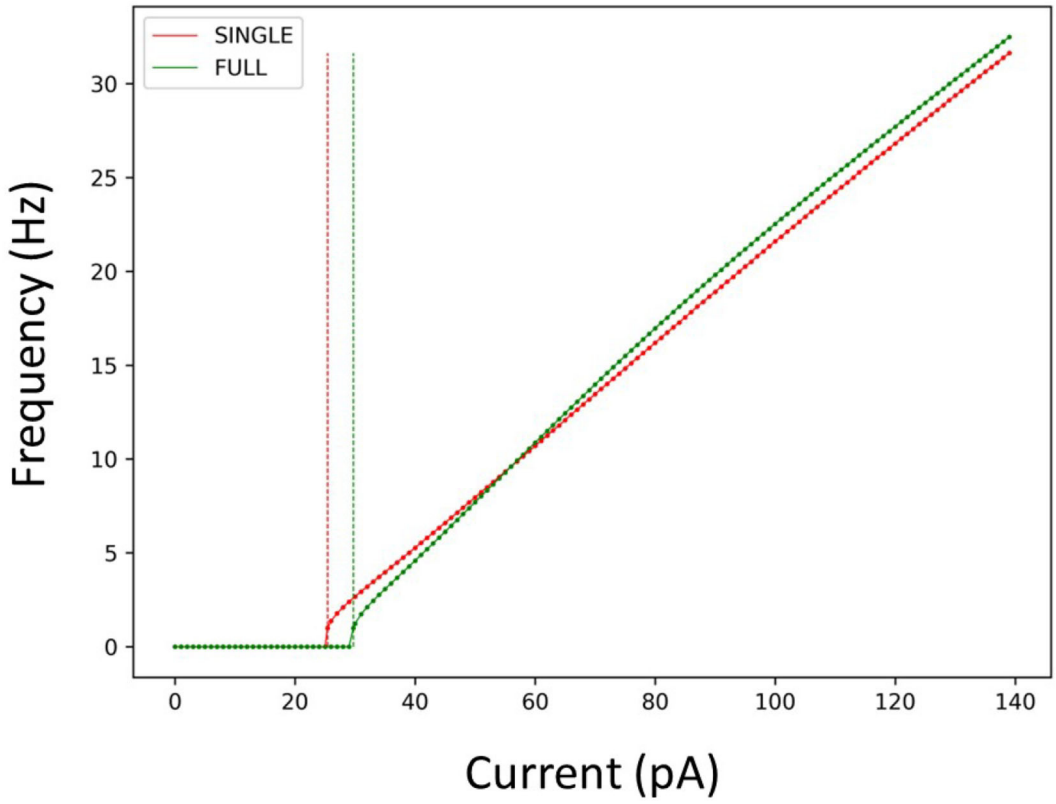

FIGURE 2
Firing rates of SINGLE and FULL. The red and green dots and lines refer to the frequency vs current (f-I) curves for SINGLE and FULL, respectively. Correspondingly, the red and green dashed lines signify the amount of injected current needed to obtain a firing rate of 1 Hz in SINGLE and FULL. 25.5 pA for SINGLE and 29.7 pA for FULL.

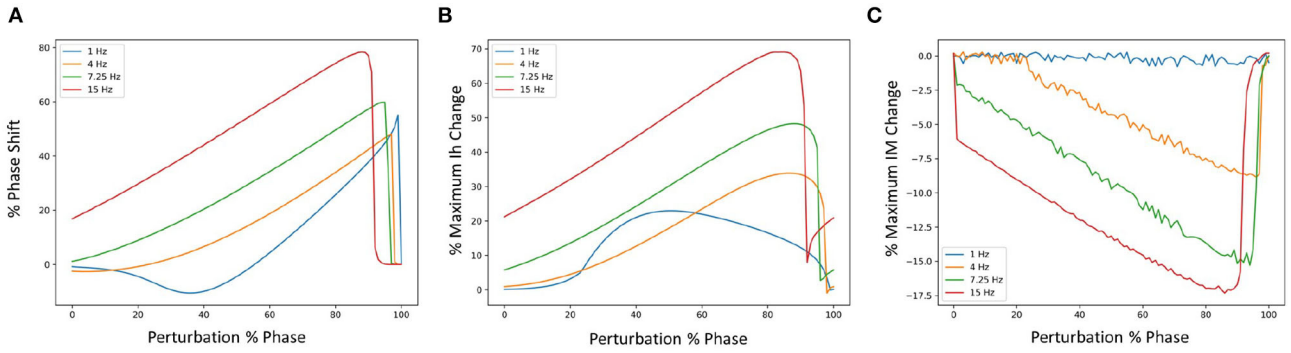

FIGURE 3
Phase response curves (PRCs) using different firing frequencies of SINGLE. **(A)** Shows PRCs at 4 different frequencies and the corresponding phase-dependent changes of Ih **(B)** and IM **(C)** when inhibitory perturbations are applied to SINGLE firing at 1, 4, 7.25, and 15 Hz, due to injected currents of 25.5, 35.1, 47.4, and 75.7 pA, respectively. Responses are similar to those obtained by Guet-McCreight and Skinner (2021).

3.2. Expanded virtual network explorations with reduced model

3.2.1. A wide range of *in vivo*-like (IVL) states is possible with SINGLE

In vivo recordings of OLM cells exhibit a range of baseline firing frequencies that span $\approx$ 3 – 25 Hz (Varga et al., 2012; Katona et al., 2014) (depending on behavioral state of movement, sleep etc.). However, our previous spiking resonance explorations in IVL states using full, detailed multi-compartment models were technically constrained to a small range of baseline firing frequencies, specifically $\approx$ 12 – 16 Hz (Guet-McCreight and Skinner, 2021), due to how different IVL states could be generated. As such, we were limited in being able to extract biophysical underpinnings of different spike frequency resonances that include theta frequencies. Here, with SINGLE, our reduced model that maintains biophysical balances for the 5 different currents it contains (see Figure 1), we are able to obtain a wide range of baseline firing rates and thus

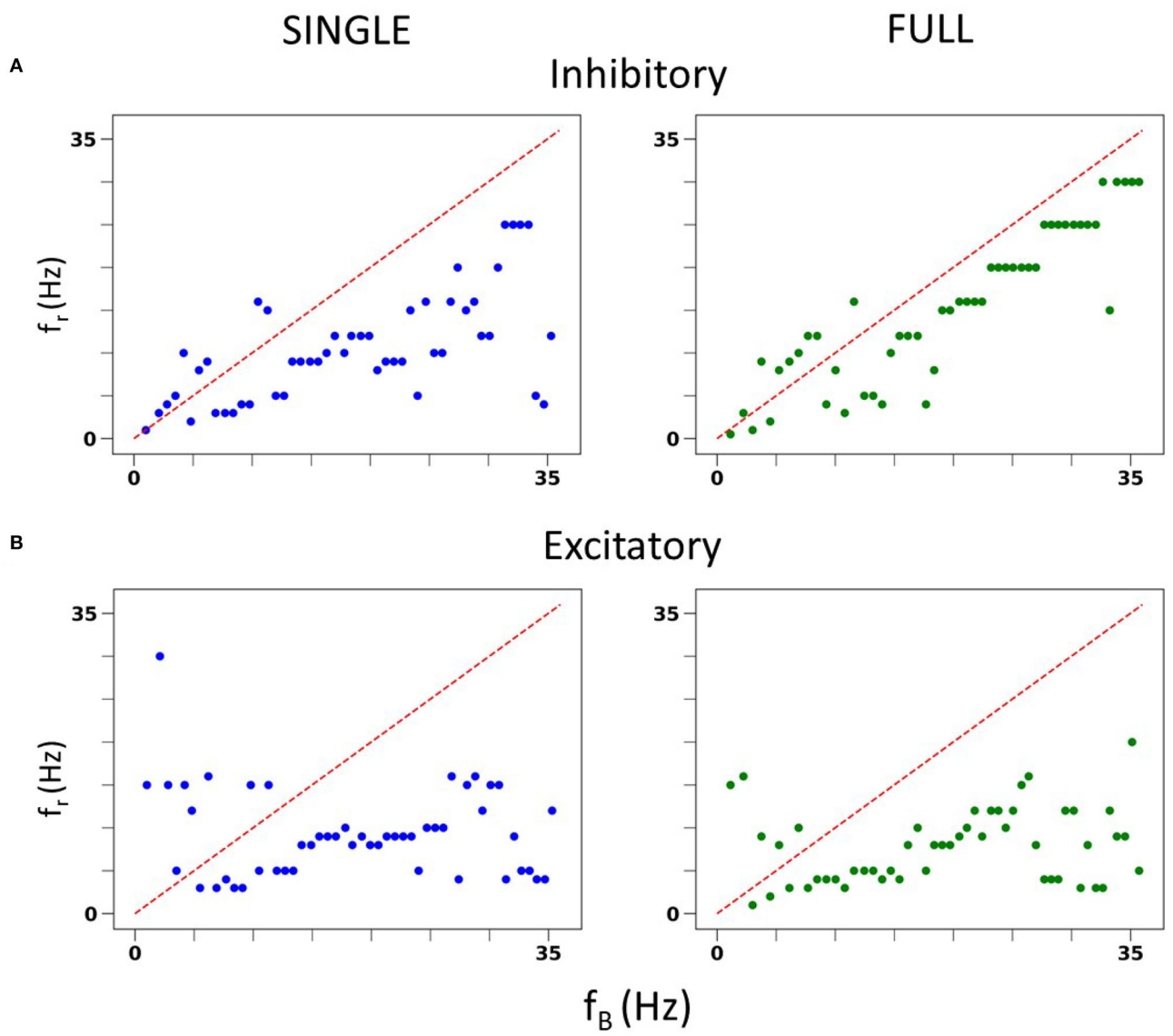

FIGURE 4
In vitro spiking resonance pattern in SINGLE is comparable to FULL. **(A)** Resonant frequency (f_r) of inhibitory perturbations at different baseline firing rates (f_B). Blue is from single compartment model, green is from full model. **(B)** Resonant frequency (f_r) of excitatory perturbations at different baseline firing rates (f_B). Blue is from single compartment model, green is from full model.

can greatly expand our explorations in IVL states. This puts us in a position to determine what the biophysical determinants underlying theta frequency spiking resonance might be.

We obtained a wide range of baseline firing rates with SINGLE by altering the parameters for the "noisy" excitatory and inhibitory currents it receives (see Section 2). From our parameter search, 414 different sets of parameters that can generate valid IVL states were found. Within these sets, the excitatory conductance and variance were generally smaller than their inhibitory counterparts, suggesting that inputs received by OLM cells *in vivo* may be inhibitory dominant. From these 414 sets, we chose 10 that could span the full range of *in vivo* firing frequencies of OLM cells, and refer to them as 10 representative parameter sets. Each representative set has a minimum and maximum baseline firing rate as given in Table 1 along with its parameter set values.

For each representative set, we generated fifty 10 s long IVL states (via 50 random seeds) to obtain 500 IVL states. In Figure 5, we plot the minimum and maximum firing rates of these 500 IVL states. To illustrate what the OLM cell firings in IVL states look like, one example of an IVL state from each of the 10 chosen representative sets is also shown in Figure 5.

We can generate as many IVL states as we desire simply by using >50 random seeds. This was also the case in our previous work using a full multi-compartment model, but the randomness was in regard to synapse placement and presynaptic spike times from specified presynaptic cell types, resulting in a limited baseline firing frequency range (Guet-McCreight and Skinner, 2021). Here, the randomness is less restrictive because of the single compartment model nature of SINGLE and is able to exhibit the needed full range of baseline firing frequencies.

TABLE 1 Representative parameter set characteristics.

Set #	Min f	Max f	g_{e0}	g_{i0}	$\sqrt{D_e}$	$\sqrt{D_i}$
0	3.1	4.6	0.00321429	0.01085714	0.00068571	0.00214286
1	4.6	6.8	0.00342857	0.01028571	0.00057143	0.00214286
2	6.5	9.3	0.00342857	0.01114286	0	0.00428571
3	8.3	10.9	0.00385714	0.01171429	0	0.00428571
4	10.4	13	0.00428571	0.01171429	0.00045714	0.00357143
5	11.8	15.2	0.00385714	0.01142857	0.00011429	0.00571429
6	13.3	16.8	0.00428571	0.01114286	0	0.00428571
7	15.2	18.6	0.00407143	0.01	0	0.00428571
8	16.7	19.9	0.00364286	0.00828571	0	0.00428571
9	18.5	22.6	0.0045	0.01085714	0.00011429	0.00571429

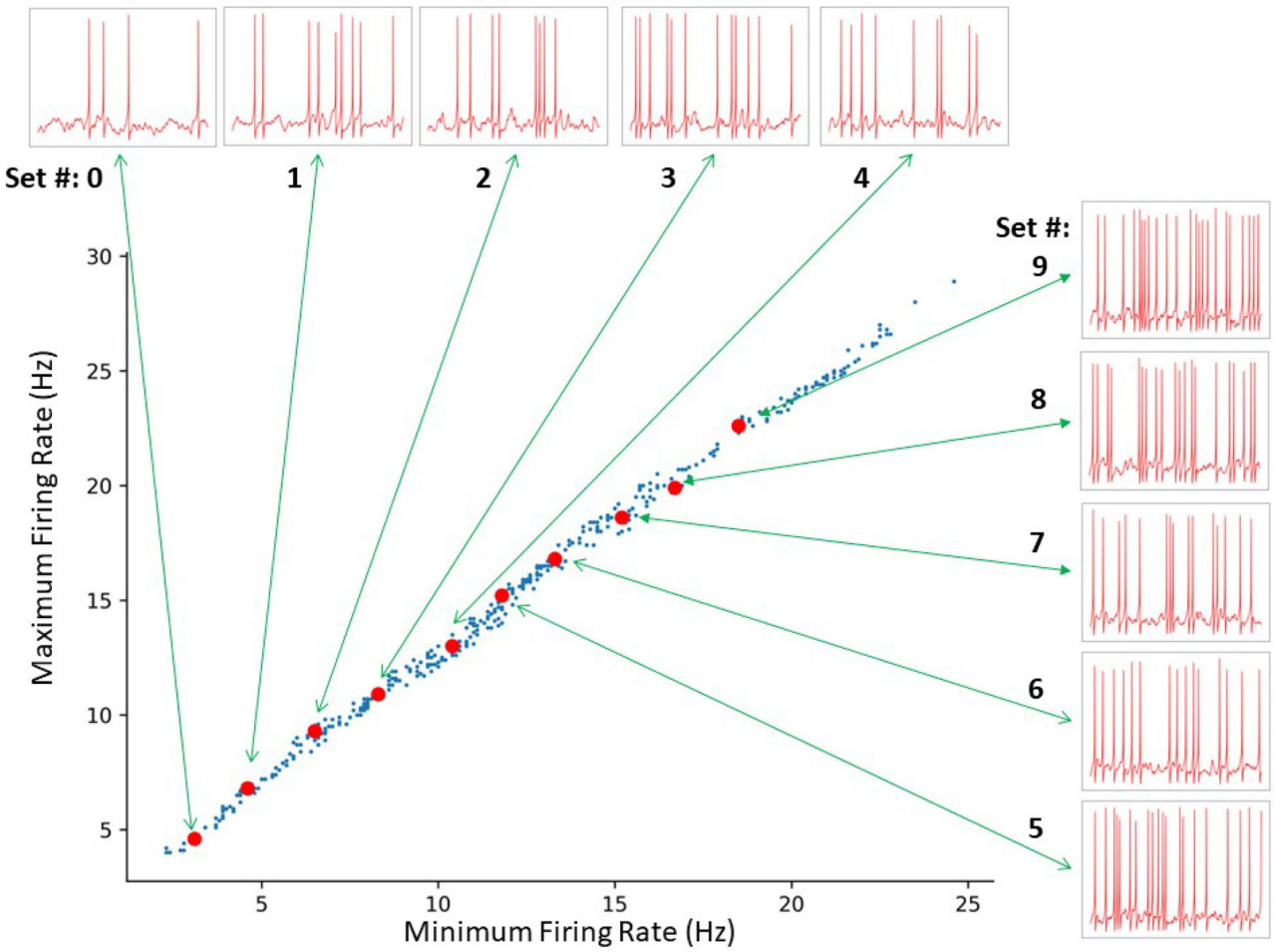

FIGURE 5
SINGLE yields a wide range of *in vivo*-like (IVL) firing frequencies as exists in experiment. A total of 414 sets of parameters were identified by a constrained search. The red dots indicate the 10 representative sets selected for further analyses. From bottom left to top right: Set # 0–9, respectively. The green arrows connect each representative set to a 1 s voltage trace example produced using the respective representative set.

3.2.2. Spiking resonances with SINGLE

We are not limited in how many random seeds we can use. We already know that we can capture the full extent of *in vivo* firing ranges, and we aimed to generate a large data set of spike frequency resonances. With a large data set, we anticipated that we could determine whether there are any particular biophysical determinants underlying *theta frequency* spiking resonance specifically. We generated 50,000 IVL states from the 10 representative sets using

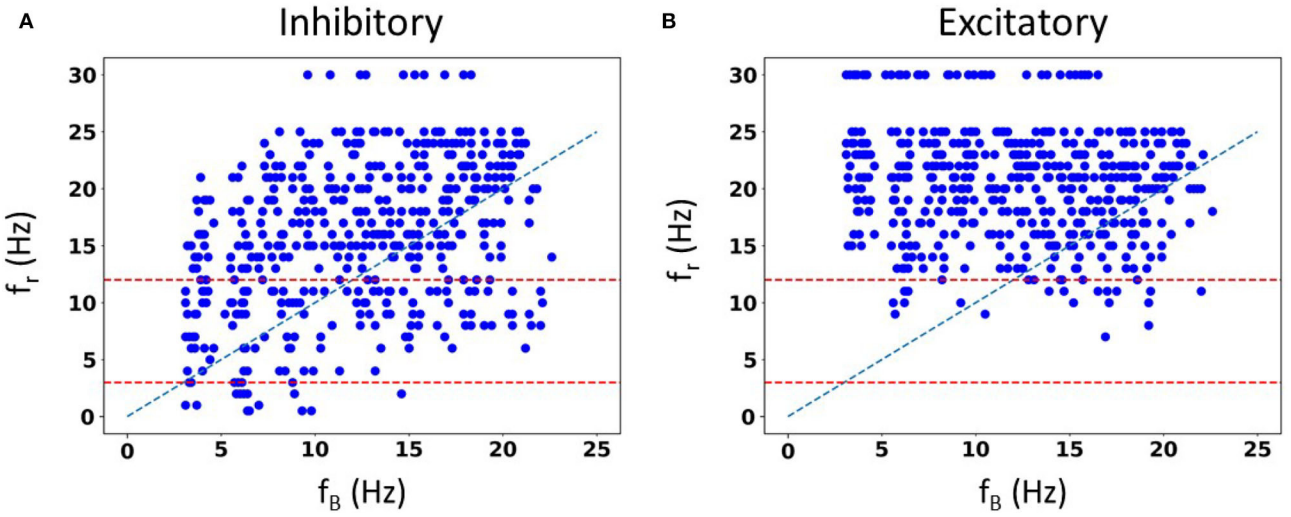

FIGURE 6
Spike resonances using SINGLE. 500 IVL states generated from the 10 representative sets are used to plot resonant frequencies (f_r's) as a function of (average) baseline firing rates (f_B's). Plots are shown for inhibitory perturbations **(A)** or excitatory perturbations **(B)**. Diagonal line is where $f_r = f_B$. Red dashed lines delineate a theta frequency (3–12 Hz) range for the f_r's.

5,000 random seeds. In Figure 6A, we show the computed spiking resonance (f_r) as a function of the baseline firing frequency (f_B) when we used inhibitory perturbations. The analogous plot for excitatory perturbations is shown in Figure 6B. To ensure that the individual dots are visible, we only used the first 50 seeds (500 IVL states) in creating the plots shown in Figure 6. As can be seen, f_B spans the range, unlike the case with FULL (see Supplementary Figure S6). In Supplementary Figure S7, we plot the mean ($\overline{V_m}$) and variance ($\sigma^2_{V_m}$) of the sub-threshold membrane potential, and the *ISICV* to show that these aspects of IVL states are not determining factors of the resulting f_r's. That is, for any given f_r, there are a range of $\overline{V_m}$, $\sigma^2_{V_m}$ and *ISICV* values. Equivalently, resonant frequencies are distributed across the ranges of $\overline{V_m}$, $\sigma^2_{V_m}$ and *ISICV* values.

Not surprisingly, one can see some dependence of f_r on f_B. That is, with a higher frequency f_B, there is an increase in the density of higher frequency f_r's. This can be seen in Figure 6, as well as in the density of colored dots representing f_B in Supplementary Figure S7. That is, IVL states with a higher f_B are more likely to have higher f_r, even though due to stochasticity of the IVL states, it is possible for some higher f_B IVL states to be resonant at low frequencies. However, this observation holds true on average. In essence, we have f_r's at many different frequencies.

Using FULL, we had previously noted that inhibitory perturbations, and not excitatory perturbations, generated f_r's that include theta frequencies during IVL states (Guet-McCreight and Skinner, 2021). Here, with SINGLE, this observation can be more clearly seen, as shown in Figure 6 where dashed red lines to delineate the theta frequency range (3–12 Hz) are drawn. With our greatly extended dataset, we can easily see that the full theta frequency range of f_r with inhibitory perturbations is exhibited. However, with excitatory perturbations, this is not the case—only minimally and at the upper end of theta frequency range are f_r's obtained. We note that the limited baseline frequencies available with FULL prevented us from being able to fully observe this.

3.2.3. STA analyses

As we would like to understand what underlies the ability of OLM cells to exhibit spiking resonance at theta frequencies, we now focus on just the inhibitory perturbations as it is inhibitory, but not excitatory, that encompass the full range of theta frequency spiking resonances (see Figure 6).

To consider this, we undertake a spike-triggered average (STA) analysis from the perspective of all of the underlying biophysical currents. Specifically, 10 different firing rates are chosen (set # 0–9 as shown in Figure 5). As noted in the Methods, since we have a mathematical model in hand, we are able to examine how the biophysical currents preceding spiking contribute for a range of baseline firing rates and spiking resonant frequencies. By performing STA analyses up to 200 ms prior to spiking, particular contributions by the various biophysical currents that influence theta frequency spiking (i.e., approximately 200 ms period) could be exposed. We examined each current type's contribution to spiking in IVL states for all of the different f_r's (27 in total from 0.5 to 30 Hz). In Figure 7A, we show STA plots for six different f_r's from these 27. For each f_r, we show normalized values in the STA plots for the five different biophysical currents (and leak) for each of the 10 representative sets (see Methods for details).

From STA plots using un-normalized values, the proportions of currents are directly comparable and it is clear, for example, that the relative proportion of Ih (to the total current) is much smaller than that of IM. From a thorough examination of STA plots of the un-normalized current values (proportion of the total current), we find that the larger the f_r, the more negative is the Ih and the less positive is the IM. In addition, STA plots with higher f_r frequencies show obvious fluctuations. These fluctuations would seem to be due to the presence of more perturbations, with the peaks and valleys of the fluctuations matching the timing of the perturbations. However, IM appears the least sensitive to the perturbations, with negligible fluctuations (see Figure 7A). Of particular note is that STA plots of IM and Ih show minimum overlap between the different representative

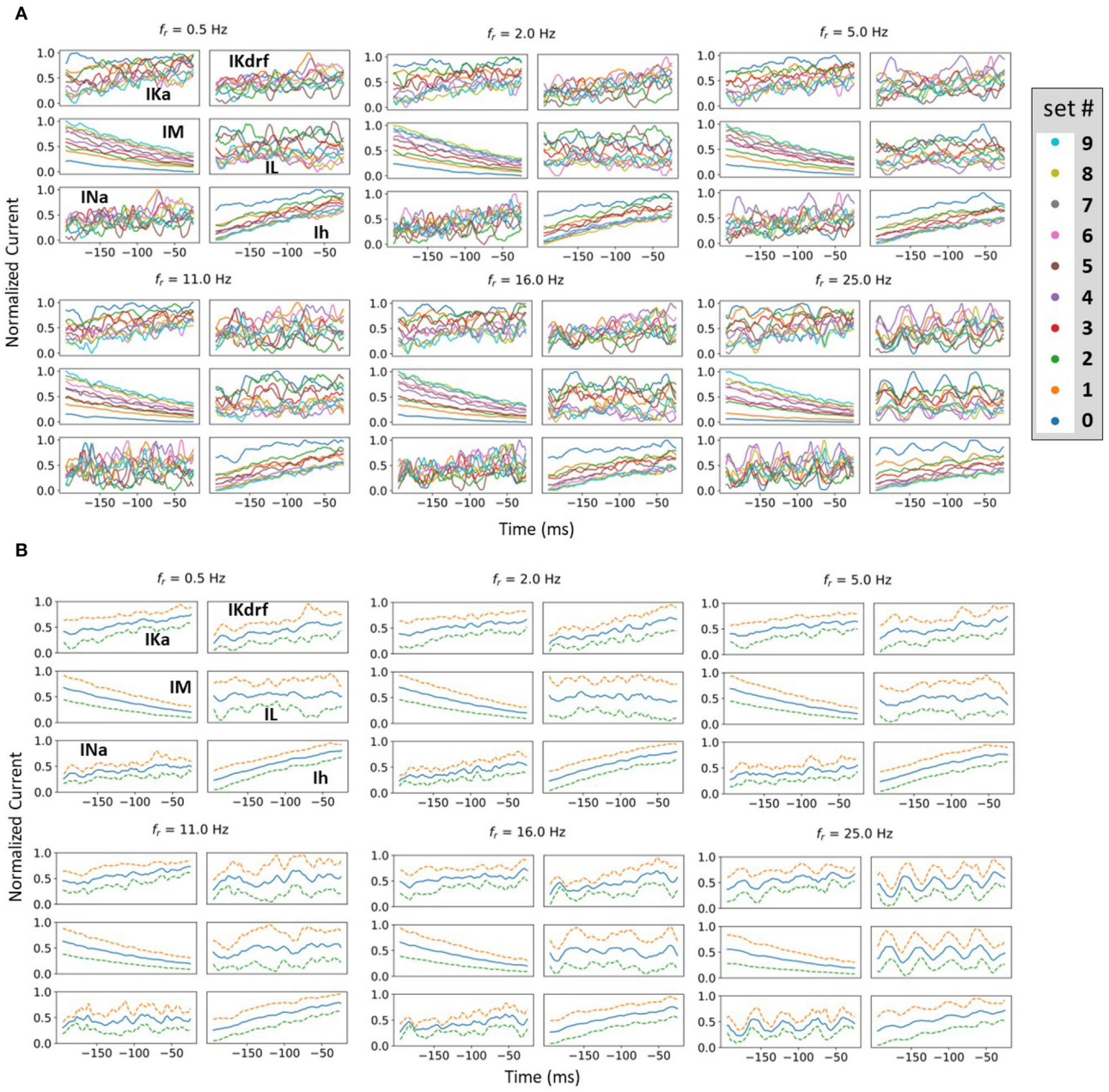

FIGURE 7
Examples of normalized STA and spread analysis. **(A)** Examples of normalized STA plots, with different colors representing different representative sets. Set numbering is the same as in Figure 5. **(B)** Blue lines in the middle of the plots are the means of normalized currents from **(A)**. The dashed lines are ± 1 standard deviation of the normalized currents from the mean. Spread is defined as the mean difference between the dashed lines.

sets relative to the other currents. This is more obviously the case for IM whose overlap is visually separable (see Figure 7A). In general, overlap is likely the result of stochasticity in the OU process which makes the currents variable and intersecting with each other. The minimal overlap in IM and Ih indicates an insensitivity to local changes, which could be attributed to them having slower time constants relative to the others. This is especially true for IM which has the slowest time constant (see equations and plots for the biophysical currents in Supplementary material). This would also explain why it does not show fluctuations for larger f_r whereas Ih does. A general interpretation of this minimal overlap is that regardless of what the *in vivo* firing rate of the OLM cell might be, IM and Ih can "tailor" their response accordingly. That is, they can perceive "global changes" and so the different firing rates are in the "history" of IM and Ih more than the other current types with faster time constants. Therefore, we now reasonably assume that if there is going to be any frequency specificity in the OLM cell's spiking resonance, Ih and IM would be the currents that could potentially control this. We now focus on Ih and IM to determine whether there are any particularities associated with theta frequency spiking resonance. To do this, we use an analysis that involves slopes and spreads. See Methods for computation details.

Let us first consider our slope analyses. We found that as f_r increased, the slope of IM's STA plot became less negative, and

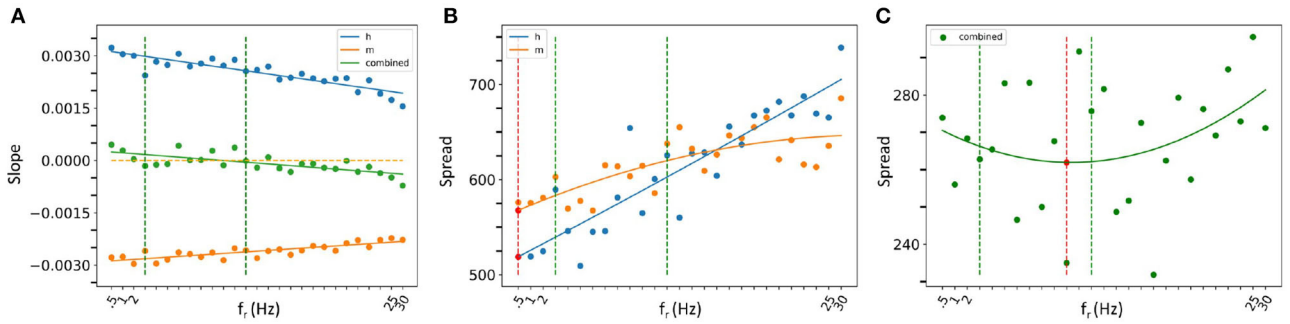

FIGURE 8
Spread and slope analysis. **(A)** Slope analysis. The lines are linear fit lines for Ih alone (blue dots), IM alone (orange dots) or IM and Ih combined (green dots). The orange dashed line is where the slope is zero. **(B, C)** Spread analysis. The curves are parabolic fits for Ih alone (blue dots), IM alone (orange dots) or IM and Ih combined (green dots) in **(C)**. The red dashed lines show where the local minima of the parabolic fits are with the minimum shown with a red dot. The theta frequency range (3–12 Hz) is delineated with vertical green dashed lines in all of the plots.

the slope of Ih's became less positive. Linear fits are statistically significant. In considering a combination of IM and Ih slopes, we again obtained a statistically significant linear fit, but now the slope crossed zero within the theta frequency range. This is all shown in Figure 8A where the 3–12 Hz theta frequency range is delineated by dashed green lines.

In our spread analysis, we found that as f_r increased, the spread in both IM and Ih STA plots increased as shown in Figure 8B. However, when we examined a combination of Ih and IM, the spread was more variable as shown in Figure 8C. Parabolic fits to each of IM, Ih and their combination were performed and the curve fits are shown in Figures 8B, C. From these fits, it is clear that the combined IM and Ih exhibits a tendency to have a minimal value in the theta frequency range, unlike IM or Ih alone, although none of these parabolic fits were found to be statistically significant. However, one can obtain a statistically significant linear fit to Ih ($R^2 = 83.1\%$). While the parabolic fits were not statistically significant, a nonlinear local polynomial regression can yield a statistically significant fit with a minimal value for the combined IM and Ih, but neither IM nor Ih alone. Overall, the findings of our spread and slope analyses imply that to specifically have spiking resonance at theta frequencies, we need to have a balance. That is, our analyses indicate that there is a "balanced sweet spot" during which the combination of Ih and IM minimally change approaching spiking (zero slope and minimal spread), regardless of the baseline firing frequency of the OLM cell *in vivo*. This suggests that the slow time constants of IM and Ih act in concert to allow a theta frequency spiking resonance to emerge despite variability in OLM baseline firing rates. That is, IM decreases and Ih increases prior to spiking in such a way to favor a response to incoming theta frequency perturbations. The combination of their biophysical characteristics is what allows this, and not either current on its own.

3.3. Parameter estimation with RAUKF

Having now determined that particular biophysical currents contribute to theta frequency spiking resonance, we move to consideration of parameter estimation directly from experimental data. That is, we examine whether we could directly estimate parameter values from experimental recordings using Kalman Filtering (KF) techniques. If so, then it may be possible to bypass the development of the detailed, multi-compartment cell models to get insights into relative differences of biophysical characteristics in various cell types under various conditions. For example, conductance or time constant values of various biophysical channels in a given cell type would vary during different neuromodulatory states to affect spiking output. To be able to do this, we first need a mathematical model structure and a set of parameters whose values are to be estimated. Using a single compartment model is ideal, but not required, in applying KF parameter estimation techniques.

For the OLM cell, we have models of SINGLE and FULL and use them as a proof of concept in doing direct parameter estimations. We carry out two sets of parameter estimations in which we assume that the experimental output is represented by the membrane potential of the model cell generated from SINGLE or FULL. That is, we use either SINGLE or FULL to generate observation data for parameter estimation. In both cases, we focus on estimating parameter values for the same four conductances that were optimized in creating the reduced single compartment model (see Methods). We use SINGLE's mathematical model structure (see Supplementary material for equations) and estimate parameter values for $g_M, g_{Kdrf}, g_{Ka}, g_{Na}$ via RAUKF (see Methods for details). The protocol we use is shown in Figure 9, and we use initial conditions that are either optimal (i.e., the optimized conductance values from SINGLE) or poor (just the order of magnitude).

Parameter estimates obtained using the RAUFK algorithm are given in Tables 2, 3. If the RAUKF algorithm is working well, then the conductance estimates obtained using SINGLE should be very close to their actual values since in this case the mathematical model structure is the same as what is being used to create the observation data. As shown in Table 2, this is clearly the case regardless of the initial conditions used. The parameter estimates are mostly <1 percent different from the actual values. How the algorithm approaches these values is shown in Figure 10A.

Table 3 shows the estimated parameters when FULL is used for the observation data (akin to actual experimental data), and how the algorithm approaches these estimated values is shown in Figure 10B. The percent differences shown in Table 3 are relative to the SINGLE parameter values. This essentially ends up being a comparison with parameter values obtained via the

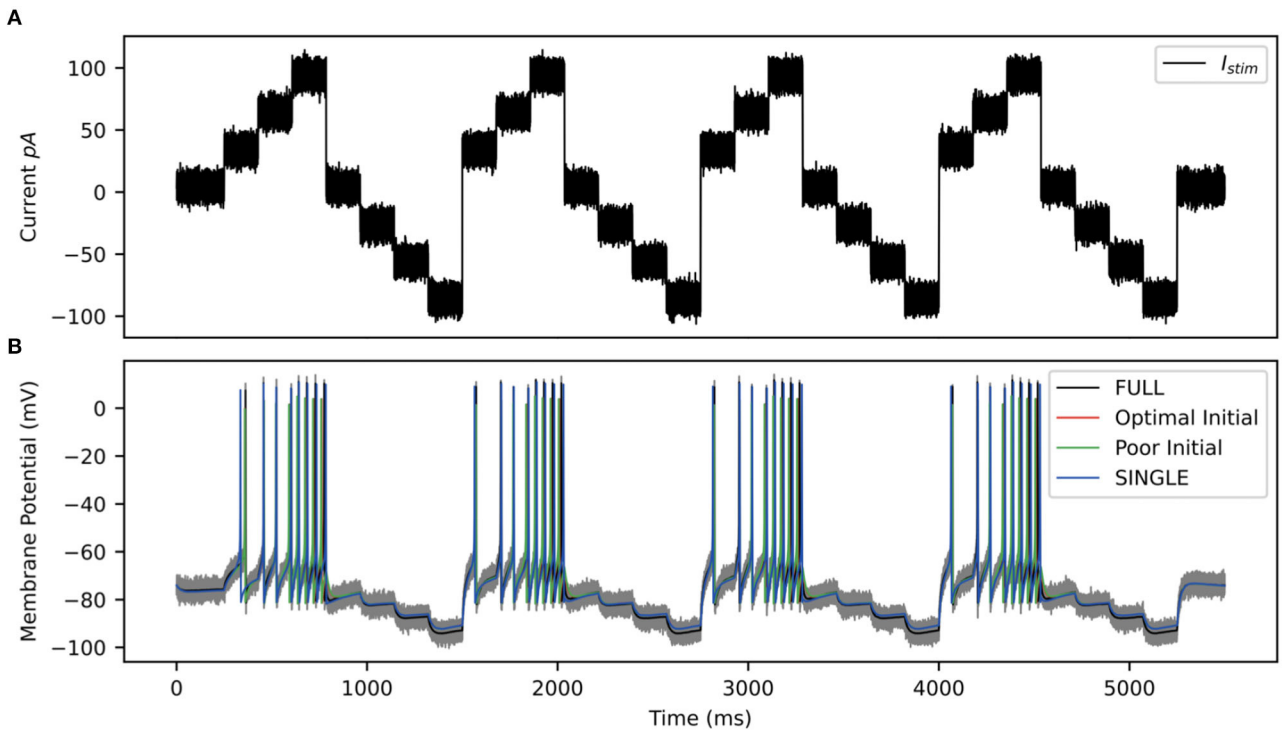

FIGURE 9
RAUKF input protocol. **(A)** Noisy input protocol applied to mathematical model to obtain parameter estimates. It is a noisy step current ($\sigma = \pm 5$ *pA*), with a mean step of 30, 60, 90, 0, −30, −60, −90 *pA*, for 196 *ms* each repeated four times beginning with 250 *ms* of noisy current. **(B)** Gray trace is observation used in filter, black trace is the real membrane potential, FULL. Red and green traces are RAUKF model estimated behavior initialized with parameters determined with optimal and poor initial estimates respectively processed observing the FULL model. Blue trace is model SINGLE, parameters determined by BluePyOpt.

TABLE 2 Using SINGLE for experimental observations.

	Optimal initial	Final	% Diff	Poor initial	Final	% Diff	Actual value
g_M	1.91e-05	1.89e-05	1.17	1.00e-05	1.88e-05	1.31	1.91e-05
g_{Kdrf}	4.33e-03	4.31e-03	0.50	1.00e-03	4.31e-03	0.63	4.33e-03
g_{Ka}	7.31e-03	7.35e-03	0.59	1.00e-03	7.35e-03	0.60	7.31e-03
g_{Na}	4.85e-03	4.84e-03	0.15	1.00e-03	4.84e-03	0.15	4.85e-03

TABLE 3 Using FULL for experimental observations.

	Optimal initial	Final	% Diff	Poor initial	Final	% Diff	SINGLE value
g_M	1.91e-05	1.84e-05	3.70	1.00e-05	1.66e-05	12.79	1.91e-05
g_{Kdrf}	4.33e-03	5.25e-03	21.07	1.00e-03	5.53e-03	27.54	4.33e-03
g_{Ka}	7.31e-03	7.17e-03	1.87	1.00e-03	7.15e-03	2.19	7.31e-03
g_{Na}	4.85e-03	4.55e-03	6.06	1.00e-03	4.56e-03	5.90	4.85e-03

BluePyOpt optimization in the reduced model development (see Section 2). In the BluePyOpt case, the optimized parameter values are obtained using metrics that include spike height, frequency etc. considering three different step current values, whereas in the RAUKF case, a noisy input protocol (Figure 9) is used to obtain parameter estimates. As shown in Figure 11 for a 60 pA input, while they are not identical, they are very similar. Comparisons for 30 and 90 pA step inputs are shown in Supplementary Figures S10, S11.

4. Discussion

In this work, we produced a reduced, single compartment model of an OLM cell that has similar biophysical current balances to a previously developed full, multi-compartment OLM cell model that was produced in a "neuron-to-model" matched fashion (Sekulić et al., 2020). Using this reduced model, we showed that it produced similar behaviors to the multi-compartment one regarding phase-dependent contributions of biophysical currents and spiking resonances in *in*

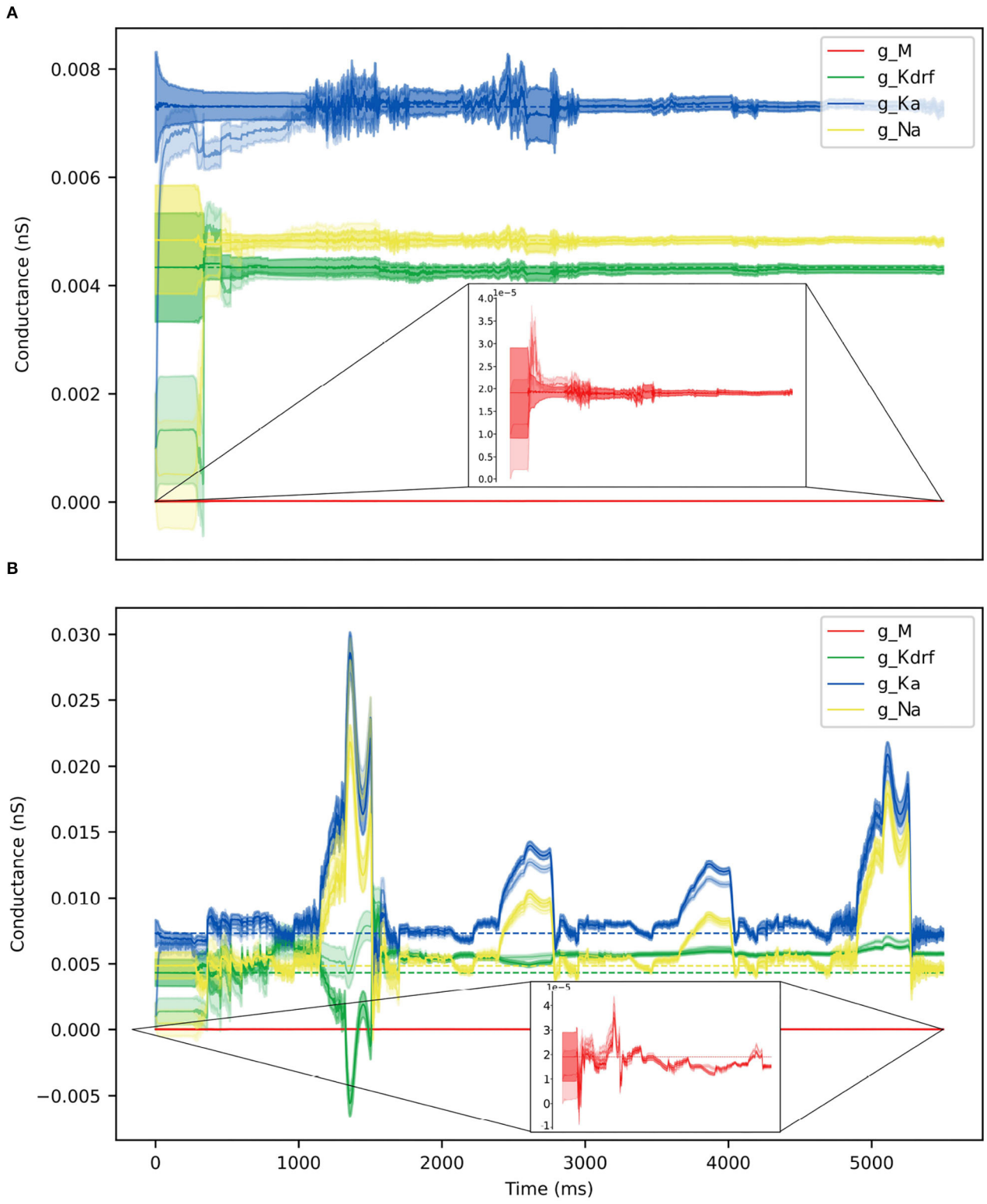

FIGURE 10
Parameter estimates over time via RAUKF algorithm. Estimate of conductance values over time, shaded region depicts the standard error of the estimate derived from the process covariance P. For each conductance, two traces are made, one transparent the other not. The transparent trace of each conductance represents the RAUKF estimates over time when initialized with a poor estimate, the opaque trace depicts conductance estimates with initial values set to the same values as in SINGLE (optimized values). The conductance estimate of g_M is presented in a zoomed frame as the order of magnitude of $g_M$is 10^{-3} less than the other values. **(A)** RAUKF estimates applied to an observation using SINGLE. **(B)** RAUKF estimates applied to observation using FULL.

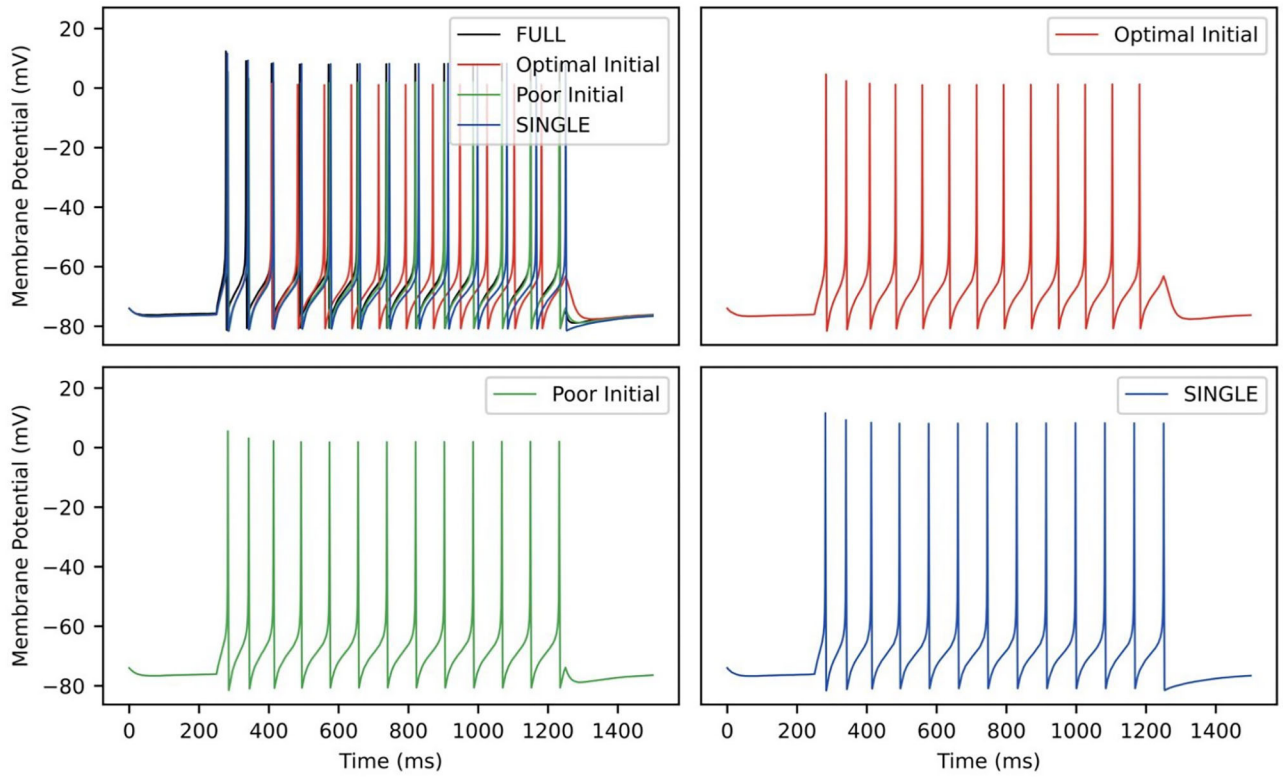

FIGURE 11
RAUKF parameter comparison. Traces of FULL (black), SINGLE (blue) and RAUKF model poor and optimal estimates (green and red) to a step 60 *pA* step current for 1 s, similar to as shown in Figure 1. The traces of SINGLE and RAUKF are overlayed atop the FULL's in the top left. The remaining corners are the traces of SINGLE and RAUKF separated for comparison.

vitro and *in vivo*-like states (Guet-McCreight and Skinner, 2021). Due to its reduced nature, we were able to produce a much wider range of firing frequencies for *in vivo*-like states to encompass OLM cell firing ranges observed experimentally. In turn, this allowed us to produce a large dataset of a wider and larger range of spike frequency resonances that could be subsequently explored from underlying biophysical perspectives. Using spike-triggered analyses, we were able to show that characteristics from a combination of M- and h-currents are what allow spiking resonances at theta frequencies specifically to be present.

Given the slower time constants of h- and M-currents relative to the other current types, it makes sense that they could play larger roles for theta frequencies in particular. It is further interesting that these channel types could be playing an oversized role in generating theta frequency spiking resonances with their distinct cholinergic profiles and prominent h-channels with location-dependent characteristics (Maccaferri, 2005; Lawrence, 2008; Hilscher et al., 2019). That is, there may be particular ways by which modulatory influences on M- and h-currents of OLM cells could control theta rhythmic activities. It is particularly interesting that we found that it is a *combination* of these two current types that is important, and not just one of them alone, suggesting that modulatory balances need to be in play for the existence of theta frequency spiking resonances. It could be that the IM and Ih of a given OLM cell are tuned and balanced to specifically allow expression of theta frequency spiking resonance. A possible next step to obtain mechanistic insight is to theoretically distill what this balance is by using an approach that separates the many parameters in the IM and Ih mathematical equations into structural and kinetic ones, potentially uncovering homeostatic control mechanisms (Ori et al., 2018).

Using our full, multi-compartment OLM cell model as an experimental proxy, we showed that it is possible to directly estimate parameter values from voltage recordings using a noisy input protocol that used multiple current steps. We limited our examination to estimating parameters of maximal conductances of four channel types but this is not a restriction of the RAUKF algorithm itself (Azzalini et al., 2022). Rather, we sought a proof of principle for the approach since we had both full, detailed multi-compartment OLM cell models and reduced single compartment models, the latter's mathematical model structure that was used with the RAUKF algorithm. Our choice to focus on extracting conductances g_M, g_{Kdrf}, g_{Ka} and g_{Na} also allowed us to directly compare these extracted parameter values with those obtained in developing the reduced model using a genetic optimization technique (BluePyOpt) to match feature values. Although the resulting parameter values were not identical, they were very similar with the most difference being in g_{Kdrf}. The RAUKF estimate was larger which would explain why the spike height is a bit less (see Figure 11). The spike height match using BluePyOpt is expected since spike height was a specific feature that was included during the optimization.

The successful demonstration of the RAUKF algorithm here is strong encouragement to expand its usage to estimate additional

parameter values in the OLM cell model and to consider application to other cell types. Indeed, these KF techniques have already been applied in various ways that include single neuron dynamics (Schiff, 2009; Ullah and Schiff, 2009; Lankarany et al., 2013, 2014). A major advantage of using the RAUKF algorithm over other optimization techniques is its speed and possibility for real-time usage. This could be particularly exciting as the modulatory nature of these h- and M-currents could be monitored in real time and changes under different conditions could be assessed.

Obtaining *in vivo* recordings of identified cells are highly non-trivial and it is important to point out how our work has built on and gone beyond previous studies. In earlier studies, artificial *in vivo* firing rates of OLM cells were restricted to 2.5 Hz (Kispersky et al., 2012; Sekulić and Skinner, 2017), but they can be much higher (Varga et al., 2012; Katona et al., 2014). Our recent modeling study that included OLM cells during IVL states produced a restricted range of firing rates using previously optimized synaptic characteristics (Guet-McCreight and Skinner, 2020). Here, with our developed reduced model, we were less restricted as we focused on having valid *in vivo* characteristics and not on optimized synaptic characteristics based on defined presynaptic cell types. The fact that our reduced single compartment model was able to capture complex behaviors to those seen with the full, multi-compartment model suggests that including dendritic OLM cell details are not overly critical for the consideration of spiking resonances, possibly due to the compact nature of OLM cells. Of course, this does not mean that dendritic details and channel distributions are not relevant. Rather, it suggests that a consideration of somatic biophysical balances of h- and M-currents is sufficient to gain insight into theta frequency spiking resonances. Further, all the different channel types present in the multi-compartment model were not retained in the reduced single compartment one. Specifically, calcium channels types were not included as we knew that they could not be biophysically balanced in a single compartment model. One can consider developing a reduced two-compartment model to include these additional biophysical currents in future studies.

In closing, we would like to heartily agree with statements that "diversity is beneficial" to have an "immense impact on our understanding of the brain," as stated in an excellent, recent review on neural modeling that pushes for combinations and not fragmentation (Eriksson et al., 2022). Our work has used developed biophysically detailed mathematical models based on *in vitro* data, created artificial *in vivo* states with reduced biophysical models to capture the range of firing frequencies *in vivo*, and directly extracted parameter values from voltage recordings of an experimental proxy (i.e., detailed, multi-compartment models). In doing this, we now have an approach and a focus to directly examine and gain insight into theta rhythms in the hippocampus from the perspective of h- and M-currents in OLM cells' control of theta frequency spiking resonances. Diversity is beneficial!

Data availability statement

The raw data supporting the conclusions of this article will be made available by the authors, without undue reservation.

Author contributions

ZS performed model simulations and all related analyses. DC performed KF analyses and usage. ZS, DC, and FS wrote the first draft of the manuscript. All authors contributed to conception and design of the study. All authors contributed to manuscript revision, read, and approved the submitted version.

Funding

This research was supported by the Natural Sciences and Engineering Research Council of Canada (NSERC) Discovery Grants (RGPIN-2016-06182 to FS and RGPIN-2020-05868 to ML) and an NSERC USRA to ZS.

Acknowledgments

We thank Miguel Barreto for statistical analyses and Alexandre Guet-McCreight for sharing original data points for comparisons, earlier technical assistance and manuscript feedback.

Conflict of interest

The authors declare that the research was conducted in the absence of any commercial or financial relationships that could be construed as a potential conflict of interest.

Publisher's note

Supplementary material

The Supplementary Material for this article can be found online at: https://www.frontiersin.org/articles/10.3389/fncir.2023.1076761/full#supplementary-material

References

Alonso, L. M., and Marder, E. (2019). Visualization of currents in neural models with similar behavior and different conductance densities. *Elife* 8, e42722. doi: 10.7554/eLife.42722.026

Azzalini, L. J., Crompton, D., D'Eleuterio, G. M. T., Skinner, F., and Lankarany, M. (2022). Adaptive unscented kalman filter for neuronal state and parameter estimation. *bioRxiv* 2022.06.29.497821 doi: 10.1101/2022.06.29.497821

Destexhe, A., Rudolph, M., Fellous, J.-M., and Sejnowski, T. J. (2001). Fluctuating synaptic conductances recreate in vivo-like activity in neocortical neurons. *Neuroscience* 107, 13–24. doi: 10.1016/S0306-4522(01)00344-X

Destexhe, A., Rudolph, M., and Paré, D. (2003). The high-conductance state of neocortical neurons *in vivo*. *Nat. Rev. Neurosci*. 4, 739–751. doi: 10.1038/nrn1198

Eriksson, O., Bhalla, U. S., Blackwell, K. T., Crook, S. M., Keller, D., Kramer, A., et al. (2022). Combining hypothesis- and data-driven neuroscience modeling in FAIR workflows. *eLife* 11, e69013. doi: 10.7554/eLife.69013

Fishell, G., and Kepecs, A. (2020). Interneuron types as attractors and controllers. *Ann. Rev. Neurosci*. 43, 1–30. doi: 10.1146/annurev-neuro-070918-050421

Guet-McCreight, A., and Skinner, F. K. (2020). Computationally going where experiments cannot: a dynamical assessment of dendritic ion channel currents during *in vivo*-like states. *F1000Res*. 9, 180. doi: 10.12688/f1000research.22584.2

Guet-McCreight, A., and Skinner, F. K. (2021). Deciphering how interneuron specific 3 cells control oriens lacunosum-moleculare cells to contribute to circuit function. *J. Neurophysiol*. 126, 997–1014. doi: 10.1152/jn.00204.2021

Hilscher, M. M., Nogueira, I., Mikulovic, S., Kullander, K., Leão, R. N., and Leão, K. E. (2019). Chrna2-OLM interneurons display different membrane properties and h-current magnitude depending on dorsoventral location. *Hippocampus* 29, 1224–1237. doi: 10.1002/hipo.23134

Ito, J. (2015). "Spike triggered average," in *Encyclopedia of Computational Neuroscience*, eds D. Jaeger and R. Jung (New York, NY: Springer New York), 2832–2835.

Katona, L., Lapray, D., Viney, T. J., Oulhaj, A., Borhegyi, Z., Micklem, B. R., et al. (2014). Sleep and movement differentiates actions of two types of somatostatin-expressing GABAergic interneuron in rat hippocampus. *Neuron* 82, 872–886. doi: 10.1016/j.neuron.2014.04.007

Kispersky, T. J., Fernandez, F. R., Economo, M. N., and White, J. A. (2012). Spike Resonance properties in hippocampal O-LM cells are dependent on refractory dynamics. *J. Neurosci*. 32, 3637–3651. doi: 10.1523/JNEUROSCI.1361-11.2012

Klausberger, T., Magill, P. J., Márton, L. F., Roberts, J. D. B., Cobden, P. M., Buzsáki, G., et al. (2003). Brain-state- and cell-type-specific firing of hippocampal interneurons *in vivo*. *Nature* 421, 844–848. doi: 10.1038/nature01374

Lankarany, M., Zhu, W.-P., Swamy, M. N. S., and Toyoizumi, T. (2013). "Blind deconvolution of hodgkin-huxley neuronal model," in *2013 35th Annual International Conference of the IEEE Engineering in Medicine and Biology Society (EMBC)* (Osaka: IEEE), 3941–3944.

Lankarany, M., Zhu, W. P., and Swamy, M. N. S. (2014). Joint estimation of states and parameters of Hodgkin-Huxley neuronal model using Kalman filtering. *Neurocomputing* 136, 289–299. doi: 10.1016/j.neucom.2014.01.003

Lawrence, J. J. (2008). Cholinergic control of GABA release: emerging parallels between neocortex and hippocampus. *Trends Neurosci*. 31, 317–327. doi: 10.1016/j.tins.2008.03.008

Lawrence, J. J., Grinspan, Z. M., Statland, J. M., and McBain, C. J. (2006a). Muscarinic receptor activation tunes mouse stratum oriens interneurones to amplify spike reliability. *J. Physiol*. 571(Pt 3), 555–562. doi: 10.1113/jphysiol.2005.103218

Lawrence, J. J., Statland, J. M., Grinspan, Z. M., and McBain, C. J. (2006b). Cell type-specific dependence of muscarinic signalling in mouse hippocampal stratum oriens interneurones. *J. Physiol*. 570(Pt 3), 595–610. doi: 10.1113/jphysiol.2005.100875

Leão, R. N., Mikulovic, S., Leão, K. E., Munguba, H., Gezelius, H., Enjin, A., et al. (2012). OLM interneurons differentially modulate CA3 and entorhinal inputs to hippocampal CA1 neurons. *Nat. Neurosci*. 15, 1524–1530. doi: 10.1038/nn.3235

Lovett-Barron, M., Kaifosh, P., Kheirbek, M. A., Danielson, N., Zaremba, J. D., Reardon, T. R., et al. (2014). Dendritic inhibition in the hippocampus supports fear learning. *Science* 343, 857–863. doi: 10.1126/science.1247485

Maccaferri, G. (2005). Stratum oriens horizontal interneurone diversity and hippocampal network dynamics. *J. Physiol*. 562(Pt 1), 73–80. doi: 10.1113/jphysiol.2004.077081

Maccaferri, G., and McBain, C. J. (1996). The hyperpolarization-activated current (Ih) and its contribution to pacemaker activity in rat CA1 hippocampal stratum oriens-alveus interneurones. *J. Physiol*. 497(Pt 1), 119–130. doi: 10.1113/jphysiol.1996.sp021754

Moradi Chameh, H., Rich, S., Wang, L., Chen, F.-D., Zhang, L., Carlen, P. L., et al. (2021). Diversity amongst human cortical pyramidal neurons revealed via their sag currents and frequency preferences. *Nat. Commun*. 12, 2497. doi: 10.1038/s41467-021-22741-9

Ori, H., Marder, E., and Marom, S. (2018). Cellular function given parametric variation in the Hodgkin and Huxley model of excitability. *Proc. Natl. Acad. Sci. U.S.A*. 115, E8211-E8218. doi: 10.1073/pnas.1808552115

Pancotti, L., and Topolnik, L. (2022). Cholinergic modulation of dendritic signaling in hippocampal GABAergic inhibitory interneurons. *Neuroscience* 489, 44–56. doi: 10.1016/j.neuroscience.2021.06.011

Pike, F. G., Goddard, R. S., Suckling, J. M., Ganter, P., Kasthuri, N., and Paulsen, O. (2000). Distinct frequency preferences of different types of rat hippocampal neurones in response to oscillatory input currents. *J. Physiol*. 529, 205–213. doi: 10.1111/j.1469-7793.2000.00205.x

Schiff, S. J. (2009). Kalman meets neuron: the emerging intersection of control theory with neuroscience. *Annu. Int. Conf. IEEE Eng. Med. Biol. Soc*. 2009, 3318–3321. doi: 10.1109/IEMBS.2009.5333752

Schwartz, O., Pillow, J. W., Rust, N. C., and Simoncelli, E. P. (2006). Spike-triggered neural characterization. *J. Vis*. 6, 13. doi: 10.1167/6.4.13

Sekulić, V., and Skinner, F. K. (2017). Computational models of O-LM cells are recruited by low or high theta frequency inputs depending on h-channel distributions. *Elife* 6, e22962. doi: 10.7554/eLife.22962

Sekulić, V., Yi, F., Garrett, T., Guet-McCreight, A., Lawrence, J. J., and Skinner, F. K. (2020). Integration of within-cell experimental data with multi-compartmental modeling predicts H-channel densities and distributions in hippocampal OLM cells. *Front. Cell. Neurosci*. 14, 277. doi: 10.3389/fncel.2020.00277

Sivagnanam, S., Majumdar, A., Yoshimoto, K., Astakhov, V., Bandrowski, A., Martone, M., et al. (2013). "Introducing the neuroscience gateway," in *IWSG, CEUR Workshop Proceedings* (CEUR-WS.org 993). Available online at: https://www.nsgportal.org/citation.html

Uhlenbeck, G. E., and Ornstein, L. S. (1930). On the theory of the brownian motion. *Phys. Rev*. 36, 823. doi: 10.1103/PhysRev.36.823

Ullah, G., and Schiff, S. J. (2009). Tracking and control of neuronal Hodgkin-Huxley dynamics. *Phys. Rev. E* 79, 040901. doi: 10.1103/PhysRevE.79.040901

Van Geit, W., Gevaert, M., Chindemi, G., Rössert, C., Courcol, J.-D., Muller, E. B., et al. (2016). BluePyOpt: leveraging open source software and cloud infrastructure to optimise model parameters in neuroscience. *Front. Neuroinform*. 10, 17. doi: 10.3389/fninf.2016.00017

Varga, C., Golshani, P., and Soltesz, I. (2012). Frequency-invariant temporal ordering of interneuronal discharges during hippocampal oscillations in awake mice. *Proc. Natl. Acad. Sci. U.S.A*. 109, E2726-E2734. doi: 10.1073/pnas.1210929109

Zemankovics, R., Káli, S., Paulsen, O., Freund, T. F., and Hájos, N. (2010). Differences in subthreshold resonance of hippocampal pyramidal cells and interneurons: the role of h-current and passive membrane characteristics. *J. Physiol*. 588, 2109–2132. doi: 10.1113/jphysiol.2009.185975

Zeng, H., and Sanes, J. R. (2017). Neuronal cell-type classification: challenges, opportunities and the path forward. *Nat. Rev. Neurosci*. 18, 530–546. doi: 10.1038/nrn.2017.85

frontiers | Frontiers in Neural Circuits

TYPE Review
PUBLISHED 23 March 2023
DOI 10.3389/fncir.2023.1122314

OPEN ACCESS

EDITED BY
Blake A. Richards,
Montreal Institute for Learning Algorithm (MILA), Canada

REVIEWED BY
Simon Chen,
University of Ottawa, Canada
Nikolaos Karalis,
Friedrich Miescher Institute for Biomedical Research (FMI), Switzerland

*CORRESPONDENCE
Lisa Topolnik
✉ lisa.topolnik@bcm.ulaval.ca

RECEIVED 12 December 2022
ACCEPTED 17 February 2023
PUBLISHED 23 March 2023

CITATION
Singh S and Topolnik L (2023) Inhibitory circuits in fear memory and fear-related disorders. Front. Neural Circuits 17:1122314. doi: 10.3389/fncir.2023.1122314

Inhibitory circuits in fear memory and fear-related disorders

Sanjay Singh[1,2] and Lisa Topolnik[1,2]*

[1]Department of Biochemistry, Microbiology and Bio-informatics, Laval University, Quebec City, QC, Canada, [2]Neuroscience Axis, CRCHUQ, Laval University, Quebec City, QC, Canada

Fear learning and memory rely on dynamic interactions between the excitatory and inhibitory neuronal populations that make up the prefrontal cortical, amygdala, and hippocampal circuits. Whereas inhibition of excitatory principal cells (PCs) by GABAergic neurons restrains their excitation, inhibition of GABAergic neurons promotes the excitation of PCs through a process called disinhibition. Specifically, GABAergic interneurons that express parvalbumin (PV+) and somatostatin (SOM+) provide inhibition to different subcellular domains of PCs, whereas those that express the vasoactive intestinal polypeptide (VIP+) facilitate disinhibition of PCs by inhibiting PV+ and SOM+ interneurons. Importantly, although the main connectivity motifs and the underlying network functions of PV+, SOM+, and VIP+ interneurons are replicated across cortical and limbic areas, these inhibitory populations play region-specific roles in fear learning and memory. Here, we provide an overview of the fear processing in the amygdala, hippocampus, and prefrontal cortex based on the evidence obtained in human and animal studies. Moreover, focusing on recent findings obtained using genetically defined imaging and intervention strategies, we discuss the population-specific functions of PV+, SOM+, and VIP+ interneurons in fear circuits. Last, we review current insights that integrate the region-specific inhibitory and disinhibitory network patterns into fear memory acquisition and fear-related disorders.

KEYWORDS

inhibition, memory, contextual fear conditioning, disinhibition, GABAergic interneuron, optogenetics

Introduction

Fear memories are associated with distressing emotions caused by anticipation of danger. Although essential for survival, when these memories persist even in the absence of threatful cues, it might lead to the development of post-traumatic stress disorder (PTSD). PTSD is a serious mental health condition that promotes reckless and self-destructive behavior due to disturbed activity within neuronal networks (Ford and Courtois, 2014). Initially, Pavlov's classic fear conditioning paradigm set a benchmark for animal studies aimed at deciphering the behavioral and neural circuits involved in fear learning (Pavlov, 1927). Since then, rodent models of fear conditioning have been extensively used in laboratory studies to understand the physiological processes that make animals more alert to traumatic events and lead to the development of associative memory. In this paradigm, the animals are trained to receive a neutral conditioning stimulus (e.g., auditory tone: CS+) paired with an aversive stimulus (mild foot shock: US) in a specific environmental context. Another neutral stimulus remains

unpaired (CS-). After the repeated presentation of CS+US pairing (generally 4–5 trials), the animals learn to associate the CS+ with the US, which is referred to as fear conditioning (Rescorla, 1988). As a result, the presentation of the CS+ evokes the fear response manifested in the form of freezing or the inhibition of motor activity. Accordingly, the aversive stimuli can be considered as a dominating cue that can elicit memory formation and even change the individual's behavior. To overcome the altered behavioral response, the extinction paradigm is routinely used by neuroscientists (Myers et al., 2006). Extinction can be defined as a form of learning, in which animals learn to inhibit retrieval (Konorski, 1948, 1967). In this paradigm, the CS+ (tone in the case of cued fear learning or context in the case of contextual fear learning) is repeatedly presented in the absence of the US leading to the reduction of fear response either by the erasure of the originally acquired CS+US association or the formation of a new association (Quirk et al., 2010). This paradigm allows for attenuating the reactivated fear memories by disrupting reconsolidation and is used in the therapy of PTSD and other related disorders.

Several decades of work have established that the experience-dependent plasticity induced by the CS-US association underlies the development of intrusive memories and causes alterations in specific brain circuits and behavior (Franke et al., 2021). To understand the circuitry involved in fear memory processes, neuroscientists have focused primarily on the triad of brain regions that includes the amygdala, hippocampus, and medial prefrontal cortex (Feng et al., 2014; McEwen et al., 2016; Kredlow et al., 2021). The amygdala is considered as the key brain region involved in the regulation of emotional responses (Phelps and LeDoux, 2005; Pape and Pare, 2010; Forster et al., 2017). This almond-shaped structure located in the medial temporal lobe is composed of >10 nuclei, with the basolateral complex (BLA) and the central amygdala (CeA, comprising the centro-lateral (CeL) and the centro-medial (CeM) regions) being intensively studied in the context of fear memory. It has been established that both acquisition and consolidation of fear memory rely on synaptic plasticity and protein synthesis in the amygdala (Schafe et al., 1999; Maren et al., 2003). The hippocampus is a second important region of the limbic system that is mainly involved in contextual (Raineki et al., 2010; Oh and Han, 2020) and traces fear learning, which relies on a temporal association between the CS and US (Curzon et al., 2009; Sharma et al., 2018). Hippocampus makes a part of the hippocampal formation comprising the hippocampus proper that consists in the CA1, CA2, and CA3 areas, the entorhinal cortex, the dentate gyrus (DG), and the subiculum (Wright, 2020). The hippocampal CA1, CA3, and DG areas have been shown to play a crucial role in contextual fear memory encoding, consolidation, and retrieval (Maren et al., 1997; Sierra-Mercado et al., 2011; Liu et al., 2012; Donato et al., 2013; Ramirez et al., 2013; Lovett-Barron et al., 2014; Stefanelli et al., 2016). Another vital region that participates in the regulation of the fear response is the prefrontal cortex (PFC), with the prelimbic area (PL-PFC) involved in the expression of fear memory, and the infralimbic area (IL-PFC) implicated in the extinction memory (Quirk et al., 2000; Runyan et al., 2004; Laviolette et al., 2005). Whereas the critical role of these brain regions in fear memory has been established, previous research focused mainly on excitatory neurons; however, with advancements in this field, it has become clear that, in addition to excitatory connections, inhibitory inputs are equally important for fear memory acquisition, consolidation, and extinction (Letzkus et al., 2011; Donato et al., 2013; Lovett-Barron et al., 2014; Stefanelli et al., 2016; Tipps et al., 2018; Krabbe et al., 2019).

Across different cortical and limbic structures, the inhibitory inputs are delivered by the GABAergic inhibitory neurons (or interneurons) that provide spatio-temporal coordination of the activity of principal cells (PCs) via the inhibition of specific subcellular domains of PCs, such as soma and dendrites (Klausberger and Somogyi, 2008; Capogna, 2014; Tremblay et al., 2016; Pelkey et al., 2017). In addition, activation of inhibitory interneurons can result in circuit disinhibition, or reduction in inhibition of PCs, because of extensive connectivity between interneurons (Cummings and Clem, 2020; Kullander and Topolnik, 2021). GABAergic neurons are highly heterogeneous and comprise a large set of specific cell types with distinct morphological, physiological, molecular, and functional properties (Ascoli et al., 2008; Klausberger and Somogyi, 2008; Capogna, 2014; Tremblay et al., 2016; Pelkey et al., 2017). Understanding the cell-type-specific roles of GABAergic neurons in different brain areas remains therefore a challenging task. Nonetheless, the development of genetic intervention strategies allowed for the selective targeting of three populations of interneurons that account for most GABAergic cells in cortical and limbic areas, i.e., cells expressing the calcium-binding protein parvalbumin (PV+), the neuropeptide somatostatin (SOM+), or the vasoactive intestinal peptide (VIP+; Rudy et al., 2011; Capogna, 2014; Kepecs and Fishell, 2014). This article will first review the evidence from human studies regarding the major brain structures involved in fear memory and fear-related disorders, such as the amygdala, hippocampus, and the prefrontal cortex, and then discuss the animal studies that allowed deciphering the circuit and cellular mechanisms underlying fear memory acquisition and extinction. As more recent research has explored the specific contributions of inhibitory interneurons in different types of memory (Topolnik and Tamboli, 2022), in the sections dealing with the related circuits, the attention will be focused on populations of PV+, SOM+, and VIP+ interneurons in order to understand their specific functions in modulating the cortical and limbic circuitry involved in fear learning.

Major brain structures involved in fear memory and related disorders: evidence from human studies

It has been established that the amygdala, PFC, and hippocampus are all involved in threat learning and are affected in individuals with PTSD (Bremner, 2006), with each of the structures playing its own role in relation to fear expression and extinction. First, studies conducted on patients with unilateral or bilateral amygdala lesions revealed impaired fear learning (Bechara et al., 1995; LaBar et al., 1995; Weike et al., 2005). Similarly, war veterans with the damaged amygdala exhibited reduced fear responses (Koenigs et al., 2008), indicating that the amygdala is critical for the physiological expression of fear learning in humans. Moreover, the amygdala showed consistent alterations in morphology and activity in fear-induced disorders. The structural magnetic resonance

imaging (MRI) conducted on patients with PTSD diagnosis showed a reduced volume of the amygdala (Morey et al., 2012; Zhang et al., 2021). The smaller amygdala volume could also make the individual more prone to the development of PTSD (Morey et al., 2012). Furthermore, the functional neuroimaging studies also demonstrated that, during fear learning in humans, the CS+ presentation resulted in high activation of the amygdala (LaBar et al., 1998; Sehlmeyer et al., 2009). Such studies also showed that the fear memory consolidation and extinction are both associated with memory traces in the BLA (Bach et al., 2011; Agren et al., 2012; Björkstrand et al., 2015). In addition, the prefrontal control of the amygdala important for fear expression and extinction can be impaired in individuals with PTSD (Forster et al., 2017). A more recent study using simultaneous positron emission tomography and functional MRI revealed an additional link between the amygdala and striatum by showing that, during conditioning, activity in the amygdala is facilitated by dopamine release, which can control the strength of conditioned fear response (Frick et al., 2021). Therefore, the amygdala is a central component in the brain threat circuitry critical for the acquisition and consolidation of fear memories and the expression of fear-related disorders.

Second, like the amygdala, the hippocampus also showed altered morphology in fear-related disorders. The reduction in hippocampal volume was observed in patients suffering from PTSD and untreated depression (Sheline et al., 2003; Kitayama et al., 2005; Zhang et al., 2021). Both the left and right hippocampi exhibited reduced volume, with case-specific variability (Pavić et al., 2007; Nelson and Tumpap, 2017). In addition to structural changes, the PTSD patients showed altered hippocampal activity, although the findings are contrasting. Both reduced (Etkin and Wager, 2007; Hayes et al., 2011) and increased hippocampal activity (Shin et al., 2004) have been observed in patients with PTSD diagnosis, likely because of the patient history-/treatment-related specifics of the examined cases. Whereas the results are contradictory, they still suggest that the hippocampus is involved in the fear response in humans. In healthy individuals, the hippocampus has been also shown to gate the extinction memory (Sevinc et al., 2019). Interestingly, various models of PTSD have revealed a compromised GABAergic inhibition in the hippocampus, which results in symptoms that are consistent with dysregulation of affective control and the extinction of conditioned fear. For example, using ^{1}H magnetic resonance spectroscopy, it has been shown that suppression of unwanted thoughts was associated with higher hippocampal GABA concentrations and a stronger fronto-hippocampal coupling, pointing to an important role of hippocampal interneurons in regulating fear extinction (Schmitz et al., 2017). Further experimental evidence will be required to understand the exact role of the human hippocampus in fear memory acquisition and extinction.

Third, different neocortical areas, including the prefrontal, insular, temporal, parietal, and occipital regions, also displayed abnormal volume in individuals with PTSD (Wang et al., 2021). The reduced volume of the ventromedial prefrontal cortex (vmPFC) is also reported in patients suffering from stress-related disorders (Greco and Liberzon, 2016). Moreover, the cued delayed and trace fear conditioning triggered an increase in the activation of the anterior cingulate and insular cortices during fear memory acquisition (Sehlmeyer et al., 2009). Further, the repetitive transcranial magnetic stimulation of the dorsal prefrontal cortex (dlPFC) during the reconsolidation window resulted in reduced fear expression and fear return after extinction (Borgomaneri et al., 2020). In a recent study conducted by Anderson and Floresco (2021), the role of prefrontal regions was investigated in the retrieval-stopping test, an assay where human volunteers were allowed to terminate the retrieval of fear memory, and significant activation was detected in the dlPFC, ventrolateral prefrontal cortex (vlPFC), posterior middle frontal gyrus (pmFG), and bilateral insular cortex. Among these regions, the dlPFC was extensively activated. The vmPFC in turn was activated during late fear conditioning (Fullana et al., 2016) and extinction learning (Phelps et al., 2004), whereas bilateral lesions in this region were associated with impaired fear conditioning (Battaglia et al., 2020). Collectively, these lines of evidence from human studies highlight the fear-induced structural and functional alterations within three primary brain regions comprising the fear network, such as amygdala, hippocampus, and the prefrontal cortex, which together regulate the fear-induced adaptive behavior but are compromised in fear-related disorders. A deeper understanding of the circuit and cellular mechanisms underlying these processes has been provided in animal studies.

Animal studies: amygdala

Similar to human studies, changes in the structure and function of the amygdala have been linked with fear learning in animal models. In particular, it has been shown that the BLA complex of the amygdala is playing a key role in fear memory (Marek et al., 2019; Ponserre et al., 2022). As such, during auditory fear learning, subjects learn an association between a tone and a mild electric foot shock. The BLA receives two streams of inputs regarding auditory (CS, tone) and somatosensory information (US, foot shock; Ponserre et al., 2022). Through the repeated temporal association of these inputs, the subjects exhibit defensive responses to the CS alone [i.e., conditioned response (CR)], which is driven by the amygdala's response to the auditory CS information entering through the BLA and going to the CeL, CeM and to the periaqueductal gray (PAG; Dejean et al., 2015; Tovote et al., 2015). The BLA model of fear conditioning suggests that the integration of CS and US information by the BLA PCs leads to long-term potentiation (LTP) at the synapses that carry the auditory CS (Schafe et al., 1999; Pape and Pare, 2010); although the auditory cortex and thalamus are also involved in fear conditioning-induced plasticity (Letzkus et al., 2011). Furthermore, blockade of the LTP in BLA using a protein synthesis inhibitor or manipulation with MAPK activity and PKA impaired fear memory consolidation. In fact, both long-term memories for contextual fear learning and auditory fear conditioning were affected, while no effect on short-term memory was observed (Atkins et al., 1998; Schafe et al., 1999). In addition to the induction of synaptic plasticity, other processes that combine enhanced intrinsic excitability and changes in the recruitment of inhibitory interneurons may occur in parallel (Han et al., 2007; Kim et al., 2013). Together, these intrinsic, synaptic, and circuit mechanisms will be responsible for assignment of some LA PCs to fear memory ensembles.

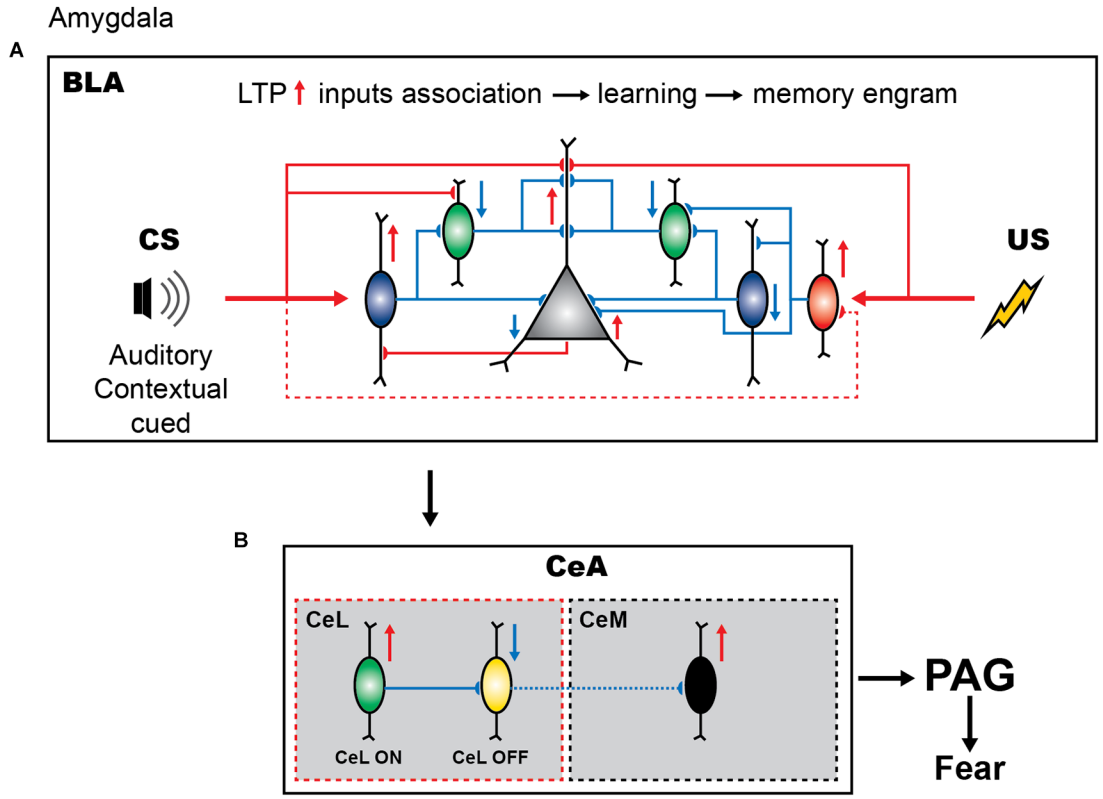

FIGURE 1
Inhibitory circuits of amygdala in fear learning. **(A)** Presentation of neutral stimulus (CS) elicits the firing of PV+ interneurons (blue) and causes the dendritic disinhibition of principal cells by inhibiting SOM+ cells (green), thus promoting the sensory response and enabling the tone-shock association. In contrast, US presentation results in the dendritic and perisomatic disinhibition due to inhibition of SOM+ and PV+ cells by the upstream VIP+ interneurons (red). **(B)** The cue-shock associated information is projected to the CeL and causes the activation of the SOM+ expressing CeL neurons (green). These GABAeric neurons regulate the CeM-PAG pathway for the expression of fear by inhibiting the PKC-delta expressing CeL cells.

Importantly, different stages of amygdala-dependent learning can be tightly controlled by synaptic inhibition mediated by the BLA GABAergic neurons (**Figure 1A**; Shumyatsky et al., 2002; Szinyei et al., 2007; Wolff et al., 2014; Krabbe et al., 2019). Several interneuron subtypes have been identified in the BLA based on cytosolic markers and physiological properties (reviewed in Spampanato et al., 2011; Hajos, 2021). Among others, the PV+, SOM+, and VIP+ populations are all involved in fear learning, albeit via distinct circuit mechanisms (**Figure 1A**; Wolff et al., 2014; Krabbe et al., 2019). Similar to cortical areas, PV+ interneurons, which comprise basket and axo-axonic cells, represent one of the largest inhibitory populations in the BLA and provide inhibitory inputs to PCs and GABAergic cells, including SOM+ interneurons (McDonald and Mascagni, 2002; Woodruff and Sah, 2007a,b; Wolff et al., 2014; Bocchio et al., 2015; Vereczki et al., 2016, 2021). BLA PV+ interneurons are primarily driven by PCs (Smith et al., 2000), and play an important role in synchronizing PC firing through feedback perisomatic inhibition (Woodruff and Sah, 2007a,b; Bienvenu et al., 2012; Veres et al., 2014, 2017). Single-unit recordings *in vivo* from opto-tagged PV+ interneurons revealed that the majority of PV+ cells are excited by CS and inhibited by shock presentation (Wolff et al., 2014; although the axo-axonic cells may be activated by the shock or hind paw pinches, see Bienvenu et al., 2012). Moreover, additional optogenetic activation of PV+ cells during fear conditioning attenuated the CS freezing response, whereas their inhibition during the US led to increased freezing during fear memory retrieval. These data indicate that the CS-induced activation and US-induced inactivation of PV+ cells are required for fear memory acquisition. Furthermore, PV+ interneurons have been shown to control the memory engram size in the BLA (Morrison et al., 2016), which may rely on the input- and/or target-specific plasticity rules at either excitatory or inhibitory connections, and require further investigation.

Local SOM+ interneurons in the BLA are primarily driven by cortical inputs providing feedforward inhibition to the distal dendrites of PCs (**Figure 1A**; Muller et al., 2007; Unal et al., 2014; Wolff et al., 2014). These cells receive inhibitory inputs from the PV+ basket cells and VIP+ interneurons (Wolff et al., 2014; Krabbe et al., 2019). Similar to the cortical SOM+ population, the BLA SOM+ family may comprise a variety of cell types with distinct functions (McDonald and Mascagni, 2002; Yu et al., 2016). For example, some SOM and neuropeptide Y (NPY) co-expressing BLA interneurons exhibit properties of cortical neurogliaform cells with slow GABA signaling (Mańko et al., 2012) that can shape hippocampo-amygdala interactions during fear memory retrieval (Seidenbecher et al., 2003). Also, some long-range GABAergic projections arising from the BLA interneurons that co-express SOM and NPY have been reported (McDonald et al., 2012). Whereas their cell-type-specific functions remain to be determined, genetically targeted manipulations at the population level revealed

an important role of SOM+ interneurons in fear memory. In particular, using the combination of optogenetic manipulations and single-unit recordings, Wolff et al. (2014) reported that, during the auditory CS presentation, the activity of SOM+ interneurons is suppressed in line with a remarkable increase in PV+ cell activity. Furthermore, the US presentation also caused the inhibition of SOM+ interneurons. Driving the SOM+ interneuron activity during the CS presentation resulted in reduced learning, whereas the inhibition of these cells led to increased learning. These data indicate that, contrary to PV+ interneurons, inhibition of SOM+ cells is important for fear memory acquisition. Thus, whereas both PV+ and SOM+ interneurons are involved in fear learning, they have opposite functions (**Figure 1A**). During CS presentation, the firing of PV+ interneurons can result in perisomatic inhibition, followed by the dendritic disinhibition of PCs via the inhibition of SOM+ cells. During US presentation, the inhibition of both the PV+ and SOM+ interneurons will result in the perisomatic and dendritic disinhibition of the PCs, respectively. Together these inhibitory and disinhibitory circuit motifs may be required to synchronize PC ensembles, support the CS-US association, and gate fear memory acquisition.

VIP+ interneurons in the BLA form a heterogeneous population and target both the PCs and interneurons, such as PV+, SOM+, cholecystokinin-expressing (CCK+), and neurogliaform cells, as well as VIP+ cells, providing synaptic inhibition with target-specific properties (Rhomberg et al., 2018; Krabbe et al., 2019). Thus, VIP+ interneurons are involved in both the inhibitory and disinhibitory circuits. Recent elegant work, using genetically targeted calcium imaging *in vivo*, revealed that the firing of BLA VIP+ interneurons is greatly enhanced during the presentation of the US, and is primarily driven by the acetylcholine released from the basal forebrain afferents (Krabbe et al., 2019). VIP+ cells have been also recruited by the CS alone but at a lower fraction as compared to the US alone or CS-US pairing. Accordingly, optogenetic inhibition of VIP+ interneurons during the US presentation prevented fear memory formation (Krabbe et al., 2019). Thus, it can be suggested that, via the target-specific inhibition of both the PV+ and SOM+ interneurons, VIP+ cells can select PV+ interneurons that will be active during conditioning and together with PV+ cells contribute to SOM+ silencing, providing a higher level regulation over inhibitory circuits required for associative fear learning.

The CeA GABAergic cells are also involved in fear encoding and defensive/aversive behaviors (McDonald and Augustine, 1993; Paré and Smith, 1993). In fact, after CS-US association in the BLA, the information is received by the CeL, which in turn regulates the CeM-to-PAG projecting neurons during the subsequent presentation of CS neutral stimulus (**Figure 1B**; Dejean et al., 2015). The CeL comprises two populations of interneurons that show excitatory and inhibitory CS responses after fear conditioning (**Figure 1B**; Ciocchi et al., 2010; Duvarci et al., 2011). As a result, with the presentation of CS, CeL SOM+ neurons (Li et al., 2013; Penzo et al., 2015; Yu et al., 2016) become activated and, *via* the inhibition of the protein kinase C delta (PKC-δ)-expressing neurons projecting to the CeM, cause disinhibition of the CeM-to-PAG pathway, leading to the expression of the fear response by the PAG (Ciocchi et al., 2010; Li et al., 2013; Dejean et al., 2015). Indeed, the inactivation of CeM neurons using a fluorescently labeled $GABA_A$ receptor agonist muscimol-bodipy impaired the freezing behavior, while optogenetic activation of CeM neurons elicited freezing (Ciocchi et al., 2010). It should be noted, however, that the CeA GABAergic population may consist of different interneuron types with specific connectivity motifs that may play an additional role in regulating the CeL-to-CeM pathway during fear conditioning; the cellular diversity of the CeA inhibitory population remains largely unstudied. For example, a population of SOM+ CeL neurons exhibited potentiated LA synapses during fear conditioning. Furthermore, optogenetic activation of these cells elicited freezing behavior whereas their silencing impaired fear learning (Li et al., 2013). These cells do not project to CeM and it is currently unknown whether they form local inhibitory or disinhibitory microcircuits with $CeL\text{-}_{ON}$ neurons to modulate their activity.

Furthermore, both BLA and CeA inhibitory circuits may be important for fear extinction (Herry et al., 2008; Duvarci et al., 2011). Enhanced inhibition can suppress fear expression by reducing the activation of "fear neurons" that exhibit a pronounced response following fear conditioning (Herry et al., 2008). In fact, an overall increase in GABAergic inhibition has been observed in the BLA after extinction training (Chhatwal et al., 2005; Heldt and Ressler, 2007). Interestingly, the PV+ interneuron synapses formed onto BLA PCs undergo long-term potentiation during contextual fear extinction, thus representing an important mechanism for silencing the "fear neurons" (Herry et al., 2008; Trouche et al., 2013). Alternatively, local disinhibitory processes may allow for the formation of the new memory traces or extinction ensembles in the BLA. Hence, it would be important to determine the relative weight of different GABAergic elements that form inhibitory and disinhibitory patterns during fear extinction. Furthermore, a recent sophisticated study combining *in vivo* calcium imaging with functional manipulations revealed a critical role of the intercalated (ITC) clusters in orchestrating the transitions between the high- and low-fear states and fear extinction (Hagihara et al., 2021). The ITC clusters are located between BLA and CeA and are populated by GABAergic neurons that comprise a mutually connected inhibitory network to control the amygdala output pathways in response to changes in the environment. The results of this work thus indicate that the balance in the activity of ITC circuits may control a wide range of amygdala functions and adaptive behavior.

Animal studies: hippocampus

Contextual fear conditioning (CFC) has been considered as a robust behavioral paradigm to investigate the role of the hippocampus in fear learning (Kim and Fanselow, 1992; Raineki et al., 2010; Liu et al., 2012; Kim and Bin, 2020; Oh and Han, 2020). During CFC, animals develop an associative memory between the neutral environmental context and the aversive stimulus, which prompts them to adopt a defensive behavior upon re-exposure to the conditioning context. The CFC paradigm combines two stages: first, the animal collects unified multisensory environmental context information; second, it associates the environmental context information with the aversive stimulus (Fanselow, 1986; Fanselow and Poulos, 2004). It has

been established that the hippocampus integrates the multisensory features of the environment into a representation of context; however, it must also exclude sensory features about aversive stimulus (Fanselow et al., 1993).

Different parts of the hippocampus appear to play different functions in these processes. The dorsal hippocampus (dHPC) is primarily involved in spatial learning and episodic memory, whereas the ventral hippocampus (vHPC) receives inputs from the amygdala and the hypothalamus, and is involved in the regulation of stress and emotional responses (Fanselow and Dong, 2010). In rodent studies, the presentation to the animals of the mild electric foot shock in a neutral context in the absence of a tone triggers the development of associative fear memory. This paradigm has been widely used for studying contextual fear memory encoding and consolidation (Curzon et al., 2009). Using this paradigm, it has been established that the CS is encoded by the dHPC, the output of which is subsequently associated with the US through synaptic plasticity in the amygdala (Kim and Fanselow, 1992). Furthermore, the role of dHPC in fear encoding was confirmed by using lesions-based studies. A lesion in the dHPC on the day after CFC greatly diminished learning, whereas lesions performed 30–100 days after fear conditioning yielded minimal disruption in the acquisition of contextual fear learning. In contrast, during extinction training, conditioned animals are only exposed to the same context in which conditioning was performed, without any shock (Curzon et al., 2009). Rosas-Vidal et al. (2014) demonstrated that the activation of the vHPC during extinction training resulted in the upregulation of the brain-derived neurotrophic factor and suggested that the vHPC, *via* connections with the IL-PFC, is involved in fear memory extinction.

Whereas the role of the amygdala in fear acquisition and extinction mechanisms as well as in interactions with other brain areas have been extensively studied, relatively little is known about the contribution of hippocampal circuitry. The primary output neurons of the hippocampus, the PCs in area CA1, are driven by the Schaffer collateral pathway from the CA3 region and the temporo-ammonic pathway from the entorhinal cortex (Ahmed and Mehta, 2009). Whereas the CA3 region is responsible for a unified representation of a multisensory context, the entorhinal cortex conveys discrete sensory information in relation to the context (Maren et al., 1997; Kesner, 2007). Electrolytic lesions of the fimbria/fornix, dHPC, or entorhinal cortex produced anterograde deficits in CFC in rats (Maren et al., 1997). At the cellular level, nonlinear interactions between the CA3 and the entorhinal cortex inputs in dendrites of PCs can result in burst-spiking output and synaptic plasticity (Golding et al., 2002; Takahashi and Magee, 2009). Although PCs can carry behaviorally relevant information in the timing of spikes (Jones and Wilson, 2005), spike rate (Ahmed and Mehta, 2009), and spike bursts (Harris et al., 2001), the information conveyed using the bursts of spikes alone is sufficient for the encoding of context in the hippocampus during fear learning (Xu et al., 2012). Importantly, the pharmacological delivery of muscimol (an agonist of the GABA-A receptor) to the dHPC prior to fear conditioning caused impairment in contextual fear memory encoding, highlighting the critical role of hippocampal interneurons in the regulation of fear acquisition (Oh and Han, 2020). Hippocampal interneurons are largely heterogeneous and exhibit distinct morphological, neurochemical, transcriptomic, and physiological properties (Klausberger and Somogyi, 2008; Pelkey et al., 2017; Harris et al., 2018). Specifically, in the hippocampal CA1 area, spike timing of PYRs is primarily regulated by PV+ interneurons that inhibit the perisomatic region of PCs, whereas burst spiking is regulated by SOM+ interneurons that inhibit PC dendrites (Losonczy et al., 2010; Royer et al., 2012). This functional dissociation between CA1 SOM+ and PV+ interneurons suggests that these cells may play distinct mnemonic functions, with SOM+ interneurons being a primary candidate for regulation of associative learning.

To enable activity recordings from genetically defined interneuronal populations in the CA1 during CFC, Lovett-Barron et al. (2014) developed a variation of CFC for head-fixed mice (hf-CFC) that is compatible with two-photon Ca^{2+} imaging. They then established that, following US presentation, SOM+ interneurons (mainly the oriens-lacunosum moleculare (OLM) cells) are excited by cholinergic projections that arrive at the CA1 from the medial septum, which in turn leads to enhanced distal dendritic inhibition onto CA1 PCs and restricts the activation of these cells by foot-shock-evoked excitation (**Figure 2**). Subsequently, the inactivation of SOM+ interneurons during the US hindered the consolidation of contextual fear memory. Another interesting study reported that contextual fear conditioning resulted in the increased density of dendritic spines in SOM+ interneurons (Schmid et al., 2016), revealing structural plasticity that can be important for enhanced recruitment of these cells during fear memory acquisition. In addition, the consolidation of fear memory required activation of the mechanistic target of rapamycin complex-1 (mTORC1) pathway, which so far has been considered a key component in the regulation of protein synthesis and induction of the long-term memory (Tang et al., 2002; Costa-Mattioli et al., 2009). Importantly, interference with mTORC1 pathway in SOM+ interneurons resulted in impaired contextual fear memory (Artinian et al., 2019). Similarly, another recent study revealed that contextual fear conditioning was associated with a reduction in phosphorylation of eIF2α, an important regulatory element for the protein synthesis-dependent LTP in PCs and SOM+ interneurons (Sharma et al., 2020). As a result, the ablation of p-eIF2α in SOM+ cells enhanced fear memory by increasing protein synthesis and lowering the threshold for LTP induction. Moreover, SOM+ interneurons' silencing immediately after the conditioning impaired fear memory (Sharma et al., 2020). Taken together, these studies indicate that encoding and consolidation of contextual fear memory in the CA1 is primarily controlled *via* activation of SOM+ interneurons that regulate burst firing of PCs and induction of long-term plasticity.

The current model furthermore suggests that the memory traces in the hippocampus are represented by a specific subset of PCs that make memory engrams because of enhanced intrinsic and synaptic excitability, which in turn can be actively regulated by specific subsets of inhibitory interneurons (reviewed in Josselyn and Tonegawa, 2020; Topolnik and Tamboli, 2022). For example, a recent tour-de-force study suggested that the non-engram cells are actively excluded from fear memory traces by dendritic inhibition provided by the SOM^+ interneurons (Szőnyi et al., 2019). Moreover, this process can be tightly regulated by GABAergic projection from the brainstem nucleus incertus (NI), which targets specifically SOM+ cells as well as the excitatory inputs from the medial septum

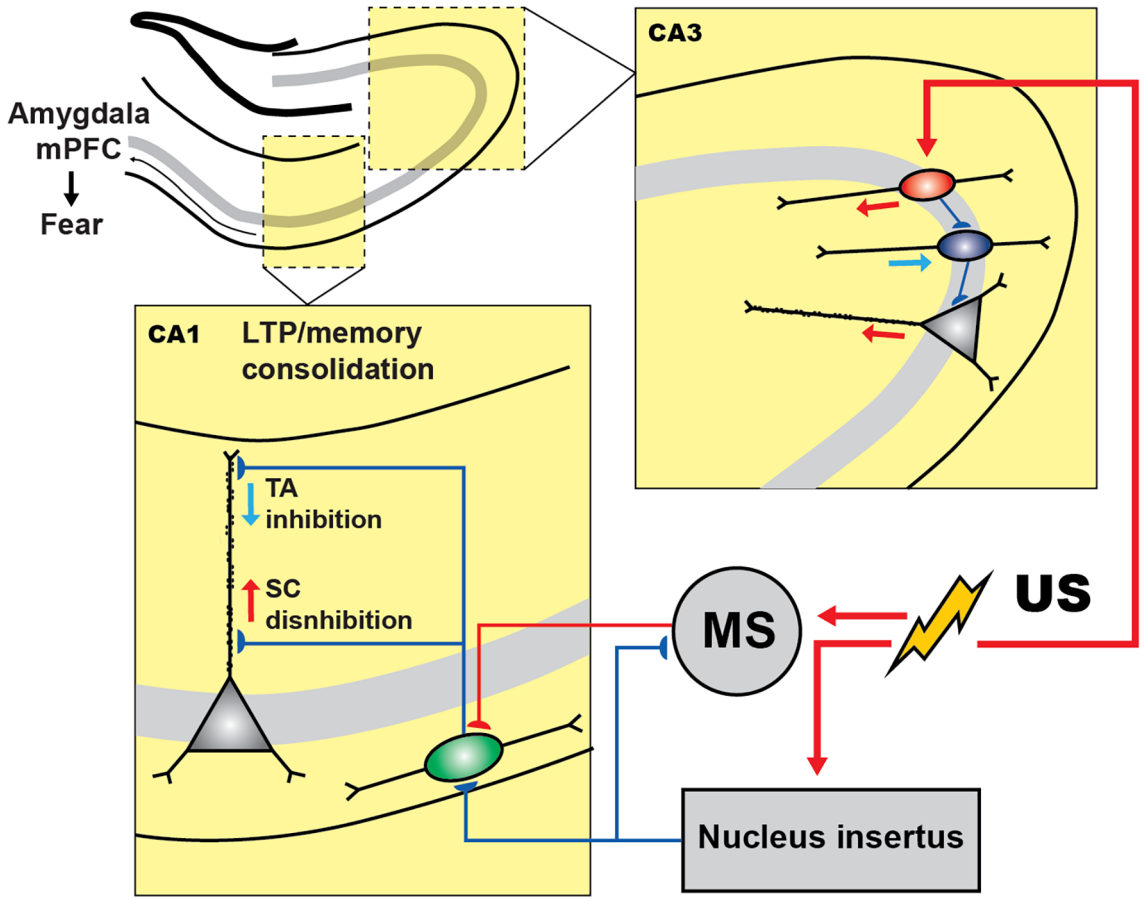

FIGURE 2
Inhibitory and disinhibitory circuit motifs in the hippocampus during fear encoding. In CA3 region of hippocampus shock presentation induces the PC disinhibition *via* inhibiting the PV+ cells (blue) by the activation of VIP+ population (red), which can control the fear expression. In CA1, during CFC, shock presentation resulted in the activation of the medial septum (MS) whose excitatory inputs to SOM+ cells (green) cause the PCs dendritic inhibition. However, the activity of SOM+ and MS are under the control of GABAergic nucleus incertus (NI) input that is also activated by the shock and regulates the fear expression.

converging onto SOM+ cells (Szőnyi et al., 2019). Optogenetic activation of NI GABAergic neurons precisely at the moment of US impaired fear memory formation, whereas optogenetic inhibition during fear conditioning led to enhanced contextual memories, indicating that NI-to-SOM+ interneuron input plays a crucial role in regulating contextual fear memory acquisition.

The role of PV+ cells in contextual fear memory remains controversial, with different results reported depending on the memory induction paradigm and manipulation strategy (Lovett-Barron et al., 2014; Ognjanovski et al., 2017; Artinian et al., 2019; Khlaifia et al., 2022). For example, in a study conducted by Ognjanovski et al. (2017), the role of CA1 PV+ interneurons had been explored during single trial contextual fear memory consolidation using chronic stereotrode recordings of the activity of fast-spiking PV+ cells continuously for 48 h. As a result, they observed increased PV+ spike field coherence along with the principal cells during the first 6 h following CFC. Furthermore, chemogenetic inhibition of PV+ cells reduced fear, indicating that PV+ cells contribute to contextual fear memory consolidation. On the other hand, optogenetic silencing of CA1 PV+ cells during US (Lovett-Barron et al., 2014) or the conditional manipulations with eIF2α or Rptor signaling in CA1 PV+ cells had no effect on contextual fear memory consolidation (Khlaifia et al., 2022). In the CA3 hippocampal region, the activity of PV+ interneurons was required for contextual fear memory consolidation (**Figure 2**; Donato et al., 2013). Whereas the underlying circuit mechanisms are still poorly understood, they likely involved increased plasticity of PV+ interneuron networks. In particular, PV+ interneurons have been found in different states, depending on their level of activity (Donato et al., 2013). A low-PV network configuration has been associated with enhanced synaptic plasticity, memory consolidation, and retrieval, whereas a high-PV network configuration resulted in the impairment of these functions. Interestingly, the switch to a low-PV network configuration was associated with an increased innervation of PV+ interneurons by VIP+ cells. These findings reveal an important role of local circuit disinhibition in memory consolidation, and a network plasticity mechanism that involves VIP–PV microcircuit reconfiguration to control the functional state of PV+ interneurons during fear memory consolidation (**Figure 2**). Nonetheless, the so far controversial findings regarding the role of hippocampal PV+ interneurons in fear memory require further detailed examination using temporally precise manipulations at different stages of fear memory acquisition.

The hippocampal DG is another critical region in fear memory formation and consolidation (Kheirbek et al., 2013; Pierson et al., 2015). The early immediate gene c-Fos has been widely used for the evaluation of neuronal activity in this region owing to its transient and rapid upregulation upon experience (Smeyne et al., 1992; Reijmers et al., 2007). cFos expression in granule cells (GCs) was induced by the exploration of a new environment (Liu et al., 2012; Deng et al., 2013). It appears that exploration can be associated with the formation of an active neuronal ensemble that becomes both necessary and sufficient for representing the context mnemonically, and can be considered the cellular engram (Ramirez et al., 2013; Denny et al., 2014). Furthermore, contextual memory can be retrieved by reactivating the cFos-expressing neuronal ensembles in the fear conditioning paradigm (Tayler et al., 2013). The fear memory has been largely assigned to excitatory neurons and was associated with the activation of the CREB transcription factor, which modulates cellular excitability, ultimately determining memory allocation (Han et al., 2007; Stefanelli et al., 2016). Whereas the selection of neuronal ensembles appears to be governed by the cell autonomous mechanisms (Rogerson et al., 2014), local circuit mechanisms may also contribute to the formation of cellular engrams. Indeed, pharmacogenetic inactivation of DG SOM+ interneurons caused impairment in the acquisition of fear memory by forcing the recruitment of GCs (Stefanelli et al., 2016).

In addition to PV+ and SOM+ interneurons, VIP+ cells that engage in both inhibitory and disinhibitory circuit motifs in the hippocampus may be involved in fear memory control by regulating a balance between inhibition and disinhibition. These cells have been broadly categorized onto VIP+ basket cells (VIP-BCs) and VIP+ cells that inhibit other interneurons and are therefore considered as VIP+ interneuron-specific (IS) cells (Acsády et al., 1996; Chamberland et al., 2010; Tyan et al., 2014; Francavilla et al., 2018; Kullander and Topolnik, 2021). In the CA1 area, VIP-BCs co-express CCK and contact the somata of PCs, thus providing local inhibition. The CCK-BCs also contact PV+ BCs (Karson et al., 2009; Dudok et al., 2021), which may result in the disinhibition of PCs; thus, VIP-BCs may play a dual function. In contrast with VIP-BCs, other VIP+ interneurons may specialize in targeting only inhibitory interneurons, thus resulting in PC disinhibition (Acsády et al., 1996; Tyan et al., 2014; Francavilla et al., 2018); although, the connectivity motifs of different VIP+ subtypes remain to be established. In the CA1 hippocampal area, VIP+ IS interneurons can be further subdivided into three subtypes: type 2 IS cells (VIP-IS2), type 3 IS cells (VIP-IS3), and long-range projecting VIP+ cells (VIP-LRP; Acsády et al., 1996; Tyan et al., 2014; Francavilla et al., 2018). VIP-IS2 cells have somata located at the stratum radiatum/lacunosum moleculare border and form synapses with interneurons located within the stratum radiatum, including calbindin-positive and VIP+ cells (Acsády et al., 1996). In turn, VIP-IS3 cells co-express calretinin and have soma located in the stratum pyramidale or radiatum; moreover, they target interneurons located within the stratum oriens/alveus, mostly the SOM+ OLM cells that provide distal dendritic inhibition to PCs (Acsády et al., 1996; Tyan et al., 2014; Luo et al., 2020). VIP-LRP cells, as suggested by their name, can project from the CA1 region of the hippocampus to more distant areas, such as the subiculum (Francavilla et al., 2018). These cells can express the muscarinic receptor 2, calretinin, and enkephalin, and by their activity patterns *in vivo* correspond to theta-off cells, as they exhibit reduced firing during theta-run episodes but show increased activity during immobility (Francavilla et al., 2018; Luo et al., 2019). By employing the paired patch-clamp recording technique, it was observed that VIP-LRP cells do not contact the CA1 PCs and prefer different types of interneurons. The local preferential targets of VIP-LRP are the OLM cells, whereas in the subiculum, they establish contacts with interneurons as well as PCs, suggesting a region-specific function (Francavilla et al., 2018). As a population, VIP+ interneurons have been instrumental in regulating the goal-directed spatial learning (Turi et al., 2019). Furthermore, due to the expression of the alpha5 $GABA_A$ receptor subunit at the IS3–OLM synapses, IS3 cells have been shown to control anxiety (Magnin et al., 2019). However, the functional role of VIP+ interneurons during fear learning remains to be determined.

Animal studies: PFC and other neocortical regions

In addition to the amygdala and hippocampus, the PFC is critically involved in fear learning and extinction. It has been reported that the dorsal PFC supports fear expression, whereas the ventral PFC mediates fear extinction in both animal and human studies (Quirk et al., 2006; Sierra-Mercado et al., 2011; Milad and Quirk, 2012; Riga et al., 2014; Singh et al., 2018). Furthermore, the mPFC lesions revealed a significant role of this area in the extinction of cued fear memory (Morgan et al., 1993), which was further supported by pharmacological studies that assessed the roles of the PL-PFC vs. that of the IL-PFC. As such, the infusion of tetrodotoxin (Na^+ channel blocker) and muscimol selectively into the PL-PFC followed by fear conditioning reduced both the cued and contextual fear expression (Laurent and Westbrook, 2009; Sierra-Mercado et al., 2011). Furthermore, electrical stimulation of the IL-PFC paired with a conditioned tone resulted in a decreased level of freezing, suggesting a role for the IL-PFC in fear extinction, in contrast with the PL-PFC, which promotes fear expression (Milad and Quirk, 2002; Milad et al., 2004). Taken together, these data highlight the region-specific roles of the PL-PFC and IL-PFC in fear learning and extinction.

The primary auditory cortex (A1) is also involved in fear learning. The role of this region has been studied using the local administration of muscimol prior to fear conditioning, which resulted in a decrease in the fear-conditioned response (Banerjee et al., 2017). Single-unit recordings together with optogenetic and pharmacological manipulations in A1 revealed an important role of a disinhibitory circuit motif for associative learning (Letzkus et al., 2011). In this case, the aversive stimulus (US) activated the inhibitory interneurons located in layer 1 (L1) *via* cholinergic projections emerging from the basal forebrain region. As L1 interneurons inhibit PV+ basket cells, the US resulted in disinhibition of the layer 2/3 (L2/3) PCs, thus highlighting the circuit disinhibition as an important mechanism in associative learning (**Figure 3**; Letzkus et al., 2011). Across cortical regions, PV+ interneurons provide a powerful perisomatic inhibition to PCs (Pfeffer et al., 2013; Lee et al., 2014). Specifically, electrophysiological recordings in brain slices have revealed that PV+ interneurons located in the mPFC mediate

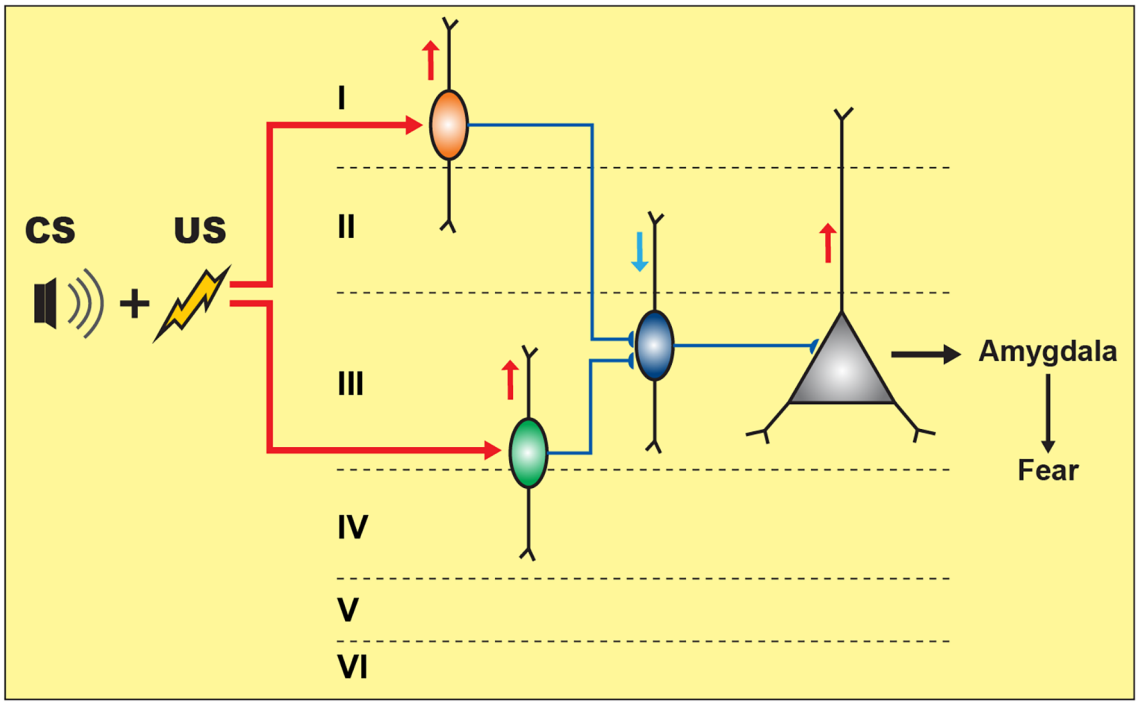

FIGURE 3
Inhibitory and disinhibitory circuit motifs in neocortical regions support fear memory formation. In the auditory cortex (A1), CS-US pairing elicits fear memory encoding by activating the L1 inhibitory neuronal population (orange) that can cause the disinhibition of L2/3 PCs by restricting the PV+ cell (blue) perisomatic inhibitory input onto the PCs, resulting in fear response expression. In the mPFC, CS-US association activates the SOM+ cells (green) that cause the disinhibition of PCs by inhibiting the PV+ cells' activity, resulting in fear expression.

feed-forward inhibition, which is crucial for maintaining the cortical excitation/inhibition balance (Lee et al., 2014). Moreover, the firing output of some PFC PV+ interneurons has been phase-locked to gamma oscillations (Kim et al., 2016). In addition, these cells regulate different types of cognitive behaviors and are affected by anxiety, panic attack, and depression (Sauer et al., 2015; Kim et al., 2016; Sauer and Bartos, 2022).

SOM+ interneurons provide inhibition to the apical dendrites of the L2/3 and layer 5 (L5) PCs. This population comprises Martinotti and non-Martinotti cell types that are distributed in layer 2 to layer 6 (Tremblay et al., 2016). The SOM+ interneurons with somata located within layer 4 (L4) and L5 receive input from thalamic projections (Naka and Adesnik, 2016). Interestingly, L2/3, L4, and L5 SOM+ interneurons receive complementary synaptic inputs to regulate the balance between top-down and bottom-up inputs (Naka et al., 2019). In the visual cortex, stimulation of a single L2/3 PC can trigger the activation of about 30% of SOM+ interneurons (Kwan and Dan, 2012). In the mouse barrel cortex, synaptic tracing using the rabies virus has demonstrated the cholinergic innervation of SOM+ cells, with presynaptic projection neurons located within the nucleus basalis of Meynert (Wall et al., 2016). In addition to neighboring PCs, SOM+ interneurons also receive input from distant brain areas (reviewed in Riedemann, 2019). The L5 non-Martinotti SOM+ cells do not inhibit L2/3 or L5 PCs; rather, they seem to contact L4 PCs (Riedemann, 2019). In addition, SOM+ cells can target VIP+ and PV+ interneurons (Pfeffer et al., 2013; Pi et al., 2013; Sohn et al., 2016). Moreover, although PCs are the primary postsynaptic target of superficial and infragranular SOM+ cells, fast-spiking interneurons are the main targets of L4 SOM+ cells (Xu et al., 2013).

In relation to fear learning, unfortunately, the roles of different types of neocortical interneurons remain largely unexplored. In L2/3 mPFC, the CS-US pairing resulted in increased spontaneous excitatory postsynaptic currents (sEPSCs) in SOM+ cells, rather than in PV+ interneurons (Cummings and Clem, 2020). These data echo the increased spine density in hippocampal CA1 SOM+ interneurons following CFC, suggesting that structural and functional plasticity of excitatory inputs to SOM+ cells may be a common sequel of fear conditioning across cortical regions. Furthermore, optogenetic activation of prefrontal SOM+ cells *in vivo* resulted in an increased freezing response. Surprisingly, in contrast to the amygdala and the hippocampus, combined optogenetic manipulations and electrophysiological recordings in brain slices revealed that prefrontal SOM+ interneurons cause disinhibition of PCs by eliciting the inhibition of PV+ interneurons (**Figure 3**; Cummings and Clem, 2020). Collectively, these data highlight a region-specific role of SOM+ interneurons.

Furthermore, the IL-PFC was involved in the suppression of fear memory *via* their excitatory projection to the BLA and GABAergic ITC clusters, which can limit the activation of the CeM output (Milad and Quirk, 2002). Moreover, the inhibitory effect of vHPC on IL-PFC PCs played a crucial role in the re-occurrence of extinguished fear. As such, activation of the vHPC projections to the IL-PFC could recruit IL-PFC PV+ interneurons and cause a

relapse of extinguished fear (Marek et al., 2018). The inactivation of either the vHPC or BLA after fear learning was associated with an increase or a decrease in the firing of selective PL-PFC neurons (PCs or interneurons; Sotres-Bayon et al., 2012). The PCs exhibited a low firing rate after the inactivation of the BLA, suggesting that the BLA provides excitatory input to the PL-PFC, whereas vHPC inactivation resulted in a decreased firing rate in interneurons, indicating that the vHPC activates local interneurons to inhibit the firing of PL-PFC PCs *via* feed-forward inhibition (Sotres-Bayon et al., 2012). Thus, it can be concluded that during fear learning the vHPC gates the BLA input *via* PL-PFC PV+ interneurons (Sotres-Bayon et al., 2012).

Finally, during fear learning, the US can activate frontal VIP+ cells, thereby promoting the disinhibition of PCs necessary to facilitate the processing of the noxious signals. In this scenario, the US presentation can limit the activation of PV+ and SOM+ interneurons *via* selective recruitment of the VIP+ cells, therefore resulting in the perisomatic and dendritic disinhibition of PCs (Lee et al., 2013; Pi et al., 2013; but see Garcia-Junco-Clemente et al., 2017 for direct inhibition of PCs exerted by VIP+ cells during arousal in addition to disinhibition, which results in push-pull frontal circuit). Given that SOM+ cells are the primary targets of VIP+ interneurons in the neocortex, the resulting dendritic disinhibition of PCs during US is likely a dominating mechanism operating in cortical circuits during associative fear learning (Lee et al., 2013; Pfeffer et al., 2013; Pi et al., 2013). Furthermore, given the SOM-to-PV connectivity motif, the VIP+ input to SOM+ interneurons may also result in disinhibition of PV+ cells and gradual recovery of perysomatic inhibition of PCs during fear conditioning. Therefore, prefrontal VIP+ interneurons are well positioned to control the timing of perisomatic inhibition and dendritic disinhibition, which may be necessary for induction of associative plasticity but also for synchronous firing and cell assignment into functional ensembles.

Conclusion and future perspectives

Although the data available thus far provide important insights regarding the structure and function of the neuronal circuits involved in fear memory, our understanding of how behavioral learning is implemented at the network level remains still limited. Several points need to be addressed to understand the mechanisms that contribute to the formation and regulation of fear circuitry. In particular, the extinction of fear memory that involves both the erasure and extinction-induced inhibition within fear circuits and allows to regulate the stability of fear memories (Herry et al., 2008) requires further investigation. How this phenomenon depends on the timing of extinction training, animal age, and sex, and specific connectivity motifs within threat circuitry still needs to be understood. Considering extinction as an important instrument in PTSD therapy (Milad and Quirk, 2012), it would be critical to explore further in human studies how the observed changes in structure and function of fear circuits affect the extinction paradigm. Likewise, in the animal models, it needs to be determined how the reduction in the volume of the amygdala, hippocampus, and PFC associated with PTSD correlates with functional deficits within specific neuronal populations that are involved in fear extinction, and how their function can be rescued in order to implement the efficient extinction paradigm in affected individuals.

In this regard, over the last few decades, the field has moved to exploring the contributions of different neuronal populations to animal behavior, thanks to rapidly developing gene targeting technologies. An increasing number of studies have investigated the functional role of inhibitory interneurons in different memory paradigms thereby revealing that interneurons are important players in diverse learning tasks. In relation to fear learning, these cells not only shaped the circuit response during fear conditioning but also showed changes in their properties during fear consolidation. Therefore, across different fear circuits, the network function appears to be tightly regulated *via* inhibitory circuit mechanisms. The PV+, SOM+ and VIP+ interneurons in the amygdala received more attention than in the other fear circuits. In BLA, perisomatic inhibition provided to PCs by the PV+ cells, and likely VIP-BCs (Rhomberg et al., 2018), during CS is followed by disinhibition during US because of VIP+ to PV+, and SOM+ connections (Wolff et al., 2014; Krabbe et al., 2019). Manipulating with these cell types impairs fear learning, indicating that they are all important for tight regulation of PC activity and induction of associative plasticity and memory to shape the amygdala fear response. Much less is known regarding the role of PV+ and VIP+ cells in the hippocampus, in particular in relation to CFC and extinction paradigms. Besides this, the role of these cell types in the prefrontal areas in fear learning, and most importantly in fear extinction, also needs to be discovered to have a complete understanding of the inhibitory components of the circuitry responsible for processing and regulation of fear memory.

Circuit disinhibition has recently emerged as an important mechanism that participates widely in memory-related paradigms by limiting the firing of the GABAergic interneuronal populations and providing additional ways for the modulation of network activity. Disinhibition phenomenon appears to be critical in fear conditioning and related long-term changes that take place in different neural circuits (Letzkus et al., 2011). So far, distinct behavioral phenomena, such as auditory fear conditioning and spatial navigation, were causally linked to disinhibition in different compartments of PCs in several cortical and limbic areas, and at time scales ranging from milliseconds to days (Sparta et al., 2014; Kim et al., 2016; Cummings and Clem, 2020; Dudok et al., 2021), suggesting that disinhibition is a conserved circuit mechanism that is required for learning and memory to occur. However, further studies are necessary to determine whether similar disinhibitory patterns exist in different circuits. In addition, abnormal disinhibition may impair memory performance and result in disruptive consequences (McGarrity et al., 2017).

In summary, a working model of fear learning can be proposed in which traumatic events recruit specific interneuronal populations that control PCs and other interneurons to create the representative PC ensembles, or memory engrams, *via* the phenomena of inhibition and disinhibition, respectively. As such, whereas some PCs are excluded from memory engrams because of active inhibition, the others become linked to engrams because of increased intrinsic and synaptic excitability facilitated by disinhibition. The changes in inhibitory connections can also shift the network balance, thus altering the coding of the fear experience.

Therefore, inhibitory neuronal populations responsible for local circuit inhibition and disinhibition are currently considered as a powerful component in the creation of mental fear representations. Further studies are required to establish the role of specific inhibitory and disinhibitory patterns in complex fear-related behavioral adaptations and a direct link between a stressful event and the functional plasticity of specific circuit elements.

Author contributions

SS wrote the first version of the manuscript and prepared the figures. LT prepared the final version of the manuscript. All authors contributed to the article and approved the submitted version.

Funding

SS was supported by the Canadian Institutes of Health Research and the Natural Sciences and Engineering Research Council of Canada Grants to LT.

Acknowledgments

We thank Dimitry Topolnik for help with figure preparation and Suhel Tamboli for comments on the manuscript.

Conflict of interest

The authors declare that the research was conducted in the absence of any commercial or financial relationships that could be construed as a potential conflict of interest.

Publisher's note

References

Acsády, L., Arabadzisz, D., and Freund, T. F. (1996). Correlated morphological and neurochemical features identify different subsets of vasoactive intestinal polypeptide-immunoreactive interneurons in rat hippocampus. *Neuroscience* 73, 299–315. doi: 10.1016/0306-4522(95)00610-9

Agren, T., Engman, J., Frick, A., Björkstrand, J., Larsson, E., Furmark, T., et al. (2012). Disruption of reconsolidation erases a fear memory trace in the human amygdala. *Science* 337, 1550–1552. doi: 10.1126/science.1223006

Ahmed, O. J., and Mehta, M. R. (2009). The hippocampal rate code: anatomy, physiology and theory. *Trends Neurosci.* 32:329. doi: 10.1016/j.tins.2009.01.009

Anderson, M. C., and Floresco, S. B. (2021). Prefrontal-hippocampal interactions supporting the extinction of emotional memories: the retrieval stopping model. *Neuropsychopharmacology* 47, 180–195. doi: 10.1038/s41386-021-01131-1

Artinian, J., Jordan, A., Khlaifia, A., Honore, E., Fontaine, A. L., Racine, A. S., et al. (2019). Regulation of hippocampal memory by mTORC1 in somatostatin interneurons. *J. Neurosci.* 39, 8439–8456. doi: 10.1523/JNEUROSCI.0728-19.2019

Ascoli, G. A., Alonso-Nanclares, L., Anderson, S. A., Barrionuevo, G., Benavides-Piccione, R., Burkhalter, A., et al. (2008). Petilla terminology: nomenclature of features of GABAergic interneurons of the cerebral cortex. *Nat. Rev. Neurosci.* 9, 557–568. doi: 10.1038/nrn2402

Atkins, C. M., Selcher, J. C., Petraitis, J. J., Trzaskos, J. M., and Sweatt, J. D. (1998). The MAPK cascade is required for mammalian associative learning. *Nat. Neurosci.* 17, 602–609. doi: 10.1038/2836

Bach, D. R., Weiskopf, N., and & Dolan, R. J. (2011). A stable sparse fear memory trace in human amygdala. *J. Neurosci.* 31, 9383–9389. doi: 10.1523/JNEUROSCI.1524-11.2011

Banerjee, S. B., Gutzeit, V. A., Baman, J., Aoued, H. S., Doshi, N. K., Liu, R. C., et al. (2017). Perineuronal nets in the adult sensory cortex are necessary for fear learning. *Neuron* 95, 169–179.e3. doi: 10.1016/J.NEURON.2017.06.007

Battaglia, S., Garofalo, S., di Pellegrino, G., and Starita, F. (2020). Revaluing the role of vmPFC in the acquisition of Pavlovian threat conditioning in humans. *J. Neurosci.* 40, 8491–8500. doi: 10.1523/JNEUROSCI.0304-20.2020

Bechara, A., Tranel, D., Damasio, H., Adolphs, R., Rockland, C., and Damasio, A. R. (1995). Double dissociation of conditioning and declarative knowledge relative to the amygdala and hippocampus in humans. *Science* 269, 1115–1118. doi: 10.1126/science.7652558

Bienvenu, T. C. M., Busti, D., Magill, P. J., Ferraguti, F., and Capogna, M. (2012). Cell-type-specific recruitment of amygdala interneurons to hippocampal theta rhythm and noxious stimuli in vivo. *Neuron* 74, 1059–1074. doi: 10.1016/j.neuron.2012.04.022

Björkstrand, J., Agren, T., Frick, A., Engman, J., Larsson, E-M., Furmark, T., et al. (2015). Disruption of memory reconsolidation erases a fear memory trace in the human amygdala: an 18-month follow-up. *PLoS One* 10:e0129393. doi: 10.1371/journal.pone.0129393

Bocchio, M., Fucsina, G., Oikonomidis, L., McHugh, S. B., Bannerman, D. M., Sharp, T., et al. (2015). Increased serotonin transporter expression reduces fear and recruitment of parvalbumin interneurons of the amygdala. *Neuropsychopharmacology* 40, 3015–3026. doi: 10.1038/npp.2015.157

Borgomaneri, S., Battaglia, S., Garofalo, S., Tortora, F., Avenanti, A., and di Pellegrino, G. (2020). State-dependent TMS over prefrontal cortex disrupts fear-memory reconsolidation and prevents the return of fear. *Curr. Biol.* 30, 3672–3679.e4. doi: 10.1016/j.cub.2020.06.091

Bremner, J. D. (2006). Traumatic stress: effects on the brain. *Dialogues Clin. Neurosci.* 8, 445–461. doi: 10.31887/DCNS.2006.8.4/jbremner

Capogna, M. (2014). GABAergic cell type diversity in the basolateral amygdala. *Curr. Opin. Neurobiol.* 26, 110–116. doi: 10.1016/j.conb.2014.01.006

Chamberland, S., Salesse, C., Topolnik, D., and Topolnik, L. (2010). Synapse-specific inhibitory control of hippocampal feedback inhibitory circuit. *Front. Cell Neurosci.* 4:130. doi: 10.3389/fncel.2010.00130

Chhatwal, J. P., Myers, K. M., Ressler, K. J., and Davis, M. (2005). Regulation of gephyrin and GABAA receptor binding within the amygdala after fear acquisition and extinction. *J. Neurosci.* 25, 502–506. doi: 10.1523/JNEUROSCI.3301-04.2005

Ciocchi, S., Herry, C., Grenier, F., Wolff, S. B. E., Letzkus, J. J., Vlachos, I., et al. (2010). Encoding of conditioned fear in central amygdala inhibitory circuits. *Nature* 468, 277–282. doi: 10.1038/nature09559

Costa-Mattioli, M., Sossin, W. S., Klann, E., and Sonenberg, N. (2009). Translational control of long-lasting synaptic plasticity and memory. *Neuron* 61, 10–26. doi: 10.1016/j.neuron.2008.10.055

Cummings, K. A., and Clem, R. L. (2020). Prefrontal somatostatin interneurons encode fear memory. *Nat. Neurosci.* 23, 61–74. doi: 10.1038/s41593-019-0552-7

Curzon, P., Rustay, N. R., and Browman, K. E. (2009). Cued and contextual fear conditioning for rodents. *Nat. Neurosci.* doi: 10.1201/noe1420052343.ch2

Dejean, C., Courtin, J., Rozeske, R. R., Bonnet, M. C., Dousset, V., Michelet, T., et al. (2015). Neuronal circuits for fear expression and recovery: recent advances and potential therapeutic strategies. *Biol. Psychiatry* 78, 298–306. doi: 10.1016/j.biopsych.2015.03.017

Deng, W., Mayford, M., and Gage, F. H. (2013). Selection of distinct populations of dentate granule cells in response to inputs as a mechanism for pattern separation in mice. *eLife* 2:e00312. doi: 10.7554/eLife.00312

Denny, C. A., Kheirbek, M. A., Alba, E. L., Tanaka, K. F., Brachman, R. A., Laughman, K. B., et al. (2014). Hippocampal memory traces are differentially

modulated by experience, time and adult neurogenesis. *Neuron* 83, 189–201. doi: 10.1016/j.neuron.2014.05.018

Donato, F., Rompani, S. B., and Caroni, P. (2013). Parvalbumin-expressing basket-cell network plasticity induced by experience regulates adult learning. *Nature* 504, 272–276. doi: 10.1038/nature12866

Dudok, B., Klein, P. M., Hwaun, E., Lee, B. R., Yao, Z., Fong, O., et al. (2021). Alternating sources of perisomatic inhibition during behavior. *Neuron* 17, 997–1012e9. doi: 10.1016/j.neuron.2021.01.003

Duvarci, S., Popa, D., and Paré, D. (2011). Central amygdala activity during fear conditioning. *J. Neurosci.* 31, 289–294. doi: 10.1523/JNEUROSCI.4985-10.2011

Etkin, A., and Wager, T. D. (2007). Functional neuroimaging of anxiety: a meta-ana lysis of emotional processing in PTSD, social anxiety disorder and specific phobia. *Am. J. Psychiatry* 164, 1476–1488. doi: 10.1176/appi.ajp.2007.07030504

Fanselow, M. S. (1986). Associative vs. topographical accounts of the immediate shock-freezing deficit in rats: implications for the response selection rules governing species-specific defensive reactions. *Learn. Motiv.* 17, 16–39.

Fanselow, M. S., and Poulos, A. M. (2004). The neuroscience of mammalian associative learning. *Annu. Rev. Psychol.* 56, 207–234. doi: 10.1146/annurev.psych.56.091103.070213

Fanselow, M. S., and Dong, H. W. (2010). Are the dorsal and ventral hippocampus functionally distinct structures? *Neuron* 65, 7–19. doi: 10.1016/j.neuron.2009.11.031

Fanselow, M. S., DeCola, J. P., and Young, S. L. (1993). Mechanisms responsible for reduced contextual conditioning with massed unsignaled unconditional stimuli. *J. Exp. Psychol. Anim. Behav. Process.* 19, 121–137.

Feng, P., Feng, T., Chen, Z., and Lei, X. (2014). Memory consolidation of fear conditioning: Bi-stable amygdala connectivity with dorsal anterior cingulate and medial prefrontal cortex. *Soc. Cogn. Affect. Neurosci.* 9, 1730–1737. doi: 10.1093/scan/nst170

Ford, J. D., and Courtois, C. A. (2014). Complex PTSD, affect dysregulation and borderline personality disorder. *Borderline Personal. Disord. Emot. Dysregulat.* 1:9. doi: 10.1186/2051-6673-1-9

Forster, G. L., Simons, R. M., and Baugh, L. A. (2017). "Revisiting the role of the amygdala in posttraumatic stress disorder," in *Amygdala. Where Emotions Shape Perception, Learning and Memories*, Ed. B. Ferry (InTechOpen). doi: 10.5772/67585

Francavilla, R., Villette, V., Luo, X., Chamberland, S., Muñoz-Pino, E., Camiré, O., et al. (2018). Connectivity and network state-dependent recruitment of long-range VIP-GABAergic neurons in the mouse hippocampus. *Nat. Commun.* 9:5043. doi: 10.1038/s41467-018-07162-5

Franke, L. K., Rattel, J. A., Miedl, S. F., Danböck, S. K., Bürkner, P. C., and Wilhelm, F. H. (2021). Intrusive memories as conditioned responses to trauma cues: an empirically supported concept? *Behav. Res. Ther.* 143:103848. doi: 10.1016/j.brat.2021.103848

Frick, A., Björkstrand, J., Lubberink, M., Eriksson, A., Fredrikson, M., and Åhs, F. (2021). Dopamine and fear memory formation in the human amygdala. *Mol. Psychiatry* 273, 1704–1711. doi: 10.1038/s41380-021-01400-x

Fullana, M. A., Harrison, B. J., Soriano-Mas, C., Vervliet, B., Cardoner, N., àvila-Parcet, A., et al. (2016). Neural signatures of human fear conditioning: an updated and extended meta-analysis of fMRI studies. *Mol. Psychiatry* 21, 500–508. doi: 10.1038/mp.2015.88

Garcia-Junco-Clemente, P., Ikrar, T., Tring, E., Xu, X., Ringach, D. L., and Trachtenberg, J. T. (2017). An inhibitory pull-push circuit in frontal cortex. *Nat. Neurosci.* 20, 389–392. doi: 10.1038/nn.4483

Golding, N. L., Staff, N. P., and Spruston, N. (2002). Dendritic spikes as a mechanism for cooperative long-term potentiation. *Nature* 418, 326–331. doi: 10.1038/nature00854

Greco, J. A., and Liberzon, I. (2016). Neuroimaging of fear-associated learning. *Neuropsychopharmacology* 41, 320–334. doi: 10.1038/npp.2015.255

Hagihara, K. M., Bukalo, O., Zeller, M., Aksoy-Aksel, A., Karalis, N., Limoges, A., et al. (2021). Intercalated amygdala clusters orchestrate a switch in fear state. *Nature* 594, 403–407. doi: 10.1038/s41586-021-03593-1

Hajos, N. (2021). Interneuron types and their circuits in the basolateral amygdala. *Front. Neural Circuits* 15:687257. doi: 10.3389/fncir.2021.687257

Han, J. H., Kushner, S. A., Yiu, A. P., Cole, C. J., Matynia, A., Brown, R. A., et al. (2007). Neuronal competition and selection during memory formation. *Science* 316, 457–460. doi: 10.1126/science.1139438

Harris, K. D., Hirase, H., Leinekugel, X., Henze, D. A., and Buzsáki, G. (2001). Temporal interaction between single spikes and complex spike bursts in hippocampal pyramidal cells. *Neuron* 32, 141–149. doi: 10.1126/science.1139438

Harris, K. D., Hochgerner, H., Skene, N. G., Magno, L., Katona, L., Bengtsson Gonzales, C., et al. (2018). Classes and continua of hippocampal CA1 inhibitory neurons revealed by single-cell transcriptomics. *PLoS Biol.* 16:e2006387. doi: 10.1371/journal.pbio.2006387

Hayes, J. P., LaBar, K. S., McCarthy, G., Selgrade, E., Nasser, J., Dolcos, F., et al. (2011). Reduced hippocampal and amygdala activity predicts memory distortions for trauma reminders in combat-related PTSD. *J. Psychiatr. Res.* 45, 600–609. doi: 10.1016/j.jpsychires.2010.10.007

Heldt, S. A., and Ressler, K. J. (2007). Training-induced changes in the expression of GABAA-associated genes in the amygdala after the acquisition and extinction of Pavlovian fear. *Eur. J. Neurosci.* 26, 3631–3644. doi: 10.1111/j.1460-9568.2007.05970.x

Herry, C., Ciocchi, S., Senn, V., Demmou, L., Müller, C., and Lüthi, A. (2008). Switching on and off fear by distinct neuronal circuits. *Nature* 454, 600–606. doi: 10.1038/nature07166

Jones, M. W., and Wilson, M. A. (2005). Theta rhythms coordinate hippocampal-prefrontal interactions in a spatial memory task. *PLoS Biol.* 3:e402. doi: 10.1371/journal.pbio.0030402

Josselyn, S. A., and Tonegawa, S. (2020). Memory engrams: recalling the past and imagining the future. *Science* 367:eaaw4325. doi: 10.1126/science.aaw4325

Karson, M. A., Tang, A. H., Milner, T. A., and Alger, B. E. (2009). Synaptic cross talk between perisomatic-targeting interneuron classes expressing cholecystokinin and parvalbumin in hippocampus. *J. Neurosci.* 29, 4140–4154. doi: 10.1523/JNEUROSCI.5264-08.2009

Kepecs, A., and Fishell, G. (2014). Interneuron cell types are fit to function. *Nature* 505, 318–326. doi: 10.1038/nature12983

Kesner, R. P. (2007). Behavioral functions of the CA3 subregion of the hippocampus. *Learn. Mem.* 14, 771–781. doi: 10.1101/lm.688207

Kheirbek, M. A., Drew, L. J., Burghardt, N. S., Costantini, D. O., Tannenholz, L., Ahmari, S. E., et al. (2013). Differential control of learning and anxiety along the dorsoventral axis of the dentate gyrus. *Neuron* 77, 955–968. doi: 10.1016/j.neuron.2012.12.038

Khlaifia, A., Honoré, E., Artinian, J., Laplante, I., and Lacaille, J. C. (2022). mTORC1 function in hippocampal parvalbumin interneurons: regulation of firing and long-term potentiation of intrinsic excitability but not long-term contextual fear memory and context discrimination. *Mol. Brain* 15:56. doi: 10.1186/s13041-022-00941-8

Kim, H., Ährlund-Richter, S., Wang, X., Deisseroth, K., and Carlén, M. (2016). Prefrontal parvalbumin neurons in control of attention. *Cell* 164, 208–218. doi: 10.1016/j.cell.2015.11.038

Kim, W., and Bin, J. H. (2020). Encoding of contextual fear memory in hippocampal-amygdala circuit. *Nat. Commun.* 11:1382. doi: 10.1038/s41467-020-15121-2

Kim, J. J., and Fanselow, M. S. (1992). Modality-specific retrograde amnesia of fear. *Science* 256, 675–677. doi: 10.1126/science.1585183

Kim, D., Pare, D., and Nair, S. S. (2013). Assignment of model amygdala neurons to the fear memory trace depends on competitive synaptic interactions. *J. Neurosci.* 33, 14354–14358. doi: 10.1523/JNEUROSCI.2430-13.2013

Kitayama, N., Vaccarino, V., Kutner, M., Weiss, P., and Bremner, J. D. (2005). Magnetic resonance imaging (MRI) measurement of hippocampal volume in posttraumatic stress disorder: a meta-analysis. *J. Affect. Disord.* 88, 79–86. doi: 10.1016/j.jad.2005.05.014

Klausberger, T., and Somogyi, P. (2008). Neuronal diversity and temporal dynamics: the unity of hippocampal circuit operations. *Science* 321, 53–57. doi: 10.1126/science.1149381

Koenigs, M., Huey, E. D., Raymont, V., Cheon, B., Solomon, J., Wassermann, E. M., et al. (2008). Focal brain damage protects against post-traumatic stress disorder in combat veterans. *Nat. Neurosci.* 11, 232–237. doi: 10.1038/nn2032

Konorski, J. (1948). *Conditioned Reflexes and Neuron Organization*. Cambridge: Cambridge University Press

Konorski, J. (1967). *Integrative Activity of the Brain; An Interdisciplinary Approach*. Chicago: University of Chicago Press

Krabbe, S., Paradiso, E., d'Aquin, S., Bitterman, Y., Courtin, J., Xu, C., et al. (2019). Adaptive disinhibitory gating by VIP interneurons permits associative learning. *Nat. Neurosci.* 22, 1834–1843. doi: 10.1038/s41593-019-0508-y

Kredlow, A. M., Fenster, R. J., Laurent, E. S., Ressler, K. J., and Phelps, E. A. (2021). Prefrontal cortex, amygdala and threat processing: implications for PTSD. *Neuropsychopharmacology* 47, 247–259. doi: 10.1038/s41386-021-01155-7

Kullander, K., and Topolnik, L. (2021). Cortical disinhibitory circuits: cell types, connectivity and function. *Trends Neurosci.* 44, 643–657. doi: 10.1016/j.tins.2021.04.009

Kwan, A. C., and Dan, Y. (2012). Dissection of cortical microcircuits by single-neuron stimulation in vivo. *Curr. Biol.* 22, 1459–1467. doi: 10.1016/j.cub.2012.06.007

LaBar, K. S., Gatenby, J. C., Gore, J. C., LeDoux, J. E., and Phelps, E. A. (1998). Human amygdala activation during conditioned fear acquisition and extinction: a mixed-trial fMRI study. *Neuron* 20, 937–945. doi: 10.1016/s0896-6273(00)80475-4

LaBar, K. S., LeDoux, J. E., Spencer, D. D., and Phelps, E. A. (1995). Impaired fear conditioning following unilateral temporal lobectomy in humans. *J. Neurosci.* 15, 6846–6855. doi: 10.1523/JNEUROSCI.15-10-06846.1995

Laurent, V., and Westbrook, R. F. (2009). Inactivation of the infralimbic but not the prelimbic cortex impairs consolidation and retrieval of fear extinction. *Learn. Mem.* 16, 520–529. doi: 10.1101/lm.1474609

Laviolette, S. R., Lipski, W. J., and Grace, A. A. (2005). A subpopulation of neurons in the medial prefrontal cortex encodes emotional learning with burst and frequency codes through a dopamine D4 receptor-dependent basolateral amygdala input. *J. Neurosci.* 25, 6066–6075. doi: 10.1523/JNEUROSCI.1168-05.2005

Lee, A. T., Gee, S. M., Vogt, D., Patel, T., Rubenstein, J. L., and Sohal, V. S. (2014). Pyramidal neurons in prefrontal cortex receive subtype-specific forms of excitation and inhibition. *Neuron* 81, 61–68. doi: 10.1016/j.neuron.2013.10.031

Lee, S., Kruglikov, I., Huang, Z. J., Fishell, G., and Rudy, B. (2013). A disinhibitory circuit mediates motor integration in the somatosensory cortex. *Nat. Neurosci.* 16, 1662–1670. doi: 10.1038/nn.3544

Letzkus, J. J., Wolff, S. B. E., Meyer, E. M. M., Tovote, P., Courtin, J., Herry, C., et al. (2011). A disinhibitory microcircuit for associative fear learning in the auditory cortex. *Nature* 480, 331–335. doi: 10.1038/nature10674

Li, H., Penzo, M. A., Taniguchi, H., Kopec, C. D., Huang, Z. J., and Li, B. (2013). Experience-dependent modification of a central amygdala fear circuit. *Nat. Neurosci.* 16, 332–339. doi: 10.1038/nn.3322

Liu, X., Ramirez, S., Pang, P. T., Puryear, C. B., Govindarajan, A., Deisseroth, K., et al. (2012). Optogenetic stimulation of a hippocampal engram activates fear memory recall. *Nature* 484, 381–385. doi: 10.1038/nature11028

Losonczy, A., Zemelman, B. V., Vaziri, A., and Magee, J. C. (2010). Network mechanisms of theta related neuronal activity in hippocampal CA1 pyramidal neurons. *Nat. Neurosci.* 13, 967–972. doi: 10.1038/nn.2597

Lovett-Barron, M., Kaifosh, P., Kheirbek, M. A., Danielson, N., Zaremba, J. D., Reardon, T. R., et al. (2014). Dendritic inhibition in the hippocampus supports fear learning. *Science* 343, 857–863. doi: 10.1126/science.1247485

Luo, X., Guet-Mccreight, A., Villette, V., Francavilla, R., Marino, B., Chamberland, S., et al. (2020). Synaptic mechanisms underlying the network state-dependent recruitment of VIP-expressing interneurons in the CA1 hippocampus. *Cereb. Cortex* 30, 3667–3685. doi: 10.1093/cercor/bhz334

Luo, X., Munoz-Pino, E., Francavilla, R., Vallée, M., Droit, A., and Topolnik, L. (2019). Transcriptomic profile of the subiculum-projecting VIP GABAergic neurons in the mouse CA1 hippocampus. *Brain Struct. Funct.* 224, 2269–2280. doi: 10.1007/s00429-019-01883-z

Magnin, E., Francavilla, R., Amalyan, S., Gervais, E., David, L. S., Luo, X., et al. (2019). Input-specific synaptic location and function of the α5 GABAA receptor subunit in the mouse CA1 hippocampal neurons. *J. Neurosci.* 39, 788–801. doi: 10.1523/JNEUROSCI.0567-18.2018

Mańko, M., Bienvenu, T. C. M., Dalezios, Y., and Capogna, M. (2012). Neurogliaform cells of amygdala: a source of slow phasic inhibition in the basolateral complex. *J. Physiol.* 590, 5611–5627. doi: 10.2186/jpr.JPR_D_22_00242

Marek, R., Jin, J., Goode, T. D., Giustino, T. F., Wang, Q., Acca, G. M., et al. (2018). Hippocampus-driven feed-forward inhibition of the prefrontal cortex mediates relapse of extinguished fear. *Nat. Neurosci.* 21, 384–392. doi: 10.1038/s41593-018-0073-9

Marek, R., Sun, Y., and Sah, P. (2019). Neural circuits for a top-down control of fear and extinction. *Psychopharmacology (Berl)* 236, 313–320. doi: 10.1007/s00213-018-5033-2

Maren, S., Aharonov, G., and Fanselow, M. S. (1997). Neurotoxic lesions of the dorsal hippocampus and Pavlovian fear conditioning in rats. *Behav. Brain Res.* 88, 261–274. doi: 10.1016/s0166-4328(97)00088-0

Maren, S., Ferrario, C. R., Corcoran, K. A., Desmond, T. J., and Frey, K. A. (2003). Protein synthesis in the amygdala, but not the auditory thalamus, is required for consolidation of Pavlovian fear conditioning in rats. *Eur. J. Neurosci.* 18, 3080–3088. doi: 10.1111/j.1460-9568.2003.03063.x

McDonald, A. J., and Augustine, J. R. (1993). Localization of GABA-like immunoreactivity in the monkey amygdala. *Neuroscience* 52, 281–294. doi: 10.1016/0306-4522(93)90156-a

McDonald, A. J., and Mascagni, F. (2002). Immunohistochemical characterization of somatostatin containing interneurons in the rat basolateral amygdala. *Brain Res.* 943, 237–244. doi: 10.1016/s0006-8993(02)02650-1

McDonald, A. J., Mascagni, F., and Zaric, V. (2012). Subpopulations of somatostatin-immunoreactive non-pyramidal neurons in the amygdala and adjacent external capsule project to the basal forebrain: evidence for the existence of GABAergic projection neurons in the cortical nuclei and basolateral nuclear com. *Front. Neural Circuits* 6:46. doi: 10.3389/fncir.2012.00046

McEwen, B. S., Nasca, C., and Gray, J. D. (2016). Stress effects on neuronal structure: hippocampus, amygdala and prefrontal cortex. *Neuropsychopharmacology* 41, 3–23. doi: 10.1038/npp.2015.171

McGarrity, S., Mason, R., Fone, K. C., Pezze, M., and Bast, T. (2017). Hippocampal neural disinhibition causes attentional and memory deficits. *Cereb. Cortex* 27, 4447–4462. doi: 10.1093/cercor/bhw247

Milad, M. R., and Quirk, G. J. (2002). Neurons in medial prefrontal cortex signal memory for fear extinction. *Nature* 420, 70–74. doi: 10.1038/nature01138

Milad, M. R., and Quirk, G. J. (2012). Fear extinction as a model for translational neuroscience: ten years of progress. *Annu. Rev. Psychol.* 63, 129–151. doi: 10.1146/annurev.psych.121208.131631

Milad, M. R., Vidal-Gonzalez, I., and Quirk, G. J. (2004). Electrical stimulation of medial prefrontal cortex reduces conditioned fear in a temporally specific manner. *Behav. Neurosci.* 118, 389–394. doi: 10.1037/0735-7044.118.2.389

Morey, R. A., Gold, A. L., LaBar, K. S., Beall, S. K., Brown, V. M., Haswell, C. C., et al. (2012). Amygdala volume changes with posttraumatic stress disorder in a large case-controlled veteran group. *Arch. Gen. Psychiatry* 69, 1169–1178. doi: 10.1001/archgenpsychiatry.2012.50

Morgan, M. A., Romanski, L. M., and LeDoux, J. E. (1993). Extinction of emotional learning: contribution of medial prefrontal cortex. *Neurosci. Lett.* 163, 109–113. doi: 10.1016/0304-3940(93)90241-c

Morrison, D. J., Rashid, A. J., Yiu, A. P., Yan, C., Frankland, P. W., and Josselyn, S. A. (2016). Parvalbumin interneurons constrain the size of the lateral amygdala engram. *Neurobiol. Learn. Mem.* 135, 91–99. doi: 10.1016/j.nlm.2016.07.007

Muller, J. F., Mascagni, F., and McDonald, A. J. (2007). Postsynaptic targets of somatostatin-containing interneurons in the rat basolateral amygdala. *J. Comp. Neurol.* 500, 513–529. doi: 10.1002/cne.21185

Myers, K. M., Ressler, K. J., and Davis, M. (2006). Different mechanisms of fear extinction dependent on length of time since fear acquisition. *Learn. Mem.* 13, 216–223. doi: 10.1101/lm.119806

Naka, A., and Adesnik, H. (2016). Inhibitory circuits in cortical layer 5. *Front. Neural Circuits* 10:35. doi: 10.3389/fncir.2016.00035

Naka, A., Veit, J., Shababo, B., Chance, R. K., Risso, D., Stafford, D., et al. (2019). Complementary networks of cortical somatostatin interneurons enforce layer specific control. *eLife* 8:e43696. doi: 10.7554/eLife.43696

Nelson, M. D., and Tumpap, A. M. (2017). Posttraumatic stress disorder symptom severity is associated with left hippocampal volume reduction: a meta-analytic study. *CNS Spectr.* 22, 363–372. doi: 10.1017/S1092852916000833

Ognjanovski, N., Schaeffer, S., Wu, J., Mofakham, S., Maruyama, D., Zochowski, M., et al. (2017). Parvalbumin-expressing interneurons coordinate hippocampal network dynamics required for memory consolidation. *Nat. Commun.* 8:15039. doi: 10.1038/ncomms15039

Oh, J. P., and Han, J. H. (2020). A critical role of hippocampus for formation of remote cued fear memory. *Mol. Brain* 13:112. doi: 10.1186/s13041-020-00652-y

Pape, H. C., and Pare, D. (2010). Plastic synaptic networks of the amygdala for the acquisition, expression and extinction of conditioned fear. *Physiol. Rev.* 90, 419–463. doi: 10.1152/physrev.00037.2009

Paré, D., and Smith, Y. (1993). The intercalated cell masses project to the central and medial nuclei of the amygdala in cats. *Neuroscience* 57, 1077–1090. doi: 10.1016/0306-4522(93)90050-p

Pavić, L. R., Gregurek, M., Rados, B., Brkljacić, L., Brajković, I., Simetin-Pavić, G., et al. (2007). Smaller right hippocampus in war veterans with posttraumatic stress disorder. *Psychiatry Res.* 154, 191–198. doi: 10.1016/j.pscychresns.2006.08.005

Pavlov, I. P. (1927). Conditioned reflexes: an investigation of the physiological activity of the cerebral cortex. *Ann. Neurosci.* 17, 136–141. doi: 10.5214/ans.0972-7531.1017309

Pelkey, K. A., Chittajallu, R., Craig, M. T., Tricoire, L., Wester, J. C., and McBain, C. J. (2017). Hippocampal GABAergic inhibitory interneurons. *Physiol. Rev* 77, 1619–1747. doi: 10.1152/physrev.00007.2017

Penzo, M. A., Robert, V., Tucciarone, J., De Bundel, D., Wang, M., Van Aelst, L., et al. (2015). The paraventricular thalamus controls a central amygdala fear circuit. *Nature* 519, 455–459. doi: 10.1038/nature13978

Pfeffer, C. K., Xue, M., He, M., Huang, Z. J., and Scanziani, M. (2013). Inhibition of inhibition in visual cortex: the logic of connections between molecularly distinct interneurons. *Nat. Neurosci.* 16, 1068–1076. doi: 10.1038/nn.3446

Phelps, E. A., Delgado, M. R., Nearing, K. I., and Ledoux, J. E. (2004). Extinction learning in humans: role of the amygdala and vmPFC. *Neuron* 43, 897–905. doi: 10.1016/j.neuron.2004.08.042

Phelps, E. A., and LeDoux, J. E. (2005). Contributions of the amygdala to emotion processing: from animal models to human behavior. *Neuron* 48, 175–187. doi: 10.1016/j.neuron.2005.09.025

Pi, H. J., Hangya, B., Kvitsiani, D., Sanders, J. I., Huang, Z. J., and Kepecs, A. (2013). Cortical interneurons that specialize in disinhibitory control. *Nature* 503, 521–524. doi: 10.1038/nature12676

Pierson, J. L., Pullins, S. E., and Quinn, J. J. (2015). Dorsal hippocampus infusions of CNQX into the dentate gyrus disrupt expression of trace fear conditioning. *Hippocampus* 25, 779–785. doi: 10.1002/hipo.22413

Ponserre, M., Fermani, F., Gaitanos, L., and Klein, R. (2022). Encoding of environmental cues in central amygdala neurons during foraging. *J. Neurosci.* 42, 3783–3796. doi: 10.1523/JNEUROSCI.1791-21.2022

Quirk, G. J., Garcia, R., and González-Lima, F. (2006). Prefrontal mechanisms in extinction of conditioned fear. *Biol. Psychiatry* 60, 337–343. doi: 10.1016/j.biopsych.2006.03.010

Quirk, G. J., Paré, D., Richardson, R., Herry, C., Monfils, M. H., Schiller, D., et al. (2010). Symposium erasing fear memories with extinction training. *J. Neurosci.* 30, 14993–14997. doi: 10.1016/j.biopsych.2006.03.010

Quirk, G. J., Russo, G. K., Barron, J. L., and Lebron, K. (2000). The role of ventromedial prefrontal cortex in the recovery of extinguished fear. *J. Neurosci.* 20, 6225–6231. doi: 10.1523/JNEUROSCI.20-16-06225.2000

Raineki, C., Holman, P. J., Debiec, J., Bugg, M., Beasley, A., and Sullivan, R. M. (2010). Functional emergence of the hippocampus in context fear learning in infant rats. *Hippocampus* 20, 1037–1046. doi: 10.1002/hipo.20702

Ramirez, S., Liu, X., Lin, P. A., Suh, J., Pignatelli, M., Redondo, R. L., et al. (2013). Creating a false memory in the hippocampus. *Science* 341, 387–391. doi: 10.1126/science.1239073

Reijmers, L. G., Perkins, B. L., Matsuo, N., and Mayford, M. (2007). Localization of a stable neural correlate of associative memory. *Science* 317, 1230–1233. doi: 10.1126/science.1143839

Rescorla, R. A. (1988). Pavlovian conditioning: it's not what you think it is. *Am. Psychol.* 43, 151–160. doi: 10.1037//0003-066x.43.3.151

Rhomberg, T., Rovira-Esteban, L., Vikór, A., Paradiso, E., Kremser, C., Nagy-Pál, P., et al. (2018). Vasoactive intestinal polypeptide-immunoreactive interneurons within circuits of the mouse basolateral amygdala. *J. Neurosci.* 38, 6983–7003. doi: 10.1523/JNEUROSCI.2063-17.2018

Riedemann, T. (2019). Diversity and function of somatostatin-expressing interneurons in the cerebral cortex. *Int. J. Mol. Sci.* 20:2952. doi: 10.3390/ijms20122952

Riga, D., Matos, M. R., Glas, A., Smit, A. B., Spijker, S., and Van den Oever, M. C. (2014). Optogenetic dissection of medial prefrontal cortex circuitry. *Front. Syst. Neurosci.* 8:230. doi: 10.3389/fnsys.2014.00230

Rogerson, T., Cai, D. J., Frank, A., Sano, Y., Shobe, J., Lopez-Aranda, M. F., et al. (2014). Synaptic tagging during memory allocation. *Nat. Rev. Neurosci.* 15, 157–169. doi: 10.1038/nrn3667

Rosas-Vidal, L., Do-Monte, F., and Sotres-Bayon, F. (2014). Hippocampal-prefrontal BDNF and memory for fear extinction. *Neuropsychopharmacology* 39, 2161–2169. doi: 10.1038/npp.2014.64

Royer, S., Zemelman, B. V., Losonczy, A., Kim, J., Chance, F., Magee, J. C., et al. (2012). Control of timing, rate and bursts of hippocampal place cells by dendritic and somatic inhibition. *Nat. Neurosci.* 15, 769–775. doi: 10.1038/nn.3077

Rudy, B., Fishell, G., Lee, S. H., and Hjerling-Leffler, J. (2011). Three groups of interneurons account for nearly 100% of neocortical GABAergic neurons. *Dev. Neurobiol.* 71, 45–61. doi: 10.1002/dneu.20853

Runyan, J. D., Moore, A. N., and Dash, P. K. (2004). A role for prefrontal cortex in memory storage for trace fear conditioning. *J. Neurosci.* 24, 1288–1295. doi: 10.1523/JNEUROSCI.4880-03.2004

Sauer, J.-F., and Bartos, M. (2022). Disrupted-in-schizophrenia-1 is required for normal pyramidal cell-interneuron communication and assembly dynamics in the prefrontal cortex. *eLife* 11:e79471. doi: 10.7554/eLife.79471

Sauer, J. F., Strüber, M., and Bartos, M. (2015). Impaired fast-spiking interneuron function in a genetic mouse model of depression. *eLife* 2015:e04979. doi: 10.7554/eLife.04979

Schafe, G. E., Nadel, N. V., Sullivan, G. M., Harris, A., and LeDoux, J. E. (1999). Memory consolidation for contextual and auditory fear conditioning is dependent on protein synthesis, PKA and MAP kinase. *Learn. Mem.* 6, 97–110.

Schmitz, T. W., Correia, M. M., Ferreira, C. S., Prescot, A. P., and Anderson, M. C. (2017). Hippocampal GABA enables inhibitory control over unwanted thoughts. *Nat. Commun.* 8:1311. doi: 10.1038/s41467-017-00956-z

Schmid, L. C., Mittag, M., Poll, S., Steffen, J., Wagner, J., Geis, H. R., et al. (2016). Dysfunction of somatostatin-positive interneurons associated with memory deficits in an Alzheimer's disease model. *Neuron* 92, 114–125. doi: 10.1016/j.neuron.2016.08.034

Sehlmeyer, C., Schöning, S., Zwitserlood, P., Pfleiderer, B., Kircher, T., Arolt, V., et al. (2009). Human fear conditioning and extinction in neuroimaging: a systematic review. *PLoS One* 4:e5865. doi: 10.1371/journal.pone.0005865

Seidenbecher, T., Laxmi, T. R., Stork, O., and Pape, H. C. (2003). Amygdalar and hippocampal theta rhythm synchronization during fear memory retrieval. *Science* 301, 846–850. doi: 10.1126/science.1085818

Sevinc, G., Holzel, B. K., Greenberg, J., Gard, T., Brunsch, V., Hashmi, J. A., et al. (2019). Strengthened hippocampal circuits underlie enhanced retrieval of extinguished fear memories following mindfulness training. *Biol. Psychiatry* 86, 693–702. doi: 10.1016/j.biopsych.2019.05.017

Sharma, V., Cohen, N., Sood, R., Ounallah-Saad, H., Gal-Ben-Ari, S., and Rosenblum, K. (2018). Trace fear conditioning: procedure for assessing complex hippocampal function in mice. *Bio. Protoc.* 8:e2475. doi: 10.21769/BioProtoc.2475

Sharma, V., Sood, R., Khlaifia, A., Eslamizade, M. J., Hung, T. Y., Lou, D., et al. (2020). eIF2α controls memory consolidation via excitatory and somatostatin neurons. *Nature* 586, 412–416. doi: 10.1038/s41586-020-2805-8

Sheline, Y. I., Gado, M. H., and Kraemer, H. C. (2003). Untreated depression and hippocampal volume loss. *Am. J. Psychiatry* 160, 1516–1518. doi: 10.1176/appi.ajp.160.8.1516

Shin, L. M., Shin, P. S., Heckers, S., Krangel, T. S., Macklin, M. L., Orr, S. P., et al. (2004). Hippocampal function in posttraumatic stress disorder. *Hippocampus* 14, 292–300. doi: 10.1002/hipo.10183

Shumyatsky, G. P., Tsvetkov, E., Malleret, G., Vronskaya, S., Hatton, M., Hampton, L., et al. (2002). Identification of a signaling network in lateral nucleus of amygdala important for inhibiting memory specifically related to learned fear. *Cell* 111, 905–918. doi: 10.1016/s0092-8674(02)01116-9

Sierra-Mercado, D., Padilla-Coreano, N., and Quirk, G. J. (2011). Dissociable roles of prelimbic and infralimbic cortices, ventral hippocampus and basolateral amygdala in the expression and extinction of conditioned fear. *Neuropsychopharmacology* 36, 529–538. doi: 10.1038/npp.2010.184

Singh, S., Siddiqui, S. A., Tripathy, S., Kumar, S., Saha, S., Ugale, R., et al. (2018). Decreased level of histone acetylation in the infralimbic prefrontal cortex following immediate extinction may result in deficit of extinction memory. *Brain Res. Bull.* 140, 355–364. doi: 10.1016/j.brainresbull.2018.06.004

Smeyne, R. J., Schilling, K., Robertson, L., Luk, D., Oberdick, J., Curran, T., et al. (1992). Fos-lacZ transgenic mice: mapping sites of gene induction in the central nervous system. *Neuron* 8, 13–23. doi: 10.1016/0896-6273(92)90105-m

Smith, Y., Ois Paré, J., and Paré, D. (2000). Differential innervation of parvalbumin-immunoreactive interneurons of the basolateral amygdaloid complex by cortical and intrinsic inputs. *J. Comp. Neurol.* 416, 496–508. doi: 10.1002/(sici)1096-9861(20000124)416:4<496::aid-cne6>3.0.co;2-n

Sohn, J., Okamoto, S., Kataoka, N., Kaneko, T., Nakamura, K., and Hioki, H. (2016). Differential inputs to the perisomatic and distal-dendritic compartments of VIP-positive neurons in layer 2/3 of the mouse barrel cortex. *Front. Neuroanat.* 10:124. doi: 10.3389/fnana.2016.00124

Sotres-Bayon, F., Sierra-Mercado, D., Pardilla-Delgado, E., and Quirk, G. J. (2012). Gating of fear in prelimbic cortex by hippocampal and amygdala inputs. *Neuron* 76, 804–812. doi: 10.1016/j.neuron.2012.09.028

Spampanato, J., Polepalli, J., and Sah, P. (2011). Interneurons in the basolateral amygdala. *Neuropharmacology* 60, 765–773. doi: 10.1016/j.neuropharm.2010.11.006

Sparta, D. R., Hovelsø, N., Mason, A. O., Kantak, P. A., Ung, R. L., Decot, H. K., et al. (2014). Activation of prefrontal cortical parvalbumin interneurons facilitates extinction of reward-seeking behavior. *J. Neurosci.* 34, 3699–3705. doi: 10.1523/JNEUROSCI.0235-13.2014

Stefanelli, T., Bertollini, C., Lüscher, C., Muller, D., and Mendez, P. (2016). Hippocampal somatostatin interneurons control the size of neuronal memory ensembles. *Neuron* 89, 1074–1085. doi: 10.1016/j.neuron.2016.01.024

Szinyei, C., Narayanan, R. T., and Pape, H. C. (2007). Plasticity of inhibitory synaptic network interactions in the lateral amygdala upon fear conditioning in mice. *Eur. J. Neurosci.* 25, 1205–1211. doi: 10.1111/j.1460-9568.2007.05349.x

Szőnyi, A., Sos, K. E., Nyilas, R., Schlingloff, D., Domonkos, A., Takács, V. T., et al. (2019). Brainstem nucleus incertus controls contextual memory formation. *Science* 25:eaaw0445. doi: 10.1126/science.aaw0445

Takahashi, H., and Magee, J. C. (2009). Pathway interactions and synaptic plasticity in the dendritic tuft regions of CA1 pyramidal neurons. *Neuron* 62, 102–111. doi: 10.1016/j.neuron.2009.03.007

Tang, S. J., Reis, G., Kang, H., Gingras, A. C., Sonenberg, N., and Schuman, E. M. (2002). A rapamycin-sensitive signaling pathway contributes to long-term synaptic plasticity in the hippocampus. *Proc. Natl. Acad. Sci. U S A* 99, 467–472. doi: 10.1073/pnas.012605299

Tayler, K. K., Tanaka, K. Z., Reijmers, L. G., and Wiltgen, B. J. (2013). Reactivation of neural ensembles during the retrieval of recent and remote memory. *Curr. Biol.* 23, 99–106. doi: 10.1016/j.cub.2012.11.019

Tipps, M., de Velasco, E. M. F., Schaeffer, A., and Wickman, K. (2018). Inhibition of pyramidal neurons in the basal amygdala promotes fear learning. *eNeuro* 23:ENEURO.0272-18.2018. doi: 10.1523/ENEURO.0272-18.2018

Topolnik, L., and Tamboli, S. (2022). The role of inhibitory circuits in hippocampal memory processing. *Nat. Rev. Neurosci.* 23, 476–492. doi: 10.1523/ENEURO.0272-18.2018

Tovote, P., Fadok, J. P., and Lüthi, A. (2015). Neuronal circuits for fear and anxiety. *Nat. Rev. Neurosci.* 16, 317–331. doi: 10.1038/nrn3945

Tremblay, R., Lee, S., and Rudy, B. (2016). GABAergic interneurons in the neocortex: from cellular properties to circuits. *Neuron* 91, 260–292. doi: 10.1016/j.neuron.2016.06.033

Trouche, S., Sasaki, J. M., Tu, T., and Reijmers, L. G. (2013). Fear extinction causes target-specific remodeling of perisomatic inhibitory synapses. *Neuron* 80, 1054–1065. doi: 10.1016/j.neuron.2013.07.047

Turi, G. F., Li, W. K., Chavlis, S., Pandi, I., O'Hare, J., Priestley, J. B., et al. (2019). Vasoactive intestinal polypeptide-expressing interneurons in the hippocampus support goal-oriented spatial learning. *Neuron* 101, 1150–1165. doi: 10.1016/j.neuron.2019.01.009

Tyan, L., Chamberland, S., Magnin, E., Camiré, O., Francavilla, R., Suzanne David, L., et al. (2014). Dendritic inhibition provided by interneuron-specific cells controls the firing rate and timing of the hippocampal feedback inhibitory circuitry. *J. Neurosci.* 34, 4534–4547. doi: 10.1523/JNEUROSCI.3813-13.2014

Unal, G., Paré, J. F., Smith, Y., and Paré, D. (2014). Cortical inputs innervate calbindin-immunoreactive interneurons of the rat basolateral amygdaloid complex. *J. Comp. Neurol.* 522, 1915–1928. doi: 10.1002/cne.23511

Vereczki, V. K., Müller, K., Krizsán, É., Máté, Z., Fekete, Z., Rovira-Esteban, L., et al. (2021). Total number and ratio of GABAergic neuron types in the mouse lateral and basal amygdala. *J. Neurosci.* 41, 4575–4595. doi: 10.1523/JNEUROSCI.2700-20.2021

Vereczki, V. K., Veres, J. M., Müller, K., Nagy, G. A., Rácz, B., Barsy, B., et al. (2016). Synaptic organization of perisomatic gabaergic inputs onto the principal cells of the mouse basolateral amygdala. *Front. Neuroanat.* 10:20. doi: 10.3389/fnana.2016.00020

Veres, J. M., Nagy, G. A., and Hájos, N. (2017). Perisomatic GABAergic synapses of basket cells effectively control principal neuron activity in amygdala networks. *eLife* 6:e20721. doi: 10.7554/eLife.20721

Veres, J. M., Nagy, G. A., Vereczki, V. K., Andrási, T., and Hájos, N. (2014). Strategically positioned inhibitory synapses of axo-axonic cells potently control principal neuron spiking in the basolateral amygdala. *J. Neurosci.* 34, 16194–16206. doi: 10.1523/JNEUROSCI.2232-14.2014

Wall, N. R., de la Parra, M., Sorokin, J. M., Taniguchi, H., Huang, Z. J., and Callaway, E. M. (2016). Brain-wide maps of synaptic input to cortical interneurons. *J. Neurosci.* 36, 4000–4009. doi: 10.1523/JNEUROSCI.3967-15.2016

Wang, X., Xie, H., Chen, T., Cotton, A. S., Salminen, L. E., Logue, M. W., et al. (2021). Cortical volume abnormalities in posttraumatic stress disorder: an ENIGMA-psychiatric genomics consortium PTSD workgroup mega-analysis. *Mol. Psychiatry* 26, 4331–4343. doi: 10.1038/s41380-020-00967-1

Weike, A. I., Hamm, A. O., Schupp, H. T., Runge, U., Schroeder, H. W. S., and Kessler, C. (2005). Fear conditioning following unilateral temporal lobectomy: dissociation of conditioned startle potentiation and autonomic learning. *J. Neurosci.* 25, 11117–11124. doi: 10.1523/JNEUROSCI.2032-05.2005

Wolff, S. B. E., Gründemann, J., Tovote, P., Krabbe, S., Jacobson, G. A., Müller, C., et al. (2014). Amygdala interneuron subtypes control fear learning through disinhibition. *Nature* 509, 453–458. doi: 10.1038/nature13258

Woodruff, A. R., and Sah, P. (2007a). Inhibition and synchronization of basal amygdala principal neuron spiking by parvalbumin-positive interneurons. *J. Neurophysiol.* 98, 2956–2961. doi: 10.1152/jn.00739.2007

Woodruff, A. R., and Sah, P. (2007b). Networks of parvalbumin-positive interneurons in the basolateral amygdala. *J. Neurosci.* 27, 553–563. doi: 10.1523/JNEUROSCI.3686-06.2007

Wright, A. (2020). "Chapter 5 - Limbic System: Hippocampus," in *Neuroscience Online: An Electronic Textbook for the Neurosciences*, Available online at: https://nba.uth.tmc.edu/neuroscience/s4/chapter05.html. Accessed August 11, 2022.

Xu, H., Jeong, H. Y., Tremblay, R., and Rudy, B. (2013). Neocortical somatostatin-expressing GABAergic interneurons disinhibit the thalamorecipient layer 4. *Neuron* 77, 155–167. doi: 10.1016/j.neuron.2012.11.004

Xu, W., Morishita, W., Buckmaster, P. S., Pang, Z. P., Malenka, R. C., and Südhof, T. C. (2012). Distinct neuronal coding schemes in memory revealed by selective erasure of fast synchronous synaptic transmission. *Neuron* 73, 990–1001. doi: 10.1016/j.neuron.2011.12.036

Yu, K., da Silva, P. G., Albeanu, D. F., and Li, B. (2016). Central amygdala somatostatin neurons gate passive and active defensive behaviors. *J. Neurosci.* 36, 6488–6496. doi: 10.1523/JNEUROSCI.4419-15.2016

Zhang, L., Lu, L., Bu, X., Li, H., Tang, S., Gao, Y., et al. (2021). Alterations in hippocampal subfield and amygdala subregion volumes in posttraumatic subjects with and without posttraumatic stress disorder. *Hum. Brain Mapp.* 42, 2147–2158. doi: 10.1002/hbm.25356

frontiers | Frontiers in Neural Circuits

TYPE Mini Review
PUBLISHED 20 April 2023
DOI 10.3389/fncir.2023.1167836

OPEN ACCESS

EDITED BY
Elsa Rossignol,
CHU Sainte-Justine, Canada

REVIEWED BY
Turgay Akay,
Dalhousie University, Canada
Patrick John Whelan,
University of Calgary, Canada

*CORRESPONDENCE
Simon Gosgnach
✉ gosgnach@ualberta.ca

RECEIVED 16 February 2023
ACCEPTED 06 April 2023
PUBLISHED 20 April 2023

CITATION
Gosgnach S (2023) Spinal inhibitory interneurons: regulators of coordination during locomotor activity.
Front. Neural Circuits 17:1167836.
doi: 10.3389/fncir.2023.1167836

Spinal inhibitory interneurons: regulators of coordination during locomotor activity

Simon Gosgnach*

Department of Physiology, University of Alberta, Edmonton, AB, Canada

Since the early 1900's it has been known that a neural network, situated entirely within the spinal cord, is capable of generating the movements required for coordinated locomotion in limbed vertebrates. Due the number of interneurons in the spinal cord, and the extent to which neurons with the same function are intermingled with others that have divergent functions, the components of this neural circuit (now referred to as the locomotor central pattern generator-CPG) have long proven to be difficult to identify. Over the past 20 years a molecular approach has been incorporated to study the locomotor CPG. This approach has resulted in new information regarding the identity of its component interneurons, and their specific role during locomotor activity. In this mini review the role of the inhibitory interneuronal populations that have been shown to be involved in locomotor activity are described, and their specific role in securing left-right, and flexor extensor alternation is outlined. Understanding how these interneuronal populations are activated, modulated, and interact with one another will help us understand how locomotor behavior is produced. In addition, a deeper understanding of the structure and mechanism of function of the locomotor CPG has the potential to assist those developing strategies aimed at enhancing recovery of motor function in spinal cord injured patients.

KEYWORDS

locomotion, interneuron, inhibitory, motor control, neural network

Introduction

The act of locomotion, or moving from place to place within one's environment, is an essential behavior in all non-sessile species. It has long been known that, in mammals, this behavior is controlled by a neural circuit, situated in the spinal cord, referred to as the locomotor central pattern generator (CPG) (Grillner et al., 1998). In limbed vertebrates, the locomotor CPG that is responsible for regulating hindlimb stepping resides in the ventral region of the lumbar spinal cord. In intact mammals descending input from the cortex and brainstem is crucial for locomotor initiation (Leiras et al., 2022), and sensory input is required to modify motor outputs to match the demands of the terrain (Prochazka and Ellaway, 2012). However, studies using the isolated spinal cord have demonstrated that the locomotor CPG, without any additional input, is able to produce intricately coordinated locomotor-like activity in flexor and extensor hindlimb motoneurons on either side of the body (Grillner, 1985; Grillner and Jessell, 2009; Kiehn, 2016). Since a comprehensive understanding of how the locomotor CPG is assembled and operates has the potential to

lead to therapeutic approaches to restore movement after spinal cord injury, investigations into the structure and mechanism of function of this neural circuit have been ongoing since its discovery, more than a century ago (Brown, 1911). Since the turn of the century, technological advances in molecular and developmental genetics have resulted in the implementation of a novel experimental approach to study the locomotor CPG. This has led to substantial insight regarding the neuronal components of this neural circuit, and the manner in which they interact with one another (reviewed in Goulding, 2009; Kiehn, 2016). The principal findings of this work is that interneurons in the developing spinal cord can be divided up into 10 "parent" populations (dI1-dI6 and V0-V3), each interneuron within a population being genetically similar to others within the same population, and genetically distinct from those belonging to other populations (Tanabe and Jessell, 1996). Investigation of the migration patterns of each population have indicated that 5 of these reside in the ventral aspect of the lumbar spinal cord postnatally, a location consistent with participation in locomotor activity. Subsequent studies on these populations have incorporated anatomical and electrophysiological techniques to characterize the properties of each. Their specific role during locomotor activity has been investigated by silencing or ablating a given cellular population and identifying locomotor defects that are apparent in their absence (Lanuza et al., 2004; Hinckley et al., 2005; Gosgnach et al., 2006; Crone et al., 2008; Zhang et al., 2008, 2014; Zagoraiou et al., 2009; Andersson et al., 2012; Talpalar et al., 2013; Britz et al., 2015; Haque et al., 2018).

Since the initial identification of these populations, subsequent investigation into their genetic makeup has led to the conclusion that, in most cases, the populations can be further subdivided into multiple subsets based on transcription factor expression downstream of those originally used to define each cell group (Gosgnach et al., 2017). In some cases multiple subpopulations, which are derived from a single "parent" cell group, have complimentary roles during locomotor activity. The integration of these subsets into the working network model of the locomotor CPG has furthered our understanding of this neural circuit by enabling us to better grasp how different groups of muscles are activated sequentially (i.e., muscle synergies recruited) in order to produce the specific locomotor outputs that are required (i.e., those responsible for slow walking vs. fast running- Rybak et al., 2015).

As it currently stands, 9 genetically- defined groups of neurons can be identified in the ventral half of the postnatal spinal cord that have a defined function during locomotor activity, five of these use excitatory neurotransmitter, and 4 populations are inhibitory. The excitatory populations ($V0_V$, V2a, V3, Shox2, and Hb9 neurons) have a variety of functions such as locomotor initiation (Dougherty et al., 2013), maintenance of locomotor stability (Zhang et al., 2008), and regulation of synchronous activity of motoneurons on either side of the spinal cord (Crone et al., 2008, 2009). In contrast, the inhibitory populations (dI6, $V0_D$, V1, and V2b groups) each play an essential role in the appropriate coordination of either left-right (Lanuza et al., 2004; Talpalar et al., 2013), or flexor-extensor (Zhang et al., 2014; Britz et al., 2015), alternation. In this mini review I will focus solely on the inhibitory populations, and describe their specific role in coordinating locomotor activity.

Inhibitory populations involved in left-right alternation: V0 and dI6 populations

Locomotor activity in bipedal mammals consists of alternation between the left and right hind limbs. This is result of a nuanced pattern of activation of various hindlimb muscles, with a great deal of variability in the onsets and offset in each (Engberg and Lundberg, 1969; Rasmussen et al., 1978). Generally speaking, however, when the left limb is on the ground (i.e., in stance phase) the extensor muscles are primarily active and the flexors are primarily silent. In the right limb (which would be in swing phase), the extensor muscles are inhibited while the flexors are active. As the speed of locomotion increases, the amount of time each limb spends in stance phase decreases while the amount of time spent in the swing phase is largely unchanged (Goslow et al., 1973; Halbertsma, 1983). Importantly, at all speeds of locomotion, alternation between the left and right hindlimbs persist. The majority of research into the structure and function of the locomotor CPG has come from quadrupedal species such as the cat or rodent, which have a unique set of muscle synergies as the speed of locomotor activity increases. Slower speed locomotion involves alternation similar to that seen in bipeds, and can be classified as either walk or trot. As speed increases there is synchronous activity across the midline and two similar locomotor gaits, gallop and bound, dominate (Bellardita and Kiehn, 2015). The current theory that accounts for the ability of this neural circuit to generate a variety of stepping patterns holds that the locomotor CPG is a two-layered circuit comprised of distinct population of interneurons. The "top" layer is responsible for rhythm generation, and activating the "lower," pattern forming layer which, in turn, activates or inhibits motoneurons in a manner appropriate for the required locomotor task (Rybak et al., 2015).

The first study to investigate the functional role of one of the molecularly defined interneuronal populations during locomotor activity was focused on the V0 neurons. These cells were shown to originate from progenitors expressing the transcription factor Dbx1, and reside in lamina VIII of the spinal cord postnatally (Pierani et al., 2001). Initially all V0 neurons were analyzed collectively, and this population was considered to be primarily comprised of inhibitory neurons which project commissural axons (Pierani et al., 2001). Subsequent work indicated that the V0 population could be divided into two subsets of neurons which could be distinguished from one another molecularly. The ventral subpopulation ($V0_V$) can be identified by expression the transcription factor Evx1 as well as Dbx1, and a dorsal population ($V0_D$) which can be identified by expression of Dbx1 but not Evx1 (Moran-Rivard et al., 2002). In the Dbx1 mutant mouse, in which all V0 neurons are absent, activity on the left and right sides of the spinal cord appeared to be "disconnected" from one another during a locomotor task. Rather that strict alternation between left and right flexor (or left and right extensor) ventral roots, contralateral activity in the Dbx1 mutant mouse drifted in and out, with left and right flexor motor axons sometimes bursting synchronously and sometimes alternating (Lanuza et al., 2004). Interestingly, in this study, mice in which only the Evx1- expressing ($V0_V$) cells were eliminated failed to show any aberrant left right alternation. This led to the suggestion that the $V0_D$ subpopulation alone were

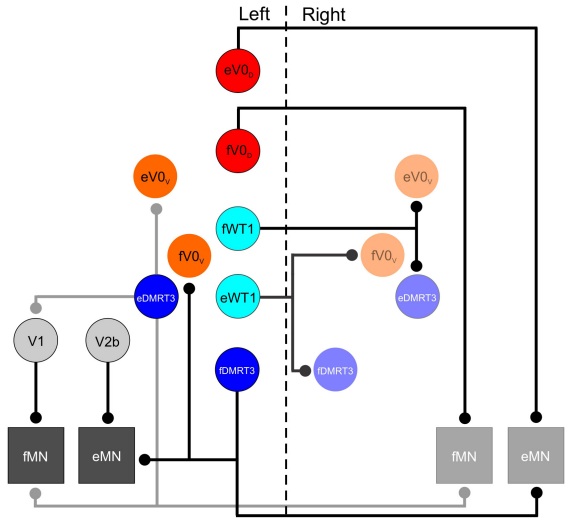

FIGURE 1
Schematic of synaptic contacts from inhibitory interneuronal populations in the lumbar spinal cord that are involved in locomotion. Vertical dashed line separates left and right side of spinal cord. In this schematic all inhibitory populations that have a defined role during locomotor activity appear on the left side, only those populations that receive inputs from these cells appear on the right side. Motoneurons are shown on both sides. Lowercase f and e indicate those members of a given population that are active during flexion and extension respectively.

responsible the coordination of motoneurons on either side of the spinal cord. Subsequent experiments indicating that V0 neurons projected axons toward, and made monosynaptic contacts onto, contralateral motoneurons suggested the circuitry responsible for this function (Lanuza et al., 2004- see **Figure 1**).

Additional investigation of the differences between the dorsal and ventral subpopulations of V0 neurons revealed a complimentary role for the two subsets during stepping. First, analysis of the neurotransmitter phenotype of each indicated that $V0_D$ cells were inhibitory while $V0_V$ cells were excitatory (Pierani et al., 2001; Talpalar et al., 2013). It was also demonstrated that ablation of the $V0_D$ cells alone resulted in inappropriate left-right alternation at slower locomotor speeds with minimal effect on coordination during faster stepping. Loss of $V0_V$ cells had the opposite effect, seemingly no impact at slower speeds, but essential for appropriate left/right alternation when locomotor speed increased (Talpalar et al., 2013). The apparent conflict with the previous study (in which removal of $V0_V$ cell function did not impact left right alternation at all) was likely due to the fact that the speeds generated in the locomotor assay used in the original study did not reach the frequencies at which the $V0_V$ subpopulation would be recruited, and thus their removal did not affect these slow locomotor outputs. The severity of the locomotor phenotype also differed between the two studies investigating V0 interneuron function during locomotion. In the initial study bilateral activity drifted in and out of phase, indicating the two sides of the spinal cord were "disconnected" from one another (Lanuza et al., 2004) while in the latter study activity on either side of the spinal cord was strictly synchronous (Talpalar et al., 2013). While the differences between the phenotypes has not been directly accounted for, they may have something to do with the mouse models implemented. The latter study used an approach in which diphtheria toxin was produced in select populations, killing cells after they had expressed specific transcription factors (Talpalar et al., 2013). In contrast, the initial study used a mutant mouse model in which V0 cells were not produced and developmental compensation occurred, increasing the number of other neuronal population such as the ipsilaterally projecting V1 cells and the commissural dI6 neurons (Lanuza et al., 2004).

dI6 interneurons have also been shown to play a role in left-right alternation. This population originates from progenitor cells expressing the transcription factors Lbx1 and Dbx1, and is situated immediately dorsal to the $V0_D$ neurons during embryonic development (Gross et al., 2002; Muller et al., 2002). dI6 neurons can be divided into 2 subsets based on the expression of the postmitotic markers WT1 or DMRT3 (Andersson et al., 2012). Unlike the V0 population, both dI6 subpopulations have been shown to be exclusively inhibitory (Andersson et al., 2012; Haque et al., 2018). A role for dI6 cells in left- right alternation was first suggested in the original study investigating the function of the V0 neurons as it was observed that the number of dI6 neurons increased in the Dbx1 mutant mouse, likely due to developmental compensation (Lanuza et al., 2004). It was suggested that the presence of these dI6 cells, which were known to be inhibitory and commissural, were perhaps responsible for the less severe locomotor phenotypes observed in some of the V0 ablated mice.

A specific role for the DMRT3- expressing neurons in gait coordination was first suggested following the observation that mutation of the DMRT3 gene in horses enabled "pacing" gaits in which the fore and hind limbs on the same side of the body move together while collectively alternating with the fore and hind limbs on the contralateral side of the body (Andersson et al., 2012). Characterization of these cells in mice indicated that, similar to $V0_D$ neurons, the DMRT3 subset of dI6 cells is primarily situated in lamina VIII of the postnatal spinal cord, and project commissural axons which release the neurotransmitter glycine. Synaptic contacts from this population were observed on motoneurons as well as on premotor neurons in laminae IX (presumably Renshaw cells which belong to the V1 population), as well as cholinergic V0 cells (derived from the $V0_V$ subpopulation) surrounding the central canal (Andersson et al., 2012- see **Figure 1**). The aforementioned gait abnormalities observed in horses lacking DMRT3 cells are strongly suggestive of a role for these subset of the dI6 population in left-right alternation. While they have been shown to be rhythmically active during a fictive locomotor task in the mouse (Perry et al., 2019), the locomotor pattern in their absence has yet to be investigated.

The WT1- expressing subset of dI6 neurons share many characteristics with DMRT3 + cells. WT1 neurons are inhibitory, and project commissural axons (Haque et al., 2018). Synaptic boutons from WT1 + cells have been found in close proximity to other commissural interneuronal populations, namely, Evx1-expressing $V0_V$, as well as DMRT3 interneurons (see **Figure 1**). Connectivity onto the $V0_D$ population was not confirmed, but cannot be ruled out as a postnatal marker for this population was not available (Haque et al., 2018). Like the DMRT3 population, WT1 cells were shown to be rhythmically active during fictive locomotion in the isolated spinal cord preparation (Haque et al., 2018; Schnerwitzki et al., 2018), and silencing of these cells

using a DREADD approach resulted in left-right alternation defects (Haque et al., 2018). The locomotor phenotype was less severe than that seen when the V0 neurons were ablated, but clear co-activation of contralateral flexor, and contralateral extensor, motor axons was regularly observed. The conclusion from this study was that the WT1 populations regulated the activity of other commissural interneurons (Haque et al., 2018). Knowing what we know now about the speed dependent regulation of the $V0_D$ and $V0_V$ interneurons, it would have been interesting to determine whether the WT1 interneurons were also modulated at different locomotor frequencies. For example, one might expect that these cells are actively regulating other commissural populations depending on whether a strictly alternating (walk/trot) or a synchronous gait (bound/gallop) is generated.

Inhibitory neurons securing flexor-extensor alternation: V1 and V2b populations

While the specific pattern flexor and extensor motoneuron and muscle activation varies during locomotor activity, one general characteristic of locomotor activity in both bipedals, and quadrupedals is the alternation of flexor and extensor motoneurons/muscles. The specific activity profile of flexor and extensor motor pools around the hip, knee, and ankle joints is complex and the peak firing phases of each has been shown to be determined by the output of the locomotor CPG, and modulated by sensory input (Patla, 1985). The specific interneuronal populations that comprise the components of the locomotor CPG which regulate the flexor/extensor alternation around hindlimb joints has only recently been revealed. The hunt for a population of neurons responsible for this alternation has involved silencing or ablating specific interneuronal populations in the hopes of identifying a locomotor phenotype in which inappropriate flexor/extensor activity could be observed, either *in vitro* or *in vivo*.

Surprisingly, ablating each of the genetically-defined interneuronal populations individually revealed no deficits in ipsilateral coordination. Given their characteristics (ipsilaterally projecting axons, and inhibitory neurotransmitter phenotype), the primary candidates to be involved in flexor/extensor alternation were the V1 (Burril et al., 1997; Sauressig et al., 1999) and V2b (Lundfald et al., 2007; Peng et al., 2007) interneurons which are defined by their expression of En1 and Gata3, respectively. Ablation or silencing of the entire V1 population leads to a marked slowing of locomotor activity (Gosgnach et al., 2006) with no change in flexor- extensor alternation when compared to the wildtype animal (Gosgnach et al., 2006; Zhang et al., 2014). From this work it was suggested that V1 INs facilitate the transition between the active and inactive phases of the step cycle (Gosgnach et al., 2006). Inhibiting activity in the V2b population alone, by arresting synaptic transmission in these cells, has only a very minor effect on left right alternation (Zhang et al., 2014). Although ablation of the function of either of these populations in isolation had little effect on ipsilateral alternation, experiments in which both of these populations were ablated simultaneously, resulted in the complete collapse of flexor- extensor alternation in the isolated spinal cord, resulting in co-activation of flexor and extensor motor axons on the same side of the body, a locomotor phenotype that is not otherwise observed in either bipeds or quadrupeds, suggesting that the V1 and V2b neurons work together to maintain flexor-extensor alternation.

Due to expression of the markers V1 (En1) and V2b populations (Gata3) throughout the CNS, inhibiting the function of these cells in the aforementioned study was lethal at either late embryonic, or early postnatal time points. This dictated that the experiments used to identify the V1 and V2b cells are required for ipsilateral alternation were carried out on isolated spinal cords removed from immature mice, which limited the understanding of how they carried out this function. A subsequent study by the same group used a tripartite genetic approach to insert a foreign diphtheria toxin receptor solely into those neurons which expressed En1 and/or Gata3, and were located in the spinal cord (Britz et al., 2015). Application of the ligand for this diphtheria toxin receptor ablated these neurons and enabled their function during locomotor activity to be examined in greater detail. Furthermore, the use of postnatal animals also allowed the synaptic connectivity of these neurons to be analyzed allowing the specific role of each to be elucidated. Using this approach it was demonstrated that mice lacking V1 cell function displayed limb hyperflexion, while the limbs of those mice lacking V2b neuronal function had their hindlimbs locked in hyperextension (Britz et al., 2015). These findings nicely complimented anatomical data which indicated that V1 neurons preferentially contacted flexor motoneurons while the V2b population tended to terminate on extensor motor pools (Britz et al., 2015- see **Figure 1**). Given the inhibitory nature of both populations the data suggests that the loss of function of the V1 cells results in lack of inhibition of flexor motor neurons (and thus hyperflexion) while loss of V2b function results in insufficient inhibition of extensor motoneurons (and excessive limb extension). A balance of the two cell populations is required in order to establish coordinated activity of flexors and extensors during locomotion.

Conclusion

The locomotor CPG had long been considered to be a "black box," a mysterious neural network that was capable of generating a wide variety of motor synergies when activated. Since the turn of the century incorporation of a multidisciplinary approach involving molecular genetics, anatomy, and electrophysiology has allowed tremendous strides forward to be taken in our ability to identify neurons that comprise this neural network, and also identify their specific function during stepping. The inhibitory neurons that have been identified to be part of this locomotor CPG have thus far been proven to be essential components required for coordination of antagonist motor pools ipsilaterally, or agonist motor pools on either side of the spinal cord in limbed vertebrates. These inhibitory populations are essential for the generation of coordinated movements. As we learn more about the axonal projection pattern of these populations, and the upstream sites that contact these inhibitory populations it is likely to help

us understand the processes by which they are modulated in order to alter the activation pattern of muscles that is required as the frequency of locomotor activities changes. Ultimately, a detailed characterization of these, and other interneurons that are components of the locomotor CPG, and a better understanding of how they regulate motoneuron activity, will help us understand how motor behavior is produced, and will provide key information to those developing therapies aimed at enhancing functional recovery of motor control after damage to the CNS.

Author contributions

The author confirms being the sole contributor of this work and has approved it for publication.

Conflict of interest

The author declares that the research was conducted in the absence of any commercial or financial relationships that could be construed as a potential conflict of interest.

Publisher's note

References

Andersson, L., Larhammar, M., Memic, F., Wootz, H., Schwochow, D., Rubin, C., et al. (2012). Mutations in DMRT3 affect locomotion in horses and spinal circuit function in mice. *Nature* 488, 642–646. doi: 10.1038/nature11399

Bellardita, C., and Kiehn, O. (2015). Phenotypic characterization of speed-associated gait changes in mice reveals modular organization of locomotor networks. *Curr Biol.* 25, 1426–1436. doi: 10.1016/j.cub.2015.04.005

Britz, O., Zhang, J., Grossmann, K. S., Dyck, J., Kim, J. C., and Dymecki, S. (2015). A genetically defined asymmetry underlies the inhibitory control of flexor-extensor locomotor movements. *eLife* 4, e04718. doi: 10.7554/eLife.04718

Brown, T. G. (1911). The intrinsic factors in the act of progression in mammals. *Proc. R. Soc.* 84, 308–319. doi: 10.1098/rspb.1911.0077

Burril, J. D., Moran, L., Goulding, M. D., and Saueressig, H. (1997). PAX2 is expressed in multiple spinal cord interneurons, including a population of EN1 interneurons that require PAX6 for their development. *Development* 124, 4493–4503. doi: 10.1242/dev.124.22.4493

Crone, S. A., Quinlan, K. A., Zagoraiou, L., Droho, S., Restrepo, C. E., and Lundfald, L. (2008). Genetic ablation of V2a ipsilateral interneurons disrupts left-right locomotor coordination in mammalian spinal cord. *Neuron* 60, 70–83. doi: 10.1016/j.neuron.2008.08.009

Crone, S. A., Zhong, G., Harris-Warrick, R., and Sharma, K. (2009). In mice lacking V2a interneurons, gait depends on speed of locomotion. *J. Neurosci.* 29, 7098–7109. doi: 10.1523/JNEUROSCI.1206-09.2009

Dougherty, K. J., Zagoraiou, L., Satoh, D., Rozani, I., Doobar, S., and Arber, S. (2013). Locomotor rhythm generation linked to the output of spinal shox2 excitatory interneurons. *Neuron* 80, 920–933. doi: 10.1016/j.neuron.2013.08.015

Engberg, I., and Lundberg, A. (1969). An electromyographic analysis of muscular activity in the hindlimb of the cat during unrestrained locomotion. *ACTA Physiol.* 75, 614–630. doi: 10.1111/j.1748-1716.1969.tb04415.x

Gosgnach, S., Bikoff, J., Dougherty, K., El Manira, A., Lanuza, G., and Zhang, Y. (2017). Delineating the diversity of spinal interneurons in locomotor circuits. *J. Neurosci.* 37, 10835–10841. doi: 10.1523/JNEUROSCI.1829-17.2017

Gosgnach, S., Lanuza, G. M., Butt, S. J., Saueressig, H., Zhang, Y., and Velasquez, T. (2006). V1 spinal neurons regulate the speed of vertebrate locomotor outputs. *Nature* 440, 215–219. doi: 10.1038/nature04545

Goslow, G. E. Jr., Reinking, R. M., and Stuart, D. G. (1973). The cat step cycle: hind limb joint angles and muscle lengths during unrestrained locomotion. *J. Morphol.* 141, 1–41. doi: 10.1002/jmor.1051410102

Goulding, M. (2009). Circuits controlling vertebrate locomotion: moving in a new direction. *Nat. Rev. Neurosci.* 10, 507–518. doi: 10.1038/nrn2608

Grillner, S. (1985). Neurobiological bases of rhythmic motor acts in vertebrates. *Science* 228, 143–149. doi: 10.1126/science.3975635

Grillner, S., and Jessell, T. (2009). Measured motion: searching for simplicity in spinal locomotor networks. *Curr. Opin Neurobiol.* 19, 572–586. doi: 10.1016/j.conb.2009.10.011

Grillner, S., El Manira, A., Lansner, A., Parker, D., Tegnér, J., and Wallén, P. (1998). Intrinsic function of a neuronal network - a vertebrate central pattern generator. *Brain Res. Brain Res. Rev.* 26, 184–197. doi: 10.1016/S0165-0173(98)00002-2

Gross, M., Dottori, M., and Goulding, M. (2002). Lbx1 specifies somatosensory associa- tion interneurons in the dorsal spinal cord. *Neuron* 34, 535–549. doi: 10.1016/S0896-6273(02)00690-6

Halbertsma, J. M. (1983). The stride cycle of the cat: the modelling of locomotion by computerized analysis of automatic recordings. *Acta Physiol. Scand.* 521, 1–75.

Haque, F., Rancic, V., Zhang, W., Clugston, R., Ballanyi, K., and Gosgnach, S. (2018). WT1-expressing interneurons regulate left-right alternation during mammalian locomotor activity. *J. Neurosci.* 36, 5666–5676. doi: 10.1523/JNEUROSCI.0328-18.2018

Hinckley, C., Hartley, R., Wu, L., Todd, A., and Ziskind-Conhaim, L. (2005). Locomotor-like rhythms in a genetically distinct cluster of interneurons in the mammalian spinal cord. *J. Neurophysiol.* 93, 1439–1449. doi: 10.1152/jn.00647.2004

Kiehn, O. (2016). Decoding the organization of spinal circuits that control locomotion. *Nat. Rev. Neurosci.* 17, 224–238. doi: 10.1038/nrn.2016.9

Lanuza, G. M., Gosgnach, S., Pierani, A., Jessell, T. M., and Goulding, M. (2004). Genetic identification of spinal interneurons that coordinate left-right locomotor activity necessary for walking movements. *Neuron* 42, 375–386. doi: 10.1016/S0896-6273(04)00249-1

Leiras, R., Cregg, J., and Kiehn, O. (2022). Brainstem circuits for locomotion. *Annu Rev. Neurosci.* 45, 63–85. doi: 10.1146/annurev-neuro-082321-025137

Lundfald, L., Restrepo, C. E., Butt, S. J., Peng, C. Y., Droho, S., and Endo, T. (2007). Phenotype of V2-derived interneurons and their relationship to the axon guidance molecule EphA4 in the developing mouse spinal cord. *Eur. J. Neurosci.* 26, 2989–3002. doi: 10.1111/j.1460-9568.2007.05906.x

Moran-Rivard, L., Kagawa, T., Saueressig, H., Gross, M. K., Burrill, J., and Goulding, M. (2002). Evx1 is a postmitotic determinant of v0 interneuron identity in the spinal cord. *Neuron* 29, 385–399. doi: 10.1016/S0896-6273(01)00213-6

Muller, T., Brohmann, H., Pierani, A., Heppenstall, A., Lewin, G., Jessell, T., et al. (2002). The homeodomain factor Lbx1 distinguishes two major programs of neuronal differentiation in the dorsal spinal cord. *Neuron* 34, 551–562. doi: 10.1016/S0896-6273(02)00689-X

Patla, A. (1985). Some characteristics of EMG patterns during locomotion: implications for the locomotor control process. *J. Mot. Behav.* 17, 443–461. doi: 10.1080/00222895.1985.10735360

Peng, C. Y., Yajima, H., Burns, C. E., Zon, L. I., Sisodia, S. S., Pfaff, S. L., et al. (2007). Notch and MAML signaling drives Scl-dependent interneuron diversity in the spinal cord. *Neuron* 53, 813–827. doi: 10.1016/j.neuron.2007.02.019

Perry, S., Larhammar, M., Vieillard, J., Nagaraja, C., Hilscher, M., Tafreshiha, A., et al. (2019). Characterization of dmrt3-derived neurons suggest a role within locomotor circuits. *J. Neurosci.* 39, 1771–1782. doi: 10.1523/JNEUROSCI.0326-18.2018

Pierani, A., Moran-Rivard, L., Sunshine, M. J., Littman, D. R., Goulding, M., and Jessell, T. M. (2001). Control of interneuron fate in the developing spinal cord by the progenitor homeodomain protein Dbx1. *Neuron* 29, 367–384. doi: 10.1016/S0896-6273(01)00212-4

Prochazka, A., and Ellaway, P. (2012). Sensory systems in the control of movement. *Comp. Physiol.* 2, 2615–2627. doi: 10.1002/cphy.c100086

Rasmussen, S., Chan, A., and Goslow, G. (1978). The cat step cycle: electromyographic patterns for hindlimb muscles during posture and unrestrained locomotion. *J. Morphol.* 155, 253–269. doi: 10.1002/jmor.1051550302

Rybak, I., Dougherty, K., and Shevtsova, N. (2015). Organization of the mammalian locomotor CPG: review of computational model and circuit architectures based on genetically identified spinal interneurons (1,2,3). *eNeuro* 2:ENEURO.0069-15.2015. doi: 10.1523/ENEURO.0069-15.2015

Sauressig, H., Burrill, J., and Goulding, M. (1999). Engrailed-1 and netrin-1 regulate axon pathfinding by association interneurons that project to motor neurons. *Development* 126, 4201–4212. doi: 10.1242/dev.126.19.4201

Schnerwitzki, D., Perry, S., Ivanova, A., Caixeta, F., Cramer, P., Günther, S., et al. (2018). Neuron-specific inactivation of Wt1 alters locomotion in mice and changes interneuron composition in the spinal cord. *Life Sci. Alliance.* 1:e201800106. doi: 10.26508/lsa.201800106

Talpalar, A. E., Bouvier, J., Borgius, L., Fortin, G., Pierani, A., and Kiehn, O. (2013). Dual-mode operation of neuronal networks involved in left-right alternation. *Nature* 500, 85–88. doi: 10.1038/nature12286

Tanabe, Y., and Jessell, T. (1996). Diversity and pattern in the developing spinal cord. *Science* 274, 1115–1123. doi: 10.1126/science.274.5290.1115

Zagoraiou, L., Akay, T., Martin, J. F., Brownstone, R. M., Jessell, T. M., and Miles, G. B. (2009). A cluster of cholinergic premotor interneurons modulates mouse locomotor activity. *Neuron* 64, 645–662. doi: 10.1016/j.neuron.2009.10.017

Zhang, J., Lanuza, G. M., Britz, O., Wang, Z., Siembab, V. C., and Zhang, Y. (2014). V1 and v2b interneurons secure the alternating flexor-extensor motor activity mice require for limbed locomotion. *Neuron* 82, 138–150. doi: 10.1016/j.neuron.2014.02.013

Zhang, Y., Narayan, S., Geiman, E., Lanuza, G. M., Velasquez, T., and Shanks, B. (2008). V3 spinal neurons establish a robust and balanced locomotor rhythm during walking. *Neuron* 60, 84–96. doi: 10.1016/j.neuron.2008.09.027

frontiers | Frontiers in Neural Circuits

TYPE Review
PUBLISHED 27 April 2023
DOI 10.3389/fncir.2023.1181032

OPEN ACCESS

EDITED BY
Graziella DiCristo,
University of Montreal, Canada

REVIEWED BY
Pablo Fuentealba,
Pontificia Universidad Católica de Chile, Chile
Manuel Francisco Lopez-Aranda,
University of California, Los Angeles,
United States

*CORRESPONDENCE
Rebecca A. Piskorowski
✉ rebecca.piskorowski@inserm.fr

RECEIVED 06 March 2023
ACCEPTED 07 April 2023
PUBLISHED 27 April 2023

CITATION
Piskorowski RA and Chevaleyre V (2023) Hippocampal area CA2: interneuron disfunction during pathological states. *Front. Neural Circuits* 17:1181032. doi: 10.3389/fncir.2023.1181032

Hippocampal area CA2: interneuron disfunction during pathological states

Rebecca A. Piskorowski[1,2]* and Vivien Chevaleyre[1,2]

[1]Université Paris Cité, INSERM UMRS 1266, Institute of Psychiatry and Neuroscience of Paris, GHU Paris Psychiatrie et Neurosciences, Paris, France, [2]Institute of Biology Paris Seine, Neuroscience Paris Seine, CNRS UMR 8246, INSERM U1130, Sorbonne Université, Paris, France

Hippocampal area CA2 plays a critical role in social recognition memory and has unique cellular and molecular properties that distinguish it from areas CA1 and CA3. In addition to having a particularly high density of interneurons, the inhibitory transmission in this region displays two distinct forms of long-term synaptic plasticity. Early studies on human hippocampal tissue have reported unique alteration in area CA2 with several pathologies and psychiatric disorders. In this review, we present recent studies revealing changes in inhibitory transmission and plasticity of area CA2 in mouse models of multiple sclerosis, autism spectrum disorder, Alzheimer's disease, schizophrenia and the 22q11.2 deletion syndrome and propose how these changes could underly deficits in social cognition observed during these pathologies.

KEYWORDS

hippocampal area CA2, inhibitory transmission, 22q11.2DS, epilepsy, multiple sclerosis, autism spectrum disorder, Alzheimer's disease, schizophrenia

1. Introduction

Several decades of human and animal lesion experiments have established that the hippocampus plays a central role in learning and memory processes (Squire and Wixted, 2011). Lorente de No (1934) defined the hippocampal subregions over 80 years ago using morphology and input targets to differentiate areas CA3, CA2, and CA1. Currently, these hippocampal subregions are now delineated by many additional criteria, including molecular expression profiles (Lein et al., 2004, 2005; Cembrowski et al., 2016). With this, prominent and long-standing models have attributed particular roles to these subregions in hippocampal-dependent learning processes. For instance, pattern separation is thought to occur in the dentate gyrus, with the large numbers of low-firing dentate granule cells forming unique representations of entorhinal cortical input, and pattern completion occurring in area CA3, with the highly plastic and recurrent network allow for auto-associative properties (Willshaw and Buckingham, 1990; McClelland et al., 1995; Lisman, 1999; Rolls, 2010, 2013). This review focuses on area CA2, a region that had been under-studied, but is now recognized as playing a key role in social recognition memory (Hitti and Siegelbaum, 2014; Stevenson and Caldwell, 2014). Furthermore, as more is learned about area CA2 and how it participates in hippocampal function, it is highly likely that the neurons in this small region play a role in memory formation in non-social learning as well

(Wintzer et al., 2014; Kay et al., 2016; Boehringer et al., 2017; Stöber et al., 2020; He et al., 2021; Lehr et al., 2021). Even though neurophysiologists have neglected hippocampal area CA2, neuroanatomists have consistently noted changes in this region in post-mortem tissue from patients with neurodegenerative or psychiatric disorders. These results have been assembled and previously reviewed (Chevaleyre and Piskorowski, 2016). Here, we aim to present recent results from mouse models demonstrating how detrimental changes in inhibitory transmission and plasticity in area CA2 underly the cognitive deficits displayed in these models, and potentially lead to better understanding of hippocampal dysfunction in patients.

2. Unique inhibitory transmission and synaptic plasticity in hippocampal area CA2

Interneurons play a critical role in tuning the balance between excitation and inhibition in all brain areas. If it can be said that one area relies more heavily on inhibitory transmission than any other, then area CA2 may qualify as a winner of the contest. In comparison to areas CA1 and CA3, there are very few studies examining the cellular composition of hippocampal area CA2. The pyramidal neurons in this region have larger soma than CA1 and dendritic arborizations that more closely resemble CA3 pyramidal neurons, except that CA2 pyramidal neurons lack the distinctive thorny excrescences that form the post-synaptic contact with mossy fibers from dentate granule cells (Ishizuka et al., 1995). There is some functional evidence that deep and superficial CA2 pyramidal cells have different firing properties during exploration (Kay et al., 2016; Oliva et al., 2016a,b). However, the cellular properties and circuitry allowing this difference to emerge are unknown.

Several anatomical studies have shown that area CA2 has the highest density of several classes of interneurons in the hippocampus in both rodents and primates. The remarkable density of parvalbumin-positive (PV+), and calbindin-positive cells in primate hippocampal CA2 was first reported in 1991 (Leranth and Ribak, 1991). A thorough and elegant study used alpha-actinin-2 and PCP4 to define the boundaries of CA2 in rat hippocampal sections, and carefully quantified the density of interneurons labeled with a large panel of markers in all the strata of all CA regions (Botcher et al., 2014). This study demonstrated that the density of both PV+ and Reelin-positive neurons were highest in *Stratum oriens* (so) of CA2, and that PV+, Reelin+ and Calbindin+ cells were the highest density in *Stratum pyramidale* (sp), as compared to areas CA3 and CA1. The high density of PV+ cells bodies in sp and so was also observed in mice using RGS14 staining as a boundary to define CA2 (Piskorowski and Chevaleyre, 2013). The morphology and physiological properties of GABAergic cells in area CA2 is vastly understudied as compared to CA1, where there are at least 21 different types of interneurons (Klausberger and Somogyi, 2008). Based on morphology, two distinct populations of basket cells have been identified in area CA2 (Mercer et al., 2007). Of these two classes, one closely resembles the basket cells of CA1, staining positive for either PV or CCK, with narrow spiny dendrites and axons that are restricted to nearby sp. The other class of basket cells were strikingly different, with long horizontal dendrites and extensive axonal arbors that extended far into CA1, CA2, and CA3 (Mercer et al., 2007). The bistratified cells in CA2 also displayed important differences from the bistratified cells in CA1. CA2 bistratified cells are PV+ and have dendrites that extend through so and sr without entering slm, entering into neighboring CA1 and CA3. The axons show a remarkable subfield preference, extensively innervating CA2 and CA1, but stopping abruptly at the CA3 border (Mercer et al., 2007). There is also a unique interneuron subtype that has been identified in area CA2, called SP-SR interneurons (Mercer et al., 2012). Similar to bistratified cells, these cells have soma in sp, and extend dendrites into so and sr. The axons of these cells, however, form dense arborizations that are restricted to sr (Mercer et al., 2012). These cells are not immunopositive for PV or CCK, and have intrinsic properties that are similar to basket cells. Thus, compared to hippocampal area CA1, the GABAergic interneurons are not well studied. However, what has been discovered reveals that this region has a distinctive local inhibitory network that can readily be recruited by intra-hippocampal inputs.

One of the remarkable aspects of the local CA2 network is the large magnitude of feed-forward inhibition that is recruited by CA3 input stimulation, especially compared to the amount of inhibitory transmission recruited in area CA1 (**Figure 1**). We postulate that the large density of interneurons in area CA2 allows for this large amount of feedforward inhibition that nearly entirely shunts the excitatory transmission when the cells are held at physiological resting membrane potentials. When GABA-ergic transmission is blocked, the excitatory transmission at the CA3-CA2 synapse is comparable to the CA3-CA1 synapse (Chevaleyre and Siegelbaum, 2010). Thus, when CA2 and CA1 are examined with the same method in acute hippocampal slice, there is an intriguing and important difference in the E/I ratio in these two regions with CA3 excitation. Furthermore, high-frequency stimulation of CA3 input readily results in action-potential firing in CA1 with inhibition intact. However, quite the opposite is true in area CA2, with high frequency trains resulting in a net hyperpolarization of the membrane potential.

Another puzzling property of CA2 pyramidal neurons that is independent of the local inhibitory network is the resistance of these cells to activity-induced long-term potentiation (LTP) at the excitatory CA3-CA2 synapse. This property was first uncovered and demonstrated in-depth by Zhao et al. (2007). Furthermore, it has since been established that this is due to the unique of expression of the regulator of g-protein signaling 14 (RGS14) (Lee et al., 2010; Evans et al., 2018) and calcium extrusion and buffering (Simons et al., 2009). This discovery and mechanism were quite puzzling given the important role of NMDA-mediated LTP in learning and memory in the hippocampus (McHugh et al., 1996, 2007; Poo et al., 2016).

So what gives? How can an entire hippocampal region be devoid of synaptic plasticity? While the glutamatergic synapses between CA3 and CA2 are resistant to activity-dependent plasticity, it is now clear that the inhibitory synapses in area CA2 express activity-induced synaptic plasticity that can powerfully shift the balance of excitation and inhibition and allow CA2 pyramidal neuron action potential firing. Specifically, there are two separate mechanisms allowing activity dependent long-term depression of GABAergic transmission (iLTD) in area CA2. One is mediated by the activation of delta-opioid receptors (DORs), and the

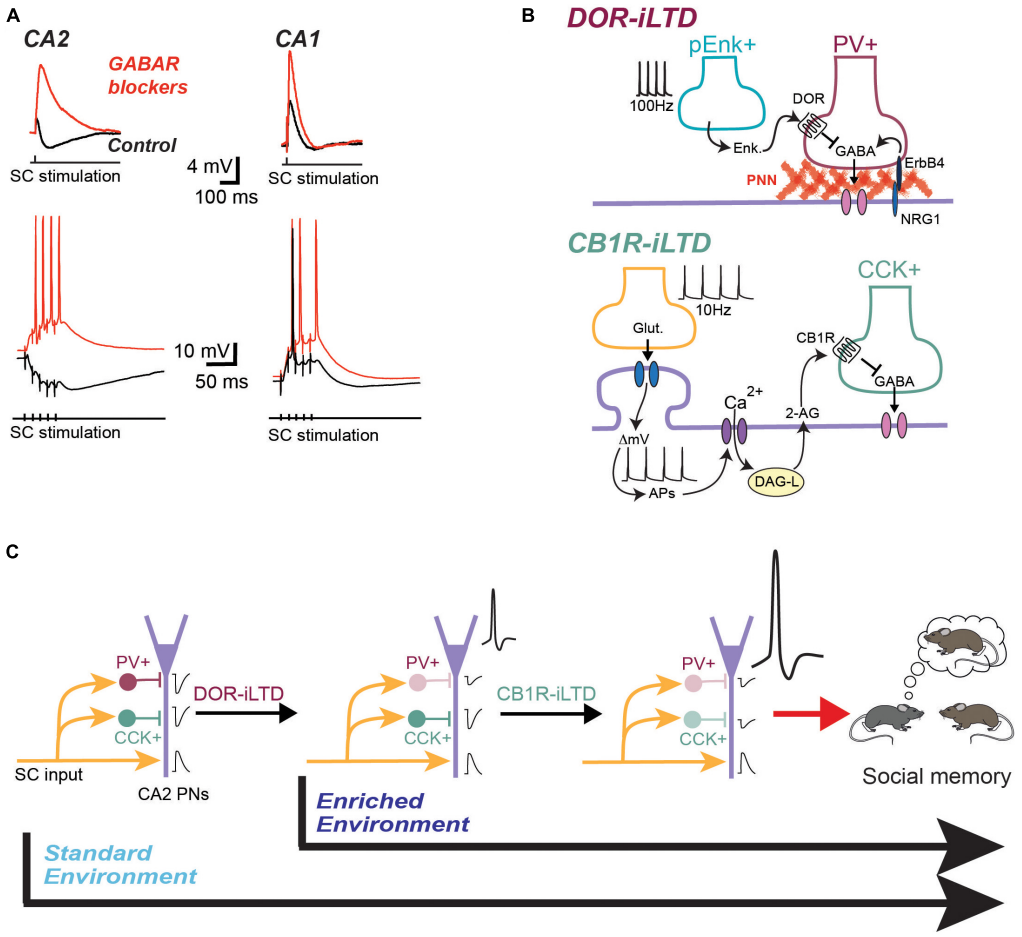

FIGURE 1
CA2 pyramidal cells receive a massive feed-forward inhibition that is plastic and modulated by environmental enrichment. **(A)** Exemple traces of synaptic responses recorded in CA2 and CA1 PN in response to CA3 input stimulation. In control condition (black traces) the inhibitory component almost completely shunts the EPSP in CA2 PNs. The inhibitory component is even more obvious during a train of stimulation of CA3 inputs. when inhibitory transmission is blocked (red traces), the EPSP becomes much larger and CA2 PN can easily fire action potentials during a train of stimulation. **(B)** Model for the DOR-iLTD and CB1R-iLTD expressed in area CA2. Top: DOR-plasticity is expressed by PV+ IN. It requires the release of enkephalins and activation of DOR located on PV+ terminals. It is also dependent on positive control of GABA release by the interaction between ErbB4 and Neureguline 1 (NRG1). This interaction is itself dependent on the PNN located around the soma of PNs. Bottom: CB1R-iLTD is expressed by CCK+ IN following activation of CB1R by the eCB 2-AG. 2-AG is released by calcium increase in the PN following stimulation of CA3 inputs and action potential firing by the PN. **(C)** Two-step model for the involvement of inhibitory plasticity in social memory formation. In mice raised in a standard environment, DOR-iLTD is induced following a single social interaction with a novel mouse. The resulting decrease in inhibition allows PNs to fire action potentials. This in turn allows the induction of CB1R-iLTD, a plasticity that is induced after several interactions with the novel mouse. Blocking CB1R in CA2 completely prevents social memory formation. In an enriched environment, DOR-iLTD is occluded and thus already induced during the enrichment. In this environmental condition, it is likely that social memory formation only requires CB1R-iLTD.

other by cannabinoid type I receptors (CB1Rs). Importantly, there is evidence that both of these plasticities play a role in social recognition memory. How is this possible? Hippocampal CA2 pyramidal neurons project strongly to ventral hippocampal CA1 (Meira et al., 2018), a region that has been demonstrated by several studies to be important for social memory encoding (Okuyama et al., 2016; Rao et al., 2019; Tsai et al., 2022). By tightly regulating CA2 pyramidal neuron output, synaptic plasticity of inhibitory transmission in area CA2 results in an enhanced excitatory drive onto CA1 with CA3 activity (Nasrallah et al., 2015, 2019). CA1 pyramidal neurons provide an important output to the hippocampus, projecting to cortical regions that are also very important for social discrimination. Furthermore, CA2 pyramidal neurons also project to extra-hippocampal structures, including hypothalamic nuclei and the septum (Cui et al., 2013; Hitti and Siegelbaum, 2014; Leroy et al., 2018). These structures, are playing central roles in social cognition and complex behaviors (Walsh et al., 2021; Wu et al., 2021; Griguoli and Pimpinella, 2022).

2.1. Parvalbumin-expressing interneurons and DOR-mediated iLTD

The DOR-mediated iLTD that occurs in hippocampal area CA2 is specific to a subset of PV+ inhibitory neurons (Piskorowski and Chevaleyre, 2013). This was determined by selective expression of channelrhodopsin in PV+ interneuron and using light to evoke an inhibitory synaptic current while recording from CA2 pyramidal

cells in voltage clamp mode. Following the application of a selective DOR agonist, the light-evoked PV-specific transmission underwent an iLTD. The same experiments performed in area CA1 resulted in a transient depression of inhibitory transmission, indicating that the DOR-mediated iLTD seen in area CA2 does not occur in CA1. It was reported later, however, that CA3 pyramidal neurons express a DOR-iLTD that is similar to area CA2 (Domínguez et al., 2019). Further evidence that the DOR-iLTD is exclusive to PV+ interneurons came from experiments in which GiDREADDs were expressed exclusively in PV+ cells. Inhibition of PV+ cells by CNO application entirely prevented induction of DOR-iLTD (Nasrallah et al., 2019). The DOR-iLTD is entirely pre-synaptic, with activation of the receptors resulting in reduced GABA release (Piskorowski and Chevaleyre, 2013). There is evidence that the resulting decrease in GABA release probability also depends on a trans-synaptic signaling between pyramidal neurons and PV+ interneurons through activation of the ErbB4 receptor located on PV+ terminals by Neuregulin 1 (Domínguez et al., 2019). This signaling is dependent on the integrity of the highly unusual and specialized perineuronal net (PNN). In many brain regions, PV+ interneurons are encased in PNNs, which are thought to regulate synaptic formation (Fawcett et al., 2019) and reduce oxidative stress (Cabungcal et al., 2013). However, in area CA2, the role of the PNN may be more complex, as this specialized extracellular matrix surrounds both PV+ interneurons as well as CA2 pyramidal cells. Furthermore, in contrast to inhibitory synapses, it has been shown the presence of the PNN in area CA2 also acts to prevent plasticity at glutamatergic synapses on CA2 pyramidal neurons (Carstens et al., 2016).

Evidence has been presented that enkephalin, the endogenous ligand for DORs, is potentially released by local vasoactive intestinal peptide-expressing (VIP+) interneurons (Leroy et al., 2017). DOR-iLTD can be induced by high-frequency, theta burst and 10 Hz stimulation of CA3 inputs (Piskorowski and Chevaleyre, 2013). Furthermore, a DOR-mediated iLTD in area CA2 has also been proposed to be inducible by a narrowly timed pairing of CA3 and distal cortical input activity, called input timing dependent plasticity (ITDP) (Leroy et al., 2017). Thus, the VIP+ cells releasing enkephalin are likely receiving input from both CA3 and cortical terminals.

There is evidence that the DOR-mediated iLTD in area CA2 contributes to social memory formation but may not be absolutely required. Selective removal of DORs in area CA2 does impair social recognition memory as tested by a 5-trial dishabituation task (Domínguez et al., 2019). In this experiment, the mice explored a familiar mouse more on the second and third exposure, but less on the fourth, indicating that with enough trials, social memory formation could occur. Similar results were observed with localized infusion of DOR-receptor antagonist into areas CA2 and CA3 (Leroy et al., 2017). Likewise with localized digestion of the PNN in area CA2, which prevents DOR-iLTD, social recognition memory was impaired, but not completely abolished (Domínguez et al., 2019). Interestingly, it was observed that the PV+ inhibitory network undergoes a maturation in area CA2 in late adolescence/early adulthood, with both the DOR-iLTD and basal ErbB4 activation emerging at ∼5 weeks after birth, around when mice start to display preference for novel conspecifics (Domínguez et al., 2019). Interestingly, though, it has been shown that very young mice need functional hippocampal CA2 activity in order to differentiate their mother from other female conspecifics (Laham et al., 2021). Thus, from these data, it seems that GABAergic plasticity at PV+ neurons in area CA2 may contribute to social memory formation but is clearly not the only mechanisms at play.

The PV+ interneurons in hippocampal area CA2 receive very strong excitatory input from the hypothalamic supramammillary nucleus (SuM) (Robert et al., 2021). This hypothalamic nucleus targets specifically the dentate gyrus and hippocampal area CA2 (Haglund et al., 1984). Strongly activated by novelty (Wirtshafter et al., 1998; Ito et al., 2009) and locomotion (Farrell et al., 2021) the SuM sends two separate projections to the dentate gyrus and hippocampal area CA2 (Chen et al., 2020). The SuM cells that project to area CA2 show increased c-fos and action potential firing with social novelty exposure. Furthermore, optogenetic activation of the CA2-projecting SuM cells increases the exploration of familiar conspecifics, supporting the hypothesis that this input conveys a novelty signal (Chen et al., 2020). Use of optogenetics and acute hippocampal slices revealed that the SuM input stimulation drives a very strong feed-forward inhibition onto CA2 pyramidal cells that not only controlled the intrinsic firing properties of CA2 pyramidal cells, but also had a significant impact on area CA1 activity via CA2 (Robert et al., 2021). Many experiments in this work provide evidence that PV+ interneurons are the primary target of the SuM hypothalamic inputs, and that the same cells that undergo the DOR-iLTD are also receiving SuM input. Thus, the PV+ neurons in area CA2 may not only be regulating the input from CA3 but are also clearly playing an important role in gating extra-hippocampal hypothalamic inputs.

2.2. Endocannabinoid-mediated depression of inhibitory transmission in area CA2, CCK+ interneurons

It has recently been reported that endocannabinoid-mediated synaptic plasticity is playing an important role in hippocampal area CA2 function. This plasticity results from the release of endocannabinoids (eCBs) by CA2 pyramidal cells and activation of cannabinoid type 1 receptors (CB1Rs) located on GABA-ergic terminals (Loisy et al., 2022). As established in CA1, the CB1Rs are likely expressed by CCK+ interneurons in area CA2. This is supported by the observation that blocking N-type calcium channels involved in GABA release from CCK+ terminals prevented this plasticity and that the chemogenetic silencing of PV+ interneurons did not alter CB1R-mediated plasticity (Loisy et al., 2022). The mechanism underlying the plasticity CB1R-iLTD in area CA2 is very different from what has been found in area CA1 (**Figure 1B**; Chevaleyre and Castillo, 2003). In CA1 pyramidal cells, the release of eCB is induced by the activation of type-I metabotropic glutamatergic receptors, activation of phospholipase C, leading to diacylglycerol (DAG) and activation of DAG-lipase activation, which results in release of the endocannabinoid 2-Arachidonoylglycerol (2-AG). This plasticity is extremely localized to the dendritic region surrounding the CA3 terminals responsible for the post-synaptic activation of mGluR-I, making this iLTD very input-specific. However, it will also likely occur on neighboring inhibitory synapses of CA1 pyramidal cells sharing the same CA3 input (Chevaleyre et al., 2006). In CA2 pyramidal cells, action

potential firing of the pyramidal cell alone is sufficient to allow sufficient calcium entry though voltage-activated calcium channels to lead to the activation of DAG-lipase and release of 2-AG along the entire dendritic arbor. Thus, this eCB-mediated iLTD is not input specific, as all GABAergic inputs with CB1Rs will undergo iLTD. However, it is very cell-specific, allowing only the CA2 pyramidal cells that were sufficiently recruited by synaptic input to fire action potentials to undergo further amplification, thus rising above the noise and having a stronger influence on the hippocampal network (Loisy et al., 2022). Thus, normally, as shown in **Figure 1**, CA3 input stimulation results in a large hyperpolarization of CA2 pyramidal cells because of recruited feed-forward inhibition from the PV+ network, and the eCB plasticity does not occur. However, following prior induction of DOR-iLTD, CA2 pyramidal cells can fire action potentials with CA3 stimulation (Nasrallah et al., 2015, 2019). The requirement of AP firing by CA2 pyramidal cells leads to a two-steps model where DOR-iLTD of the PV+ network is permissive for the induction of CB1R-iLTD (**Figure 1C**). Critically, this model also suggests that CB1R-plasticity may be enabled after any physiological change that enables AP firing in CA2 pyramidal cells, whether is it through a decrease in inhibitory transmission (i.e., iLTD), an increase in excitatory transmission (i.e., LTP) or a change in pyramidal cell intrinsic excitability by neuromodulators such as oxytocin (Tirko et al., 2018).

We hypothesize that the eCB-iLTD is critical and necessary for area CA2 to allow for social memory formation, and likely playing a more prominent role than the DOR-iLTD. The DOR-mediated iLTD was found to be occluded after a single social interaction (Leroy et al., 2017; Loisy et al., 2022). However, as mentioned earlier, blocking DOR-iLTD by several strategies only impedes social memory formation, but does not prevent it. In contrast, CB1R-iLTD is occluded after four social interactions (Loisy et al., 2022). Furthermore, social memory formation was shown to be completely impaired even after 4 presentations of a familiar conspecific when CB1 R antagonist was locally infused into area CA2 (Loisy et al., 2022). Additional evidence for the central importance of the CB1R-iLTD in social memory comes from the recent finding that DOR-plasticity cannot be induced after mice have spent 3 weeks in an enriched environment (EE) (Loisy et al., 2023). In fact, we postulate that the DOR-iLTD is occluded after EE. Evidence for this come from the reduced GABA release and neither DOR activation or ErbB4 block (two pathways that modulate GABA release from PV+ INs) have significant effect on GABA transmission in EE-housed mice. It is well-established that 3 weeks in an EE environment enhances many aspects of hippocampal-dependent learning, improving performance in numerous animal models of neurodegenerative and psychiatric disorders (Hannan, 2014). Interestingly, DOR-plasticity can be induced in EE-housed animals following 24 h of social isolation (Loisy et al., 2023). Thus, it is possible that he PV+ inhibitory network in area CA2 may be linked to internal state. When mice are stressed or raised in an impoverished environment, transmission from PV+ INs increases, thus allowing DOR-iLTD to be induced and preventing the recruitment of CA2 pyramidal cells by CA3 activity. CA2 pyramidal cells do not fire action potentials and social recognition memory is impaired. This is in fact what is seen when social recognition memory is tested in socially isolated animals (Kogan et al., 2000). Thus, as numerous psychiatric disorders and neuropathologies are linked to stress-induced worsening of symptoms, it seems fitting that the inhibitory network in area CA2 will be compromised.

3. Alterations of inhibitory transmission in area CA2 during pathological states

Given the critical role of inhibitory transmission and plasticity in controlling pyramidal cell firing in area CA2, it is not surprising that inhibitory transmission has been found to be altered in several neurodevelopmental and neurodegenerative diseases (Chevaleyre and Piskorowski, 2016). While most early findings on area CA2 where derived from studies on human tissue (Williamson and Spencer, 1994; Benes et al., 1998), recent evidence using mouse models of diverse pathologies have provided a more detailed descriptions of the alterations present in area CA2. In the following sections, we summarize the changes that are observed in area CA2 during several pathologies where the function of inhibitory networks is clearly impaired.

3.1. Multiple sclerosis

Multiple sclerosis (MS) is an autoimmune disease often associated with severe cognitive symptoms including deficits in social cognition and facial emotion recognition. Interestingly, these symptoms can be observed early in the disease progression, even before appearance of other cognitive symptoms (Pöttgen et al., 2013). Some of the deficits have been linked to a structural and functional disconnection of the hippocampus from several brain networks, a change that might result from an aberrant loss of synapse during synaptic pruning and extensive demyelination. Components of the complement such as C1q and C3, which are part of the immune system, have been implicated in the process of pruning during development but also in re-shaping neuronal networks during forgetting in adults (Schafer et al., 2013; Wang et al., 2020). In the hippocampus of post-mortem MS patients, the C1q and C3 components accumulate predominantly in the CA2/3 area at synapses that are engulfed by microglial processes (Michailidou et al., 2015). C1q accumulation in CA2 was also shown to be higher in patients with cognitive impairment compared to those with normal cognition (Ramaglia et al., 2021). Using the cuprizone model of demyelination, this study also characterized the changes occurring in area CA2 (**Figure 2A**). C1q accumulation was larger in the CA2 pyramidal layer and was colocalized with inhibitory synapses engulfed by microglia/macrophages. Stimulation of CA3 input led to normal excitatory transmission but feed-forward inhibitory transmission was strongly reduced. In agreement with a loss of inhibitory synapses, a decrease in the number of puncta for the GABA transporter VGAT was also observed in the pyramidal layer. However, pyramidal cells fire less action potentials in response to trains of stimulation of CA3 inputs (in presence of blockers of GABA transmission) and to depolarizing steps. Pyramidal cells also display a larger sag during hyperpolarizing steps, indicating an increase in the current mediated by HCN channels. Finally, in

agreement with the impaired inhibition and CA2 pyramidal cell excitability, this study reported that social recognition memory was strongly impaired in this mouse model of MS. Altogether, this study reveal how accumulation of the C1q component of the complement in area CA2 can result in memory deficits in mice but also potentially in humans.

3.2. Autism spectrum disorders

Autism spectrum disorders (ASD) include neurodevelopmental diseases characterized by deficits in verbal and non-verbal communication, stereotyped behaviors and impaired social cognition. Many genes involved in synaptic function have been linked to the development of ASD, including mutations or deletions in genes encoding for Neuroligins (NGLs). NGLs are expressed by the postsynaptic elements and interact with their presynaptic partners Neurexins. Mice lacking NGL3 have been used as a model for a non-syndromic form of autism and NGL3 KO mice display strong deficits in social behaviors.

Using electrophysiological recordings *in vivo* and *ex vivo*, a recent study performed with these mice has focused on the potential alterations in hippocampal area CA2 (Modi et al., 2019). First, using extracellular recordings *in vivo*, this study reported a significant reduction in oscillatory activity in the theta and gamma frequencies in both areas CA3 and CA2, as well as a more specific decrease in the amplitude of local field potential oscillation recorded in CA2. Using juxtacellular recordings of putative pyramidal cells, a large increase in spike frequency as well as bursting activity was reported in area CA2 but not in CA3. This data suggested an increased excitability specific to CA2 pyramidal cells (**Figure 2B**).

To address more precisely the change in CA2 activity, the authors used whole cell recordings in hippocampal slices. These experiments revealed that the frequency but not the amplitude of isolated spontaneous EPSCs (recorded in presence of blockers of GABA transmission) was increased in CA2 pyramidal cells (Modi et al., 2019). Conversely, isolated spontaneous IPSCs frequency (but not amplitude) recorded in CA2 pyramidal cells was decreased in NLG3 KO mice. To address which class of interneuron might be responsible for the decrease in inhibitory drive, the authors used the fact that GABA release from PV+ and CCK+ interneurons is mediated by different calcium channels (respectively, P/Q and N types). They found that the component of evoked IPSCs abolished by a blocker of N type channels was strongly reduced in NLG3 KO mice, while the component of IPSCs dependent on P/Q type channel was unaltered. These data indicated that inhibitory transmission from CCK+ INs, but not from PV+ INs, was reduced in the NLG3 KO mice. However, quantification of PV+ and CCK+ puncta in the pyramidal layer of CA2 suggested that the number of synapses from these 2 classes of interneurons was not altered, suggesting that the reduced inhibitory transmission resulted from a decrease in GABA release probability and not from a reduced number of synapses.

Finally, this study also shows that NLGN3 KO have a deficit in social memory formation, i.e., they spend the same amount of time exploring a novel and a familiar mouse. However, while these mice might indeed have an impairment in the capacity to remember a conspecific, an effect that would be consistent with a disfunction in the CA2 network, caution should be taken when interpreting this result. Indeed, the same study clearly showed that NLGN3 KO mice also have a deficit in sociability, an effect that could potentially result from a deficit in olfactory functions as described previously in a NLGN3-deficient mice (Radyushkin et al., 2009). Thus, it is unclear whether the apparent lack of social memory results from an impairment in remembering a familiar conspecific, or just from a general alteration in sociability. In any case, this study convincingly shows that alteration in CA2 inhibitory transmission from a specific class of interneuron can result in more global disfunction of the CA2 network, thus likely contributing to some of the hippocampal-dependent phenotypes observed in this mouse model of ASD.

3.3. Alzheimer's disease

Alzheimer's disease (AD) is a neurodegenerative disease leading to dementia in the elderly population. Symptoms include impairments in acquisition and retrieval of memories that are linked to alterations in hippocampal function (Hirjak et al., 2017). In particular, the inability to remember and recognize other individuals, including family members, is a particularly strong burden on patients. This deficit in social recognition memory suggested that area CA2 might be altered during AD (**Figure 2C**). Indeed, the largest and earliest decrease in INs expressing PV and surrounded by the PNN in the hippocampus is observed in area CA2 of the Tg2576 mouse model of AD (Cattaud et al., 2018).

A recent study focused on area CA2 has shown that PV+ and PNN+ cell density is strongly reduced in area CA2. This was accompanied by a large decrease in inhibitory transmission between CA3 and CA2, leading to a large increase in EPSP amplitude and the emergence of action potential firing in CA2 PNs in response to CA3 input stimulation. Impaired inhibitory transmission from PV+ interneurons likely contribute to the reduced inhibitory transmission because DOR-iLTD as well as the DOR-mediated disinhibitory increase in PSP amplitude was strongly reduced in this mice. In agreement with a role of this plasticity in social memory formation, social recognition memory was completely abolished in Tg2576 mice.

Interestingly, degradation of the PNN following ChABC injection in area CA2 also completely prevented social memory formation (Domínguez et al., 2019; Rey et al., 2022). The PNN in area CA2 was previously shown to be required not only for social memory formation, but also for the induction of DOR-iLTD onto PV+ IN, likely by allowing a *trans*-synaptic signaling through interaction between the Neuregulin 1 (expressed by PNs) and its receptor ErbB4 expressed by PV+ INs (**Figure 1**). degradation of the PNN prevents the positive control of ErbB4 on GABA release probability, a mechanism that could potentially underly the decreased inhibitory transmission in Tg2576 mice. Accordingly, restoring activation of the ErbB4 receptor via a local injection of NRG1 in area CA2 was found to also restore some of the deficits observed in Tg2576 mice. Not only PV and PNN expression were found to be normalized after NRG1 injection, indicating that PV+ INs were not dead but just expressing less PV, but also social memory formation was completely rescued. While inhibitory

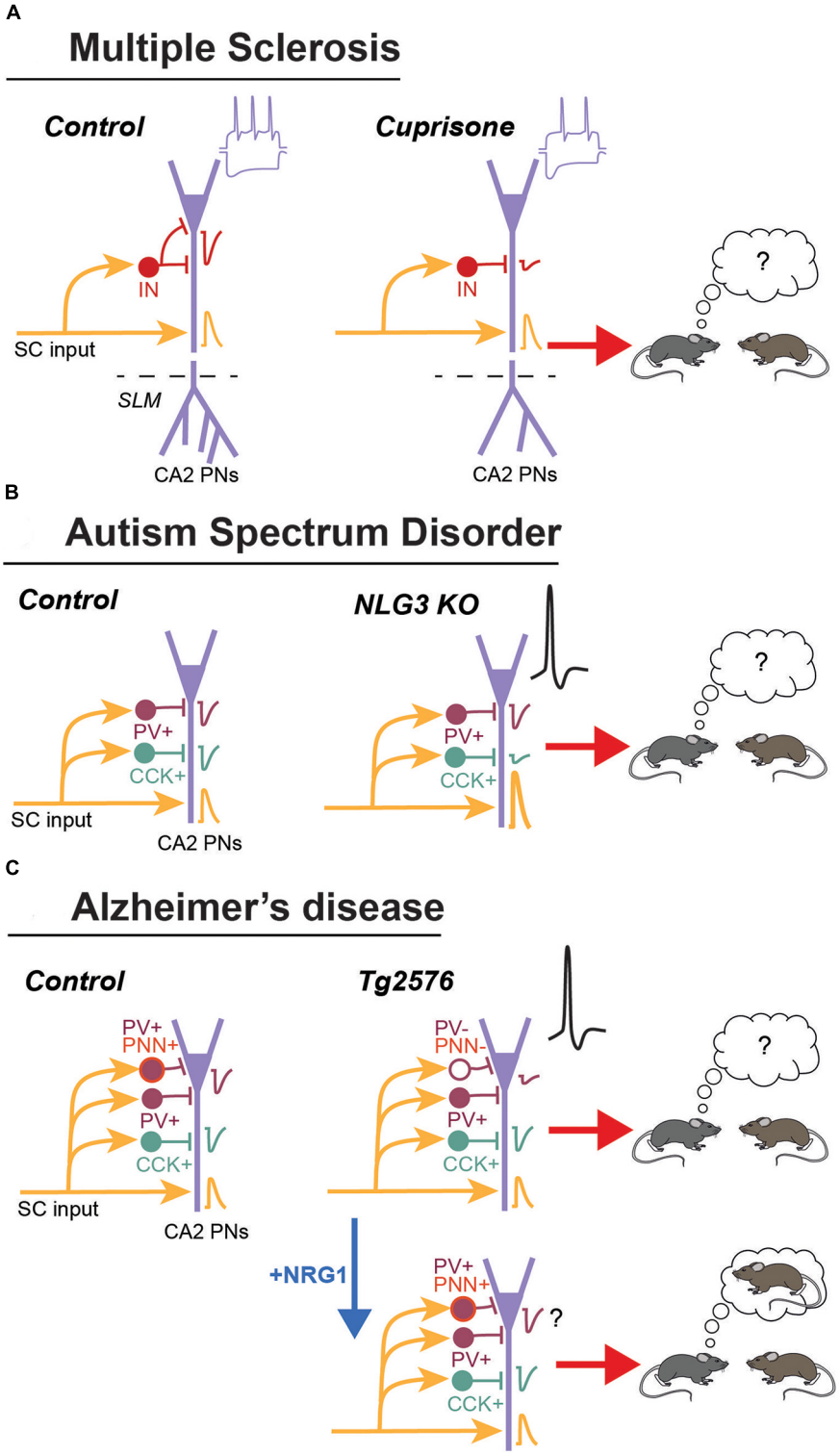

FIGURE 2
Summary of the main changes observed in area CA2 during MS, ASD and AD. **(A)** In the cortisone mouse model of demyelination. These mice display an accumulation of the C1q component of the complement around inhibitory synapses in CA2. Excitatory transmission from CA3 (Shaffer collaterals: SC) is normal but inhibitory transmission is reduced. The distal dendritic branching is also reduced. Pyramidal neurons have and increased sag during hyperpolarization and fire less action potential. This lower PN excitability could explain the deficit in social memory formation. **(B)** In the Neuroligin 3 KO mice, excitatory transmission for CA3 is increased. Inhibitory transmission from CCK+ but not from PV+ IN is reduced. This resulted in an increased excitability and bursting activity of PNs *in vivo*. This mice have a deficit in social memory formation. **(C)** In the Tg2576 mouse model schizophrenia, there is a decrease in PV and in the PNN expression. This could explain the decrease in inhibitory transmission and DOR-plasticity, as well as the large increase in action potential firing by PNs. This mice display a strong deficit in social memory formation. Injection of Neuregulin 1 in area CA2 restores PV and PNN expression, as well as social memory formation.

transmission and plasticity was not tested after NRG1 injection, one can speculate that increasing ErbB4 receptor activation in PV+ INs will also restore GABA release probability and induction of DOR-iLTD from PV+ cells, hence re-allowing the emergence of sequential inhibitory plasticities and the formation of social recognition memory.

Independently of the exact mechanism engaged following NRG1 injection, it is striking to consider that in a pathology affecting many brain structures, a manipulation of excitability specifically in area CA2 was sufficient to fully restore the formation of social memory in Tg2576 mice. This further strengthen the critical role of this area and of inhibitory transmission and plasticity in the formation of social memory in the normal brain, but also the contribution of this area in the development of cognitive symptoms in pathologies leading to impairments in social cognition. It is also interesting to note that a transient exposure of Tg2576 mice to and enriched environment had lasting beneficial effect on PV/PNN expression and memory formation. Although social memory was not tested after enrichment in Tg2576 mice, one can speculate that it could also be improved, once again though a normalization of PV+ IN synaptic transmission and DOR-mediated plasticity (Cattaud et al., 2018).

3.4. Epilepsy

One of the earliest study on area CA2 revealed that this region might play an important role in the pathology of epilepsy (Williamson and Spencer, 1994). Performed on hippocampal samples from epileptic patients, this study revealed that the vast majority of CA2 PNs recorded in current clamp display no apparent inhibitory transmission. The same study also observed an excitatory transmission between granule cell mossy fiber's axons and CA2 PNs in epileptic tissues from medial temporal lobe sclerosis patients but not from tumor-associated temporal lobe epilepsy patients. Other studies also performed in human tissue from epileptic patients confirmed the important decrease in spontaneous inhibitory transmission (Wittner et al., 2009) and the sprouting of mossy fiber terminals (Arellano et al., 2004; Freiman et al., 2021) with the appearance of excitatory synapses on the soma of CA2 PNs resembling mossy fiber boutons (Wittner et al., 2009). Several studies from human tissues also observed that the density of PV+ IN was reduced in area CA2 of epileptic samples (Arellano et al., 2004; Andrioli et al., 2007; Wittner et al., 2009), and this decrease was ascribed potentially to a reduced expression of PV by INs rather than their death (Wittner et al., 2009).

Subsequent studies performed on mouse models of Temporal Lobe Epilepsy (TLE) have confirmed key data observed in human tissues from epileptic patients and also provided a detailed description of the anatomical and functional changes observed in area CA2 during the course of the disease. Specifically, aberrant mossy fiber sprouting in area CA2 was observed in the kainate mouse model of TLE (Häussler et al., 2015; Freiman et al., 2021). This extra connectivity is likely functional as *in vivo* recording revealed epileptic activities in CA2 that were shortly preceded by epileptic activities in the dentate gyrus (Häussler et al., 2015). Subsequent studies using unilateral kainate injection has shown that CA2 plays an active role in the generation of epileptic activity and in the propagation of these activity to the non-sclerotic contralateral hippocampus, including the contralateral CA2 (Kilias et al., 2022). Another study performed on the Pilocarpine mouse model of epilepsy confirmed that DG-CA2 PN excitatory transmission was increased and that feed-forward inhibitory transmission from CA3 and from CA2 recurrent connections were decreased (Whitebirch et al., 2022). Furthermore, reducing the hyper-excitability of CA2 PNs following inhibitory DREADD expression in Amigo2-cre+ mice was sufficient to reduce the number but not the duration of convulsive seizures in pilocarpine treated mice (Whitebirch et al., 2022).

Epilepsy has long been thought to result from an imbalance between excitation and inhibition. Although anatomical and functional changes have been observed in all hippocampal areas, CA2 is unique in that it is much more resistant to cell death in comparison to area CA1 or CA3. Furthermore, while acutely reducing inhibitory transmission in rodent hippocampal slices was by itself sufficient to trigger the generation of epileptic-like activities that originated in area CA2 (Wong and Traub, 1983; Knowles et al., 1987), it is likely that both the increased excitatory drive from mossy fiber sprouting and the reduced inhibitory transmission cooperate in the generation of spontaneous interictal-like activity observed in area CA2 of TLE patient (Wittner et al., 2009). Therefore, both an increase in excitation and a decrease in inhibition in this region contribute to strongly shift the E/I balance toward a hyper-excitable and pathological state (**Figure 3A**).

3.5. Schizophrenia and the 22q11.2 deletion syndrome

Early studies on post-mortem hippocampal tissues from schizophrenic patients have reveal that CA2 is uniquely altered. In particular, a large decrease in the density of interneurons was reported in area CA2 during schizophrenia (Benes et al., 1998; Zhang and Reynolds, 2002). A meta-analysis reported that a decrease in PV+ INs in area CA2 was one of the very few parameters significantly changed in the hippocampus during schizophrenia (Knable et al., 2004).

A decrease in interneuron density in area CA2 was also reported in several rodent models of schizophrenia. One model consists in transiently over-activating the basolateral amygdala (BLA) inputs that project to the basal dendrites of CA2 and CA3 pyramidal cells. This manipulation during adolescence results in a lasting decrease in the density of interneurons expressing PV, calretinin and calbindin located in *Stratum oriens* of CA2 and CA3 (Gisabella et al., 2009). The density of basket terminals arising from PV+ interneurons was also reduced. This anatomical changes were accompanied by a decrease in both spontaneous inhibitory currents and IPSCs evoked by stimulation in *Stratum radiatum* (Gisabella et al., 2005). Furthermore, these studies also show that the intrinsic properties of remaining interneurons in so were altered. In particular, an increase in 1h (current that mediates the sag observed during hyperpolarization of the cell), a decrease in action potential duration and an increase action potential firing frequency were observed following over-activation of the BLA (Gisabella et al., 2009).

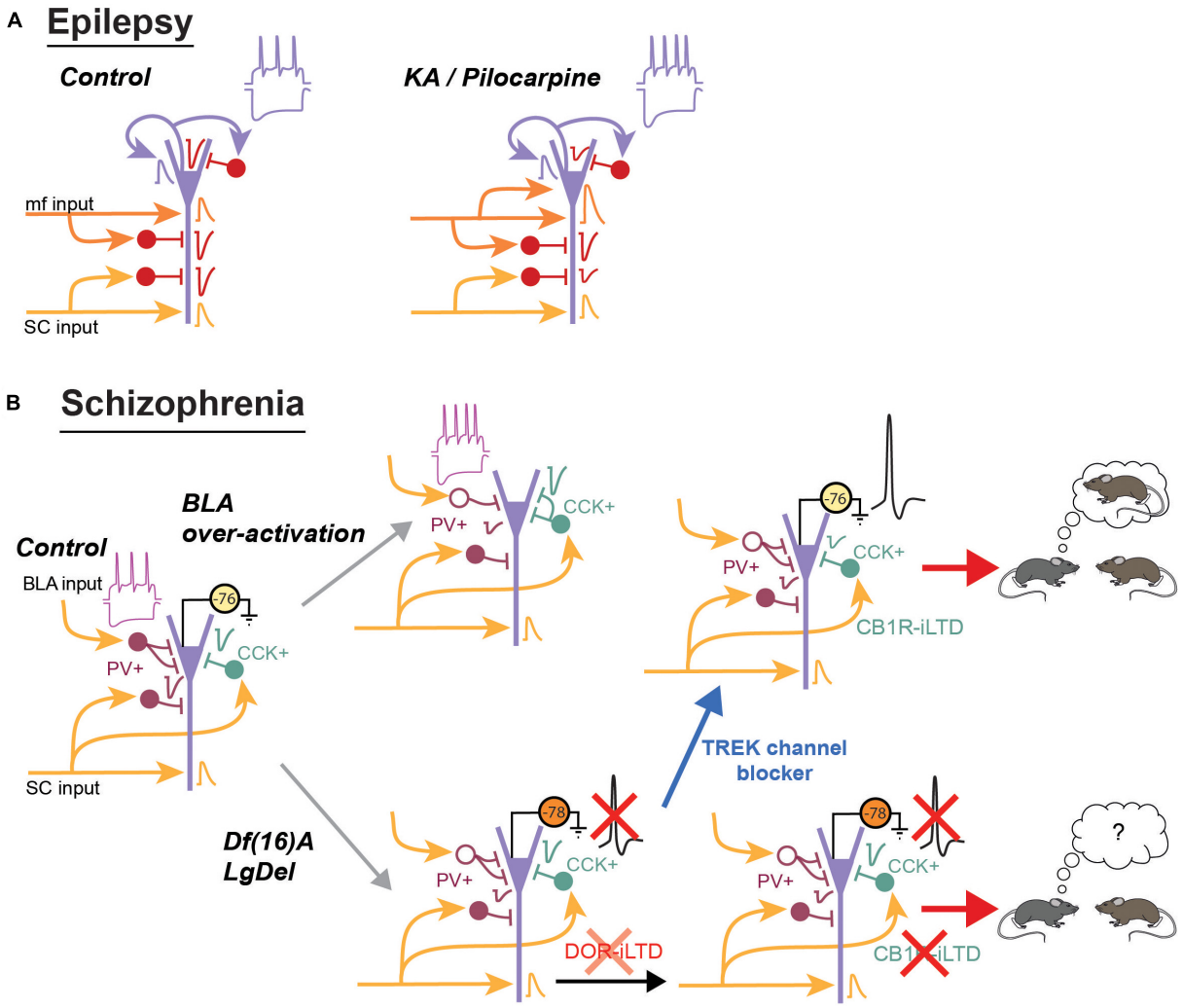

FIGURE 3
Summary of the main changes observed in area CA2 during schizophrenia and epilepsy. **(A)** In the kainate model of epilepsy, there is a sprouting of the mossy fibers terminals in area CA2 and *in vivo* recordings indicate an increased connectivity between the dentate gyrus and CA2. In the pilocarpine mouse model, excitatory transmission from the dentate gyrus is increased. Conversely, feed-forward inhibitory transmission from CA3 and from CA2 is reduced. PNs also have an increased sag during hyperpolarization and fire more easily action potentials. **(B)** The mouse model of schizophrenia resulting from over-activation of the BLA display a decrease in PV expression and inhibitory transmission. The number of PV+ terminals is also reduced while the number of CCK+ terminals is increased. IN in SO display an increase in their sag and an increase in action potential firing frequency. In the Df(16)A or LgDel mouse model of schizophrenia, the number of PV+ IN is reduced and inhibitory transmission is decreased. DOR-iLTD is reduced and because PNs are also more hyperpolarized, they do not fire action potentials following DOR-plasticity. As a consequence, CB1R-iLTD is also strongly reduced. Blocking TREK channels depolarizes PNs and allow them to fire action potentials. This depolarization is sufficient to restore CB1R-iLTD and social memory formation.

Changes in interneuron properties have also been observed in mouse models of the 22q11.2 deletion syndrome (**Figure 3B**). This spontaneous deletion of around 30 genes is one of the highest genetic factors for schizophrenia diagnosis (Drew et al., 2011). Mice that have an equivalent genetic deletion on chromosome 16 have been generated [Df(16)A and LgDel mice]. Similar to the social cognition deficits observed in humans, Df(16)A mice have impaired social memory formation. Furthermore, they display a decreased density of PV+ interneurons in area CA2 but not in CA1 or CA3 (Piskorowski et al., 2016). This decrease in PV density was accompanied by a decrease in feed-forward inhibitory transmission from CA3 inputs, while excitatory CA3 transmission was not altered. However, despite the decrease in inhibitory transmission, CA2 pyramidal cells were found to be less likely to fire action potentials when stimulated by CA3. This is because CA2 pyramidal cells are more hyperpolarized due to an increased conductance of the TREK potassium channel that is highly expressed in area CA2 and known to control resting membrane potential (Talley et al., 2001; Honoré, 2007; Piskorowski et al., 2016). Interestingly, the decrease in PV expression, the change in membrane potential and the decrease in inhibitory transmission are age dependent: they were not altered during early adolescence (up to post-natal week 5) but started to change after this period. PV+ interneurons likely contribute to the global decrease in inhibitory transmission because DOR-plasticity is reduced in these mice. In the LgDel mice that carry a similar deletion as the Df(16)A mice, CB1R-plasticity was also shown to be impaired (Loisy et al., 2022). This impairment likely results from the reduced DOR plasticity, preventing CA3

activity from inducing DOR-iLTD in area CA2 as efficiently as in WT, and further, the resting membrane potential of pyramidal cells start from a more hyperpolarized potential, preventing action potential firing. Interestingly, if sufficient current was injected into the cells to evoke action potential firing, CA2 pyramidal cells from LgDel mice were capable of undergoing CB1R-iLTD.

In vivo recordings have shown that CA2 PNs can encode social information (i.e., distinction between familiar and novel mouse). In Df(16)A mice, this coding was impaired while spatial coding, initially weak in WT mice, was enhanced (Donegan et al., 2020). Furthermore this study also showed that increasing CA2 PN excitability by blocking TREK channels, either through unspecific pharmacological manipulation or through expression of a dominant negative of TREK channels specifically in CA2 pyramidal cells, was sufficient to rescue social memory formation in Df(16)A mice. We postulate that this rescue at least partially relied on the restoration of CB1R-plasticity by permitting action potential firing in CA2 PNs. Indeed, in a similar animal model, the acute blockade of TREK channels in slice preparation was sufficient to restore CB1R-mediated plasticity (Loisy et al., 2022).

Altogether, these data show that interneuron density is reduced in both a pharmacological and a genetic model of schizophrenia. These studies also revealed that intrinsic properties of both INs and PNs can be altered, thus resulting in specific alterations in CA2 PN activity. Schizophrenia englobes multiple pathologies and using different models might be necessary in order to reveal the different facets of this complex set of diseases.

4. Conclusion

Despite an important lag in the number of studies investigating CA2 area in comparison to the other hippocampal regions, significant progress has been made during the last decade in understanding the role of CA2 in controlling the activity and function of the hippocampus in normal conditions. Recent studies have also revealed how alterations in CA2 neurons during diverse pathological states can result in aberrant hippocampal activity and social memory deficits. Gain-of-function (assessed as an increased CA2 pyramidal cells firing such as in AD, ASD, and epilepsy) and lost-of-function (MS, Schizophrenia) have been reported and they both ultimately result in social cognition deficits. This suggests that a fine, bidirectional tuning of CA2 activity is required for the normal function of this region. Unquestionably, inhibition plays a major role in controlling CA2 pyramidal cell activity in normal condition, and alterations in inhibitory transmission and plasticity likely contributes to the deficits in hippocampal function observed during these neurodegenerative and neurodevelopmental disorders. Alterations have often been reported in PV+ and CCK+ interneurons, but other classes of interneurons are also affected. Thus, understanding the precise contribution of diverse populations of interneurons during each specific pathology is one of the challenges of future studies.

Author contributions

Both authors listed have made a substantial, direct, and intellectual contribution to the work, and approved it for publication.

Conflict of interest

The authors declare that the research was conducted in the absence of any commercial or financial relationships that could be construed as a potential conflict of interest.

Publisher's note

References

Andrioli, A., Alonso-Nanclares, L., Arellano, J., and DeFelipe, J. (2007). Quantitative analysis of parvalbumin-immunoreactive cells in the human epileptic hippocampus. *Neuroscience* 149, 131–143. doi: 10.1016/j.neuroscience.2007.07.029

Arellano, J., Muñoz, A., Ballesteros-Yáñez, I., Sola, R., and DeFelipe, J. (2004). Histopathology and reorganization of chandelier cells in the human epileptic sclerotic hippocampus. *Brain* 127, 45–64. doi: 10.1093/brain/awh004

Benes, F., Kwok, E., Vincent, S., and Todtenkopf, M. (1998). A reduction of nonpyramidal cells in sector CA2 of schizophrenics and manic depressives. *Biol. Psychiatry* 44, 88–97. doi: 10.1016/S0006-3223(98)00138-3

Boehringer, R., Polygalov, D., Huang, A., Middleton, S., Robert, V., Wintzer, M., et al. (2017). Chronic loss of CA2 transmission leads to hippocampal hyperexcitability. *Neuron* 94, 642.e9–655.e9. doi: 10.1016/j.neuron.2017.04.014

Botcher, N., Falck, J., Thomson, A., and Mercer, A. (2014). Distribution of interneurons in the CA2 region of the rat hippocampus. *Front. Neuroanat.* 8:104. doi: 10.3389/fnana.2014.00104

Cabungcal, J., Steullet, P., Morishita, H., Kraftsik, R., Cuenod, M., Hensch, T., et al. (2013). Perineuronal nets protect fast-spiking interneurons against oxidative stress. *Proc. Natl. Acad. Sci. U.S.A.* 110, 9130–9135. doi: 10.1073/pnas.1300454110

Carstens, K., Phillips, M., Pozzo-Miller, L., Weinberg, R., and Dudek, S. (2016). Perineuronal nets suppress plasticity of excitatory synapses on CA2 pyramidal neurons. *J. Neurosci.* 36, 6312–6320. doi: 10.1523/JNEUROSCI.0245-16.2016

Cattaud, V., Bezzina, C., Rey, C., Lejards, C., Dahan, L., and Verret, L. (2018). Early disruption of parvalbumin expression and perineuronal nets in the hippocampus of the Tg2576 mouse model of Alzheimer's disease can be rescued by enriched environment. *Neurobiol. Aging* 72, 147–158. doi: 10.1016/j.neurobiolaging.2018.08.024

Cembrowski, M., Wang, L., Sugino, K., Shields, B., Spruston, N., and Marder, E. (2016). Hipposeq: a comprehensive RNA-seq database of gene expression in hippocampal principal neurons. *eLife* 5:e14997. doi: 10.7554/eLife.14997

Chen, S., He, L., Huang, A., Boehringer, R., Robert, V., Wintzer, M., et al. (2020). A hypothalamic novelty signal modulates hippocampal memory. *Nature* 586, 270–274. doi: 10.1038/s41586-020-2771-1

Chevaleyre, V., and Castillo, P. (2003). Heterosynaptic LTD of hippocampal GABAergic synapses: a novel role of endocannabinoids in regulating excitability. *Neuron* 38, 461–472. doi: 10.1016/S0896-6273(03)00235-6

Chevaleyre, V., and Piskorowski, R. (2016). Hippocampal area CA2: an overlooked but promising therapeutic target. *Trends Mol. Med.* 22, 645–655. doi: 10.1016/j.molmed.2016.06.007

Chevaleyre, V., and Siegelbaum, S. (2010). Strong CA2 pyramidal neuron synapses define a powerful disynaptic cortico-hippocampal loop. *Neuron* 66, 560–572. doi: 10.1016/j.neuron.2010.04.013

Chevaleyre, V., Takahashi, K., and Castillo, P. (2006). Endocannabinoid-mediated synaptic plasticity in the CNS. *Annu. Rev. Neurosci.* 29, 37–76. doi: 10.1146/annurev.neuro.29.051605.112834

Cui, Z., Gerfen, C., and Young, W. (2013). Hypothalamic and other connections with dorsal CA2 area of the mouse hippocampus. *J. Comp. Neurol.* 521, 1844–1866. doi: 10.1002/cne.23263

Domínguez, S., Rey, C., Therreau, L., Fanton, A., Massotte, D., Verret, L., et al. (2019). Maturation of PNN and ErbB4 signaling in area CA2 during adolescence underlies the emergence of pv interneuron plasticity and social memory. *CellReports* 29, 1099.e4–1112.e4. doi: 10.1016/j.celrep.2019.09.044

Donegan, M., Stefanini, F., Meira, T., Gordon, J., Fusi, S., and Siegelbaum, S. (2020). Coding of social novelty in the hippocampal CA2 region and its disruption and rescue in a 22q11.2 microdeletion mouse model. *Nat. Neurosci.* 23, 1365–1375. doi: 10.1038/s41593-020-00720-5

Drew, L., Crabtree, G., Markx, S., Stark, K., Chaverneff, F., Xu, B., et al. (2011). The 22q11.2 microdeletion: fifteen years of insights into the genetic and neural complexity of psychiatric disorders. *Int. J. Dev. Neurosci.* 29, 259–281. doi: 10.1016/j.ijdevneu.2010.09.007

Evans, P., Parra-Bueno, P., Smirnov, M., Lustberg, D., Dudek, S., Hepler, J., et al. (2018). RGS14 restricts plasticity in hippocampal CA2 by limiting postsynaptic calcium signaling. *eNeuro* 5:ENEURO.0353-17.2018. doi: 10.1523/ENEURO.0353-17.2018

Farrell, J., Lovett-Barron, M., Klein, P., Sparks, F., Gschwind, T., Ortiz, A., et al. (2021). Supramammillary regulation of locomotion and hippocampal activity. *Science* 374, 1492–1496. doi: 10.1126/science.abh4272

Fawcett, J., Oohashi, T., and Pizzorusso, T. (2019). The roles of perineuronal nets and the perinodal extracellular matrix in neuronal function. *Nat. Rev. Neurosci.* 20, 451–465. doi: 10.1038/s41583-019-0196-3

Freiman, T., Häussler, U., Zentner, J., Doostkam, S., Beck, J., Scheiwe, C., et al. (2021). Mossy fiber sprouting into the hippocampal region CA2 in patients with temporal lobe epilepsy. *Hippocampus* 31, 580–592. doi: 10.1002/hipo.23323

Gisabella, B., Bolshakov, V., and Benes, F. (2005). Regulation of synaptic plasticity in a schizophrenia model. *Proc. Natl. Acad. Sci. U.S.A.* 102, 13301–13306. doi: 10.1073/pnas.0506034102

Gisabella, B., Cunningham, M., Bolshakov, V., and Benes, F. (2009). Amygdala-dependent regulation of electrical properties of hippocampal interneurons in a model of schizophrenia. *Biol. Psychiatry* 65, 464–472. doi: 10.1016/j.biopsych.2008.09.016

Griguoli, M., and Pimpinella, D. (2022). Medial septum: relevance for social memory. *Front. Neural Circuits* 16:965172. doi: 10.3389/fncir.2022.965172

Haglund, L., Swanson, L., and Köhler, C. (1984). The projection of the supramammillary nucleus to the hippocampal formation: an immunohistochemical and anterograde transport study with the lectin PHA-L in the rat. *J. Comp. Neurol.* 229, 171–185. doi: 10.1002/cne.902290204

Hannan, A. (2014). Environmental enrichment and brain repair: harnessing the therapeutic effects of cognitive stimulation and physical activity to enhance experience-dependent plasticity. *Neuropathol. Appl. Neurobiol.* 40, 13–25. doi: 10.1111/nan.12102

Häussler, U., Rinas, K., Kilias, A., Egert, U., and Haas, C. (2015). Mossy fiber sprouting and pyramidal cell dispersion in the hippocampal CA2 region in a mouse model of temporal lobe epilepsy. *Hippocampus* 26, 577–588. doi: 10.1002/hipo.22543

He, H., Boehringer, R., Huang, A., Overton, E., Polygalov, D., Okanoya, K., et al. (2021). CA2 inhibition reduces the precision of hippocampal assembly reactivation. *Neuron* 109, 3674.e7–3687.e7. doi: 10.1016/j.neuron.2021.08.034

Hirjak, D., Wolf, R., Remmele, B., Seidl, U., Thomann, A., and Kubera, K. (2017). Hippocampal formation alterations differently contribute to autobiographic memory deficits in mild cognitive impairment and Alzheimer's disease. *Hippocampus* 27, 702–715. doi: 10.1002/hipo.22726

Hitti, F., and Siegelbaum, S. (2014). The hippocampal CA2 region is essential for social memory. *Nature* 508, 88–92. doi: 10.1038/nature13028

Honoré, E. (2007). The neuronal background K2P channels: focus on TREK1. *Nat. Rev. Neurosci.* 8, 251–261. doi: 10.1038/nrn2117

Ishizuka, N., Cowan, W., and Amaral, D. (1995). A quantitative analysis of the dendritic organization of pyramidal cells in the rat hippocampus. *J. Comp. Neurol.* 362, 17–45. doi: 10.1002/cne.903620103

Ito, M., Shirao, T., Doya, K., and Sekino, Y. (2009). Three-dimensional distribution of Fos-positive neurons in the supramammillary nucleus of the rat exposed to novel environment. *Neurosci. Res.* 64, 397–402. doi: 10.1016/j.neures.2009.04.013

Kay, K., Sosa, M., Chung, J., Karlsson, M., Larkin, M., and Frank, L. (2016). A hippocampal network for spatial coding during immobility and sleep. *Nature* 531, 185–190. doi: 10.1038/nature17144

Kilias, A., Tulke, S., Barheier, N., Ruther, P., and Häussler, U. (2022). Integration of the CA2 region in the hippocampal network during epileptogenesis. *Hippocampus* 33, 223–240. doi: 10.1002/hipo.23479

Klausberger, T., and Somogyi, P. (2008). Neuronal diversity and temporal dynamics: the unity of hippocampal circuit operations. *Science* 321, 53–57. doi: 10.1126/science.1149381

Knable, M., Barci, B., Webster, M., Meador-Woodruff, J., Torrey, E., and Consortium, S. (2004). Molecular abnormalities of the hippocampus in severe psychiatric illness: postmortem findings from the stanley neuropathology consortium. *Mol. Psychiatry* 9, 609–620. doi: 10.1038/sj.mp.4001471

Knowles, W., Traub, R., and Strowbridge, B. (1987). The initiation and spread of epileptiform bursts in the *in vitro* hippocampal slice. *Neuroscience* 21, 441–455. doi: 10.1016/0306-4522(87)90134-5

Kogan, J., Frankland, P., and Silva, A. (2000). Long-term memory underlying hippocampus-dependent social recognition in mice. *Hippocampus* 10, 47–56. doi: 10.1002/(SICI)1098-1063(2000)10:1<47::AID-HIPO5>3.0.CO;2-6

Laham, B., Diethorn, E., and Gould, E. (2021). Newborn mice form lasting CA2-dependent memories of their mothers. *Cell Rep.* 34, 108668–108668. doi: 10.1016/j.celrep.2020.108668

Lee, S., Simons, S., Heldt, S., Zhao, M., Schroeder, J., Vellano, C., et al. (2010). RGS14 is a natural suppressor of both synaptic plasticity in CA2 neurons and hippocampal-based learning and memory. *Proc. Natl. Acad. Sci. U.S.A.* 107, 16994–16998. doi: 10.1073/pnas.1005362107

Lehr, A., Kumar, A., Tetzlaff, C., Hafting, T., Fyhn, M., and Stöber, T. (2021). CA2 beyond social memory: evidence for a fundamental role in hippocampal information processing. *Neurosci. Biobehav. Rev.* 126, 398–412. doi: 10.1016/j.neubiorev.2021.03.020

Lein, E., Callaway, E., Albright, T., and Gage, F. (2005). Redefining the boundaries of the hippocampal CA2 subfield in the mouse using gene expression and 3-dimensional reconstruction. *J. Comp. Neurol.* 485, 1–10. doi: 10.1002/cne.20426

Lein, E., Zhao, X., and Gage, F. (2004). Defining a molecular atlas of the hippocampus using DNA microarrays and high-throughput *in situ* hybridization. *J. Neurosci.* 24, 3879–3889. doi: 10.1523/JNEUROSCI.4710-03.2004

Leranth, C., and Ribak, C. (1991). Calcium-binding proteins are concentrated in the CA2 field of the monkey hippocampus: a possible key to this region's resistance to epileptic damage. *Exp. Brain Res.* 85, 129–136. doi: 10.1007/BF00229993

Leroy, F., Brann, D., Meira, T., and Siegelbaum, S. (2017). Input-timing-dependent plasticity in the hippocampal CA2 region and its potential role in social memory. *Neuron* 95, 1089.e5–1102.e5. doi: 10.1016/j.neuron.2017.07.036

Leroy, F., Park, J., Asok, A., Brann, D., Meira, T., Boyle, L., et al. (2018). A circuit from hippocampal CA2 to lateral septum disinhibits social aggression. *Nature* 564, 213–218. doi: 10.1038/s41586-018-0772-0

Lisman, J. (1999). Relating hippocampal circuitry to function: recall of memory sequences by reciprocal dentate-CA3 interactions. *Neuron* 22, 233–242. doi: 10.1016/S0896-6273(00)81085-5

Loisy, M., Bouisset, G., Lopez, S., Muller, M., Spitsyn, A., Duval, J., et al. (2022). Sequential inhibitory plasticities in hippocampal area CA2 and social memory formation. *Neuron* 110, 2854.e4–2866.e4. doi: 10.1016/j.neuron.2022.06.013

Loisy, M., Farah, A., Fafouri, A., Fanton, A., Ahmadi, M., Therreau, L., et al. (2023). Environmental enrichment and social isolation modulate inhibitory transmission and plasticity in hippocampal area CA2. *Hippocampus* 33, 197–207. doi: 10.1002/hipo.23478

Lorente de No, R. (1934). Studies on the structure of the cerebral cortex. II. Continuation of the study of the ammonic system. *J. Psychol. Neurol.* 46, 113–175.

McClelland, J., McNaughton, B., and O'Reilly, R. (1995). Why there are complementary learning systems in the hippocampus and neocortex: insights from the successes and failures of connectionist models of learning and memory. *Psychol. Rev.* 102, 419–457. doi: 10.1037/0033-295X.102.3.419

McHugh, T., Blum, K., Tsien, J., Tonegawa, S., and Wilson, M. (1996). Impaired hippocampal representation of space in CA1-specific NMDAR1 knockout mice. *Cell* 87, 1339–1349. doi: 10.1016/S0092-8674(00)81828-0

McHugh, T., Jones, M., Quinn, J., Balthasar, N., Coppari, R., Elmquist, J., et al. (2007). Dentate gyrus NMDA receptors mediate rapid pattern separation in the hippocampal network. *Science* 317, 94–99. doi: 10.1126/science.1140263

Meira, T., Leroy, F., Buss, E., Oliva, A., Park, J., and Siegelbaum, S. (2018). A hippocampal circuit linking dorsal CA2 to ventral CA1 critical for social memory dynamics. *Nat. Commun.* 9, 1–14. doi: 10.1038/s41467-018-06501-w

Mercer, A., Botcher, N., Eastlake, K., and Thomson, A. (2012). SP–SR interneurones: a novel class of neurones of the CA2 region of the hippocampus. *Hippocampus* 22, 1758–1769. doi: 10.1002/hipo.22010

Mercer, A., Trigg, H., and Thomson, A. (2007). Characterization of neurons in the CA2 subfield of the adult rat hippocampus. *J. Neurosci.* 27, 7329–7338. doi: 10.1523/JNEUROSCI.1829-07.2007

Michailidou, I., Willems, J., Kooi, E., van Eden, C., Gold, S., Geurts, J., et al. (2015). Complement C1q-C3–associated synaptic changes in multiple sclerosis hippocampus. *Ann. Neurol.* 77, 1007–1026. doi: 10.1002/ana.24398

Modi, B., Pimpinella, D., Pazienti, A., Zacchi, P., Cherubini, E., and Griguoli, M. (2019). Possible implication of the CA2 hippocampal circuit in social cognition deficits observed in the neuroligin 3 Knock-out mouse, a non-syndromic animal model of autism. *Front. Psychiatry* 10:513. doi: 10.3389/fpsyt.2019.00513

Nasrallah, K., Piskorowski, R., and Chevaleyre, V. (2015). Inhibitory plasticity permits the recruitment of CA2 pyramidal neurons by CA3(1,2,3). *eNeuro* 2, 1–12. doi: 10.1523/ENEURO.0049-15.2015

Nasrallah, K., Therreau, L., Robert, V., Huang, A., McHugh, T., Piskorowski, R., et al. (2019). Routing hippocampal information flow through parvalbumin interneuron plasticity in area CA2. *CellReports* 27, 86.e3–98.e3. doi: 10.1016/j.celrep.2019.03.014

Okuyama, T., Kitamura, T., Roy, D., Itohara, S., and Tonegawa, S. (2016). Ventral CA1 neurons store social memory. *Science* 353, 1536–1541. doi: 10.1126/science.aaf7003

Oliva, A., Fernández-Ruiz, A., Buzsáki, G., and Berényi, A. (2016a). Role of hippocampal CA2 region in triggering sharp-wave ripples. *Neuron* 91, 1342–1355. doi: 10.1016/j.neuron.2016.08.008

Oliva, A., Fernández-Ruiz, A., Buzsáki, G., and Berényi, A. (2016b). Spatial coding and physiological properties of hippocampal neurons in the cornu ammonis subregions. *Hippocampus* 26, 1593–1607. doi: 10.1002/hipo.22659

Piskorowski, R., and Chevaleyre, V. (2013). Delta-opioid receptors mediate unique plasticity onto parvalbumin-expressing interneurons in area CA2 of the hippocampus. *J. Neurosci.* 33, 14567–14578. doi: 10.1523/JNEUROSCI.0649-13.2013

Piskorowski, R., Nasrallah, K., Diamantopoulou, A., Mukai, J., Hassan, S., Siegelbaum, S., et al. (2016). Age-dependent specific changes in area CA2 of the hippocampus and social memory deficit in a mouse model of the 22q11.2 deletion syndrome. *Neuron* 89, 163–176. doi: 10.1016/j.neuron.2015.11.036

Poo, M., Pignatelli, M., Ryan, T., Tonegawa, S., Bonhoeffer, T., Martin, K., et al. (2016). What is memory? The present state of the engram. *BMC Biol.* 14:40. doi: 10.1186/s12915-016-0261-6

Pöttgen, J., Dziobek, I., Reh, S., Heesen, C., and Gold, S. (2013). Impaired social cognition in multiple sclerosis. *J. Neurol. Neurosurg. Psychiatry* 84, 523–528. doi: 10.1136/jnnp-2012-304157

Radyushkin, K., Hammerschmidt, K., Boretius, S., Varoqueaux, F., El-Kordi, A., Ronnenberg, A., et al. (2009). Neuroligin-3-deficient mice: model of a monogenic heritable form of autism with an olfactory deficit. *Genes Brain Behav.* 8, 416–425. doi: 10.1111/j.1601-183x.2009.00487.x

Ramaglia, V., Dubey, M., Malpede, M., Petersen, N., de Vries, S., Ahmed, S., et al. (2021). Complement-associated loss of CA2 inhibitory synapses in the demyelinated hippocampus impairs memory. *Acta Neuropathol.* 142, 643–667. doi: 10.1007/s00401-021-02338-8

Rao, R., von Heimendahl, M., Bahr, V., and Brecht, M. (2019). Neuronal responses to conspecifics in the ventral CA1. *Cell Rep.* 27, 3460.e3–3472.e3. doi: 10.1016/j.celrep.2019.05.081

Rey, C., Robert, V., Bouisset, G., Loisy, M., Lopez, S., Cattaud, V., et al. (2022). Altered inhibitory function in hippocampal CA2 contributes in social memory deficits in Alzheimer's mouse model. *iScience* 25:103895. doi: 10.1016/j.isci.2022.103895

Robert, V., Therreau, L., Chevaleyre, V., Lepicard, E., Viollet, C., Cognet, J., et al. (2021). Local circuit allowing hypothalamic control of hippocampal area CA2 activity and consequences for CA1. *eLife* 10:e63352. doi: 10.7554/eLife.63352

Rolls, E. (2010). A computational theory of episodic memory formation in the hippocampus. *Behav. Brain Res.* 215, 180–196. doi: 10.1016/j.bbr.2010.03.027

Rolls, E. (2013). The mechanisms for pattern completion and pattern separation in the hippocampus. *Front. Syst. Neurosci.* 7:74. doi: 10.3389/fnsys.2013.00074

Schafer, D., Lehrman, E., and Stevens, B. (2013). The "quad-partite" synapse: microglia-synapse interactions in the developing and mature CNS. *Glia* 61, 24–36. doi: 10.1002/glia.22389

Simons, S., Escobedo, Y., Yasuda, R., and Dudek, S. (2009). Regional differences in hippocampal calcium handling provide a cellular mechanism for limiting plasticity. *Proc. Natl. Acad. Sci. U.S.A.* 106, 14080–14084. doi: 10.1073/pnas.0904775106

Squire, L., and Wixted, J. (2011). The cognitive neuroscience of human memory since H.M. *Annu. Rev. Neurosci.* 34, 259–288. doi: 10.1146/annurev-neuro-061010-113720

Stevenson, E., and Caldwell, H. (2014). Lesions to the CA2 region of the hippocampus impair social memory in mice. *Eur. J. Neurosci.* 40, 3294–3301. doi: 10.1111/ejn.12689

Stöber, T., Lehr, A., Hafting, T., Kumar, A., and Fyhn, M. (2020). Selective neuromodulation and mutual inhibition within the CA3–CA2 system can prioritize sequences for replay. *Hippocampus* 30, 1228–1238. doi: 10.1002/hipo.23256

Talley, E., Solorzano, G., Lei, Q., Kim, D., and Bayliss, D. (2001). Cns distribution of members of the two-pore-domain (KCNK) potassium channel family. *J. Neurosci.* 21, 7491–7505. doi: 10.1523/JNEUROSCI.21-19-07491.2001

Tirko, N., Eyring, K., Carcea, I., Mitre, M., Chao, M., Froemke, R., et al. (2018). Oxytocin transforms firing mode of CA2 hippocampal neurons. *Neuron* 100, 593.e3–608.e3. doi: 10.1016/j.neuron.2018.09.008

Tsai, T., Fang, Y., Hung, Y., Hung, L., and Hsu, K. (2022). A dorsal CA2 to ventral CA1 circuit contributes to oxytocinergic modulation of long-term social recognition memory. *J. Biomed. Sci.* 29:50. doi: 10.1186/s12929-022-00834-x

Walsh, J., Christoffel, D., Wu, X., Pomrenze, M., and Malenka, R. (2021). Dissecting neural mechanisms of prosocial behaviors. *Curr. Opin. Neurobiol.* 68, 9–14. doi: 10.1016/j.conb.2020.11.006

Wang, C., Yue, H., Hu, Z., Shen, Y., Ma, J., Li, J., et al. (2020). Microglia mediate forgetting via complement-dependent synaptic elimination. *Science* 367, 688–694. doi: 10.1126/science.aaz2288

Whitebirch, A., LaFrancois, J., Jain, S., Leary, P., Santoro, B., Siegelbaum, S., et al. (2022). Enhanced excitability of the hippocampal CA2 region and its contribution to seizure activity in a mouse model of temporal lobe epilepsy. *Neuron* 110, 3121.e8–3138.e8. doi: 10.1016/j.neuron.2022.07.020

Williamson, A., and Spencer, D. (1994). Electrophysiological characterization of CA2 pyramidal cells from epileptic humans. *Hippocampus* 4, 226–237. doi: 10.1002/hipo.450040213

Willshaw, D., and Buckingham, J. (1990). An assessment of Marr's theory of the hippocampus as a temporary memory store. *Philos. Trans. R. Soc. Lon. Ser. B Biol. Sci.* 329, 205–215. doi: 10.1098/rstb.1990.0165

Wintzer, M., Boehringer, R., Polygalov, D., and McHugh, T. (2014). The hippocampal CA2 ensemble is sensitive to contextual change. *J. Neurosci.* 34, 3056–3066. doi: 10.1523/JNEUROSCI.2563-13.2014

Wirtshafter, D., Stratford, T., and Shim, I. (1998). Placement in a novel environment induces Fos-like immunoreactivity in supramammillary cells projecting to the hippocampus and midbrain. *Brain Res.* 789, 331–334. doi: 10.1016/S0006-8993(97)01555-2

Wittner, L., Huberfeld, G., Clémenceau, S., Eross, L., Dezamis, E., Entz, L., et al. (2009). The epileptic human hippocampal cornu ammonis 2 region generates spontaneous interictal-like activity *in vitro*. *Brain* 132, 3032–3046. doi: 10.1093/brain/awp238

Wong, R., and Traub, R. (1983). Synchronized burst discharge in disinhibited hippocampal slice. I. Initiation in CA2-CA3 region. *J. Neurophysiol.* 49, 442–458. doi: 10.1152/jn.1983.49.2.442

Wu, X., Morishita, W., Beier, K., Heifets, B., and Malenka, R. (2021). 5-HT modulation of a medial septal circuit tunes social memory stability. *Nature* 599, 96–101. doi: 10.1038/s41586-021-03956-8

Zhang, Z., and Reynolds, G. (2002). A selective decrease in the relative density of parvalbumin-immunoreactive neurons in the hippocampus in schizophrenia. *Schizophr. Res.* 55, 1–10. doi: 10.1016/S0920-9964(01)00188-8

Zhao, M., Choi, Y., Obrietan, K., and Dudek, S. (2007). Synaptic plasticity (and the lack thereof) in hippocampal CA2 neurons. *J. Neurosci.* 27, 12025–12032. doi: 10.1523/JNEUROSCI.4094-07.2007

frontiers | Frontiers in Neural Circuits

TYPE Original Research
PUBLISHED 19 May 2023
DOI 10.3389/fncir.2023.1093066

OPEN ACCESS

EDITED BY
Lisa Topolnik,
Laval University, Canada

REVIEWED BY
Klas Kullander,
Uppsala University, Sweden
Jochen Ferdinand Staiger,
University of Göttingen, Germany

*CORRESPONDENCE
Simon X. Chen
✉ schen2@uottawa.ca

†These authors have contributed equally to this work

RECEIVED 08 November 2022
ACCEPTED 05 May 2023
PUBLISHED 19 May 2023

CITATION
Lee C, Côté SL, Raman N, Chaudhary H, Mercado BC and Chen SX (2023) Whole-brain mapping of long-range inputs to the VIP-expressing inhibitory neurons in the primary motor cortex.
Front. Neural Circuits 17:1093066.
doi: 10.3389/fncir.2023.1093066

Whole-brain mapping of long-range inputs to the VIP-expressing inhibitory neurons in the primary motor cortex

Candice Lee[1†], Sandrine L. Côté[1†], Nima Raman[1], Hritvic Chaudhary[1], Bryan C. Mercado[1] and Simon X. Chen[1,2,3*]

[1]Department of Cellular and Molecular Medicine, University of Ottawa, Ottawa, ON, Canada, [2]Brain and Mind Research Institute, University of Ottawa, Ottawa, ON, Canada, [3]Center for Neural Dynamics, University of Ottawa, Ottawa, ON, Canada

The primary motor cortex (MOp) is an important site for motor skill learning. Interestingly, neurons in MOp possess reward-related activity, presumably to facilitate reward-based motor learning. While pyramidal neurons (PNs) and different subtypes of GABAergic inhibitory interneurons (INs) in MOp all undergo cell-type specific plastic changes during motor learning, the vasoactive intestinal peptide-expressing inhibitory interneurons (VIP-INs) in MOp have been shown to preferentially respond to reward and play a critical role in the early phases of motor learning by triggering local circuit plasticity. To understand how VIP-INs might integrate various streams of information, such as sensory, pre-motor, and reward-related inputs, to regulate local plasticity in MOp, we performed monosynaptic rabies tracing experiments and employed an automated cell counting pipeline to generate a comprehensive map of brain-wide inputs to VIP-INs in MOp. We then compared this input profile to the brain-wide inputs to somatostatin-expressing inhibitory interneurons (SST-INs) and parvalbumin-expressing inhibitory interneurons (PV-INs) in MOp. We found that while all cell types received major inputs from sensory, motor, and prefrontal cortical regions, as well as from various thalamic nuclei, VIP-INs received more inputs from the orbital frontal cortex (ORB) – a region associated with reinforcement learning and value predictions. Our findings provide insight on how the brain leverages microcircuit motifs by both integrating and partitioning different streams of long-range input to modulate local circuit activity and plasticity.

KEYWORDS

monosynaptic circuit tracing, inhibitory neurons, motor cortex, associative learning, orbital frontal cortex (ORB)

Introduction

The primary motor cortex (MOp) has a well-established role in the execution of voluntary movement (Guo et al., 2015). Recent studies have also identified it as a critical site for motor learning (Xu et al., 2009; Peters et al., 2014; Chen et al., 2015; Kawai et al., 2015). Like other cortical areas, MOp is primarily composed of glutamatergic pyramidal neurons

(PNs) and different subtypes of GABAergic inhibitory interneurons (INs), which together form distinctive patterns of local connectivity. In particular, parvalbumin-expressing INs (PV-INs) primarily inhibit the perisomatic region of PNs, somatostatin-expressing INs (SST-INs) primarily inhibit the apical dendrites of PNs, while vasoactive intestinal peptide-expressing inhibitory interneurons (VIP-INs) mainly inhibit SST-INs and thereby disinhibit PNs. While there are preferential connections between these cell types, the microcircuit connectivity is not entirely unique and specific among cell types (Pfeffer et al., 2013; Pi et al., 2013; Tremblay et al., 2016; Staiger and Petersen, 2021).

During motor learning, both PNs and INs in MOp undergo structural and functional plastic changes (Xu et al., 2009; Peters et al., 2014; Chen et al., 2015; Ren et al., 2022, Yang et al., 2022). Recently, a selective disinhibitory mechanism acting through VIP-IN mediated inhibition of SST-INs has been suggested to promote motor learning by enhancing PN excitability (Adler et al., 2019; Ren et al., 2022). In line with this idea, Ren et al. (2022) have shown that VIP-INs are highly active in the early phase of motor learning while SST-INs show weak activation. Inactivation of VIP-INs in MOp during this early phase impairs learning, demonstrating the importance of VIP-INs for the acquisition of new motor skills (Ren et al., 2022). Interestingly, VIP-INs in MOp have also been shown to represent reward and undergo plastic changes following reward-based associative learning in a non-motor related task. When compared to PNs, PV-INs, and SST-INs, VIP-INs preferentially respond to reward and become more reliably responsive to reward during the associative learning process (Lee et al., 2022). While the plastic changes attributed to VIP-INs in MOp underscore their importance for motor learning, it remains unclear where motor- and reward-related signals to VIP-INs arise from.

Primary motor cortex is heavily interconnected with many cortical and sub-cortical regions (Mao et al., 2011; Hooks et al., 2013; Luo et al., 2019; Duan et al., 2020; Okoro et al., 2022), several of which have been shown to be plastic during motor learning, including the secondary motor cortex (MOs; Cao et al., 2015), anterior lateral motor area (ALM; Chabrol et al., 2019), retrosplenial cortex (RSP; Makino et al., 2017), and thalamus (Biane et al., 2016; Tanaka et al., 2018). In addition, many input regions that project to MOp have also been shown to undergo plastic changes after reward-based associative learning such as the primary somatosensory cortex (Chen et al., 2015), auditory cortex (AUD) (Kisley and Gerstein, 2001; Lee and Rothschild, 2021), RSP (Hattori et al., 2019), ALM, and MOs (Komiyama et al., 2010). Importantly, thus far, these input regions have not been shown to provide preferential input to a specific neuron subtype in MOp.

Here, we utilized a monosynaptic rabies tracing strategy and performed brain-wide mapping of long-range inputs to the four major cell types in MOp (VIP-INs, PV-INs, SST-INs, and PNs). By systematically comparing the proportion of inputs from different brain regions to VIP-INs with the inputs to PV-INs and SST-INs, we found that VIP-INs received significantly more inputs from the orbital frontal cortex (ORB). Considering that both ORB and VIP-INs have been shown to respond to reward (Baltz et al., 2018; Namboodiri et al., 2019; Zhou et al., 2019; Wang et al., 2020; Lee et al., 2022), our results point toward ORB serving as an important node in a reward-related input stream projecting to VIP-INs in MOp. In contrast, SST-INs received more input from the RSP, demonstrating that different IN subtypes receive preferential long-range input from specific brain regions. Taken together, our comprehensive whole-brain mapping uncovers input from ORB that could be responsible for activating VIP-INs in MOp in response to reward and may thereby gate local circuit plasticity during reward-based motor learning.

Results

To identify long-range input regions that are specific to VIP-INs, PV-INs, and SST-INs in the caudal forelimb area of MOp, we utilized the monosynaptic rabies virus (RV) tracing system (Wickersham et al., 2007; Callaway and Luo, 2015; Wall et al., 2016). Helper virus (AAV1-EF1a-DIO-TVA950-T2A-CVS11G or AAV2/DJ-hSyn-FLEX-TVA-P2A-eGFP-2A-oG) was first injected into the right MOp forelimb area of VIP-Cre, PV-Cre, or SST-Cre mice to express avian TVA receptors, rabies glycoprotein (G) and GFP in each cell type, respectively. Three weeks after the helper virus injection, we injected pseudotyped G-deleted RV (EnvA-RVdG-mCherry) into the same site (**Figure 1A**). One week after the injection of the pseudotyped G-deleted RV, animals were perfused, and coronal sections were imaged at a 120 μm increment across the entire brain (see section "Materials and methods"). It has been shown that the helper virus could have potential leak expression of TVA and subsequent rabies infection in the absence of Cre (Seidler et al., 2008; Callaway and Luo, 2015; Hafner et al., 2019); hence, we conducted control experiments by injecting the helper virus (AAV2/DJ-hSyn-FLEX-TVA-P2A-eGFP-2A-oG) as well as the pseudotyped G-deleted RV (RVdG-EnvA-mCherry, University of Berlin Viral Core Facility) into wild-type (WT) mice and examined whether there were GFP-expressing (GFP^+) and/or mCherry expressing ($mCherry^+$) cells in MOp. We found 0 GFP^+ cells and an average of 10 $mCherry^+$ cells in MOp (**Figures 1B, C**). When we only injected pseudotyped G-deleted RV in WT mice, we found 0 GFP^+ and $mCherry^+$ cells. Together, these control experiments indicate that there were negligible amounts of TVA leakage at the volume and titer we employed. In contrast to the control experiments, we observed many GFP^+ cells in PV-, SST-, and VIP-Cre animals, and these GFP^+ cells were all constrained within the injection site in the MOp. Many of them also co-localized with mCherry, indicating the presence of starter cells (**Figures 1D–I**). To ensure the specificity of the helper virus to Cre-expressing (Cre^+) cells, we conducted another set of control experiments, where we injected the helper virus (AAV2/DJ-hSyn-FLEX-TVA-P2A-eGFP-2A-oG) in VIP-Cre:tdTomato mice and examined the fraction of GFP^+ cells that co-localized with tdTomato. We found that 99% of the GFP^+ cells co-localized with tdTomato, confirming the specificity of the helper virus to Cre^+ cells (**Supplementary Figures 1A, B**).

To automatically and unbiasedly quantify RV-labeled cells throughout the brain, we employed the software "Wholebrain" (Fürth et al., 2018), which enables automated detection and quantification of labeled neurons. Most importantly, Wholebrain enables scale-invariant registration of brain sections to the Allen Mouse Brain Atlas (**Figures 2A–C**), thus providing a method to identify all the brain regions from different brain samples within a standardized framework. By applying the Wholebrain software to sections from 2.945 mm anterior to bregma through

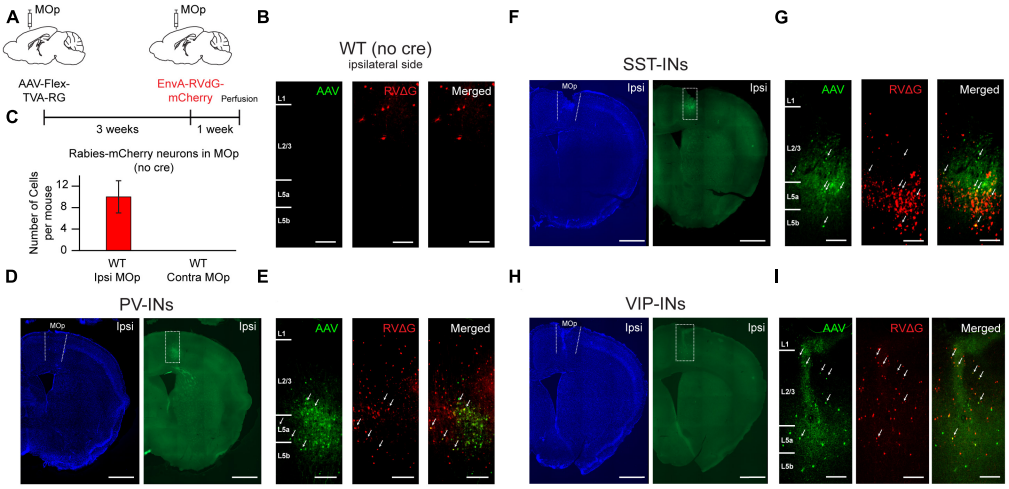

FIGURE 1
Helper AAV and RV system for retrograde tracing of monosynaptic inputs to PV-INs, SST-INs, and VIP-INs in MOp. **(A)** Helper virus was injected unilaterally into right MOp (ipsilateral) followed by pseudotyped G-deleted rabies virus 3 weeks later. Animals were sacrificed 1 week after the rabies viral injection. **(B)** Example images from a control wild-type mouse injected with AAV2/DJ-hSyn-FLEX-TVA-P2A-eGFP-2A-oG and EnvA-G-deleted-Rabies-mCherry (University of Berlin Viral Core Facility) into ipsilateral MOp. No GFP^+ labeled cells from the helper virus (left), a small amount of $mCherry^+$ labeled cells from the rabies virus (middle), and no co-localized cells (right). The presence of $mCherry^+$ cells indicates small TVA leakage. Scale bar, 100 μm. **(C)** Mean number of $mCherry^+$ cells in ipsilateral and contralateral MOp of control animals (n = 5 mice, 3 sections per mouse). Representative images of the injection sites for PV-Cre **(D,E)**, SST-Cre **(F,G)**, and VIP-Cre **(H,I)** mice injected with AAV2/DJ-hSyn-FLEX-TVA-P2A-eGFP-2A-oG and EnvA-G-deleted-Rabies-mCherry (University of Berlin Viral Core Facility) into ipsilateral MOp. Neurotrace Blue staining (**D,F,H**, left) and GFP fluorescence (**D,F,H**, right) show confinement of GFP^+ cells to MOp. Zoomed in images **(E,G,I)** from the injection site (dashed rectangle in GFP fluorescent images in panels **D,F,H**) shows GFP^+ cells (left), $mCherry^+$ cells (middle), and colocalized GFP^+ and $mCherry^+$ starter cells (right). Arrows show example starter cells. Scale bars, 1 mm for **(D,F,H)** and 100 μm for **(E,G,I)**.

to 5.055 mm posterior to bregma (cells were not found outside of these coordinates), we generated comprehensive and comparative maps of whole-brain input to VIP-INs, PV-INs, and SST-INs (VIP-INs: 5 mice, ∼35 slices/mouse; PV-INs: 4 mice, ∼48 brain slices/mouse; SST-INs: 4 mice, ∼40 slices/mouse; Figures 2D–F and Supplementary Table 1). To test the reliability of the Wholebrain software in counting the input cells, we compared it to the manual counts done by an experimenter prior to the adoption of the Wholebrain software and found that both methods produced similar counts (Supplementary Figure 2). We first quantified the number of input cells ($mCherry^+$ cells outside of MOp) within each region identified in the Allen Brain Atlas, including subdivisions and cortical layers. We found that the total number of labeled input cells varied between each IN subtype (VIP-INs, 3,887 ± 2,021 cells; PV-INs, 1,593 ± 234 cells; SST-INs, 1,253 ± 344 cells). Since the total number of input cells could be dependent on the number of starter cells that were labeled from the viral injection, we also counted the number of starter cells (colocalized GFP^+ and $mCherry^+$ cells within MOp) and calculated an approximate ratio of starter cells to the total number of input cells in the entire brain. We found that the ratio of starter-to-input cells were very similar between the IN subtypes (VIP-INs, 1:15; PV-INs, 1:17; SST-INs, 1:18; Supplementary Table 1).

Long-range inputs to different IN subtypes in MOp from the cortex

We next examined which brain regions each IN subtype receives its input from, beginning with broad subdivisions within the brain. We observed that for all IN subtypes, the majority of input originated in the cortex (Figures 2G–I); in particular, the greatest source of cortical input came from the sensorimotor regions (Figures 3A, C). It is known that ascending tactile sensory information propagates sequentially from the primary somatosensory cortex (SSp) to the secondary somatosensory cortex (SSs). While both regions encode stimulus features, SSp encodes the stimulus more strongly and SSs encodes higher order information such as stimulus-related recall (Condylis et al., 2020) and decision-related activity (Kwon et al., 2016), which is then conveyed back to SSp. Our results show that on the ipsilateral side, the SSp was the largest source of input for all IN subtypes in MOp and comprised 40.99 ± 2.04, 48.64 ± 2.76, and 40.40 ± 4.29% of input to VIP-INs, PV-INs, and SST-INs, respectively (Figure 3A). In contrast, all IN subtypes received substantially less input from SSs (SSp compared to SSs: $p < 1 \times 10^{-3}$ for all cell types). We also identified major cortical input from the MOs and ALM (also known as frontal MOs). MOs and ALM are two motor regions that show preparatory activity preceding movement and are thought to be akin to the primate premotor cortex (Guo et al., 2015; Li et al., 2015; Chen et al., 2017). We found that MOs provided inputs to all IN subtypes in MOp, and PV-INs received the most among them. Interestingly, we observed that MOs provided more inputs to the INs in MOp than ALM. Specifically, on the ipsilateral side, PV-INs and SST-INs but not VIP-INs received greater input from MOs compared to ALM (VIP-INs, $p = 0.084$; PV-INs and SST-INs, $p < 1 \times 10^{-3}$; Figure 3A). In contrast, while input from ALM was relatively low compared to MOs, it projected substantially more to PV-INs and VIP-INs than to SST-INs (VIP-IN vs. SST-INs: $p < 1 \times 10^{-3}$; PV-INs vs. SST-INs:

10.3389/fncir.2023.1093066

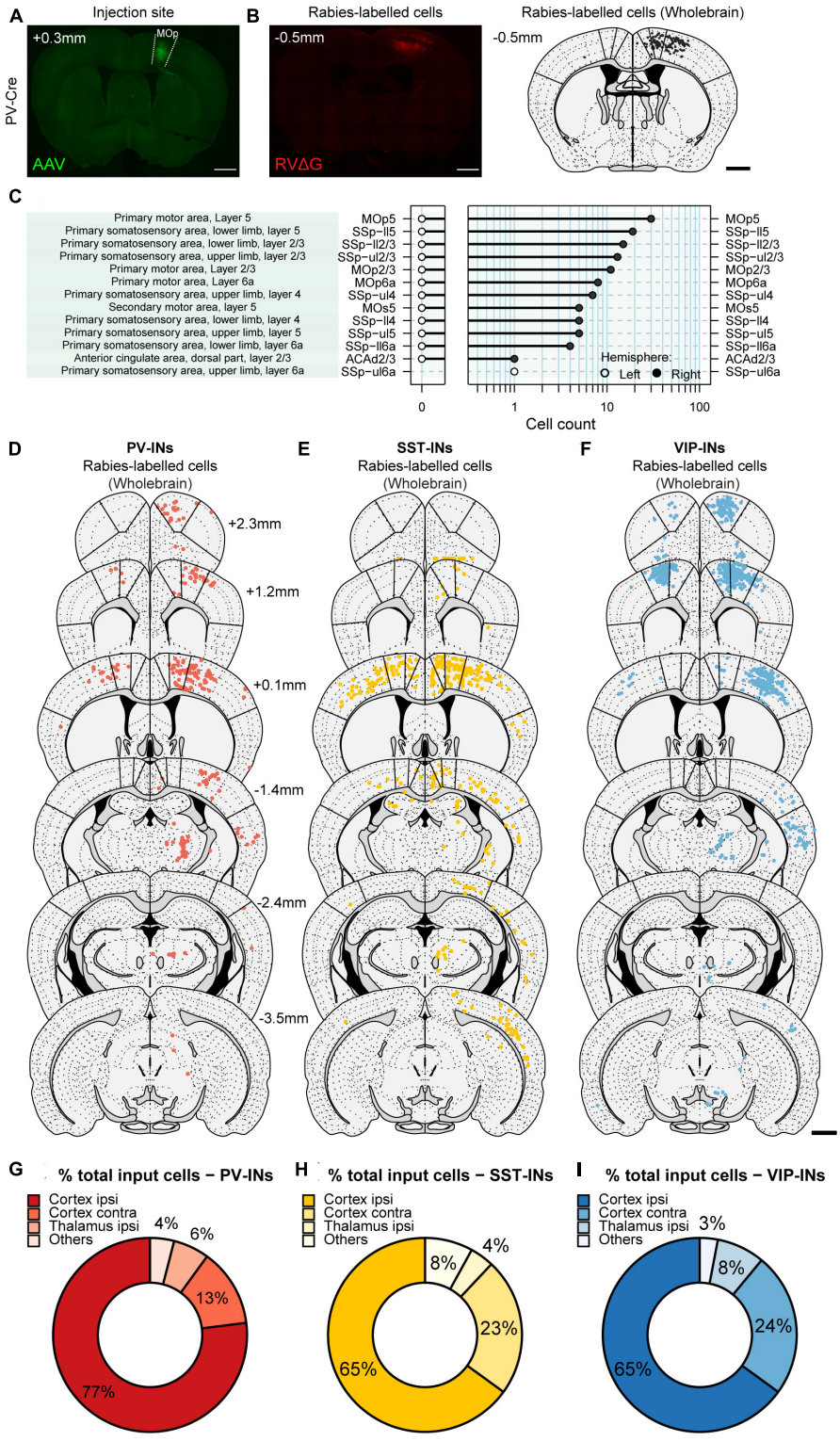

FIGURE 2
Generating brain-wide input maps to VIP-INs, PV-INs, and SST-INs in MOp. **(A)** Example image of a brain section showing GFP$^+$ labeled cells in ipsilateral MOp from the helper virus (AAV2/DJ-hSyn-FLEX-TVA-P2A-eGFP-2A-oG). **(B)** Example image of the same mouse showing mCherry$^+$ labeled cells from the rabies virus (EnvA-G-deleted-Rabies-mCherry, University of Berlin Viral Core Facility) (left). Registration of the same section to the Allen Brain Atlas with the Wholebrain software (right). Each black dot is a mCherry$^+$ input cell that was automatically detected by the software. **(C)** Cell quantification within different regions, subdivisions, and layers for the example section in panel **(B)**. Example sections showing detected input cells projecting to PV-INs **(D)**, SST-INs **(E)**, and VIP-INs **(F)**. Bold lines indicate the delineation between MOs, MOp, and SSp. Scale bar, 1 mm. Mean percentage of brain-wide inputs to PV-INs **(G)**, SST-INs **(H)**, and VIP-INs **(I)** from broad subdivisions of the brain. Regions with small proportions were grouped together in others. PV-INs, n = 4 mice; SST-INs, n = 4 mice; VIP-INs, n = 5 mice.

$p < 1 \times 10^{-3}$; Figure 3A). Hence, unlike SSp and SSs which had similar proportions of input to all IN subtypes in MOp, MOs, and ALM demonstrated some subtype-specific differences. Since MOs and ALM have been shown to have differential roles in movement preparation and execution (Siniscalchi et al., 2016; Chen et al., 2017), our results suggest that specific IN subtypes in MOp may be involved in processing different movement-related information.

Within ipsilateral cortex, we also found other cortical regions that provide differential input biased toward specific IN subtypes in MOp, although they represented a smaller proportion of brain-wide inputs compared to SSp, SSs, MOs, and ALM. The anterior cingulate area (ACA) projected to all IN subtypes but significantly more to SST-INs than to PV-INs, while no significant difference was found between SST-INs and VIP-INs (Figure 3B). The AUD was a major source of input to all three IN subtypes with no significant differences in the proportion of input cells. Intriguingly, the ORB projected significantly more to VIP-INs compared to either PV-INs or SST-INs, and ORB was one of the most pronounced inputs to VIP-INs outside of the SSp (Figure 3B). Lastly, SST-INs received significantly more input from RSP than PV-INs and VIP-INs. In addition, SST-INs also received significantly more inputs from the posterior parietal cortex (PTLp) compared to VIP-INs (Figure 3B). Overall, among ipsilateral cortex, MOs and SSp account for a substantial proportion of brain-wide input to INs in MOp. In addition, we identified biased input from ORB to VIP-INs and RSP to SST-INs.

In the contralateral cortex, MOp was a major source of input to all three IN subtypes (Figure 3C). ALM, MOs, and SS (SSp and SSs combined) had substantially less input cells compared to the ipsilateral side. Unlike ipsilateral ALM which projected similarly to both VIP-INs and PV-INs, contralateral ALM projected more to VIP-INs than to the other two subtypes. Intriguingly, contralateral MOs projected more to VIP-INs and SST-INs than to PV-INs; this is in contrast to ipsilateral MOs, which had a greater proportion of input to PV-INs and less input to SST-INs and VIP-INs. The relative proportion of input from MOs and ALM also differed; unlike the ipsilateral side, where PV-INs and SST-INs but not VIP-INs received more input from MOs compared to ALM, all IN subtypes received more input from contralateral MOs compared to ALM (VIP-INs: $p = 0.006$; SST-INs and PV-INs: $p < 1 \times 10^{-3}$). These findings demonstrate that subtype-specificity of long-range input from the same region can vary between hemispheres. Outside of ALM, MOs, and SS, the proportion of input from other regions within the contralateral cortex were mostly minimal with some exceptions (Figure 3D). Noticeably, the contralateral ACA trended toward providing more input to SST-INs compared to both PV-INs and VIP-INs, akin to its ipsilateral homolog In addition, contralateral ORB was another exception, as it had a proportion of input cells comparable to its ipsilateral counterpart and also projected significantly more to VIP-INs compared to PV-INs and SST-INs (Figure 3D). Hence, the numerous bilateral inputs from ORB further highlight the importance of this projection to VIP-INs.

To test for the possibility that cre-independent leak expression of TVA could result in non-specific trans-synaptic labeling, we also examined mCherry$^+$ cells in the major labeled areas (ipsi and contra MOs and SSp) from our control experiments, in which we injected the helper virus and the pseudotyped G-deleted RV in WT mice (Figure 1B). We observed almost no cells in either region (Figures 3E, F), demonstrating that there was a negligible amount of non-specific trans-synaptic labeling from the TVA leakage at the volume and titer we employed.

Distinct subregion- and layer-specific inputs to different IN subtypes in MOp

Orbital frontal cortex has been shown to encode and predict value and reward (Baltz et al., 2018; Namboodiri et al., 2019; Zhou et al., 2019; Wang et al., 2020), and previous work has also demonstrated that VIP-INs in MOp undergo plastic changes in response to reward after associative learning (Lee et al., 2022). To better understand this projection, we sought to further examine the location of the input cells within the ORB (Figure 4A). ORB is comprised of three main subdivisions – the lateral, medial, and ventrolateral regions (ORBl, ORBm, and ORBvl). While the function of individual subregions is still unclear, in monkeys, ORBl has been implicated in reward-guided learning, and ORBm has been implicated in reward-guided decision making (Noonan et al., 2010). In rats, ORBvl has been shown to be involved in goal-directed behavior following contingency switches (Parkes et al., 2018; Zimmermann et al., 2018). In our results, we found that on the ipsilateral side, VIP-INs received almost all of its input from ORBl with no detectable input from ORBm and minimal input from ORBvl. The proportion of input cells from ORBl to VIP-INs was significantly higher than to PV-INs and SST-INs (VIP-IN vs. PV-IN: $p < 0.002$; VIP-IN vs. SST-INs: $p < 1 \times 10^{-3}$; Figures 4B, D, F). Similar observations were made on the contralateral side; VIP-INs also received more input from cells in the contralateral ORBl and barely any input from ORBm and ORBvl. The proportion of input cells from the contralateral ORBl to VIP-INs was also significantly higher than to PV-INs and SST-INs (VIP-IN vs. PV-IN: $p = 0.007$; VIP-IN vs. SST-INs: $p < 1 \times 10^{-3}$; Figures 4C, E, G). These results indicate that VIP-INs in MOp receive a considerable amount of input from both ipsilateral and contralateral ORBl but not ORBm and ORBvl, consistent with the hypothesis that VIP-INs may be involved in reward-guided motor learning (Figures 4F, G). Since VIP-INs received the most input from ORB, we next asked which layers of ORB project to VIP-INs. We found that on both the ipsilateral and contralateral sides, most of the VIP-IN projecting cells were located in L2/3 of ORBl (Figure 4H). On the ipsilateral side, VIP-INs also received some input from L1, L5, and L6a of ORBl, whereas on the contralateral side, VIP-INs received similar proportions of input from L1 compared to the ipsilateral side but not as much from L5 and L6a (Figure 4H).

In addition to ORB, RSP was another region that was identified to be unique as it provided more input to SST-INs compared to both PV-INs and VIP-INs (on the ipsilateral side, SST-INs vs. VIP-INs: $p < 1 \times 10^{-3}$; SST-INs vs. PV-INs: $p = 0.015$; Figure 3B). RSP is a complex brain region that has been implicated in spatial navigation (Vann et al., 2009), associative learning (Lukoyanov and Lukoyanova, 2006; Makino and Komiyama, 2015; Makino et al., 2017; Hattori et al., 2019; Hattori and Komiyama, 2022),

10.3389/fncir.2023.1093066

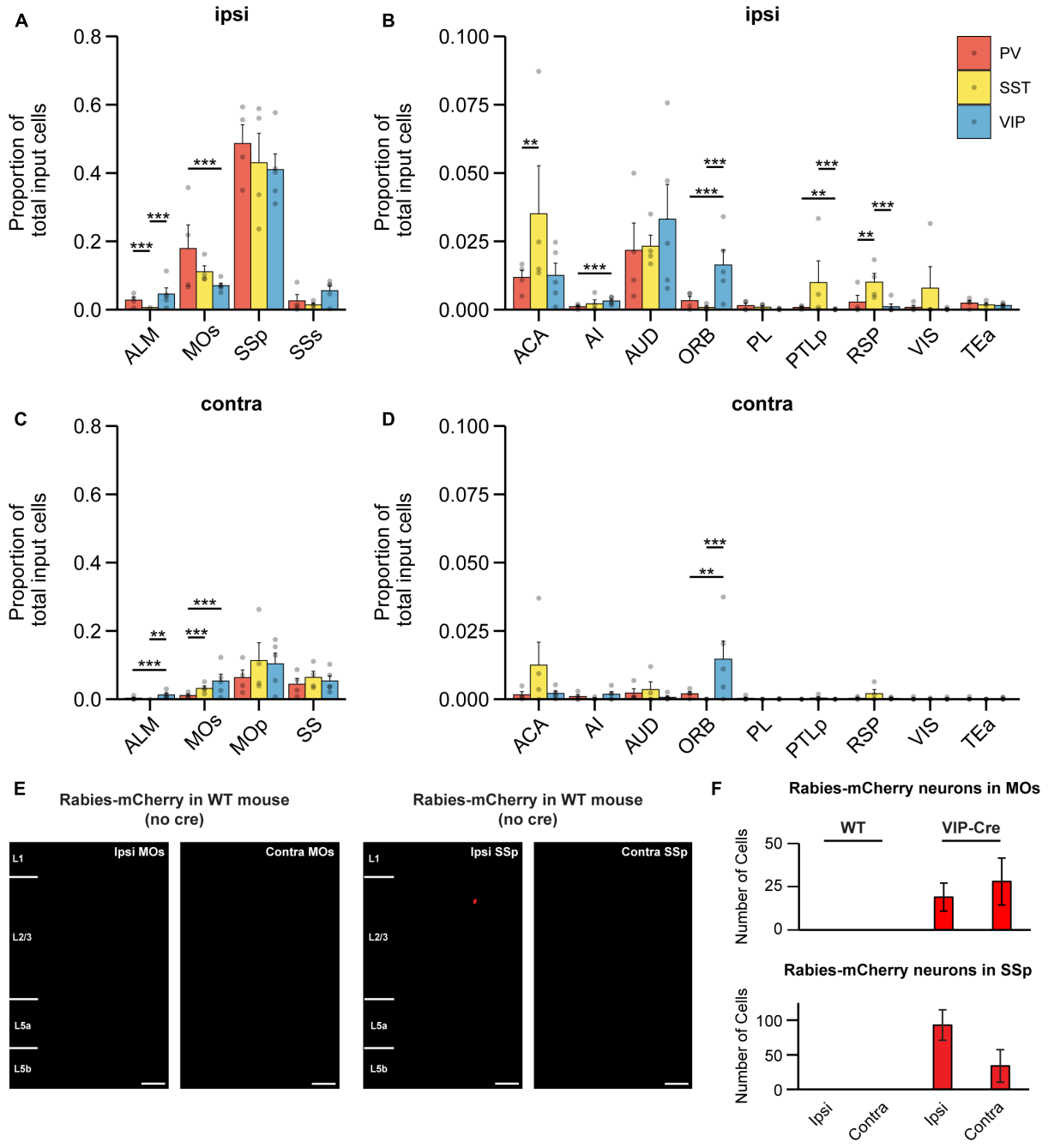

FIGURE 3
Cortical input to different IN subtypes in MOp. **(A)** Mean proportion of input cells in ipsilateral somatosensory and motor cortices. **(B)** Mean proportion of input cells in other ipsilateral cortical regions. Regions with negligible cell counts are not shown. **(C)** Mean proportion of input cells in contralateral somatosensory and motor cortices. **(D)** Mean proportion of input cells in other contralateral cortical regions. Regions with negligible cell counts are not shown. PV-INs, n = 4 mice; SST-INs, n = 4 mice; VIP-INs, n = 5 mice. Bootstrap with Bonferroni correction for multiple comparisons. Each point represents a mouse. **(E)** Example images of wild-type mice injected with AAV2/DJ-hSyn-FLEX-TVA-P2A-eGFP-2A-oG and EnvA-G-deleted-Rabies-mCherry (University of Berlin Viral Core Facility) into right (ipsilateral) MOp. Almost no mCherry$^+$ cells were labeled in MOs and SSp (n = 5 mice, 3 sections per mouse). Scale bar, 100 μm. **(F)** mCherry$^+$ cells found in MOs and SSp of control and experimental animals (VIP-Cre mice). Error bars show the SEM. $^{**}p < 0.01$, $^{***}p < 0.001$.

and motor learning (Makino et al., 2017). RSP can be further subdivided into the lateral agranular, dorsal, and ventral parts (RSPagl, RSPd, and RSPv; Figure 5A). Therefore, we also sought to further examine the location of the input cells to SST-INs within the RSP. On the ipsilateral side, SST-INs received the most input from RSPv, followed by RSPd and small amounts of input from RSPagl (Figure 5D). In contrast, PV-INs and VIP-INs received no input from RSPagl and minimal inputs from RSPd and RSPv (Figures 5B, F). On the contralateral side, SST-INs mainly received input from RSPv and almost no input from RSPd and RSPagl (Figure 5E) while PV-INs and VIP-INs received minimal or no inputs from all subdivisions (Figures 5C, G). Given the biased input to SST-INs

10.3389/fncir.2023.1093066

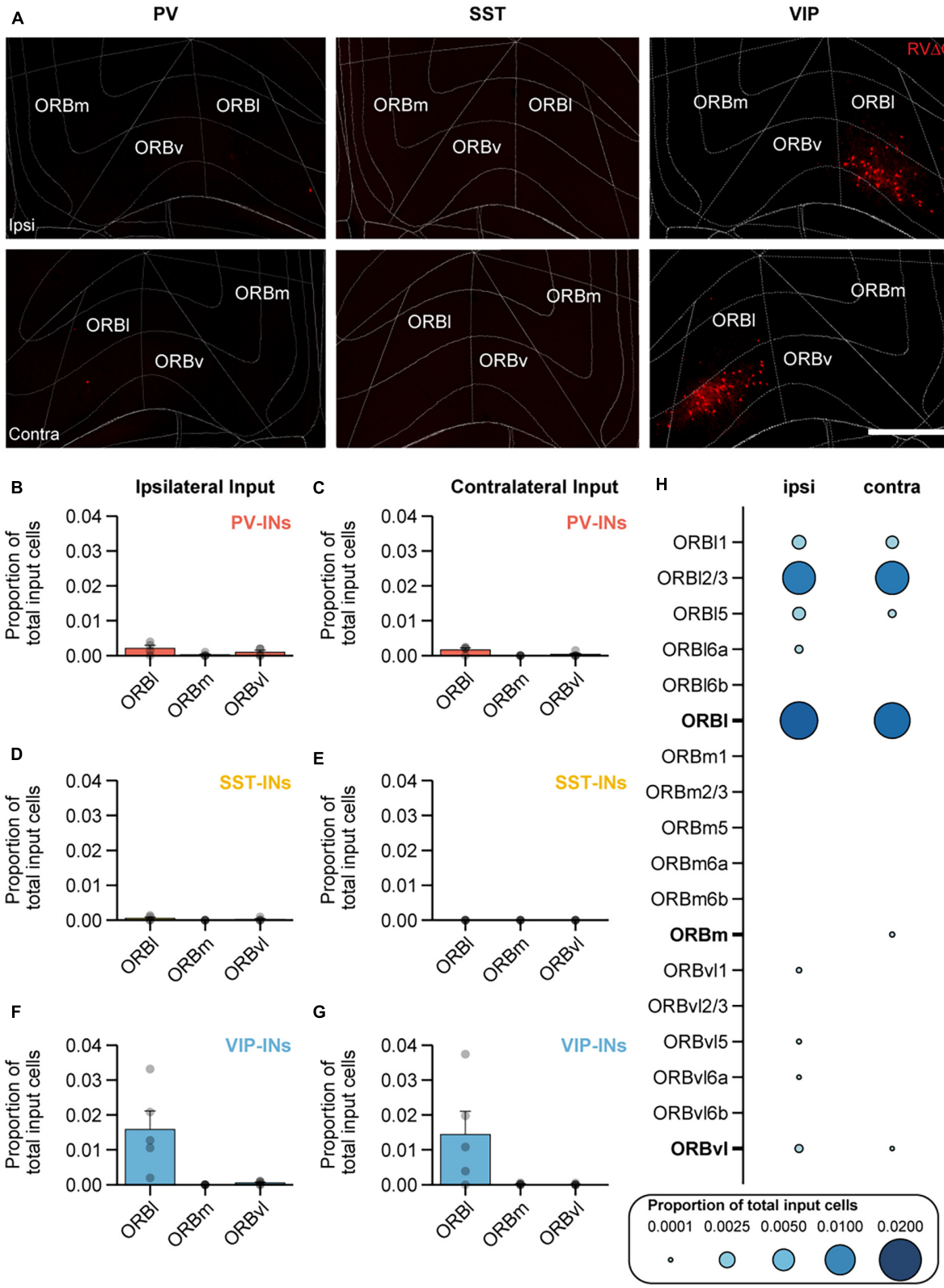

FIGURE 4
ORBl preferentially projects to VIP-INs in MOp. **(A)** Example images of mCherry^{+} input cells in ORB that project to PV-INs (left), SST-INs (middle), and VIP-INs (right) in MOp. Top row, ipsilateral ORB. Bottom row, contralateral ORB. Scale bar, 500 μm. Mean proportion of brain-wide inputs from ipsilateral and contralateral ORB to PV-INs **(B,C)**, SST-INs **(D,E)**, and VIP-INs **(F,G)**. **(H)** Mean proportion of brain-wide inputs to VIP-INs found within different layers of ORBl, ORBm, and ORBvl. Bolded labels show the sum across all layers for each subdivision. PV-INs, n = 4 mice; SST-INs, n = 4 mice; VIP-INs, n = 5 mice. Each point represents a mouse. Error bars show the SEM.

from RSP, we then sought to determine the laminar distribution of RSP projection neurons to SST-INs (**Figure 5H**). We observed that in RSPv, input cells were found in all layers on the ipsilateral side except in L6b. Interestingly, on the contralateral side, input neurons were only found in L1 and L2/3.

Long-range inputs to different IN subtypes in MOp from the thalamus

While the majority of brain-wide input to all three IN subtypes originated from cortex, ipsilateral thalamus was the next largest source of input to VIP-INs, PV-INs, and SST-INs and provided 8, 6, and 4% of the total inputs to VIP-INs, PV-INs, and SST-INs, respectively (**Figures 2G–I**). In contrast, we did not find many input cells in the contralateral thalamus. Inputs from various thalamic nuclei to MOp have been shown before, including significant input from motor-related nuclei such as ventral anterior lateral (VAL) and ventromedial (VM) nuclei (Hooks et al., 2013; Lam and Sherman, 2015; Duan et al., 2020; Muñoz-Castañeda et al., 2021), as well as some input from sensory thalamic nuclei such as the ventral posterior (VP) nuclei (Hunnicutt et al., 2014; Muñoz-Castañeda et al., 2021) and posterior (PO) nuclei (Hooks et al., 2013) among others. From all the nuclei in the thalamus, we observed that a greater proportion of inputs arose from the mediodorsal (MD), parafascicular (PF), PO, VAL, and VP nuclei of thalamus, while relatively small amounts of inputs arose from the central lateral (CL), central medial (CM), lateral dorsal (LD), lateral habenula (LH), paracentral nucleus (PCN), reticular nucleus (RT), and ventromedial (VM) nuclei of thalamus (**Figure 6A**). Intriguingly, we also observed some subtype specificity in the proportion of input. For example, CL projected more to VIP-INs than to SST-INs, and CM provided modest but significantly more input to VIP-INs than to either PV-INs or SST-INs. MD projected significantly more to VIP-INs compared to SST-INs but not to PV-INs, and PCN also provided modest input that was biased to VIP-INs. PO and VM projected significantly more to VIP-INs and PV-INs compared to SST-INs. Lastly, LD, LH, PF, RT, VAL, and VP did not show any subtype specific biases.

It has been shown that various nuclei within thalamus are topographically organized (Angaut et al., 1985; Pierret et al., 2000; Veinante et al., 2000; Lam and Sherman, 2015); hence, we mapped the input neurons within each of the major input nuclei in three-dimensional space to assess whether there is spatial specificity or clustering among the input neurons. Previous work has shown that MD neurons projecting to PV-INs and VIP-INs in the prefrontal cortex occupy distinct locations along the medial-lateral axis (Mukherjee et al., 2021). Here, we found that MD neurons projecting to PV-INs and VIP-INs in MOp were intermingled along the medial-lateral axis (**Figure 6B**). However, MD neurons projecting to VIP-INs appeared to be more widely distributed along the anterior-posterior axis while neurons projecting to PV-INs were located more toward the posterior end of the nucleus (**Figures 6B, C**). Previous work has shown that first-order POm (the medial division of PO) receives direct input from the brainstem and is located more anteriorly (centered around ∼1.7 mm posterior to bregma). Higher-order POm, on the other hand, does not receive input from the brainstem and is located more posteriorly (centered on 2.2 mm posterior to bregma; El-Boustani et al., 2020). We found that input neurons to VIP-INs were located within both of these subdivisions, while neurons providing input to PV-INs lay in between these two subdivisions (**Figures 6D, E**). The ventral group of thalamic nuclei including VAL, VM, and VP show primarily sensory- and motor-related activity. In addition, within the ventral-lateral subdivision, the anterior regions strongly represent whisking-related activity, and more posterior regions are more limb-related (Tlamsa and Brumberg, 2010). We found that VAL was among the most largest source of input to all three IN subtypes, and a cluster of PV-IN projecting neurons was found in the most anterior parts of VAL. In contrast, VIP-IN projecting neurons were found to be more distributed throughout the middle and most posterior regions of VAL (**Figures 6F, G**). Noticeably, SST-INs received a smaller proportion of input from MD, PO, and VAL (**Figure 6A**). The posterior division of the ventral group (VP) relays sensory-related input to the somatosensory cortex (Jensen and Killackey, 1987; Lee and Sherman, 2008). VP neurons projecting to PV-INs were located in the most anterior parts through to the center of the nucleus along the anterior-posterior axis. VIP-IN-projecting neurons in VP were found more uniformly throughout the anterior-posterior length of VP, and SST-IN-projecting neurons were sparser and located just anterior to the center of the nucleus (**Figures 6H, I**). Interestingly, the center region (∼−1.555 mm posterior to bregma) appears to have the largest concentration of input neurons, regardless of the IN subtype. Overall, these results demonstrate that INs in M1 receive input from both first and higher order thalamic nuclei, as well as from sensory, motor, and polymodal nuclei. Moreover, neurons in thalamus projecting to different IN cell types in MOp can occupy distinct regions within the same nucleus.

Brain-wide long-range inputs to PNs in MOp

Lastly, we performed a similar experiment and generated a brain-wide map of input to PNs to examine if any regions send exclusive inputs to IN subtypes but not to PNs. We injected AAV-CaMKII-Cre and the AAV helper virus (AAV2/DJ-hSyn-FLEX-TVA-P2A-eGFP-2A-oG) in WT mice, and 3 weeks after the helper virus injection, we injected the pseudotyped G-deleted RV (EnvA-RVdG-mCherry) into the same site (**Figure 7A**). Starter cells were constrained to MOp (**Figure 7B**). We again used the Wholebrain software to unbiasedly count the labeled input cells in all brain regions (**Figures 7C, D**). We found a starter-to-input cell ratio of 1:9, and the total number of input cells for PNs was 3,431 ± 1,671 cells (PNs: 5 mice, ∼47 slices/mouse). We found that PNs in MOp received very similar inputs compared to all IN subtypes, which includes a large proportion of input from the ipsilateral SSp and MOs (**Figures 7E, H**) and a smaller proportion from the ACA and AUD (**Figures 7F, I**). PNs also received a considerable amount of input from ORB as previously shown (Hooks et al., 2013); however in contrast to VIP-INs, ORB input to PNs was primarily ipsilateral, and input cells were located throughout all the layers in ORBl except for L6b (**Figure 7G**). In addition, similar to SST-INs, PNs also received input from RSP but it was proportionally distributed across RSPd and RSPv

10.3389/fncir.2023.1093066

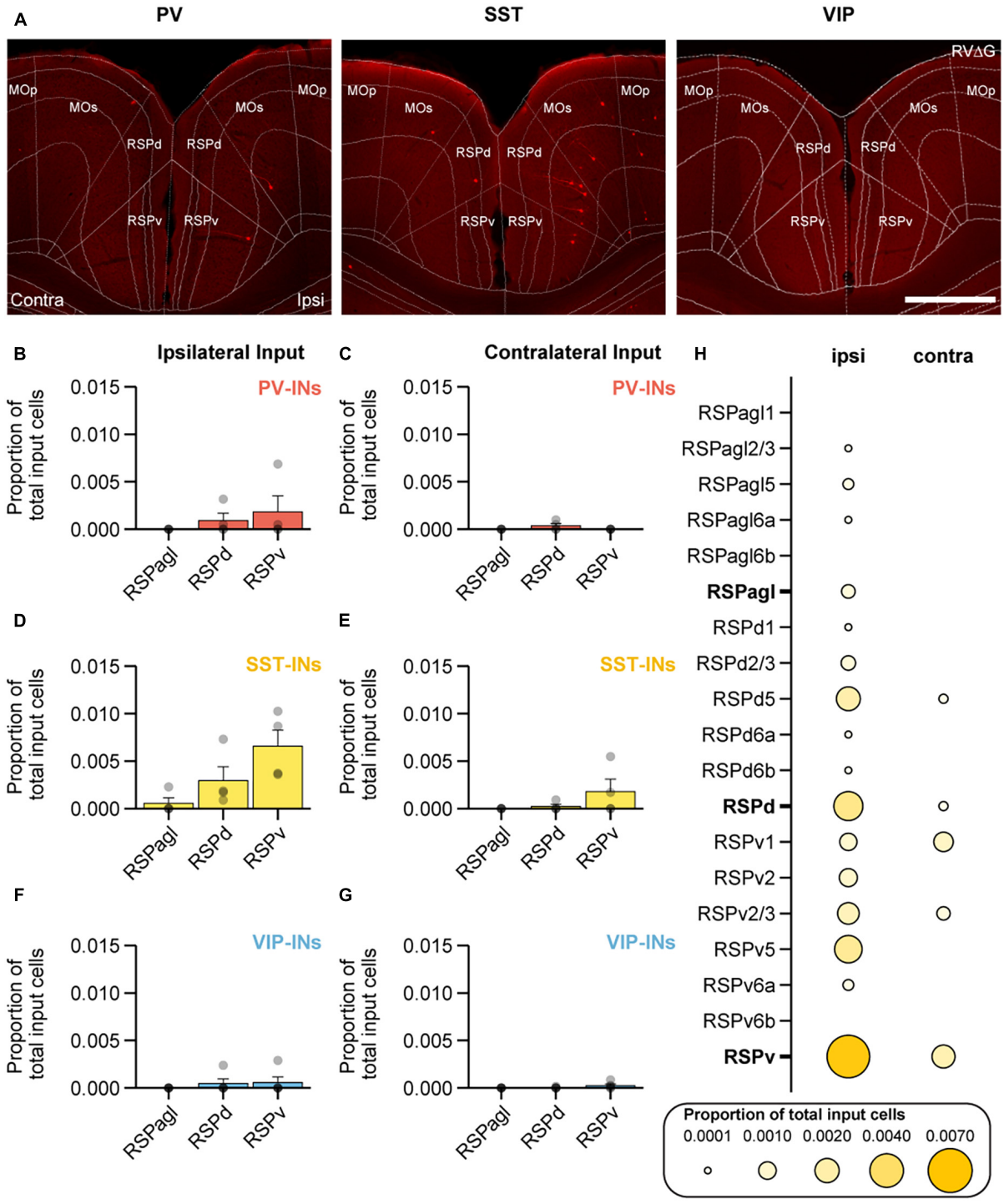

FIGURE 5
RSPd and RSPv preferentially project to SST-INs in MOp. **(A)** Example images of mCherry$^+$ input cells in RSP that project to PV-INs (left), SST-INs (middle), and VIP-INs (right) in MOp. Scale bar, 500 μm. Mean proportion of brain-wide input from ipsilateral and contralateral RSP to PV-INs **(B,C)**, SST-INs **(D,E)**, and VIP-INs **(F,G)**. **(H)** Mean proportion of brain-wide inputs to SST-INs found within different layers of RSPagl, RSPd, and RSPv. Bolded labels show the sum across all layers for each subdivision. PV-INs, n = 4 mice; SST-INs, n = 4 mice; VIP-INs, n = 5 mice. Each point represents a mouse. Each point represents a mouse. Error bars show the SEM.

(Figure 7J). Lastly, many of the major thalamic input nuclei to INs in MOp also projected to PNs, including PO, VAL, and VP, which is consistent with the literature (Hooks et al., 2013; Hunnicutt et al., 2014; Tanaka et al., 2018; **Figure 7K**). It has been shown that CaMKII can be detected in INs (Veres et al., 2023); therefore, we also performed control experiments to examine if we also see AAV helper virus expression in INs. We injected AAV-CaMKII-Cre and the AAV helper virus (AAV2/DJ-hSyn-FLEX-TVA-P2A-eGFP-2A-oG) in WT mice and then stained for GABA to identify INs. We found that ∼14% of the GFP-expressing cells were GABA

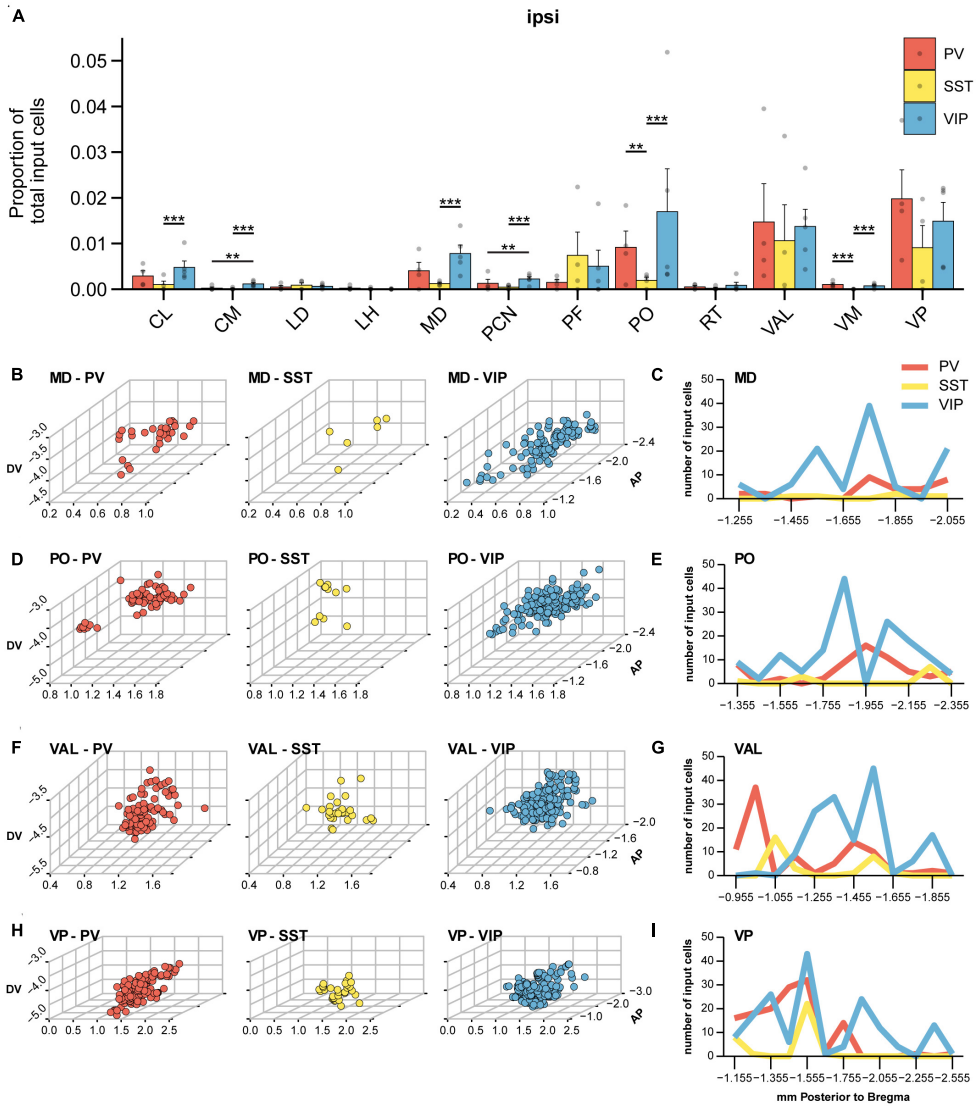

FIGURE 6
Thalamic input to IN subtypes in MOp. **(A)** Mean proportion of brain-wide input found in different thalamic nuclei. Nuclei with a negligible number of cells are not shown. Bootstrap with Bonferroni correction for multiple comparisons. Each point represents a mouse. **(B)** Three-dimensional spatial distribution of input cells within MD of PV-INs (left), SST-INs (middle), and VIP-INs (right). Axes correspond to the medial-lateral (ML), dorsal-ventral (DV), and anterior-posterior (AP) coordinates relative to bregma. Each point represents a cell. **(C)** Number of cells within MD along the anterior-posterior axis for different IN subtypes. **(D)** Three-dimensional spatial distribution of input cells within PO of PV-INs (left), SST-INs (middle), and VIP-INs (right). **(E)** Number of cells within PO along the anterior-posterior axis. **(F)** Three-dimensional spatial distribution of input cells within VAL of PV-INs (left), SST-INs (middle), and VIP-INs (right). **(G)** Number of cells within VAL along the anterior-posterior axis. **(H)** Three-dimensional spatial distribution of input cells within VP of PV-INs (left), SST-INs (middle), and VIP-INs (right). **(I)** Number of cells within VP along the anterior-posterior axis. PV-INs, $n = 4$ mice; SST-INs, $n = 4$ mice; VIP-INs, $n = 5$ mice. Error bars show the SEM. $^{**}p < 0.01$, $^{***}p < 0.001$.

positive (Supplementary Figures 1C, D). Since the ratio of starter cells ($GFP^+/mCherry^+$) to TVA-expressing cells (GFP^+) in the PN brain samples is 1:3, our results suggest that only a tiny proportion of the starter cells (~4.7%) will be INs in this experiment. Overall, from our tracing experiments, we observed that the majority of the input regions to PNs were similar to IN subtypes.

Discussion

It is well-established that MOp is involved in the execution of volitional movement; however, recent observations that MOp also exhibits reward-related activity that could facilitate reward-based motor learning have only begun to be explored. Previous work using *in vivo* two-photon imaging to compare reward representations among PNs, VIP-INs, PV-INs, and SST-INs, revealed that VIP-INs in MOp are preferentially responsive to reward compared to the other cell types in MOp, and their responses to reward become more reliable after associative learning (Lee et al., 2022). Hence, in this study, we employed monosynaptic rabies tracing and brain-wide mapping to identify candidate brain regions with preferential projections to VIP-INs in MOp, which might confer reward-related input to VIP-INs. By generating a comprehensive and subtype-specific map of brain-wide inputs to

10.3389/fncir.2023.1093066

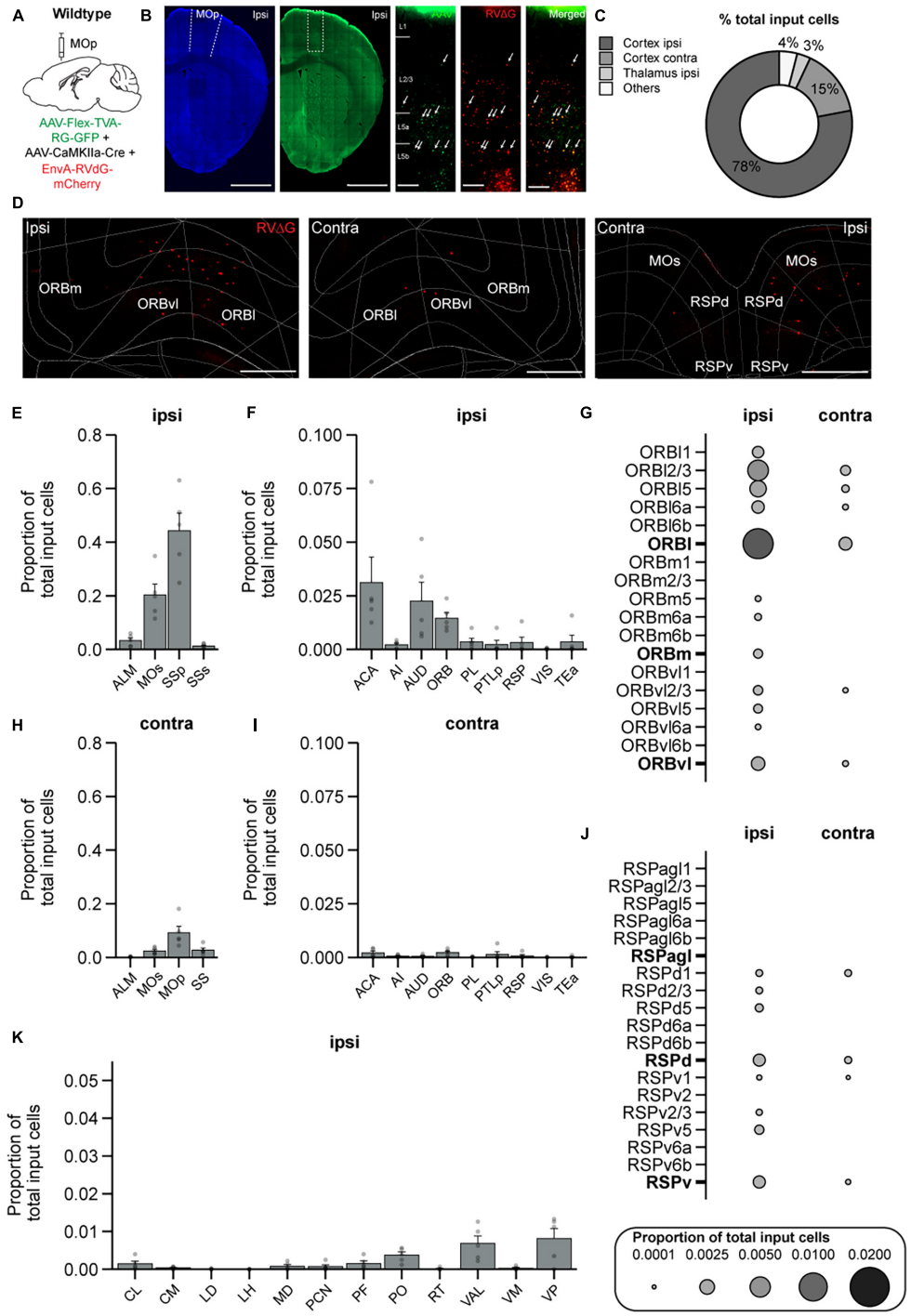

FIGURE 7

Brain-wide input to PNs in MOp. **(A)** Helper virus (AAV2/DJ-hSyn-FLEX-TVA-P2A-eGFP-2A-oG) and CaMKII-Cre were injected unilaterally into right (ipsilateral) MOp of wild-type mice followed by EnvA-G-deleted-Rabies-mCherry (University of Berlin Viral Core Facility) 3 weeks later. Animals were sacrificed 1 week after the rabies viral injection. **(B)** Representative images of the injection site. Neurotrace Blue staining and GFP fluorescence show confinement of GFP^+ cells to MOp. Zoomed in view from the injection site (dashed rectangle in GFP fluorescent image) shows GFP^+ cells (left), $mCherry^+$ cells (middle), and colocalized GFP^+ and $mCherry^+$ starter cells (right). Arrows show example starter cells. Scale bars = 1mm and 100 μm. **(C)** Mean percentage of brain-wide inputs to PNs from broad subdivisions of the brain. **(D)** Example images of $mCherry^+$ input cells in ipsilateral ORB (left), contralateral ORB (middle), and bilateral RSP that project to PNs (right). Scale bars, 500 μm **(E)** Mean proportion of brain-wide input cells in ipsilateral somatosensory and motor cortices. **(F)** Mean proportion of input cells in other ipsilateral cortical regions. Regions with negligible cell counts are not shown. **(G)** Mean proportion of input cells in contralateral somatosensory and motor cortices. **(H)** Mean proportion of input cells in other contralateral cortical regions. Regions with negligible cell counts are not included. **(I)** Mean proportion of brain-wide inputs to PNs found within different layers of ORBl, ORBm, and ORBvl. Bolded labels show the sum across all layers of each subdivision. **(J)** Mean proportion of brain-wide inputs to PNs found within different layers of RSPagl, RSPd, and RSPv. Bolded labels show the sum across all layers of each subdivision. **(K)** Mean proportion of brain-wide input to PNs found in different thalamic nuclei. *n* = 5 mice. Each point represents a mouse. Error bars show the SEM.

VIP-INs and comparing it to the input maps for PV-INs and SST-INs, we demonstrated that the major inputs to all three IN subtypes originated from sensory, motor, prefrontal cortices, as well as thalamus. While many of the identified brain regions provided input to all three IN cell types, some regions were significantly biased toward one particular IN cell type. Among these, we observed dense bilateral input from ORB projecting primarily to VIP-INs. In comparison, we also found biased input from the ipsilateral RSP to SST-INs. Through the generation of IN subtype-specific brain-wide input maps to MOp, this study provides a framework for future investigations exploring how different IN subtypes in MOp integrate long-range inputs from various brain regions and consequently, influence motor output and motor learning.

While the use of monosynaptic rabies tracing provides a number of unique advantages, there are several important technical considerations. It has previously been shown that TVA – EnvA interactions are extremely efficient; hence, very small levels of cre-independent leak expression of TVA can be sufficient for viral infection by EnvA-pseudotyped virus (Seidler et al., 2008; Callaway and Luo, 2015; Hafner et al., 2019). For example, Hafner et al. (2019) conducted a series of control experiments where they injected cre-dependent and flp-dependent helper virus to express TVA but not rabies glycoprotein in WT mice followed by EnvA-RVdG injection. The authors found that there were still cells in the injection site labeled by RVdG virus, demonstrating that small amounts of TVA "invisible leak" expression can enable RVdG infection, and these cells could be mistakenly deemed to be local pre-synaptic inputs. However, cells with cre-independent leak of TVA did not show any trans-synaptic labeling. We also conducted control experiments by injecting the helper virus and RVdG in WT animals. While we did observe some mCherry-only expressing cells in MOp, we did not observe any trans-synaptic spread resulting from TVA-leakage (**Figures 3E, F**). To avoid potential confounds, we refrained from quantifying mCherry-only expressing cells in ipsilateral MOp in our analyses.

It is also important to mention that the transfection efficiency can vary significantly as the result of numerous factors (promoter, viral titer, injection protocols, injection efficacy, the cell type targeted, and transgenic mouse lines used); therefore, the number of starter cells can vary between different studies as well as between animals within a single study (Callaway and Luo, 2015; Roelofs et al., 2021). For this reason, it is convention to view the results as ratios instead of absolute numbers. We found our ratio of starter:input cells comparable to other studies that examined presynaptic input to interneurons in cortical regions (Wall et al., 2016; Gehrlach et al., 2020). In other studies that did not report the starter:input cell ratio, we found that we had a similar number of starter cells per section (Duan et al., 2020). Moreover, Yao et al. (2023) found that differences in the number of starter cells do not drastically alter the proportions of inputs from pre-synaptic input regions, likely due to cells receiving convergent input. With these technical caveats and considerations in mind, we discuss the conceptual implications of our findings below.

One major finding from our work is that ORB provides dense bilateral input preferentially to VIP-INs, and ipsilateral input to PNs. Although previous work identified ORB input to PNs in the vibrissal region of MOp, it remained unclear whether ORB inputs also synapse onto other cell types. Using fluorescent retrograde microbeads, Hooks et al. (2013) found that ipsilateral ORB input neurons projecting to MOp largely originated in deep layers of ORB, while contralateral input was predominantly from superficial layers of ORB. In addition, anterograde tracing of ORBl and ORBvl projections demonstrated the presence of ORB axons throughout all layers of ipsilateral MOp with the greatest presence of axons in deep L5B and L6 (Hooks et al., 2013). In the present study, we found that PNs and VIP-INs are the major recipient cell types of ORB input to MOp, and that both receive input mainly from the lateral part of ORB (ORBl). Interestingly, ORBl neurons projecting to PNs were more numerous on the ipsilateral side and were more evenly distributed throughout L1 to L6a. In contrast, ORB input neurons projecting to VIP-INs were unique in that they resided mainly in the L2/3 of both ipsilateral and contralateral ORBl. These results suggest that the anatomical differences in laminar and hemispheric connectivity from ORB to PNs and VIP-INs in MOp could be related to different roles in processing reward-related signals during learning.

The exact functional role of ORB is still unclear but it is thought to be involved in predicting or updating expected outcomes or values during learning (Baltz et al., 2018; Zhou et al., 2019). Neurons in ORB have been shown to persistently represent both cue and reward throughout learning in an auditory-cued reward associative learning task, and photoinhibition of ORB specifically during the reward-predicting cue period impaired behavioral performance during learning (Namboodiri et al., 2019). Another study found that during an odor-cued reward associative learning task, 29% of ORB neurons demonstrated large amplitude responses to the cue odor after associative learning (Wang et al., 2020). Interestingly, if naïve mice were exposed to the same odor prior to learning and in the absence of reward, only 11% of neurons in ORB showed a response, and these responses were lower in amplitude and trial-to-trial consistency compared to after learning. In line with the notion that ORB represents value, the authors found that ORB neuron responses to the cue were greater when the mice were thirsty compared to when they were satiated. Furthermore, optogenetic silencing of ORB during the cue and response period reduced cue-evoked anticipatory licking, suggesting ORB is involved in encoding the relative value of a stimulus and choosing an appropriate response (Wang et al., 2020). Together with our anatomical results, these findings signify that neurons in ORB represent value by integrating internal state with learned associations and might be involved in reward-based motor skill learning.

It has also been hypothesized that ORB may have a role in regulating reinforcement learning through top-down modulation of cortex (Banerjee et al., 2020; Liu et al., 2020). However, the different subdivisions of ORB are infrequently investigated in isolation, and their individual functions remain unclear. One study found that in monkeys, ORBl is necessary for reward-based learning while ORBm is necessary for reward-based decision making (Noonan et al., 2010). In SSp, ORBl has been shown to project strongly to L2/3 and L5 (Banerjee et al., 2020). Similar to the cue and reward-related responses we observed in MOp during an auditory-cued classical conditioning task (Lee et al., 2022), a subpopulation of neurons in SSp showed outcome or reward-related activity during a texture-based go/no-go task. Furthermore, these outcome-related responses in SSp underwent ORB-dependent remapping during a reversal learning

task, indicating that ORBl input to SSp may function as a teaching signal to modulate and remap SSp activity during reward-based reversal learning. In line with their findings, our results suggest that during motor learning, a bilateral teaching signal from ORBl to VIP-INs in MOp could mediate broad disinhibition. Recent findings from Ren et al. (2022) and Szadai et al. (2022) show that VIP-INs are key regulators in gating a cortex-wide response to reward. Therefore, input from ORB to VIP-INs in MOp during cue and reward could be a potential mechanism for driving VIP-INs and gating plastic changes in MOp during reward-based motor learning.

Generally, other studies mapping presynaptic inputs to different GABAergic inhibitory interneurons in cortex have not found biased input to specific cell types (Wall et al., 2016; but see Leinweber et al., 2017; Ährlund-Richter et al., 2019; Duan et al., 2020; Yao et al., 2023). One possibility is that there are region-specific differences in long-range connectivity. A previous study also used rabies tracing to map presynaptic inputs to VIP-INs, PV-INs, and SST-INs in MOp; however, the results are discordant with some of our key findings. In Duan et al. (2020), they did not observe preferential inputs from ORB to VIP-INs in MOp, but instead, they found that ORB projected mostly to PV-INs, followed by VIP-INs, and then SST-INs. The authors also found that ipsilateral input from ORB to VIP-INs was substantially more abundant than contralateral input, while we found ipsilateral and contralateral inputs from ORB to VIP-INs were comparable in proportion (**Figures 4F, G**). Additionally, Duan et al. found that ORBvl was the primary source of ORB input to MOp, followed by ORBl input, and little to no input from ORBm. Incongruously, we found that ORB input to MOp arose mainly from ORBl with very small amounts of input from ORBvl and ORBm (**Figures 4F, G**). After carefully examining the experimental procedures, we observed several differences in methods including a significant difference in the injection coordinates. In our study, we targeted MOp using the coordinates 0.3 mm anterior and 1.5 mm lateral to bregma. This coordinate was determined based on previous motor mapping studies (defined by measuring evoked forelimb movement) using either optogenetic (Harrison et al., 2012) or electrical (Tennant et al., 2011; Brown et al., 2022) stimulation. This coordinate evoked forelimb movement most reliably (Harrison et al., 2012) and is near the center of the forelimb motor representations (Tennant et al., 2011; Brown et al., 2022). Furthermore, using *in vivo* two-photon imaging, several studies have observed motor learning-related plasticity during forelimb motor learning tasks using this coordinate (Peters et al., 2014, 2017; Chen et al., 2015; Yang et al., 2022), and optogenetic inhibition at this coordinate impairs forelimb function (Peters et al., 2014). Lastly, we also previously observed reward responses in VIP-INs and associative learning-related plasticity in different neuronal subtypes at this coordinate (Lee et al., 2022), which supports our observations that input from ORB to VIP-INs in MOp could provide reward-related signals during reward-based motor learning. In contrast to our injection site, Duan et al. used the coordinate of 1.34 mm anterior and 1.75 mm lateral to bregma. While stimulation at this coordinate can evoke forelimb movement, it is located at the edge of the forelimb representation (Tennant et al., 2011; Harrison et al., 2012; Brown et al., 2022) and is more strongly associated with jaw movement (Tennant et al., 2011). Additionally, Duan et al. used a dorsal-ventral coordinate of −1.5 mm which would target L6. While INs can be found throughout all layers of cortex, VIP-INs, SST-INs, and PV-INs are most numerous in L2–5 (Kawaguchi and Kubota, 1996; Kawaguchi, 1997; Prönneke et al., 2015; Tremblay et al., 2016); therefore, we performed our injections at two depths of −0.3 and −0.5 mm, targeting both L2/3 and L5 of MOp, respectively. Hence, the differential observations from the two studies regarding the cell-type specificity of post-synaptic targets in MOp and bilateral projection patterns may further highlight how different IN subtypes are uniquely involved in regulating local circuitry in different layers and regions of MOp. Finally, we noticed that the two studies utilized different viruses from different sources. Duan et al. used two helper viruses, one to express TVA receptors and another to express RG whereas we utilized a single helper virus to express both TVA and RG concurrently; hence, different serotypes of AAV could also possibly introduce unforeseen biases.

In this study, we have identified a multitude of inputs that target different cell types within MOp. The brain-wide maps of inputs revealed long-range connectivity onto different IN subtypes and provide insight on how input from different regions is parsed within the MOp microcircuitry. Importantly, we identify ORB as a putative candidate region that could drive the reward representation among VIP-INs within MOp. This suggests that MOp is not only involved in producing motor commands, but also integrates numerous streams of complex input, including sensory and reinforcement-related information, to modulate motor behavior and motor learning. Many inputs from a single brain region project onto several IN subtypes; therefore, these streams could engage different cell types in MOp based on the behavioral state or context. Future work will involve detailed investigation of the functional connectivity of these long-range inputs during behavior to examine whether and how they engage distinct modules within MOp during associative and motor learning.

Materials and methods

Mouse lines

All animal experiments were approved by the University of Ottawa Animal Care Committee and in accordance with the Canadian Council on Animal Care guidelines. Experimental mice were group-housed in plastic cages with food and water *ad libitum* in a room with a reversed light cycle (12–12 h). PV-Cre (JAX 008069), SST-Cre (JAX 013044), VIP-Cre (JAX 010908), Ai14 (JAX 007914), and B6129SF1/J (JAX 101043) mouse lines were acquired from Jackson Laboratory (Bar Harbor, ME, USA). VIP-Cre:Ai14 mouse colonies were generated by crossing VIP-Cre females with Ai14 males. All Cre mouse lines were homozygous and in C57BL/6 × 129S4 background, and both male and female mice were used.

Surgery

Mice underwent two surgeries. In the first surgery, they were injected with a helper virus. After 3 weeks, in the second surgery, animals were injected with an engineered RV. The same surgical procedures were used for both surgeries on the same injection

site. Mice were deeply anesthetized using 1–2% isoflurane and given a subcutaneous injection of buprenorphine (0.05 mg/kg) for analgesia. An incision was made, and a small craniotomy was performed at the coordinate 1.5 mm lateral and 0.3 mm anterior to bregma above the forelimb area of MOp. A glass pipette was loaded and lowered to 500 μm below the pia and 100 nl of the virus was injected at a rate of 10 nl/min. The pipette was left in place for 10 min to avoid backflow, then the pipette was raised to 300 μm below the pia and an additional 100 nl of the virus was injected. The pipette was again left in place for 10 min. All injections were performed on the right hemisphere only. The incision was then sutured, bupivacaine ointment was applied topically, and mice recovered on a heated pad. Four hours following surgery, an additional subcutaneous injection of buprenorphine (0.05 mg/kg) was given. For the helper virus injections in PV-Cre, SST-Cre, and VIP-Cre, either AAV1-EF1a-DIO-TVA950-T2A-CVS11G (plasmid obtained from Friedrich Miescher Institute for Biomedical Research Vector Core, titer 3.11×10^{13} GC/ml) or AAV2/DJ-hSyn-FLEX-TVA-P2A-eGFP-2A-oG (Canadian Neurophotonics Platform Viral Vector Core Facility, titer 1.2×10^{13} GC/ml) was used. We switched to a new helper virus as the initial one became unavailable during the span of our experiments. For the helper virus injections targeting PNs, a 1:1 mixture of AAV2/DJ-hSyn-FLEX-TVA-P2A-eGFP-2A-oG and AAV9.CamKII-Cre.SV40 (Addgene, titer 2.1×10^{13} GC/ml or UPenn Vector Core, titer 2.8×10^{12} GC/ml) was used. For the engineered RV injection, EnvA-G-deleted-Rabies-mCherry (Salk Institute for Biological Studies, titer 3.95×10^{8} or 4.24×10^{7} GC/ml or University of Berlin Viral Core Facility, titer 2.4×10^{8} GC/ml) was used.

Histology

One week after the rabies injection, mice were deeply anesthetized and transcardial perfusion was performed with 4% paraformaldehyde (PFA). Brains were kept in 4% PFA overnight at 4°C and transferred to a 30% sucrose and 0.1% sodium azide in phosphate buffered saline (PBS) solution at 4°C. The bottom right side of the brain was cut approximately 1–2 mm deep to mark the injected hemisphere. Brains were then sectioned with a microtome with the thickness of 40 μm and kept in 0.1% sodium azide in PBS solution. Every fourth section was mounted such that the entire brain was screened at 120 μm intervals. Sections were then counterstained using either Neurotrace Blue 435/455 Blue Fluorescent Nissl Stain (Thermo Fisher Scientific) or Vectashield Hardset Antifade Mounting Medium with DAPI (Vector Laboratories).

Control experiments

For all the control experiments, the same surgery, histology and imaging methods were consistent with the experimental groups described above. To test for TVA leakage, AAV2/DJ-hSyn-FLEX-TVA-P2A-eGFP-2A-oG (Canadian Neurophotonics Platform Viral Vector Core Facility) and EnvA-G-deleted-Rabies-mCherry (University of Berlin Viral Core Facility) were injected in WT (B6129SF1/J) mice. After 3 weeks, mice were perfused, and histology, imaging and analyses were performed. To test that helper virus expression was specific to Cre-expressing cells, AAV2/DJ-hSyn-FLEX-TVA-P2A-eGFP-2A-oG (Canadian Neurophotonics Platform Viral Vector Core Facility) was injected in *VIP-Cre:Ail4* mice. After 3 weeks, mice were perfused, and histology, imaging and analyses were performed. To test for RVdG leakage, EnvA-G-deleted-Rabies-mCherry (University of Berlin Viral Core Facility) was injected in WT mice. After 1 week, mice were perfused, and histology, imaging and analyses were performed. To test if the CaMKII promoter is specific to PNs, we injected a 1:1 mixture of AAV2/DJ-hSyn-FLEX-TVA-P2A-eGFP-2A-oG and AAV9.CamKII-Cre.SV40 (Addgene #105558). After 3 weeks, mice were perfused and sectioned. For immunofluorescence targeting GABA, rabbit anti-GABA (1:500; Millipore, A2052) was used for the primary antibody and Alexa Fluor Plus 594 donkey anti-rabbit (1:500; Invitrogen, A21207) was used for the secondary antibody.

Imaging

Images were obtained at 10× with either the Zeiss AxioImager M2, Zeiss AxioScanner Z1 or Zeiss AxioObserver 7 microscopes. Entire brain sections were tiled using motorized stage controls and stitched using Zeiss ZEN Microscope Software.

Data analysis

Starter cells were identified as cells with colocalized eGFP, mCherry, and DAPI/Neurotrace Blue and counted manually using the multi-point tool in Fiji (**Supplementary Figure 1**; Schindelin et al., 2012). Input cells were identified as cells outside of right MOp with colocalized mCherry and DAPI/Neurotrace Blue. Input cells were detected, counted, and registered to brain regions using WholeBrain Software Suite (Fürth et al., 2018) in R. All cell quantifications and image registrations were manually inspected and adjusted as needed. Any incorrectly detected cells that did not colocalize with the counterstain (DAPI or Neurotrace Blue) were removed from the dataset. These incorrectly detected "cells" were mainly autofluorescence signals with fluorescent intensities similar to those of the real cells. Subsequent analysis and figures were made using custom-written code in R and Matlab. All analyses were performed on the proportion of total input cells for each region unless otherwise stated. To calculate the proportion, the number of input cells in a specified region was divided by the total number of input cells in the entire brain for each animal.

Statistics

Comparisons between IN subtypes were performed using one-sided bootstrap. Briefly, distributions F and G, were sampled with replacement and compared under the null hypothesis H_0 : $F = G$ for 1,000 replications. The achieved significance level was calculated as the proportion of replications supporting the null hypothesis (Efron and Tibshirani, 1994). p-Values were corrected for multiple comparisons using the Bonferroni correction. All statistics were performed in Matlab.

Data availability statement

The original contributions presented in this study are included in the article/**Supplementary material**, further inquiries can be directed to the corresponding author.

Ethics statement

The animal study was reviewed and approved by the Animal Care and Veterinary Service (ACVS).

Author contributions

CL, SLC, and SXC conceived the project and wrote the manuscript. CL and SLC conducted the experiments. CL, SLC, NR, HC, and BM performed the image registration and cell quantifications. CL and SLC analyzed the data under the supervision of SXC. All authors contributed to the article and approved the submitted version.

Funding

This work was supported by grants for SXC from Canada Research Chair (CRC) (grant no. 950-231274) and Natural Sciences and Engineering Research Council of Canada (NSERC) (grant no. 05308). CL was supported by Ontario Graduate Scholarship and Queen Elizabeth II Graduate Scholarship. SLC was supported by Fonds de Recherche du Québec Natural Sciences, Mathematics, Sciences and Engineering Post-doctoral Training Scholarship (FRQNT). Imaging was performed using microscopes from the University of Ottawa Cell Biology and Image Acquisition Core Facility (RRID:SCR_021845), funded by the University of Ottawa, Ottawa, Natural Sciences and Engineering Research Council of Canada, and the Canada Foundation for Innovation.

Acknowledgments

We thank the members of the Chen Lab for discussions and providing feedback on the manuscript.

Conflict of interest

The authors declare that the research was conducted in the absence of any commercial or financial relationships that could be construed as a potential conflict of interest.

Publisher's note

Supplementary material

The Supplementary Material for this article can be found online at: https://www.frontiersin.org/articles/10.3389/fncir.2023.1093066/full#supplementary-material

SUPPLEMENTARY FIGURE 1
Control experiments assessing the specificity of the viruses. **(A)** Example images from a VIP-Cre-tdTomato mouse injected with AAV2/DJ-hSyn-FLEX-TVA-P2A-eGFP-2A-oG showing the injection site in right MOp and a zoomed in view with GFP^+ cells labeled from the helper virus (left), $tdTomato^+$ cells (middle), and a merged image showing co-localized GFP^+ and $tdTomato^+$ cells (right). Scale bars, 1 mm and 50 μm. **(B)** Mean percentage of GFP^+ cells co-localizing with tdTomato (n = 4 mice, 2 sections per mouse). **(C)** Example images from a wild-type mouse injected with AAV2/DJ-hSyn-FLEX-TVA-P2A-eGFP-2A-oG and CaMKII-Cre showing the injection site in right MOp and a zoomed in view with of GFP^+ cells (left), $GABA^+$ cells (middle), and a merged image showing co-localized GFP^+ cells and $GABA^+$ cells (right). **(D)** Mean percentage of GFP^+ cells co-localized with GABA (n = 4 mice, 2 sections per mouse).

SUPPLEMENTARY FIGURE 2
Comparison of manual and Wholebrain software counts. Example whole brain sections from VIP-Cre **(A)**, PV-Cre **(B)**, SST-Cre **(C)**, and B6129SF1/J (PN) **(D)** animals displaying manual counts, automatic counts made by the Wholebrain software and the number of "cells" that were removed manually due to being incorrectly detected by the software.

SUPPLEMENTARY TABLE 1
Individual counts of $mCherry^+$ cells outside of MOp and starter cells for each cell type and their ratio. Summary of the animals, $mCherry^+$ cells, starter cells, and number of brain slices with cells that were analyzed for each experimental group in this study.

References

Adler, A., Zhao, R., Shin, M. E., Yasuda, R., and Gan, W.-B. (2019). Somatostatin-expressing interneurons enable and maintain learning-dependent sequential activation of pyramidal neurons. *Neuron* 102, 202–216. doi: 10.1016/j.neuron.2019.01.036

Ährlund-Richter, S., Xuan, Y., van Lunteren, J. A., Kim, H., Ortiz, C., Pollak Dorocic, I., et al. (2019). A whole-brain atlas of monosynaptic input targeting four different cell types in the medial prefrontal cortex of the mouse. *Nat. Neurosci.* 22, 657–668. doi: 10.1038/s41593-019-0354-y

Angaut, P., Cicirata, F., and Serapide, F. (1985). Topographic organization of the cerebellothalamic projections in the rat. An autoradiographic study. *Neuroscience* 15, 389–401. doi: 10.1016/0306-4522(85)90221-0

Baltz, E. T., Yalcinbas, E. A., Renteria, R., and Gremel, C. M. (2018). Orbital frontal cortex updates state-induced value change for decision-making. *eLife* 7:e35988. doi: 10.7554/eLife.35988

Banerjee, A., Parente, G., Teutsch, J., Lewis, C., Voigt, F. F., and Helmchen, F. (2020). Value-guided remapping of sensory cortex by lateral orbitofrontal cortex. *Nature* 585, 245–250. doi: 10.1038/s41586-020-2704-z

Biane, J. S., Takashima, Y., Scanziani, M., Conner, J. M., and Tuszynski, M. H. (2016). Thalamocortical projections onto behaviorally relevant neurons exhibit plasticity during adult motor learning. *Neuron* 89, 1173–1179. doi: 10.1016/j.neuron.2016.02.001

Brown, A. R., Mitra, S., Teskey, G. C., and Boychuk, J. A. (2022). Complex forelimb movements and cortical topography evoked by intracortical microstimulation in male and female mice. *Cereb. Cortex* 33, 1866–1875. doi: 10.1093/cercor/bhac178

Callaway, E. M., and Luo, L. (2015). Monosynaptic circuit tracing with glycoprotein-deleted rabies viruses. *J. Neurosci.* 35, 8979–8985. doi: 10.1523/JNEUROSCI.0409-15.2015

Cao, V. Y., Ye, Y., Mastwal, S., Ren, M., Coon, M., Liu, Q., et al. (2015). Motor learning consolidates arc-expressing neuronal ensembles in secondary motor cortex. *Neuron* 86, 1385–1392. doi: 10.1016/j.neuron.2015.05.022

Chabrol, F. P., Blot, A., and Mrsic-Flogel, T. D. (2019). Cerebellar contribution to preparatory activity in motor neocortex. *Neuron* 103, 506–519.e4. doi: 10.1016/j.neuron.2019.05.022

Chen, S. X., Kim, A. N., Peters, A. J., and Komiyama, T. (2015). Subtype-specific plasticity of inhibitory circuits in motor cortex during motor learning. *Nat. Neurosci.* 18, 1109–1115. doi: 10.1038/nn.4049

Chen, T.-W., Li, N., Daie, K., and Svoboda, K. (2017). A map of anticipatory activity in mouse motor cortex. *Neuron* 94, 866–879.e4. doi: 10.1016/j.neuron.2017.05.005

Condylis, C., Lowet, E., Ni, J., Bistrong, K., Ouellette, T., Josephs, N., et al. (2020). Context-dependent sensory processing across primary and secondary somatosensory cortex. *Neuron* 106, 515–525.e5. doi: 10.1016/j.neuron.2020.02.004

Duan, Z., Li, A., Gong, H., and Li, X. (2020). A whole-brain map of long-range inputs to gabaergic interneurons in the mouse caudal forelimb area. *Neurosci. Bull.* 36, 493–505. doi: 10.1007/s12264-019-00458-6

Efron, B., and Tibshirani, R. J. (1994). *An introduction to the bootstrap*. Boca Raton, FL: Chapman and Hall/CRC. doi: 10.1201/9780429246593

El-Boustani, S., Sermet, B. S., Foustoukos, G., Oram, T. B., Yizhar, O., and Petersen, C. C. H. (2020). Anatomically and functionally distinct thalamocortical inputs to primary and secondary mouse whisker somatosensory cortices. *Nat. Commun.* 11:3342. doi: 10.1038/s41467-020-17087-7

Fürth, D., Vaissière, T., Tzortzi, O., Xuan, Y., Märtin, A., Lazaridis, I., et al. (2018). An interactive framework for whole-brain maps at cellular resolution. *Nat. Neurosci.* 21, 139–149. doi: 10.1038/s41593-017-0027-7

Gehrlach, D. A., Weiand, C., Gaitanos, T. N., Cho, E., Klein, A. S., Hennrich, A. A., et al. (2020). A whole-brain connectivity map of mouse insular cortex. *eLife* 9:e55585. doi: 10.7554/eLife.55585

Guo, J.-Z., Graves, A. R., Guo, W. W., Zheng, J., Lee, A., Rodríguez-González, J., et al. (2015). Cortex commands the performance of skilled movement. *eLife* 4:e10774. doi: 10.7554/eLife.10774

Hafner, G., Witte, M., Guy, J., Subhashini, N., Fenno, L. E., Ramakrishnan, C., et al. (2019). Mapping brain-wide afferent inputs of parvalbumin-expressing GABAergic neurons in barrel cortex reveals local and long-range circuit motifs. *Cell Rep.* 28, 3450–3461.e8. doi: 10.1016/j.celrep.2019.08.064

Harrison, T. C., Ayling, O. G. S., and Murphy, T. H. (2012). Distinct cortical circuit mechanisms for complex forelimb movement and motor map topography. *Neuron* 74, 397–409. doi: 10.1016/j.neuron.2012.02.028

Hattori, R., Danskin, B., Babic, Z., Mlynaryk, N., and Komiyama, T. (2019). Area-specificity and plasticity of history-dependent value coding during learning. *Cell* 177, 1858–1872.e15. doi: 10.1016/j.cell.2019.04.027

Hattori, R., and Komiyama, T. (2022). Context-dependent persistency as a coding mechanism for robust and widely distributed value coding. *Neuron* 110, 502–515.e11. doi: 10.1016/j.neuron.2021.11.001

Hooks, B. M., Mao, T., Gutnisky, D. A., Yamawaki, N., Svoboda, K., and Shepherd, G. M. G. (2013). Organization of cortical and thalamic input to pyramidal neurons in mouse motor cortex. *J. Neurosci.* 33, 748–760. doi: 10.1523/JNEUROSCI.4338-12.2013

Hunnicutt, B. J., Long, B. R., Kusefoglu, D., Gertz, K. J., Zhong, H., and Mao, T. (2014). A comprehensive thalamocortical projection map at the mesoscopic level. *Nat. Neurosci.* 17, 1276–1285. doi: 10.1038/nn.3780

Jensen, K., and Killackey, H. (1987). Terminal arbors of axons projecting to the somatosensory cortex of the adult rat. II. The altered morphology of thalamocortical afferents following neonatal infraorbital nerve cut. *J. Neurosci.* 7, 3544–3553. doi: 10.1523/JNEUROSCI.07-11-03544.1987

Kawaguchi, Y. (1997). GABAergic cell subtypes and their synaptic connections in rat frontal cortex. *Cereb. Cortex* 7, 476–486. doi: 10.1093/cercor/7.6.476

Kawaguchi, Y., and Kubota, Y. (1996). Physiological and morphological identification of somatostatin- or vasoactive intestinal polypeptide-containing cells among GABAergic cell subtypes in rat frontal cortex. *J. Neurosci.* 16, 2701–2715. doi: 10.1523/JNEUROSCI.16-08-02701.1996

Kawai, R., Markman, T., Poddar, R., Ko, R., Fantana, A. L., Dhawale, A. K., et al. (2015). Motor cortex is required for learning but not for executing a motor skill. *Neuron* 86, 800–812. doi: 10.1016/j.neuron.2015.03.024

Kisley, M. A., and Gerstein, G. L. (2001). Daily variation and appetitive conditioning-induced plasticity of auditory cortex receptive fields: Variation and plasticity of receptive fields. *Eur. J. Neurosci.* 13, 1993–2003. doi: 10.1046/j.0953-816x.2001.01568.x

Komiyama, T., Sato, T. R., O'Connor, D. H., Zhang, Y.-X., Huber, D., Hooks, B. M., et al. (2010). Learning-related fine-scale specificity imaged in motor cortex circuits of behaving mice. *Nature* 464, 1182–1186. doi: 10.1038/nature08897

Kwon, S. E., Yang, H., Minamisawa, G., and O'Connor, D. H. (2016). Sensory and decision-related activity propagate in a cortical feedback loop during touch perception. *Nat. Neurosci.* 19, 1243–1249. doi: 10.1038/nn.4356

Lam, Y.-W., and Sherman, S. M. (2015). Functional topographic organization of the motor reticulothalamic pathway. *J. Neurophysiol.* 113, 3090–3097. doi: 10.1152/jn.00847.2014

Lee, C., Harkin, E. F., Yin, X., Naud, R., and Chen, S. (2022). Cell-type-specific responses to associative learning in the primary motor cortex. *eLife* 11:e72549. doi: 10.7554/eLife.72549

Lee, C. C., and Sherman, S. M. (2008). Synaptic properties of thalamic and intracortical inputs to layer 4 of the first- and higher-order cortical areas in the auditory and somatosensory systems. *J. Neurophysiol.* 100, 317–326. doi: 10.1152/jn.90391.2008

Lee, J., and Rothschild, G. (2021). Encoding of acquired sound-sequence salience by auditory cortical offset responses. *Cell Rep.* 37:109927. doi: 10.1016/j.celrep.2021.109927

Leinweber, M., Ward, D. R., Sobczak, J. M., Attinger, A., and Keller, G. B. (2017). A sensorimotor circuit in mouse cortex for visual flow predictions. *Neuron* 95, 1420–1432.e5. doi: 10.1016/j.neuron.2017.08.036

Li, N., Chen, T.-W., Guo, Z. V., Gerfen, C. R., and Svoboda, K. (2015). A motor cortex circuit for motor planning and movement. *Nature* 519, 51–56. doi: 10.1038/nature14178

Liu, D., Deng, J., Zhang, Z., Zhang, Z.-Y., Sun, Y.-G., Yang, T., et al. (2020). Orbitofrontal control of visual cortex gain promotes visual associative learning. *Nat. Commun.* 11:2784. doi: 10.1038/s41467-020-16609-7

Lukoyanov, N., and Lukoyanova, E. (2006). Retrosplenial cortex lesions impair acquisition of active avoidance while sparing fear-based emotional memory. *Behav. Brain Res.* 173, 229–236. doi: 10.1016/j.bbr.2006.06.026

Luo, P., Li, A., Zheng, Y., Han, Y., Tian, J., Xu, Z., et al. (2019). Whole brain mapping of long-range direct input to glutamatergic and GABAergic neurons in motor cortex. *Front. Neuroanat.* 13:44. doi: 10.3389/fnana.2019.00044

Makino, H., and Komiyama, T. (2015). Learning enhances the relative impact of top-down processing in the visual cortex. *Nat. Neurosci.* 18, 1116–1122. doi: 10.1038/nn.4061

Makino, H., Ren, C., Liu, H., Kim, A. N., Kondapaneni, N., Liu, X., et al. (2017). Transformation of cortex-wide emergent properties during motor learning. *Neuron* 94, 880–890.e8. doi: 10.1016/j.neuron.2017.04.015

Mao, T., Kusefoglu, D., Hooks, B. M., Huber, D., Petreanu, L., and Svoboda, K. (2011). Long-range neuronal circuits underlying the interaction between sensory and motor cortex. *Neuron* 72, 111–123. doi: 10.1016/j.neuron.2011.07.029

Mukherjee, A., Lam, N. H., Wimmer, R. D., and Halassa, M. M. (2021). Thalamic circuits for independent control of prefrontal signal and noise. *Nature* 600, 100–104. doi: 10.1038/s41586-021-04056-3

Muñoz-Castañeda, R., Zingg, B., Matho, K. S., Chen, X., Wang, Q., Foster, N. N., et al. (2021). Cellular anatomy of the mouse primary motor cortex. *Nature* 598, 159–166. doi: 10.1038/s41586-021-03970-w

Namboodiri, V. M. K., Otis, J. M., van Heeswijk, K., Voets, E. S., Alghorazi, R. A., Rodriguez-Romaguera, J., et al. (2019). Single-cell activity tracking reveals that orbitofrontal neurons acquire and maintain a long-term memory to guide behavioral adaptation. *Nat. Neurosci.* 22, 1110–1121. doi: 10.1038/s41593-019-0408-1

Noonan, M. P., Walton, M. E., Behrens, T. E. J., Sallet, J., Buckley, M. J., and Rushworth, M. F. S. (2010). Separate value comparison and learning mechanisms in macaque medial and lateral orbitofrontal cortex. *Proc. Natl. Acad. Sci. U.S.A.* 107, 20547–20552. doi: 10.1073/pnas.1012246107

Okoro, S. U., Goz, R. U., Njeri, B. W., Harish, M., Ruff, C. F., Ross, S. E., et al. (2022). Organization of cortical and thalamic input to inhibitory neurons in mouse motor cortex. *J. Neurosci.* 42, 8095–8112. doi: 10.1523/JNEUROSCI.0950-22.2022

Parkes, S. L., Ravassard, P. M., Cerpa, J.-C., Wolff, M., Ferreira, G., and Coutureau, E. (2018). Insular and ventrolateral orbitofrontal cortices differentially contribute to goal-directed behavior in rodents. *Cereb. Cortex* 28, 2313–2325. doi: 10.1093/cercor/bhx132

Peters, A. J., Chen, S. X., and Komiyama, T. (2014). Emergence of reproducible spatiotemporal activity during motor learning. *Nature* 510, 263–267. doi: 10.1038/nature13235

Peters, A. J., Lee, J., Hedrick, N. G., O'Neil, K., and Komiyama, T. (2017). Reorganization of corticospinal output during motor learning. *Nat. Neurosci.* 20, 1133–1141. doi: 10.1038/nn.4596

Pfeffer, C. K., Xue, M., He, M., Huang, Z. J., and Scanziani, M. (2013). Inhibition of inhibition in visual cortex: The logic of connections between molecularly distinct interneurons. *Nat. Neurosci.* 16, 1068–1076. doi: 10.1038/nn.3446

Pi, H.-J., Hangya, B., Kvitsiani, D., Sanders, J. I., Huang, Z. J., and Kepecs, A. (2013). Cortical interneurons that specialize in disinhibitory control. *Nature* 503, 521–524. doi: 10.1038/nature12676

Pierret, T., Lavallée, P., and Deschênes, M. (2000). Parallel streams for the relay of vibrissal information through thalamic barreloids. *J. Neurosci.* 20, 7455–7462. doi: 10.1523/JNEUROSCI.20-19-07455.2000

Prönneke, A., Scheuer, B., Wagener, R. J., Möck, M., Witte, M., and Staiger, J. F. (2015). Characterizing VIP neurons in the barrel cortex of VIPcre/tdTomato mice reveals layer-specific differences. *Cereb. Cortex* 25, 4854–4868. doi: 10.1093/cercor/bhv202

Ren, C., Peng, K., Yang, R., Liu, W., Liu, C., and Komiyama, T. (2022). Global and subtype-specific modulation of cortical inhibitory neurons regulated by acetylcholine during motor learning. *Neuron* 110, 2334–2350.e8. doi: 10.1016/j.neuron.2022.04.031

Roelofs, T. J. M., Menting-Henry, S., Gol, L. M., Speel, A. M., Wielenga, V. H., Garner, K. M., et al. (2021). Optimization of whole-brain rabies virus tracing technology for small cell populations. *Sci. Rep.* 11:10400. doi: 10.1038/s41598-021-89862-5

Schindelin, J., Arganda-Carreras, I., Frise, E., Kaynig, V., Longair, M., Pietzsch, T., et al. (2012). Fiji: An open-source platform for biological-image analysis. *Nat. Methods* 9, 676–682. doi: 10.1038/nmeth.2019

Seidler, B., Schmidt, A., Mayr, U., Nakhai, H., Schmid, R. M., Schneider, G., et al. (2008). A Cre-loxP-based mouse model for conditional somatic gene expression and knockdown in vivo by using avian retroviral vectors. *Proc. Natl. Acad. Sci. U.S.A.* 105, 10137–10142. doi: 10.1073/pnas.0800487105

Siniscalchi, M. J., Phoumthipphavong, V., Ali, F., Lozano, M., and Kwan, A. C. (2016). Fast and slow transitions in frontal ensemble activity during flexible sensorimotor behavior. *Nat. Neurosci.* 19, 1234–1242. doi: 10.1038/nn.4342

Staiger, J. F., and Petersen, C. C. H. (2021). Neuronal circuits in barrel cortex for whisker sensory perception. *Physiol. Rev.* 101, 353–415. doi: 10.1152/physrev.00019.2019

Szadai, Z., Pi, H.-J., Chevy, Q., Ócsai, K., Albeanu, D. F., Chiovini, B., et al. (2022). Cortex-wide response mode of VIP-expressing inhibitory neurons by reward and punishment. *eLife* 11:e78815. doi: 10.7554/eLife.78815

Tanaka, Y. H., Tanaka, Y. R., Kondo, M., Terada, S.-I., Kawaguchi, Y., and Matsuzaki, M. (2018). Thalamocortical axonal activity in motor cortex exhibits layer-specific dynamics during motor learning. *Neuron* 100, 244–258.e12. doi: 10.1016/j.neuron.2018.08.016

Tennant, K. A., Adkins, D. L., Donlan, N. A., Asay, A. L., Thomas, N., Kleim, J. A., et al. (2011). The organization of the forelimb representation of the C57BL/6 mouse motor cortex as defined by intracortical microstimulation and cytoarchitecture. *Cereb. Cortex* 21, 865–876. doi: 10.1093/cercor/bhq159

Tlamsa, A. P., and Brumberg, J. C. (2010). Organization and morphology of thalamocortical neurons of mouse ventral lateral thalamus. *Somatosens. Mot. Res.* 27, 34–43. doi: 10.3109/08990221003646736

Tremblay, R., Lee, S., and Rudy, B. (2016). GABAergic interneurons in the neocortex: From cellular properties to circuits. *Neuron* 91, 260–292. doi: 10.1016/j.neuron.2016.06.033

Vann, S. D., Aggleton, J. P., and Maguire, E. A. (2009). What does the retrosplenial cortex do? *Nat. Rev. Neurosci.* 10, 792–802. doi: 10.1038/nrn2733

Veinante, P., Jacquin, M. F., and Deschênes, M. (2000). Thalamic projections from the whisker-sensitive regions of the spinal trigeminal complex in the rat. *J. Comp. Neurol.* 420, 233–243. doi: 10.1002/(sici)1096-9861(20000501)420:2<233::aid-cne6>3.0.co;2-t

Veres, J. M., Andrasi, T., Nagy-Pal, P., and Hajos, N. (2023). CaMKIIα promoter-controlled circuit manipulations target both pyramidal cells and inhibitory interneurons in cortical networks. *eNeuro* 10:ENEURO.0070-23.2023. doi: 10.1523/ENEURO.0070-23.2023

Wall, N. R., De La Parra, M., Sorokin, J. M., Taniguchi, H., Huang, Z. J., and Callaway, E. M. (2016). Brain-wide maps of synaptic input to cortical interneurons. *J. Neurosci.* 36, 4000–4009. doi: 10.1523/JNEUROSCI.3967-15.2016

Wang, P. Y., Boboila, C., Chin, M., Higashi-Howard, A., Shamash, P., Wu, Z., et al. (2020). Transient and persistent representations of odor value in prefrontal cortex. *Neuron* 108, 209–224.e6. doi: 10.1016/j.neuron.2020.07.033

Wickersham, I. R., Lyon, D. C., Barnard, R. J. O., Mori, T., Finke, S., Conzelmann, K.-K., et al. (2007). Monosynaptic restriction of transsynaptic tracing from single, genetically targeted neurons. *Neuron* 53, 639–647. doi: 10.1016/j.neuron.2007.01.033

Xu, T., Yu, X., Perlik, A. J., Tobin, W. F., Zweig, J. A., Tennant, K., et al. (2009). Rapid formation and selective stabilization of synapses for enduring motor memories. *Nature* 462, 915–919. doi: 10.1038/nature08389

Yang, J., Serrano, P., Yin, X., Sun, X., Lin, Y., and Chen, S. X. (2022). Functionally distinct NPAS4-expressing somatostatin interneuron ensembles critical for motor skill learning. *Neuron* 110, 3339–3355.e8. doi: 10.1016/j.neuron.2022.08.018

Yao, S., Wang, Q., Hirokawa, K. E., Ouellette, B., Ahmed, R., Bomben, J., et al. (2023). A whole-brain monosynaptic input connectome to neuron classes in mouse visual cortex. *Nat. Neurosci.* 26, 350–364. doi: 10.1038/s41593-022-01219-x

Zhou, J., Montesinos-Cartagena, M., Wikenheiser, A. M., Gardner, M. P. H., Niv, Y., and Schoenbaum, G. (2019). Complementary task structure representations in hippocampus and orbitofrontal cortex during an odor sequence task. *Curr. Biol.* 29, 3402–3409.e3. doi: 10.1016/j.cub.2019.08.040

Zimmermann, K. S., Li, C., Rainnie, D. G., Ressler, K. J., and Gourley, S. L. (2018). Memory retention involves the ventrolateral orbitofrontal cortex: Comparison with the basolateral amygdala. *Neuropsychopharmacology* 43, 373–383. doi: 10.1038/npp.2017.139

frontiers | Frontiers in Neural Circuits

TYPE Original Research
PUBLISHED 02 June 2023
DOI 10.3389/fncir.2023.1138358

OPEN ACCESS

EDITED BY
Lisa Topolnik,
Laval University, Canada

REVIEWED BY
Ivo Spiegel,
Weizmann Institute of Science, Israel
Maximiliano Jose Nigro,
Norwegian University of Science and Technology, Norway

*CORRESPONDENCE
Bianca A. Silva
✉ bianca.silva@in.cnr.it
Anthony Holtmaat
✉ anthony.holtmaat@unige.ch

†These authors have contributed equally to this work

‡Deceased

RECEIVED 05 January 2023
ACCEPTED 16 May 2023
PUBLISHED 02 June 2023

CITATION
Fossati G, Kiss-Bodolay D, Prados J, Chéreau R, Husi E, Cadilhac C, Gomez L, Silva BA, Dayer A and Holtmaat A (2023) Bimodal modulation of L1 interneuron activity in anterior cingulate cortex during fear conditioning.
Front. Neural Circuits 17:1138358.
doi: 10.3389/fncir.2023.1138358

Bimodal modulation of L1 interneuron activity in anterior cingulate cortex during fear conditioning

Giuliana Fossati[1,2†], Daniel Kiss-Bodolay[1,3,4†], Julien Prados[1,5], Ronan Chéreau[1], Elodie Husi[1], Christelle Cadilhac[1,5], Lucia Gomez[1,5], Bianca A. Silva[2,6*], Alexandre Dayer[1,5‡] and Anthony Holtmaat[1*]

[1]Department of Basic Neurosciences, and Neurocenter, Faculty of Medicine, University of Geneva, Geneva, Switzerland, [2]Neuro Center, IRCCS Humanitas Research Hospital, Milan, Italy, [3]Department of Neurosurgery, Geneva University Hospitals, Geneva, Switzerland, [4]Lemanic Neuroscience Doctoral School, University of Geneva, Geneva, Switzerland, [5]Department of Psychiatry, University of Geneva, Geneva, Switzerland, [6]National Research Council of Italy, Institute of Neuroscience, Milan, Italy

The anterior cingulate cortex (ACC) plays a crucial role in encoding, consolidating and retrieving memories related to emotionally salient experiences, such as aversive and rewarding events. Various studies have highlighted its importance for fear memory processing, but its circuit mechanisms are still poorly understood. Cortical layer 1 (L1) of the ACC might be a particularly important site of signal integration, since it is a major entry point for long-range inputs, which is tightly controlled by local inhibition. Many L1 interneurons express the ionotropic serotonin receptor 3a (5HT3aR), which has been implicated in post-traumatic stress disorder and in models of anxiety. Hence, unraveling the response dynamics of L1 interneurons and subtypes thereof during fear memory processing may provide important insights into the microcircuit organization regulating this process. Here, using 2-photon laser scanning microscopy of genetically encoded calcium indicators through microprisms in awake mice, we longitudinally monitored over days the activity of L1 interneurons in the ACC in a tone-cued fear conditioning paradigm. We observed that tones elicited responses in a substantial fraction of the imaged neurons, which were significantly modulated in a bidirectional manner after the tone was associated to an aversive stimulus. A subpopulation of these neurons, the neurogliaform cells (NGCs), displayed a net increase in tone-evoked responses following fear conditioning. Together, these results suggest that different subpopulations of L1 interneurons may exert distinct functions in the ACC circuitry regulating fear learning and memory.

KEYWORDS

anterior cingulate cortex, serotonin receptor 3a, neurogliaform cells, fear learning, 2-photon laser scanning microscopy, microprism

Introduction

Fear and anxiety-related disorders impose a major burden on people and society. Despite the high prevalence of these disorders, their mechanistic underpinnings remain largely unknown. Defensive responses upon perception of fearful stimuli are in large part innate, but they can also be learned through the association of threats and harmful events with concomitantly presented stimuli (Gross and Canteras, 2012; Silva et al., 2016; LeDoux and Daw, 2018).

The neuronal circuits underlying fear and fear learning have been studied in animals and humans (Tovote et al., 2015), mostly using Pavlovian fear conditioning (FC) paradigms. In these paradigms, a mild electric foot shock is typically used as an unconditioned stimulus (US) that elicits an innate fear response. Repeated pairing of the US with a neutral stimulus (conditioned stimulus–CS) leads to a conditioned response (CR) upon subsequent presentation of the CS alone, which in rodents presents itself as freezing behavior. Such studies have revealed major roles for the amygdala, the hippocampus, and various cortical structures in fear learning and memory (Herry and Johansen, 2014; Tovote et al., 2015; Greco and Liberzon, 2016). Of these, high order prefrontal cortical areas were found to play important roles in assessing the severity and controllability of stressors or threats and to bidirectionally modulate fear expression, fear memory encoding and extinction (Amat et al., 2005; Giustino and Maren, 2015).

The medial prefrontal cortex (mPFC) comprises various executive centers implicated in the control of cognitive, emotional and social behaviors (Yizhar et al., 2011; Coley et al., 2021; Howland et al., 2022). Specifically, all its three subdivisions, the infralimbic (IL), prelimbic (PL) and anterior cingulate cortices (ACC), represent crucial nodes in the cortico-hippocampal-amygdala circuit that regulate fear learning and have been selectively implicated in the acquisition, retrieval and extinction of fear memories (Dejean et al., 2015). While the functional circuit organization of the PL and IL subdivisions in relation to fear learning has been investigated in detail, including layer and cell type specific interrogation of function (Courtin et al., 2014; Dejean et al., 2015), the contribution of the ACC to fear learning has been dissected with far less detail. Specifically, the ACC shows a global activity increase upon fear learning in both rodents and humans (Etkin et al., 2011; Steenland et al., 2012; Greco and Liberzon, 2016; Roy et al., 2022). Direct stimulation of the ACC in mice produces long-term fear memories, while its inhibition impairs them (Tang et al., 2005; Einarsson and Nader, 2012; de Lima et al., 2022). However, due to its location deep in the medial bank of the cortex, imaging and electrophysiology studies have mostly been performed at a relatively low resolution and without clear identification of the cell types that displayed activity upon fear conditioning. Therefore, the specific contribution of the different neuronal cell types to the global fear memory-related increase of ACC activity have not yet been disentangled. In particular, the role of inhibitory interneuron types remains elusive, yet they are critical for cortical processing. For example, inhibitory microcircuits in a number of limbic areas have been identified as key regulators of the amount of excitation that a particular stimulus elicits and are essential modulators of the CS-US association coding (Ehrlich et al., 2009; Donato et al., 2013; Courtin et al., 2014; Wolff et al., 2014; Tovote et al., 2015). Therefore, characterizing the evolution of interneuron activity is important for understanding how the ACC processes and encodes information over the course of fear learning.

Interneurons in cortical layer 1 (L1) play an important role in balancing the long-range and local excitation (Tremblay et al., 2016; Ibrahim et al., 2021) and have been shown to regulate fear learning processes (Letzkus et al., 2011, 2015). This suggests that L1 interneurons in the ACC could also play a fundamental role in fear learning and memory. In addition, a subpopulation of L1 interneurons has been shown to express the ionotropic serotonergic receptor 3A (5HT3aR) (Zhou and Hablitz, 1999; Ferezou et al., 2002; Lee et al., 2010; Vucurovic et al., 2010; the Allen Cell Type database: https://portal.brain-map.org/atlases-and-data/rnaseq), a gene which has been linked to fear-related pathologies by genetic and epigenetic studies (Kelmendi et al., 2016; Perroud et al., 2016; Schechter et al., 2017). However, unlike in sensory cortices (Letzkus et al., 2011, 2015) there is a paucity of information about the activity of L1 interneurons in the prefrontal cortex in general and during fear learning in particular. L1 cortical interneurons can be divided into two anatomically and functionally distinct classes: single bouquet cells and neurogliaform cells (NGCs) (Lee et al., 2015). The former display distinct morphological and electrophysiological properties, are characterized by a simple axonal arbor, and preferentially target deeper layer interneurons (Schuman et al., 2019); the latter are characterized by axonal arbors restricted to L1 and contact both interneurons and principal neurons distal dendrites (Letzkus et al., 2011; Jiang et al., 2013; Abs et al., 2018; Niquille et al., 2018; Schuman et al., 2019). NGCs are part of a population of interneurons that have been identified in the auditory cortex as regulators of plasticity in fear conditioning (Abs et al., 2018). However, their activity during fear learning has never been specifically investigated in the ACC.

Here, we utilized transgenic mice and AAV vectors to drive the expression of genetically encoded calcium sensors in the 5HT3aR and NGCs subpopulations of L1 interneurons, and applied 2-photon laser scanning microscopy (2PLSM) through microprism implants to longitudinally image these neurons in the ACC before and after cued FC (Andermann et al., 2013; Low et al., 2014; Pattwell et al., 2016). We show that FC changes their response dynamics. Within both populations, we identified distinct neuronal assemblies that either increase (positively modulated) or decrease (negatively modulated) their responses to the CS following FC and found more positively modulated neurons among the NGC population. These results suggest that fear learning is associated with a net increase in inhibitory activity of a cell type that targets pyramidal cell apical dendrites, potentially impacting the integration of long-range inputs that project to L1 of the ACC.

Materials and methods

Animals and viral vectors

Animals were group housed at the University of Geneva's animal husbandry facility on a 12-h light cycle (lights on at 8:00 a.m.). All procedures were carried out in accordance with protocols approved by the ethics committee of the University of Geneva

and the authorities of the Canton of Geneva (license numbers GE/28/14, GE/61/17).

For all the experiments we used 12 weeks-old male mice. To target 5HT3aR-expressing interneurons we used the Tg(Htr3a-cre)NO152Gsat line produced by the Gene Expression Nervous System Atlas [GENSAT] project at the Rockefeller University (New York, NY) (MGI: 5435492; J:100256).[1] To target NGCs, we used an in-house bred NGC-Flippase line. This line was created by crossing the Tg(Hmx3-icre)1Kess line (MGI: 5566775; MGI:5566775)[2] (Niquille et al., 2018), with the Cre-conditional Rosa-26-CAG-LSL-Flp line [B6;129S4-Gt(ROSA)26Sortm5(CAG-flpo)Zjh/J].[3] This strategy allowed robust and local viral vector-mediated expression of a genetically encoded calcium sensor, which was preferable to direct crossing of the Hmx3-Cre line with a Cre-dependent reporter line. For the L1 5HT3aR cell targeting experiments, AAV9-hSyn-DIO-GcaMP6s was injected (Penn Vector Core, PA, USA; 90 nl per injection). For the L1 NGC cell targeting experiments, AAV1/2-hSyn.fDIO.GCaMP6s was injected (EMBL viral core facility, Rome, Italy; 90 nl per injection).

Surgery for microprism implantation

All surgeries were performed in a dedicated separate surgery room equipped with an intermediary animal housing station and heating pads. Before the surgery, all micro instruments and the surgical bench were cleaned with 70% ethanol (Sigma). Anesthesia induction was done with a mix of O2 and 4% isoflurane at 0.4 L/min (Baxter) followed by an intraperitoneal injection of MMF solution, consisting of 0.2 mg/kg medetomidine (Dormitory, Orion Pharma, Milan, Italy), 5 mg/kg midazolam (Dormicum, Roche, Basel, Switzerland), and 0.05 mg/kg fentanyl (Fentanyl, Sintetica, Münster, Germany) diluted in sterile 0.9% NaCl producing deep anesthesia and analgesia for a minimum of 2 h. After stable deep anesthesia was confirmed by using toe pinching, a 2 μg/g IP injection of dexamethasone was given to reduce brain swelling and inflammation (Mephameson, Mepha Pharma, Aesch, Switzerland). Animals were then placed on a heating pad (MIO Star thermocare 100) set at 37°C and head fixed in stereotaxic frame (Stoelting) equipped with one-axis oil hydraulic micromanipulator (MO-10, Narishige, London, United Kingdom). Sterile lubricant eye ointment was applied (Lacryvisc, Alcon, Geneva, Switzerland). Betadine (Mundipharma, Cambridge, United Kingdom) skin surface disinfection followed by local anesthesia using subcutaneous scalp injection of Lidocaine 1% (Streuli, Uznach, Switzerland) was performed before skin incisions were made. After termination of the surgery, a wake solution composed of Atipamezole 2.5 mg/Kg (Antisedan, Orion Pharma, Milan, Italy), Flumazenil 0.5 mg/Kg (Anexate flumazenil, Roche, Basel, Switzerland), Buprenorphine 0.1 mg/Kg (Temgesic buprenorphinum, Schering-Plough, NJ, USA) was delivered subcutaneously and 500 μl of intraperitoneal sterile saline was injected for rehydration. Animals were then placed on a heating pad set to 37°C with food and water *ad libitum*. Animals were returned to the home cage when diuresis and gastrointestinal transit had restarted and signs of acute pain were absent. Anesthesia for the entire surgery in general lasted 1 h–1 h 30.

Microprism surgical implantation was performed based on a modified protocol described previously (Low et al., 2014). Specifically, 1.5 mm sized microprisms with aluminum coating on the hypotenuse (BK7 glass, TowerOptical, CT, USA, MPCH-1.5) were used. These 1.5 mm microprisms were inserted in the interhemispheric fissure, in the subdural space of the left hemisphere, with the lateral face flush with the dural falx and facing the right ACC. In this configuration, the excitation light entered the microprism through the top face and the emitted fluorescence light through the lateral face (**Figure 1A**). Both were reflected on the aluminum-coated hypotenuse. Before surgery, the microprisms and coverslips were cleaned using sterile saline and dried with microscope paper (Kimtech 7552) to reduce dust layers. Under a surgery stereo microscope (M80, Leica, Wetzlar, Germany) the microprisms were then bonded to a 3 mm coverslip (64-0720, Multi-channel systems) using one drop of UV-curing glue (Norland, PA, USA) which was placed with the tip of a needle on the center of the window. Care was taken to have the glue evenly distributed over the entire surface of the prisms to avoid unequal transparencies. Curing was performed using a UVA lamp. Surgical loop was used (M80, Leica, Wetzlar, Germany) and surgical field illumination was done using fiber lights (MI-150, Dolan-Jenner). The craniotomy was performed using a 0.6 mm dental drill (HM1 006, Meisinger, Düsseldorf, Germany). Sterile cortex buffer [125 mM NaCl (7.21 g NaCl), 5 mM KCl (0.372 g KCl), 10 mM glucose (1.802 g glucose), 10 mM HEPES (2.38 g HEPES), 2 mM CaCl2 (2 ml 1M CaCl2) and 2 mM MgSO4 (2 ml 1M MgSO4) in distilled 1l H2O] to moisturize the tissue. For hemostasis, small pieces of sterilized microscope paper were combined with humidified Gelfoam (Pfizer, New York, NY, USA). A surgical tray sterilized with ethanol 70% was used to contain the following micro instruments during the procedure: Vannas Spring Scissors (15070-08, Fine Science Tools, Heidelberg, Germany), Extra Fine Bonn Scissors (14083-08, Fine Science Tools, Heidelberg, Germany), two Student Dumont #5 Forceps (91150-20, Fine Science Tools, Heidelberg, Germany) angle sharp microtool (Ergobrobe 202660, M + W dental), two standard blue forceps (DumontAA 11210-10, Fine Science Tools, Heidelberg, Germany, microblade), microspatula (orban scaler, World Precision Instrument, FL, USA), 3 mm disposable biopsy puncher (801818, World Precision Instrument), two plastic forceps (11700-00, Fine Science Tools, Heidelberg, Germany), and a skin tissue forceps (Adson 14226-G, World Precision Instrument, FL, USA). The window was sealed using acrylic superglue (110-41-180, Patex), and a head cap was created out of dental acrylic (Jet repair, Lang Dental, NY, USA), which was adhered to the skull by applying the liquid mix to the superglue-covered skull surface. The aluminum holders (1269-7475-001, Protolab, MN, USA) were fixed to the head cap by using another layer of dental acrylic.

Stereotaxic injections of adeno-associated viral (AAV) vectors were performed in the contralateral, intact hemisphere right after the craniotomy and before microprism implantation. Injection pipettes were made from Drummond Wiretrol II 1–5 μl capillaries (DRUM5-000-2005, Drummond). Stereotaxic injections were delivered to the ACC through two separate injection points on the

1 http://www.informatics.jax.org/reference/

2 http://www.informatics.jax.org/allele/

3 https://www.jax.org/strain/028584

rostro-caudal axis in order to avoid tissue trauma-related gliosis in the center of the future imaged area. The ACC spans a cortical area extending from the caudal edge of the PL cortex to the rostral edge of the retrosplenial cortex (RSP). The surface vasculature over this region is dense and the size of the sagittal sinus greatly varies in different mice. To avoid penetrating the vasculature, the injection slightly varied between mice along the rosto-caudal axis, but always well within the range of the ACC. The injection coordinates were the following: rostro-caudal, between +1.5 mm and −0.7 mm around bregma; dorso-ventral between 0.7 and 0.8 mm from the pia; medio-lateral, between 0.2 and 0.3 mm from the sagittal suture. Therefore, all the injections were centered in the dorsal part of the ACC, centered in the Cg1 subregion as defined by Paxinos atlas (or the ACAd according to the Allen Brain Atlas), which aligns with the well characterized parcellation of the cingulate cortex in rodents (van Heukelum et al., 2020). Expression of GCaMP6s was allowed to ramp up for at least 2–3 weeks after surgery. Imaging was started if the brain's vasculature and surface maintained a clear and healthy appearance 2–3 weeks after the microprism implantation. The intradural and subdural and intracortical vasculature was used to register regions of interest and to re-identify neurons at different time points.

Fear conditioning protocol

Mice were handled for at least 7 days (10 min, twice a day) to allow familiarization with the experimenter and microscope enclosure. Subsequently, mice underwent four habituation sessions (Hab1-4, 1 session/day), during which they were awake and head-fixed in the microscope setup and exposed to the conditioning tones (conditioned stimulus, CS). This protocol was composed of a 5-min silent baseline period followed by 10 tones (70 dB, 7.5 kHz, 200 ms duration) delivered at 1 Hz for 30 s (Grewe et al., 2017) with variable inter-stimulus intervals (ISI) of 60–90 s. Neuronal calcium signals in the ACC were imaged during the last 2 days of habituation (Hab-3 and Hab-4). On day 5, mice underwent a cued fear conditioning (FC) protocol while freely moving in a different context, which consisted of a 25 cm × 25 cm × 35 cm custom made plexiglass enclosure built around a stainless-steel electrified grid placed in a custom made soundproof 50 cm × 50 cm × 50 cm box equipped with two speakers and LED lighting (100 Lux). The conditioning protocol was run by ANY-maze software (Stoelting Europe), which paired a series of 5 tones (70 dB, 7.5 kHz freq, 200 ms duration delivered at 1 Hz for 30 s) with an electric shock (the unconditioned stimulus, US; 0.6 mA). The shock was delivered in the last 2 s of each tone period. The inter-stimulus intervals randomly varied from 60 to 90 s. After conditioning, the animals were returned to the home cage. The conditioning box was cleaned with 70% ethanol before and after each session. Animals were monitored using a camera positioned above the conditioning enclosure. Freezing was scored automatically by the ANY-maze software using a 2-s threshold for the absence of movement (based on pixel variance detection). As controls, a different set of mice underwent a pseudo-conditioning protocol in which the US was randomly given during the ISI following the CS. On day 6, conditioned mice were again head-fixed in the microscope setup and tested for fear memory. This memory recall session (Rec-1) was performed similarly to Hab-3 and Hab-4, i.e., calcium signals were imaged while presenting 10× the CS with randomly varied ISI durations (60–90 s). 24 h after Rec-1, a second recall session (Rec-2) was performed while mice were freely moving. The mice were placed in a novel chamber, exposed to tones, and freezing was evaluated as described for the FC session.

All statistical analyses were performed using R-Studio and GraphPad Prism. Significance levels were denoted as $^{*}p < 0.05$, $^{**}p < 0.01$, $^{***}p < 0.001$, $^{****}p < 0.0001$. No statistical calculation was made to estimate sample sizes. Comparison tests were performed as two-sided.

Post hoc histology and immunostaining

For regular *post hoc* assessment, mice were anaesthetized with 3–4% isoflurane (mixed with O_2) induction followed by an intraperitoneal injection of Pentobarbital (150 mg/Kg, Esconarkon ad us. Vet. Streuli, Uznach, Switzerland) combined with subcutaneous injection of buprenorphine (0.1 mg/kg, Temgesic, Schering-Plough, NJ, USA) analgesia. After reaching deep anesthesia checked by toe pinching, before reaching cardiorespiratory arrest, transcardiac perfusion (4% paraformaldehyde (PFA), 1× PBS, pH 7.4) was performed. The brains were extracted and post-fixed overnight at 4°C in 4% PFA and subsequently transferred in PBS. *Post hoc* 50–100 µm-thick axial coronal sections were produced using a vibratome (Leica VT 1000, Germany) and stored in PBS 0.1% Na-azide. The sections were imaged using a Zeiss Confocal LSM800 Airyscan (Axio Imager.Z2 Basis LSM 800 microscope).

For the immunohistological characterization the NGC-Flp mouse line, mice (n = 3) received an injection of AAV1/2-hSyn.fDIO.GCaMP6s as above, but without a microprism implant. 20 days post-surgery they were anaesthetized and fixed as above. The brains were collected and left in 4% PFA 3h at RT for further fixation. Coronal brain sections (40 µm thickness) were produced using a vibratome (Leica VT1200S; Leica Microsystems). First, the sections were pre-incubated in PBS 1% BSA, 0.3% Triton X-100 for 1 h at room temperature. Then, the following primary antibodies were used: mouse anti-GFP 1:500 (Abcam, Cambridge, United Kingdom, #ab1218), rabbit anti-VIP 1:500 (Immunostar, WI, USA, #20077), rabbit anti-SST 1:1000 (Invitrogen, MA, USA, #PA5-82678), goat anti-PV 1:2000 (Swant, Burgdorf, Switzerland, #PVG-214) diluted in the pre-incubation solution and applied for overnight at 4°C. As secondary antibodies we used Alexa anti-mouse 488 (1:1000); anti-rabbit 568 (1:1000); anti-goat 568 (1:1000) diluted in PBS 1%BSA and applied for 1 h in the dark at room temperature. Finally, for cell nuclei staining, Hoechst 1:5000 (Invitrogen, MA, USA, #H3570) was applied for 20 min in the dark at room temperature. Images were taken using a Leica Stellaris confocal microscope 20× objective. Image analysis on these images was performed in Fiji (NIH, Bethesda). Regions of interest (ROI) contours were drawn around neuronal somata, and the mean pixel value at the focal plane with the highest value for each cell was measured. PV, SST, and VIP antibody-stained (red) cells and GFP antibody-stained (green) cells were selected, as well as red cells in an area outside of the injection zone (controls for GFP-background). Number of analyzed cells: VIP: 297; SST: 316; PV: 539.

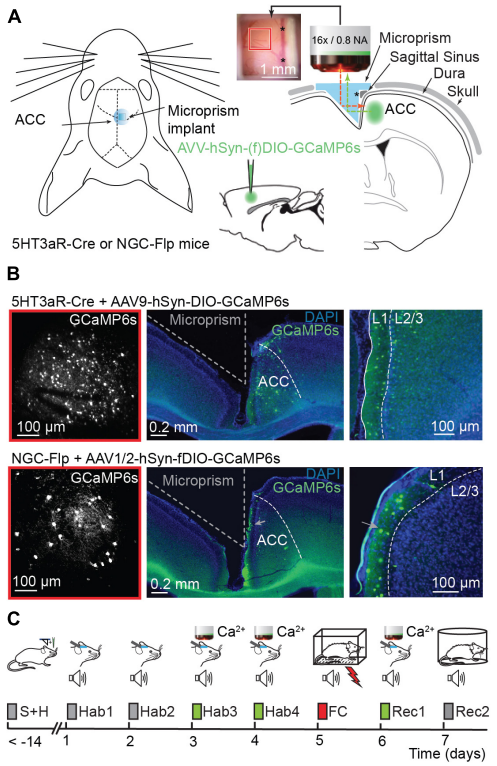

FIGURE 1

Calcium imaging in the ACC before and after fear conditioning. **(A)** Left, schematic representation of prism implantation in 5HT3aR-Cre or NGC-Flp mice. Right, AAV9-hSyn-DIO.GCaMP6s or AAV1/2-hSyn-fDIO.GCaMP6s viral vectors were injected in the ACC of 5HT3aR-Cre or NGC-Flp mice, respectively. Immediately after the injection, a microprism was implanted in the contralateral hemisphere. The inset shows an example of the cranial window with the underlying cortex and vasculature 2 weeks after surgery. The red and green dotted lines represent the excitation beam and the emitted light path, respectively, through the implanted prism. Note that the reflective hypotenuse of the prism converts the horizontal plane into a vertical imaging plane. The asterisk indicates the sagittal sinus, which is also visible on the right-hand side of the inset. **(B)** Left, example of the field of view with 2PLSM in GCaMP6-expressing 5HT3aR-Cre (top) or in NGC-Flp (bottom) mice. The red square compares the field of view to the size of the cranial window in panel **(A)**. Right, representative *post hoc* immunostaining showing GCaMP6s expression (green) in the ACC. The integrity of the targeted cortex for imaging remains intact. In blue, DAPI-staining. **(C)** The FC paradigm. After surgery, mice are handled daily for at least 7 days. The experimental paradigm starts with 4 days of habituation (Hab1-4) where the mice are head-fixed and exposed to tones. In the last 2 days of habituation (Hab-3 and Hab-4) this is combined with 2PLSM. On day 5, the mice are subjected to fear conditioning (FC) in a conditioning box while freely moving. 24 h later a recall session (Rec-1) is performed while mice are head-fixed and imaged. On day 7, animals undergo a second recall session (Rec-2) while freely moving, allowing the scoring of freezing behavior.

2-photon laser scanning microscopy

For the detection of calcium signals, mice were head-fixed under the microscope and imaged while awake. We used a custom-built 2-photon laser scanning microscope [2PLSM; (Holtmaat et al., 2009)], equipped with a 16 × 0.8NA water immersion-objective (Nikon, CFI75), and controlled with Scanimage 2016b.[4] Fluorophores were excited using a Ti: Sapphire laser (Chameleon Ultra II, Coherent, CA, USA) tuned to λ = 980 m. Fluorescent signals were collected with GaAsP photomultiplier tubes (10770PB-40, Hamamatsu, Japan). GCaMP6s signals were collected through a dichroic mirror (565dcxr, Chroma) and emission filter (ET525/50 m, Chroma). Images were acquired at a 8 Hz-scanning rate, and each image consisted of a single plane (723 × 675 µm; 512 × 256 pixels). The imaging plane was between 10–100 µm below the pia and therefore well within L1.

Image processing and calcium signal analysis

Images were processed using custom-written MATLAB (Mathworks, MA, USA) script and ImageJ (NIH, Bethesda, MD, USA). Lateral and axial motion errors were corrected using the ImageJ plugin Stack Aligner by performing a rigid image registration across all frames of the movie. To extract the GCaMP6s fluorescence signals from individual neurons, regions of interest (ROIs) were drawn manually for each session. The fluorescence time-course of each neuron was measured as the average of all pixel values of the GCaMP6s signal within the ROI. Calcium activity was then evaluated as ΔF/F, where F is the lowest 30th percentile mean intensity of all the trace. ΔF/F signals of all cells were subsequently log-transformed with the formula $v_i' = \log_2(\max(0, v_i) + 1)$. For each tone, the obtained signals were averaged over 10-s periods: 20–10 s pre-tone (ISI), 10–0 s pre-tone (ISI), and 0–10 s from tone onset (Tone).

Cell classification and exclusion

We generated scatterplots of the 10 s-average-signals to visually inspect the difference between the signal during tones (y-axis: signal average of 0–10 s from tone onset) with the signal during the preceding ISI (x-axis: signal average of 10–0 s pre-tone). Because of the above log-transformation, the distance to the diagonal on this plot is an estimate of the $\log_2$ ("fold-change") during the tone. A tone-associated response was considered significant if it had a $\log_2$ ("fold-change") distance to the diagonal higher than a predetermined threshold (see below). Based on this, neurons were subdivided into three classes: increase–cells displaying a $\log_2$ ("fold-change") increase above the threshold in at least 6 out of the 10 tones within a session; decrease–cells displaying a $\log_2$ ("fold-change") decrease above the threshold in at least 6 out of the 10 tones within a session, no change–all remaining cells. A cell was considered non-responsive to tones if it belonged to the "no change" class in all recording sessions (Hab-3, Hab-4, Rec-1) (indicated in black in Figures 2C, 3C). These cells were excluded from cell activity change enrichment test. The threshold was independently determined for each group of mice (NGC, 5HT3aR, pseudo-conditioned 5HT3aR), and set such that it excluded 33% of the cells when only habituation sessions (Hab-3, Hab-4) were considered.

To verify the specificity of this approach, the same analysis was performed to estimate the $\log_2$ ("fold-change") between two ISI

4 http://www.scanimage.org

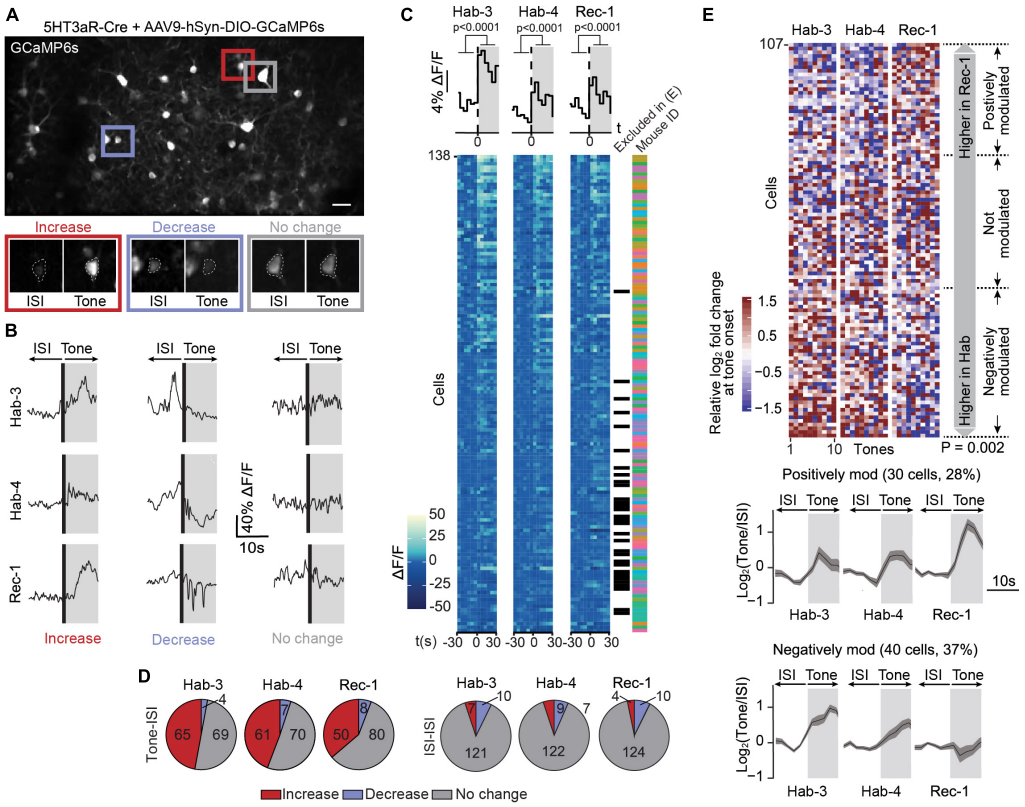

FIGURE 2
Calcium signals in 5HT3aR interneurons are bimodally modulated following fear conditioning. **(A)** A field of view containing GCaMP6s-expressing 5HT3aR neurons in L1 of ACC (scale bar: 50 μm). The image is an average projection of the full-length imaging period. The insets show examples of cells displaying an increase, decrease or no change in calcium signals at tone onset. Insets were generated from the average projection of the first 10 s of tone and the last 10 s of the preceding ISI. **(B)** Example ΔF/F traces of individual neurons over a 20-s window spanning one ISI-tone transition in each imaging session (Hab-3, Hab-4, Rec-1). **(C)** Tone-evoked 5HT3aR neuron activity. The heatmaps represent calcium signals (ΔF/F) in neurons before and after tone onset. Each row represents a single cell. Each square represents a 5-s bin averaged across all 10 tone presentations. Cells are sorted according to their responsiveness in Hab3, with the highest responses on top. Above the heatmaps, the grand average ΔF/F during tone vs. ISI (mean activity during first and last 30 s, *t*-test $P < 0.0001$, $n = 138$). Next to the heatmaps, the black checkmarks indicate cells that did not significantly respond in any of the recording sessions and were therefore excluded from further analysis (31). The color-coded checkmarks identify the mouse from which the recorded cell was derived. **(D)** Fraction of cells that increase, decrease, or do not show changes in activity at tone presentation (left) or during ISIs (right) for each recording session. **(E)** Top, heatmap of the 107 responding cells (8 mice) sorted according to the difference of the median response to tones in Rec-1 relative to Hab-3 and Hab-4. Each square represents the relative $\log_2$-fold change of the calcium signal at tone onset. Margin analysis revealed two groups of neurons whose activity is dynamically modulated following fear learning (random permutation analysis $P = 0.002$). A total of 30 cells are positively modulated by fear learning (median activity difference > 0.3) and 40 cells are negatively modulated (median activity difference < -0.3). Bottom, for both groups of neurons, the lower panel shows the average calcium trace (with SEM) of the tone-evoked calcium signals during all three imaging sessions. Gray areas represent the 10-s tone duration.

periods (i.e., comparing the average-signals over 20–10 s pre-tone with the average-signals over 10–0 s pre-tone).

Cell activity change enrichment test

To test whether there was a significant change in tone responses between habituation and recall sessions, we first generated a heatmap with the $\log_2$ ("fold-changes") of each cell for the 30 tones of all sessions (Hab-3, Hab-4, Rec-1) (Figures 2E, 3E). In this heatmap, cells were sorted according to the difference in the signal between the habituation and recall sessions (detail of the criterion used for sorting in next section). The color of each square is the $\log_2$ fold-change between the first 10 s of the tone vs. the last 10 s of the ISI. The colors are saturated, with fold-changes above 1.5 (resp. below −1.5) being assigned the 1.5 color (resp. −1.5 color). A cutoff was chosen (see below) to classify a cell as 'modulated' or 'not modulated' between habituation and recall days, and we counted the number of cells satisfying this criterion. Subsequently, a simulated dataset of 10^4 cells was generated by randomly selecting cells from the initial dataset and randomly permuting their responses to 30 tones. Then, the same criterion was applied as above, and we performed a binomial test to assert that the number of cells changing their activity in the real dataset was higher than the amount in the simulated dataset.

Cell activity change criterion

The criterion that was used to sort the heatmap and classify a cell as modulated or not between habituation and recall conditions is the difference of the medians, slightly adapted to be more rigid and so that it defines three groups of cells: increasing, decreasing, no-change. The exact formula of our sorting criteria is:

$$\delta_i = \max\left(0, 5^{th}(r_i) + 9^{th}(-h_i)\right) - \max(0, 9^{th}(h_i) + 5^{th}(-r_i))$$

where:

n^{th} (x) is the n^{th} smallest value of vector x.

r_i (resp. h_i) is the vector of fold-changes of the i^{th} cell, at the 10 (resp. 20) tones during recall (resp. habituation).

In other words, δ_i is:

positive if the i^{th} cell has an activity that is higher in 6 recall tones than in 12 habituation tones.

negative if the i^{th} cell has an activity that is smaller in 6 recall tones than in 12 habituation tones.

zero otherwise

In our enrichment test, a cell was considered to have changed its response between habituation and recall if δ_i was not zero.

Results

Labeling and imaging of ACC L1 interneurons in a fear conditioning paradigm

In order to investigate neuronal activity of ACC L1 interneurons, we expressed the genetically-encoded calcium indicator GCaMP6s using recombinase-dependent AAV vectors in two different genetically modified mouse lines. In a first approach, the vectors were injected in 5HT3aR-Cre mice that constitutively express Cre in a heterogenous population of interneurons in L1, albeit a more precise functional characterization is gradually building (Lee et al., 2010; Gerfen et al., 2013; Takesian et al., 2018; Gouwens et al., 2020; Anastasiades and Carter, 2021). Hence, we will refer to the cells that are labeled using 5HT3aR-Cre mice in combination with AAV vectors as 5HT3aR neurons. In a second set of experiments, we specifically targeted NGCs which form a distinct subgroup of interneurons in L1 that largely belong to 5HT3aR-Cre neuron population (Niquille et al., 2018; Tasic et al., 2018; Gouwens et al., 2020; Ibrahim et al., 2021). To accomplish this, we took advantage of an Hmx3-Cre mouse line, a reporter line previously shown to fate map NGCs by targeting cortical interneurons originating from the preoptic area (Gelman et al., 2009; Niquille et al., 2018). Since in this line Cre is only expressed at embryonic stages, we crossed it with a LSL-Flp mouse line that harbors a Cre-conditional Rosa-26-CAG-LSL-Flp allele (Gelman et al., 2009; Niquille et al., 2018). The offspring of this crossing transiently expresses Cre in NGC precursors, which subsequently switches on the constitutive Rosa-26-CAG-driven expression of Flp recombinase in the mature population of NGCs (**Supplementary Figure 1A**). This offspring, which we hereafter refer to as NGC-Flp mice, allowed targeted expression of GCaMP6s in NGCs in the adult brain using Flp dependent AAV vectors. The characteristics of the labeled cells indeed strongly resembled those of NGCs, i.e., they were enriched in L1, had an elongated morphology, and projected thin axons with elaborate branches (**Supplementary Figures 1B, C**). The presumptive NGC identity in these mice was further confirmed using an immunolabeling of interneuron molecular markers. Due to the absence of a general molecular marker of NGCs, sections were labeled using antibodies for three other main classes of interneurons: PV, SST, and VIP. The absence of co-labeling of any of these markers indicates that the GCaMP6s-expressing cells were molecularly distinct from the PV, SST, and VIP interneuron population (**Supplementary Figure 1D**), further corroborating their putative NGC identity (Jiang et al., 2013; Lee et al., 2015; Overstreet-Wadiche and McBain, 2015; Niquille et al., 2018; Schuman et al., 2019; Gouwens et al., 2020).

To longitudinally track L1 interneuron activity, we implanted a microprism into the interhemispheric longitudinal fissure and used 2PLSM in head-fixed awake mice (Low et al., 2014; **Figure 1A**). *Post hoc* assessment of microprism-implanted brains confirmed that GCaMP6s expressing neurons were abundantly present in L1 in both 5HT3aR-Cre and NGC-Flp mice (**Figure 1B**). The labeled NGC population showed a strong enrichment in L1 relative to the other cortical layers, in accordance with previous findings (Jiang et al., 2015; Tremblay et al., 2016; Niquille et al., 2018). The *post hoc* assessment also indicated that the microprism implant had left the microanatomy and layers of the injected right hemisphere intact (**Figure 1B**).

Once mice were recovered from surgery (>7 days), they were handled for 7 days and then habituated for 4 days (Hab-1-4; 1 session/day) to the head fixation in the microscope during which they were exposed to 10 tones (10× CS) per session without shocks (US) (**Figure 1C**; **Supplementary Figure 2A**). The fear conditioning paradigm (FC; 5× CS-US pairing) was performed on freely moving mice in a different environment. The subsequent memory recall session (Rec-1; 10× CS) was again performed while mice were head-fixed under the microscope. A second recall session (Rec-2) was performed in freely moving mice in a further different context to assess the CS-US associative memory using the freezing time as a measure. Calcium signals were imaged in the last two habituation sessions (Hab-3 and 4) as well as in the first recall session (Rec-1) (**Figure 1C**).

During the FC session, the average duration of freezing upon tone presentation increased starting after the second CS-US pairing and was significantly higher by the fifth tone (**Supplementary Figure 2B**). When mice were re-exposed to the CS in Rec-2, they displayed a selective increase in conditioned freezing (**Supplementary Figure 2C**) and the level of freezing remained high for the whole duration of the protocol (**Supplementary Figures 2C, D**). Mice subjected to pseudo-conditioning, in which the CS and US were not paired (**Supplementary Figure 2A**), tended to gradually increase the duration of freezing during tone presentation, even if such increase was not significant (**Supplementary Figure 2E**). Most importantly, pseudo-conditioned mice did not display increased freezing in Rec-2, indicating that they had not produced a CS-US associative memory (**Supplementary Figures 2F, G**).

NGC-Flp mice showed a similar behavioral response to FC as the 5HT3aR-Cre mice, i.e., they started to increase freezing duration after the second CS-US pairing (**Supplementary Figure 2H**), and they had significantly longer freezing durations in Rec-2 (**Supplementary Figures 2I, J**).

Together, these data show that the fear conditioning protocol created a specific and robust CS-US associative memory, which lasted throughout and beyond the Rec-1 imaging session. Therefore, by comparing the calcium signal dynamics during Hab-3, Hab-4, and Rec-1 in the conditioned versus the pseudo-conditioned mice, we were able to identify the interneurons that are putatively involved in the successful formation or recall of a CS-US associative memory.

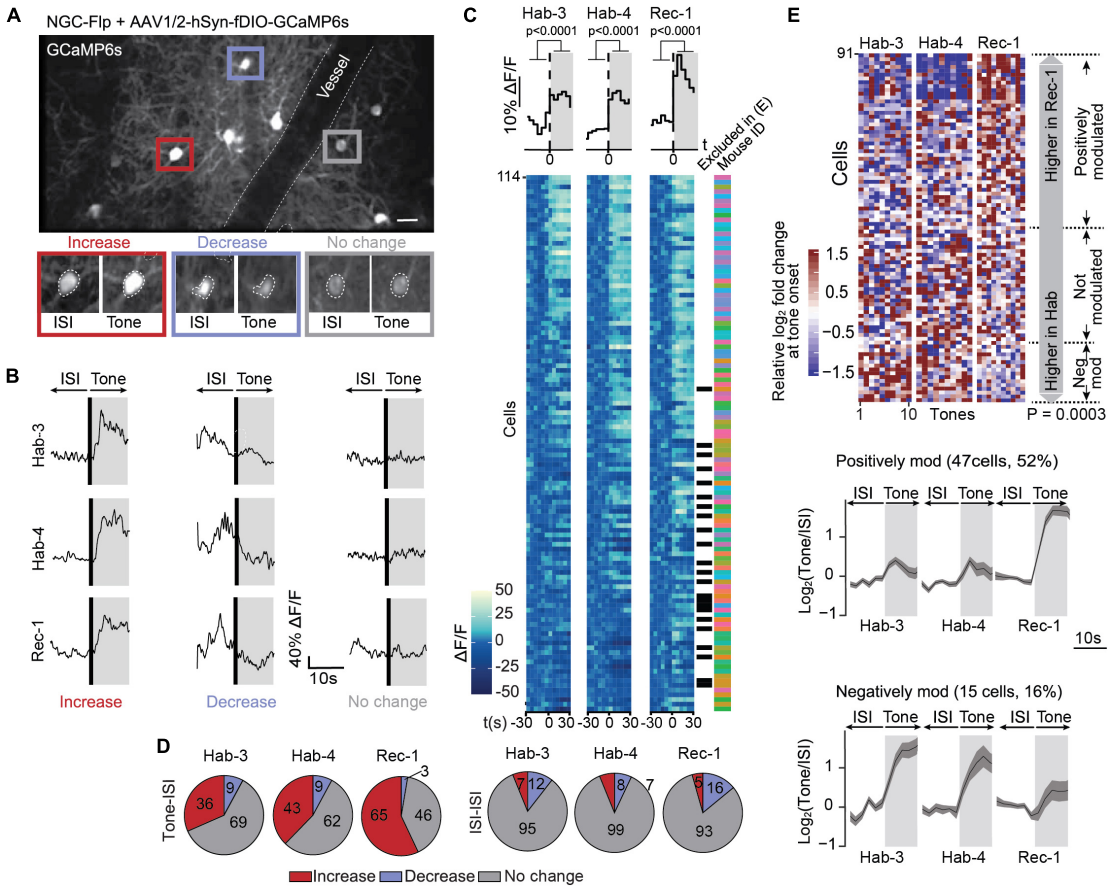

FIGURE 3
Calcium signals in NGCs are mostly positively modulated following fear conditioning. **(A)** A field of view containing GCaMP6s-expressing NGCs in L1 of the ACC (scale bar: 50 μm). This image is an average projection of the full-length imaging period. The insets show examples of cells displaying an increase, decrease or no change in calcium signals at tone onset. Insets were generated from the average projection of the first 10 s of tone and the last 10 s of the preceding ISI. **(B)** Example ΔF/F traces of individual neurons over a 20-s window spanning one ISI-tone transition in each imaging session (Hab-3, Hab-4, Rec-1). **(C)** Tone-evoked NGC activity. The heatmaps represent calcium signals (ΔF/F) in neurons before and after tone onset. Each row represents a single cell. Each square represents a 5-s bin averaged across all 10 tone presentations. Cells are sorted according to their responsiveness in Hab-3, with the highest responses on top. Above the heatmaps, the grand average ΔF/F during tone vs. ISI (mean activity during first and last 30 s, *t*-test $P < 0.0001$, $n = 114$). Next to the heatmaps, the black checkmarks indicate cells that did not significantly respond in any of the recording sessions and were therefore excluded from further analysis (23). The color-coded checkmarks identify the mouse from which the recorded cell was derived. **(D)** Fraction of cells that increase, decrease, or do not show changes in activity at tone presentation (left) or during ISIs (right) for each recording session. **(E)** Top, heatmap of the 91 responding cells (9 mice) sorted according to the difference of the median response to tones in Rec-1 relative to Hab-3 and Hab-4. Each square represents the relative $\log_2$-fold change of the calcium signal at tone onset. Margin analysis revealed two groups of neurons whose activity is dynamically modulated following fear learning (random permutation analysis $P = 0.0003$). A total of 47 cells are positively modulated by fear learning (median activity difference > 0.3) and 15 cells are negatively modulated (median activity difference < -0.3). Bottom, for both groups of neurons, the lower panel shows the average calcium trace (with SEM) of the tone-evoked calcium signals during all three imaging sessions. Gray areas represent the 10-s tone duration.

Tone-evoked calcium signals in 5HT3aR neurons are bimodally modulated by fear conditioning

In order to investigate the evolution of L1 5HT3aR interneuron activity in response to conditioned tones during fear learning, we longitudinally recorded calcium signals in 138 cells from eight 5HT3aR-Cre mice during three sessions (Hab-3, Hab-4, and Rec-1; Supplementary Figure 3A). Neurons displayed heterogeneous responses across all sessions, including increases, decreases and no change in calcium signals upon tone presentations (Figures 2B, C). On average the calcium signals increased upon tones, indicating that a substantial fraction of this population of L1 ACC neurons responds to auditory stimuli (Figure 2C). To further classify individual responses, we averaged for each cell the ΔF/F over a 10-s period immediately before and after tone onset and calculated the post-pre $\log_2$-fold change (see Section "Materials and methods"). In all sessions we found a substantial fraction of neurons that increased their activity upon tone presentations while only a few did not change or decrease their activity (Figure 2D) indicating that 5HT3aR interneuron activity can be evoked by tones. When the same classification was performed on the post-pre $\log_2$-fold change between 10 s periods outside tones, most cells showed no activity change, confirming that the responses were tone-specific (Figure 2D). Based on this analysis, we found 31 out of 138 cells that showed no response in any session. They were excluded for further analysis (see Section "Materials and methods"). To assess

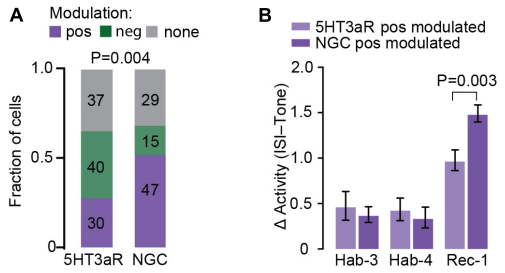

FIGURE 4

Comparison of 5HT3aR neurons and NGC activity upon FC. **(A)** Fraction of the cells whose activity is positively, negatively or not modulated following fear learning in the 5HT3aR and NGC populations. The number of neurons populating each cluster is indicated inside each color-coded box. Positively modulated neurons are enriched in the NGC population (Chi square test; $P = 0.004$). **(B)** Direct comparison of tone-evoked responses between positively 5HT3aR neurons and NGCs. Δ activity was calculated for each cell as an average across all tones of the difference in the $\log_2$-fold change during the first 10s of CS and the $\log_2$-fold change during the last 10s of ISI. While the average tone-evoked response in habituation sessions does not differ between both groups, it is higher in NGC population during Rec-1 [RM-Two-Way ANOVA, $F(2,150) = 6.681$, $P = 0.003$; *Post hoc* analysis Sidak, $N = 30–47$ cells].

whether tone-responsive cells dynamically modified their activity following CS-US association, we compared their responses during Hab-3 + 4 to the responses in Rec-1. First, we sorted the 107 responding cells according to the difference in their tone responses between habituation and recall (Figure 2E). In order to assess if FC affects those responses, we performed margin analysis to find clusters of differentially modulated neurons. We obtained three groups of neurons: a positively modulated cluster (30 cells; 30%), in which 60% of the tone responses during Rec-1 (i.e., 6 out of 10 tones) are higher than 60% of the tone responses during Hab-3 and 4 (i.e., 12 of 20 tones); a negatively modulated cluster (40 cells; 37%) where 60% of the tone response during Rec-1 are smaller than 60% of the tone responses during Hab-3 and 4; and a third non-modulated cluster of the remaining cells (Figure 2E). All clusters were populated by neurons obtained from different mice (Supplementary Figure 4A), confirming that these types of modulation are transversally present. Importantly, random permutation analysis confirmed the significant separation of the obtained neuronal clusters (positively or negatively modulated neurons following fear conditioning; $P = 0.002$). These results demonstrate that 67% of tone-responding ACC L1 5HT3aR cells are bimodally modulated by fear learning. To verify whether this modulation was specifically induced by the CS following FC, we performed the same margin and permutation analysis using the calcium signals observed in between tone presentations [two periods of 10 s each within the inter-stimulus interval (ISI)]. ISI analysis did not reveal any clusters ($P = 0.778$), indicating that FC does not cause a generalized (CS-unrelated) modulation of activity in these cells (Supplementary Figure 4B).

To validate that the modulation of the responses is specifically associated with FC, we performed the same analysis in the pseudo-conditioned mice (6 mice, 111 cells; Supplementary Figure 3B). Again, results did not reveal any positively or negatively modulated clusters (88 responsive cells, $P = 0.301$; Supplementary Figure 4C). Similarly, no clusters were found when activity in 10-s ISIs were considered in pseudo-conditioned mice ($P = 0.900$; Supplementary Figure 4D).

Overall, these data demonstrate that 5HT3aR ACC L1 INs can selectively respond to auditory stimuli and these responses are bidirectionally modulated by FC.

Tone-evoked responses of NGCs increase upon fear conditioning

Similar to the global 5HT3aR neuron population, NGCs recorded during different days (Supplementary Figure 3C) displayed heterogeneous responses upon CS presentation, i.e., cells either increased, decreased or showed no change in calcium signals during tones across sessions (Hab-3, 4 and Rec-1; Figures 3A, B). At the population level, NGCs also showed a marked tone-evoked increase in activity across all sessions (Figure 3C). Single cell analysis revealed that a substantial fraction of neurons increased their activity while only a few decreased their activity (Figure 3D). When the same classification analysis was performed on 10-s periods during ISIs, most cells showed no change in activity, confirming the tone-specificity of the responses (Figure 3D). From the 114 recorded cells (9 mice), 91 (80%) responders were kept for further analysis (see Section "Materials and methods"). As before, we compared the neurons' responses during Hab-3 + 4 to those in Rec-1 to assess whether FC had a modulating effect on tone-evoked responses in NGCs. Cells were sorted according to the difference in responses between habituation and recall (Figure 3E). Margin and random permutation analysis ($P = 0.0003$) revealed the emergence of three clusters of FC-modulated responses. Differently to what we observed for the 5HT3aR neuronal population, NGCs were enriched in positively modulated cells (47/91; 52%), with only a small fraction decreasing CS-evoked responses following FC (15/91; 16%) (Figure 3E). The positively modulated cluster contained cells from all mice, the negatively modulated cluster did not (Supplementary Figure 5A). Like what was observed for the 5HT3aR population, no clusters were detected when analyzing 10-s segments of ISIs in the same group of cells ($P = 0.958$; Supplementary Figure 5B), confirming that FC had specifically modulated the tone-evoked responsiveness in NGCs.

The positively modulated NGCs did not only constitute a larger fraction of the population as compared to those of the 5HT3aR population (52 vs. 28%; Figure 4A), they also showed larger calcium signals during Rec-1 (no difference was observed for Hab-3 and 4; Figure 4B). Conversely, negatively modulated neurons were less abundant within the NGC population as compared to the 5HT3aR population (16 vs. 37%; Figure 4A), suggesting that NGCs may represent a functionally distinct type when compared to 5HT3aR L1 INs. Together, the data suggest that interneuron subpopulations in L1 of ACC may differentially contribute to FC memory formation and recall.

Discussion

We repeatedly imaged calcium signals in two L1 interneuron subtypes of the ACC in a mouse model for fear learning. We

observed that tones (CS) evoked activity in ∼80% of the L1 5HT3aR cells and NGCs before and after the conditioning protocol. Of these tone responsive populations, ∼70% of the total responsive neurons were bidirectionally modulated by FC, i.e., some cells increased and others decreased their responses to the CS upon fear learning. The NGC population was relatively enriched in positively modulated neurons. Altogether, the data indicate that auditory stimuli evoke responses in subpopulations of ACC L1 INs, which can be modified by fear learning. In particular, our data show that fear learning is associated with a net increase in the activity of an inhibitory motif constituted of NGCs which are known to target pyramidal cell apical dendrites and to be targeted by long-range excitatory inputs (Muralidhar et al., 2013; Hou and Capogna, 2018). Together, this suggests that the integration of sensory inputs and/or executive outputs of the ACC are modulated by fear learning. This may have important implications for the understanding of how aversive memories are encoded and stored in cortical circuits.

Tone-evoked responses in ACC

The first remarkable observation provided by this work is the strong activation of subpopulations of L1 interneurons upon the presentation of the auditory CS, even before learning (**Figures 2B–D**, **3B–D**). Previous studies have shown that the ACC can be activated by visual and somatosensory inputs, in particular when they are noxious (Johansen et al., 2001; Wei and Zhuo, 2001; Blom et al., 2014; Ma et al., 2016; Sidorov et al., 2020). Such responses may originate from afferents of the medial thalamus (MT) (Hsu and Shyu, 1997; Hsu et al., 2000), or somatosensory and visual cortices (Sidorov et al., 2020; Singh et al., 2020).

Our data suggest that auditory information is processed by the ACC as well. Auditory signals may also derive from thalamic and cortical sensory areas. However, the responses may not necessarily represent low-order inputs from the auditory stream to the ACC, but rather be the result of high-order processing of the sound as a contextual stimulus. In addition, it is also possible that tone-evoked activity that we observed did not merely represent the perceptual processing of auditory input *per se* but rather a sound-evoked increase in attention levels, known to increase and depend on activity in the ACC (Petersen and Posner, 2012; Wu et al., 2017).

Since the auditory stimulus in our paradigm was delivered as pips for a period of 30 s, the temporal relationship between the sound and neuronal activity was difficult to disentangle. To circumvent this, we focused our analysis around tone onset, and assessed how this was modulated by fear learning.

Bidirectional modulation of responses upon fear learning

The second main observation was the bidirectional modulation of the CS-evoked responses in subpopulations of the L1 interneurons (**Figures 2**, **3**). We demonstrated that this modulation is a specific learning effect. First, because a pseudo-conditioning protocol in which mice received shocks in a dissociated manner from the CS did not result in significant CS-evoked response alterations (**Supplementary Figure 4**); and second because spontaneous calcium signals during ISIs were not changed (**Supplementary Figure 4**). A bimodal response in fear learning-related activity is not unique to the ACC. Our results align with observations in L1 interneurons of the auditory cortex (Letzkus et al., 2011; Abs et al., 2018), pyramidal neurons in the amygdala (Grewe et al., 2017) and PV neurons in the dmPFC (Courtin et al., 2014).

In addition, activity of the ACC has been reported in association with various subcomponents of fear learning (see for reviews: Jovanovic and Norrholm, 2011; Hinojosa et al., 2019). It has been implicated in storage of fear memories (Descalzi et al., 2012; Einarsson et al., 2015), but also in fear termination (Steenland et al., 2012; de Lima et al., 2022) and resistance to extinction (Louzolo et al., 2022). Taken together, these findings suggest that specific subpopulations of projecting neurons in the ACC may be bimodally regulated by fear learning, allowing targeted facilitation of fear-encoding neurons and a suppression of antagonistic neuronal subsets. Such bimodal regulation may be achieved by inhibition derived from either up-regulated or down-regulated L1 interneuron activity, which may be directed to different subsets of principal neurons.

The role of L1 interneurons subtypes

Using the intersectional genetic strategy described in the Results, we were able to specifically monitor the activity of the NGC subpopulation of L1 5HT3aR interneurons. NGCs are *Hmx3*-derived 5HT3aR neurons, which belong to the reelin$^+$, VIP$^-$ IN population and are characterized by the expression of NDNF (Cadwell et al., 2016; Tasic et al., 2016; Abs et al., 2018; Poorthuis et al., 2018; Cohen-Kashi Malina et al., 2021). NDNF is also present in some non-NGC cells which share the same morphology as NGCs but show a reduced connectivity to L2 principal cells (Schuman et al., 2019). Therefore, in our study we were able to more specifically target the NGC subpopulation of 5HT3aR neurons than in most other functional studies of L1 interneurons. However, it should be noted that the use of viral vectors to label neurons may result in biased labeling of cellular subtypes within both 5HT3aR and NGC populations due to variations in Cre and GCaMP6 expression levels as well as differences in viral tropism between cells.

The NGC population displayed a different response than the general 5HT3aR population. Whereas 5HT3aR cells consisted of an equal fraction that up-regulated and down-regulated their activity upon learning, the NGC population displayed a larger fraction of neurons with increased activity. This suggests that conditioned tones recruit NGCs to produce a net increase in inhibitory activity on the cortical microcircuit upon presentation of a conditioned cue. The role of this presumed net increase in inhibition of pyramidal neurons by NGC in our fear learning paradigm remains unclear. This could affect integration of long-range excitatory inputs through L1 (such as from other cortical areas or thalamus), but also suppresses the output of particular pyramidal neurons. One possible interpretation would entail that increased inhibition through NGC may lead to specific suppression of outputs that normally play a role in the termination of freezing, as described in a previous study (Steenland et al., 2012). It would be interesting

to investigate such a relationship by scoring freezing behavior (or general fear responses) while NGCs are imaged in head-fixed mice. Along similar lines, the decrease in activity of other neurons within the 5HT3aR population may serve to specifically promote the activity of pyramidal neurons that mediate the fear memory-related information to other brain regions such as amygdala (Skelly et al., 2017; Tipps et al., 2018) and auditory cortex (Letzkus et al., 2011).

It is also well possible that the distinct modulation of different L1 inhibitory neuron subpopulations ultimately converge to a similar effect in fear-memory formation. For example, NGCs may serve direct inhibition of pyramidal cell dendrites, whereas other 5HT3aR neurons, such as single bouquet cells (SBC), may promote disinhibition (Rudy et al., 2011; Jiang et al., 2015; Tremblay et al., 2016; Hou and Capogna, 2018; Huang and Paul, 2019). Such an effect can be envisioned since various subpopulations of 5HT3aR neurons target different components of the cortical circuits (Jiang et al., 2013; Lee et al., 2015; Markram et al., 2015; Schuman et al., 2019; Ibrahim et al., 2020; Cohen-Kashi Malina et al., 2021) and thereby exert distinct effects on pyramidal cell activity. In such distinct wiring motifs, the net upregulation of NGC activity and the net down-regulation of SBC may mutually cause a general dampening of pyramidal cell activity in ACC upon fear memory recall. Alternatively, the distinct responses may lead to inhibition and disinhibition of different cellular compartments, similar to a recent study showing that the concerted activation of VIP and PV neurons causes somato-dendritic decoupling in pyramidal neurons of the dPFC during REM sleep (Aime et al., 2022).

What could be the source of the bidirectional response modulation? In sensory cortex, higher order thalamocortical projections to L1 have been found to target inhibitory neurons such as NGCs (Pardi et al., 2020; Ibrahim et al., 2021). Along the same lines, studies in the medial prefrontal cortex indicate that projections of ventromedial (VM) nucleus of the thalamus arrive in L1a where they preferentially target NDNF cells, whereas the mediodorsal (MD) thalamus projects to L1b and targets VIP neurons (Anastasiades and Carter, 2021; Anastasiades et al., 2021). It is possible that in our paradigm the positively modulated NGCs receive preferential inputs from VM, whereas the negatively modulated 5HT3aR neurons receive inputs from the MD. Since VM likely relays information related to arousal (Schiff, 2008; Honjoh et al., 2018; Petty et al., 2021), and MD is involved in working memory (Stokes and Best, 1990; Cardoso-Cruz et al., 2013; Bolkan et al., 2017; Schmitt et al., 2017), these two pathways to the ACC may be differentially regulated during fear learning.

Data availability statement

The raw data supporting the conclusions of this article will be made available by the authors, without undue reservation.

Ethics statement

This animal study was reviewed and approved by the Ethics Committee of the University of Geneva and the authorities of the Canton of Geneva (license numbers: GE/28/14 and GE/61/17).

Author contributions

GF, DK-B, AD, and AH designed the experiments and defined and built experimental setups. GF and DK-B performed the experiments and analyzed the data. JP designed and performed the cluster analysis. CC generated the transgenic NGC-Flp mouse line. EH performed the immuno-labeling characterization of NGC-Flp brains. LG managed mice colonies. RC generated the Matlab script for calcium analysis. BS implemented data analysis and interpretation. AH provided equipment and technical expertise. GF, DK-B, BS, and AH wrote the manuscript. AD and AH supervised the research. All authors except AD edited the manuscript.

Funding

This work was financially supported by the Swiss National Science Foundation (grants: 310030-204562, 31003A_173125, CRSII3_154453, and NCCR Synapsy 51NF40-158776/185897) and a gift from a private foundation with public interest through the International Foundation for Research in Paraplegia. DK-B was supported by a fellowship from the Swiss National Science Foundation (323530_171142). The laboratory of BS was supported by the Cariplo Foundation (Cariplo Giovani 2020-3632).

Acknowledgments

We thank the members of the Dayer-lab and Holtmaat-lab for their support, discussions, and help with the experiments.

Conflict of interest

The authors declare that the research was conducted in the absence of any commercial or financial relationships that could be construed as a potential conflict of interest.

Publisher's note

Supplementary material

The Supplementary Material for this article can be found online at: https://www.frontiersin.org/articles/10.3389/fncir.2023.1138358/full#supplementary-material

References

Abs, E., Poorthuis, R. B., Apelblat, D., Muhammad, K., Pardi, M. B., Enke, L., et al. (2018). Learning-related plasticity in dendrite-targeting layer 1 interneurons. *Neuron* 100, 684–699.e6. doi: 10.1016/j.neuron.2018.09.001

Aime, M., Calcini, N., Borsa, M., Campelo, T., Rusterholz, T., Sattin, A., et al. (2022). Paradoxical somatodendritic decoupling supports cortical plasticity during REM sleep. *Science* 376, 724–730. doi: 10.1126/science.abk2734

Amat, J., Baratta, M. V., Paul, E., Bland, S. T., Watkins, L. R., and Maier, S. F. (2005). Medial prefrontal cortex determines how stressor controllability affects behavior and dorsal raphe nucleus. *Nat. Neurosci.* 8, 365–371. doi: 10.1038/nn1399

Anastasiades, P. G., and Carter, A. G. (2021). Circuit organization of the rodent medial prefrontal cortex. *Trends Neurosci.* 44, 550–563. doi: 10.1016/j.tins.2021.03.006

Anastasiades, P. G., Collins, D. P., and Carter, A. G. (2021). Mediodorsal and ventromedial thalamus engage distinct L1 circuits in the prefrontal cortex. *Neuron* 109, 314–330.e4. doi: 10.1016/j.neuron.2020.10.031

Andermann, M. L., Gilfoy, N. B., Goldey, G. J., Sachdev, R. N., Wolfel, M., Mccormick, D. A., et al. (2013). Chronic cellular imaging of entire cortical columns in awake mice using microprisms. *Neuron* 80, 900–913. doi: 10.1016/j.neuron.2013.07.052

Blom, S. M., Pfister, J. P., Santello, M., Senn, W., and Nevian, T. (2014). Nerve injury-induced neuropathic pain causes disinhibition of the anterior cingulate cortex. *J. Neurosci.* 34, 5754–5764. doi: 10.1523/JNEUROSCI.3667-13.2014

Bolkan, S. S., Stujenske, J. M., Parnaudeau, S., Spellman, T. J., Rauffenbart, C., Abbas, A. I., et al. (2017). Thalamic projections sustain prefrontal activity during working memory maintenance. *Nat. Neurosci.* 20, 987–996. doi: 10.1038/nn.4568

Cadwell, C. R., Palasantza, A., Jiang, X., Berens, P., Deng, Q., Yilmaz, M., et al. (2016). Electrophysiological, transcriptomic and morphologic profiling of single neurons using Patch-seq. *Nat. Biotechnol.* 34, 199–203. doi: 10.1038/nbt.3445

Cardoso-Cruz, H., Sousa, M., Vieira, J. B., Lima, D., and Galhardo, V. (2013). Prefrontal cortex and mediodorsal thalamus reduced connectivity is associated with spatial working memory impairment in rats with inflammatory pain. *Pain* 154, 2397–2406. doi: 10.1016/j.pain.2013.07.020

Cohen-Kashi Malina, K., Tsivourakis, E., Kushinsky, D., Apelblat, D., Shtiglitz, S., Zohar, E., et al. (2021). NDNF interneurons in layer 1 gain-modulate whole cortical columns according to an animal's behavioral state. *Neuron* 109, 2150–2164.e5. doi: 10.1016/j.neuron.2021.05.001

Coley, A. A., Padilla-Coreano, N., Patel, R., and Tye, K. M. (2021). Valence processing in the PFC: Reconciling circuit-level and systems-level views. *Int. Rev. Neurobiol.* 158, 171–212. doi: 10.1016/bs.irn.2020.12.002

Courtin, J., Chaudun, F., Rozeske, R. R., Karalis, N., Gonzalez-Campo, C., Wurtz, H., et al. (2014). Prefrontal parvalbumin interneurons shape neuronal activity to drive fear expression. *Nature* 505, 92–96. doi: 10.1038/nature12755

de Lima, M. A. X., Baldo, M. V. C., Oliveira, F. A., and Canteras, N. S. (2022). The anterior cingulate cortex and its role in controlling contextual fear memory to predatory threats. *eLife* 11:e67007. doi: 10.7554/eLife.67007

Dejean, C., Courtin, J., Rozeske, R. R., Bonnet, M. C., Dousset, V., Michelet, T., et al. (2015). Neuronal circuits for fear expression and recovery: Recent advances and potential therapeutic strategies. *Biol. Psychiatry* 78, 298–306. doi: 10.1016/j.biopsych.2015.03.017

Descalzi, G., Li, X. Y., Chen, T., Mercaldo, V., Koga, K., and Zhuo, M. (2012). Rapid synaptic potentiation within the anterior cingulate cortex mediates trace fear learning. *Mol. Brain* 5:6. doi: 10.1186/1756-6606-5-6

Donato, F., Rompani, S. B., and Caroni, P. (2013). Parvalbumin-expressing basket-cell network plasticity induced by experience regulates adult learning. *Nature* 504, 272–276. doi: 10.1038/nature12866

Ehrlich, I., Humeau, Y., Grenier, F., Ciocchi, S., Herry, C., and Luthi, A. (2009). Amygdala inhibitory circuits and the control of fear memory. *Neuron* 62, 757–771. doi: 10.1016/j.neuron.2009.05.026

Einarsson, E. O., and Nader, K. (2012). Involvement of the anterior cingulate cortex in formation, consolidation, and reconsolidation of recent and remote contextual fear memory. *Learn. Mem.* 19, 449–452. doi: 10.1101/lm.027227.112

Einarsson, E. O., Pors, J., and Nader, K. (2015). Systems reconsolidation reveals a selective role for the anterior cingulate cortex in generalized contextual fear memory expression. *Neuropsychopharmacology* 40, 480–487. doi: 10.1038/npp.2014.197

Etkin, A., Egner, T., and Kalisch, R. (2011). Emotional processing in anterior cingulate and medial prefrontal cortex. *Trends Cogn. Sci.* 15, 85–93.

Ferezou, I., Cauli, B., Hill, E. L., Rossier, J., Hamel, E., and Lambolez, B. (2002). 5-HT3 receptors mediate serotonergic fast synaptic excitation of neocortical vasoactive intestinal peptide/cholecystokinin interneurons. *J. Neurosci.* 22, 7389–7397. doi: 10.1523/JNEUROSCI.22-17-07389.2002

Gelman, D. M., Martini, F. J., Nobrega-Pereira, S., Pierani, A., Kessaris, N., and Marin, O. (2009). The embryonic preoptic area is a novel source of cortical GABAergic interneurons. *J. Neurosci.* 29, 9380–9389.

Gerfen, C. R., Paletzki, R., and Heintz, N. (2013). GENSAT BAC cre-recombinase driver lines to study the functional organization of cerebral cortical and basal ganglia circuits. *Neuron* 80, 1368–1383. doi: 10.1016/j.neuron.2013.10.016

Giustino, T. F., and Maren, S. (2015). The role of the medial prefrontal cortex in the conditioning and extinction of fear. *Front. Behav. Neurosci.* 9:298. doi: 10.3389/fnbeh.2015.00298

Gouwens, N. W., Sorensen, S. A., Baftizadeh, F., Budzillo, A., Lee, B. R., Jarsky, T., et al. (2020). Integrated morphoelectric and transcriptomic classification of cortical GABAergic cells. *Cell* 183, 935–953.e19.

Greco, J. A., and Liberzon, I. (2016). Neuroimaging of fear-associated learning. *Neuropsychopharmacology* 41, 320–334. doi: 10.1038/npp.2015.255

Grewe, B. F., Grundemann, J., Kitch, L. J., Lecoq, J. A., Parker, J. G., Marshall, J. D., et al. (2017). Neural ensemble dynamics underlying a long-term associative memory. *Nature* 543, 670–675.

Gross, C. T., and Canteras, N. S. (2012). The many paths to fear. *Nat. Rev. Neurosci.* 13, 651–658. doi: 10.1038/nrn3301

Herry, C., and Johansen, J. P. (2014). Encoding of fear learning and memory in distributed neuronal circuits. *Nat. Neurosci.* 17, 1644–1654. doi: 10.1038/nn.3869

Hinojosa, C. A., Kaur, N., Vanelzakker, M. B., and Shin, L. M. (2019). Cingulate subregions in posttraumatic stress disorder, chronic stress, and treatment. *Handb. Clin. Neurol.* 166, 355–370. doi: 10.1016/B978-0-444-64196-0.00020-0

Holtmaat, A., Bonhoeffer, T., Chow, D. K., Chuckowree, J., De Paola, V., Hofer, S. B., et al. (2009). Long-term, high-resolution imaging in the mouse neocortex through a chronic cranial window. *Nat. Protoc.* 4, 1128–1144.

Honjoh, S., Sasai, S., Schiereck, S. S., Nagai, H., Tononi, G., and Cirelli, C. (2018). Regulation of cortical activity and arousal by the matrix cells of the ventromedial thalamic nucleus. *Nat. Commun.* 9:2100. doi: 10.1038/s41467-018-04497-x

Hou, W. H., and Capogna, M. (2018). Dendritic inhibition in layer 1 cortex gates associative memory. *Neuron* 100, 516–519. doi: 10.1016/j.neuron.2018.10.029

Howland, J. G., Ito, R., Lapish, C. C., and Villaruel, F. R. (2022). The rodent medial prefrontal cortex and associated circuits in orchestrating adaptive behavior under variable demands. *Neurosci. Biobehav. Rev.* 135:104569. doi: 10.1016/j.neubiorev.2022.104569

Hsu, M. M., Kung, J. C., and Shyu, B. C. (2000). Evoked responses of the anterior cingulate cortex to stimulation of the medial thalamus. *Chin. J. Physiol.* 43, 81–89.

Hsu, M. M., and Shyu, B. C. (1997). Electrophysiological study of the connection between medial thalamus and anterior cingulate cortex in the rat. *Neuroreport* 8, 2701–2707. doi: 10.1097/00001756-199708180-00013

Huang, Z. J., and Paul, A. (2019). The diversity of GABAergic neurons and neural communication elements. *Nat. Rev. Neurosci.* 20, 563–572. doi: 10.1038/s41583-019-0195-4

Ibrahim, L. A., Huang, S., Fernandez-Otero, M., Sherer, M., Qiu, Y., Vemuri, S., et al. (2021). Bottom-up inputs are required for establishment of top-down connectivity onto cortical layer 1 neurogliaform cells. *Neuron* 109, 3473–3485.e5. doi: 10.1016/j.neuron.2021.08.004

Ibrahim, L. A., Schuman, B., Bandler, R., Rudy, B., and Fishell, G. (2020). Mining the jewels of the cortex's crowning mystery. *Curr. Opin. Neurobiol.* 63, 154–161. doi: 10.1016/j.conb.2020.04.005

Jiang, X., Shen, S., Cadwell, C. R., Berens, P., Sinz, F., Ecker, A. S., et al. (2015). Principles of connectivity among morphologically defined cell types in adult neocortex. *Science* 350:aac9462.

Jiang, X., Wang, G., Lee, A. J., Stornetta, R. L., and Zhu, J. J. (2013). The organization of two new cortical interneuronal circuits. *Nat. Neurosci.* 16, 210–218.

Johansen, J. P., Fields, H. L., and Manning, B. H. (2001). The affective component of pain in rodents: Direct evidence for a contribution of the anterior cingulate cortex. *Proc. Natl. Acad. Sci. U.S.A.* 98, 8077–8082. doi: 10.1073/pnas.141218998

Jovanovic, T., and Norrholm, S. D. (2011). Neural mechanisms of impaired fear inhibition in posttraumatic stress disorder. *Front. Behav. Neurosci.* 5:44. doi: 10.3389/fnbeh.2011.00044

Kelmendi, B., Adams, T. G., Yarnell, S., Southwick, S., Abdallah, C. G., and Krystal, J. H. (2016). PTSD: From neurobiology to pharmacological treatments. *Eur. J. Psychotraumatol.* 7:31858.

LeDoux, J., and Daw, N. D. (2018). Surviving threats: Neural circuit and computational implications of a new taxonomy of defensive behaviour. *Nat. Rev. Neurosci.* 19, 269–282. doi: 10.1038/nrn.2018.22

Lee, A. J., Wang, G., Jiang, X., Johnson, S. M., Hoang, E. T., Lanté, F., et al. (2015). Canonical organization of layer 1 neuron-led cortical inhibitory and disinhibitory interneuronal circuits. *Cereb. Cortex* 25, 2114–2126. doi: 10.1093/cercor/bhu020

Lee, S., Hjerling-Leffler, J., Zagha, E., Fishell, G., and Rudy, B. (2010). The largest group of superficial neocortical GABAergic interneurons expresses ionotropic

serotonin receptors. *J. Neurosci.* 30, 16796–16808. doi: 10.1523/JNEUROSCI.1869-10.2010

Letzkus, J. J., Wolff, S. B., and Luthi, A. (2015). Disinhibition, a circuit mechanism for associative learning and memory. *Neuron* 88, 264–276.

Letzkus, J. J., Wolff, S. B., Meyer, E. M., Tovote, P., Courtin, J., Herry, C., et al. (2011). A disinhibitory microcircuit for associative fear learning in the auditory cortex. *Nature* 480, 331–335. doi: 10.1038/nature10674

Louzolo, A., Lebedev, A. V., Björnsdotter, M., Acar, K., Ahrends, C., Kringelbach, M. L., et al. (2022). Resistance to extinction of evaluative fear conditioning in delusion proneness. *Schizophr. Bull. Open* 3:sgac033.

Low, R. J., Gu, Y., and Tank, D. W. (2014). Cellular resolution optical access to brain regions in fissures: Imaging medial prefrontal cortex and grid cells in entorhinal cortex. *Proc. Natl. Acad. Sci. U.S.A.* 111, 18739–18744. doi: 10.1073/pnas.1421753111

Ma, L. Q., Ning, L., Wang, Z., and Wang, Y. W. (2016). Visual and noxious electrical stimulus-evoked membrane-potential responses in anterior cingulate cortical neurons. *Mol. Brain* 9:82. doi: 10.1186/s13041-016-0262-y

Markram, H., Muller, E., Ramaswamy, S., Reimann, M. W., Abdellah, M., Sanchez, C. A., et al. (2015). Reconstruction and simulation of neocortical microcircuitry. *Cell* 163, 456–492.

Muralidhar, S., Wang, Y., and Markram, H. (2013). Synaptic and cellular organization of layer 1 of the developing rat somatosensory cortex. *Front. Neuroanat.* 7:52. doi: 10.3389/fnana.2013.00052

Niquille, M., Limoni, G., Markopoulos, F., Cadilhac, C., Prados, J., Holtmaat, A., et al. (2018). Neurogliaform cortical interneurons derive from cells in the preoptic area. *eLife* 7:e32017. doi: 10.7554/eLife.32017

Overstreet-Wadiche, L., and McBain, C. J. (2015). Neurogliaform cells in cortical circuits. *Nat. Rev. Neurosci.* 16, 458–468.

Pardi, M. B., Vogenstahl, J., Dalmay, T., Spano, T., Pu, D. L., Naumann, L. B., et al. (2020). A thalamocortical top-down circuit for associative memory. *Science* 370, 844–848.

Pattwell, S. S., Liston, C., Jing, D., Ninan, I., Yang, R. R., Witztum, J., et al. (2016). Dynamic changes in neural circuitry during adolescence are associated with persistent attenuation of fear memories. *Nat. Commun.* 7:11475. doi: 10.1038/ncomms11475

Perroud, N., Zewdie, S., Stenz, L., Adouan, W., Bavamian, S., Prada, P., et al. (2016). Methylation of serotonin receptor 3a in Adhd, borderline personality, and bipolar disorders: Link with severity of the disorders and childhood maltreatment. *Depress. Anxiety* 33, 45–55. doi: 10.1002/da.22406

Petersen, S. E., and Posner, M. I. (2012). The attention system of the human brain: 20 years after. *Annu. Rev. Neurosci.* 35, 73–89.

Petty, G. H., Kinnischtzke, A. K., Hong, Y. K., and Bruno, R. M. (2021). Effects of arousal and movement on secondary somatosensory and visual thalamus. *eLife* 10:e67611. doi: 10.7554/eLife.67611

Poorthuis, R. B., Muhammad, K., Wang, M., Verhoog, M. B., Junek, S., Wrana, A., et al. (2018). Rapid neuromodulation of layer 1 interneurons in human neocortex. *Cell Rep.* 23, 951–958. doi: 10.1016/j.celrep.2018.03.111

Roy, D. S., Park, Y. G., Kim, M. E., Zhang, Y., Ogawa, S. K., Dinapoli, N., et al. (2022). Brain-wide mapping reveals that engrams for a single memory are distributed across multiple brain regions. *Nat. Commun.* 13:1799. doi: 10.1038/s41467-022-29384-4

Rudy, B., Fishell, G., Lee, S., and Hjerling-Leffler, J. (2011). Three groups of interneurons account for nearly 100% of neocortical GABAergic neurons. *Dev. Neurobiol.* 71, 45–61. doi: 10.1002/dneu.20853

Schechter, D. S., Moser, D. A., Pointet, V. C., Aue, T., Stenz, L., Paoloni-Giacobino, A., et al. (2017). The association of serotonin receptor 3A methylation with maternal violence exposure, neural activity, and child aggression. *Behav. Brain Res.* 325, 268–277. doi: 10.1016/j.bbr.2016.10.009

Schiff, N. D. (2008). Central thalamic contributions to arousal regulation and neurological disorders of consciousness. *Ann. N. Y. Acad. Sci.* 1129, 105–118. doi: 10.1196/annals.1417.029

Schmitt, L. I., Wimmer, R. D., Nakajima, M., Happ, M., Mofakham, S., and Halassa, M. M. (2017). Thalamic amplification of cortical connectivity sustains attentional control. *Nature* 545, 219–223.

Schuman, B., Machold, R. P., Hashikawa, Y., Fuzik, J., Fishell, G. J., and Rudy, B. (2019). Four unique interneuron populations reside in neocortical layer 1. *J. Neurosci.* 39, 125–139. doi: 10.1523/JNEUROSCI.1613-18.2018

Sidorov, M. S., Kim, H., Rougie, M., Williams, B., Siegel, J. J., Gavornik, J. P., et al. (2020). Visual sequences drive experience-dependent plasticity in mouse anterior cingulate cortex. *Cell Rep.* 32:108152. doi: 10.1016/j.celrep.2020.108152

Silva, B. A., Mattucci, C., Krzywkowski, P., Cuozzo, R., Carbonari, L., and Gross, C. T. (2016). The ventromedial hypothalamus mediates predator fear memory. *Eur. J. Neurosci.* 43, 1431–1439.

Singh, A., Patel, D., Li, A., Hu, L., Zhang, Q., Liu, Y., et al. (2020). Mapping cortical integration of sensory and affective pain pathways. *Curr. Biol.* 30, 1703–1715.e5.

Skelly, M. J., Ariwodola, O. J., and Weiner, J. L. (2017). Fear conditioning selectively disrupts noradrenergic facilitation of GABAergic inhibition in the basolateral amygdala. *Neuropharmacology* 113, 231–240. doi: 10.1016/j.neuropharm.2016.10.003

Steenland, H. W., Li, X. Y., and Zhuo, M. (2012). Predicting aversive events and terminating fear in the mouse anterior cingulate cortex during trace fear conditioning. *J. Neurosci.* 32, 1082–1095. doi: 10.1523/JNEUROSCI.5566-11.2012

Stokes, K. A., and Best, P. J. (1990). Mediodorsal thalamic lesions impair "reference" and "working" memory in rats. *Physiol. Behav.* 47, 471–476. doi: 10.1016/0031-9384(90)90111-g

Takesian, A. E., Bogart, L. J., Lichtman, J. W., and Hensch, T. K. (2018). Inhibitory circuit gating of auditory critical-period plasticity. *Nat. Neurosci.* 21, 218–227.

Tang, J., Ko, S., Ding, H. K., Qiu, C. S., Calejesan, A. A., and Zhuo, M. (2005). Pavlovian fear memory induced by activation in the anterior cingulate cortex. *Mol. Pain* 1:6. doi: 10.1186/1744-8069-1-6

Tasic, B., Menon, V., Nguyen, T. N., Kim, T. K., Jarsky, T., Yao, Z., et al. (2016). Adult mouse cortical cell taxonomy revealed by single cell transcriptomics. *Nat. Neurosci.* 19, 335–346.

Tasic, B., Yao, Z., Graybuck, L. T., Smith, K. A., Nguyen, T. N., Bertagnolli, D., et al. (2018). Shared and distinct transcriptomic cell types across neocortical areas. *Nature* 563, 72–78. doi: 10.1038/s41586-018-0654-5

Tipps, M., Marron Fernandez de Velasco, E., Schaeffer, A., and Wickman, K. (2018). Inhibition of pyramidal neurons in the basal amygdala promotes fear learning. *eNeuro* 5:ENEURO.0272-18.2018. doi: 10.1523/ENEURO.0272-18.2018

Tovote, P., Fadok, J. P., and Luthi, A. (2015). Neuronal circuits for fear and anxiety. *Nat. Rev. Neurosci.* 16, 317–331. doi: 10.1038/nrn3945

Tremblay, R., Lee, S., and Rudy, B. (2016). GABAergic interneurons in the neocortex: From cellular properties to circuits. *Neuron* 91, 260–292. doi: 10.1016/j.neuron.2016.06.033

van Heukelum, S., Mars, R. B., Guthrie, M., Buitelaar, J. K., Beckmann, C. F., Tiesinga, P. H. E., et al. (2020). Where is cingulate cortex? A cross-species view. *Trends Neurosci.* 43, 285–299. doi: 10.1016/j.tins.2020.03.007

Vucurovic, K., Gallopin, T., Ferezou, I., Rancillac, A., Chameau, P., van Hooft, J. A., et al. (2010). Serotonin 3A receptor subtype as an early and protracted marker of cortical interneuron subpopulations. *Cereb. Cortex* 20, 2333–2347. doi: 10.1093/cercor/bhp310

Wei, F., and Zhuo, M. (2001). Potentiation of sensory responses in the anterior cingulate cortex following digit amputation in the anaesthetised rat. *J. Physiol.* 532, 823–833. doi: 10.1111/j.1469-7793.2001.0823e.x

Wolff, S. B., Grundemann, J., Tovote, P., Krabbe, S., Jacobson, G. A., Muller, C., et al. (2014). Amygdala interneuron subtypes control fear learning through disinhibition. *Nature* 509, 453–458.

Wu, D., Deng, H., Xiao, X., Zuo, Y., Sun, J., and Wang, Z. (2017). Persistent neuronal activity in anterior cingulate cortex correlates with sustained attention in rats regardless of sensory modality. *Sci. Rep.* 7:43101. doi: 10.1038/srep43101

Yizhar, O., Fenno, L. E., Prigge, M., Schneider, F., Davidson, T. J., O'SHEA, D. J., et al. (2011). Neocortical excitation/inhibition balance in information processing and social dysfunction. *Nature* 477, 171–178. doi: 10.1038/nature10360

Zhou, F. M., and Hablitz, J. J. (1999). Activation of serotonin receptors modulates synaptic transmission in rat cerebral cortex. *J. Neurophysiol.* 82, 2989–2999.

frontiers | Frontiers in Neural Circuits

TYPE Review
PUBLISHED 14 September 2023
DOI 10.3389/fncir.2023.1256455

OPEN ACCESS

EDITED BY
Jean-François Cloutier,
McGill University Health Centre, Canada

REVIEWED BY
Nicoletta Kessaris,
University College London, United Kingdom
Nathalie Dehorter,
The University of Queensland, Australia

*CORRESPONDENCE
Elsa Rossignol
✉ elsa.rossignol@umontreal.ca

†These authors have contributed equally to this work and share first authorship

RECEIVED 10 July 2023
ACCEPTED 21 August 2023
PUBLISHED 14 September 2023

CITATION
Toudji I, Toumi A, Chamberland É and Rossignol E (2023) Interneuron odyssey: molecular mechanisms of tangential migration. *Front. Neural Circuits* 17:1256455. doi: 10.3389/fncir.2023.1256455

Interneuron odyssey: molecular mechanisms of tangential migration

Ikram Toudji[1,2†], Asmaa Toumi[1,3†], Émile Chamberland[1,2] and Elsa Rossignol[1,2,4*]

[1]Centre Hospitalier Universitaire (CHU) Sainte-Justine Research Center, Montréal, QC, Canada, [2]Department of Neurosciences, Université de Montréal, Montréal, QC, Canada, [3]Department of Biochemistry and Molecular Medicine, Université de Montréal, Montréal, QC, Canada, [4]Department of Pediatrics, Université de Montréal, Montréal, QC, Canada

Cortical GABAergic interneurons are critical components of neural networks. They provide local and long-range inhibition and help coordinate network activities involved in various brain functions, including signal processing, learning, memory and adaptative responses. Disruption of cortical GABAergic interneuron migration thus induces profound deficits in neural network organization and function, and results in a variety of neurodevelopmental and neuropsychiatric disorders including epilepsy, intellectual disability, autism spectrum disorders and schizophrenia. It is thus of paramount importance to elucidate the specific mechanisms that govern the migration of interneurons to clarify some of the underlying disease mechanisms. GABAergic interneurons destined to populate the cortex arise from multipotent ventral progenitor cells located in the ganglionic eminences and pre-optic area. Post-mitotic interneurons exit their place of origin in the ventral forebrain and migrate dorsally using defined migratory streams to reach the cortical plate, which they enter through radial migration before dispersing to settle in their final laminar allocation. While migrating, cortical interneurons constantly change their morphology through the dynamic remodeling of actomyosin and microtubule cytoskeleton as they detect and integrate extracellular guidance cues generated by neuronal and non-neuronal sources distributed along their migratory routes. These processes ensure proper distribution of GABAergic interneurons across cortical areas and lamina, supporting the development of adequate network connectivity and brain function. This short review summarizes current knowledge on the cellular and molecular mechanisms controlling cortical GABAergic interneuron migration, with a focus on tangential migration, and addresses potential avenues for cell-based interneuron progenitor transplants in the treatment of neurodevelopmental disorders and epilepsy.

KEYWORDS

GABA, interneurons, migration, blood vessels, oligodendrocytes, cytoskeleton, neurodevelopmental disorders, therapy

1. Introduction

Brain function requires the balanced and coordinated activity of excitatory glutamatergic projection neurons and cortical inhibitory GABAergic interneurons. The cortical excitatory projection neurons, often referred to as pyramidal cells, are generated from dorsal progenitors located in the pallium. On the other hand, cINs are generated from several progenitor pools

located outside the pallium, in the ventral telencephalon (subpallium; Anderson et al., 1997; Wonders and Anderson, 2006). Consequently, pyramidal cells and cINs follow distinct migratory journeys during embryonic development to converge in the mature cerebral cortex. Pyramidal cells migrate radially over relatively short distances into the developing cortical plate, whereas cINs follow a complex process involving multiple consecutive phases: a tangential migration from their embryonic origin to the pallium, a switch to radial migration with intracortical dispersion and subsequent integration in their final laminar allocation in the cortex (Marin and Rubenstein, 2001; Marin, 2013). Mounting evidence suggests that alterations in cIN development or function contributes to the pathogenesis of several neurodevelopmental and psychiatric disorders including autism spectrum disorders (Vogt et al., 2018; Chen et al., 2020; Smith et al., 2020a; Amegandjin et al., 2021; Nomura, 2021; Juarez and Martinez Cerdeno, 2022), intellectual deficiency/learning disabilities/attention deficit disorders (Lupien-Meilleur et al., 2021; Ferguson et al., 2023), epilepsy (Rossignol et al., 2013; Jiang et al., 2016, 2018; Tran et al., 2020; Gertler et al., 2022; Ryner et al., 2023) and schizophrenia (Sohal and Rubenstein, 2019; Shen et al., 2021). Furthermore, *in utero* ethanol exposure was recently shown to disrupt cIN migration in a mouse model of fetal alcohol spectrum disorder (FASD; Skorput et al., 2015; Lee et al., 2022), suggesting that environmental factors, together with perturbations of intrinsic molecular programs, both play critical roles in cIN development, relevant to a range of neurodevelopmental disorders. This review aims to summarize some of the molecular and environmental mechanisms regulating cIN migration.

2. Extrinsic guidance cues directing cIN migration

2.1. Repulsion from the proliferative zone and onset of migration

The majority of cINs arise in the embryonic subpallium from multipotent progenitors in the medial (MGE) and caudal (CGE) ganglionic eminences, while a smaller fraction originates from the preoptic area (POA). MGE lineages produce parvalbumin- and somatostatin-expressing cINs which account for ~70% of the total GABAergic cIN population, while CGE-derived INs expressing the serotoninergic receptor 5-HT-3A comprise ~30% of the total cortical interneuron population (Fogarty et al., 2007; Lee et al., 2010; Miyoshi et al., 2010; Rubin et al., 2010; Yu et al., 2021). Regardless of their embryonic origin, newborn interneurons adopt a highly polarized morphology as they initiate their tangential migration, and they display an astonishing ability to move and interact with environmental cues: they extend, branch and remodel their leading process, retract unselected branches and orient in space in response to chemoattractant and repulsive cues. Although multiple mechanisms are shared between MGE and CGE-derived cINs, recent evidence suggests that distinct transcriptional programs regulate the migration and laminar positioning of CGE-derived cINs (Murthy et al., 2014; Miyoshi et al., 2015; Touzot et al., 2016; Wei et al., 2019; Limoni et al., 2021; Venkataramanappa et al., 2022). This review focuses on mechanisms governing MGE-derived cIN migration, which have been more extensively studied.

Newborn postmitotic cINs are actively repulsed from the proliferative zone by guidance cues expressed within the MGE ventricular (VZ) and subventricular (SVZ) zones, which triggers the onset of cIN tangential migration (Zhu et al., 1999; Marin et al., 2001; see Figure 1A). The diffusible cues Slit homologs 1 and 2 (Slit1 and 2), expressed in the VZ and SVZ zones of the MGE, were shown to repulse cINs *in vitro* and were though to contribute to the onset of migration away from the VZ and towards the cortical plate (CP; Yuan et al., 1999; Zhu et al., 1999). However, migration of cINs was unaffected in *Slit1*$^{-/-}$ and *Slit2*$^{-/-}$ mutant mice, although the repulsive effect of ventral structures remained (Marin et al., 2003), suggesting that other factors originating from the basal forebrain contribute to the initiation of cIN migration. Ephrins and their receptors Eph tyrosine kinases appear critical in this process. EphrinA5, expressed in the VZ, exerts a repulsive effect on migrating cINs expressing the EphA4 receptor, contributing to VZ avoidance (Zimmer et al., 2008). In addition to repulsive cues, cINs also encounter motogenic cues that stimulate their motility. For instance, EphrinA2 expressed by cINs interacts with its EphA4 receptor expressed by glial cells and exerts a reverse signaling effect that increases the speed of cIN migration (Steinecke et al., 2014). Other motogenic factors that promote cIN migration include hepatocyte growth factor/scatter factor (HGF/SF; Powell et al., 2001), brain-derived neurotrophic factor (BDNF) and neurotrophin 4 (NT4; Polleux et al., 2002), and glial-derived neurotrophic factor (GDNF; Pozas and Ibanez, 2005).

En route to the dorsal pallium, cINs must avoid entering the striatum to pursue their dorsal migration, contrary to striatal interneurons, which end their trajectory in this structure [see review (Villar-Cervino et al., 2015)]. The avoidance of the striatum by cINs is mostly due to the chemorepulsive effect of semaphorin 3A and 3F, expressed in the striatal mantle, as well as EphrinA3, expressed by striatal cells (Marin et al., 2001; Rudolph et al., 2010). Indeed, migrating interneurons destined to populate the cortex, but not those directed to the striatum, express the semaphorin receptors neuropilin 1 and 2 (Nrp1 and 2) and the EphA4 receptor. Thus, they are directed away from the striatum in response to semaphorin 3A/3F (Marin et al., 2001) and EphrinA3 (Rudolph et al., 2010). Interestingly, the loss of the Slit receptor Roundabout homolog 1 (Robo1) leads to a failure of this repulsive effect, resulting in an aberrant accumulation of cINs in the developing striatum (Andrews et al., 2006), a phenotype that was absent from *Slit1*$^{-/-}$ and *Slit2*$^{-/-}$ mutants (Marin et al., 2003), suggesting that Robo signaling regulates cIN migration independently of Slits. Indeed, it was since shown that the repulsive effect of semaphorin 3A/3F requires binding of Robo1 to Nrp1, such that the loss of Robo1 function in cINs leads to their aberrant accumulation in the striatum through a loss of sensitivity to the repulsive effect of semaphorins 3A/3F (Hernández-Miranda et al., 2011).

2.2. Guidance towards the dorsal pallium

Chemoattractive molecules create permissive corridors for migrating cINs (see Figure 1A). Neuregulin-1 (Nrg1), a protein containing an epidermal growth factor (EGF)-like motif which dimerizes and activates transmembrane tyrosine kinases related to the EGF receptor, was the first factor described as having a chemoattractive effect on migrating cINs (Flames et al., 2004). The *NRG1* gene, identified as a schizophrenia susceptibility gene [as

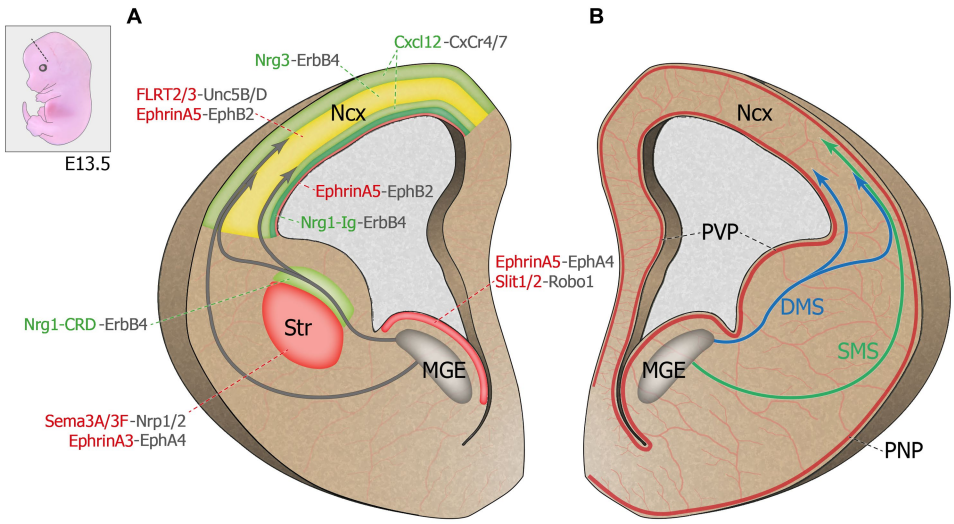

FIGURE 1
Molecular regulation of cortical interneuron migration. Top left corner: Representation of an E13.5 mouse embryo. Dash line illustrates the coronal plane through the telencephalon. **(A)** Schematic representation of a coronal hemi-section (left) highlighting the chemorepulsive (red) and chemoattractive (green) molecules guiding MGE-derived INs migrating towards the developing cortical plate. The cortical plate hosts both chemoattractive and chemorepulsive cues and is represented in yellow. **(B)** Schematic representation of a coronal hemi-section (right) showing the spatial proximity between the developing brain principal vascular networks and the MGE-derived IN migratory streams. DMS: deep migratory stream. E13.5: Embryonic day 13.5. MGE: medial ganglionic eminence. Ncx: neocortex. PNP: perineural vascular plexus. PVP: periventricular vascular plexus. SMS: superficial migratory stream. Str: striatum.

reviewed in Rossignol, 2011; Marin, 2012], is subject to alternative splicing (Falls, 2003), resulting in the expression of two distinct protein isoforms in the developing telencephalon: Nrg1-Ig, a diffusible protein expressed in the pallium, and Nrg1-CRD, a membrane-bound protein expressed along the dorsal migratory streams, which, respectively, act as long- and short-range attractors for MGE-derived INs. The Nrg1 receptor tyrosine-protein kinase ErbB4, a member of the epidermal growth factor receptor family, is required for this process as interneurons lacking ErbB4 largely fail to enter the Nrg1-CRD+ corridor as they migrate towards the cortex (Flames et al., 2004). Interestingly, ErbB4 is not ubiquitously expressed in all migrating cINs, suggesting that different subtypes of cINs might be guided by distinct extracellular factors (Yau et al., 2003). Recent work has revealed that Nrg1/ErbB4-mediated chemoattraction of migrating cINs involves two molecular cascades: PI3-kinase/PTEN/AKT and p35/Cdk5, which both play keys roles in cIN migration (Rakić et al., 2015). Like Nrg1, ErbB4 receptor exists in two different isoforms, one with a binding site for PI3-kinase (cyt1) and one without (cyt2). At embryonic day (E)13.5, the cyt1 isoform is selectively expressed by migrating cINs entering the dorsal pallium, not in those still in the ganglionic eminences, and it seems critical for their ability to traverse the pallial-subpallial boundary (Rakić et al., 2015). Furthermore, Cdk5 positively regulates the ErbB4/PI3-kinase/AKT pathway by phosphorylating ErbB4 (Rakić et al., 2015). Thus, altering of ErbB4 signaling through defective Cdk5 phosphorylation, PI3-kinase binding or alterations in both molecular pathways impair leading process morphology, directionality and polarity of MGE-derived INs, as well as their ability to enter the dorsal pallium (Rakić et al., 2015). This cascade is clinically relevant since disruption of Nrg1-ErbB4 signaling is associated with epilepsy, intellectual disability and schizophrenia (Li et al., 2011; Tan et al., 2011; Marin, 2012; Del Pino et al., 2013; Hyder et al., 2021).

2.3. Integration into migratory streams, intracortical dispersion, and laminar allocation

Once they cross the pallial-subpallial boundary, cINs integrate migratory streams on either side of the cortical plate. In early stages of cortical development (E12-E13), most interneurons migrate towards the developing cortex via two parallel routes, a superficial migratory stream (SMS) that passes through the marginal zone (Bastaki et al., 2017). and a deep migratory stream (DMS) localized in the subventricular zone (SVZ). Between E15 and E16 in mice, a third migratory stream appears in the subplate (SP) between the MZ and the SVZ streams (Lavdas et al., 1999; Wichterle et al., 2001; Marin, 2013; Peyre et al., 2015). Although earlier evidence suggested that migratory route allocation is independent of an interneuron's birthplace (Miyoshi and Fishell, 2011), recent evidence suggests that cell identity may actually determine, at least in part, the chosen migratory stream. Indeed, somatostatin-expressing Martinotti cells as well as translaminar parvalbumin-expressing cells preferentially migrate through the MZ (Lim et al., 2018). Interestingly, these interneurons send axonal projections to cortical layer I post-natally, a region arising from the MZ. Hence, integration into a migratory stream seems linked to cell fate (early specification) and may contribute to axonal targeting (Lim et al., 2018). It is thus likely that cINs migrate through the MZ or SVZ depending on their response to different extracellular guidance cues, although the identity of these signals as well as the underlying mechanisms remain largely unknown.

Transcriptomics data from migrating cINs showed differential gene expression profiles between cINs migrating within the superficial or deep migratory streams, including different sets of guidance receptors (Antypa et al., 2011). Further, a recent study demonstrated that EphB2/EphrinA5 signaling maintains the segregation of the SVZ and SP migratory routes. EphrinA5, highly expressed in the deep ventricular zone (VZ), upper SVZ, deep intermediate zone (IZ) and the CP of the developing telencephalon, confines EphB2-expressing interneurons to the SVZ and SP streams through a repulsive effect (Liu et al., 2017). Similarly, fibronectin leucine-rich transmembrane proteins (FLRT2 and 3), expressed by pyramidal cells and previously known for their roles in axon guidance, excitatory neuron migration and synaptogenesis (Yamagishi et al., 2011; O'Sullivan et al., 2012; Leyva-Díaz et al., 2014; Del Toro et al., 2017, 2020), have recently been shown to exert repulsive effects on Unc5B/D-expressing cINs *in vitro* (Fleitas et al., 2021). *In vivo*, these repulsive cues cooperate to maintain the integrity of the SP stream, as the loss of both FLRT2 and 3 in pyramidal cells affects the cortical distribution of cINs. In *Flrt2/3* double knockout mouse model, cINs normally found in the SP stream abnormally accumulate in the IZ, while the organization of the SVZ stream remains intact (Fleitas et al., 2021).

Neurotransmitter signaling can also modulate cIN migration. *In vivo*, mice lacking the glycine receptor α2 subunit homomers specifically in cINs show migration defects in the SVZ, but not the MZ or SP streams (Avila et al., 2013). Furthermore, pharmacological blockade of $GABA_B$ receptors leads to an aberrant accumulation of cINs in the SVZ stream and a decrease in the MZ stream, suggesting that GABA signaling is also important for migratory route selection (Lopez-Bendito et al., 2003).

Intracortical dispersion involves the timed exit from migratory streams and a switch of migration modes from tangential to radial migration. Chemokine Cxcl12 (previously known as Sdf-1), expressed by meningeal and progenitor cells in the SVZ (Stumm et al., 2003; Tiveron et al., 2006) exerts a dual role in interneuron migration, confining migrating cINs to the migratory streams and controlling the timing of CP invasion. Its function in migrating cINs is mediated by two G protein-coupled receptors, Cxcr4 and Cxcr7, both essential for proper sensing of this chemokine. Indeed, the absence of either receptor leads to the premature departure of cINs from the migratory streams and their precocious invasion of the CP, perturbing cIN laminar positioning in the postnatal cortex (Li et al., 2008; López-Bendito et al., 2008; Tanaka et al., 2010; Wang et al., 2011). These findings suggest that the CP exerts a chemoattractive effect on migrating cINs. Interestingly, Cxcl12 reduces the branching dynamics of cIN leading process through the regulation of actin and microtubules (Lysko et al., 2011, 2014), thus decreasing the ability of cINs to sense short-range environmental cues present at significant distance from the tangential migratory streams. It was later discovered that the developing CP is highly enriched in neuregulin-3 (Nrg3), a short-range chemoattractant expressed by pyramidal cells. The *NRG3* gene has been linked to schizophrenia in human genetic studies and *Nrg3* knockout mice display behavioral deficits mirroring those observed in patients (Meier et al., 2013; Hayes et al., 2016). *In vitro*, tangentially migrating MGE-derived INs are attracted by both Cxcl12 and Nrg3, but they display a preference for Cxcl12. However, overexpressing Nrg3 hastens the invasion of the CP by MGE-derived INs expressing the receptor ErbB4. These experiments suggest that the timed invasion of the CP, which is essential for the proper lamination of cINs, depends on the fine-tuned balance between Cxcl12 and Nrg3 (Bartolini et al., 2017).

Moreover, disrupting the fate of cortical pyramidal cells changes the laminar distribution of cINs, suggesting that pyramidal cells instruct cIN positioning through specific guidance cues. For instance, deep layer pyramidal tract neurons, which typically project to the thalamus, brainstem and spinal cord, inform the positioning of MGE-derived cINs (the parvalbumin-and the somatostatin-expressing cINs) in cortical layer V. Thus, the deletion of *Fezf2*, inducing a fate-switch from subcerebral projection neurons towards callosal projection neurons, results in massive reduction of MGE-derived cINs in layer V (Lodato et al., 2011). In explants and *in vivo*, cortical pyramidal cells specifically attract cINs that would typically target them, such that deep-layer corticofugal pyramidal neurons tend to attract early-born MGE-neurons while callosal projecting pyramidal neurons attract later-born cINs (Lodato et al., 2011). Notably, the subtype of PC and cIN seems more important for their proper pairing than their chronological appearance (Lodato et al., 2011). Similarly, the deletion of *Satb2* to reprogram intratelencephalic pyramidal neurons that usually project to other cortical areas and the striatum into pyramidal tract neurons projecting to subcortical structures selectively disrupts the lamination of CGE-derived INs (Wester et al., 2019). Thus, distinct populations of cortical projection neurons might control the lamination of cINs, likely through their release of specific cues, which must be further be identified.

Interestingly, cINs interact with other cIN populations and this crosstalk also regulates the final distribution of specific cIN populations. For instance, MGE-derived cINs, which populate deep cortical layers, secrete semaphorin 3A that repulses PlexinA4 receptor-expressing CGE-derived INs, ultimately confining CGE-INs to superficial cortical layers as they enter the cortical plate (Limoni et al., 2021).

Emerging neuronal network activity also plays an essential role in cIN development and migration (Zimmer-Bensch, 2018). For instance, before postnatal day (P)3 when radial migration is ongoing, a decrease in neuronal excitability through overexpression of the inward rectifier potassium channel Kir2.1 in CGE-derived INs leads to a shift in the cortical distribution of calretinin-positive and reelin-positive cells, but not VIP-positive cells, from superficial to deep cortical layers (De Marco Garcia et al., 2011). Interestingly, the level of activity after P3 regulates the morphology, but not the positioning, of these same cell types (De Marco Garcia et al., 2011). Furthermore, the source of input seems critical to regulate these processes. For instance, glutamatergic inputs from the thalamus specifically regulates the morphological maturation of reelin-expressing INs, without affecting VIP-positive cells, while manipulating cortical glutamatergic inputs does not affect the morphology of either cell types (De Marco Garcia et al., 2015). Thus, distinct subtypes of cINs might rely on specific sources of neuronal activity for their development, migration, and maturation in cortical circuits.

2.4. Termination of interneuron migration

Once settled in the appropriate cortical layers, cINs must stop their migratory behavior. In mice, this phenomenon occurs during the first postnatal week (Bortone and Polleux, 2009). It was first suggested that migrating cINs perceive GABA as a stop signal during early postnatal development, when the expression of potassium/chloride

exchanger KCC2 is upregulated in these cells (Bortone and Polleux, 2009). KCC2 mediates the inversion of the intracellular chloride gradient. Consequently, GABA becomes hyperpolarizing and, through its activation of $GABA_A$ receptors, decreases the frequency of intracellular calcium transients and slows IN motility (Bortone and Polleux, 2009). Although it was initially proposed that KCC2 expression suffices to trigger the arrest of cIN migration, it was recently demonstrated that the lack of KCC2 in cINs does not alter their ability to migrate to their final cortical allocation, arguing that other molecular actors might determine the arrest of cIN migration (Zavalin et al., 2022). Moreover, reduction of cIN motility is also observed when migrating cINs are co-cultured with postnatal cortical cells, suggesting that unknown extrinsic cues secreted by cortical cells might also act as stop signals for migrating cINs through yet elusive mechanisms (Inamura et al., 2012).

3. Blood vessels as a source of guidance cues for migrating interneurons

Several recent studies have demonstrated that the development of the vascular system is crucial for many aspects of cortical maturation, including neuronal migration (Paredes et al., 2018). Two distinct types of vascular structures are found in the embryonic brain: the periventricular vascular plexus (PVP) and the pial network, also known as perineural vascular plexus (PNP; see Figure 1B). These two blood vessel systems are different in their anatomical location, developmental timeline, and gene expression (Vasudevan and Bhide, 2008). The PNP is generated by the neural tube and covers the pial surface of the cortex around embryonic day 10 (E10) in mice (Hogan et al., 2004). In comparison, PVP formation begins at E11 following a ventro-dorsal angiogenic gradient, aligned with the future direction of cINs migration starting a day later (Vasudevan et al., 2008). The PVP was recently shown to regulate neurogenesis and the generation of MGE-derived cINs (Tan et al., 2016). Migration of MGE-derived INs in mice starts at E13.5 (Lavdas et al., 1999; Marin and Rubenstein, 2001), corresponding roughly to humans IN migration that has been shown to be in progress during the late stage of gestation (Xu et al., 2011). Both in mice and humans, vascular development slightly precedes the onset of IN migration, suggesting a potential role for early brain vascular structures in instructing migrating INs. Moreover, these two vascular structures are in close proximity to the two migratory routes followed by cINs, the PNP lining the edge of the SMS, and the PVP closely aligned with the DMS (see Figure 1B; Won et al., 2013). This spatial proximity as well as the temporal coincidence of PVP development with cIN migration suggests opportunities for potential interactions between the developing brain vasculature and migrating cINs, as detailed below.

3.1. Vascular-neuronal interactions and the roles of endothelial cells in guiding cINs migration

Endothelial cells (ECs) from cortical blood vessels impact neocortex formation by secreting molecular cues that influence neuronal cell behavior (Karakatsani et al., 2019). Interestingly, the MGE becomes actively vascularized in the days preceding the initiation of MGE-IN migration, suggesting that vessels in the MGE may secrete cues that will help initiate cIN migration. The work of Genestine et al. (2021) helped identify two EC-derived paracrine factors released in the MGE, SPARC and SerpinE1, which promote the tangential migration of MGE-derived cINs in mice MGE explants and organotypic slice cultures at E11.5, and also favour cIN migration from human stem cell derived organoïds. SPARC protein has been previously shown to be implicated in multiple different cellular events, such as migration of malignant cells (Arnold and Brekken, 2009). SerpinE1, on the other hand, is implicated in the uPA/urokinase pathway (Mahmood et al., 2018), which plays a known role in IN tangential migration (Powell et al., 2001). In addition to their intracellular contribution, these proteins likely also participate in IN migration by reducing the cell adherence to the extracellular matrix (Gongidi et al., 2004). SPARC and SerpinE1 are enriched in brain ECs compared to the rest of the brain and to EC of other organs (Hupe et al., 2017). Notably, Genestine et al. (2021) showed that the inactivation of either SPARC or SerpinE1 using antibody-mediated interference reduces the ability of MGE-derived medium to stimulate cIN migration *in vitro*, and that both proteins likely act in a complementary fashion within the same molecular pathway.

In addition, the vascular endothelial growth factor Vegfa, a pro-angiogenic factor expressed by ECs and neural progenitors and critical for the formation of the brain's vasculature (Ruhrberg et al., 2002), also appears to play a critical role in cIN migration (Haigh et al., 2003; Raab et al., 2004). Vegfa exists in three isoforms, Vegfa120, Vegfa165, and Vegfa188, differing in their expression of a heparan sulfate proteoglycan binding domain and their ability to bind the extracellular matrix. Vegfa ablation was shown to reduce the number of cINs (Li et al., 2013), partly by impairing the expression of *Dlx1/2*, a transcription factor required for IN specification and migration (Darland et al., 2011; Cain et al., 2014). Using a mouse model carrying a deletion of the Vegfa165/188 isoforms and ubiquitously expressing the Vegfa120 isoform, circumventing the early lethality of pan Vegfa knockout models, Barber et al. (2018) found that cINs populate the cortex at mid-gestation, despite aberrant brain vascularization and angiogenesis, although migration of cINs in late gestation is greatly impaired, resulting in a net reduction of cIN numbers at birth, with altered distribution and proximity to developing vessels (Barber et al., 2018).

Early during cIN migration, both GABA and glutamate act as motogenic factors that promote cIN migration (Bortone and Polleux, 2009). Furthermore, cINs require the functional expression of $GABA_A$ receptor subunits to ensure their tangential migration (Cuzon Carlson and Yeh, 2011). However, the exact source of GABA that triggers this effect was unclear. Li et al. (2018) recently demonstrated that endothelial derived GABA is essential for this process. First, endothelial cells require functional $GABA_A$ receptors and a GABA release mechanism (*Vgat*) for appropriate brain angiogenesis Li et al. (2018). Secondly, GABA release from PVP blood vessels promotes cIN migration (Li et al., 2018), while neuronal-derived GABA could not compensate for the reduced ($Gabrb3^{ECKO}$) or null ($Vgat^{ECKO}$) release of endothelial cell-derived GABA in ensuring these processes (Li et al., 2018). Nonetheless, further research is required to determine how, precisely, GABA influence IN migration at the cellular and molecular levels.

Glutamate also influences the interaction between the vascular network and migrating cINs. Recent findings suggest that ECs NMDA receptor subunits expression is region-specific and coincides with late cIN migration (Legros et al., 2009; Luhmann et al., 2015). Glutamate

activation of endothelial NMDA receptors leads to the recruitment of two proteases, matrix metalloproteinase-9 (MMP-9) and tissue-plasminogen activator (t-PA), who in turn increase cIN migratory speed alongside the PNP and radial-microvessels in the mouse superficial cortex (Léger et al., 2020). Medications altering this process, such as NMDA antagonist anesthetics, could thus potentially interrupt the process of late cIN migration in neonates at a time when a portion of cINs are still migrating along radial microvessels, warranting caution at this age (Xu et al., 2011; Léger et al., 2020). Subsequent studies at a subcellular level are needed to address how theses proteases are able to promote cIN migration speed.

3.2. Crosstalk between blood vessels, glial cells and migrating interneurons

Recent discoveries in the field of vascular guidance of cIN migration revealed the critical role of ventrally-derived oligodendrocyte precursor cells (vOPCs). First-wave vOPCs undergo substantial cell death shortly after birth. Their contribution to cIN development was thus unclear (Kessaris et al., 2006). However, Lepiemme et al. (2022) recently described significant contributions of these vOPCs to the guidance of cIN tangential migration. Both cINs and vOPCs emerge from common embryonic origins (MGE, POA) and follow parallel migratory routes, responding to the chemoattractant Cxcl12 at the level of the cortical plate (Lepiemme et al., 2022). However, despite these similarities, there is minimal overlap between cINs and vOPCs migratory streams. While vOPCs migrate along the cortical blood vessels expressing Cxcl12, cINs remain in organized streams within the parenchyma (Tsai et al., 2016; Lepiemme et al., 2022). Upon depletion of first-wave vOPCs, cINs start to cluster around Cxcl12-expressing blood vessels and halt their migration (Lepiemme et al., 2022). vOPCs thus prevent migrating cINs from aggregating to the Cxcl12-enriched blood vessels through a unilateral contact repulsion (UCoRe) mechanism (Lepiemme et al., 2022). Importantly, this critical function cannot be performed by second-wave vOPCs, which fail to rescue the cINs migration deficit in mutants devoid of first wave vOPCs, suggesting either age-specific mechanisms in earlier born cINs or first-wave vOPC-specific signaling molecules (Lepiemme et al., 2022).

4. Cell-intrinsic regulation of cIN migration dynamics

4.1. Transcriptional regulation of cIN migration

cIN migration is under the control of both extracellular signals and cell-autonomous intrinsic programs. Transcription factors, in addition to their fundamental roles in cell specification and differentiation, regulate cIN migration in part by controlling the expression of critical receptors and downstream molecular signaling cascades. During forebrain development, the generation of MGE-derived INs relies on the expression of several TFs including the *Dlx* homeobox genes *Dlx1/2* and *Dlx5/6*, the *NK2* homeobox 1 gene (*Nkx2-1*) and the *LIM* homeobox protein 6 [*Lhx-6*; see reviews (Bandler et al., 2017; Hu et al., 2017; Christodoulou et al., 2022; see Figure 2)].

The distal-less (*Dlx*) homeobox genes *Dlx1/2* and *Dlx5/6* are at the core of the genetic cascade controlling prenatal and postnatal IN development (Wang et al., 2010; Le et al., 2017; Pla et al., 2018). In *Dlx1/2* knockout mice, which die at birth, cINs fail to migrate out of the ganglionic eminences, resulting in a reduction of IN numbers in the cortex and hippocampus (Anderson et al., 1997). These migratory deficits were rescued upon overexpression of *Arx* or by decreasing the levels of *Gsh1*, suggesting that these downstream transcription factors are necessary for mediating *Dlx*-dependent regulation of IN migration (Colasante et al., 2008; Wang et al., 2013).

Moreover, *Dlx1/2* promotes the subpallial expression of the *Sip1* transcription factor (McKinsey et al., 2013). Notably, the deletion of *Sip1* from MGE-derived INs severely comprises their migration and maturation (van den Berghe et al., 2013). This is largely due to an upregulation of the guidance receptor Unc5b in *Sip* knockout INs, which misguides migrating INs towards ventral regions away from the cortex. Thus, downregulating Unc5b rescues the cIN migratory deficit in *Sip1* mutants (van den Berghe et al., 2013), suggesting that *Sip1* acts as a critical regulator of cIN migration by controlling Unc5b expression in a cell-autonomous manner (van den Berghe et al., 2013).

Upstream of *Dlx1/2* is the Achaete-scute family bHLH transcription factor (*Ascl1*) and Forkhead box G1 transcription factor (*Foxg1*; Poitras et al., 2007; Yang et al., 2017). *In utero* electroporation of both *Ascl1* and *Dlx2* in the dorsal telencephalon of mice promotes tangential migration along the SVZ/VZ and IZ. Further, knockdown of *Dlx2* and overexpression of *Ascl1* leads to a reduction in the number of INs migrating through the SVZ/VZ, but increases the number of INs migrating through the IZ (Liu et al., 2017). Moreover, chromatin immunoprecipitation assays confirmed that EphB2 receptor, which binds to the repulsive molecule EphrinA5, is a direct downstream target of *Ascl1*. Disruption of EphB2/EphrinA5 signaling alters tangential migration as INs fail to confine to the DMS (Liu et al., 2017). These results indicate that *Ascl1* promotes tangential migration in two distinct ways: through the induction of *Dlx2* expression and in a *Dlx2*-independent fashion through the induction of *Ephb2* expression.

Foxg1, encoding a transcription factor associated with autism, Rett syndrome, epilepsy and intellectual disability (Seltzer et al., 2014; Wong et al., 2019; Miyoshi et al., 2021), acts upstream of *Dlx1/2* and *Ascl1* to regulate their expression levels and control IN migration (Yang et al., 2017). Indeed, conditional deletion of *Foxg1* in the SVZ and mantle zone of the MGE at E13.5 impairs the formation of tangential migratory streams. At E18.5, both MGE- and CGE-derived INs fail to reach the cortex and abnormally accumulate in the subpallium. Loss of *Foxg1* in migrating INs led to morphological defects (shorter neurites and decreased branching). Additionally, several receptors required for proper guidance of migrating INs, such as *Robo1, EphA4* and *Cxcr4/7*, were significantly downregulated in absence of *Foxg1* (Yang et al., 2017).

Nkx2-1, expressed in the MGE and POA, maintains regional identity by repressing other transcription factors in adjacent embryonic regions and initiates, through a permissive chromatin state, the expression in SVZ and mantle zone progenitors of transcription factors which regulate MGE-derived lineages (Sandberg et al., 2016). A direct downstream target of *Nkx2-1* is *Lhx6* (Liodis et al., 2007), whose expression starts around E11.5 and persists during IN migration and maturation, suggesting that it plays roles beyond IN specification. *Lhx6* null mutant display significant delays in

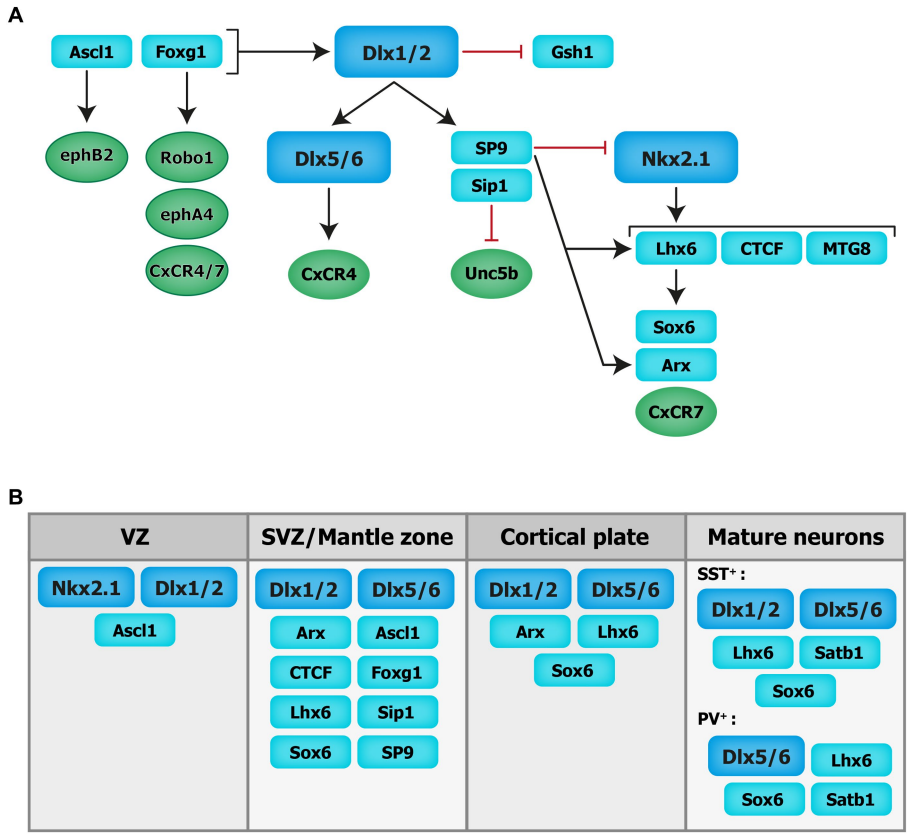

FIGURE 2
Transcriptional regulation of cortical interneuron migration. Schematics of the molecular cascade that regulates cIN migration. Several transcription factors contribute to the regulation of cIN migration, in part by controlling the expression of key guidance receptors (in circles). VZ: ventricular zone. SVZ: subventricular zone.

MGE-derived cIN migration resulting in severe reductions and abnormal positioning of somatostatin- and parvalbumin-expressing INs in superficial and deep cortical layers in the post-natal cortex (Liodis et al., 2007). Similar phenotypes were seen when the Sry-related HMG box transcription factor *Sox6*, acting downstream of *Lhx6*, was conditionally ablated from MGE cells (Batista-Brito et al., 2009). However, in *Lhx6* null mutants, transduction of mutant MGE cells with viruses expressing *Sox6* did not rescue the cellular and laminar phenotypes of these mice, suggesting that other molecular mechanisms are at play (Vogt et al., 2014). Notably, chromatin immunoprecipitation experiments revealed that *Lhx6* directly binds enhancers near the Aristaless-related homeobox transcription factor (*Arx*) and *CXCR7* gene locus, therefore promoting their expression. Interestingly, transduction of *Lhx6* mutant MGE cells with viruses expressing *Arx* or *CXCR7* rescues the expression of somatostatin and parvalbumin and the laminar distribution of cINs, respectively, suggesting that *Arx* activity is important for IN differentiation while *CXCR7* plays a key role in laminar allocation, in addition to its roles in tangential and radial migration (discussed above; Vogt et al., 2014).

Myeloid translocation gene 8 (MTG8) is a non-DNA binding transcriptional regulator expressed in the SVZ of the MGE, CGE and LGE at an early embryonic stage (E11.5), with progressive broader expression in the cortical plate and PC progenitors (E16.5; Asgarian et al., 2022). During early embryonic stages MTG8 interacts with *Lhx6* in MGE-derived cIN to specifically promote somatostatin- NPY-expressing cINs cell-fate before the onset of migration (Asgarian et al., 2022). Other regulators of *Lhx6* expression, acting upstream in the molecular cascade, include the zinc-finger CCCTC-binding factor (CTCF), acting as a regulator of chromatin organization (Merkenschlager and Nora, 2016). Recently, *de novo* mutations in the *CTCF* gene were associated with ASD, microcephaly, schizophrenia, and intellectual disability (Gregor et al., 2013; Iossifov et al., 2014; Juraeva et al., 2014; Bastaki et al., 2017). Conditional inactivation of *Ctcf* in early neural progenitors reduces the expression of *Lhx6* and a few of its downstream effectors, including *Sst* and *Cxcr4*, while *Nkx2-1* transcript levels remain unchanged. This reduction in *Lhx6* transcripts is associated with a delay in tangential migration prenatally (possibly due to the loss of Cxcr4) as well as a significant reduction in the number of somatostatin- and parvalbumin-expressing INs in the postnatal cortex along with lamination defects (Elbert et al., 2019). Notably, the re-expression of *Lhx6* in CTCF-null MGE cells rescues the number of somatostatin-expressing INs but not parvalbumin-expressing INs (Elbert et al., 2019). Further, recent transcriptomics data have shown zinc-finger transcription factor *Sp9*, expressed in the ganglionic eminences (Zhang et al., 2016b), as an upstream regulator of the transcription factors *Lhx6*, *Nkx2-1*, *Arx* and *Zeb2*. In mice, the conditional loss of *Sp9* in MGE-derived INs leads to disorganized migratory streams, with more cells in the DMS vs. the SMS and an abnormal increase in the ratio of somatostatin- vs.

parvalbumin-expressing cells. At the molecular level, *Lhx6*, *CXCR7* and *Arx* transcripts levels are significantly reduced in the mutant mouse compared to controls at different developmental timepoints (E12.5, E13.5, and E15.5; Liu et al., 2019). Interestingly, *Sp8* is significantly upregulated in the MGE of *Sp9* mutant mice, offering some degree of functional compensation, whereas the combined deletion of *Sp8* and *Sp9* results in greater defects in MGE-derived cINs numbers and distribution (Tao et al., 2019).

4.2. Cytoskeletal reorganization during migration

From a cellular point of view, cINs migration is a cyclic process comprising three stages during which the morphology of cINs dynamically changes to allow saltatory movement. During the first step, cINs elongate their leading process and extend several branches to sense the surrounding environment through filopodia and lamellipodia. Once a branch stabilizes in a specific direction, a swelling containing the centrosome and Golgi apparatus advances toward the leading process. The second step involves nucleokinesis, which consists of a fast anterograde nuclear translocation into the swelling. Lastly, in most cases, cINs retract their trailing process (Bellion et al., 2005; Lepiemme et al., 2020). Each step is controlled by the rearrangements of the cytoskeleton in response to extracellular and intracellular signals. The cytoskeleton is mainly composed of two major components: actin filaments (F-actin) and microtubules (MT). F-actin results from the polymerization of small globular proteins called g-actin. F-actin is highly dynamic and continuously assembles and disassembles, preferentially at the barbed (+) end (Lehtimäki et al., 2017).

Among the proteins that regulate actin filaments, we find the non-muscle myosin II that forms actomyosin networks. During migration, INs are pulled forward by contractile forces generated by the actomyosin network (Bellion et al., 2005; Martini et al., 2009; Martini and Valdeolmillos, 2010). Multiple factors acting on the actomyosin network in migrating cINs have been described. Elongator is a protein complex composed of six subunits including the Elp1 scaffold subunits and the Elp3 enzymatic core (Li et al., 2001; Winkler et al., 2001). Elongator is implicated in several processes such as the control of mRNA translation efficiency (Nedialkova and Leidel, 2015) and paternal genome demethylation (Okada et al., 2010). Pathogenic variants in Elongator subunits have been associated with moderate to severe neurodevelopmental disorders (Toral-Lopez et al., 2020; Duan et al., 2021; Kojic et al., 2021; Gaik et al., 2022; Kojic et al., 2023). Elongator promotes cIN tangential migration during corticogenesis by regulating nucleokinesis and the dynamics of leading process branching (Tielens et al., 2016). In the normal state, non-phosphorylated (active) cofilin induces a depolymerization of actin filaments into globular actin. A balance between the phosphorylated (inactive) and non-phosphorylated (active) form is typically maintained. Cofilin, together with Myosin II activated by the phosphorylation of the myosin light chain (MLC), regulates the nucleokinesis and branching of cINs leading process. However, the conditional deletion of the *Elp3* subunit in newborn cINs reduces cofilin phosphorylation and increases MLC phosphorylation in the soma and growth cone of migrating cINs, resulting in altered actin cytoskeletal reorganization and reduced actomyosin contractility, impairing nucleokinesis and branching (Tielens et al., 2016).

MT, the second component of the cytoskeleton, are composed of β-tubulin and α-tubulin, located, respectively, at their plus and minus ends (Janke and Magiera, 2020). The centrosome acts as a major assembly points for MT, with assembly and disassembly occurring at MT plus ends (Garcin and Straube, 2019). MT dynamics are crucial to all neuronal development steps including migration (Kuijpers and Hoogenraad, 2011). During cIN migration, MT form a cage-like structure around the nucleus that facilitates nuclear translocation (Godin et al., 2012). MT are also required for the extension of the leading process (Godin et al., 2012). Several microtubule-associated proteins (MAPs), including the doublecortin (DCX) and Lissencephaly-1 (Lis-1) proteins, participate in the organization and function of MT and are key regulators of pyramidal cell radial migration. Their loss results in brain malformations known as lissencephaly, characterized by altered lamination and gyration of the neocortex, resulting in developmental delay, intellectual disability and sometimes epilepsy (Matsumoto et al., 2001; Reiner and Sapir, 2013). Both DCX and Lis-1 have been shown to play critical roles in cIN migration, likely contributing to the global clinical manifestations of these disorders. DCX stabilizes and bundles MT within the leading process and regulates the interaction between MT and actin. Accordingly, cINs lacking DCX display MT instability that results in excessively branched leading processes (Lysko et al., 2014). Lis-1 regulates dynein, a cytoplasmic motor protein implicated in the transport of vesicles towards the minus ends of MT (Roberts et al., 2013). Loss of *Lis-1* in cINs alters their tangential migration (McManus et al., 2004). $p27^{kip1}$ is another MAP implicated in the coordination of both MT network and actomyosin contractility. The conditional deletion of $p27^{kip1}$ impacts cIN migration through an overactivation of myosin II (Godin et al., 2012).

MT are subject to several posttranslational modifications that regulate their biological functions, including during cell migration (van Dijk et al., 2008; Creppe et al., 2009; Hahn et al., 2013; Tanco et al., 2013). Polyglutamylation adds a peptide chain of glutamate to the target protein by enzymes known as polyglutamylases (ex: TTLL1; Janke et al., 2005; Janke and Kneussel, 2010). As this modification is reversible, the glutamate chain is removed by a cytosolic carboxypeptidase (CCP) enzyme (van Dijk et al., 2007). Pathogenic variants of *CCP1* have been associated with developmental delay (Firth et al., 2009). *Ccp1* mRNA is highly expressed in the developing subpallium (Silva et al., 2018). The conditional loss of *Ccp1* from post-mitotic cINs impairs cytoskeletal remodelling and actomyosin dynamics, leading to a decrease in the amplitude of nucleokinesis and reduced pause duration, without affecting speed (Silva et al., 2018). Notably, whereas actomyosin contraction is usually polarised at the rear of the nucleus to push the nucleus forward, *Ccp1* cKO cINs display a failure of actomyosin polarization resulting in a switch from saltatory migration to a "treadmill-like motion" (Silva et al., 2018). This abnormal phenotype is due to the aberrant enzymatic regulation of MLCK in the absence of CCP1 by mechanisms dependent of its function on MT depolyglutamylation (Silva et al., 2018). Interestingly, this reduction of pause duration dominates the phenotype, such that the loss of *Ccp1* ultimately leads to a net increase of cIN invasion in the cortical plate while also enhancing the proliferation of intermediate progenitors giving rise to upper layer projection neurons in the dorsal

pallium, ultimately altering the balance of excitation and inhibition in the cortex (Silva et al., 2018).

Microtubule-actin cross-linking factor 1 (MACF1) is a member of the ubiquitous plakin family of cytoskeletal linker proteins (Suozzi et al., 2012). By coordinating the organization of both MT and actin filaments, MACF1 is implicated in many cellular processes such as axonal growth and cell migration (Goryunov and Liem, 2016). Recently, *MACF1* mutations have been associated with lissencephaly, severe intellectual disability and epilepsy (Dobyns et al., 2018). MACF1 has several isoforms, some of which are highly expressed in the brain. At E12.5, MACF1 is enriched in the ventricular zone, whereas it becomes mostly expressed in the cortical plate at E15.5 (Ka et al., 2017). MACF1 regulates the migration of pyramidal cells (Ka et al., 2014) and cINs (Ka et al., 2017). Indeed, the conditional deletion of *Macf1* in mouse cINs progenitors leads to a reduction and an abnormal distribution of cINs, which accumulate in the intermediate zone during migration and largely fail to populate the dorsal pallium (neocortex and hippocampus), due to a premature switch from tangential to radial migration (Ka et al., 2017). The loss of *Macf1* also impacts the morphology of cINs by promoting aberrantly complex neurites, which are shorter and more branched, largely due to a defect in MT stabilization in *Macf1* knockout INs (Ka et al., 2017). This reflects the role of MACF1 as an actin-MT linker that coordinates MT dynamics (Kodama et al., 2003).

4.3. Rho GTPases and their regulators and effectors involved in cIN migration

Genomic studies in patients with autism spectrum disorders, epilepsy or intellectual deficiency have identified pathogenic mutations in multiple Rho GTPases-encoding genes, but also in various Rho GTPase regulators and effectors (*RAC1, CDC42, PAK*; Michaud et al., 2014; Tastet et al., 2019; Barbosa et al., 2020; Halder et al., 2022; Dobrigna et al., 2023). Deregulation of Rho GTPases thus seems to be a shared molecular mechanism between several monogenic forms of neurodevelopmental disorders. Interestingly, recent evidence suggests that Rho GTPases, as well as their regulators and effectors, play essential roles during IN migration by coordinating cytoskeletal dynamics. Small GTPases of the Rho classes (Rho GTPases) are highly conserved signal transducing enzymes that switch between GTP and GDP-bound states in response to stimuli (Bos et al., 2007). The GTPases are highly regulated by the Rho guanine nucleotide exchange factors (RhoGEFs) and Rho GTPase activating proteins (RhoGAP). RhoGEF activate GTPases by promoting the switch from an inactive GDP-bound conformation to an active GTP-bound conformation, while RhoGAP downregulate GTPase signaling by enhancing the intrinsic GTP hydrolysis activity of GTPases (Rossman et al., 2005; Hodge and Ridley, 2016). Rho GTPases integrate different extracellular and intracellular cues to reorganize the actin cytoskeleton and are critical in several cellular aspects of brain development, including neuronal migration, axonal guidance, and synaptic plasticity (Govek et al., 2005; Ba et al., 2013; Cannet et al., 2014; Herring and Nicoll, 2016; Gentile et al., 2022; see Figure 3).

The best-characterized members of the Rho family in the brain are Rac1 (ras related C3 botulinum toxin substrate 1), RhoA (ras homologous member A) and Cdc42 (cell division cycle 42; Azzarelli et al., 2014) Rac1 plays a key role in the formation of lamellipodia and membrane protrusion at the front of migrating cells (Bisaria et al., 2020). RhoA regulates cell retraction during migration and induces the formation of actin stress fiber via Rho-associated protein kinase (Riedl et al., 2008 that phosphorylates myosin light chain (MLC) required for myosin II activation. RhoA also activates diaphanous-related formin mDia1/2 to control cell retraction (Watanabe et al., 1999). Cdc42 induces the formation of filopodia in the leading edge through the activation of mDia2 (Peng et al., 2003). Cdc42 and Rac1 activate Wasp/WAVE complex, which in turn activates Arp2/3 protein (Takenawa and Suetsugu, 2007). During leading process branching, Arp2/3 together with contractin allow the formation of new membrane protrusions by the assembly of F-actin. These protrusions are then stabilized by MT and support the formation of new branches (Martini et al., 2009; Spillane et al., 2011; Lysko et al., 2014; Peyre et al., 2015). In addition, Wasp/WAVE complex also activate ROCK which phosphorylates profilin, a key protein implicated in F-actin nucleation in filopodia (Witke, 2004).

The ablation of *Rac1* in MGE-derived IN progenitors at E13.5 induces a reduction of cIN progenitor proliferation due to defects in actin cytoskeleton organization, which prolongs the cell cycles, resulting in a 50% reduction of cINs in the postnatal cortex. Proliferating MGE-derived IN progenitors aggregate in their place of birth and fail to properly exit the cell cycle (Vidaki et al., 2012). Notably, *Rac1* is required for the transition from the G1 phase to S phase in MGE-derived progenitors as it regulates cyclin D protein expression and the phosphorylation of the retinoblastoma protein (Vidaki et al., 2012). The deletion of *Rac1* in postmitotic MGE-derived INs does not impact the final number of cINs in the mature cortex, suggesting that *Rac1* acts at the proliferation stage, but not during migration (Vidaki et al., 2012).

Rac3 (Ras-related C3 botulinum toxin substrate 3), another member of the Rac family, is highly expressed in the developing nervous system (Katayama et al., 2013). *Rac1* and *Rac3* double mutants display a significant loss of parvalbumin-expressing INs in the cortex and hippocampus, leading to reduced spontaneous inhibitory currents (IPSCs) and epilepsy (Tivodar et al., 2014; Vaghi et al., 2014). In *Rac1/Rac3* double-mutant mice, the usual migratory streams fail to form adequately and cINs travel shorter distances, while cell cycle exit is also delayed, resulting in a mixed proliferation and migration phenotype, ultimately decreasing the density of cINs in the mature cortex (Tivodar et al., 2014). In addition, a morphological defect is also observed, in part due to a decrease in acetylated tubulin, a post-translational modification involved in the stabilization of MT, resulting in a shorter but more branched leading process, together with impaired lamellipodia formation and reduced growth cone development (Tivodar et al., 2014). These morphological phenotypes likely contribute to the slowing of tangential migration. In addition, the dynamics of tangential migration is grossly impaired in dual *Rac1*/*Rac3* mutants, with decreased velocity, frequency and amplitude of translocations, as well as duration of migratory cycles and of leading process swelling (Kounoupa et al., 2023). The centrosome and Golgi complex are closer together and to the cell body in *Rac1*/*Rac3* mutants, correlating with shorter translocations (Kounoupa et al., 2023). Actomyosin contractility is also impaired, given reduced phosphorylation of MLC (pMLC) and decreased RhoA levels, leading to slower nuclear translocation in dual *Rac1*/*Rac3* mutants cINs (Kounoupa et al., 2023). This is partly due to MT instability as

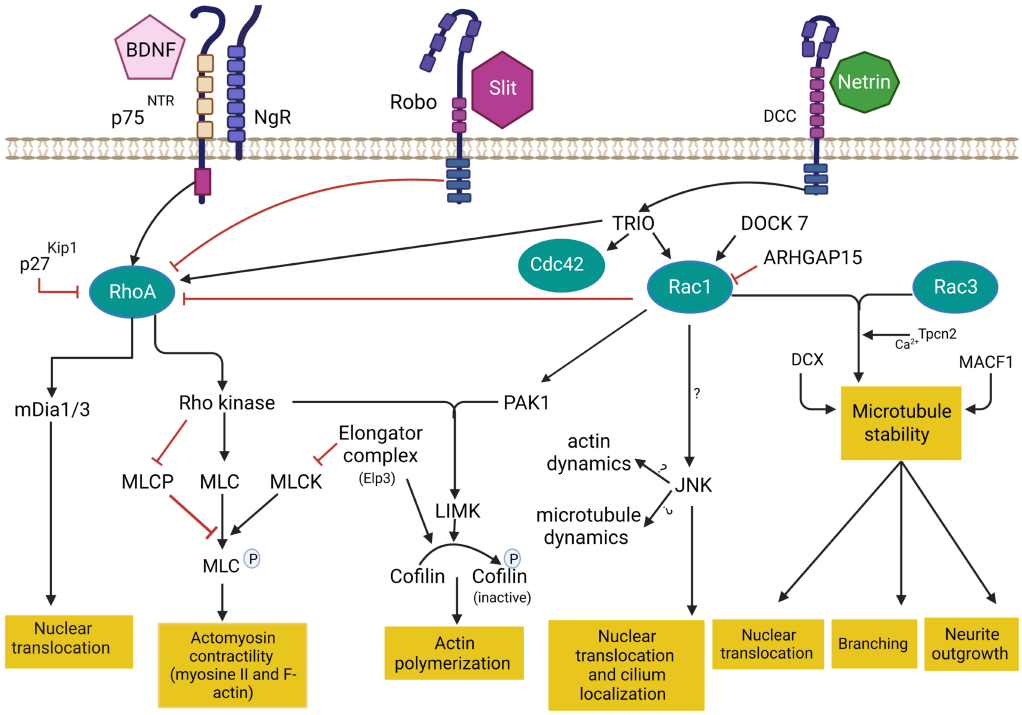

FIGURE 3
Cytoskeleton remodeling during IN migration is regulated by extrinsic cues and intracellular molecular cascades that relay these signals to the cytoskeleton. Various intracellular molecular cascades signal from the cell membrane to the actin and microtubule cytoskeleton. Rho GTPases are key regulators of these processes. This figure was created using BioRender.com. DCC: deleted in colorectal cancer. BDNF: Brain-derived neurotrophic factor. NgR: Nogo-66-Receptor. $P75^{NTR}$: The neurotrophin receptor p75. Rac1: ras related C3 botulinum toxin substrate 1. RhoA: ras homologous member A. Cdc42: cell division cycle 42. mDia: diaphanous-related formin. MLC: myosin light chain. MLCP: myosin light chain phosphorylated. MLCK: myosin light chain kinase. PAK1: p21-activated serine/threonine kinase 1. LIMK: lim domains kinase. JNK: c-jun N-terminal kinase. DCX: doublecortin protein. MACF1: Microtubule-actin cross-linking factor 1. Tpcn1: two pore segment channel 2. DOCK7: (Dedicator of cytokenesis7). ARHGAP15: GTPase-activating protein 15. TRIO: Trio Rho Guanine Nucleotide Exchange Factor.

described before with the deletion of *Dcx* or nocodazole treatment impacting nuclear translocation (Tanaka et al., 2004; Baudoin et al., 2007). Finally, axonal outgrowth is defective in dual *Rac1*/*Rac3* mutants (Kounoupa et al., 2023), a process dependent on the activation of Rac1 by the EB1 (end binding1)-induced TRIO-NAV1 (neuron navigator 1) complex at the end of growing MT (van Haren et al., 2014). Notably, RNA sequencing in Rac1/Rac3 double mutant INs showed reduced expression of the two pore segment channel 2 (*Tpcn2*), a voltage-gated ion channel that mediates calcium release from lysosome-related stores upon activation by nicotinic acid adenine dinucleotide phosphate (NAADP) and c-jun N-terminal kinase (JNK; Calcraft et al., 2009; Jha et al., 2014; Lee et al., 2016; Ogunbayo et al., 2018). TPC2 is implicated in metastatic cell migration (Nguyen et al., 2017; Kounoupa et al., 2023). The pharmacological inhibition of *Tpcn2* by NAADP antagonists (trans-Ned19) in MGE-derived cINs induces a reduction in axon length and surface, as well as reduced nuclear translocation frequency, impairing migration (Kounoupa et al., 2023). Altogether, *Rac1* and *Rac3,* together with *Tpnc2* play key synergistic roles in cIN development by regulating their cell cycle progression as well as their migration and morphology.

The p21-activated serine/threonine kinase (PAKs) family, that includes 6 members (Pak1-6), are downstream effectors of Cdc42 and Rac1 (Hofmann et al., 2004). During neuronal migration, PAK1 activation induces the phosphorylation of LIM Kinase (LMK), which phosphorylates cofilin and tubulin cofactor B, both required for the reorganization of actin filaments and MT polymerization (Arber et al., 1998; Vadlamudi et al., 2005; Chen et al., 2011). PAK also phosphorylates myosin II by inhibiting MLC kinase (MLCK; Sanders et al., 1999). Mutations in PAK1 are associated with developmental delay, macrocephaly, and seizures (Cartwright et al., 2017; Hertecant et al., 2017; Harms et al., 2018; Horn et al., 2019). In cINs, *Dlx1/2* represses PAK3 to promote cell migration, while it is activated once cINs reach their final position when it regulates dendritic growth and postsynaptic differentiation (Cobos et al., 2007; Dai et al., 2014).

JNK (c-Jun N-terminal kinase) also acts downstream of Rac1/Pak1 signaling pathway (Kawauchi et al., 2003). JNK belongs to the mitogen-activated protein kinase (MAPK) superfamily, known to regulate several important physiological processes including cortical development and neuronal migration (Davis, 2000; Zhang et al., 2016a). JNK is regulated by the thousand and one amino-acid kinase 2 (TAOK2), involved in 16p11.2 duplication syndrome and schizophrenia (Davis, 2000; Coffey, 2014; Richter et al., 2019). The deregulation of the TAOK-JNK pathway impacts cINs by accelerating their development, as reported in 16p11.2 duplication mouse models (Willis et al., 2021). Notably, parvalbumin is downregulated in this model, an adaptative mechanism that aims to re-establish a proper balance between excitation and inhibition (Willis et al., 2021). The conditional deletion of *Jnk 1* in *Jnk 2* knockout mice impairs the morphology and tangential migration of cINs, with blurred migratory streams (MZ and SVZ/IZ), resulting in misplaced cINs (Myers et al.,

2014). This occurs due to an early switch from tangential to radial migration and premature entry in the cortical plate (Myers et al., 2020). Further, the loss of *Jnk* in cINs leads to alterations of leading process branching dynamics through reduced growth cone splitting and shortening of the swelling extension in the leading process, together with an aberrant localization of the centrosome and primary cilium to the trailing process (Smith et al., 2020b). Overall, JNK plays critical roles in regulating cIN migration, downstream of Rac1/Pak1.

By contrast, RhoA is typically inhibited in migratory cells, including in cINs (Pacary et al., 2011). In this context, the deletion of *RhoA* in migrating cINs, after they exit the VZ, does not significantly impair their migration (Katayama et al., 2013). However, RhoA activation seems required during neurogenesis as its deletion in cINs progenitors in the VZ results in significant reduction of final cINs numbers (Katayama et al., 2013). Similarly, the deletion of Cdc42 in MGE-derived cINs does not alter their migration but it is required in the VZ for their normal differentiation (Katayama et al., 2013). Nonetheless, more studies are needed to understand the role of RhoA and Cdc42 in cIN migration since local activation of RhoA may be required to regulate actomyosin contractility and actin polymerisation that promote neurite and membrane retraction during migration (Etienne-Manneville and Hall, 2002; Ito et al., 2014). Notably, mDia, a downstream effector of RhoA, is actively involved in the nucleation and polymerization of actin (Higashida et al., 2004). Thus, deletion of *mDia1* and *mDia3* in cIN neuroblasts in mice results in striking impairments of tangential migration, with reduced distance between the centrosome and the cell body and decreased movements of the swelling in the leading process before nuclear translocations. On the other hand, *mDia* deficiency does not impair the radial migration of excitatory neurons (Shinohara et al., 2012), suggesting it plays a more selective role in tangentially migrating cINs.

Upstream regulators of RhoGTPases also play a critical role in neuronal development, including cIN migration. TRIO (Trio Rho Guanine Nucleotide Exchange Factor) is a dual GEF protein known to activate Rac1 and RhoA (Bellanger et al., 1998; Chhatriwala et al., 2007). *TRIO* mutations have been identified in patients with autism spectrum disorder, microcephaly, and intellectual disability, with or without epilepsy (Michaud et al., 2014; Sadybekov et al., 2017). While most described mutations are loss-of-function variants that selectively impact the GEFD1 domain, thus preventing Rac1 activation, some variants appear to induce a gain-of-function and enhanced Rac1 activation (Pengelly et al., 2016), and selected few variants involve the GEFD2-RhoA activating domain (Barbosa et al., 2020; Bonnet et al., 2023). Studies demonstrated that TRIO is critical for multiple aspects of brain development. In mice, complete knock-out of the gene is embryonically lethal while surviving mice show an aberrant cellular organization of the hippocampus and the olfactory bulb (O'Brien et al., 2000). Further, the deletion of *Trio* specifically in the nervous system induces a reduced brain size (microcephaly), with abnormal brain and hippocampal morphology, defective cerebellar granule cell migration and spatial learning deficits (Peng et al., 2010; Zong et al., 2015). At the cellular level, TRIO is known to regulate cell migration, axonal guidance, and dendritic development of pyramidal cells, mostly through its function as a Rac1 activator (Schmidt and Debant, 2014; Ba et al., 2016; Wei et al., 2022). However, recent evidence suggests that TRIO also plays critical roles in cIN migration and that targeted deletion in post-mitotic cINs suffices to induce autism-like behavior and epilepsy (Sun et al., 2021). Recent data indicate that the conditional deletion of *Trio* specifically in cINs alters the migration dynamics and morphogenesis of tangentially migrating cINs, with increased neurite complexity and reduced responses to guidance cues, resulting in impaired cortical inhibition and autism-like behaviors in mice (Sun et al., 2021).

DOCK7 (dedicator of cytokinesis 7), a member of the DOCK180 family, is another Rac GEF implicated in the differentiation and genesis of both pyramidal cells and cINs (Yang et al., 2012). Mutations in *DOCK7* are associated with epileptic encephalopathy and intellectual disability (Perrault et al., 2014). Recently, the loss of DOCK7 has been shown to disrupt the movement of the centrosome leading to slower tangential migration of the olfactory bulb INs (Nakamuta et al., 2017).

ARHGAP15 (GTPase-activating protein 15) is a GAP protein known to downregulate Rac1 and switch off the downstream signaling pathway (Seoh et al., 2003; Radu et al., 2013). Overexpression of this protein results in cell retraction due to the increase of stress fiber formation (Costa et al., 2011). *De novo* mutations in *ARHGAP15* have been associated with autism spectrum disorders and intellectual disability (O'Roak et al., 2011; Mulatinho et al., 2012). The targeted deletion of *Arhgap15* in cINs in conditional knock-out mice increases their susceptibility to seizures after treatment with pro-epileptic drug pilocarpine (Liaci et al., 2022). Furthermore, this deletion disrupts cIN migration, morphology and laminar distribution (Liaci et al., 2022). This suggests a critical role of these various GAPs in the development of inhibition by negative regulation of Rac1.

5. Clinical prospect of MGE-cIN progenitor transplants as cell-based therapies for neurodevelopmental disorders and epilepsy

Given the growing evidence that various monogenic forms of neurodevelopmental disorders, such as autism spectrum disorders, childhood epilepsy, severe developmental epileptic encephalopathies, intellectual disabilities and schizophrenia, may reflect primary disorders of cIN development, migration or function, the development of cell-based therapies involving the transplantation of cIN progenitors has gained momentum. Indeed, current pharmaceutical approaches are mostly symptomatic and have limited benefits, emphasizing the importance of exploring new therapeutic avenues. Thus, cell-based therapies, for instance transplantation of MGE-derived progenitors, have been extensively studied in animal models of genetic interneuronopathies, autism spectrum disorders and epilepsy (Anderson and Baraban, 2012; Hunt et al., 2013; Li et al., 2022; Righes Marafiga and Baraban, 2023). MGE-derived progenitors transplanted in neonatal and juvenile mice brains maintain an ability to migrate, disperse and integrate in the host circuits, often spanning great distances from the injection site, an interesting property when targeting multifocal complex circuits disorders (Alvarez-Dolado et al., 2006; Tong et al., 2014; Upadhya et al., 2019). Upon integration in the cortical circuitry, transplanted MGE-derived cINs selectively enhance local inhibition in a functionally relevant fashion (Wichterle et al., 1999; Alvarez-Dolado et al., 2006). Transplanted MGE-derived progenitors survive up to 1 year after transplantation, even in unfavorable environments (Zipancic et al., 2010; Tong et al., 2014; Lu et al., 2020). MGE-cell transplants have been shown to rescue behavioural deficits

and prevent or reduce seizures in multiple mice models of autism-spectrum disorders or epilepsy (Alvarez-Dolado et al., 2006; Hunt et al., 2013). Additionally, MGE transplants are considered relatively safe, having minimal proliferative potential, compared to induced pluripotent stem cells (PSCs), which are prone to result in tumor formation (De la Cruz et al., 2011). Although ethical issues preclude the use of human-derived MGE cells, human-induced PSCs (hiPSCs) derived "MGE" cells are actively being considered, as are other mammalian sources of MGE cells (Righes Marafiga and Baraban, 2023).

6. Conclusion

Decades after the initial discovery of the origin of cortical interneurons in the subpallium of rodents, remarkable research efforts have helped advance our understanding of interneuron migration, focusing on identifying environmental guidance molecules as well as intrinsic factors implicated in this process. Yet, many questions remain open, awaiting further investigation. In particular, further studies are needed to clarify the intracellular signaling pathways activated by guidance cues in migrating interneurons as well as their impact on cytoskeletal remodeling. In addition, although some mechanisms of radial migration are shared between cINs and pyramidal neurons, such as gap-junction mediated attachment to an intact radial glia scaffold (Poluch and Juliano, 2007; Yokota et al., 2007; Elias et al., 2010), other mechanisms are specific for cIN radial migration, including attachment to vessels (Léger et al., 2020), inputs from thalamocortical projections (Zechel et al., 2016) and pyramidal cells (as detailed above). These cell-type specific molecular mechanisms guiding cIN radial migration must be further clarified. Further, the mechanisms underlying CGE- and POA-derived IN migration remain less well studied and must be further explored.

Most of our current knowledge about IN development and migration arises from animal studies using rodent models given limitations using human tissue. Although many aspects of cIN development, transcriptomic identity and migration are maintained across species (Ma et al., 2013; Krienen et al., 2020), some differences have been highlighted and it remains unclear to what extend evolution has altered these processes. For instance, the human brain has a much longer and complex developmental period compared to rodents. Primate studies found that cINs originate from both the ventral and dorsal forebrain, while only ventrally-derived cINs have been described in rodents (Jakovcevski et al., 2011; Hansen et al., 2013; Ma et al., 2013). How do these primate-specific cINs develop and migrate? What are the mechanisms involved? The development of hiPSCs and more recently forebrain assembloids (Birey et al., 2022) has opened new research avenues that will enable us to answer these questions as well as to further study human pathologies involving cIN development, so-called interneuronopathies, both from a mechanistic and translational point of view, using patient-derived INs. Nonetheless, testing these novel mechanisms and future therapies in whole animal models remains essential to provide adequate pre-clinical data for future therapeutic trials.

Author contributions

IT: Conceptualization, Writing – original draft. AT: Conceptualization, Writing – original draft. ÉC: Writing – original draft. ER: Conceptualization, Funding acquisition, Resources, Writing – original draft.

Funding

The author(s) declare financial support was received for the research, authorship, and/or publication of this article. This work was supported by the Canadian Institutes for Health Research (CIHR award #: PJT-173284). EC receives a Guy-Geoffroy Scholarship from the CHU Ste-Justine and PREMIER Scholarship from Montreal University. ER holds the Canadian Research Chair on the Neurobiology of Epilepsy and is a FRQS senior research scholar.

Acknowledgments

We are grateful to Marisol Lavertu-Jolin who provided critical input on the manuscript.

Conflict of interest

The authors declare that the research was conducted in the absence of any commercial or financial relationships that could be construed as a potential conflict of interest.

Publisher's note

References

Alvarez-Dolado, M., Calcagnotto, M. E., Karkar, K. M., Southwell, D. G., Jones-Davis, D. M., Estrada, R. C., et al. (2006). Cortical inhibition modified by embryonic neural precursors grafted into the postnatal brain. *J. Neurosci.* 26, 7380–7389. doi: 10.1523/JNEUROSCI.1540-06.2006

Amegandjin, C. A., Choudhury, M., Jadhav, V., Carrico, J. N., Quintal, A., Berryer, M., et al. (2021). Sensitive period for rescuing parvalbumin interneurons connectivity and social behavior deficits caused by TSC1 loss. *Nat. Commun.* 12:3653. doi: 10.1038/s41467-021-23939-7

Anderson, S. A., and Baraban, S. C. (2012). "Cell therapy using GABAergic neural progenitors" in *Jasper's basic mechanisms of the epilepsies. 4th edn*. J. L. Noebels, M. Avoli, M. A. Rogawski, R. W. Olsen and A. V. Delgado-Escueta. (Bethesda MD, US: National Center for Biotechnology Information).

Anderson, S. A., Eisenstat, D. D., Shi, L., and Rubenstein, J. L. (1997). Interneuron migration from basal forebrain to neocortex: dependence on Dlx genes. *Science* 278, 474–476. doi: 10.1126/science.278.5337.474

Andrews, W., Liapi, A., Plachez, C., Camurri, L., Zhang, J., Mori, S., et al. (2006). Robo1 regulates the development of major axon tracts and interneuron migration in the forebrain. *Development* 133, 2243–2252. doi: 10.1242/dev.02379

Antypa, M., Faux, C., Eichele, G., Parnavelas, J. G., and Andrews, W. D. (2011). Differential gene expression in migratory streams of cortical interneurons. *Eur. J. Neurosci.* 34, 1584–1594. doi: 10.1111/j.1460-9568.2011.07896.x

Arber, S., Barbayannis, F. A., Hanser, H., Schneider, C., Stanyon, C. A., Bernard, O., et al. (1998). Regulation of actin dynamics through phosphorylation of cofilin by LIM-kinase. *Nature* 393, 805–809. doi: 10.1038/31729

Arnold, S. A., and Brekken, R. A. (2009). SPARC: a matricellular regulator of tumorigenesis. *J. Cell Commun. Signal.* 3, 255–273. doi: 10.1007/s12079-009-0072-4

Asgarian, Z., Oliveira, M. G., Stryjewska, A., Maragkos, I., Rubin, A. N., Magno, L., et al. (2022). MTG8 interacts with LHX6 to specify cortical interneuron subtype identity. *Nat. Commun.* 13:5217. doi: 10.1038/s41467-022-32898-6

Avila, A., Vidal, P. M., Dear, T. N., Harvey, R. J., Rigo, J. M., and Nguyen, L. (2013). Glycine receptor alpha2 subunit activation promotes cortical interneuron migration. *Cell Rep.* 4, 738–750. doi: 10.1016/j.celrep.2013.07.016

Azzarelli, R., Kerloch, T., and Pacary, E. (2014). Regulation of cerebral cortex development by rho GTPases: insights from in vivo studies. *Front. Cell. Neurosci.* 8:445. doi: 10.3389/fncel.2014.00445

Ba, W., van der Raadt, J., and Nadif Kasri, N. (2013). Rho GTPase signaling at the synapse: implications for intellectual disability. *Exp. Cell Res.* 319, 2368–2374. doi: 10.1016/j.yexcr.2013.05.033

Ba, W., Yan, Y., Reijnders, M. R., Schuurs-Hoeijmakers, J. H., Feenstra, I., Bongers, E. M., et al. (2016). TRIO loss of function is associated with mild intellectual disability and affects dendritic branching and synapse function. *Hum. Mol. Genet.* 25, 892–902. doi: 10.1093/hmg/ddv618

Bandler, R. C., Mayer, C., and Fishell, G. (2017). Cortical interneuron specification: the juncture of genes, time and geometry. *Curr. Opin. Neurobiol.* 42, 17–24. doi: 10.1016/j.conb.2016.10.003

Barber, M., Andrews, W. D., Memi, F., Gardener, P., Ciantar, D., Tata, M., et al. (2018). Vascular-derived Vegfa promotes cortical interneuron migration and proximity to the vasculature in the developing forebrain. *Cereb. Cortex* 28, 2577–2593. doi: 10.1093/cercor/bhy082

Barbosa, S., Greville-Heygate, S., Bonnet, M., Godwin, A., Fagotto-Kaufmann, C., Kajava, A. V., et al. (2020). Opposite modulation of RAC1 by mutations in TRIO is associated with distinct, domain-specific neurodevelopmental disorders. *Am. J. Hum. Genet.* 106, 338–355. doi: 10.1016/j.ajhg.2020.01.018

Bartolini, G., Sanchez-Alcaniz, J. A., Osorio, C., Valiente, M., Garcia-Frigola, C., and Marin, O. (2017). Neuregulin 3 mediates cortical Plate invasion and laminar allocation of GABAergic interneurons. *Cell Rep.* 18, 1157–1170. doi: 10.1016/j.celrep.2016.12.089

Bastaki, F., Nair, P., Mohamed, M., Malik, E. M., Helmi, M., al-Ali, M. T., et al. (2017). Identification of a novel CTCF mutation responsible for syndromic intellectual disability - a case report. *BMC Med. Genet.* 18:68. doi: 10.1186/s12881-017-0429-0

Batista-Brito, R., Rossignol, E., Hjerling-Leffler, J., Denaxa, M., Wegner, M., Lefebvre, V., et al. (2009). The cell-intrinsic requirement of Sox6 for cortical interneuron development. *Neuron* 63, 466–481. doi: 10.1016/j.neuron.2009.08.005

Baudoin, J.-P., Alvarez, C., Gaspar, P., and Métin, C. (2007). Nocodazole-induced changes in microtubule dynamics impair the morphology and directionality of migrating medial ganglionic Eminence cells. *Dev. Neurosci.* 30, 132–143. doi: 10.1159/000109858

Bellanger, J. M., Lazaro, J. B., Diriong, S., Fernandez, A., Lamb, N., and Debant, A. (1998). The two guanine nucleotide exchange factor domains of Trio link the Rac1 and the RhoA pathways in vivo. *Oncogene* 16, 147–152. doi: 10.1038/sj.onc.1201532

Bellion, A., Baudoin, J. P., Alvarez, C., Bornens, M., and Metin, C. (2005). Nucleokinesis in tangentially migrating neurons comprises two alternating phases: forward migration of the Golgi/centrosome associated with centrosome splitting and myosin contraction at the rear. *J. Neurosci.* 25, 5691–5699. doi: 10.1523/JNEUROSCI.1030-05.2005

Birey, F., Li, M. Y., Gordon, A., Thete, M. V., Valencia, A. M., Revah, O., et al. (2022). Dissecting the molecular basis of human interneuron migration in forebrain assembloids from Timothy syndrome. *Cell Stem Cell* 29, 248–264.e7. doi: 10.1016/j.stem.2021.11.011

Bisaria, A., Hayer, A., Garbett, D., Cohen, D., and Meyer, T. (2020). Membrane-proximal F-actin restricts local membrane protrusions and directs cell migration. *Science* 368, 1205–1210. doi: 10.1126/science.aay7794

Bonnet, M., Roche, F., Fagotto-Kaufmann, C., Gazdagh, G., Truong, I., Comunale, F., et al. (2023). Pathogenic TRIO variants associated with neurodevelopmental disorders perturb the molecular regulation of TRIO and axon pathfinding in vivo. *Mol. Psychiatry* 28, 1527–1544. doi: 10.1038/s41380-023-01963-x

Bortone, D., and Polleux, F. (2009). KCC2 expression promotes the termination of cortical interneuron migration in a voltage-sensitive calcium-dependent manner. *Neuron* 62, 53–71. doi: 10.1016/j.neuron.2009.01.034

Bos, J. L., Rehmann, H., and Wittinghofer, A. (2007). GEFs and GAPs: critical elements in the control of small G proteins. *Cells* 129, 865–877. doi: 10.1016/j.cell.2007.05.018

Cain, J. T., Berosik, M. A., Snyder, S. D., Crawford, N. F., Nour, S. I., Schaubhut, G. J., et al. (2014). Shifts in the vascular endothelial growth factor isoforms result in transcriptome changes correlated with early neural stem cell proliferation and differentiation in mouse forebrain. *Dev. Neurobiol.* 74, 63–81. doi: 10.1002/dneu.22130

Calcraft, P. J., Ruas, M., Pan, Z., Cheng, X., Arredouani, A., Hao, X., et al. (2009). NAADP mobilizes calcium from acidic organelles through two-pore channels. *Nature* 459, 596–600. doi: 10.1038/nature08030

Cannet, A., Schmidt, S., Delaval, B., and Debant, A. (2014). Identification of a mitotic Rac-GEF, Trio, that counteracts MgcRacGAP function during cytokinesis. *Mol. Biol. Cell* 25, 4063–4071. doi: 10.1091/mbc.E14-06-1153

Cartwright, A., Smith, K., and Balasubramanian, M. (2017). Short case report: Xq23 deletion involving PAK3 as a novel cause of developmental delay in a 6-year-old boy. *Clin. Dysmorphol.* 26, 38–40. doi: 10.1097/mcd.0000000000000154

Chen, Q., Deister, C. A., Gao, X., Guo, B. L., Lynn-Jones, T., Chen, N. Y., et al. (2020). Dysfunction of cortical GABAergic neurons leads to sensory hyper-reactivity in a Shank3 mouse model of ASD. *Nat. Neurosci.* 23:520. doi: 10.1038/s41593-020-0598-6

Chen, S. Y., Huang, P. H., and Cheng, H. J. (2011). Disrupted-in-schizophrenia 1-mediated axon guidance involves TRIO-RAC-PAK small GTPase pathway signaling. *Proc. Natl. Acad. Sci. U. S. A.* 108, 5861–5866. doi: 10.1073/pnas.1018128108

Chhatriwala, M. K., Betts, L., Worthylake, D. K., and Sondek, J. (2007). The DH and PH domains of Trio coordinately engage rho GTPases for their efficient activation. *J. Mol. Biol.* 368, 1307–1320. doi: 10.1016/j.jmb.2007.02.060

Christodoulou, O., Maragkos, I., Antonakou, V., and Denaxa, M. (2022). The development of MGE-derived cortical interneurons: An Lhx6 tale. *Int. J. Dev. Biol.* 66, 43–49. doi: 10.1387/ijdb.210185md

Cobos, I., Borello, U., and Rubenstein, J. L. (2007). Dlx transcription factors promote migration through repression of axon and dendrite growth. *Neuron* 54, 873–888. doi: 10.1016/j.neuron.2007.05.024

Coffey, E. T. (2014). Nuclear and cytosolic JNK signalling in neurons. *Nat. Rev. Neurosci.* 15, 285–299. doi: 10.1038/nrn3729

Colasante, G., Collombat, P., Raimondi, V., Bonanomi, D., Ferrai, C., Maira, M., et al. (2008). Arx is a direct target of Dlx2 and thereby contributes to the tangential migration of GABAergic interneurons. *J. Neurosci.* 28, 10674–10686. doi: 10.1523/Jneurosci.1283-08.2008

Costa, C., Germena, G., Martin-Conte, E. L., Molineris, I., Bosco, E., Marengo, S., et al. (2011). The RacGAP ArhGAP15 is a master negative regulator of neutrophil functions. *Blood* 118, 1099–1108. doi: 10.1182/blood-2010-12-324756

Creppe, C., Malinouskaya, L., Volvert, M.-L., Gillard, M., Close, P., Malaise, O., et al. (2009). Elongator controls the migration and differentiation of cortical neurons through acetylation of α-tubulin. *Cells* 136, 551–564. doi: 10.1016/j.cell.2008.11.043

Cuzon Carlson, V. C., and Yeh, H. H. (2011). GABAA receptor subunit profiles of tangentially migrating neurons derived from the medial ganglionic eminence. *Cereb. Cortex* 21, 1792–1802. doi: 10.1093/cercor/bhq247

Dai, X., Iwasaki, H., Watanabe, M., and Okabe, S. (2014). Dlx1 transcription factor regulates dendritic growth and postsynaptic differentiation through inhibition of neuropilin-2 and PAK3 expression. *Eur. J. Neurosci.* 39, 531–547. doi: 10.1111/ejn.12413

Darland, D. C., Cain, J. T., Berosik, M. A., Saint-Geniez, M., Odens, P. W., Schaubhut, G. J., et al. (2011). Vascular endothelial growth factor (VEGF) isoform regulation of early forebrain development. *Dev. Biol.* 358, 9–22. doi: 10.1016/j.ydbio.2011.06.045

Davis, R. J. (2000). Signal transduction by the JNK group of MAP kinases. *Cells* 103, 239–252. doi: 10.1016/s0092-8674(00)00116-1

De la Cruz, E., Zhao, M., Guo, L., Ma, H., Anderson, S. A., and Schwartz, T. H. (2011). Interneuron progenitors attenuate the power of acute focal ictal discharges. *Neurotherapeutics* 8, 763–773. doi: 10.1007/s13311-011-0058-9

De Marco Garcia, N. V., Karayannis, T., and Fishell, G. (2011). Neuronal activity is required for the development of specific cortical interneuron subtypes. *Nature* 472, 351–355. doi: 10.1038/nature09865

De Marco Garcia, N. V., Priya, R., Tuncdemir, S. N., Fishell, G., and Karayannis, T. (2015). Sensory inputs control the integration of neurogliaform interneurons into cortical circuits. *Nat. Neurosci.* 18, 393–401. doi: 10.1038/nn.3946

del Pino, I., García-Frigola, C., Dehorter, N., Brotons-Mas, J. R., Alvarez-Salvado, E., Martínez de Lagrán, M., et al. (2013). Erbb4 deletion from fast-spiking interneurons causes schizophrenia-like phenotypes. *Neuron* 79, 1152–1168. doi: 10.1016/j.neuron.2013.07.010

del Toro, D., Carrasquero-Ordaz, M. A., Chu, A., Ruff, T., Shahin, M., Jackson, V. A., et al. (2020). Structural basis of Teneurin-Latrophilin interaction in repulsive guidance of migrating neurons. *Cells* 180, 323–339.e19. doi: 10.1016/j.cell.2019.12.014

del Toro, D., Ruff, T., Cederfjäll, E., Villalba, A., Seyit-Bremer, G., Borrell, V., et al. (2017). Regulation of cerebral cortex folding by controlling neuronal migration via FLRT adhesion molecules. *Cells* 169, 621–635.e16. doi: 10.1016/j.cell.2017.04.012

Dobrigna, M., Poëa-Guyon, S., Rousseau, V., Vincent, A., Toutain, A., and Barnier, J. V. (2023). The molecular basis of p21-activated kinase-associated neurodevelopmental disorders: from genotype to phenotype. *Front. Neurosci.* 17:1123784. doi: 10.3389/fnins.2023.1123784

Dobyns, W. B., Aldinger, K. A., Ishak, G. E., Mirzaa, G. M., Timms, A. E., Grout, M. E., et al. (2018). MACF1 mutations encoding highly conserved zinc-binding residues of the

GAR domain cause defects in neuronal migration and axon guidance. *Am. J. Hum. Genet.* 103, 1009–1021. doi: 10.1016/j.ajhg.2018.10.019

Duan, Y., Leng, X., Liu, C., Qi, X., Zhang, L., Tan, W., et al. (2021). The correlation of ELP4-PAX6 with Rolandic spike sources in idiopathic Rolandic epilepsy syndromes. *Front. Neurol.* 12:643964. doi: 10.3389/fneur.2021.643964

Elbert, A., Vogt, D., Watson, A., Levy, M., Jiang, Y., Brûlé, E., et al. (2019). CTCF governs the identity and migration of MGE-derived cortical interneurons. *J. Neurosci.* 39, 177–192. doi: 10.1523/Jneurosci.3496-17.2018

Elias, L. A., Turmaine, M., Parnavelas, J. G., and Kriegstein, A. R. (2010). Connexin 43 mediates the tangential to radial migratory switch in ventrally derived cortical interneurons. *J. Neurosci.* 30, 7072–7077. doi: 10.1523/JNEUROSCI.5728-09.2010

Etienne-Manneville, S., and Hall, A. (2002). Rho GTPases in cell biology. *Nature* 420, 629–635. doi: 10.1038/nature01148

Falls, D. L. (2003). Neuregulins: functions, forms, and signaling strategies. *Exp. Cell Res.* 284, 14–30. doi: 10.1016/s0014-4827(02)00102-7

Ferguson, B., Glick, C., and Huguenard, J. R. (2023). Prefrontal PV interneurons facilitate attention and are linked to attentional dysfunction in a mouse model of absence epilepsy. *eLife* 12:e78349. doi: 10.7554/eLife.78349

Firth, H. V., Richards, S. M., Bevan, A. P., Clayton, S., Corpas, M., Rajan, D., et al. (2009). DECIPHER: database of chromosomal imbalance and phenotype in humans using Ensembl resources. *Am. J. Hum. Genet.* 84, 524–533. doi: 10.1016/j.ajhg.2009.03.010

Flames, N., Long, J. E., Garratt, A. N., Fischer, T. M., Gassmann, M., Birchmeier, C., et al. (2004). Short- and long-range attraction of cortical GABAergic interneurons by neuregulin-1. *Neuron* 44, 251–261. doi: 10.1016/j.neuron.2004.09.028

Fleitas, C., Marfull-Oromí, P., Chauhan, D., del Toro, D., Peguera, B., Zammou, B., et al. (2021). FLRT2 and FLRT3 cooperate in maintaining the tangential migratory streams of cortical interneurons during development. *J. Neurosci.* 41, 7350–7362. doi: 10.1523/JNEUROSCI.0380-20.2021

Fogarty, M., Grist, M., Gelman, D., Marín, O., Pachnis, V., and Kessaris, N. (2007). Spatial genetic patterning of the embryonic neuroepithelium generates GABAergic interneuron diversity in the adult cortex. *J. Neurosci.* 27, 10935–10946. doi: 10.1523/jneurosci.1629-07.2007

Gaik, M., Kojic, M., Stegeman, M. R., Öncü-Öner, T., Kościelniak, A., Jones, A., et al. (2022). Functional divergence of the two Elongator subcomplexes during neurodevelopment. *EMBO Mol. Med.* 14:e15608. doi: 10.15252/emmm.202115608

Garcin, C., and Straube, A. (2019). Microtubules in cell migration. *Essays Biochem.* 63, 509–520. doi: 10.1042/ebc20190016

Genestine, M., Ambriz, D., Crabtree, G. W., Dummer, P., Molotkova, A., Quintero, M., et al. (2021). Vascular-derived SPARC and SerpinE1 regulate interneuron tangential migration and accelerate functional maturation of human stem cell-derived interneurons. *eLife* 10:e56063. doi: 10.7554/eLife.56063

Gentile, J. E., Carrizales, M. G., and Koleske, A. J. (2022). Control of synapse structure and function by actin and its regulators. *Cells* 11:603. doi: 10.3390/cells11040603

Gertler, T. S., Cherian, S., DeKeyser, J. M., Kearney, J. A., and George, A. L. Jr. (2022). K(Na)1.1 gain-of-function preferentially dampens excitability of murine parvalbumin-positive interneurons. *Neurobiol. Dis.* 168:105713. doi: 10.1016/j.nbd.2022.105713

Godin, J. D., Thomas, N., Laguesse, S., Malinouskaya, L., Close, P., Malaise, O., et al. (2012). p27Kip1 is a microtubule-associated protein that promotes microtubule polymerization during neuron migration. *Dev. Cell* 23, 729–744. doi: 10.1016/j.devcel.2012.08.006

Gongidi, V., Ring, C., Moody, M., Brekken, R., Sage, E. H., Rakic, P., et al. (2004). SPARC-like 1 regulates the terminal phase of radial glia-guided migration in the cerebral cortex. *Neuron* 41, 57–69. doi: 10.1016/s0896-6273(03)00818-3

Goryunov, D., and Liem, R. K. H. (2016). Microtubule-actin cross-linking factor 1: domains, interaction partners, and tissue-specific functions *Meth. Enzymol.* 569, 331–353. doi: 10.1016/bs.mie.2015.05.022

Govek, E. E., Newey, S. E., and Van Aelst, L. (2005). The role of the rho GTPases in neuronal development. *Genes Dev.* 19, 1–49. doi: 10.1101/gad.1256405

Gregor, A., Oti, M., Kouwenhoven, E. N., Hoyer, J., Sticht, H., Ekici, A. B., et al. (2013). De novo mutations in the genome organizer CTCF cause intellectual disability. *Am. J. Hum. Genet.* 93, 124–131. doi: 10.1016/j.ajhg.2013.05.007

Hahn, M. A., Qiu, R., Wu, X., Li, A. X., Zhang, H., Wang, J., et al. (2013). Dynamics of 5-hydroxymethylcytosine and chromatin marks in mammalian neurogenesis. *Cell Rep.* 3, 291–300. doi: 10.1016/j.celrep.2013.01.011

Haigh, J. J., Morelli, P. I., Gerhardt, H., Haigh, K., Tsien, J., Damert, A., et al. (2003). Cortical and retinal defects caused by dosage-dependent reductions in VEGF-A paracrine signaling. *Dev. Biol.* 262, 225–241. doi: 10.1016/s0012-1606(03)00356-7

Halder, S. K., Rafi, M. O., Shahriar, E. B., Albogami, S., el-Shehawi, A. M., Daullah, S., et al. (2022). Identification of the most damaging nsSNPs in the human CFL1 gene and their functional and structural impacts on cofilin-1 protein. *Gene* 819:146206. doi: 10.1016/j.gene.2022.146206

Hansen, D. V., Lui, J. H., Flandin, P., Yoshikawa, K., Rubenstein, J. L., Alvarez-Buylla, A., et al. (2013). Non-epithelial stem cells and cortical interneuron production in the human ganglionic eminences. *Nat. Neurosci.* 16, 1576–1587. doi: 10.1038/nn.3541

Harms, F. L., Kloth, K., Bley, A., Denecke, J., Santer, R., Lessel, D., et al. (2018). Activating mutations in PAK1, encoding p21-activated kinase 1, cause a neurodevelopmental disorder. *Am. J. Hum. Genet.* 103, 579–591. doi: 10.1016/j.ajhg.2018.09.005

Hayes, L. N., Shevelkin, A., Zeledon, M., Steel, G., Chen, P. L., Obie, C., et al. (2016). Neuregulin 3 knockout mice exhibit behaviors consistent with psychotic disorders. *Mol. Neuropsychiatry* 2, 79–87. doi: 10.1159/000445836

Hernández-Miranda, L. R., Cariboni, A., Faux, C., Ruhrberg, C., Cho, J. H., Cloutier, J. F., et al. (2011). Robo1 regulates semaphorin signaling to guide the migration of cortical interneurons through the ventral forebrain. *J. Neurosci.* 31, 6174–6187. doi: 10.1523/JNEUROSCI.5464-10.2011

Herring, B. E., and Nicoll, R. A. (2016). Kalirin and Trio proteins serve critical roles in excitatory synaptic transmission and LTP. *Proc. Natl. Acad. Sci. U. S. A.* 113, 2264–2269. doi: 10.1073/pnas.1600179113

Hertecant, J., Komara, M., Nagi, A., al-Zaabi, O., Fathallah, W., Cui, H., et al. (2017). A de novo mutation in the X-linked PAK3 gene is the underlying cause of intellectual disability and macrocephaly in monozygotic twins. *Eur. J. Med. Genet.* 60, 212–216. doi: 10.1016/j.ejmg.2017.01.004

Higashida, C., Miyoshi, T., Fujita, A., Oceguera-Yanez, F., Monypenny, J., Andou, Y., et al. (2004). Actin polymerization-driven molecular movement of mDia1 in living cells. *Science* 303, 2007–2010. doi: 10.1126/science.1093923

Hodge, R. G., and Ridley, A. J. (2016). Regulating rho GTPases and their regulators. *Nat. Rev. Mol. Cell Biol.* 17, 496–510. doi: 10.1038/nrm.2016.67

Hofmann, C., Shepelev, M., and Chernoff, J. (2004). The genetics of Pak. *J. Cell Sci.* 117, 4343–4354. doi: 10.1242/jcs.01392

Hogan, K. A., Ambler, C. A., Chapman, D. L., and Bautch, V. L. (2004). The neural tube patterns vessels developmentally using the VEGF signaling pathway. *Development* 131, 1503–1513. doi: 10.1242/dev.01039

Horn, S., Au, M., Basel-Salmon, L., Bayrak-Toydemir, P., Chapin, A., Cohen, L., et al. (2019). De novo variants in PAK1 lead to intellectual disability with macrocephaly and seizures. *Brain* 142, 3351–3359. doi: 10.1093/brain/awz264%JBrain

Hu, J. S., Vogt, D., Sandberg, M., and Rubenstein, J. L. (2017). Cortical interneuron development: a tale of time and space. *Development* 144, 3867–3878. doi: 10.1242/dev.132852

Hunt, R. F., Girskis, K. M., Rubenstein, J. L., Alvarez-Buylla, A., and Baraban, S. C. (2013). GABA progenitors grafted into the adult epileptic brain control seizures and abnormal behavior. *Nat. Neurosci.* 16, 692–697. doi: 10.1038/nn.3392

Hupe, M., Li, M. X., Kneitz, S., Davydova, D., Yokota, C., Kele, J., et al. (2017). Gene expression profiles of brain endothelial cells during embryonic development at bulk and single-cell levels. *Sci. Signal.* 10:eaag2476. doi: 10.1126/scisignal.aag2476

Hyder, Z., van Paesschen, W., Sabir, A., Sansbury, F. H., Burke, K. B., Khan, N., et al. (2021). ERBB4 exonic deletions on chromosome 2q34 in patients with intellectual disability or epilepsy. *Eur. J. Hum. Genet.* 29, 1377–1383. doi: 10.1038/s41431-021-00815-y

Inamura, N., Kimura, T., Tada, S., Kurahashi, T., Yanagida, M., Yanagawa, Y., et al. (2012). Intrinsic and extrinsic mechanisms control the termination of cortical interneuron migration. *J. Neurosci.* 32, 6032–6042. doi: 10.1523/JNEUROSCI.3446-11.2012

Iossifov, I., O'Roak, B. J., Sanders, S. J., Ronemus, M., Krumm, N., Levy, D., et al. (2014). The contribution of de novo coding mutations to autism spectrum disorder. *Nature* 515, 216–221. doi: 10.1038/nature13908

Ito, H., Morishita, R., Tabata, H., and Nagata, K. (2014). Roles of rho small GTPases in the tangentially migrating neurons. *Histol. Histopathol.* 29, 871–879. doi: 10.14670/hh-29.871

Jakovcevski, I., Mayer, N., and Zecevic, N. (2011). Multiple origins of human neocortical interneurons are supported by distinct expression of transcription factors. *Cereb. Cortex* 21, 1771–1782. doi: 10.1093/cercor/bhq245

Janke, C., and Kneussel, M. (2010). Tubulin post-translational modifications: encoding functions on the neuronal microtubule cytoskeleton. *Trends Neurosci.* 33, 362–372. doi: 10.1016/j.tins.2010.05.001

Janke, C., and Magiera, M. M. (2020). The tubulin code and its role in controlling microtubule properties and functions. *Nat. Rev. Mol. Cell Biol.* 21, 307–326. doi: 10.1038/s41580-020-0214-3

Janke, C., Rogowski, K., Wloga, D., Regnard, C., Kajava, A. V., Strub, J. M., et al. (2005). Tubulin polyglutamylase enzymes are members of the TTL domain protein family. *Science* 308, 1758–1762. doi: 10.1126/science.1113010

Jha, A., Ahuja, M., Patel, S., Brailoiu, E., and Muallem, S. (2014). Convergent regulation of the lysosomal two-pore channel-2 by Mg^{2+}, NAADP, $PI(3,5)P_2$ and multiple protein kinases. *EMBO J.* 33, 501–511. doi: 10.1002/embj.201387035

Jiang, X., Lachance, M., and Rossignol, E. (2016). Involvement of cortical fast-spiking parvalbumin-positive basket cells in epilepsy. *Prog. Brain Res.* 226, 81–126. doi: 10.1016/bs.pbr.2016.04.012

Jiang, X., Lupien-Meilleur, A., Tazerart, S., Lachance, M., Samarova, E., Araya, R., et al. (2018). Remodeled cortical inhibition prevents motor seizures in generalized epilepsy. *Ann. Neurol.* 84, 436–451. doi: 10.1002/ana.25301

Juarez, P., and Martinez Cerdeno, V. (2022). Parvalbumin and parvalbumin chandelier interneurons in autism and other psychiatric disorders. *Front. Psychol.* 13:913550. doi: 10.3389/fpsyt.2022.913550

Juraeva, D., Haenisch, B., Zapatka, M., Frank, J., GROUP Investigators, PSYCH-GEMS SCZ working groupWitt, S. H., et al. (2014). Integrated pathway-based approach identifies association between genomic regions at CTCF and CACNB2 and schizophrenia. *PLoS Genet.* 10:e1004345. doi: 10.1371/journal.pgen.1004345

Ka, M., Jung, E. M., Mueller, U., and Kim, W. Y. (2014). MACF1 regulates the migration of pyramidal neurons via microtubule dynamics and GSK-3 signaling. *Dev. Biol.* 395, 4–18. doi: 10.1016/j.ydbio.2014.09.009

Ka, M., Moffat, J. J., and Kim, W. Y. (2017). MACF1 controls migration and positioning of cortical GABAergic interneurons in mice. *Cereb. Cortex* 27, 5525–5538. doi: 10.1093/cercor/bhw319

Karakatsani, A., Shah, B., and Ruiz de Almodovar, C. (2019). Blood vessels as regulators of neural stem cell properties. *Front. Mol. Neurosci.* 12:85. doi: 10.3389/fnmol.2019.00085

Katayama, K.-I., Imai, F., Campbell, K., Lang, R. A., Zheng, Y., and Yoshida, Y. (2013). RhoA and Cdc42 are required in pre-migratory progenitors of the medial ganglionic eminence ventricular zone for proper cortical interneuron migration. *Development* 140, 3139–3145. doi: 10.1242/dev.092585

Kawauchi, T., Chihama, K., Nabeshima, Y.-I., and Hoshino, M. (2003). The in vivo roles of STEF/Tiam1, Rac1 and JNK in cortical neuronal migration. *EMBO J.* 22, 4190–4201. doi: 10.1093/emboj/cdg413

Kessaris, N., Fogarty, M., Iannarelli, P., Grist, M., Wegner, M., and Richardson, W. D. (2006). Competing waves of oligodendrocytes in the forebrain and postnatal elimination of an embryonic lineage. *Nat. Neurosci.* 9, 173–179. doi: 10.1038/nn1620

Kodama, A., Karakesisoglou, I., Wong, E., Vaezi, A., and Fuchs, E. (2003). ACF7: An essential integrator of microtubule dynamics. *Cells* 115, 343–354. doi: 10.1016/S0092-8674(03)00813-4

Kojic, M., Abbassi, N. E. H., Lin, T.-Y., Jones, A., Wakeling, E. L., Clement, E., et al. (2023). A novel ELP1 mutation impairs the function of the Elongator complex and causes a severe neurodevelopmental phenotype. *J. Hum. Genet.* 68, 445–453. doi: 10.1038/s10038-023-01135-3

Kojic, M., Gawda, T., Gaik, M., Begg, A., Salerno-Kochan, A., Kurniawan, N. D., et al. (2021). Elp2 mutations perturb the epitranscriptome and lead to a complex neurodevelopmental phenotype. *Nat. Commun.* 12:2678. doi: 10.1038/s41467-021-22888-5

Kounoupa, Z., Tivodar, S., Theodorakis, K., Kyriakis, D., Denaxa, M., and Karagogeos, D. (2023). Rac1 and Rac3 GTPases and TPC2 are required for axonal outgrowth and migration of cortical interneurons. *J. Cell Sci.* 136:jcs260373. doi: 10.1242/jcs.260373

Krienen, F. M., Goldman, M., Zhang, Q., del Rosario, R., Florio, M., Machold, R., et al. (2020). Innovations present in the primate interneuron repertoire. *Nature* 586, 262–269. doi: 10.1038/s41586-020-2781-z

Kuijpers, M., and Hoogenraad, C. C. (2011). Centrosomes, microtubules and neuronal development. *Mol. Cell. Neurosci.* 48, 349–358. doi: 10.1016/j.mcn.2011.05.004

Lavdas, A. A., Grigoriou, M., Pachnis, V., and Parnavelas, J. G. (1999). The medial ganglionic eminence gives rise to a population of early neurons in the developing cerebral cortex. *J. Neurosci.* 19, 7881–7888. doi: 10.1523/JNEUROSCI.19-18-07881.1999

le, T. N., Zhou, Q. P., Cobos, I., Zhang, S. Z., Zagozewski, J., Japoni, S., et al. (2017). GABAergic interneuron differentiation in the basal forebrain is mediated through direct regulation of glutamic acid decarboxylase isoforms by dlx Homeobox transcription factors. *J. Neurosci.* 37, 8816–8829. doi: 10.1523/Jneurosci.2125-16.2017

Lee, S., Hjerling-Leffler, J., Zagha, E., Fishell, G., and Rudy, B. (2010). The largest group of superficial neocortical GABAergic interneurons expresses ionotropic serotonin receptors. *J. Neurosci.* 30, 16796–16808. doi: 10.1523/JNEUROSCI.1869-10.2010

Lee, C. S., Tong, B. C., Cheng, C. W., Hung, H. C., and Cheung, K. H. (2016). Characterization of two-Pore Channel 2 by nuclear membrane electrophysiology. *Sci. Rep.* 6:20282. doi: 10.1038/srep20282

Lee, S. M., Yeh, P. W. L., and Yeh, H. H. (2022). L-type calcium channels contribute to ethanol-induced aberrant tangential migration of primordial cortical GABAergic interneurons in the embryonic medial prefrontal cortex. *eNeuro* 9:0359–21.2021. doi: 10.1523/ENEURO.0359-21.2021

Léger, C., Dupré, N., Aligny, C., Bénard, M., Lebon, A., Henry, V., et al. (2020). Glutamate controls vessel-associated migration of GABA interneurons from the pial migratory route via NMDA receptors and endothelial protease activation. *Cell. Mol. Life Sci.* 77, 1959–1986. doi: 10.1007/s00018-019-03248-5

Legros, H., Launay, S., Roussel, B. D., Marcou-Labarre, A., Calbo, S., Catteau, J., et al. (2009). Newborn- and adult-derived brain microvascular endothelial cells show age-related differences in phenotype and glutamate-evoked protease release. *J. Cereb. Blood Flow Metab.* 29, 1146–1158. doi: 10.1038/jcbfm.2009.39

Lehtimäki, J., Hakala, M., and Lappalainen, P. (2017). Actin filament structures in migrating cells. *Handb. Exp. Pharmacol.* 235, 123–152. doi: 10.1007/164_2016_28

Lepiemme, F., Silva, G. C., and Nguyen, L. (2020). "Chapter 16 - mechanisms of tangential migration of interneurons in the developing forebrain" in *Cellular migration and formation of axons and dendrites*. eds. J. Rubenstein, P. Rakic, B. Chen, K. Y. Kwan, A. Kolodkin and E. Anton. *Second* ed (Academic Press), 345–363.

Lepiemme, F., Stoufflet, J., Javier-Torrent, M., Mazzucchelli, G., Silva, C. G., and Nguyen, L. (2022). Oligodendrocyte precursors guide interneuron migration by unidirectional contact repulsion. *Science* 376:eabn6204. doi: 10.1126/science.abn6204

Leyva-Díaz, E., del Toro, D., Menal, M. J., Cambray, S., Susín, R., Tessier-Lavigne, M., et al. (2014). FLRT3 is a Robo1-interacting protein that determines Netrin-1 attraction in developing axons. *Curr. Biol.* 24, 494–508. doi: 10.1016/j.cub.2014.01.042

Li, G., Adesnik, H., Li, J., Long, J., Nicoll, R. A., Rubenstein, J. L., et al. (2008). Regional distribution of cortical interneurons and development of inhibitory tone are regulated by Cxcl12/Cxcr4 signaling. *J. Neurosci.* 28, 1085–1098. doi: 10.1523/JNEUROSCI.4602-07.2008

Li, S., Haigh, K., Haigh, J. J., and Vasudevan, A. (2013). Endothelial VEGF sculpts cortical cytoarchitecture. *J. Neurosci.* 33, 14809–14815. doi: 10.1523/JNEUROSCI.1368-13.2013

Li, S., Kumar, T. P., Joshee, S., Kirschstein, T., Subburaju, S., Khalili, J. S., et al. (2018). Endothelial cell-derived GABA signaling modulates neuronal migration and postnatal behavior. *Cell Res.* 28, 221–248. doi: 10.1038/cr.2017.135

Li, K. X., Lu, Y. M., Xu, Z. H., Zhang, J., Zhu, J. M., Zhang, J. M., et al. (2011). Neuregulin 1 regulates excitability of fast-spiking neurons through Kv1.1 and acts in epilepsy. *Nat. Neurosci.* 15, 267–273. doi: 10.1038/nn.3006

Li, Y., Takagi, Y., Jiang, Y., Tokunaga, M., Erdjument-Bromage, H., Tempst, P., et al. (2001). A multiprotein complex that interacts with RNA polymerase II elongator. *J. Biol. Chem.* 276, 29628–29631. doi: 10.1074/jbc.C100274200

Li, D., Wu, Q., and Han, X. (2022). Application of medial ganglionic Eminence cell transplantation in diseases associated with interneuron disorders. *Front. Cell. Neurosci.* 16:939294. doi: 10.3389/fncel.2022.939294

Liaci, C., Camera, M., Zamboni, V., Sarò, G., Ammoni, A., Parmigiani, E., et al. (2022). Loss of ARHGAP15 affects the directional control of migrating interneurons in the embryonic cortex and increases susceptibility to epilepsy. *Front. Cell Dev. Biol.* 10:875468. doi: 10.3389/fcell.2022.875468

Lim, L., Pakan, J. M. P., Selten, M. M., Marques-Smith, A., Llorca, A., Bae, S. E., et al. (2018). Optimization of interneuron function by direct coupling of cell migration and axonal targeting. *Nat. Neurosci.* 21, 920–931. doi: 10.1038/s41593-018-0162-9

Limoni, G., Murthy, S., Jabaudon, D., Dayer, A., and Niquille, M. (2021). PlexinA4-Semaphorin3A-mediated crosstalk between main cortical interneuron classes is required for superficial interneuron lamination. *Cell Rep.* 34:108644. doi: 10.1016/j.celrep.2020.108644

Liodis, P., Denaxa, M., Grigoriou, M., Akufo-Addo, C., Yanagawa, Y., and Pachnis, V. (2007). Lhx6 activity is required for the normal migration and specification of cortical interneuron subtypes. *J. Neurosci.* 27, 3078–3089. doi: 10.1523/Jneurosci.3055-06.2007

Liu, Y. H., Tsai, J. W., Chen, J. L., Yang, W. S., Chang, P. C., Cheng, P. L., et al. (2017). Ascl1 promotes tangential migration and confines migratory routes by induction of Ephb2 in the telencephalon. *Mech. Dev.* 145, S126–S127. doi: 10.1016/j.mod.2017.04.347

Liu, Z. D., Zhang, Z. Z., Lindtner, S., Li, Z. M. Y., Xu, Z. J., Wei, S., et al. (2019). Sp9 regulates medial ganglionic Eminence-derived cortical interneuron development. *Cereb. Cortex* 29, 2653–2667. doi: 10.1093/cercor/bhy133

Lodato, S., Rouaux, C., Quast, K. B., Jantrachotechatchawan, C., Studer, M., Hensch, T. K., et al. (2011). Excitatory projection neuron subtypes control the distribution of local inhibitory interneurons in the cerebral cortex. *Neuron* 69, 763–779. doi: 10.1016/j.neuron.2011.01.015

Lopez-Bendito, G., Lujan, R., Shigemoto, R., Ganter, P., Paulsen, O., and Molnar, Z. (2003). Blockade of GABA(B) receptors alters the tangential migration of cortical neurons. *Cereb. Cortex* 13, 932–942. doi: 10.1093/cercor/13.9.932

López-Bendito, G., Sánchez-Alcañiz, J. A., Pla, R., Borrell, V., Picó, E., Valdeolmillos, M., et al. (2008). Chemokine signaling controls intracortical migration and final distribution of GABAergic interneurons. *J. Neurosci.* 28, 1613–1624. doi: 10.1523/JNEUROSCI.4651-07.2008

Lu, M. H., Zhao, X. Y., Xu, D. E., Chen, J. B., Ji, W. L., Huang, Z. P., et al. (2020). Transplantation of GABAergic interneuron progenitor attenuates cognitive deficits of Alzheimer's disease model mice. *J. Alzheimers Dis.* 75, 245–260. doi: 10.3233/jad-200010

Luhmann, H. J., Fukuda, A., and Kilb, W. (2015). Control of cortical neuronal migration by glutamate and GABA. *Front. Cell. Neurosci.* 9:4. doi: 10.3389/fncel.2015.00004

Lupien-Meilleur, A., Jiang, X., Lachance, M., Taschereau-Dumouchel, V., Gagnon, L., Vanasse, C., et al. (2021). Reversing frontal disinhibition rescues behavioural deficits in models of CACNA1A-associated neurodevelopment disorders. *Mol. Psychiatry* 26, 7225–7246. doi: 10.1038/s41380-021-01175-1

Lysko, D. E., Putt, M., and Golden, J. A. (2011). SDF1 regulates leading process branching and speed of migrating interneurons. *J. Neurosci.* 31, 1739–1745. doi: 10.1523/JNEUROSCI.3118-10.2011

Lysko, D. E., Putt, M., and Golden, J. A. (2014). SDF1 reduces interneuron leading process branching through dual regulation of actin and microtubules. *J. Neurosci.* 34, 4941–4962. doi: 10.1523/JNEUROSCI.4351-12.2014

Ma, T., Wang, C., Wang, L., Zhou, X., Tian, M., Zhang, Q., et al. (2013). Subcortical origins of human and monkey neocortical interneurons. *Nat. Neurosci.* 16, 1588–1597. doi: 10.1038/nn.3536

Mahmood, N., Mihalcioiu, C., and Rabbani, S. A. (2018). Multifaceted role of the Urokinase-type plasminogen activator (uPA) and its receptor (uPAR): diagnostic, prognostic, and therapeutic applications. *Front. Oncol.* 8:24. doi: 10.3389/fonc.2018.00024

Marin, O. (2012). Interneuron dysfunction in psychiatric disorders. *Nat. Rev. Neurosci.* 13, 107–120. doi: 10.1038/nrn3155

Marin, O. (2013). Cellular and molecular mechanisms controlling the migration of neocortical interneurons. *Eur. J. Neurosci.* 38, 2019–2029. doi: 10.1111/ejn.12225

Marin, O., Plump, A. S., Flames, N., Sanchez-Camacho, C., Tessier-Lavigne, M., and Rubenstein, J. L. (2003). Directional guidance of interneuron migration to the cerebral cortex relies on subcortical Slit1/2-independent repulsion and cortical attraction. *Development* 130, 1889–1901. doi: 10.1242/dev.00417

Marin, O., and Rubenstein, J. L. (2001). A long, remarkable journey: tangential migration in the telencephalon. *Nat. Rev. Neurosci.* 2, 780–790. doi: 10.1038/35097509

Marin, O., Yaron, A., Bagri, A., Tessier-Lavigne, M., and Rubenstein, J. L. (2001). Sorting of striatal and cortical interneurons regulated by semaphorin-neuropilin interactions. *Science* 293, 872–875. doi: 10.1126/science.1061891

Martini, F. J., and Valdeolmillos, M. (2010). Actomyosin contraction at the cell rear drives nuclear translocation in migrating cortical interneurons. *J. Neurosci.* 30, 8660–8670. doi: 10.1523/jneurosci.1962-10.2010

Martini, F. J., Valiente, M., López Bendito, G., Szabó, G̈., Moya, F., Valdeolmillos, M., et al. (2009). Biased selection of leading process branches mediates chemotaxis during tangential neuronal migration. *Development* 136, 41–50. doi: 10.1242/dev.025502

Matsumoto, N., Leventer, R., Kuc, J., Mewborn, S., Dudlicek, L. L., Ramocki, M. B., et al. (2001). Mutation analysis of the DCX gene and genotype/phenotype correlation in subcortical band heterotopia. *Eur. J. Hum. Genet.* 9, 5–12. doi: 10.1038/sj.ejhg.5200548

McKinsey, G. L., Lindtner, S., Trzcinski, B., Visel, A., Pennacchio, L. A., Huylebroeck, D., et al. (2013). Dlx1&2-dependent expression of Zfhx1b (Sip1, Zeb2) regulates the fate switch between cortical and striatal interneurons. *Neuron* 77, 83–98. doi: 10.1016/j.neuron.2012.11.035

McManus, M. F., Nasrallah, I. M., Pancoast, M. M., Wynshaw-Boris, A., and Golden, J. A. (2004). Lis1 is necessary for Normal non-radial migration of inhibitory interneurons. *Am. J. Pathol.* 165, 775–784. doi: 10.1016/S0002-9440(10)63340-8

Meier, S., Strohmaier, J., Breuer, R., Mattheisen, M., Degenhardt, F., Mühleisen, T. W., et al. (2013). Neuregulin 3 is associated with attention deficits in schizophrenia and bipolar disorder. *Int. J. Neuropsychopharmacol.* 16, 549–556. doi: 10.1017/S1461145712000697

Merkenschlager, M., and Nora, E. P. (2016). CTCF and Cohesin in genome folding and transcriptional gene regulation. *Annu. Rev. Genomics Hum. Genet.* 17, 17–43. doi: 10.1146/annurev-genom-083115-022339

Michaud, J. L., Lachance, M., Hamdan, F. F., Carmant, L., Lortie, A., Diadori, P., et al. (2014). The genetic landscape of infantile spasms. *Hum. Mol. Genet.* 23, 4846–4858. doi: 10.1093/hmg/ddu199

Miyoshi, G., and Fishell, G. (2011). GABAergic interneuron lineages selectively sort into specific cortical layers during early postnatal development. *Cereb. Cortex* 21, 845–852. doi: 10.1093/cercor/bhq155

Miyoshi, G., Hjerling-Leffler, J., Karayannis, T., Sousa, V. H., Butt, S. J. B., Battiste, J., et al. (2010). Genetic fate mapping reveals that the caudal ganglionic Eminence produces a large and diverse population of superficial cortical interneurons. *Rapid Commun.* 30, 1582–1594. doi: 10.1523/JNEUROSCI.4515-09.2010

Miyoshi, G., Ueta, Y., Natsubori, A., Hiraga, K., Osaki, H., Yagasaki, Y., et al. (2021). FoxG1 regulates the formation of cortical GABAergic circuit during an early postnatal critical period resulting in autism spectrum disorder-like phenotypes. *Nat. Commun.* 12:3773. doi: 10.1038/s41467-021-23987-z

Miyoshi, G., Young, A., Petros, T., Karayannis, T., McKenzie Chang, M., Lavado, A., et al. (2015). Prox1 regulates the subtype-specific development of caudal ganglionic eminence-derived GABAergic cortical interneurons. *J. Neurosci.* 35, 12869–12889. doi: 10.1523/JNEUROSCI.1164-15.2015

Mulatinho, M. V., de Carvalho Serao, C. L., Scalco, F., Hardekopf, D., Pekova, S., Mrasek, K., et al. (2012). Severe intellectual disability, omphalocele, hypospadia and high blood pressure associated to a deletion at 2q22.1q22.3: case report. *Mol. Cytogenet.* 5:30. doi: 10.1186/1755-8166-5-30

Murthy, S., Niquille, M., Hurni, N., Limoni, G., Frazer, S., Chameau, P., et al. (2014). Serotonin receptor 3A controls interneuron migration into the neocortex. *Nat. Commun.* 5:5524. doi: 10.1038/ncomms6524

Myers, A. K., Cunningham, J. G., Smith, S. E., Snow, J. P., Smoot, C. A., and Tucker, E. S. (2020). JNK signaling is required for proper tangential migration and laminar allocation of cortical interneurons. *Development* 147:dev180646. doi: 10.1242/dev.180646

Myers, A. K., Meechan, D. W., Adney, D. R., and Tucker, E. S. (2014). Cortical interneurons require Jnk1 to enter and navigate the developing cerebral cortex. *J. Neurosci.* 34, 7787–7801. doi: 10.1523/JNEUROSCI.4695-13.2014

Nakamuta, S., Yang, Y. T., Wang, C. L., Gallo, N. B., Yu, J. R., Tai, Y., et al. (2017). Dual role for DOCK7 in tangential migration of interneuron precursors in the postnatal forebrain. *J. Cell Biol.* 216, 4313–4330. doi: 10.1083/jcb.201704157

Nedialkova, D. D., and Leidel, S. A. (2015). Optimization of codon translation rates via tRNA modifications maintains proteome integrity. *Cells* 161, 1606–1618. doi: 10.1016/j.cell.2015.05.022

Nguyen, O. N. P., Grimm, C., Schneider, L. S., Chao, Y.-K., Atzberger, C., Bartel, K., et al. (2017). Two-Pore Channel function is crucial for the migration of invasive Cancer cells. *Cancer Res.* 77, 1427–1438. doi: 10.1158/0008-5472.CAN-16-0852

Nomura, T. (2021). Interneuron dysfunction and inhibitory deficits in autism and fragile X syndrome. *Cells* 10:2610. doi: 10.3390/cells10102610

O'Brien, S. P., Seipel, K., Medley, Q. G., Bronson, R., Segal, R., and Streuli, M. (2000). Skeletal muscle deformity and neuronal disorder in Trio exchange factor-deficient mouse embryos. *Proc. Natl. Acad. Sci. U. S. A.* 97, 12074–12078. doi: 10.1073/pnas.97.22.12074

Ogunbayo, O. A., Duan, J., Xiong, J., Wang, Q., Feng, X., Ma, J., et al. (2018). mTORC1 controls lysosomal Ca²⁺ release through the two-pore channel TPC2 11, eaao5775. doi: 10.1126/scisignal.aao5775

Okada, Y., Yamagata, K., Hong, K., Wakayama, T., and Zhang, Y. (2010). A role for the elongator complex in zygotic paternal genome demethylation. *Nature* 463, 554–558. doi: 10.1038/nature08732

O'Roak, B. J., Deriziotis, P., Lee, C., Vives, L., Schwartz, J. J., Girirajan, S., et al. (2011). Exome sequencing in sporadic autism spectrum disorders identifies severe de novo mutations. *Nat. Genet.* 43, 585–589. doi: 10.1038/ng.835

O'Sullivan, M. L., de Wit, J., Savas, J. N., Comoletti, D., Otto-Hitt, S., Yates, J. R. 3rd, et al. (2012). FLRT proteins are endogenous latrophilin ligands and regulate excitatory synapse development. *Neuron* 73, 903–910. doi: 10.1016/j.neuron.2012.01.018

Pacary, E., Heng, J., Azzarelli, R., Riou, P., Castro, D., Lebel-Potter, M., et al. (2011). Proneural transcription factors regulate different steps of cortical neuron migration through Rnd-mediated inhibition of RhoA signaling. *Neuron* 69, 1069–1084. doi: 10.1016/j.neuron.2011.02.018

Paredes, I., Himmels, P., and Ruiz de Almodovar, C. (2018). Neurovascular communication during CNS development. *Dev. Cell* 45, 10–32. doi: 10.1016/j.devcel.2018.01.023

Peng, Y. J., He, W. Q., Tang, J., Tao, T., Chen, C., Gao, Y. Q., et al. (2010). Trio is a key guanine nucleotide exchange factor coordinating regulation of the migration and morphogenesis of granule cells in the developing cerebellum. *J. Biol. Chem.* 285, 24834–24844. doi: 10.1074/jbc.M109.096537

Peng, J., Wallar, B. J., Flanders, A., Swiatek, P. J., and Alberts, A. S. (2003). Disruption of the diaphanous-related Formin Drf1 gene encoding mDia1 reveals a role for Drf3 as an effector for Cdc42. *Curr. Biol.* 13, 534–545. doi: 10.1016/S0960-9822(03)00170-2

Pengelly, R. J., Greville-Heygate, S., Schmidt, S., Seaby, E. G., Jabalameli, M. R., Mehta, S. G., et al. (2016). Mutations specific to the Rac-GEF domain of TRIO cause intellectual disability and microcephaly. *J. Med. Genet.* 53, 735–742. doi: 10.1136/jmedgenet-2016-103942

Perrault, I., Hamdan, F. F., Rio, M., Capo-Chichi, J.-M., Boddaert, N., Décarie, J.-C., et al. (2014). Mutations in DOCK7 in individuals with epileptic encephalopathy and cortical blindness. *Am. J. Hum. Genet.* 94, 891–897. doi: 10.1016/j.ajhg.2014.04.012

Peyre, E., Silva, C. G., and Nguyen, L. (2015). Crosstalk between intracellular and extracellular signals regulating interneuron production, migration and integration into the cortex. *Front. Cell. Neurosci.* 9:129. doi: 10.3389/fncel.2015.00129

Pla, R., Stanco, A., Howard, M. A., Rubin, A. N., Vogt, D., Mortimer, N., et al. (2018). Dlx1 and Dlx2 promote interneuron GABA synthesis, synaptogenesis, and Dendritogenesis. *Cereb. Cortex* 28, 3797–3815. doi: 10.1093/cercor/bhx241

Poitras, L., Ghanem, N., Hatch, G., and Ekker, M. (2007). The proneural determinant MASH1 regulates forebrain Dlx1/2 expression through the I12b intergenic enhancer. *Development* 134, 1755–1765. doi: 10.1242/dev.02845

Polleux, F., Whitford, K. L., Dijkhuizen, P. A., Vitalis, T., and Ghosh, A. (2002). Control of cortical interneuron migration by neurotrophins and PI3-kinase signaling. *Development* 129, 3147–3160. doi: 10.1242/dev.129.13.3147

Poluch, S., and Juliano, S. L. (2007). A normal radial glial scaffold is necessary for migration of interneurons during neocortical development. *Glia* 55, 822–830. doi: 10.1002/glia.20488

Powell, E. M., Mars, W. M., and Levitt, P. (2001). Hepatocyte growth factor/scatter factor is a motogen for interneurons migrating from the ventral to dorsal telencephalon. *Neuron* 30, 79–89. doi: 10.1016/s0896-6273(01)00264-1

Pozas, E., and Ibanez, C. F. (2005). GDNF and GFRalpha1 promote differentiation and tangential migration of cortical GABAergic neurons. *Neuron* 45, 701–713. doi: 10.1016/j.neuron.2005.01.043

Raab, S., Beck, H., Gaumann, A., Yüce, A., Gerber, H. P., Plate, K., et al. (2004). Impaired brain angiogenesis and neuronal apoptosis induced by conditional homozygous inactivation of vascular endothelial growth factor. *Thromb. Haemost.* 91, 595–605. doi: 10.1160/th03-09-0582

Radu, M., Rawat, S. J., Beeser, A., Iliuk, A., Tao, W. A., and Chernoff, J. (2013). ArhGAP15, a Rac-specific GTPase-activating protein, plays a dual role in inhibiting small GTPase signaling. *J. Biol. Chem.* 288, 21117–21125. doi: 10.1074/jbc.M113.459719

Rakić, S., Kanatani, S., Hunt, D., Faux, C., Cariboni, A., Chiara, F., et al. (2015). Cdk5 phosphorylation of ErbB4 is required for tangential migration of cortical interneurons. *Cereb. Cortex* 25, 991–1003. doi: 10.1093/cercor/bht290

Reiner, O., and Sapir, T. (2013). LIS1 functions in normal development and disease. *Curr. Opin. Neurobiol.* 23, 951–956. doi: 10.1016/j.conb.2013.08.001

Richter, M., Murtaza, N., Scharrenberg, R., White, S. H., Johanns, O., Walker, S., et al. (2019). Altered TAOK2 activity causes autism-related neurodevelopmental and cognitive abnormalities through RhoA signaling. *Mol. Psychiatry* 24, 1329–1350. doi: 10.1038/s41380-018-0025-5

Riedl, J., Crevenna, A. H., Kessenbrock, K., Yu, J. H., Neukirchen, D., Bista, M., et al. (2008). Lifeact: a versatile marker to visualize F-actin. *Nat. Methods* 5, 605–607. doi: 10.1038/nmeth.1220

Righes Marafiga, J., and Baraban, S. C. (2023). Cell therapy for neurological disorders: Progress towards an embryonic medial ganglionic eminence progenitor-based treatment. *Front. Neurosci.* 17:1177678. doi: 10.3389/fnins.2023.1177678

Roberts, A. J., Kon, T., Knight, P. J., Sutoh, K., and Burgess, S. A. (2013). Functions and mechanics of dynein motor proteins. *Nat. Rev. Mol. Cell Biol.* 14, 713–726. doi: 10.1038/nrm3667

Rossignol, E. (2011). Genetics and function of neocortical GABAergic interneurons in neurodevelopmental disorders. *Neural Plast.* 2011:649325. doi: 10.1155/2011/649325

Rossignol, E., Kruglikov, I., van den Maagdenberg, A. M., Rudy, B., and Fishell, G. (2013). CaV 2.1 ablation in cortical interneurons selectively impairs fast-spiking basket cells and causes generalized seizures. *Ann. Neurol.* 74, 209–222. doi: 10.1002/ana.23913

Rossman, K. L., Der, C. J., and Sondek, J. (2005). GEF means go: turning on RHO GTPases with guanine nucleotide-exchange factors. *Nat. Rev. Mol. Cell Biol.* 6, 167–180. doi: 10.1038/nrm1587

Rubin, A. N., Alfonsi, F., Humphreys, M. P., Choi, C. K., Rocha, S. F., and Kessaris, N. (2010). The germinal zones of the basal ganglia but not the septum generate GABAergic interneurons for the cortex. *J. Neurosci.* 30, 12050–12062. doi: 10.1523/jneurosci.6178-09.2010

Rudolph, J., Zimmer, G., Steinecke, A., Barchmann, S., and Bolz, J. (2010). Ephrins guide migrating cortical interneurons in the basal telencephalon. *Cell Adhes. Migr.* 4, 400–408. doi: 10.4161/cam.4.3.11640

Ruhrberg, C., Gerhardt, H., Golding, M., Watson, R., Ioannidou, S., Fujisawa, H., et al. (2002). Spatially restricted patterning cues provided by heparin-binding VEGF-A control blood vessel branching morphogenesis. *Genes Dev.* 16, 2684–2698. doi: 10.1101/gad.242002

Ryner, R. F., Derera, I. D., Armbruster, M., Kansara, A., Sommer, M. E., Pirone, A., et al. (2023). Cortical Parvalbumin-positive interneuron development and function are altered in the APC conditional knockout mouse model of infantile and epileptic spasms syndrome. *J. Neurosci.* 43, 1422–1440. doi: 10.1523/JNEUROSCI.0572-22.2022

Sadybekov, A., Tian, C., Arnesano, C., Katritch, V., and Herring, B. E. (2017). An autism spectrum disorder-related de novo mutation hotspot discovered in the GEF1 domain of Trio. *Nat. Commun.* 8:601. doi: 10.1038/s41467-017-00472-0

Sandberg, M., Flandin, P., Silberberg, S., Su-Feher, L., Price, J. D., Hu, J. S., et al. (2016). Transcriptional networks controlled by NKX2-1 in the development of forebrain GABAergic neurons. *Neuron* 91, 1260–1275. doi: 10.1016/j.neuron.2016.08.020

Sanders, L. C., Matsumura, F., Bokoch, G. M., and de Lanerolle, P. (1999). Inhibition of myosin light chain kinase by p21-activated kinase. *Science* 283, 2083–2085. doi: 10.1126/science.283.5410.2083

Schmidt, S., and Debant, A. (2014). Function and regulation of the rho guanine nucleotide exchange factor Trio. *Small GTPases* 5:e29769. doi: 10.4161/sgtp.29769

Seltzer, L. E., Ma, M. D., Ahmed, S., Bertrand, M., Dobyns, W. B., Wheless, J., et al. (2014). Epilepsy and outcome in FOXG1-related disorders. *Epilepsia* 55, 1292–1300. doi: 10.1111/epi.12648

Seoh, M. L., Ng, C. H., Yong, J., Lim, L., and Leung, T. (2003). ArhGAP15, a novel human RacGAP protein with GTPase binding property 1. *FEBS Lett.* 539, 131–137. doi: 10.1016/S0014-5793(03)00213-8

Shen, M. J., Guo, Y., Dong, Q. P., Gao, Y., Stockton, M. E., Li, M., et al. (2021). FXR1 regulation of parvalbumin interneurons in the prefrontal cortex is critical for schizophrenia-like behaviors. *Mol. Psychiatry* 26, 6845–6867. doi: 10.1038/s41380-021-01096-z

Shinohara, R., Thumkeo, D., Kamijo, H., Kaneko, N., Sawamoto, K., Watanabe, K., et al. (2012). A role for mDia, a rho-regulated actin nucleator, in tangential migration of interneuron precursors. *Nat. Neurosci.* 15, 373–380. doi: 10.1038/nn.3020

Silva, C. G., Peyre, E., Adhikari, M. H., Tielens, S., Tanco, S., van Damme, P., et al. (2018). Cell-intrinsic control of interneuron migration drives cortical morphogenesis. *Cells* 172, 1063–1078.e19. doi: 10.1016/j.cell.2018.01.031

Skorput, A. G., Gupta, V. P., Yeh, P. W., and Yeh, H. H. (2015). Persistent Interneuronopathy in the prefrontal cortex of Young adult offspring exposed to ethanol in utero. *J. Neurosci.* 35, 10977–10988. doi: 10.1523/JNEUROSCI.1462-15.2015

Smith, S. E., Coker, N. K., and Tucker, E. S. (2020b). JNK signaling regulates cellular mechanics of cortical interneuron migration. *eNeuro* 7, ENEURO.0132–ENEU20.2020. doi: 10.1523/eneuro.0132-20.2020

Smith, A. L., Jung, E. M., Jeon, B. T., and Kim, W. Y. (2020a). Arid1b haploinsufficiency in parvalbumin- or somatostatin-expressing interneurons leads to distinct ASD-like and ID-like behavior. *Sci. Rep.* 10:7834. doi: 10.1038/s41598-020-64066-5

Sohal, V. S., and Rubenstein, J. L. R. (2019). Excitation-inhibition balance as a framework for investigating mechanisms in neuropsychiatric disorders. *Mol. Psychiatry* 24, 1248–1257. doi: 10.1038/s41380-019-0426-0

Spillane, M., Ketschek, A., Jones, S. L., Korobova, F., Marsick, B., Lanier, L., et al. (2011). The actin nucleating Arp2/3 complex contributes to the formation of axonal filopodia and branches through the regulation of actin patch precursors to filopodia. *J. Neurobiol.* 71, 747–758. doi: 10.1002/dneu.20907

Steinecke, A., Gampe, C., Zimmer, G., Rudolph, J., and Bolz, J. (2014). EphA/ephrin a reverse signaling promotes the migration of cortical interneurons from the medial ganglionic eminence. *Development* 141, 460–471. doi: 10.1242/dev.101691

Stumm, R. K., Zhou, C., Ara, T., Lazarini, F., Dubois-Dalcq, M., Nagasawa, T., et al. (2003). CXCR4 regulates interneuron migration in the developing neocortex. *J. Neurosci.* 23, 5123–5130. doi: 10.1523/JNEUROSCI.23-12-05123.2003

Sun, X., Wang, L., Wei, C., Sun, M., Li, Q., Meng, H., et al. (2021). Dysfunction of Trio GEF1 involves in excitatory/inhibitory imbalance and autism-like behaviors through regulation of interneuron migration. *Mol. Psychiatry* 26, 7621–7640. doi: 10.1038/s41380-021-01109-x

Suozzi, K. C., Wu, X., and Fuchs, E. (2012). Spectraplakins: master orchestrators of cytoskeletal dynamics. *J. Cell Biol.* 197, 465–475. doi: 10.1083/jcb.201112034

Takenawa, T., and Suetsugu, S. (2007). The WASP–WAVE protein network: connecting the membrane to the cytoskeleton. *Nat. Rev. Mol. Cell Biol.* 8, 37–48. doi: 10.1038/nrm2069

Tan, G. H., Liu, Y. Y., Hu, X. L., Yin, D. M., Mei, L., and Xiong, Z. Q. (2011). Neuregulin 1 represses limbic epileptogenesis through ErbB4 in parvalbumin-expressing interneurons. *Nat. Neurosci.* 15, 258–266. doi: 10.1038/nn.3005

Tan, X., Liu, W. A., Zhang, X. J., Shi, W., Ren, S. Q., Li, Z., et al. (2016). Vascular influence on ventral Telencephalic progenitors and neocortical interneuron production. *Dev. Cell* 36, 624–638. doi: 10.1016/j.devcel.2016.02.023

Tanaka, D. H., Mikami, S., Nagasawa, T., Miyazaki, J., Nakajima, K., and Murakami, F. (2010). CXCR4 is required for proper regional and laminar distribution of cortical somatostatin-, calretinin-, and neuropeptide Y-expressing GABAergic interneurons. *Cereb. Cortex* 20, 2810–2817. doi: 10.1093/cercor/bhq027

Tanaka, T., Serneo, F. F., Higgins, C., Gambello, M. J., Wynshaw-Boris, A., and Gleeson, J. G. (2004). Lis1 and doublecortin function with dynein to mediate coupling of the nucleus to the centrosome in neuronal migration. *J. Cell Biol.* 165, 709–721. doi: 10.1083/jcb.200309025

Tanco, S., Lorenzo, J., Garcia-Pardo, J., Degroeve, S., Martens, L., Aviles, F. X., et al. (2013). Proteome-derived peptide libraries to study the substrate specificity profiles of carboxypeptidases. *Mol. Cell. Proteomics* 12, 2096–2110. doi: 10.1074/mcp.M112.023234

Tao, G. X., Li, Z. M. Y., Wen, Y., Song, X. L., Wei, S., du, H., et al. (2019). Transcription factors Sp8 and Sp9 regulate medial ganglionic Eminence-derived cortical interneuron migration. *Front. Mol. Neurosci.* 12:75. doi: 10.3389/fnmol.2019.00075

Tastet, J., Cuberos, H., Vallée, B., Toutain, A., Raynaud, M., Marouillat, S., et al. (2019). LIMK2-1 is a Hominidae-specific isoform of LIMK2 expressed in central nervous system and associated with intellectual disability. *Neuroscience* 399, 199–210. doi: 10.1016/j.neuroscience.2018.12.017

Tielens, S., Huysseune, S., Godin, J. D., Chariot, A., Malgrange, B., and Nguyen, L. (2016). Elongator controls cortical interneuron migration by regulating actomyosin dynamics. *Cell Res.* 26, 1131–1148. doi: 10.1038/cr.2016.112

Tiveron, M. C., Rossel, M., Moepps, B., Zhang, Y. L., Seidenfaden, R., Favor, J., et al. (2006). Molecular interaction between projection neuron precursors and invading interneurons via stromal-derived factor 1 (CXCL12)/CXCR4 signaling in the cortical subventricular zone/intermediate zone. *J. Neurosci.* 26, 13273–13278. doi: 10.1523/JNEUROSCI.4162-06.2006

Tivodar, S., Kalemaki, K., Kounoupa, Z., Vidaki, M., Theodorakis, K., Denaxa, M., et al. (2014). Rac-GTPases regulate microtubule stability and axon growth of cortical GABAergic interneurons. *Cereb. Cortex* 25, 2370–2382. doi: 10.1093/cercor/bhu037

Tong, L. M., Djukic, B., Arnold, C., Gillespie, A. K., Yoon, S. Y., Wang, M. M., et al. (2014). Inhibitory interneuron progenitor transplantation restores normal learning and memory in ApoE4 knock-in mice without or with Aβ accumulation. *J. Neurosci.* 34, 9506–9515. doi: 10.1523/jneurosci.0693-14.2014

Toral-Lopez, J., Huerta, L. M. G., Messina-Baas, O., and Cuevas-Covarrubias, S. A. (2020). Submicroscopic 11p13 deletion including the elongator acetyltransferase complex subunit 4 gene in a girl with language failure, intellectual disability and congenital malformations: a case report. *World J. Clin. Cases* 8, 5296–5303. doi: 10.12998/wjcc.v8.i21.5296

Touzot, A., Ruiz-Reig, N., Vitalis, T., and Studer, M. (2016). Molecular control of two novel migratory paths for CGE-derived interneurons in the developing mouse brain. *Development* 143, 1753–1765. doi: 10.1242/dev.131102

Tran, C. H., Vaiana, M., Nakuci, J., Somarowthu, A., Goff, K. M., Goldstein, N., et al. (2020). Interneuron desynchronization precedes seizures in a mouse model of Dravet syndrome. *J. Neurosci.* 40, 2764–2775. doi: 10.1523/Jneurosci.2370-19.2020

Tsai, H. H., Niu, J., Munji, R., Davalos, D., Chang, J., Zhang, H., et al. (2016). Oligodendrocyte precursors migrate along vasculature in the developing nervous system. *Science* 351, 379–384. doi: 10.1126/science.aad3839

Upadhya, D., Hattiangady, B., Castro, O. W., Shuai, B., Kodali, M., Attaluri, S., et al. (2019). Human induced pluripotent stem cell-derived MGE cell grafting after status epilepticus attenuates chronic epilepsy and comorbidities via synaptic integration. *Proc. Natl. Acad. Sci. U. S. A.* 116, 287–296. doi: 10.1073/pnas.1814185115

Vadlamudi, R. K., Barnes, C. J., Rayala, S., Li, F., Balasenthil, S., Marcus, S., et al. (2005). p21-activated kinase 1 regulates microtubule dynamics by phosphorylating tubulin cofactor B. *Mol. Cell. Biol.* 25, 3726–3736. doi: 10.1128/MCB.25.9.3726-3736.2005

Vaghi, V., Pennucci, R., Talpo, F., Corbetta, S., Montinaro, V., Barone, C., et al. (2014). Rac1 and rac3 GTPases control synergistically the development of cortical and hippocampal GABAergic interneurons. *Cereb. Cortex* 24, 1247–1258. doi: 10.1093/cercor/bhs402

van den Berghe, V., Stappers, E., Vandesande, B., Dimidschstein, J., Kroes, R., Francis, A., et al. (2013). Directed migration of cortical interneurons depends on the cell-autonomous action of Sip1. *Neuron* 77, 70–82. doi: 10.1016/j.neuron.2012.11.009

van Dijk, J., Miro, J., Strub, J. M., Lacroix, B., van Dorsselaer, A., Edde, B., et al. (2008). Polyglutamylation is a post-translational modification with a broad range of substrates. *J. Biol. Chem.* 283, 3915–3922. doi: 10.1074/jbc.M705813200

van Dijk, J., Rogowski, K., Miro, J., Lacroix, B., Eddé, B., and Janke, C. (2007). A targeted multienzyme mechanism for selective microtubule Polyglutamylation. *Mol. Cell* 26, 437–448. doi: 10.1016/j.molcel.2007.04.012

van Haren, J., Boudeau, J., Schmidt, S., Basu, S., Liu, Z., Lammers, D., et al. (2014). Dynamic microtubules catalyze formation of navigator-TRIO complexes to regulate neurite extension. *Curr. Biol.* 24, 1778–1785. doi: 10.1016/j.cub.2014.06.037

Vasudevan, A., and Bhide, P. G. (2008). Angiogenesis in the embryonic CNS: a new twist on an old tale. *Cell Adhes. Migr.* 2, 167–169. doi: 10.4161/cam.2.3.6485

Vasudevan, A., Long, J. E., Crandall, J. E., Rubenstein, J. L., and Bhide, P. G. (2008). Compartment-specific transcription factors orchestrate angiogenesis gradients in the embryonic brain. *Nat. Neurosci.* 11, 429–439. doi: 10.1038/nn2074

Venkataramanappa, S., Saaber, F., Abe, P., Schutz, D., Kumar, P. A., and Stumm, R. (2022). Cxcr4 and Ackr3 regulate allocation of caudal ganglionic eminence-derived interneurons to superficial cortical layers. *Cell Rep.* 40:111157. doi: 10.1016/j.celrep.2022.111157

Vidaki, M., Tivodar, S., Doulgeraki, K., Tybulewicz, V., Kessaris, N., Pachnis, V., et al. (2012). Rac1-dependent cell cycle exit of MGE precursors and GABAergic interneuron migration to the cortex. *Cereb. Cortex* 22, 680–692. doi: 10.1093/cercor/bhr145

Villar-Cervino, V., Kappeler, C., Nobrega-Pereira, S., Henkemeyer, M., Rago, L., Nieto, M. A., et al. (2015). Molecular mechanisms controlling the migration of striatal interneurons. *J. Neurosci.* 35, 8718–8729. doi: 10.1523/JNEUROSCI.4317-14.2015

Vogt, D., Cho, K. K. A., Shelton, S. M., Paul, A., Huang, Z. J., Sohal, V. S., et al. (2018). Mouse Cntnap2 and human CNTNAP2 ASD alleles cell autonomously regulate PV+ cortical interneurons. *Cereb. Cortex* 28, 3868–3879. doi: 10.1093/cercor/bhx248

Vogt, D., Hunt, R. F., Mandal, S., Sandberg, M., Silberberg, S. N., Nagasawa, T., et al. (2014). Lhx6 directly regulates Arx and CXCR7 to determine cortical interneuron fate and laminar position. *Neuron* 82, 350–364. doi: 10.1016/j.neuron.2014.02.030

Wang, Y. L., Dye, C. A., Sohal, V., Long, J. E., Estrada, R. C., Roztocil, T., et al. (2010). Dlx5 and Dlx6 regulate the development of Parvalbumin-expressing cortical interneurons. *J. Neurosci.* 30, 5334–5345. doi: 10.1523/Jneurosci.5963-09.2010

Wang, Y., Li, G., Stanco, A., Long, J. E., Crawford, D., Potter, G. B., et al. (2011). CXCR4 and CXCR7 have distinct functions in regulating interneuron migration. *Neuron* 69, 61–76. doi: 10.1016/j.neuron.2010.12.005

Wang, B., Long, J. E., Flandin, P., Pla, R., Waclaw, R. R., Campbell, K., et al. (2013). Loss of Gsx1 and Gsx2 function rescues distinct phenotypes in Dlx1/2 mutants. *J. Comp. Neurol.* 521, 1561–1584. doi: 10.1002/cne.23242

Watanabe, N., Kato, T., Fujita, A., Ishizaki, T., and Narumiya, S. (1999). Cooperation between mDia1 and ROCK in rho-induced actin reorganization. *Nat. Cell Biol.* 1, 136–143. doi: 10.1038/11056

Wei, S., du, H., Li, Z., Tao, G., Xu, Z., Song, X., et al. (2019). Transcription factors Sp8 and Sp9 regulate the development of caudal ganglionic eminence-derived cortical interneurons. *J. Comp. Neurol.* 527, 2860–2874. doi: 10.1002/cne.24712

Wei, C., Sun, M., Sun, X., Meng, H., Li, Q., Gao, K., et al. (2022). RhoGEF Trio regulates radial migration of projection neurons via its distinct domains. *Neurosci. Bull.* 38, 249–262. doi: 10.1007/s12264-021-00804-7

Wester, J. C., Mahadevan, V., Rhodes, C. T., Calvigioni, D., Venkatesh, S., Maric, D., et al. (2019). Neocortical projection neurons instruct inhibitory interneuron circuit development in a lineage-dependent manner. *Neuron* 102, 960–975.e6. doi: 10.1016/j.neuron.2019.03.036

Wichterle, H., Garcia-Verdugo, J. M., Herrera, D. G., and Alvarez-Buylla, A. (1999). Young neurons from medial ganglionic eminence disperse in adult and embryonic brain. *Nat. Neurosci.* 2, 461–466. doi: 10.1038/8131

Wichterle, H., Turnbull, D. H., Nery, S., Fishell, G., and Alvarez-Buylla, A. (2001). In utero fate mapping reveals distinct migratory pathways and fates of neurons born in the mammalian basal forebrain. *Development* 128, 3759–3771. doi: 10.1242/dev.128.19.3759

Willis, A., Pratt, J. A., and Morris, B. J. (2021). BDNF and JNK signaling modulate cortical interneuron and Perineuronal net development: implications for schizophrenia-linked 16p11.2 duplication syndrome. *Schizophr. Bull.* 47, 812–826. doi: 10.1093/schbul/sbaa139

Winkler, G. S., Petrakis, T. G., Ethelberg, S., Tokunaga, M., Erdjument-Bromage, H., Tempst, P., et al. (2001). RNA polymerase II Elongator holoenzyme is composed of two discrete subcomplexes*. *J. Biol. Chem.* 276, 32743–32749. doi: 10.1074/jbc.M105303200

Witke, W. (2004). The role of profilin complexes in cell motility and other cellular processes. *Trends Cell Biol.* 14, 461–469. doi: 10.1016/j.tcb.2004.07.003

Won, C., Lin, Z., Kumar, T. P., Li, S., Ding, L., Elkhal, A., et al. (2013). Autonomous vascular networks synchronize GABA neuron migration in the embryonic forebrain. *Nat. Commun.* 4:2149. doi: 10.1038/ncomms3149

Wonders, C. P., and Anderson, S. A. (2006). The origin and specification of cortical interneurons. *Nat. Rev. Neurosci.* 7, 687–696. doi: 10.1038/nrn1954

Wong, L. C., Singh, S., Wang, H. P., Hsu, C. J., Hu, S. C., and Lee, W. T. (2019). FOXG1-related syndrome: from clinical to molecular genetics and pathogenic mechanisms. *Int. J. Mol. Sci.* 20:4176. doi: 10.3390/ijms20174176

Xu, G., Broadbelt, K. G., Haynes, R. L., Folkerth, R. D., Borenstein, N. S., Belliveau, R. A., et al. (2011). Late development of the GABAergic system in the human cerebral cortex and white matter. *J. Neuropathol. Exp. Neurol.* 70, 841–858. doi: 10.1097/NEN.0b013e31822f471c

Yamagishi, S., Hampel, F., Hata, K., del Toro, D., Schwark, M., Kvachnina, E., et al. (2011). FLRT2 and FLRT3 act as repulsive guidance cues for Unc5-positive neurons. *EMBO J.* 30, 2920–2933. doi: 10.1038/emboj.2011.189

Yang, Y., Shen, W., Ni, Y., Su, Y., Yang, Z. Y., and Zhao, C. J. (2017). Impaired interneuron development after Foxg1 disruption. *Cereb. Cortex* 27, 793–808. doi: 10.1093/cercor/bhv297

Yang, Y.-T., Wang, C.-L., and Van Aelst, L. (2012). DOCK7 interacts with TACC3 to regulate interkinetic nuclear migration and cortical neurogenesis. *Nat. Neurosci.* 15, 1201–1210. doi: 10.1038/nn.3171

Yau, H. J., Wang, H. F., Lai, C., and Liu, F. C. (2003). Neural development of the neuregulin receptor ErbB4 in the cerebral cortex and the hippocampus: preferential expression by interneurons tangentially migrating from the ganglionic eminences. *Cereb. Cortex* 13, 252–264. doi: 10.1093/cercor/13.3.252

Yokota, Y., Gashghaei, H. T., Han, C., Watson, H., Campbell, K. J., and Anton, E. S. (2007). Radial glial dependent and independent dynamics of interneuronal migration in the developing cerebral cortex. *PLoS One* 2:e794. doi: 10.1371/journal.pone.0000794

Yu, Y., Zeng, Z., Xie, D., Chen, R., Sha, Y., Huang, S., et al. (2021). Interneuron origin and molecular diversity in the human fetal brain. *Nat. Neurosci.* 24, 1745–1756. doi: 10.1038/s41593-021-00940-3

Yuan, W., Zhou, L., Chen, J. H., Wu, J. Y., Rao, Y., and Ornitz, D. M. (1999). The mouse SLIT family: secreted ligands for ROBO expressed in patterns that suggest a role in morphogenesis and axon guidance. *Dev. Biol.* 212, 290–306. doi: 10.1006/dbio.1999.9371

Zavalin, K., Hassan, A., Fu, C., Delpire, E., and Lagrange, A. H. (2022). Loss of KCC2 in GABAergic neurons causes seizures and an imbalance of cortical interneurons. *Front. Mol. Neurosci.* 15:826427. doi: 10.3389/fnmol.2022.826427

Zechel, S., Nakagawa, Y., and Ibanez, C. F. (2016). Thalamo-cortical axons regulate the radial dispersion of neocortical GABAergic interneurons. *eLife* 5:e20770. doi: 10.7554/eLife.20770

Zhang, F., Yu, J., Yang, T., Xu, D., Chi, Z., Xia, Y., et al. (2016a). A novel c-Jun N-terminal kinase (JNK) signaling complex involved in neuronal migration during brain development. *J. Biol. Chem.* 291, 11466–11475. doi: 10.1074/jbc.M116.716811

Zhang, Q. Q., Zhang, Y., Wang, C. Y., Xu, Z. J., Liang, Q. F., An, L., et al. (2016b). The zinc finger transcription factor Sp9 is required for the development of Striatopallidal projection neurons. *Cell Rep.* 16, 1431–1444. doi: 10.1016/j.celrep.2016.06.090

Zhu, Y., Li, H., Zhou, L., Wu, J. Y., and Rao, Y. (1999). Cellular and molecular guidance of GABAergic neuronal migration from an extracortical origin to the neocortex. *Neuron* 23, 473–485. doi: 10.1016/s0896-6273(00)80801-6

Zimmer, G., Garcez, P., Rudolph, J., Niehage, R., Weth, F., Lent, R., et al. (2008). Ephrin-A5 acts as a repulsive cue for migrating cortical interneurons. *Eur. J. Neurosci.* 28, 62–73. doi: 10.1111/j.1460-9568.2008.06320.x

Zimmer-Bensch, G. (2018). Diverse facets of cortical interneuron migration regulation - implications of neuronal activity and epigenetics. *Brain Res.* 1700, 160–169. doi: 10.1016/j.brainres.2018.09.001

Zipancic, I., Calcagnotto, M. E., Piquer-Gil, M., Mello, L. E., and Alvarez-Dolado, M. (2010). Transplant of GABAergic precursors restores hippocampal inhibitory function in a mouse model of seizure susceptibility. *Cell Transplant.* 19, 549–564. doi: 10.3727/096368910x491383

Zong, W., Liu, S., Wang, X., Zhang, J., Zhang, T., Liu, Z., et al. (2015). Trio gene is required for mouse learning ability. *Brain Res.* 1608, 82–90. doi: 10.1016/j.brainres.2015.02.040

frontiers | Frontiers in Neural Circuits

TYPE Mini Review
PUBLISHED 29 September 2023
DOI 10.3389/fncir.2023.1223891

OPEN ACCESS

EDITED BY
Lisa Topolnik,
Laval University, Canada

REVIEWED BY
Claudio Elgueta,
University of Freiburg, Germany
Balint Lasztoczi,
Medical University of Vienna, Austria

*CORRESPONDENCE
Jayeeta Basu
✉ jayeeta.basu@nyulangone.org
Arjun V. Masurkar
✉ arjun.masurkar@nyulangone.org

RECEIVED 16 May 2023
ACCEPTED 08 September 2023
PUBLISHED 29 September 2023

CITATION
Hernández-Frausto M, Bilash OM, Masurkar AV and Basu J (2023) Local and long-range GABAergic circuits in hippocampal area CA1 and their link to Alzheimer's disease. *Front. Neural Circuits* 17:1223891. doi: 10.3389/fncir.2023.1223891

Local and long-range GABAergic circuits in hippocampal area CA1 and their link to Alzheimer's disease

Melissa Hernández-Frausto[1,2], Olesia M. Bilash[1,3], Arjun V. Masurkar[1,2,4]* and Jayeeta Basu[1,2,5,6]*

[1]Neuroscience Institute, New York University Langone Health, New York, NY, United States, [2]Department of Neuroscience and Physiology, New York University Grossman School of Medicine, New York, NY, United States, [3]Meinig School of Biomedical Engineering, Cornell University, Ithaca, NY, United States, [4]Center for Cognitive Neurology, Department of Neurology, New York University Grossman School of Medicine, New York, NY, United States, [5]Department of Psychiatry, New York University Grossman School of Medicine, New York, NY, United States, [6]Center for Neural Science, New York University, New York, NY, United States

GABAergic inhibitory neurons are the principal source of inhibition in the brain. Traditionally, their role in maintaining the balance of excitation-inhibition has been emphasized. Beyond homeostatic functions, recent circuit mapping and functional manipulation studies have revealed a wide range of specific roles that GABAergic circuits play in dynamically tilting excitation-inhibition coupling across spatio-temporal scales. These span from gating of compartment- and input-specific signaling, gain modulation, shaping input–output functions and synaptic plasticity, to generating signal-to-noise contrast, defining temporal windows for integration and rate codes, as well as organizing neural assemblies, and coordinating inter-regional synchrony. GABAergic circuits are thus instrumental in controlling single-neuron computations and behaviorally-linked network activity. The activity dependent modulation of sensory and mnemonic information processing by GABAergic circuits is pivotal for the formation and maintenance of episodic memories in the hippocampus. Here, we present an overview of the local and long-range GABAergic circuits that modulate the dynamics of excitation-inhibition and disinhibition in the main output area of the hippocampus CA1, which is crucial for episodic memory. Specifically, we link recent findings pertaining to GABAergic neuron molecular markers, electrophysiological properties, and synaptic wiring with their function at the circuit level. Lastly, given that area CA1 is particularly impaired during early stages of Alzheimer's disease, we emphasize how these GABAergic circuits may contribute to and be involved in the pathophysiology.

KEYWORDS

GABAergic circuits, Alzheimer's disease, hippocampus (CA1), long-range GABAergic neurons, disinhibition

Introduction

Gamma-aminobutyric acid (GABA) is the primary inhibitory neurotransmitter in the mammalian central nervous system. It is released by GABAergic inhibitory neurons (INs), which serve as one of the main sources of inhibition (Caputi et al., 2013; Le Magueresse and Monyer, 2013). GABAergic INs modulate the activity of other neurons to maintain a

homeostatic excitation-inhibition balance. This is a striking feature of the cortex where E/I ratios are tightly maintained within various layers (Pfeffer et al., 2013; Xue et al., 2014; Adesnik, 2018; Yen et al., 2022). Do GABAergic inputs just act to balance excitation, or do they have specific roles in organizing information flow? The balance of excitation and inhibition is critical for normal brain function. Disruptions to excitation-inhibition balance can result in hyperexcitability, runaway excitation, and disturbance of oscillatory synchrony, which can be seen in epilepsy, neuropsychiatric disorders such as post-traumatic stress disorder (PTSD), schizophrenia, anxiety, and depression (Marín, 2012), and neurodegenerative diseases such as Alzheimer's disease (AD; Han et al., 2012; Busche et al., 2015; Busche and Konnerth, 2016; O'Donnell et al., 2017; Bridi et al., 2020). However, during learning, shifts in the weight of excitation and inhibition are important to discriminate and store only the relevant information based on contexts. A precise model of how excitatory and inhibitory neurons cooperate to tune information flow is crucial to our understanding of the brain. In this context, hippocampal area CA1 is particularly interesting to study- it provides the main output of the hippocampus and thus critical for memory-guided behavior. Interestingly, CA1 is also the part of hippocampus affected earliest and the most in AD (Braak and Braak, 1991).

A single hippocampal CA1 pyramidal neuron receives several different inputs (glutamatergic, GABAergic) from various sources (hippocampus, entorhinal cortex, prefrontal cortex). Glutamatergic inputs drive excitation in a circuit; GABAergic inputs typically inhibit the propagation of excitation. ***How do local and long-range GABAergic circuits interact to change the dynamics of excitation and inhibition for acquiring important information?*** The hippocampal CA1 region alone has >21 different types of local GABAergic neurons with distinct molecular make-up and physiological properties. However, we know little about how these GABAergic neurons contribute to hippocampal functions such as plasticity or learning behavior.

Several lines of evidence suggest that local and long-range circuit interactions between pyramidal neurons (PNs) and GABAergic INs are poised to play a prominent role in higher-order cognitive functions. Within the hippocampus, dynamically controlling the excitation-inhibition (E/I) balance – tilting it in favor of excitation or inhibition in a context-specific manner at the single cell and network levels – can influence memory processing, multisensory coding, and fine-tuning of behaviorally-relevant neuronal activity (Klausberger and Somogyi, 2008; Joshi et al., 2017; Szabo et al., 2022). For example, functional interactions between the prefrontal cortex, entorhinal cortex, and hippocampus that support formation of episodic memories of context and events in the hippocampus rely on the activity of long-range GABAergic projection neurons from the cortex and local GABAergic microcircuits in the hippocampus (Basu et al., 2013, 2016; Malik et al., 2022).

At the single-neuron level, the distribution of specific types of inhibitory synapses varies along the somato-dendritic axis of pyramidal neurons found in hippocampal area CA1, even within a dendritic branch (Megías et al., 2001; Bloss et al., 2016; Cembrowski et al., 2016). Surprisingly, the electrophysiological, neurochemical, and functional characteristics of the inhibitory synapses correlate with their axo-dendritic distribution. At the network level, the interaction between local and long-range excitation and inhibition in the cortex and hippocampus could be important for supporting context-dependent stability and flexibility of memory representations encoding familiar and novel experiences and generating adaptive learned behaviors. Furthermore, GABAergic circuits may substantially coordinate oscillations (Somogyi et al., 2014), such as gamma oscillations during learning (Wulff et al., 2009), theta oscillations during locomotion (Csicsvari et al., 1999; Buzsáki, 2002; Bezaire et al., 2016; Melzer and Monyer, 2020), and sharp wave ripples (SWR; Cutsuridis and Taxidis, 2013; Schlingloff et al., 2014; Stark et al., 2014; Evangelista et al., 2020; Noguchi et al., 2022) in quiet wakefulness, and sleep (Eichenbaum, 2000; Squire, 2004; Basu and Siegelbaum, 2015; Francavilla et al., 2018; Eyre and Bartos, 2019; Udakis et al., 2020; Malik et al., 2022; Yen et al., 2022).

In the present review, we describe the local and long-range GABAergic circuits in hippocampal area CA1. However, rather than describing inhibitory neuron types based on their expressed molecular markers, we focus on a functional classification approach. We present our perspective on how specific inhibitory microcircuits modulate compartment-specific activity, as well as how the dynamic interaction between excitation, inhibition, and disinhibition shapes dendritic integration, plasticity, and behavior. We particularly showcase the recently described GABAergic disinhibitory circuit motifs to emphasize the role of 'inhibitory' neurons in boosting excitatory signaling rather than curbing it, and coordinating long-range inter-regional interactions beyond local 'interneuron' domains. Finally, we highlight how these circuits may contribute to the neurodegeneration seen during Alzheimer's disease.

General GABAergic circuit motifs in CA1

Within the hippocampus, local inhibition is mediated by GABAergic microcircuits comprising of INs that target PNs directly to suppress their activity. Within these GABAergic microcircuits that drive inhibition there are two organizational motifs.

Feed-forward inhibition

Within hippocampal area CA1, feed-forward inhibition (FFI) is locally mediated by INs that are directly excited by the glutamatergic inputs arriving from the EC or by intra-hippocampal glutamatergic inputs from CA3 or CA2 (Chevaleyre and Siegelbaum, 2010; Basu and Siegelbaum, 2015; Ferrante and Ascoli, 2015; Zemla and Basu, 2017; Bilash et al., 2023). These INs then target PNs to limit their activity and the propagation of information (Buzsaki, 1984; Pouille and Scanziani, 2001; Price et al., 2008; Kullmann, 2011; Basu et al., 2013, 2016; Figure 1).

Feed-back inhibition

Feedback inhibition (FBI) occurs when CA1 PNs recurrently target INs through direct monosynaptic connections and the INs in turn target the PNs (Tremblay et al., 2016). Thus, FBI is driven by recurrent excitation and the overall effect is auto-inhibition of PN

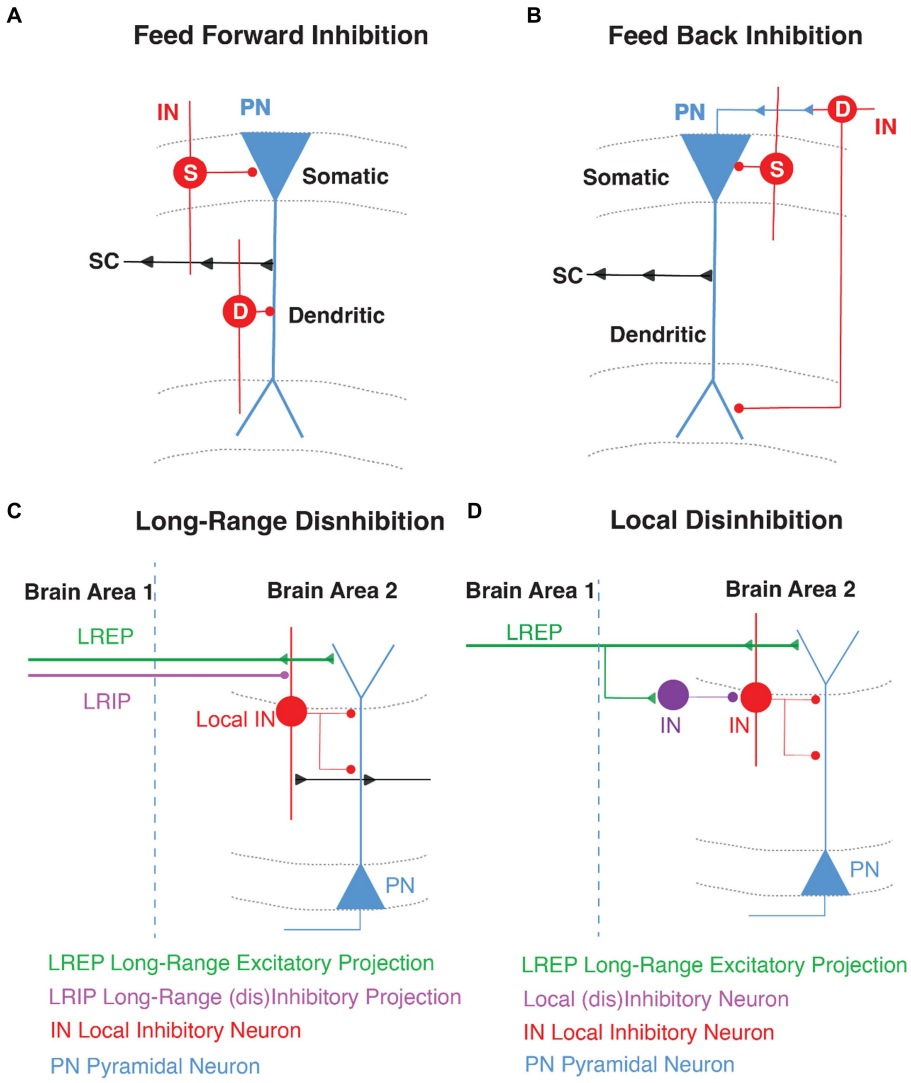

FIGURE 1
General GABAergic Circuit Motifs in area CA1. Schematic representations of **(A)** feed-forward inhibition (FFI) and **(B)** feed-back inhibition (FBI) in CA1 highlighting the pyramidal neuron (PN, in blue) with the Schaffer Collateral inputs (SC, arrows in black) and the inhibition of local interneurons (IN, in red) in somatic (S) and dendritic (D) compartments. **(C)** Long-range disinhibition **(D)** Local disinhibition in hippocampal area CA1.

activity. The initial drive for the PN spiking to trigger FBI arises from strong activity of the proximal CA3 or CA2 excitatory inputs and on occasion from distal EC (Buzsaki, 1984; Kullmann, 2011; Tyan et al., 2014; Figure 1).

Disinhibition

Disinhibition is a circuit motif that results from an IN directly targeting another IN, which releases the inhibition from a downstream PN (Basu et al., 2013, 2016; Francavilla et al., 2015; Guet-McCreight et al., 2020; Bilash et al., 2023). So rather than inhibiting a PN, the GABAergic IN-specific-IN (ISI) mediates inhibition of inhibition and thereby disinhibition of coincident excitatory transmission. In the hippocampus, disinhibitory gating can be local (LEC driven VIP INs) or long-range (direct GABAergic projections from EC). Curiously, most long-range GABAergic projection neurons synapse onto INs in their target region and are therefore primarily disinhibitory in nature (Fuchs et al., 2007; Melzer et al., 2012; Caputi et al., 2013; Tyan et al., 2014; Basu et al., 2016; Melzer and Monyer, 2020; Yen et al., 2022; Figure 1).

Hippocampal circuit organization and layer specific inhibition

The hippocampus is anatomically divided into different sub-regions, namely dentate gyrus (DG), CA3, CA2, CA1 and subiculum, which are each believed to perform distinct roles in memory operations. Each of these subregions have a laminar organization through the dorso-ventral axis (Amaral and Witter, 1989; Zemla and Basu, 2017). Hippocampal area CA1 consists of four layers. The pyramidal cell layer, or *stratum pyramidale*, is where all the PN somata are located. These PNs are innervated exclusively by GABAergic synapses from perisomatic basket interneurons. The *stratum oriens*

(SO) is where the basal dendrites and axonal arborizations of CA1 PNs are located. SO hosts oriens lacunosom moleculare (OLM) interneurons and basket cell soma and axo-axonic interneurons (Maccaferri, 2005), and receives input from area CA2 (Chevaleyre and Siegelbaum, 2010), and medial septum (Lovett-Barron et al., 2014). The *stratum radiatum* (SR), where PN apical dendrites are located, receives excitatory input from CA3 PNs via the Schaffer Collateral (SC) synapses and is embedded with some bistratified dendrite-targeting GABAergic neurons. Lastly, the *stratum lacunosum moleculare* (SLM), where most distal tuft dendrites are located, receives input from the entorhinal cortex (EC) and has cell bodies of several dendrite-targeting and some soma-targeting INs (Amaral and Witter, 1989; Witter et al., 2000; Basu and Siegelbaum, 2015). The SR/SLM border region is particularly rich in GABAergic neuron cell bodies that control the flow of direct cortical inputs arriving distally upon CA1 PNs and their integration with proximal inputs carrying content processed through the indirect intra-hippocampal trisynaptic circuit (DG → CA3 → CA1). Both the direct EC and indirect trisynaptic pathways have been implicated in learning and memory storage (Barnes et al., 1977; Van Strien et al., 2009; Basu et al., 2013, 2016; Jonas and Lisman, 2014; Eyre and Bartos, 2019; Figure 2).

Classification of GABAergic interneurons

GABAergic INs constitute ~10-20% of all neurons in cortex (Bartos et al., 2007; Klausberger and Somogyi, 2008; Caputi et al., 2013) and ~10–15% of all neurons in the hippocampus (Bezaire and Soltesz, 2013; Pelkey et al., 2017). Within the hippocampus, area CA1 contains more than 21 types of GABAergic INs (Klausberger and Somogyi, 2008). Each of these GABAergic IN types can be classified based on single cell transcriptome analyses and according to their morphology, molecular markers, intrinsic physiological properties, postsynaptic target cells, developmental origin, and function in the adult brain (Ascoli et al., 2008; Klausberger and Somogyi, 2008; Le Magueresse and Monyer, 2013; Pelkey et al., 2017; Harris et al., 2018). However, the integrated classification of interneuron types remains a daunting challenge in cellular and circuit neuroscience (Ascoli et al., 2008; Kepecs and Fishell, 2014; Pelkey et al., 2017; Zeng, 2022). Circuit mapping studies have greatly benefitted from classifying INs based on the expression of specific molecular markers, and the development of transgenic animals based on these molecular markers has provided a relatively precise and consistent strategy to label and manipulate major interneuron populations selectively (Taniguchi et al., 2011; Dimidschstein et al., 2016).

In terms of their expression of molecular markers, GABAergic INs have been traditionally categorized as parvalbumin (PV), vasoactive intestinal peptide (VIP), cholecystokinin (CCK), somatostatin (SST), neuropeptide Y (NPY), and neuron-derived neurotrophic factor (NDNF) and/or nitric oxide synthase (nNOS), among others. These interneuron types generally possess characteristic intrinsic properties and short-term synaptic plasticity dynamics due to their unique molecular make up. Moreover, they can perform specific functions in modulating compartment-specific and behaviorally-relevant activity based on their layer specificity location, connectivity onto downstream PNs and responses to neuromodulators (Figure 3). Each of these interneuron populations can be further subdivided based on co-expressed molecular markers, intrinsic properties, morphology, location within a particular CA1 layer, or input–output connectivity [thoroughly reviewed in (Pelkey et al., 2017)]. Here we provide a brief overview of these sub-classes.

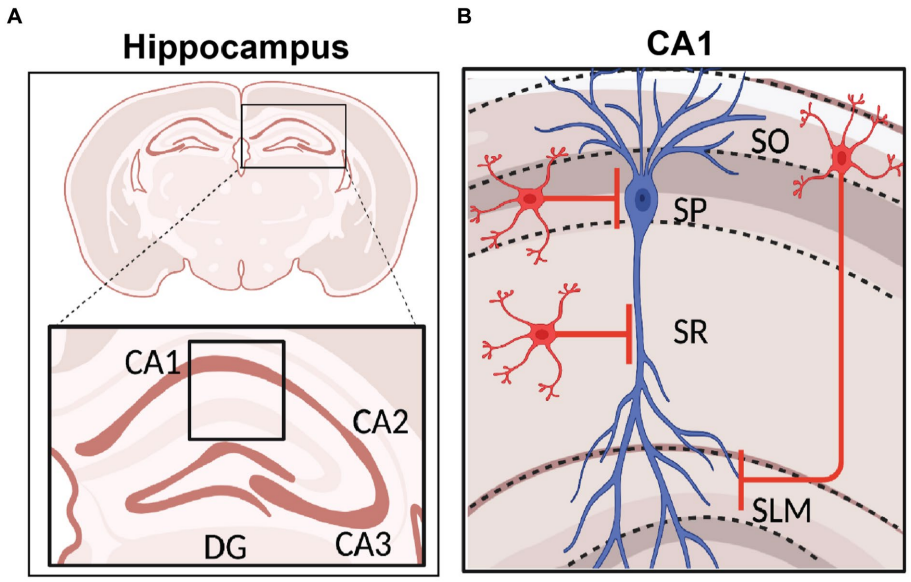

FIGURE 2
Hippocampal Formation and area CA1 Circuitry. **(A)** Schematic representation of coronal section of a rodent brain highlighting the hippocampal region with its sub-areas dentate gyrus (DG), CA3, CA2, and CA1. **(B)** Stratification of hippocampal area CA1 namely stratum oriens (SO), *stratum pyramidale* (SP), *stratum radiatum* (SR), and *stratum lacunosum moleculare* (SLM). The CA1 pyramidal neuron soma and dendrites organization are shown in blue, and INs in red. Created with BioRender.

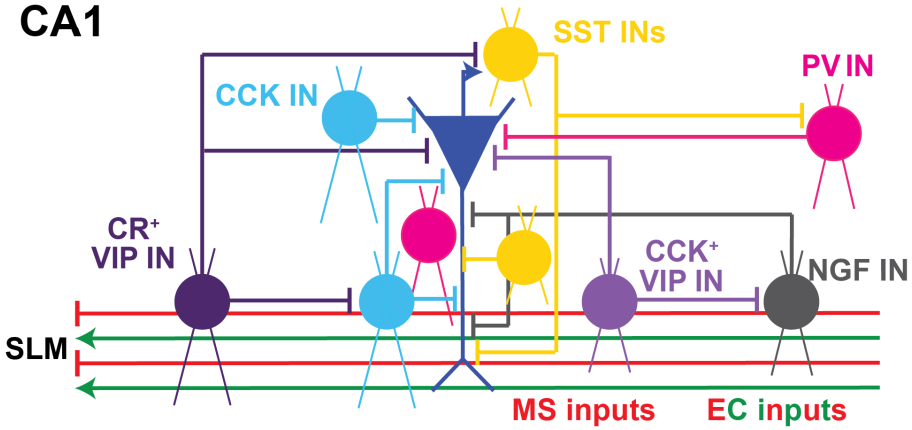

FIGURE 3
Local Inhibitory microcircuits in area CA1. Schematic representation of CA1 microcircuit connectivity, the CA1 pyramidal neuron (blue) is surrounded by local GABAergic microcircuitry: PV$^+$ IN (pink), SST$^+$ IN (yellow), soma-targeting CCK$^+$ basket cell and SR/SLM border CCK IN (light blue), CR$^+$ VIP IN (dark purple), CCK$^+$ VIP$^+$ IN (light purple), and NPY$^+$ IN (gray). Excitatory and inhibitory inputs from EC into SLM of area CA1 shown in green and red, respectively. Inhibitory inputs from the Medial septum (MS) into SLM of area CA1 shown in red.

PV INs

Parvalbumin-expressing (PV) INs are classically considered to provide perisomatic inhibition onto a neighboring CA1 PN by surrounding its soma with a basket-like axon morphology (Sik et al., 1995; Cope et al., 2002; Pawelzik et al., 2002; Klausberger et al., 2005; Takács et al., 2015; Dudok et al., 2021a). Moreover, PV INs can also have bistratified morphological subtypes that specifically target the proximal apical dendrites to mediate dendritic feed-forward inhibition (FFI; Basu et al., 2013, 2016; Udakis et al., 2020; Bilash et al., 2023; Chamberland et al., 2023). PV INs also participate in FBI circuit motifs. Few recurrent collaterals of CA1 PNs make functional synaptic contacts onto PV basket cells that target basal dendrites in *stratum oriens* (Ribak et al., 1993; Hu et al., 2014). Furthermore, the apical dendrite targeting OLM neurons, which are a classical FBI also express low levels of parvalbumin (Klausberger, 2009). Recent studies in CA1 show that PV INs particularly target PNs in the deep layer, while being driven by PNs the superficial layer (Lee A. T. et al., 2014). Lastly, parvalbumin is also expressed in axo-axonic interneurons that directly inhibit the axon initial segment of a pyramidal neuron (Pawelzik et al., 2002; Takács et al., 2015). Functionally, fast-spiking PV INs in CA1 are involved in networking oscillations modulating the PN synchrony particularly in the gamma frequency regime (English et al., 2017) and spatial working memory (Murray et al., 2011; Hu et al., 2014; Harris et al., 2018). PV IN synapses undergo inhibitory long-term depression (i-LTD) during theta burst stimulation (TBS) as well as a spike-timing-dependent plasticity (STDP) paradigm, which is mediated via the activation of $GABA_A$ receptors and T-type voltage-gated calcium channels (VGCCs; Udakis et al., 2020). In area CA1, the activity of PV INs is modulated by opioids, specifically via the μ-opioid receptors (Glickfeld et al., 2008). Furthermore, neuromodulation of PV INs is mediated by oxytocin, which increases PV IN firing rate through $GABA_A$ receptors (Owen et al., 2013) and by D4-dopamine receptors that enhances the CA3 SC input-driven from CA1 to mediate PV FFI upon PNs to suppress SC pathway output (Rosen et al., 2015).

CCK INs

Cholecystokinin-expressing (CCK) INs were classically considered to mediate FBI (Glickfeld and Scanziani, 2006) at the CA1 pyramidal neuron soma because of their slower responses compared to PV basket cells. Furthermore, these INs are known for their asynchronous GABA release (Hefft and Jonas, 2005), where they fail to keep up with fidelity during high-frequency trains of activation. However, recent studies using optogenetic activation and pharmacogenetic silencing (Basu et al., 2013) show that CCK INs are recruited in a FFI manner by the Schaffer Collateral inputs from CA3, as well as by the perforant path inputs from the entorhinal cortex. In fact, CCK INs can mediated robust and fast FFI both at the soma and dendrites to considerably suppress the amplitude of coincident EPSPs. *In vivo* juxtacellular recordings of single CCK INs in area CA1 reveals their preferred theta phase firing precedes that of CA1 PNs, putting them in a strategic position to modulate place cell firing at the peak of the theta cycle (Klausberger and Somogyi, 2008). Recent *in vivo* two-photon imaging studies show that CCK INs (Geiller et al., 2020; Dudok et al., 2022; Dudok and Soltesz, 2022) are particularly active during rest or when animals are stationary, creating a potential functional link to quiet, awake behavioral states associated with sharp wave ripples (Buzsáki, 2015). A well-characterized feature of the CCK INs, is their sensitivity to cannabinoid modulation by virtue of the cannabinoid 1 receptors (CB1Rs) they express (Chevaleyre and Castillo, 2003; Glickfeld and Scanziani, 2006; Freund and Katona, 2007; Castillo et al., 2012). Release of retrograde endocannabinoid messengers upon activation and depolarization of CA1 PNs allows for local and rapid suppression of GABA release from CCK basket cells, which are particularly enriched in CB1Rs (Freund and Katona, 2007). This can occur across shorter time scales, e.g., depolarization induced suppression of inhibition (DSI; Wilson et al., 2001; Yoshida et al., 2002) as well as longer time scales, e.g., inhibitory long-term depression (iLTD) time scales (Chevaleyre et al., 2007; Heifets and Castillo, 2009; Castillo et al., 2012; Basu et al., 2013). Notably, the genetic targeting of CCK INs has been challenging considering CCK pre- pro- hormone is

widely expressed in glutamatergic pyramidal neurons as well. Thus, targeting CCK INs exclusively requires intersectional strategies (Taniguchi et al., 2011; Basu et al., 2013, 2016). Finally, recent studies suggest that immediate early gene NPAS4 preferentially modulates CCK IN activity and synaptic output during exposure to enriched environments (Hartzell et al., 2018) and contextual fear learning (Sun et al., 2020).

SST INs

Somatostatin-expressing (SST) INs classically mediate dendritic inhibition onto pyramidal neurons either in a FFI or FBI manner (Oliva et al., 2000; Leão et al., 2012; Lovett-Barron et al., 2012, 2014; Müller and Remy, 2014; Udakis et al., 2020). SST INs in area CA1 consist of two main subpopulations: OLM INs, which mediate FBI (Leão et al., 2012), and bistratified SST INs, which modulate CA3-driven FFI (Lovett-Barron et al., 2012). OLM INs are recruited by spiking CA1 PNs and inhibit the distal dendrites of CA1 PNs. OLM neurons modulate SC input plasticity (Leão et al., 2012) and gate EC inputs that are relevant for contextual fear learning (Cutsuridis et al., 2010; Lovett-Barron et al., 2014). The OLM neurons have been more extensively studied, and can be characterized by the specific expression of nicotinic acetylcholine receptor α2 subunit (CHRNA2; Leão et al., 2012; Lovett-Barron et al., 2014). Their cell bodies are located in the oriens layer with the axons projecting to the *stratum lacunosum moleculare*, and known to be modulated by cholinergic input (Leão et al., 2012; Lovett-Barron et al., 2014), and the effect of this modulation is amplified by gap junctions interconnecting the OLM cells. SST IN synapses upon CA1 PN have also been shown to undergo LTP during theta burst stimulation (Udakis et al., 2020) through voltage-gated T- and L-type calcium channel modulation. Imaging studies comparing SST IN and PV IN activity in animals navigating between familiar and novel environments, have shown that the activity of SST INs is transiently suppressed when animals are exposed to novel environments to disinhibit dendrites, while somatic inhibition is dialed up by boosting PV IN activity (Sheffield et al., 2017).

VIP INs

Vasoactive intestinal peptide-expressing (VIP) INs generally target other inhibitory neurons, thereby disinhibiting downstream pyramidal neurons (Acsády et al., 1996; Chamberland and Topolnik, 2012). They have an important role in the modulation of distal dendritic inhibition of PNs with specific target of bistratified and oriens INs controlling the firing rate and FFI (Tyan et al., 2014). They are strongly stimulated by cholinergic modulation (Bell et al., 2015; Askew et al., 2019; Ren et al., 2022) through α4β2 nicotinic acetylcholine (Ach) receptors (Bell et al., 2015). VIP INs can be divided into sub-populations based on their additional expression of calretinin (CR), CCK, or muscarinic acetylcholine receptor 2 (Tyan et al., 2014; Francavilla et al., 2018; Guet-McCreight et al., 2020). Genetically targeting these VIP IN subtypes requires intersectional tools, so dissociating their specific functions has been challenging. Nevertheless, a couple of recent studies have used intersectional tools and modeling to dissociate the function of VIP/CR+ and VIP/CCK INs. The VIP/CR+ INs are primarily disinhibitory and target a host of different interneurons types in area CA1, particularly the dendrite-targeting OLM INs (Tyan et al., 2014; Bilash et al., 2023). On the other hand, the CCK-expressing VIP INs can target PNs and mediate perisomatic FFI (Turi et al., 2019; Guet-McCreight et al., 2020; Kullander and Topolnik, 2021) through asynchronous GABA release (Tyan et al., 2014). For detailed information regarding their disinhibitory function please see Disinhibitory GABAergic Circuits section.

Neurogliaform cells – INs expressing NDNF, NPY, and/or nNos

Neurogliaform cells (NGF) express neuron-derived neurotrophic factor (NDNF) but can also be defined by NPY and/or nNOS expression (Price et al., 2005; Tricoire et al., 2010; Armstrong et al., 2012; Milstein et al., 2015; Tasic et al., 2016; Guo et al., 2021). NGF INs soma are predominantly restricted to the distal dendritic SLM layer in CA1, with a smaller distinct subset residing at the border of SLM/SR (Capogna, 2011). Given their position, NGF INs are likely predominantly driven by glutamatergic inputs from EC, as well as thalamus. However, NPY+ NGF neurons have been shown to modulate integration of SC and EC inputs (Milstein et al., 2015). A unique feature of NGF INs is their volume transmission of GABA to provide slow-acting inhibition, via activation of both $GABA_A$ and $GABA_B$ receptors onto neurons within a particular radius (Price et al., 2005, 2008; Tasic et al., 2016; Abs et al., 2018; Mercier et al., 2022).

In conclusion, molecular markers can be a helpful tool to classify the different GABAergic INs and determine their modulation of excitation-inhibition balance. Nevertheless, they can co-express similar molecular markers and have specific locations throughout the various layers of area CA1. For instance, the expression of molecular markers PV, SST, or NPY can overlap in morphologically-defined *oriens-lacunosum moleculare* (OLM) interneurons or bistratified neurons (Klausberger and Somogyi, 2008; Klausberger, 2009; Katona et al., 2014; Müller and Remy, 2014). This calls for IN classification and nomenclature systems to use a combination of the molecular markers and their localization in laminar stratification of hippocampal area CA1 (Figure 3).

GABAergic microcircuits in modulating compartment-specific activity in hippocampal area CA1

Synaptic inhibition can powerfully influence the dendritic and somatic activity of a pyramidal neuron (PN; Miles et al., 1996; Gidon and Segev, 2012; Müller et al., 2012; Pouille et al., 2013; Marlin and Carter, 2014; Müllner et al., 2015). Arranged in specialized microcircuit motifs, interneurons can provide axonal (Kiss et al., 1996; Dudok et al., 2021b), perisomatic (Pawelzik et al., 2002; Klausberger et al., 2005; Dudok et al., 2021a), or dendritic (Lacaille and Schwartzkroin, 1988; Klausberger, 2009; Lovett-Barron et al., 2012; Müller and Remy, 2014) inhibition onto specific compartments of CA1 pyramidal neurons. Other interneurons specifically target GABAergic interneurons, thereby serving a disinhibitory function within the larger neural circuit in area CA1 (Acsády et al., 1996; Chamberland and Topolnik, 2012). GABAergic synapses that densely

surround the perisomatic region of a CA1 PNs strongly modulate somatic output (Pouille and Scanziani, 2001), while those found along the dendritic tree can serve to precisely modulate EC- or CA3-driven dendritic computations (Klausberger, 2009; Lovett-Barron et al., 2012; Basu et al., 2013, 2016; Bloss et al., 2016; Schulz et al., 2018; Bilash et al., 2023; Chamberland et al., 2023). Ultimately, by affecting the entire span of a CA1 pyramidal neuron (Buhl et al., 1994; Glickfeld et al., 2009; Bloss et al., 2016), GABAergic INs can serve as powerful circuit switches to rapidly, precisely, and flexibly shape single-cell and network computations (Lovett-Barron et al., 2012; Royer et al., 2012; Milstein et al., 2015; Basu et al., 2016; Grienberger et al., 2017).

PV INs mediate FFI in area CA1, modulating somatic and axonal activity in an apparent temporarily silent state (Sik et al., 1995; Pawelzik et al., 2002; Takács et al., 2015; Pelkey et al., 2017; Dudok et al., 2021a; Chamberland et al., 2023). On the other hand, CCK IN subpopulations provide FFI onto the somata and dendrites of downstream pyramidal neurons, curbing compartment-specific activity. Although soma-targeting CCK INs basket cells have been more widely investigated (Mátyás et al., 2004; Somogyi et al., 2004; Glickfeld and Scanziani, 2006; Bartos and Elgueta, 2012; Del Pino et al., 2017; Whissell et al., 2019; Dudok et al., 2021a), non-basket cell CCK-expressing INs have been shown to target the dendrites of CA1 PNs (Cope et al., 2002; Pawelzik et al., 2002; Klausberger, 2009) and likely mediate dendritic inhibition (Basu et al., 2016; Bilash et al., 2023). Neurogliaform INs release GABA through volume transmission (Oláh et al., 2009; Armstrong et al., 2012), a non-specific form of neurotransmitter release that affects many downstream neurons within a particular radius, producing a slow, $GABA_B$ receptor ($GABA_BR$)-mediated inhibitory response (Price et al., 2005, 2008). Additionally, they can form gap junctions with a variety of interneuron types in area CA1 (Zsiros and Maccaferri, 2005; Armstrong et al., 2012). Studies have demonstrated that NDNF INs in area CA1 modulate learning and recall (Guo et al., 2021) and that SST INs in area CA1 modulate input-specific plasticity (Leão et al., 2012), as well as object- and fear-related memory encoding (Siwani et al., 2018). In area CA1, NPY+ neurons receive converging inputs from EC and CA3 (Milstein et al., 2015) and bistratified SST INs mediate CA3-driven FFI (Lovett-Barron et al., 2012), to shape dendritic activity and somatic firing in CA1 PNs. Therefore, NDNF INs and SST INs could feasibly modulate the integration of extrahippocampal and intrahippocampal (CA3) inputs within CA1 PNs dendrites. This may influence input-timing-dependent plasticity mechanisms (Basu et al., 2013). Neurogliaform cells may additionally modulate the soma-dendrite coupling or dendritic excitability in large populations of CA1 PNs, given that they release GABA through volume transmission and given that $GABA_BRs$ are enriched in the distal dendrites of CA1 PNs (Degro et al., 2015).

GABAergic inhibitory neurons modulate information flow in the cortico-hippocampal circuit

As described above, GABAergic INs allow for the precise modulation of pyramidal neuron activity (Basu et al., 2013; Francavilla et al., 2015; Guet-McCreight et al., 2020; Bilash et al., 2023). Within the cortico-hippocampal circuit, long-range excitatory projections from the entorhinal cortex recruit specific inhibitory neurons within the hippocampus to influence local computations. For example, Milstein et al. (2015) found that EC inputs recruit NPY-expressing neurogliaform neurons in area CA1 (Milstein et al., 2015). Using optogenetics to selectively activate projections from each EC subdivision, Li et al. (2017) found that medial entorhinal cortex (MEC) and lateral entorhinal cortex (LEC) inputs target local GABAergic INs in area CA1, including morphologically-defined axo-axonic cells, basket cells, and bistratified cells. This circuit organization likely enables EC subdivisions to drive inhibition onto the axon initial segment, soma, and dendrites of CA1 PNs, respectively (Li et al., 2017). Combining optogenetics and pharmacology, Bilash et al. (2023) found that glutamatergic LEC inputs drive strong amounts of FFI onto both the somatic and dendritic compartments of CA1 PNs by recruiting CCK-expressing INs, while also recruiting disinhibition by exciting local CR co-expressing VIP INs in area CA1 (Bilash et al., 2023).

Disinhibitory GABAergic circuits

Beyond FFI and FBI, some particular INs can modulate disinhibition by directly inhibiting other INs and thereby activating the downstream PNs (Basu et al., 2013, 2016; Francavilla et al., 2015, 2018; Guet-McCreight et al., 2020; Bilash et al., 2023). In hippocampal CA1 area, this phenomenon can occur at the local microcircuit level and through long-range inhibitory projections (LRIPs). Locally, VIP INs are classically a disinhibitory IN subtype. However, disinhibitory roles of SST, CCK, and PV INs have also been described (Karson et al., 2009; Chamberland et al., 2023). Across the brain, most LRIPs described to date act in a disinhibitory manner by targeting local INs (Karson et al., 2009; Leão et al., 2012; Melzer et al., 2012; Basu et al., 2016; Pelkey et al., 2017; Artinian and Lacaille, 2018). Here, we provide an updated view of local and long-range disinhibitory GABAergic circuits.

Local Disinhibitory GABAergic microcircuits

VIP INs are famous for their role in mediating disinhibition in the hippocampus (Acsády et al., 1996; Tyan et al., 2014; Guet-McCreight et al., 2020) and cortex (Lee et al., 2013; Pfeffer et al., 2013; Pi et al., 2013). They inhibit other interneurons, thereby relieving downstream principal cells from inhibitory forces (Chamberland and Topolnik, 2012; Kepecs and Fishell, 2014). Tyan et al. (2014), a pioneering study in hippocampal area CA1 that defined the functional connectivity of the interneuron-specific calretinin co-expressing VIP INs (CR+/VIP+ INs) using paired recordings and optogenetics. This study showed that when synchronously activated these VIP neurons target OLM INs to control their firing rate and timing (Tyan et al., 2014). In a more recent study, Bilash et al. (2023) used intersectional genetics to confirm that CR co-expressing VIP INs (CR+/VIP+ INs) are disinhibitory. These INs are mainly located in SLM and primarily target other INs including, CCK INs and SST INs in area CA1 (Bilash et al., 2023). Whereas the CCK+/VIP+ INs target CA1 PNs and modulate somatic inhibition. Curiously, this study found that both the disinhibitory CR+/VIP+ INs and the inhibitory CCK+/VIP+ INs are recruited by glutamatergic LEC inputs, raising the question of whether these

opposing IN subtypes are differentially or simultaneously recruited during behavior to modulate cortico-hippocampal excitation-inhibition dynamics. *In vivo*, VIP INs are recruited during quiescent states and are weakly active during theta oscillations in locomotion (Magnin et al., 2019; Luo et al., 2020; Kullander and Topolnik, 2021). General optogenetic silencing of VIP INs highlight their role in goal-directed spatial learning (Turi et al., 2019).

SST INs can also play a disinhibitory role within the hippocampal area CA1 to regulate synaptic plasticity and activity of PNs. They make direct contact with PV, VIP, CCK, and CR INs in *lacunosum moleculare (LM)* as well as with NDNF INs in SR and in LM strata (Katona et al., 1999; Elfant et al., 2008; Leão et al., 2012; Artinian and Lacaille, 2018). Leão et al. (2012), observed that optogenetic stimulation of SST INs in OLM disinhibits SC inputs upon the PNs to increase the magnitude of LTP (Leão et al., 2012). A recent study showed using brief inhibition mediated by optogenetic activation of SST INs persistently interrupts firing of PV INs, so as to disinhibit spike generation in CA1 PNs (Chamberland et al., 2023).

Beyond their classical role in mediating FFI and FBI, CCK and PV INs show bidirectional synaptic coupling. Karson et al. (2009) demonstrated that PV INs anatomically project onto CCK INs and that CCK INs make functional synaptic connections onto PV INs. Such coupling exists at the level of axo-somatic, axo-dendritic, and axo-axonic synapses, between the perisomatic-targeting CCK and PV INs (Karson et al., 2009). This is of great relevance, considering that local disinhibitory circuit motifs can operate with sub-layer specific precision. This is because CCK INs show stronger inhibition upon superficial layer CA1 PNs (Valero et al., 2015), whereas PV INs preferentially target and inhibit the deep layer CA1 PNs (Lee A. T. et al., 2014). The immediate early gene, NPAS4 strengthens CB1R-expressing CCK synapses upon superficial PNs in CA1 in an experience-dependent manner (Hartzell et al., 2018). Hence CCK and PV neurons may orchestrate a fine-tuned modulation of sub-layer specific inhibition and disinhibition between the deep and superficial layer PNs in a behavioral or experience state-dependent manner. More recently, Dudok et al. (2021a) demonstrated that in area CA1, CCK and PV INs are capable of scaling their activities with respect to ensemble neuronal activity in opposite paths but both within brain states and their transitions, leading to a mechanism that PV inhibits the CCK IN activity (Dudok et al., 2021a).

In general, novel tools and transgenic rodents have allowed for the functional and circuit interrogation of the different subtypes of GABAergic neurons that play an important but non-canonical role in disinhibiting the activity of PNs. The favorable impact of rapid and context-selective disinhibitory gating of sensory and mnemonic information flow warrants further investigation into how these disinhibitory microcircuits in hippocampal area CA1 contribute to memory function and adaptive learnt behaviors relying on one trial learning and efficient recall.

Long-range GABAergic disinhibitory circuits

While GABAergic inhibitory neurons are typically attributed to maintaining local excitation-inhibition balance and dynamically modulate activity at the microcircuit level, there is surmounting evidence that GABAergic neurons also send long-range inhibitory projections (LRIPs) between different brain areas (Jinno et al., 2007; Melzer et al., 2012; Caputi et al., 2013; Lee A. T. et al., 2014; Basu et al., 2016; Joshi et al., 2017; Melzer and Monyer, 2020; Sans-Dublanc et al., 2020; Szabo et al., 2022; Yen et al., 2022; Schroeder et al., 2023). It has been postulated that LRIPs exist to coordinate activity across longer distances within the brain and are important for generating inter-regional synchrony. An emerging principle for connectivity of LRIPs is that they usually target local GABAergic INs, thereby acting as a disinhibitory system of the principal neurons, found in the downstream target brain region (Melzer et al., 2012; Caputi et al., 2013; Basu et al., 2016; Joshi et al., 2017; Melzer and Monyer, 2020; Malik et al., 2022). Within the cortico-hippocampal circuit, LRIPs from medial and lateral entorhinal cortex (MEC and LEC), medial septum (MS), prefrontal cortex (PFC) and retrosplenial cortex (RS) have been found. In fact, LRIPs mediate bidirectionally connectivity between MEC (Ino et al., 1990; Melzer et al., 2012), MS, PFC and RS (Gulyás et al., 2003; Fanselow and Dong, 2010; Joshi et al., 2017; Yuan et al., 2017) and the hippocampus. Although LRIPs have been found to project from LEC into CA1 (Basu et al., 2016), it has yet to be determined whether similar to glutamatergic cortico-hippocampal loop there exists a GABAergic reciprocal loop counterpart from CA1 to LEC.

Hippocampal area CA1 also sends LRIPs to other sub-cortical regions as amygdala, nucleus accumbens, subiculum and band of Broca (Cohen and Squire, 1980; Jinno et al., 2007; Eichenbaum et al., 2012; Melzer et al., 2012; Caputi et al., 2013; Lee S. H. et al., 2014; Lübkemann et al., 2015; Basu et al., 2016; Witter et al., 2017; Wick et al., 2019). Given the extensive regions that interact with CA1 by sending and receiving GABAergic projections, here we discuss recent findings about the heterogeneity and functionality in circuit computations and episodic memory functions of the different LRIPs.

Entorhinal cortex-hippocampal long-range inhibitory inputs

Within the cortico-hippocampal circuit, most LRIP axons from EC terminate in SR and SLM of hippocampal area CA1, where information is integrated in the distal dendrites of CA1 PNs (Melzer et al., 2012; Basu et al., 2016; Xu et al., 2020). Melzer et al. (2012) reported that MEC sends LRIPs to the dorsal and intermediate hippocampal areas into SLM and deep SR. These MEC LRIPs consist of axons from PV INs but likely include other GABAergic subtypes as well (Melzer et al., 2012). Although retrograde labelling experiments previously uncovered the existence of GABAergic LRIPs from EC into the hippocampus (Germroth et al., 1989), Melzer et al. (2012) was the first to address the molecular composition and functional connectivity of MEC LRIPs, as well as their potential function in modulating local GABAergic neuron theta synchrony in the hippocampus.

Basu et al. (2016) discovered that LEC also sends long-range inhibitory inputs into hippocampal area CA1. Interestingly, *in vivo* two-photon imaging of a pan-GABAergic neuron Cre line (Gad2-Cre) shows that these LEC LRIPs are strongly activated by behaviorally-salient cues such as water rewards and air-puffs. Neutral sensory cue-driven presynaptic activity in these LEC LRIP boutons is boosted supra-linearly when combined with appetitive or aversive stimuli. Accordingly, LEC LRIPs are important for novelty and contextual salience discrimination: silencing the LEC LRIPs leads to impaired

novel object recognition and to the over-generalization of context-dependent fear memory. At the circuit level, LEC LRIPs prominently target Schaffer collateral-associated, dendrite-targeting CCK INs in CA1 to effectively relieve dendritic FFI. This long-range disinhibitory circuit motif facilitates the integration of EC and CA3 inputs within CA1 PNs to boost dendritic spike probability and induce input-timing-dependent plasticity. Interestingly, LRIPs from MEC and LEC are differentially distributed within hippocampal area CA1. MEC LRIPs target mostly proximal area CA1, similar to excitatory MEC projections. Meanwhile, LEC LRIPs distribute uniformly along the proximal-distal axis of CA1, in contrast to the excitatory LEC long range excitatory projections (LREP) that target mostly distal area CA1 (Melzer et al., 2012; Basu et al., 2016). It is therefore possible that long-range GABAergic projections from LEC could serve to modulate the integration of MEC, LEC, and CA3 inputs within CA1 PNs, thereby influencing the output of area CA1. This circuit organization could provide LEC LRIPs with the means to influence contextual and spatial information processing. For example, perhaps the long-range disinhibition of dendritic spikes by this salience detection circuit may contribute to context-dependent spatial tuning or remapping of place cells (Bittner et al., 2015, 2017; Figure 4).

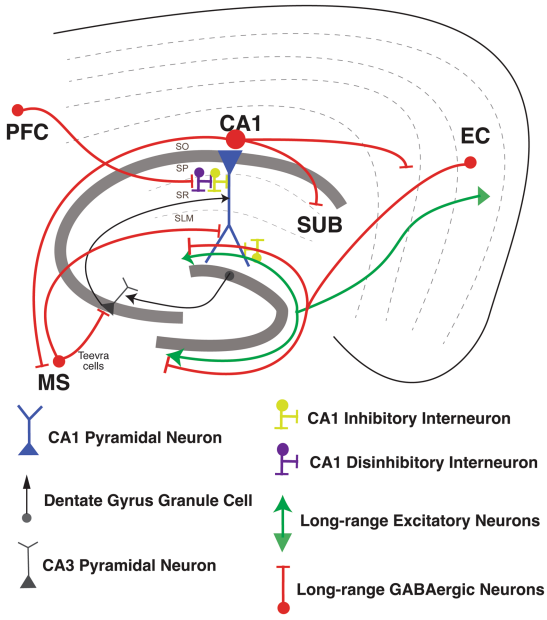

FIGURE 4
Long-range Inhibitory projections circuits in the hippocampus. Long-range Inhibitory projections (LRIPs) into hippocampal area CA1 and LRIPs outputs from hippocampal area. Inhibition or disinhibition of hippocampal CA1 pyramidal neuron (in blue), with GABAergic inhibitory interneurons (in yellow) and disinhibitory interneurons (in purple). Inputs into hippocampal area CA1 from dentate gyrus granule cells and CA3 pyramidal neurons (in black).

Other hippocampal long-range inhibitory inputs

Besides the LRIPs from the entorhinal cortex into the hippocampus, LRIPs have also been found from other brain regions that modulate hippocampal information processing (Joshi et al., 2017; Malik et al., 2022). Joshi et al. (2017) reported a new set of LRIPs neurons, named "Teevra cells," that originate in the medial septum with general IN targets in CA3 with a few inputs into CA1. Teevra cells target axo-axonic GABAergic neurons (likely PV INs) and CCK INs in hippocampal area CA3. Teevra cells were themselves positive for parvalbumin, as well as for the transcription factor SATB1. These cells increase their rhythmicity during run and rest periods, coincident with heightened excitation in area CA1 (Joshi et al., 2017). Medial septum LRIPs are recruited for recall of contextual fear memory. Photostimulation of these projections, selectively inhibited local PV INs in area CA1, whereas chemogenetic silencing blocked memory retrieval (Sans-Dublanc et al., 2020). Furthermore, Malik et al. (2022) described a new form of LRIPs from PFC to PNs from dorsal CA1. These projections directly synapse onto VIP INs, so activating the PFC LRIPs increases FFI, enhancing the signal-to-noise ratio for hippocampus to encode object locations with increasing spatial information. Furthermore, silencing of these projections suppresses object exploration (Malik et al., 2022; Figure 4).

Hippocampal long-range inhibitory outputs

Once information is integrated in area CA1, hippocampal output is sent back to EC, as well as to various other cortical and sub-cortical areas (Cohen and Squire, 1980; Eichenbaum et al., 2012; Melzer et al., 2012; Basu et al., 2016; Witter et al., 2017). LRIPs from the hippocampus to retrosplenial cortex (Jinno et al., 2007), amygdala (Lübkemann et al., 2015), frontal cortex (Wick et al., 2019) and nucleus accumbens (Lee S. H. et al., 2014) have also been reported. GABAergic LRIPs from CA1 have diverse molecular identities and firing properties (Melzer and Monyer, 2020). GABAergic INs originating in SO of area CA1 project to subiculum and medial septum, and increase the firing during sharp wave ripples (SWR; Jinno et al., 2007; Caputi et al., 2013; Melzer and Monyer, 2020). GABAergic INs originating in SP of area CA1 project to band of Broca and the frontal cortex, express the nNOS and NPY markers and connect to PNs and other local IN subtypes (Wick et al., 2019). GABAergic LRIPs from CA1 also project to retrosplenial cortex (RS), and to MEC, which are part of the brain's navigation system. Both of these projections include a sub-population expressing somatostatin (Jinno et al., 2007; Miyashita and Rockland, 2007; Melzer et al., 2012). Within the CA1-subiculum circuit, LRIP from VIP INs mostly restricted in stratum oriens (SO), stratum pyramidale (SP) and radiatum (SR) of CA1 target INs in subiculum through gap junctions. These VIP IN LRIP have sparse spiking *in vitro* but are highly active during quiet wakefulness (Francavilla et al., 2018; Figure 4).

In summary, the cortico-hippocampal network for memory and navigation has bidirectional functional interactions mediated by glutamatergic and GABAergic circuits that can drive excitation, inhibition, and disinhibition in hippocampal area, locally and across long-distances. The diversity of activity-dependent and neuromodulatory tuning of specific subsets of INs contributes to a wide dynamic range for spatio-temporal modulation of balance of excitation-inhibition-disinhibition. This will allow for gating of cortico-hippocampal information flow and CA1 ensemble output by GABAergic circuits *in vivo* in a behavioral state- or task-selective manner.

GABAergic circuits in Alzheimer's disease

Clinical AD is staged across normal, preclinical, mild cognitive impairment (MCI), and dementia stages that are defined by worsening biomarkers, cognition, and function (Jack et al., 2018). These clinical stages are grossly associated with the spatiotemporal progression of AD pathology through the brain. In particular, memory impairment becomes first evident at the pre-dementia MCI stage when AD pathology progresses from EC to CA1, the region of hippocampus first and most affected during the course of AD (Braak and Braak, 1991; Bennett et al., 2005; Lace et al., 2009). Histological analysis has demonstrated that this correlates with synaptic loss and neurodegeneration initiated by this AD pathology in area CA1 (Price et al., 2001; Scheff et al., 2007; Kerchner et al., 2010). Molecular pathways associated with these changes relate to spine integrity, glutamate receptor loss, cellular stress response, inflammation and calcium dyshomeostasis (imbalance of the homeostasis system; Colangelo et al., 2002; Ginsberg et al., 2010, 2012; Counts et al., 2014; Hondius et al., 2016). The advent of transgenic and, more recently, knock-in rodent models of AD has further established a link between various forms of memory deficits and aspects of AD pathology within the hippocampus (Webster et al., 2014). Studies using these models have elucidated neuronal mechanisms that relate to synaptic dysfunction (Pozueta et al., 2013), aberrant synaptic plasticity (Cuestas Torres and Cardenas, 2020), and altered information coding properties (Zhao et al., 2014; Mably et al., 2017; Jun et al., 2020). Human and rodent models studies have also suggested disruption of network activity and oscillations (Zott et al., 2018; Giustiniani et al., 2022).

Excitatory pyramidal neurons have primarily drawn the focus of such cellular-level AD research, as they carry the main output from brain areas and are the principal cell type that develop neurofibrillary tangles (NFTs; Braak and Braak, 1991). Moreover, surmounting evidence of pyramidal neuron heterogeneity has suggested further studies to elucidate how these subgroups are differentially impacted by AD (Masurkar, 2018). However, as delineated above, inhibitory GABAergic neurons play a critical role in shaping and transforming information processing by pyramidal neurons through local and long-range interactions. Pyramidal neuron functional heterogeneity can in part be mediated by differential associations with specific GABAergic neuron subtypes (Lee S. H. et al., 2014; Valero et al., 2015). Therefore, the loss or degeneration of GABAergic neurons due to AD pathology can play a significant role in driving symptomatology. Moreover, reduction of GABAergic tone can increase net excitability of a network. This may impact the development and progression of AD pathology itself, as tau and amyloid can be released by activity and/or exert their effects across synapses (Kamenetz et al., 2003; Cirrito et al., 2005; De Calignon et al., 2012; Liu et al., 2012; Khan et al., 2014; Wu et al., 2016).

Broad interrogation of the GABAergic system in AD has indeed revealed relevant changes that leads to alterations. The temporal lobe in human AD features a reduction of $GABA_A$ mRNA and protein, and reduced physiologic function of $GABA_A$ receptors (Limon et al., 2012). Rodent AD models also show alteration of GABA function in the hippocampus (Palop et al., 2007) that can associate with disruptions in hippocampal theta oscillations and sharp wave ripples (Mahar et al., 2016; Caccavano et al., 2020), as well as disruption of hippocampal excitation-inhibition balance that impairs spatial learning (Yang et al., 2018). Moreover, recent studies in the APP-KI (amyloid-beta precursor protein-knock in) mice show that GABAergic neurons in area CA1 contribute to 30% of amyloid plaque load, highlighting the bidirectional relationship between GABAergic interneurons (INs) and AD pathology (Rice et al., 2020). While global measures of $GABA_AR$ dysfunction and altered excitatory/inhibitory balance were not as prominent in an analysis of human AD hippocampal regions (Scaduto et al., 2023), this does not rule out alterations in specific hippocampal IN populations and/or compensatory changes resulting from such IN-specific changes. Given the heterogeneity of IN function delineated above, here we discuss the cell type specific IN vulnerability in the hippocampus in human patients of AD, as well as in AD mouse models. A summary of these findings are described in Table 1.

PV INs

PV INs are the most extensively studied of the hippocampal INs in the setting of AD. While overall there is no difference in PV INs counts in AD versus control human cases (Waller et al., 2020), there is region-specific loss of PV INs and/or PV immunoreactivity limited to DG, CA1, and CA2 (Brady and Mufson, 1997; Takahashi et al., 2010). In rodent AD models, PV INs can develop tau pathology (Soler et al., 2017; Siddhartha et al., 2018), and are found to degenerate, with loss in CA1 observed most consistently (Takahashi et al., 2010; Loreth et al., 2012; Silva Albequerque et al., 2015; Verdaguer et al., 2015; Huh et al., 2016; Mahar et al., 2016; Cattaud et al., 2018; Zallo et al., 2018; Giesers and Wirths, 2020; Seo et al., 2021; Li et al., 2022). In contrast, a few studies using different amyloid and tau models show resilience (Verdaguer et al., 2015; Ahnaou et al., 2017; Sos et al., 2020; Morrone et al., 2022). Comparing the CA1 layers, PV INs in *stratum pyramidale* are most vulnerable to degeneration, followed by those in *stratum oriens* (Villette et al., 2012; Silva Albequerque et al., 2015; Mahar et al., 2016).

TABLE 1 Summary of interneuron changes and impact in human AD and AD rodent models.

Interneuron subtype	Loss in human AD	Loss in rodent AD models	Excitability change	Network hyperexcitability	Disrupted oscillations	LTP deficits
PV	Loss in CA1	Loss in CA1	Hypoactivity	Yes	Yes	Yes
CCK	?	Inconsistent	Hyperactivity	?	?	?
SST	Unchanged in hippocampus	Loss in CA1-3	Hyperactivity	?	Yes	?
VIP CR^+	Loss in DG	Inconsistent	Hypoactivity	Yes	?	?
NPY	Loss in DG, CA1, S	Loss in DG, CA1-3, S	?	?	?	?

Table of the heterogeneity of IN vulnerability in the hippocampus in human patients of AD, as well as in AD mouse models.

The degenerating or remaining PV INs appear to also have a critical role in modulating excitation-inhibition balance, plasticity, and network oscillations during the course of disease. Loss of excitatory drive to PV INs, in particular from EC Layer 2, leads to excitation-inhibition balance disruption, which can be rescued with optogenetically-driven plasticity (Xiao et al., 2017; Yang et al., 2018). Intrinsically, PV INs show an NaV1.1 channelopathy in the J20 amyloid model, which reduces their function and leads to epileptiform activity in the brain (Verret et al., 2012). With regard to plasticity, PV INs also mediate amyloid-induced suppression of CA3 → CA1 long term potentiation (Huh et al., 2016; Zhang et al., 2017). Oscillatory behavior of the hippocampus is altered in AD models, and amyloid impact on PV interneurons appears to play a critical role (Hollnagel et al., 2019; Chung et al., 2020; Park et al., 2020).

PV INs also appear to have relationship to AD pathology that are intriguing areas for future work. Through their impact on network excitability, PV INs not only promote hyperexcitability, a process that may give rise more pathology, but also can induce vulnerability to further amyloid-induced damage (Hijazi et al., 2019, 2020). Moreover, in APP/PS1 mice (AD model with human amyloid-beta precursor protein and presenilin-1 mutations), PV INs show close interactions with microglia (Gervais et al., 2022). However, another study has called in to question the relationship between PV INs and AD pathogenesis (Mackenzie-Gray Scott et al., 2022). Of note, PV INs also express amyloid-degrading enzymes which would indeed be counterintuitive (Pacheco-Quinto et al., 2016).

While PV INs have been extensively studied in the context of AD, many further questions have arisen. In particular, reconciling how they promote hyperexcitability while also suppressing plasticity is needed to better understand how chronic PV IN dysfunction alters the course of disease. Furthermore, PV INs are themselves heterogeneous, and it is not clear if subtypes are differentially affected. Notably, in 5×FAD mice, an AD model harboring 5 familial AD mutations, the soma-targeting PV basket cells are affected, reducing their activity during sharp wave ripples, whereas the bistratified and axo-axonic subpopulations were unchanged (Caccavano et al., 2020). Lastly, there has been limited study on the physiologic impact of tauopathy on PV INs.

CCK INs

CCK hormone, highly expressed in the hippocampus, has been suggested to enhance healthy mnemonic functions and serves as a biomarker of cognitive and neuronal integrity in neurodegenerative disease (Plagman et al., 2019; Zhang et al., 2022). There have been few studies specifically examining CCK INs, relative to their extensive study in non-pathologic settings, and these are primarily limited to rodent models featuring or exposed to amyloid pathology. Those examining CCK expression or total number show varied results. Whereas intraventricular injection of amyloid does not alter CCK mRNA levels in the hippocampus (Aguado-Llera et al., 2018), and the number of CCK INs in CA1 (in SO) remained unchanged with intrahippocampal injection of amyloid (Villette et al., 2012), APP/PS1 mice feature a reduction of CB1R-expressing CCK interneurons in DG and CA1 (He et al., 2021). While these differences may arise from exogenous versus endogenous exposure to amyloid, it is also possible that CCK IN subpopulations show a differential vulnerability. In addition, CCK INs appear to undergo physiologic changes to their synaptic drive and overall excitability. In the APP KI model, these interneurons feature signs of reduced inhibitory input (Petrache et al., 2020; Shi et al., 2020) and show early hyperactivity that precedes amyloid accumulation, which is then followed by reduction in GABA production (Shi et al., 2020). The above studies suggest that AD-induced changes in CCK INs function may play a critical role in cognitive deficits and promoting disease progression. Of note, cannabinoids (CB) that target CB1R-expressing CCK INs show promising effects in reducing amyloid plaque deposition and hyperphosphorylation of tau (Aso and Ferrer, 2014; Aguirre-Rueda et al., 2015; Abate et al., 2021; Xiong and Lim, 2021; Khavandi et al., 2023). As such, further studies examining subtypes of CCK INs and their impact on function and pathology are needed. Moreover, the relationship between tau pathology and these interneurons have not been studied, despite suggestion of a relationship in human AD (Lenders et al., 1989). Further study of CCK INs in human AD is also needed.

SST INs

As a critical modulator of pyramidal neuron dendritic excitability, SST INs have been the focus of several studies. Importantly, there is no difference in SST INs counts in AD and control human cases (Waller et al., 2020), suggesting that they may be largely resilient to neurodegeneration. This finding is recapitulated in the TauPS2APP (Loreth et al., 2012) and hAPP (Palop et al., 2007) rodent models. In contrast, loss of SST mRNA is found with intraventricular injection of amyloid in rat (Aguado-Llera et al., 2018), and SST INs loss appears in the mouse 5xFAD and PS1xAPP and rat TgF344-AD models (Ramos et al., 2006; Li et al., 2022; Morrone et al., 2022). A reason for these discrepancies, beyond choice of animal model, may because SST INs vulnerability is location- and subtype-specific. Indeed, hippocampal amyloid injection causes loss of subset of SST INs in CA1 *stratum oriens* that do no co-express NPY or PV (Villette et al., 2012). In the TgCRND8 amyloid model, there is a subregion- and lamina-specific decrease of SST-expressing interneurons primarily in *stratum oriens* of CA1, CA2 and stratum radiatum of CA3 (Silva Albequerque et al., 2015).

SST INs may also play a more active role in AD as other studies have evaluated SST INs physiology and relationship to AD pathogenesis. For example, CA1 SST INs show early hyperactivity in the APP KI model preceding amyloid accumulation, which is then followed by reduction in GABA production (Shi et al., 2020). Relatedly, the impact of A-beta oligomers on hippocampal oscillations is suggested to be mediated by effects on SST INs (Chung et al., 2020; Park et al., 2020). In APP/PS1 mice, SST INs show increased interactions with microglia (Gervais et al., 2022). Interestingly, SST INs may directly modulate AD pathology. SST INs express amyloid-degrading enzymes (Pacheco-Quinto et al., 2016). Examination of human AD pathology suggests a relationship of SST INs to the development of tau pathology (Lenders et al., 1989).

In summary, SST INs present an intriguing target for modulating AD pathophysiology due to their targeting of pyramidal neuron dendrites, partial resilience to neurodegeneration, and potential influence over amyloidosis and tauopathy. Open questions remain

over their exact influence on cognitive and behavioral deficits in the context of hippocampal circuits and the efficacy of leveraging this knowledge to improve hippocampal function and counteract AD pathogenesis.

CR co-expressing VIP INs

There are several studies examining CR-expressing INs, which often co-express VIP and mediate disinhibition, as discussed above. In human AD hippocampus, loss of CR immunoreactivity is found in DG (Takahashi et al., 2010). In rodent models of AD featuring amyloid or both amyloid and tau, evidence is inconsistent that CR INs degenerate in various hippocampal subregions (Baglietto-Vargas et al., 2010; Takahashi et al., 2010; Loreth et al., 2012; Aguado-Llera et al., 2018; Zallo et al., 2018; Giesers and Wirths, 2020; Shi et al., 2020; Li et al., 2022). Physiologic characterization has demonstrated that in CA1 they have unchanged intrinsic excitability but show hyper-inhibition through upregulated purinoreceptors in an APP KI model (Shi et al., 2020). Given their targeting of interneuron, this associates with pyramidal neuron hyperexcitability. Together, these results imply that CR-expressing INs may be spared during AD in some subregions, and could thus be a potential target for pharmacological and therapeutic intervention. Furthermore, there is promising evidence that VIP peptide secreted by VIP INs alongside GABA contributes to neuroprotection and neurotrophic processes, and inhibits Aβ induced neurodegeneration by suppressing microglial secreted neurotoxic factors (Song et al., 2012; Korkmaz et al., 2019). Further studies are needed to more directly elucidate the impact of altered disinhibition by CR, VIP, and CR^+/VIP^+ INs populations on hippocampal function and related behaviors.

NPY INs

As mentioned above, NPY expression defines a heterogeneous population of INs that co-express other molecular markers and have unique functions in non-pathologic settings. Most work on NPY interneurons has been centered on quantifying expression levels or neurodegeneration. In human AD there is a reduction in NPY that is most prominent in the DG hilus, CA1, and parasubiculum (Chan-Palay et al., 1986). Intraventricular injection of amyloid in rat reduces NPY mRNA levels in the hippocampus (Aguado-Llera et al., 2018). At a subregion level, the human pattern is largely mimicked in rodent AD models with amyloidosis and dual pathology, with some models also demonstrating CA3 and CA2 vulnerability (Palop et al., 2007; Loreth et al., 2012; Silva Albequerque et al., 2015; Mahar et al., 2016). Additional complexity to alteration of the NPY INs network is suggested by laminar-specific vulnerability, with stratum pyramidale most consistently vulnerable (Villette et al., 2012; Mahar et al., 2016), alterations of NPY-subtype expression (Palop et al., 2007), and findings that NPY-expression identifies SST INs most vulnerable to degeneration (Ramos et al., 2006). Open questions remain on the impact of this region-specific vulnerability on hippocampal function and related behaviors. Furthermore, as NPY can subcategorize other IN types, it is unclear if AD-related physiologic alterations also occur based on NPY expression. Additional work is also needed to investigate possible changes in their excitability and impact of this on plasticity and network activity.

Conclusion

Given their diversity, GABAergic circuits play a wide range of critical roles – from modulation of single-neuron and network activity in a compartment- and layer-specific manner, to acting as gain control switches or knobs to modulate the dynamics between excitation-inhibition-disinhibition, to synchronizing distant brain areas and creating spatio-temporal windows for integration, coincidence-detection and signal-to-noise modulation. As highlighted above, there is surmounting evidence that specific GABAergic circuits in the hippocampus may be involved in the pathology and progression of AD. In this context, several open questions remain regarding their differential engagement with pyramidal neuron subtypes (Masurkar, 2018), their role in dysregulated information processing, plasticity, and network activity, and their impact on behavioral deficits and disease progression. Notably, while their specific role in AD is yet to be explored, the more recently discovered long-range GABAergic projections support inter-regional coordination of activity and context discrimination. Given their disinhibitory role in area CA1, the dysfunction of these LRIPs in AD might disrupt spatial and non-spatial memory processing. These modifications, may elicit hyperactivity and increased plasticity to exacerbate the spread of AD pathology and neurodegeneration. This warrants future studies using mouse models of AD as well as proteomics and transcriptomics-based studies in human patients to examine the pathological vulnerability of specific types of long-range inhibitory projections (regional: MEC vs. LEC; cell-type: SST- vs. PV- vs. VIP-expressing) and their downstream interactions. Such information will be important for correlating their dysfunction with disease pathology and cognitive and physiological phenotypes and identifying potential targets for therapeutic intervention (Figure 5).

Author contributions

MH-F, AM, and JB: planning and conceptualization. MH-F, OB, AM, and JB: manuscript preparation. MH-F prepared the figures with input from OB and JB. AM prepared the table. All authors contributed to the article and approved the submitted version.

Funding

This work was supported by NIH NINDS 1R01NS109362-01, BRAIN INITIATIVE NIH NINDS 1R01NS109994, Mathers Charitable Foundation Investigator Award, McKnight Scholar Award in Neuroscience, Klingenstein-Simons Fellowship Award in Neuroscience, Alfred P. Sloan Research Fellowship, Whitehall Research Grant, American Epilepsy Society Junior Investigator Award, Blas Frangione Young Investigator Research Grant, New York University Whitehead Fellowship for Junior Faculty in Biomedical and Biological Sciences, and Leon Levy Foundation Award to JB. JB was supported by Alzheimer's Association grant AARGD-NTF-23-1151101, NIH NCATS NYU Clinical and Translational Science Institute (CTSI) Pilot Project: UL1TR001445 and Parekh Center for Interdisciplinary Neurology (PCIN) Pilot Research Program 2023. AM and JB were jointly supported by an NIH RF1AG072507. AM was supported by NIH grants RF1AG072507, R21AG070880, and P30AG066512, Alzheimer's Association grant AACF-17-524288, BrightFocus Foundation grant A2019602S, and support from

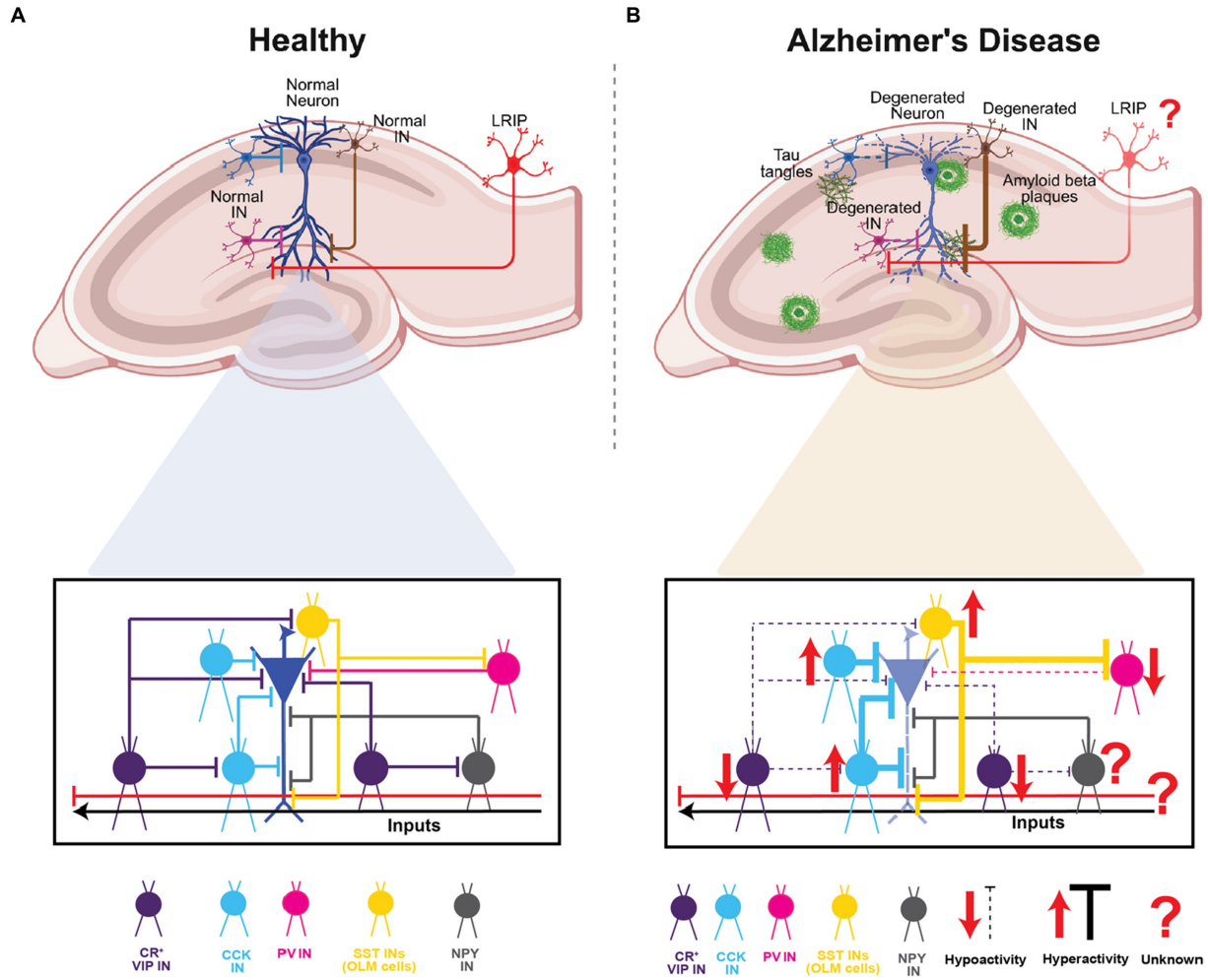

FIGURE 5
Summary of CA1 INs in health and Alzheimer's disease. **(A)** Schematic representation of the hippocampal area and a normal pyramidal neuron of CA1 highlighting the INs subtypes and the inhibition and disinhibition processes in healthy circuit. **(B)** Schematic representation of the hippocampal area and a degenerated pyramidal neuron of CA with amyloid plaques depositions and Tau tangles. In lower panel highlighting the INs subtypes and the dysregulation of hyperexcitability or hypoexcitability processes found in AD. Top panels of **(A,B)**, created with BioRender.

the Blas Frangione and Leon Levy Foundations. MH-F was supported by REC Scholar Program of NYU Alzheimer's Disease Center (ADRC) P30 AG066512 and the Alzheimer's Association grant 23AARFD-1026841. OB was supported by the NIH 5T32NS86750 and REC Scholar Program of NYU Alzheimer's Disease Center (ADRC) P30 AG066512.

Conflict of interest

The authors declare that the research was conducted in the absence of any commercial or financial relationships that could be construed as a potential conflict of interest.

Publisher's note

All claims expressed in this article are solely those of the authors and do not necessarily represent those of their affiliated organizations, or those of the publisher, the editors and the reviewers. Any product that may be evaluated in this article, or claim that may be made by its manufacturer, is not guaranteed or endorsed by the publisher.

References

Abate, G., Uberti, D., and Tambaro, S. (2021). Potential and limits of cannabinoids in Alzheimer's disease therapy. *Biology* 10. doi: 10.3390/biology 10060542

Abs, E., Poorthuis, R. B., Apelblat, D., Muhammad, K., Pardi, M. B., Enke, L., et al. (2018). Learning-related plasticity in dendrite-targeting layer 1 interneurons. *Neuron* 100, 684–699.e6. doi: 10.1016/j.neuron.2018.09.001

Acsády, L., Görcs, T. J., and Freund, T. F. (1996). Different populations of vasoactive intestinal polypeptide-immunoreactive interneurons are specialized to control pyramidal cells or interneurons in the hippocampus. *Neuroscience* 73, 317–334. doi: 10.1016/0306-4522(95)00609-5

Adesnik, H. (2018). Layer-specific excitation/inhibition balances during neuronal synchronization in the visual cortex. *J. Physiol.* 596, 1639–1657. doi: 10.1113/JP274986

Aguado-Llera, D., Canelles, S., Frago, L. M., Chowen, J. A., Argente, J., Arilla, E., et al. (2018). The protective effects of IGF-I against β-amyloid-related downregulation of hippocampal somatostatinergic system involve activation of Akt and protein kinase a. *Neuroscience* 374, 104–118. doi: 10.1016/j.neuroscience.2018.01.041

Aguirre-Rueda, D., Guerra-Ojeda, S., Aldasoro, M., Iradi, A., Obrador, E., Mauricio, M. D., et al. (2015). WIN 55, 212-2, agonist of cannabinoid receptors, prevents amyloid β1-42 effects on astrocytes in primary culture. *PLoS One* 10, 1–42. doi: 10.1371/JOURNAL.PONE.0122843

Ahnaou, A., Moechars, D., Raeymaekers, L., Biermans, R., Manyakov, N. V., Bottelbergs, A., et al. (2017). Emergence of early alterations in network oscillations and functional connectivity in a tau seeding mouse model of Alzheimer's disease pathology. *Sci. Rep.* 7, 1–14. doi: 10.1038/s41598-017-13839-6

Amaral, D. G., and Witter, M. P. (1989). The three-dimensional organization of the hippocampal formation: a review of anatomical data. *Neuroscience* 31, 571–591. doi: 10.1016/0306-4522(89)90424-7

Armstrong, C., Krook-Magnuson, E., and Soltesz, I. (2012). Neurogliaform and ivy cells: a major family of nNOS expressing GABAergic neurons. *Front. Neural Circ.* 6, 1–10. doi: 10.3389/FNCIR.2012.00023

Artinian, J., and Lacaille, J. C. (2018). Disinhibition in learning and memory circuits: new vistas for somatostatin interneurons and long-term synaptic plasticity. *Brain Res. Bull.* 141, 20–26. doi: 10.1016/j.brainresbull.2017.11.012

Ascoli, G. A., Alonso-Nanclares, L., Anderson, S. A., Barrionuevo, G., Benavides-Piccione, R., Burkhalter, A., et al. (2008). Petilla terminology: nomenclature of features of GABAergic interneurons of the cerebral cortex. *Neuroscience* 9, 557–568. doi: 10.1038/nrn2402

Askew, C. E., Lopez, A. J., Wood, M. A., and Metherate, R. (2019). Nicotine excites VIP interneurons to disinhibit pyramidal neurons in auditory cortex. *Synapse* 73. doi: 10.1002/syn.22116

Aso, E., and Ferrer, I. (2014). Cannabinoids for treatment of Alzheimer's disease: moving toward the clinic. *Front. Pharmacol.* 5:37. doi: 10.3389/fphar.2014.00037

Baglietto-Vargas, D., Moreno-Gonzalez, I., Sanchez-Varo, R., Jimenez, S., Trujillo-Estrada, L., Sanchez-Mejias, E., et al. (2010). Calretinin interneurons are early targets of extracellular amyloid-beta pathology in PS1/AbetaPP Alzheimer mice hippocampus. *J. Alzheimer's Dis.* 21, 119–132. doi: 10.3233/JAD-2010-100066

Barnes, C. A., Mcnaughton, B. L., Goddard, G. V., Douglas, R. M., and Adamec, R. (1977). Circadian rhythm of synaptic excitability in rat and monkey central nervous system. *Science* 197, 91–92. doi: 10.1126/science.194313

Bartos, M., and Elgueta, C. (2012). Functional characteristics of parvalbumin- and cholecystokinin-expressing basket cells. *J. Physiol.* 590, 669–681. doi: 10.1113/jphysiol.2011.226175

Bartos, M., Vida, I., and Jonas, P. (2007). Synaptic mechanisms of synchronized gamma oscillations in inhibitory interneuron networks. *Nat. Rev. Neurosci.* 8, 45–56. doi: 10.1038/nrn2044

Basu, J., and Siegelbaum, S. A. (2015). The Corticohippocampal circuit, synaptic plasticity, and memory. *Cold Spring Harb. Perspect. Biol.* 7, 1–27. doi: 10.1101/cshperspect.a021733

Basu, J., Srinivas, K. V., Cheung, S. K., Taniguchi, H., Huang, Z. J., and Siegelbaum, S. A. (2013). A Cortico-hippocampal learning rule shapes inhibitory microcircuit activity to enhance hippocampal information flow. *Neuron* 79, 1208–1221. doi: 10.1016/j.neuron.2013.07.001

Basu, J., Zaremba, J. D., Cheung, S. K., Hitti, F. L., Zemelman, B. V., Losonczy, A., et al. (2016). Gating of hippocampal activity, plasticity, and memory by entorhinal cortex long-range inhibition. *Science* 351. doi: 10.1126/science.aaa5694

Bell, L. A., Bell, K. A., and McQuiston, A. R. (2015). Acetylcholine release in mouse hippocampal CA1 preferentially activates inhibitory-selective interneurons via α4β2* nicotinic receptor activation. *Front. Cell. Neurosci.* 9:134226. doi: 10.3389/FNCEL.2015.00115/BIBTEX

Bennett, D. A., Schneider, J. A., Bienias, J. L., Evans, D. A., and Wilson, R. S. (2005). Mild cognitive impairment is related to Alzheimer disease pathology and cerebral infarctions. *Neurology* 64, 834–841. doi: 10.1212/01.WNL.0000152982.47274.9E

Bezaire, M. J., Raikov, I., Burk, K., Vyas, D., and Soltesz, I. (2016). Interneuronal mechanisms of hippocampal theta oscillations in a full-scale model of the rodent CA1 circuit. *elife* 5. doi: 10.7554/ELIFE.18566

Bezaire, M. J., and Soltesz, I. (2013). Quantitative assessment of CA1 local circuits: knowledge base for interneuron-pyramidal cell connectivity. *Hippocampus* 23, 751–785. doi: 10.1002/hipo.22141

Bilash, O. M., Chavlis, S., Johnson, C. D., Poirazi, P., and Basu, J. (2023). Lateral entorhinal cortex inputs modulate hippocampal dendritic excitability by recruiting a local disinhibitory microcircuit. *Cell Rep.* 42. doi: 10.1016/j.celrep.2022.111962

Bittner, K. C., Grienberger, C., Vaidya, S. P., Milstein, A. D., Macklin, J. J., Suh, J., et al. (2015). Conjunctive input processing drives feature selectivity in hippocampal CA1 neurons. *Nat. Neurosci.* 18, 1133–1142. doi: 10.1038/nn.4062

Bittner, K. C., Milstein, A. D., Grienberger, C., Romani, S., and Magee, J. C. (2017). Behavioral time scale synaptic plasticity underlies CA1 place fields. *Science* 357, 1033–1036. doi: 10.1126/science.aan3846

Bloss, E. B., Cembrowski, M. S., Karsh, B., Colonell, J., Fetter, R. D., and Spruston, N. (2016). Structured dendritic inhibition supports branch-selective integration in CA1 pyramidal cells. *Neuron* 89, 1016–1030. doi: 10.1016/j.neuron.2016.01.029

Braak, H., and Braak, E. (1991). Neuropathological stageing of Alzheimer-related changes. *Acta Neuropathol.* 82, 239–259. doi: 10.1007/BF00308809

Brady, D. R., and Mufson, E. J. (1997). Parvalbumin-immunoreactive neurons in the hippocampal formation of Alzheimer's diseased brain. *Neuroscience* 80, 1113–1125. doi: 10.1016/S0306-4522(97)00068-7

Bridi, M. C. D., Zong, F. J., Min, X., Luo, N., Tran, T., Qiu, J., et al. (2020). Daily oscillation of the excitation-inhibition balance in visual cortical circuits. *Neuron* 105, 621–629.e4. doi: 10.1016/j.neuron.2019.11.011

Buhl, E. H., Halasy, K., and Somogyi, P. (1994). Diverse sources of hippocampal unitary inhibitory postsynaptic potentials and the number of synaptic release sites. *Nature* 368, 823–828. doi: 10.1038/368823a0

Busche, M. A., Kekuš, M., Adelsberger, H., Noda, T., Förstl, H., Nelken, I., et al. (2015). Rescue of long-range circuit dysfunction in Alzheimer's disease models. *Nat. Neurosci.* 18, 1623–1630. doi: 10.1038/nn.4137

Busche, M. A., and Konnerth, A. (2016). Impairments of neural circuit function in Alzheimer's disease. *Philos. Trans. R. Soc. Lond., B, Biol. Sci.* 371. doi: 10.1098/rstb.2015.0429

Buzsaki, G. (1984). Feed-forward inhibition in the hippocampal formation. *Prog. Neurobiol.* 22, 131–153. doi: 10.1016/0301-0082(84)90023-6

Buzsáki, G. (2002). Theta oscillations in the hippocampus. *Neuron* 33, 325–340. doi: 10.1016/S0896-6273(02)00586-X

Buzsáki, G. (2015). Hippocampal sharp wave-ripple: a cognitive biomarker for episodic memory and planning. *Hippocampus* 25, 1073–1188. doi: 10.1002/hipo.22488

Caccavano, A., Lorenzo Bozzelli, P., Forcelli, P. A., Pak, D. T. S., Wu, J. Y., Conant, K., et al. (2020). Inhibitory Parvalbumin basket cell activity is selectively reduced during hippocampal sharp wave ripples in a mouse model of familial Alzheimer's disease. *J. Neurosci.* 40, 5116–5136. doi: 10.1523/JNEUROSCI.0425-20.2020

Capogna, M. (2011). Neurogliaform cells and other interneurons of stratum lacunosum-moleculare gate entorhinal-hippocampal dialogue. *J. Physiol.* 589, 1875–1883. doi: 10.1113/jphysiol.2010.201004

Caputi, A., Melzer, S., Michael, M., and Monyer, H. (2013). The long and short of GABAergic neurons. *Curr. Opin. Neurobiol.* 23, 179–186. doi: 10.1016/j.conb.2013.01.021

Castillo, P. E., Younts, T. J., Chávez, A. E., and Hashimotodani, Y. (2012). Endocannabinoid signaling and synaptic function. *Neuron* 76, 70–81. doi: 10.1016/j.neuron.2012.09.020

Cattaud, V., Bezzina, C., Rey, C. C., Lejards, C., Dahan, L., and Verret, L. (2018). Early disruption of parvalbumin expression and perineuronal nets in the hippocampus of the Tg2576 mouse model of Alzheimer's disease can be rescued by enriched environment. *Neurobiol. Aging* 72, 147–158. doi: 10.1016/j.neurobiolaging.2018.08.024

Cembrowski, M. S., Wang, L., Sugino, K., Shields, B. C., and Spruston, N. (2016). Hipposeq: a comprehensive RNA-seq database of gene expression in hippocampal principal neurons. *elife* 5. doi: 10.7554/ELIFE.14997

Chamberland, S., Nebet, E. R., Valero, M., Hanani, M., Egger, R., Larsen, S. B., et al. (2023). Brief synaptic inhibition persistently interrupts firing of fast-spiking interneurons. *Neuron*. 111, 1264–1281. doi: 10.1016/j.neuron.2023.01.017

Chamberland, S., and Topolnik, L. (2012). Inhibitory control of hippocampal inhibitory neurons. *Front. Neurosci.* 6:165. doi: 10.3389/FNINS.2012.00165/BIBTEX

Chan-Palay, V., Lang, W., Haesler, U., Köhler, C., and Yasargil, G. (1986). Distribution of altered hippocampal neurons and axons immunoreactive with antisera against neuropeptide Y in Alzheimer's-type dementia. *J. Comp. Neurol.* 248, 376–394. doi: 10.1002/cne.902480307

Chevaleyre, V., and Castillo, P. E. (2003). Heterosynaptic LTD of hippocampal GABAergic synapses: a novel role of endocannabinoids in regulating excitability. *Neuron* 38, 461–472. doi: 10.1016/S0896-6273(03)00235-6

Chevaleyre, V., Heifets, B. D., Kaeser, P. S., Südhof, T. C., Purpura, D. P., and Castillo, P. E. (2007). Endocannabinoid-mediated long-term plasticity requires cAMP/PKA signaling and RIM1alpha. *Neuron* 54, 801–812. doi: 10.1016/j.neuron.2007.05.020

Chevaleyre, V., and Siegelbaum, S. A. (2010). Strong CA2 pyramidal neuron synapses define a powerful disynaptic cortico-hippocampal loop. *Neuron* 66, 560–572. doi: 10.1016/j.neuron.2010.04.013

Chung, H., Park, K., Jang, H. J., Kohl, M. M., and Kwag, J. (2020). Dissociation of somatostatin and parvalbumin interneurons circuit dysfunctions underlying hippocampal theta and gamma oscillations impaired by amyloid β oligomers in vivo. *Brain Struct. Funct.* 225, 935–954. doi: 10.1007/s00429-020-02044-3

Cirrito, J. R., Yamada, K. A., Finn, M. B., Sloviter, R. S., Bales, K. R., May, P. C., et al. (2005). Synaptic activity regulates interstitial fluid amyloid-beta levels in vivo. *Neuron* 48, 913–922. doi: 10.1016/j.neuron.2005.10.028

Cohen, N. J., and Squire, L. R. (1980). Preserved learning and retention of pattern-analyzing skill in amnesia: dissociation of knowing how and knowing that. *Science* 210, 207–210. doi: 10.1126/science.7414331

Colangelo, V., Schurr, J., Ball, M. J., Pelaez, R. P., Bazan, N. G., and Lukiw, W. J. (2002). Gene expression profiling of 12633 genes in Alzheimer hippocampal CA1: transcription and neurotrophic factor down-regulation and up-regulation of apoptotic and pro-inflammatory signaling. *J. Neurosci. Res.* 70, 462–473. doi: 10.1002/jnr.10351

Cope, D. W., Maccaferri, G., Márton, L. F., Roberts, J. D. B., Cobden, P. M., and Somogyi, P. (2002). Cholecystokinin-immunopositive basket and Schaffer collateral-associated interneurones target different domains of pyramidal cells in the CA1 area of the rat hippocampus. *Neuroscience* 109, 63–80. doi: 10.1016/S0306-4522(01)00440-7

Counts, S. E., Alldred, M. J., Che, S., Ginsberg, S. D., and Mufson, E. J. (2014). Synaptic gene dysregulation within hippocampal CA1 pyramidal neurons in mild cognitive impairment. *Neuropharmacology* 79, 172–179. doi: 10.1016/j.neuropharm.2013.10.018

Csicsvari, J., Hirase, H., Czurkó, A., Mamiya, A., and Buzsáki, G. (1999). Oscillatory coupling of hippocampal pyramidal cells and interneurons in the behaving rat. *J. Neurosci.* 19:274. doi: 10.1523/JNEUROSCI.19-01-00274.1999

Cuestas Torres, D. M., and Cardenas, F. P. (2020). Synaptic plasticity in Alzheimer's disease and healthy aging. *Rev. Neurosci.* 31, 245–268. doi: 10.1515/REVNEURO-2019-0058

Cutsuridis, V., Cobb, S., and Graham, B. P. (2010). Encoding and retrieval in a model of the hippocampal CA1 microcircuit. *Hippocampus* 20, 423–446. doi: 10.1002/hipo.20661

Cutsuridis, V., and Taxidis, J. (2013). Deciphering the role of CA1 inhibitory circuits in sharp wave-ripple complexes. *Front. Syst. Neurosci.* 7:13. doi: 10.3389/FNSYS.2013.00013

De Calignon, A., Polydoro, M., Suárez-Calvet, M., William, C., Adamowicz, D. H., Kopeikina, K. J., et al. (2012). Propagation of tau pathology in a model of early Alzheimer's disease. *Neuron* 73, 685–697. doi: 10.1016/j.neuron.2011.11.033

Degro, C. E., Kulik, A., Booker, S. A., and Vida, I. (2015). Compartmental distribution of GABAB receptor-mediated currents along the somatodendritic axis of hippocampal principal cells. *Front. Synap. Neurosci.* 7:6. doi: 10.3389/FNSYN.2015.00006

Del Pino, I., Brotons-Mas, J. R., Marques-Smith, A., Marighetto, A., Frick, A., Marín, O., et al. (2017). Abnormal wiring of CCK+ basket cells disrupts spatial information coding. *Nat. Neurosci.* 20:784. doi: 10.1038/nn.4544

Dimidschstein, J., Chen, Q., Tremblay, R., Rogers, S. L., Saldi, G. A., Guo, L., et al. (2016). A viral strategy for targeting and manipulating interneurons across vertebrate species. *Nat. Neurosci.* 19:1743. doi: 10.1038/nn.4430

Dudok, B., Klein, P. M., Hwaun, E., Lee, B. R., Yao, Z., Fong, O., et al. (2021a). Alternating sources of perisomatic inhibition during behavior. *Neuron* 109, 997–1012.e9. doi: 10.1016/J.NEURON.2021.01.003

Dudok, B., Klein, P. M., and Soltesz, I. (2022). Toward understanding the diverse roles of Perisomatic interneurons in epilepsy. *Epilepsy Curr.* 22:54. doi: 10.1177/15357597211053687

Dudok, B., and Soltesz, I. (2022). Imaging the endocannabinoid signaling system. *J. Neurosci. Methods* 367:109451. doi: 10.1016/j.jneumeth.2021.109451

Dudok, B., Szoboszlay, M., Paul, A., Klein, P. M., Liao, Z., Hwaun, E., et al. (2021b). Recruitment and inhibitory action of hippocampal axo-axonic cells during behavior. *Neuron* 109, 3838–3850.e8. doi: 10.1016/J.NEURON.2021.09.033

Eichenbaum, H. (2000). A cortical-hippocampal system for declarative memory. *Neuroscience* 1, 41–50. doi: 10.1038/35036213

Eichenbaum, H., Sauvage, M., Fortin, N., Komorowski, R., and Lipton, P. (2012). Towards a functional organization of episodic memory in the medial temporal lobe. *Neurosci. Biobehav. Rev.* 36, 1597–1608. doi: 10.1016/j.neubiorev.2011.07.006

Elfant, D., Pál, B. Z., Emptage, N., and Capogna, M. (2008). Specific inhibitory synapses shift the balance from feedforward to feedback inhibition of hippocampal CA1 pyramidal cells. *Eur. J. Neurosci.* 27, 104–113. doi: 10.1111/j.1460-9568.2007.06001.x

English, D. F., McKenzie, S., Evans, T., Kim, K., Yoon, E., and Buzsáki, G. (2017). Pyramidal cell-interneuron circuit architecture and dynamics in hippocampal networks. *Neuron* 96, 505–520.e7. doi: 10.1016/j.neuron.2017.09.033

Evangelista, R., Cano, G., Cooper, C., Schmitz, D., Maier, N., and Kempter, R. (2020). Generation of sharp wave-ripple events by disinhibition. *J. Neurosci.* 40, 7811–7836. doi: 10.1523/JNEUROSCI.2174-19.2020

Eyre, M. D., and Bartos, M. (2019). Somatostatin-expressing interneurons form axonal projections to the contralateral Hippocampus. *Front. Neural Circ.* 13:56. doi: 10.3389/fncir.2019.00056

Fanselow, M. S., and Dong, H. W. (2010). Are the dorsal and ventral hippocampus functionally distinct structures? *Neuron* 65, 7–19. doi: 10.1016/j.neuron.2009.11.031

Ferrante, M., and Ascoli, G. A. (2015). Distinct and synergistic feedforward inhibition of pyramidal cells by basket and bistratified interneurons. *Front. Cell. Neurosci.* 9:165037. doi: 10.3389/FNCEL.2015.00439/BIBTEX

Francavilla, R., Luo, X., Magnin, E., Tyan, L., and Topolnik, L. (2015). Coordination of dendritic inhibition through local disinhibitory circuits. *Front. Synap. Neurosci.* 7:5. doi: 10.3389/FNSYN.2015.00005/BIBTEX

Francavilla, R., Villette, V., Luo, X., Chamberland, S., Muñoz-Pino, E., Camiré, O., et al. (2018). Connectivity and network state-dependent recruitment of long-range VIP-GABAergic neurons in the mouse hippocampus. *Nat. Commun.* 9. doi: 10.1038/s41467-018-07162-5

Freund, T. F., and Katona, I. (2007). Perisomatic inhibition. *Neuron* 56, 33–42. doi: 10.1016/j.neuron.2007.09.012

Fuchs, E. C., Zivkovic, A. R., Cunningham, M. O., Middleton, S., LeBeau, F. E. N., Bannerman, D. M. M., et al. (2007). Recruitment of parvalbumin-positive interneurons determines hippocampal function and associated behavior. *Neuron* 53, 591–604. doi: 10.1016/j.neuron.2007.01.031

Geiller, T., Vancura, B., Terada, S., Troullinou, E., Chavlis, S., Tsagkatakis, G., et al. (2020). Large-scale 3D two-photon imaging of molecularly identified CA1 interneuron dynamics in behaving mice. *Neuron* 108, 968–983.e9. doi: 10.1016/j.neuron.2020.09.013

Germroth, P., Schwerdtfeger, W. K., and Buhl, E. H. (1989). GABAergic neurons in the entorhinal cortex project to the hippocampus. *Brain Res.* 494, 187–192. doi: 10.1016/0006-8993(89)90162-5

Gervais, É., Iloun, P., Martianova, E., Gonçalves Bessa, A. C., Rivest, S., and Topolnik, L. (2022). Structural analysis of the microglia–interneuron interactions in the CA1 hippocampal area of the APP/PS1 mouse model of Alzheimer's disease. *J. Comp. Neurol.* 530, 1423–1437. doi: 10.1002/cne.25289

Gidon, A., and Segev, I. (2012). Principles governing the operation of synaptic inhibition in dendrites. *Neuron* 75, 330–341. doi: 10.1016/j.neuron.2012.05.015

Giesers, N. K., and Wirths, O. (2020). Loss of hippocampal calretinin and parvalbumin interneurons in the 5XFAD mouse model of Alzheimer's disease. *ASN Neuro* 12. doi: 10.1177/1759091420925356

Ginsberg, S. D., Alldred, M. J., and Che, S. (2012). Gene expression levels assessed by CA1 pyramidal neuron and regional hippocampal dissections in Alzheimer's disease. *Neurobiol. Dis.* 45, 99–107. doi: 10.1016/j.nbd.2011.07.013

Ginsberg, S. D., Alldred, M. J., Counts, S. E., Cataldo, A. M., Neve, R. L., Jiang, Y., et al. (2010). Microarray analysis of hippocampal CA1 neurons implicates early endosomal dysfunction during Alzheimer's disease progression. *Biol. Psychiatry* 68, 885–893. doi: 10.1016/j.biopsych.2010.05.030

Giustiniani, A., Danesin, L., Bozzetto, B., Macina, A., Benavides-Varela, S., and Burgio, F. (2022). Functional changes in brain oscillations in dementia: a review. *Rev. Neurosci.* 34, 25–47. doi: 10.1515/REVNEURO-2022-0010

Glickfeld, L. L., Atallah, B. V., and Scanziani, M. (2008). Complementary modulation of somatic inhibition by opioids and cannabinoids. *J. Neurosci.* 28, 1824–1832. doi: 10.1523/JNEUROSCI.4700-07.2008

Glickfeld, L. L., Roberts, J. D., Somogyi, P., and Scanziani, M. (2009). Interneurons hyperpolarize pyramidal cells along their entire somatodendritic axis. *Nat. Neurosci.* 12, 21–23. doi: 10.1038/nn.2230

Glickfeld, L. L., and Scanziani, M. (2006). Distinct timing in the activity of cannabinoid-sensitive and cannabinoid-insensitive basket cells. *Nat. Neurosci.* 9:807. doi: 10.1038/nn1688

Grienberger, C., Milstein, A. D., Bittner, K. C., Romani, S., and Magee, J. C. (2017). Inhibitory suppression of heterogeneously tuned excitation enhances spatial coding in CA1 place cells. *Nat. Neurosci.* 20, 417–426. doi: 10.1038/nn.4486

Guet-McCreight, A., Skinner, F. K., and Topolnik, L. (2020). Common principles in functional organization of VIP/Calretinin cell-driven Disinhibitory circuits across cortical areas. *Front. Neural Circ.* 14:32. doi: 10.3389/FNCIR.2020.00032/BIBTEX

Gulyás, A. I., Hájos, N., Katona, I., and Freund, T. F. (2003). Interneurons are the local targets of hippocampal inhibitory cells which project to the medial septum. *Eur. J. Neurosci.* 17, 1861–1872. doi: 10.1046/j.1460-9568.2003.02630.x

Guo, J., Oliveros, H., Jung, O. S., Liang, B., Li, Y., Kavalali, E., et al. (2021). Stratum Lacunosum-moleculare interneurons of the Hippocampus coordinate memory encoding and retrieval. *bioRxiv*. doi: 10.21203/rs.3.rs-310894/v1

Han, S., Tai, C., Westenbroek, R. E., Yu, F. H., Cheah, C. S., Potter, G. B., et al. (2012). Autistic-like behaviour in Scn1a+/− mice and rescue by enhanced GABA-mediated neurotransmission. *Nature* 489, 385–390. doi: 10.1038/nature11356

Harris, K. D., Hochgerner, H., Skene, N. G., Magno, L., Katona, L., Bengtsson Gonzales, C., et al. (2018). Classes and continua of hippocampal CA1 inhibitory neurons revealed by single-cell transcriptomics. *PLoS Biol.* 16:e2006387. doi: 10.1371/journal.pbio.2006387

Hartzell, A. L., Martyniuk, K. M., Brigidi, G. S., Heinz, D. A., Djaja, N. A., Payne, A., et al. (2018). NPAS4 recruits CCK basket cell synapses and enhances cannabinoid-sensitive inhibition in the mouse hippocampus. *elife* 7. doi: 10.7554/eLife.35927

He, Q., Jiang, L., Zhang, Y., Yang, H., Zhou, C. N., Xie, Y., et al. (2021). Anti-LINGO-1 antibody ameliorates cognitive impairment, promotes adult hippocampal neurogenesis, and increases the abundance of CB1R-rich CCK-GABAergic interneurons in AD mice. *Neurobiology of Disease* 156:105406. doi: 10.1016/J.NBD.2021.105406

Hefft, S., and Jonas, P. (2005). Asynchronous GABA release generates long-lasting inhibition at a hippocampal interneuron–principal neuron synapse. *Nat. Neurosci.* 8, 1319–1328. doi: 10.1038/nn1542

Heifets, B. D., and Castillo, P. E. (2009). Endocannabinoid signaling and long-term synaptic plasticity. *Annu. Rev. Physiol.* 71, 283–306. doi: 10.1146/annurev.physiol.010908.163149

Hijazi, S., Heistek, T. S., Scheltens, P., Neumann, U., Shimshek, D. R., Mansvelder, H. D., et al. (2019). Early restoration of parvalbumin interneuron activity prevents memory loss and network hyperexcitability in a mouse model of Alzheimer's disease. *Mol. Psychiatry* 25, 3380–3398. doi: 10.1038/s41380-019-0483-4

Hijazi, S., Heistek, T. S., van der Loo, R., Mansvelder, H. D., Smit, A. B., and van Kesteren, R. E. (2020). Hyperexcitable Parvalbumin interneurons render hippocampal circuitry vulnerable to amyloid Beta. *iScience* 23. doi: 10.1016/j.isci.2020.101271

Hollnagel, J. O., Elzoheiry, S., Gorgas, K., Kins, S., Beretta, C. A., Kirsch, J., et al. (2019). Early alterations in hippocampal perisomatic GABAergic synapses and network oscillations in a mouse model of Alzheimer's disease amyloidosis. *PLoS One* 14. doi: 10.1371/journal.pone.0209228

Hondius, D. C., Van Nierop, P., Li, K. W., Hoozemans, J. J. M., Van Der Schors, R. C., Van Haastert, E. S., et al. (2016). Profiling the human hippocampal proteome at all pathologic stages of Alzheimer's disease. *Alzheimers Dement.* 12, 654–668. doi: 10.1016/J.JALZ.2015.11.002

Hu, H., Gan, J., and Jonas, P. (2014). Fast-spiking, parvalbumin+ GABAergic interneurons: from cellular design to microcircuit function. *Science* 345. doi: 10.1126/science.1255263

Huh, S., Baek, S. J., Lee, K. H., Whitcomb, D. J., Jo, J., Choi, S. M., et al. (2016). The reemergence of long-term potentiation in aged Alzheimer's disease mouse model. *Sci. Rep.* 6. doi: 10.1038/srep29152

Ino, T., Matsuzaki, S., Shinonaga, Y., Ohishi, H., Ogawa-Meguro, R., and Mizuno, N. (1990). Direct projections of non-pyramidal neurons of Ammon's horn to the amygdala and the entorhinal cortex. *Neurosci. Lett.* 115, 161–166. doi: 10.1016/0304-3940(90)90448-I

Jack, C. R., Bennett, D. A., Blennow, K., Carrillo, M. C., Dunn, B., Haeberlein, S. B., et al. (2018). NIA-AA research framework: toward a biological definition of Alzheimer's disease. *Alzheimer's Dement.* 14, 535–562. doi: 10.1016/j.jalz.2018.02.018

Jinno, S., Klausberger, T., Marton, L. F., Dalezios, Y., Roberts, J. D. B., Fuentealba, P., et al. (2007). Neuronal diversity in GABAergic long-range projections from the hippocampus. *J. Neurosci.* 27, 8790–8804. doi: 10.1523/JNEUROSCI.1847-07.2007

Jonas, P., and Lisman, J. (2014). Structure, function, and plasticity of hippocampal dentate gyrus microcircuits. *Front. Neural Circ.* 8:107. doi: 10.3389/fncir.2014.00107

Joshi, A., Salib, M., Viney, T. J., Dupret, D., and Somogyi, P. (2017). Behavior-dependent activity and synaptic Organization of Septo-hippocampal GABAergic neurons selectively targeting the hippocampal CA3 area. *Neuron* 96, 1342–1357.e5. doi: 10.1016/j.neuron.2017.10.033

Jun, H., Bramian, A., Soma, S., Saito, T., Saido, T. C., and Igarashi, K. M. (2020). Disrupted place cell remapping and impaired grid cells in a knockin model of Alzheimer's disease. *Neuron* 107, 1095–1112.e6. doi: 10.1016/j.neuron.2020.06.023

Kamenetz, F., Tomita, T., Hsieh, H., Seabrook, G., Borchelt, D., Iwatsubo, T., et al. (2003). APP processing and synaptic function. *Neuron* 37, 925–937. doi: 10.1016/S0896-6273(03)00124-7

Karson, M. A., Tang, A. H., Milner, T. A., and Alger, B. E. (2009). Synaptic cross talk between perisomatic-targeting interneuron classes expressing cholecystokinin and parvalbumin in hippocampus. *J. Neurosci.* 29, 4140–4154. doi: 10.1523/JNEUROSCI.5264-08.2009

Katona, I., Acsády, L., and Freund, T. F. (1999). Postsynaptic targets of somatostatin-immunoreactive interneurons in the rat hippocampus. *Neuroscience* 88, 37–55. doi: 10.1016/S0306-4522(98)00302-9

Katona, L., Lapray, D., Viney, T. J., Oulhaj, A., Borhegyi, Z., Micklem, B. R., et al. (2014). Sleep and movement differentiates actions of two types of somatostatin-expressing GABAergic interneuron in rat hippocampus. *Neuron* 82, 872–886. doi: 10.1016/j.neuron.2014.04.007

Kepecs, A., and Fishell, G. (2014). Interneuron cell types are fit to function. *Nature* 505, 318–326. doi: 10.1038/nature12983

Kerchner, G. A., Hess, C. P., Hammond-Rosenbluth, K. E., Xu, D., Rabinovici, G. D., Kelley, D. A. C., et al. (2010). Hippocampal CA1 apical neuropil atrophy in mild Alzheimer disease visualized with 7-T MRI. *Neurology* 75, 1381–1387. doi: 10.1212/WNL.0b013e3181f736a1

Khan, U. A., Liu, L., Provenzano, F. A., Berman, D. E., Profaci, C. P., Sloan, R., et al. (2014). Molecular drivers and cortical spread of lateral entorhinal cortex dysfunction in preclinical Alzheimer's disease. *Nat. Neurosci.* 17:304. doi: 10.1038/nn.3606

Khavandi, M., Rao, P. P. N., and Beazely, M. A. (2023). Differential effects of endocannabinoids on amyloid-Beta aggregation and toxicity. *Int. J. Mol. Sci.* 24. doi: 10.3390/ijms24020911

Kiss, J., Buzsaki, G., Morrow, J. S., Glantz, S. B., and Leranth, C. (1996). Entorhinal cortical innervation of Parvalbumin-containing neurons (basket and chandelier cells) in the rat Ammon's horn. *Hippocampus* 6, 239–246. doi: 10.1002/(SICI)1098-1063(1996)6:3<239::AID-HIPO3>3.0.CO;2-I

Klausberger, T. (2009). GABAergic interneurons targeting dendrites of pyramidal cells in the CA1 area of the hippocampus. *Eur. J. Neurosci.* 30, 947–957. doi: 10.1111/j.1460-9568.2009.06913.x

Klausberger, T., Marton, L. F., O'Neill, J., Huck, J. H. J., Dalezios, Y., Fuentealba, P., et al. (2005). Complementary roles of cholecystokinin- and parvalbumin-expressing GABAergic neurons in hippocampal network oscillations. *J. Neurosci.* 25, 9782–9793. doi: 10.1523/JNEUROSCI.3269-05.2005

Klausberger, T., and Somogyi, P. (2008). Neuronal diversity and temporal dynamics: the unity of hippocampal circuit operations. *Science* 321, 53–57. doi: 10.1126/science.1149381

Korkmaz, O. T., Ay, H., Aytan, N., Carreras, I., Kowall, N. W., Dedeoglu, A., et al. (2019). Vasoactive intestinal peptide decreases β-amyloid accumulation and prevents brain atrophy in the 5xFAD mouse model of Alzheimer's disease. *J. Mol. Neurosci.* 68, 389–396. doi: 10.1007/s12031-018-1226-8

Kullander, K., and Topolnik, L. (2021). Cortical disinhibitory circuits: cell types, connectivity and function. *Trends Neurosci.* 44, 643–657. doi: 10.1016/j.tins.2021.04.009

Kullmann, D. M. (2011). Interneuron networks in the hippocampus. *Curr. Opin. Neurobiol.* 21, 709–716. doi: 10.1016/j.conb.2011.05.006

Lacaille, J. C., and Schwartzkroin, P. A. (1988). Stratum lacunosum-moleculare interneurons of hippocampal CA1 region. II. Intrasomatic and intradendritic recordings of local circuit synaptic interactions. *J. Neurosci.* 8, 1411–1424. doi: 10.1523/JNEUROSCI.08-04-01411.1988

Lace, G., Savva, G. M., Forster, G., De Silva, R., Brayne, C., Matthews, F. E., et al. (2009). Hippocampal tau pathology is related to neuroanatomical connections: an ageing population-based study. *Brain J. Neurol.* 132, 1324–1334. doi: 10.1093/brain/awp059

Le Magueresse, C., and Monyer, H. (2013). GABAergic interneurons shape the functional maturation of the cortex. *Neuron* 77, 388–405. doi: 10.1016/j.neuron.2013.01.011

Leão, R. N., Mikulovic, S., Leão, K. E., Munguba, H., Gezelius, H., Enjin, A., et al. (2012). OLM interneurons differentially modulate CA3 and entorhinal inputs to hippocampal CA1 neurons. *Nat. Neurosci.* 15, 1524–1530. doi: 10.1038/nn.3235

Lee, S., Kruglikov, I., Huang, Z. J., Fishell, G., and Rudy, B. (2013). A disinhibitory circuit mediates motor integration in the somatosensory cortex. *Nat. Neurosci.* 16:1662. doi: 10.1038/nn.3544

Lee, S. H., Marchionni, I., Bezaire, M., Varga, C., Danielson, N., Lovett-Barron, M., et al. (2014). Parvalbumin-positive basket cells differentiate among hippocampal pyramidal cells. *Neuron* 82, 1129–1144. doi: 10.1016/j.neuron.2014.03.034

Lee, A. T., Vogt, D., Rubenstein, J. L., and Sohal, V. S. (2014). A class of GABAergic neurons in the prefrontal cortex sends long-range projections to the nucleus Accumbens and elicits acute avoidance behavior. *J. Neurosci.* 34, 11519–11525. doi: 10.1523/JNEUROSCI.1157-14.2014

Lenders, M. B., Peers, M. C., Tramu, G., Delacourte, A., Defossez, A., Petit, H., et al. (1989). Dystrophic peptidergic neurites in senile plaques of Alzheimer's disease hippocampus precede formation of paired helical filaments. *Brain Res.* 481, 344–349. doi: 10.1016/0006-8993(89)90812-3

Li, Y., Xu, J., Liu, Y., Zhu, J., Liu, N., Zeng, W., et al. (2017). A distinct entorhinal cortex to hippocampal CA1 direct circuit for olfactory associative learning. *Nat. Neurosci.* 20, 559–570. doi: 10.1038/nn.4517

Li, H., Zhao, J., Lai, L., Xia, Y., Wan, C., Wei, S., et al. (2022). Loss of SST and PV positive interneurons in the ventral hippocampus results in anxiety-like behavior in 5xFAD mice. *Neurobiol. Aging* 117, 165–178. doi: 10.1016/j.neurobiolaging.2022.05.013

Limon, A., Reyes-Ruiz, J. M., and Miledi, R. (2012). Loss of functional GABA a receptors in the Alzheimer diseased brain. *Proc. Natl. Acad. Sci. U. S. A.* 109, 10071–10076. doi: 10.1073/pnas.1204606109

Liu, L., Drouet, V., Wu, J. W., Witter, M. P., Small, S. A., Clelland, C., et al. (2012). Trans-synaptic spread of tau pathology in vivo. *PLoS One* 7. doi: 10.1371/journal.pone.0031302

Loreth, D., Ozmen, L., Revel, F. G., Knoflach, F., Wetzel, P., Frotscher, M., et al. (2012). Selective degeneration of septal and hippocampal GABAergic neurons in a mouse model of amyloidosis and tauopathy. *Neurobiol. Dis.* 47, 1–12. doi: 10.1016/j.nbd.2012.03.011

Lovett-Barron, M., Kaifosh, P., Kheirbek, M. A., Danielson, N., Zaremba, J. D., Reardin, T. R., et al. (2014). Dendritic inhibition in the Hippocampus supports fear learning. *Science* 343, 857–863. doi: 10.1126/science.1247485

Lovett-Barron, M., Turi, G. F., Kaifosh, P., Lee, P. H., Bolze, F., Sun, X. H., et al. (2012). Regulation of neuronal input transformations by tunable dendritic inhibition. *Nat. Neurosci.* 15, 423–430. doi: 10.1038/nn.3024

Lübkemann, R., Eberhardt, J., Röhl, F. W., Janitzky, K., Nullmeier, S., Stork, O., et al. (2015). Identification and characterization of GABAergic projection neurons from ventral hippocampus to amygdala. *Brain Sci.* 5, 299–317. doi: 10.3390/brainsci5030299

Luo, X., Guet-Mccreight, A., Villette, V., Francavilla, R., Marino, B., Chamberland, S., et al. (2020). Synaptic mechanisms underlying the network state-dependent recruitment of VIP-expressing interneurons in the CA1 Hippocampus. *Cereb. Cortex* 30:3667. doi: 10.1093/cercor/bhz334

Mably, A. J., Gereke, B. J., Jones, D. T., and Colgin, L. L. (2017). Impairments in spatial representations and rhythmic coordination of place cells in the 3xTg mouse model of Alzheimer's disease. *Hippocampus* 27, 378–392. doi: 10.1002/hipo.22697

Maccaferri, G. (2005). Stratum oriens horizontal interneurone diversity and hippocampal network dynamics. *J. Physiol.* 562, 73–80. doi: 10.1113/jphysiol.2004.077081

Mackenzie-Gray Scott, C. A., Pelkey, K. A., Caccavano, A. P., Abebe, D., Lai, M., Black, K. N., et al. (2022). Resilient hippocampal gamma rhythmogenesis and parvalbumin-expressing interneuron function before and after plaque burden in 5xFAD Alzheimer's disease model. *Front. Synap. Neurosci.* 14:857608. doi: 10.3389/fnsyn.2022.857608

Magnin, E., Francavilla, R., Amalyan, S., Gervais, E., David, L. S., Luo, X., et al. (2019). Input-specific synaptic location and function of the α5 GABAA receptor subunit in the mouse CA1 hippocampal neurons. *J. Neurosci.* 39, 788–801. doi: 10.1523/JNEUROSCI.0567-18.2018

Mahar, I., Albuquerque, M. S., Mondragon-Rodriguez, S., Cavanagh, C., Davoli, M. A., Chabot, J. G., et al. (2016). Phenotypic alterations in hippocampal NPY- and PV-expressing interneurons in a Presymptomatic transgenic mouse model of Alzheimer's disease. *Front. Aging Neurosci.* 8:327. doi: 10.3389/FNAGI.2016.00327

Malik, R., Li, Y., Schamiloglu, S., and Sohal, V. S. (2022). Top-down control of hippocampal signal-to-noise by prefrontal long-range inhibition. *Cells* 185, 1602–1617.e17. doi: 10.1016/j.cell.2022.04.001

Marín, O. (2012). Interneuron dysfunction in psychiatric disorders. *Nat. Rev. Neurosci.* 13, 107–120. doi: 10.1038/nrn3155

Marlin, J. J., and Carter, A. G. (2014). GABA-A receptor inhibition of local calcium signaling in spines and dendrites. *J. Neurosci.* 34, 15898–15911. doi: 10.1523/JNEUROSCI.0869-13.2014

Masurkar, A. V. (2018). Towards a circuit-level understanding of hippocampal CA1 dysfunction in Alzheimer's disease across anatomical axes. *J. Alzheimer's Dis. Parkin.* 8. doi: 10.4172/2161-0460.1000412

Mátyás, F., Freund, T. F., and Gulyás, A. I. (2004). Convergence of excitatory and inhibitory inputs onto CCK-containing basket cells in the CA1 area of the rat hippocampus. *Eur. J. Neurosci.* 19, 1243–1256. doi: 10.1111/j.1460-9568.2004.03225.x

Megías, M., Emri, Z., Freund, T. F., and Gulyás, A. I. (2001). Total number and distribution of inhibitory and excitatory synapses on hippocampal CA1 pyramidal cells. *Neuroscience* 102, 527–540. doi: 10.1016/S0306-4522(00)00496-6

Melzer, S., Michael, M., Caputi, A., Eliava, M., Fuchs, E. C., Whittington, M., et al. (2012). Long-range–projecting GABAergic neurons modulate inhibition in Hippocampus and entorhinal cortex. *Science* 335, 1506–1510. doi: 10.1126/science.1217139

Melzer, S., and Monyer, H. (2020). Diversity and function of corticopetal and corticofugal GABAergic projection neurons. *Nat. Rev. Neurosci.* 21, 499–515. doi: 10.1038/s41583-020-0344-9

Mercier, M. S., Magloire, V., Cornford, J. H., and Kullmann, D. M. (2022). Long-term potentiation in neurogliaform interneurons modulates excitation–inhibition balance in the temporoammonic pathway. *J. Physiol.* 600:4001. doi: 10.1113/JP282753

Miles, R., Tóth, K., Gulyás, A. I., Hájos, N., and Freund, T. F. (1996). Differences between somatic and dendritic inhibition in the hippocampus. *Neuron* 16, 815–823. doi: 10.1016/S0896-6273(00)80101-4

Milstein, A. D., Bloss, E. B., Apostolides, P. F., Vaidya, S. P., Dilly, G. A., Zemelman, B. V., et al. (2015). Inhibitory gating of input comparison in the CA1 microcircuit. *Neuron* 87, 1274–1289. doi: 10.1016/j.neuron.2015.08.025

Miyashita, T., and Rockland, K. S. (2007). GABAergic projections from the hippocampus to the retrosplenial cortex in the rat. *Eur. J. Neurosci.* 26, 1193–1204. doi: 10.1111/j.1460-9568.2007.05745.x

Morrone, C. D., Lai, A. Y., Bishay, J., Hill, M. E., and McLaurin, J. A. (2022). Parvalbumin neuroplasticity compensates for somatostatin impairment, maintaining cognitive function in Alzheimer's disease. *Trans. Neurodegen.* 11. doi: 10.1186/s40035-022-00300-6

Müller, M., Faber-Zuschratter, H., Yanagawa, Y., Stork, O., Schwegler, H., and Linke, R. (2012). Synaptology of ventral CA1 and subiculum projections to the basomedial nucleus of the amygdala in the mouse: relation to GABAergic interneurons. *Brain Struct. Funct.* 217, 5–17. doi: 10.1007/s00429-011-0326-9

Müller, C., and Remy, S. (2014). Dendritic inhibition mediated by O-LM and bistratified interneurons in the hippocampus. *Front. Synap. Neurosci.* 6:23. doi: 10.3389/FNSYN.2014.00023

Müllner, F. E., Wierenga, C. J., and Bonhoeffer, T. (2015). Precision of inhibition: dendritic inhibition by individual GABAergic synapses on hippocampal pyramidal cells is confined in space and time. *Neuron* 87, 576–589. doi: 10.1016/j.neuron.2015.07.003

Murray, A. J., Sauer, J. F., Riedel, G., McClure, C., Ansel, L., Cheyne, L., et al. (2011). Parvalbumin-positive CA1 interneurons are required for spatial working but not for reference memory. *Nat. Neurosci.* 14, 297–299. doi: 10.1038/nn.2751

Noguchi, A., Huszár, R., Morikawa, S., Buzsáki, G., and Ikegaya, Y. (2022). Inhibition allocates spikes during hippocampal ripples. *Nat. Commun.* 13, 1–14. doi: 10.1038/s41467-022-28890-9

O'Donnell, C., Tiago Gonçalves, J., Portera-Cailliau, C., and Sejnowski, T. J. (2017). Beyond excitation/inhibition imbalance in multidimensional models of neural circuit changes in brain disorders. *elife* 6. doi: 10.7554/eLife.26724

Oláh, S., Füle, M., Komlósi, G., Varga, C., Báldi, R., Barzó, P., et al. (2009). Regulation of cortical microcircuits by unitary GABAergic volume transmission. *Nature* 461:1278. doi: 10.1038/nature08503

Oliva, A. A., Jiang, M., Lam, T., Smith, K. L., and Swann, J. W. (2000). Novel hippocampal interneuronal subtypes identified using transgenic mice that express green fluorescent protein in GABAergic interneurons. *J. Neurosci.* 20:3354. doi: 10.1523/JNEUROSCI.20-09-03354.2000

Owen, S. F., Tuncdemir, S. N., Bader, P. L., Tirko, N. N., Fishell, G., and Tsien, R. W. (2013). Oxytocin enhances hippocampal spike transmission by modulating fast-spiking interneurons. *Nature* 500, 458–462. doi: 10.1038/nature12330

Pacheco-Quinto, J., Eckman, C. B., and Eckman, E. A. (2016). Major amyloid-β-degrading enzymes, endothelin-converting enzyme-2 and neprilysin, are expressed by distinct populations of GABAergic interneurons in hippocampus and neocortex. *Neurobiol. Aging* 48, 83–92. doi: 10.1016/j.neurobiolaging.2016.08.011

Palop, J. J., Chin, J., Roberson, E. D., Wang, J., Thwin, M. T., Bien-Ly, N., et al. (2007). Aberrant excitatory neuronal activity and compensatory remodeling of inhibitory hippocampal circuits in mouse models of Alzheimer's disease. *Neuron* 55:697. doi: 10.1016/j.neuron.2007.07.025

Park, K., Lee, J., Jang, H. J., Richards, B. A., Kohl, M. M., and Kwag, J. (2020). Optogenetic activation of parvalbumin and somatostatin interneurons selectively restores theta-nested gamma oscillations and oscillation-induced spike timing-dependent long-term potentiation impaired by amyloid β oligomers. *BMC Biol.* 18. doi: 10.1186/s12915-019-0732-7

Pawelzik, H., Hughes, D. I., and Thomson, A. M. (2002). Physiological and morphological diversity of immunocytochemically defined parvalbumin- and cholecystokinin-positive interneurones in CA1 of the adult rat hippocampus. *J. Comp. Neurol.* 443, 346–367. doi: 10.1002/cne.10118

Pelkey, K. A., Chittajallu, R., Craig, M. T., Tricoire, L., Wester, J. C., and McBain, C. J. (2017). Hippocampal gabaergic inhibitory interneurons. *Physiol. Rev.* 97, 1619–1747. doi: 10.1152/physrev.00007.2017

Petrache, A. L., Khan, A. A., Nicholson, M. W., Monaco, A., Kuta-Siejkowska, M., Haider, S., et al. (2020). Selective modulation of α5 GABAA receptors exacerbates aberrant inhibition at key hippocampal neuronal circuits in APP mouse model of Alzheimer's disease. *Front. Cell. Neurosci.* 14:568194. doi: 10.3389/fncel.2020.568194

Pfeffer, C. K., Xue, M., He, M., Huang, Z. J., and Scanziani, M. (2013). Inhibition of inhibition in visual cortex: the logic of connections between molecularly distinct interneurons. *Nat. Neurosci.* 16:1068. doi: 10.1038/nn.3446

Pi, H. J., Hangya, B., Kvitsiani, D., Sanders, J. I., Huang, Z. J., and Kepecs, A. (2013). Cortical interneurons that specialize in disinhibitory control. *Nature* 503:521. doi: 10.1038/nature12676

Plagman, A., Hoscheidt, S., McLimans, K. E., Klinedinst, B., Pappas, C., Anantharam, V., et al. (2019). Cholecystokinin and Alzheimer's disease: a biomarker of metabolic function, neural integrity, and cognitive performance. *Neurobiol. Aging* 76, 201–207. doi: 10.1016/j.neurobiolaging.2019.01.002

Pouille, F., and Scanziani, M. (2001). Enforcement of temporal fidelity in pyramidal cells by somatic feed-forward inhibition. *Science* 293, 1159–1163. doi: 10.1126/science.1060342

Pouille, F., Watkinson, O., Scanziani, M., and Trevelyan, A. J. (2013). The contribution of synaptic location to inhibitory gain control in pyramidal cells. *Phys. Rep.* 1:67. doi: 10.1002/PHY2.67

Pozueta, J., Lefort, R., and Shelanski, M. L. (2013). Synaptic changes in Alzheimer's disease and its models. *Neuroscience* 251, 51–65. doi: 10.1016/j.neuroscience.2012.05.050

Price, C. J., Cauli, B., Kovacs, E. R., Kulik, A., Lambolez, B., Shigemoto, R., et al. (2005). Neurogliaform neurons form a novel inhibitory network in the hippocampal CA1 area. *J. Neurosci.* 25:6775. doi: 10.1523/JNEUROSCI.1135-05.2005

Price, J. L., Ko, A. I., Wade, M. J., Tsou, S. K., McKeel, D. W., and Morris, J. C. (2001). Neuron number in the entorhinal cortex and CA1 in preclinical Alzheimer disease. *Arch. Neurol.* 58, 1395–1402. doi: 10.1001/archneur.58.9.1395

Price, C. J., Scott, R., Rusakov, D. A., and Capogna, M. (2008). GABAB receptor modulation of feedforward inhibition through hippocampal neurogliaform cells. *J. Neurosci.* 28:6974. doi: 10.1523/JNEUROSCI.4673-07.2008

Ramos, B., Baglietto-Vargas, D., del Rio, J. C., Moreno-Gonzalez, I., Santa-Maria, C., Jimenez, S., et al. (2006). Early neuropathology of somatostatin/NPY GABAergic cells in the hippocampus of a PS1xAPP transgenic model of Alzheimer's disease. *Neurobiol. Aging* 27, 1658–1672. doi: 10.1016/j.neurobiolaging.2005.09.022

Ren, C., Peng, K., Yang, R., Liu, W., Liu, C., and Komiyama, T. (2022). Global and subtype-specific modulation of cortical inhibitory neurons regulated by acetylcholine during motor learning. *Neuron* 110, 2334–2350.e8. doi: 10.1016/j.neuron.2022.04.031

Ribak, C. E., Seress, L., and Leranth, C. (1993). Electron microscopic immunocytochemical study of the distribution of parvalbumin-containing neurons and axon terminals in the primate dentate gyrus and Ammon's horn. *J. Comp. Neurol.* 327, 298–321. doi: 10.1002/cne.903270211

Rice, H. C., Marcassa, G., Chrysidou, I., Horré, K., Young-Pearse, T. L., Müller, U. C., et al. (2020). Contribution of GABAergic interneurons to amyloid-β plaque pathology in an APP knock-in mouse model. *Mol. Neurodegener.* 15, 1–8. doi: 10.1186/S13024-019-0356-Y/FIGURES/3

Rosen, Z. B., Cheung, S., and Siegelbaum, S. A. (2015). Midbrain dopamine neurons bidirectionally regulate CA3-CA1 synaptic drive. *Nat. Neurosci.* 18, 1763–1771. doi: 10.1038/nn.4152

Royer, S., Zemelman, B. V., Losonczy, A., Kim, J., Chance, F., Magee, J. C., et al. (2012). Control of timing, rate and bursts of hippocampal place cells by dendritic and somatic inhibition. *Nat. Neurosci.* 15, 769–775. doi: 10.1038/nn.3077

Sans-Dublanc, A., Razzauti, A., Desikan, S., Pascual, M., Monyer, H., and Sindreu, C. (2020). Septal GABAergic inputs to CA1 govern contextual memory retrieval. *Sci. Adv.* 6:5003. doi: 10.1126/sciadv.aba5003

Scaduto, P., Lauterborn, J. C., Cox, C. D., Fracassi, A., Zeppillo, T., Gutierrez, B. A., et al. (2023). Functional excitatory to inhibitory synaptic imbalance and loss of cognitive performance in people with Alzheimer's disease neuropathologic change. *Acta Neuropathol.* 145, 303–324. doi: 10.1007/s00401-022-02526-0

Scheff, S. W., Price, D. A., Schmitt, F. A., Dekosky, S. T., and Mufson, E. J. (2007). Synaptic alterations in CA1 in mild Alzheimer disease and mild cognitive impairment. *Neurology* 68, 1501–1508. doi: 10.1212/01.wnl.0000260698.46517.8f

Schlingloff, D., Káli, S., Freund, T. F., Hájos, N., and Gulyás, A. I. (2014). Mechanisms of sharp wave initiation and ripple generation. *J. Neurosci.* 34:11385. doi: 10.1523/JNEUROSCI.0867-14.2014

Schroeder, A., Pardi, M. B., Keijser, J., Dalmay, T., Groisman, A. I., Schuman, E. M., et al. (2023). Inhibitory top-down projections from zona incerta mediate neocortical memory. *Neuron* 111, 727–738.e8. doi: 10.1016/j.neuron.2022.12.010

Schulz, J. M., Knoflach, F., Hernandez, M. C., and Bischofberger, J. (2018). Dendrite-targeting interneurons control synaptic NMDA-receptor activation via nonlinear α5-GABAA receptors. *Nat. Commun.* 9, 1–16. doi: 10.1038/s41467-018-06004-8

Seo, H. J., Park, J. E., Choi, S. M., Kim, T., Cho, S. H., Lee, K. H., et al. (2021). Inhibitory neural Network's impairments at hippocampal CA1 LTP in an aged transgenic mouse model of Alzheimer's disease. *Int. J. Mol. Sci.* 22, 1–15. doi: 10.3390/IJMS22020698

Sheffield, M. E. J., Adoff, M. D., and Dombeck, D. A. (2017). Increased prevalence of calcium transients across the dendritic arbor during place field formation. *Neuron* 96:490. doi: 10.1016/j.neuron.2017.09.029

Shi, A., Petrache, A. L., Shi, J., and Ali, A. B. (2020). Preserved Calretinin interneurons in an app model of Alzheimer's disease disrupt hippocampal inhibition via upregulated P2Y1 purinoreceptors. *Cereb. Cortex* 30, 1272–1290. doi: 10.1093/cercor/bhz165

Siddhartha, M. R., Anahi, S. G., Perla, G. P., Macías, M., Ordaz, B., Fernando, P. O., et al. (2018). Phosphorylation of tau protein correlates with changes in hippocampal theta oscillations and reduces hippocampal excitability in Alzheimer's model. *J. Biol. Chem.* 293, 8462–8472. doi: 10.1074/jbc.RA117.001187

Sik, A., Penttonen, M., Ylinen, A., and Buzsáki, G. (1995). Hippocampal CA1 interneurons: an in vivo intracellular labeling study. *J. Neurosci.* 15, 6651–6665. doi: 10.1523/JNEUROSCI.15-10-06651.1995

Silva Albequerque, M., Mahar, I., Davoli, M. A., Chabot, J. G., Mechawar, N., Quirion, R., et al. (2015). Regional and sub-regional differences in hippocampal GABAergic neuronal vulnerability in the TgCRND8 mouse model of Alzheimer's disease. *Front. Aging Neurosci.* 7:30. doi: 10.3389/FNAGI.2015.00030

Siwani, S., França, A. S. C., Mikulovic, S., Reis, A., Hilscher, M. M., Edwards, S. J., et al. (2018). OLMα2 cells bidirectionally modulate learning. *Neuron* 99, 404–412.e3. doi: 10.1016/j.neuron.2018.06.022

Soler, H., Dorca-Arévalo, J., González, M., Rubio, S. E., Ávila, J., Soriano, E., et al. (2017). The GABAergic septohippocampal connection is impaired in a mouse model of tauopathy. *Neurobiol. Aging* 49, 40–51. doi: 10.1016/j.neurobiolaging.2016.09.006

Somogyi, J., Baude, A., Omori, Y., Shimizu, H., El Mestikawy, S., Fukaya, M., et al. (2004). GABAergic basket cells expressing cholecystokinin contain vesicular glutamate transporter type 3 (VGLUT3) in their synaptic terminals in hippocampus and isocortex of the rat. *Eur. J. Neurosci.* 19, 552–569. doi: 10.1111/j.0953-816X.2003.03091.x

Somogyi, P., Katona, L., Klausberger, T., Lasztóczi, B., and Viney, T. J. (2014). Temporal redistribution of inhibition over neuronal subcellular domains underlies state-dependent rhythmic change of excitability in the hippocampus. *Philos. Trans. R. Soc. Lond., B, Biol. Sci.* 369. doi: 10.1098/rstb.2012.0518

Song, M., Xiong, J., Wang, Y. Y., Tang, J., Zhang, B., and Bai, Y. (2012). VIP enhances phagocytosis of fibrillar beta-amyloid by microglia and attenuates amyloid deposition in the brain of APP/PS1 mice. *PLoS One* 7. doi: 10.1371/journal.pone.0029790

Sos, K. E., Mayer, M. I., Takács, V. T., Major, A., Bardóczi, Z., Beres, B. M., et al. (2020). Amyloid β induces interneuron-specific changes in the hippocampus of APPNL-F mice. *PLoS One* 15. doi: 10.1371/journal.pone.0233700

Squire, L. R. (2004). Memory systems of the brain: a brief history and current perspective. *Neurobiol. Learn. Mem.* 82, 171–177. doi: 10.1016/j.nlm.2004.06.005

Stark, E., Roux, L., Eichler, R., Senzai, Y., Royer, S., and Buzsáki, G. (2014). Pyramidal cell-interneuron interactions underlie hippocampal ripple oscillations. *Neuron* 83, 467–480. doi: 10.1016/j.neuron.2014.06.023

Sun, X., Bernstein, M. J., Meng, M., Rao, S., Sørensen, A. T., Yao, L., et al. (2020). Functionally distinct neuronal ensembles within the memory engram. *Cells* 181:410. doi: 10.1016/j.cell.2020.02.055

Szabo, G. G., Farrell, J. S., Dudok, B., Hou, W. H., Ortiz, A. L., Varga, C., et al. (2022). Ripple-selective GABAergic projection cells in the hippocampus. *Neuron* 110, 1959–1977.e9. doi: 10.1016/j.neuron.2022.04.002

Takács, V. T., Szőnyi, A., Freund, T. F., Nyiri, G., and Gulyás, A. I. (2015). Quantitative ultrastructural analysis of basket and axo-axonic cell terminals in the mouse hippocampus. *Brain Struct. Funct.* 220, 919–940. doi: 10.1007/s00429-013-0692-6

Takahashi, H., Brasnjevic, I., Rutten, B. P. F., Van Der Kolk, N., Perl, D. P., Bouras, C., et al. (2010). Hippocampal interneuron loss in an APP/PS1 double mutant mouse and in Alzheimer's disease. *Brain Struct. Funct.* 214:145. doi: 10.1007/S00429-010-0242-4

Taniguchi, H., He, M., Wu, P., Kim, S., Paik, R., Sugino, K., et al. (2011). A resource of Cre driver lines for genetic targeting of GABAergic neurons in cerebral cortex. *Neuron* 71, 995–1013. doi: 10.1016/j.neuron.2011.07.026

Tasic, B., Menon, V., Nguyen, T. N., Kim, T. K., Jarsky, T., Yao, Z., et al. (2016). Adult mouse cortical cell taxonomy by single cell transcriptomics. *Nat. Neurosci.* 19:335. doi: 10.1038/nn.4216

Tremblay, R., Lee, S., and Rudy, B. (2016). GABAergic interneurons in the neocortex: from cellular properties to circuits. *Neuron* 91:260. doi: 10.1016/j.neuron.2016.06.033

Tricoire, L., Pelkey, K. A., Daw, M. I., Sousa, V. H., Miyoshi, G., Jeffries, B., et al. (2010). Common origins of hippocampal ivy and Nitric oxide synthase expressing Neurogliaform cells. *J. Neurosci.* 30:2165. doi: 10.1523/JNEUROSCI.5123-09.2010

Turi, G. F., Li, W. K., Chavlis, S., Pandi, I., O'Hare, J., Priestley, J. B., et al. (2019). Vasoactive intestinal polypeptide-expressing interneurons in the hippocampus support goal-oriented spatial learning. *Neuron* 101, 1150–1165.e8. doi: 10.1016/j.neuron.2019.01.009

Tyan, L., Chamberland, S., Magnin, E., Camiré, O., Francavilla, R., Suzanne David, L., et al. (2014). Dendritic inhibition provided by interneuron-specific cells controls the firing rate and timing of the hippocampal feedback inhibitory circuitry. *J. Neurosci.* 34, 4534–4547. doi: 10.1523/JNEUROSCI.3813-13.2014

Udakis, M., Pedrosa, V., Chamberlain, S. E. L., Clopath, C., and Mellor, J. R. (2020). Interneuron-specific plasticity at parvalbumin and somatostatin inhibitory synapses onto CA1 pyramidal neurons shapes hippocampal output. *Nat. Commun.* 11. doi: 10.1038/s41467-020-18074-8

Valero, M., Cid, E., Averkin, R. G., Aguilar, J., Sanchez-Aguilera, A., Viney, T. J., et al. (2015). Determinants of different deep and superficial CA1 pyramidal cell dynamics during sharp-wave ripples. *Nat. Neurosci.* 18, 1281–1290. doi: 10.1038/nn.4074

Van Strien, N. M., Cappaert, N. L. M., and Witter, M. P. (2009). The anatomy of memory: an interactive overview of the parahippocampal–hippocampal network. *Nat. Rev. Neurosci.* 10, 272–282. doi: 10.1038/nrn2614

Verdaguer, E., Brox, S., Petrov, D., Olloquequi, J., Romero, R., de Lemos, M. L., et al. (2015). Vulnerability of calbindin, calretinin and parvalbumin in a transgenic/knock-in APPswe/PS1dE9 mouse model of Alzheimer disease together with disruption of hippocampal neurogenesis. *Exp. Gerontol.* 69, 176–188. doi: 10.1016/j.exger.2015.06.013

Verret, L., Mann, E. O., Hang, G. B., Barth, A. M. I., Cobos, I., Ho, K., et al. (2012). Inhibitory interneuron deficit links altered network activity and cognitive dysfunction in Alzheimer model. *Cells* 149, 708–721. doi: 10.1016/j.cell.2012.02.046

Villette, V., Poindessous-Jazat, F., Bellessort, B., Roullot, E., Peterschmitt, Y., Epelbaum, J., et al. (2012). A new neuronal target for beta-amyloid peptide in the rat hippocampus. *Neurobiol. Aging* 33, 1126.e1–1126.e14. doi: 10.1016/j.neurobiolaging.2011.11.024

Waller, R., Mandeya, M., Viney, E., Simpson, J. E., and Wharton, S. B. (2020). Histological characterization of interneurons in Alzheimer's disease reveals a loss of somatostatin interneurons in the temporal cortex. *Neuropathology* 40, 336–346. doi: 10.1111/neup.12649

Webster, S. J., Bachstetter, A. D., Nelson, P. T., Schmitt, F. A., and Van Eldik, L. J. (2014). Using mice to model Alzheimer's dementia: an overview of the clinical disease and the preclinical behavioral changes in 10 mouse models. *Front. Genet.* 5:88. doi: 10.3389/FGENE.2014.00088

Whissell, P. D., Bang, J. Y., Khan, I., Xie, Y. F., Parfitt, G. M., Grenon, M., et al. (2019). Selective activation of cholecystokinin-expressing GABA (CCK-GABA) neurons enhances memory and cognition. *eNeuro* 6. doi: 10.1523/ENEURO.0360-18.2019

Wick, Z. C., Tetzlaff, M. R., and Krook-Magnuson, E. (2019). Novel long-range inhibitory nNOS-expressing hippocampal cells. *elife* 8. doi: 10.7554/eLife.46816

Wilson, R. I., Kunos, G., and Nicoll, R. A. (2001). Presynaptic specificity of endocannabinoid signaling in the hippocampus. *Neuron* 31, 453–462. doi: 10.1016/S0896-6273(01)00372-5

Witter, M. P., Doan, T. P., Jacobsen, B., Nilssen, E. S., and Ohara, S. (2017). Architecture of the entorhinal cortex a review of entorhinal anatomy in rodents with some comparative notes. *Front. Syst. Neurosci.* 11:46. doi: 10.3389/fnsys.2017.00046

Witter, M. P., Wouterlood, F. G., Naber, P. A., and Van Haeften, T. (2000). Anatomical Organization of the Parahippocampal-Hippocampal Network. *Ann. N. Y. Acad. Sci.* 911, 1–24. doi: 10.1111/J.1749-6632.2000.TB06716.X

Wu, J. W., Hussaini, S. A., Bastille, I. M., Rodriguez, G. A., Mrejeru, A., Rilett, K., et al. (2016). Neuronal activity enhances tau propagation and tau pathology in vivo. *Nat. Neurosci.* 19:1085. doi: 10.1038/nn.4328

Wulff, P., Ponomarenko, A. A., Bartos, M., Korotkova, T. M., Fuchs, E. C., Bähner, F., et al. (2009). Hippocampal theta rhythm and its coupling with gamma oscillations

require fast inhibition onto parvalbumin-positive interneurons. *Proc. Natl. Acad. Sci. U. S. A.* 106, 3561–3566. doi: 10.1073/pnas.0813176106

Xiao, M. F., Xu, D., Craig, M. T., Pelkey, K. A., Chien, C. C., Shi, Y., et al. (2017). NPTX2 and cognitive dysfunction in Alzheimer's disease. *elife* 6, 1–27. doi: 10.7554/ELIFE.23798

Xiong, Y., and Lim, C. S. (2021). Understanding the modulatory effects of Cannabidiol on Alzheimer's disease. *Brain Sci.* 11. doi: 10.3390/brainsci11091211

Xu, Y., Zhao, M., Han, Y., and Zhang, H. (2020). GABAergic inhibitory interneuron deficits in Alzheimer's disease: implications for treatment. *Front. Neurosci.* 14:660. doi: 10.3389/fnins.2020.00660

Xue, M., Atallah, B. V., and Scanziani, M. (2014). Equalizing excitation-inhibition ratios across visual cortical neurons. *Nature* 511, 596–600. doi: 10.1038/nature13321

Yang, X., Yao, C., Tian, T., Li, X., Yan, H., Wu, J., et al. (2018). A novel mechanism of memory loss in Alzheimer's disease mice via the degeneration of entorhinal-CA1 synapses. *Mol. Psychiatry* 23, 199–210. doi: 10.1038/mp.2016.151

Yen, T. Y., Huang, X., MacLaren, D. A. A., Schlesiger, M. I., Monyer, H., and Lien, C. C. (2022). Inhibitory projections connecting the dentate gyri in the two hemispheres support spatial and contextual memory. *Cell Rep.* 39. doi: 10.1016/j.celrep.2022.110831

Yoshida, T., Hashimoto, K., Zimmer, A., Maejima, T., Araishi, K., and Kano, M. (2002). The cannabinoid CB1 receptor mediates retrograde signals for depolarization-induced suppression of inhibition in cerebellar Purkinje cells. *J. Neurosci.* 22:1690. doi: 10.1523/JNEUROSCI.22-05-01690.2002

Yuan, M., Meyer, T., Benkowitz, C., Savanthrapadian, S., Ansel-Bollepalli, L., Foggetti, A., et al. (2017). Somatostatin-positive interneurons in the dentate gyrus of mice provide local-and long-range septal synaptic inhibition. *elife* 6. doi: 10.7554/eLife.21105

Zallo, F., Gardenal, E., Verkhratsky, A., and Rodríguez, J. J. (2018). Loss of calretinin and parvalbumin positive interneurones in the hippocampal CA1 of aged Alzheimer's disease mice. *Neurosci. Lett.* 681, 19–25. doi: 10.1016/j.neulet.2018.05.027

Zemla, R., and Basu, J. (2017). Hippocampal function in rodents. *Curr. Opin. Neurobiol.* 43, 187–197. doi: 10.1016/j.conb.2017.04.005

Zeng, H. (2022). What is a cell type and how to define it? *Cells* 185, 2739–2755. doi: 10.1016/j.cell.2022.06.031

Zhang, Z., Li, H., Su, Y., Ma, J., Yuan, Y., Yu, Z., et al. (2022). Neuroprotective effects of a cholecystokinin analogue in the 1-methyl-4-phenyl-1,2,3,6-tetrahydropyridine Parkinson's disease mouse model. *Front. Neurosci.* 16:814430. doi: 10.3389/fnins.2022.814430

Zhang, H., Zhang, L., Zhou, D., He, X., Wang, D., Pan, H., et al. (2017). Ablating ErbB4 in PV neurons attenuates synaptic and cognitive deficits in an animal model of Alzheimer's disease. *Neurobiol. Dis.* 106, 171–180. doi: 10.1016/j.nbd.2017.07.001

Zhao, R., Fowler, S. W., Chiang, A. C. A., Ji, D., and Jankowsky, J. L. (2014). Impairments in experience-dependent scaling and stability of hippocampal place fields limit spatial learning in a mouse model of Alzheimer's disease. *Hippocampus* 24, 963–978. doi: 10.1002/hipo.22283

Zott, B., Busche, M. A., Sperling, R. A., and Konnerth, A. (2018). What happens with the circuit in Alzheimer's disease in mice and humans? *Annu. Rev. Neurosci.* 41, 277–297. doi: 10.1146/annurev-neuro-080317-061725

Zsiros, V., and Maccaferri, G. (2005). Electrical coupling between interneurons with different excitable properties in the stratum lacunosum-moleculare of the juvenile CA1 rat hippocampus. *J. Neurosci. Off. J. Soc. Neurosci.* 25, 8686–8695. doi: 10.1523/JNEUROSCI.2810-05.2005

frontiers | Frontiers in Neural Circuits

TYPE Review
PUBLISHED 20 October 2023
DOI 10.3389/fncir.2023.1218737

OPEN ACCESS

EDITED BY
Elsa Rossignol,
CHU Sainte-Justine, Canada

REVIEWED BY
Sheketha R. Hauser,
Indiana University Bloomington, United States
Benjamin Rolland,
Université Claude Bernard Lyon 1, France
Serge McGraw,
Montreal University, Canada

*CORRESPONDENCE
Thomas D. Prevot
✉ thomas.prevot@camh.ca

RECEIVED 08 May 2023
ACCEPTED 04 September 2023
PUBLISHED 20 October 2023

CITATION
Dharavath RN, Pina-Leblanc C, Tang VM, Sloan ME, Nikolova YS, Pangarov P, Ruocco AC, Shield K, Voineskos D, Blumberger DM, Boileau I, Bozinoff N, Gerretsen P, Vieira E, Melamed OC, Sibille E, Quilty LC and Prevot TD (2023) GABAergic signaling in alcohol use disorder and withdrawal: pathological involvement and therapeutic potential.
Front. Neural Circuits 17:1218737.
doi: 10.3389/fncir.2023.1218737

GABAergic signaling in alcohol use disorder and withdrawal: pathological involvement and therapeutic potential

Ravinder Naik Dharavath[1], Celeste Pina-Leblanc[1,2], Victor M. Tang[1,3,4,5,7,8], Matthew E. Sloan[1,2,4,5,6,7,8], Yuliya S. Nikolova[1,3], Peter Pangarov[1], Anthony C. Ruocco[1,3,9,10], Kevin Shield[8], Daphne Voineskos[1,3,9], Daniel M. Blumberger[1,3,9], Isabelle Boileau[1,2,3,11], Nikki Bozinoff[1,12], Philip Gerretsen[1,3,7,11], Erica Vieira[1,3], Osnat C. Melamed[1,12], Etienne Sibille[1,2,3], Lena C. Quilty[1,3] and Thomas D. Prevot[1,3]*

[1]Campbell Family Mental Health Research Institute of CAMH, Toronto, ON, Canada, [2]Department of Pharmacology and Toxicology, University of Toronto, Toronto, ON, Canada, [3]Department of Psychiatry, University of Toronto, Toronto, ON, Canada, [4]Addiction Division, CAMH, Toronto, ON, Canada, [5]Division of Neurosciences and Clinical Translation, Department of Psychiatry, University of Toronto, Toronto, ON, Canada, [6]Department of Psychological Clinical Science, University of Toronto Scarborough, Toronto, ON, Canada, [7]Institute of Medical Science, University of Toronto, Toronto, ON, Canada, [8]Institute of Mental Health Policy Research, CAMH, Toronto, ON, Canada, [9]Temerty Centre for Therapeutic Brain Intervention, CAMH, Toronto, ON, Canada, [10]Department of Psychology, University of Toronto Scarborough, Toronto, ON, Canada, [11]Brain Health Imaging Centre, CAMH, Toronto, ON, Canada, [12]Department of Family and Community Medicine, University of Toronto, Toronto, ON, Canada

Alcohol is one of the most widely used substances. Alcohol use accounts for 5.1% of the global disease burden, contributes substantially to societal and economic costs, and leads to approximately 3 million global deaths yearly. Alcohol use disorder (AUD) includes various drinking behavior patterns that lead to short-term or long-lasting effects on health. Ethanol, the main psychoactive molecule acting in alcoholic beverages, directly impacts the GABAergic system, contributing to GABAergic dysregulations that vary depending on the intensity and duration of alcohol consumption. A small number of interventions have been developed that target the GABAergic system, but there are promising future therapeutic avenues to explore. This review provides an overview of the impact of alcohol on the GABAergic system, the current interventions available for AUD that target the GABAergic system, and the novel interventions being explored that in the future could be included among first-line therapies for the treatment of AUD.

KEYWORDS

alcohol use disorders, clinical trials, GABA, integrative approach, interventions, pharmacotherapy, translational, unmet need

1. Introduction

Alcoholic beverages have been consumed for recreational purposes in most parts of the world since before recorded history began. According to the latest World Health Organization (WHO) global estimates (WHO, 2021), about 5.1% of the global adult population is living with alcohol use disorders (AUD). Another study by the global burden

of disease (GBD) collaborative network reported a 1.5% global AUD prevalence in 2019, highlighting variabilities between countries (Castaldelli-Maia and Bhugra, 2022). Ethanol, the main active component of alcoholic beverages, is currently one of the most used psychoactive drugs on the market. Ethanol produces a state of anxiolysis and disinhibition, which is commonly sought after in social situations or in individuals with AUD (Gilman et al., 2008). Alcohol consumption is also causally related to the development of approximately 230 diseases or disorders, including infectious diseases, malignant neoplasms, cardiovascular system due to ethanol's effect on blood pressure and inflammation (Chiva-Blanch and Badimon, 2019), mental and behavioral disorders, neurological diseases, digestive diseases, and injuries (Rehm et al., 2017). While consumption patterns vary, the impact of ethanol at low doses on overall health remains unclear (Larsson et al., 2020; Zhao et al., 2023). A recent systematic meta-analysis of cohort studies showed no statistically significant protective effect of alcohol on all-cause mortality at low ethanol intakes (Zhao et al., 2023). Studies have highlighted that abstinence from alcohol has many health benefits, including improved sleep. On the contrary, the risk of certain types of cancer, heart disease, and stroke increases with increased alcohol consumption (Savin et al., 2018; Paradis et al., 2022), and chronic consumption of ethanol in high doses is also linked to feelings of dysphoria, cognitive deficits, and an increased risk of developing AUD (Trantham-Davidson and Chandler, 2015).

Two major diagnostic classification systems are used to define AUD. The Diagnostic and Statistical Manual of Mental Disorders, Fifth Edition (DSM-5), developed by the American Psychiatric Association, defines AUD as a cluster of behavioral and physical symptoms, including withdrawal, tolerance, and craving (American Psychological Association, 2013). The International Classification of Diseases 11th Revision (ICD-11), developed by the World Health Organization, divides AUD into a harmful pattern of alcohol use and alcohol dependence. Alcohol dependence is characterized by "a strong internal drive to use alcohol, which is manifested by an impaired ability to control use, increasing priority given to use over other activities, and persistence of use despite harm or negative consequences" (WHO-ICD11, 2022). According to the ICD-10 definition of AUD, it was estimated that in 2016, approximately 8.6% of adult men and 1.7% of adult women suffered from AUD globally (Carvalho et al., 2019).

AUD may be characterized by the development of tolerance due to homeostatic adaptation in the brain compulsive seeking and withdrawal upon cessation of consumption (Liang and Olsen, 2014). AUD symptomatology includes a wide range of behaviors such as poor control over drinking and impulsivity (a failure to inhibit excessive drive), reward deficiency (a reduced response to natural rewards), maladaptive learning (the growing incentive salience of a drug's predictive cues with chronic use), the emergence of opponent processes (the power of negative motivational states underlying withdrawal), faulty decision making (inaccurate computation in preparation for action) or automaticity of responses (inflexibility of stimulus–response habits) (Volkow et al., 2013). Due to neuronal dependency on alcohol for regular activity in individuals with AUD, cessation of alcohol consumption often leads to withdrawal (Littleton, 1998). Sudden cessation might result in acute withdrawal symptoms, including delirium, seizures, and cognitive dysfunctions (Jesse et al., 2017; Laniepce et al., 2020). However, the symptoms seen in alcohol withdrawal range in severity depending on the volume and duration of ethanol consumption and inter-individual variability (Newman et al., 2023). Withdrawal symptoms are often related to hyperexcitability, such as insomnia, anxiety, palpitations, agitation, and even seizures (Saunders et al., 2019), likely related to alteration in the functioning of the brain inhibition system.

Due to its hydrophilic nature, ethanol readily penetrates all biological membranes and crosses the blood–brain barrier. Once in the organism, ethanol metabolism happens in the liver but also in the brain due to the presence of alcohol dehydrogenase (ADH), catalase, and P450 (CYP2E1) in both organs. Such metabolism routes produce mainly three metabolites: acetaldehyde, salsolinol, and acetate (Gil-Mohapel et al., 2019; Wilson and Matschinsky, 2020). After reaching the brain, ethanol and its metabolites induce diverse disturbances such as reduced glucose uptake, increased monocarboxylate uptake, dopaminergic, GABAergic, and glutamatergic alterations (Peana et al., 2017).

Since, ethanol and its metabolites act on multiple biological pathways of the central nervous system (CNS), therapeutic interventions relying on various approaches have been developed with variable degrees of efficacy. However, there is still a significant need to understand better the underlying mechanism leading to AUD and associated symptoms and develop more efficient intervention strategies. While impacting many CNS pathways, one of the main pathways altered by alcohol is the inhibitory pathway utilizing gamma-aminobutyric acid (GABA).

This review provides an overview of the impact of ethanol on brain functions related to GABA, describes existing therapeutic interventions, lists their shortcomings, and summarizes the existing knowledge around GABAergic functions in AUD involved in the expression of symptoms and outcomes before providing insight into the development of future therapeutic interventions acting on the GABAergic system.

2. Impact of ethanol on brain

Ethanol produces a wide variety of behavioral and physiological effects in the body, but exactly how it acts to produce these effects is still poorly understood. Like most dependence-producing substances, ethanol binds and acts on multiple proteins, receptors, and signaling pathways throughout the brain (Figure 1A), including amino acids, opioids, enzymes, and ion channels (Heinz et al., 2009; Koob and Volkow, 2016). The primary targets behind ethanol-induced behavioral phenotypes (disinhibition, hyperlocomotion, and anxiolysis) are $GABA_A$ receptors. Besides modulating $GABA_A$ receptor activity, ethanol can directly bind and modulate the activity of several proteins, including ionotropic glutamatergic (NMDA) receptors, alcohol dehydrogenase (ADH), and glycine receptors (Grant and Lovinger, 2018). Further, it has been observed that ethanol is capable of indirect modulation of other neurotransmitters (dopamine, serotonin, opioid, and cholinergic), particularly in brain regions involved in the mesolimbic reward system [i.e., amygdala, hippocampus, striatum, and ventral tegmental area (VTA)] via GABAergic/glutamatergic neurons or their respective receptors present on other types of neurons

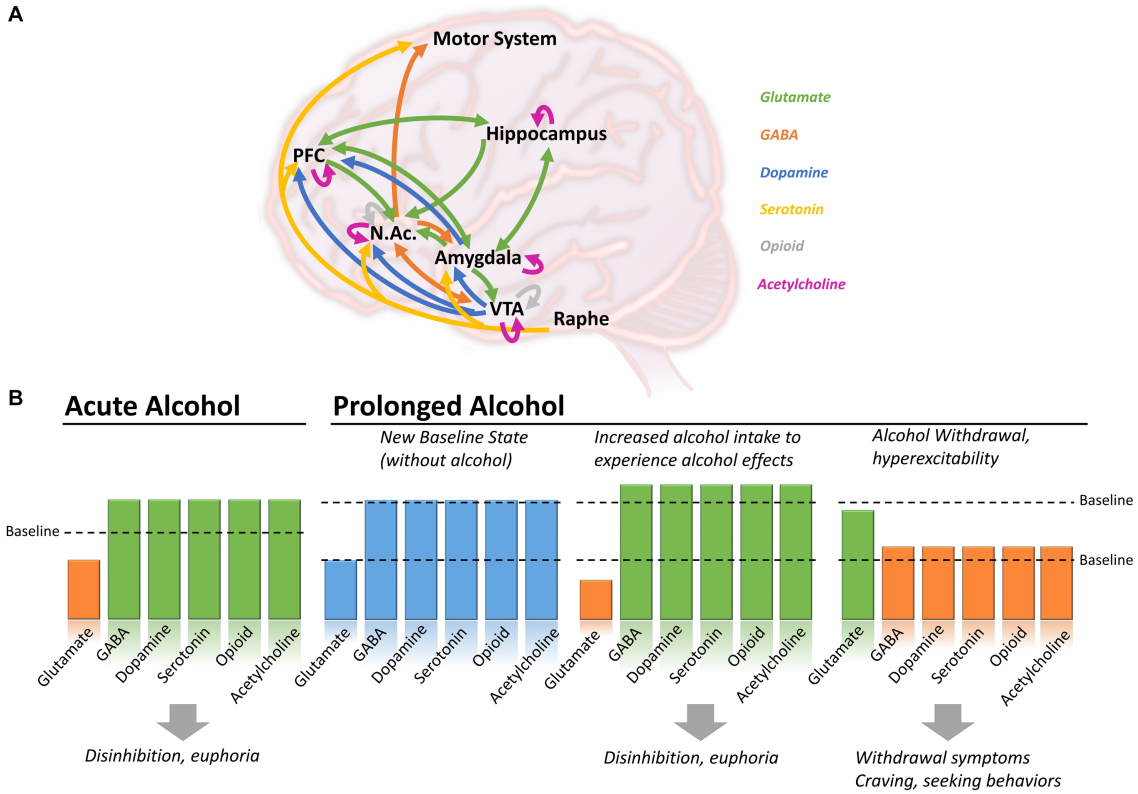

FIGURE 1
Brain circuits affected by alcohol consumption in the context of acute or prolonged exposure. **(A)** Alcohol induces changes in neutrotransmitters including glutamate (green), GABA (orange), dopamine (blue), serotonin (yellow), opioid (grey) and acetylcholine (purple), in various brain regions. **(B)** During acute alcohol consumption, ethanol induces a decrease in glutamatergic activity and an increased of GABAergic, dopaminergic, serotoninergic, opioid and cholinergic systems. With prolonged alcohol consumption, the different systems establish themselves at a new baseline level. To experience the effect of alcohol, individuals have to further increase their consumption leading to disinhibition and euphoria, but increasing the risk of AUD and dependence. During withdrawal, glutamatergic activity increases above the newly-set baseline, while GABAergic, dopaminergic, serotoninergic, opioid and cholinergic activity decrease, causing withdrawal symptoms, craving and seeking behaviors. Arrows in panel A shows direction of the projections between brain regions. NAc, Nucleus accumbens; PFC, Prefrontal cortex; VTA, Ventral tegmental area.

(Abrahao et al., 2017). Therefore, chronic ethanol consumption in large volumes drives a chemical imbalance in the brain and forces a homeostatic response to maintain neurochemical equilibrium and functionality (De Witte, 2004). As the brain chemically adapts to excess ethanol, it forms a new equilibrium in which ethanol becomes integral in neuronal function (Figure 1B; Valenzuela, 1997; Pérez-Ramírez et al., 2022). In individuals with AUD, this is manifested through increased tolerance to the effects of ethanol, which can lead to the consumption of alcohol near toxicity levels to experience the effects of alcohol, such as relaxation, anxiolysis, or disinhibition. Consistent with this notion, magnetic resonance spectroscopy (MRS) studies generally demonstrate lower cortical GABA levels in individuals with AUD, specifically during withdrawal, than in control participants (Prisciandaro et al., 2019; Kirkland et al., 2022; Shyu et al., 2022).

Therefore, the main activity of ethanol is thought to be on glutamatergic and GABAergic signaling pathways, with an increase or decrease of function depending on the state (acute consumption, chronic consumption, or withdrawal), inducing a cascade of events acting on dopamine, serotonin, and endogenous opioid release (Ferraguti et al., 2015).

2.1. Impact of ethanol on glutamate and GABA

Preclinical and clinical studies showed that ethanol binds to and inhibits the functions of the glutamatergic receptors (NMDA, AMPA, Kainate, and mGluR5) (Möykkynen and Korpi, 2012; Ferraguti et al., 2015). It also binds to and facilitates the functions of the $GABA_A$ and $GABA_B$ receptors (Valenzuela and Jotty, 2015; Olsen and Liang, 2017), which, combined with the effect of glutamatergic receptors, causes an overall imbalance in neuronal activity, thought to be responsible for "blackout" moments after acute heavy drinking (Wetherill and Fromme, 2016; Yang et al., 2022) and contributing to excitotoxicity and loss of synaptic plasticity (Chandrasekar, 2013). Data from studies using human transcranial magnetic stimulation (TMS), a non-invasive neuromodulation approach that probes GABA-receptor-mediated cortical inhibition, confirmed that alcohol intake increases GABA-inhibitory neurotransmission and decreases NMDA-receptor-activated excitatory neurotransmission (Ziemann et al., 2015). Interestingly, the activity of ethanol metabolites on glutamatergic and GABAergic targets seems different, which could explain the

dynamic changes happening during drinking episodes (see Section 2.6 below).

Preclinical studies in rats have also confirmed the critical impact of ethanol on the regulation of ethanol-maintained responses through $GABA_A$ receptor-dependent signaling in the central nucleus of the amygdala (Avegno et al., 2018; Barchiesi et al., 2021; Kisby et al., 2021). Preclinical studies have also confirmed the impact of alcohol on behavioral outcomes [compulsive behavior (Giuliano et al., 2018), withdrawal-induced hyperalgesia (Avegno et al., 2018), increased anxiety (Barchiesi et al., 2021), altered cognitive functions], and biological pathways [GABA and glutamine (McCunn et al., 2022), glutamate (Vengeliene et al., 2005; Mira et al., 2019), dopamine (Ma and Zhu, 2014; Solanki et al., 2020)] as well as provided insights onto therapeutic interventions (Foo et al., 2019).

2.2. Impact of ethanol on acetylcholine

Ethanol intake in rats was also shown to bind to the nicotinic-subtype receptor of acetylcholine (Davis and de Fiebre, 2006) and to increase acetylcholine levels in the VTA (Larsson et al., 2005), facilitating the influx of dopamine onto the nucleus accumbens (NAc). Such activity in the VTA and NAc is thought to contribute to positive reinforcement of alcohol. In contrast, modulation of the nicotinic receptors of the hippocampus and amygdala is thought to be involved in negative effects (Tarren et al., 2016). Ethanol's binding and activity at nicotinic receptors are also thought to interfere with nicotine-induced desensitization, which could explain the high prevalence of co-use of alcohol and tobacco (Davis and de Fiebre, 2006; Addolorato et al., 2012).

2.3. Impact of ethanol on dopamine

As a downstream effect of alcohol consumption, ethanol induces an indirect increase in dopamine release and acetylcholine activity from the VTA to the NAc, a brain region strongly associated with reward and motivation (Boehm II et al., 2004). Preclinical Studies have also shown that dopamine is released in the ventral striatum and NAc, contributing to drug reward, which could be further increased by nicotine co-administration (Tizabi et al., 2007). The activation of central GABAergic neurotransmission, particularly through $GABA_B$ receptors, is also linked to the mesolimbic dopaminergic neurotransmission during rewarding processes, altogether contributing to the addictive properties of ethanol (Addolorato et al., 2012).

2.4. Impact of ethanol on serotonin

Acute alcohol consumption increases serotonin release, contributing to the rewarding aspect of consuming alcohol (Banerjee, 2014). Previous studies showed that acute ethanol augments the firing rate of the serotoninergic 5-HT_3 receptors, and longer consumption can affect the expression and function of various other subtypes, including 5-HT_2, without a clear understanding of whether it is a direct effect or mediated by a cascade of events or adaptation (Lovinger, 1997).

2.5. Impact of ethanol on opioids

Consumption of alcoholic beverages has also been shown to increase the levels of endogenous opioids (Mitchell et al., 2012), which are subsequently drastically reduced during withdrawal, leading to craving and increasing the risk of opioid-seeking behaviors (Turton et al., 2020). The activity of ethanol at $GABA_A$ receptors in the VTA and NAc facilitates endogenous opioid release in the VTA, contributing to the alcohol-induced feeling of euphoria (Colasanti et al., 2012). Opioid-targeting treatments such as naltrexone or nalmefene diminish these effects of alcohol (Turton et al., 2020), providing further evidence of the impact of alcohol on the opioid system.

2.6. Impact of ethanol metabolism on various neurotransmitters

Acetaldehyde, salsolinol, and acetate, metabolites of ethanol, seem to participate in the effect of alcohol, but their contribution is less understood. Acetaldehyde in the brain causes euphoria at low doses and plays a vital role in ethanol's reinforcing properties, thereby facilitating alcohol addiction (Quertemont et al., 2005; Peana et al., 2017). One of the primary studies reported that acetaldehyde increased GABA uptake but did not affect both its release and synthesis (Bobrova and Covaltchuk, 1980). Acetaldehyde has been shown to stimulate dopaminergic neurons (Melis et al., 2007) and μ opioid receptors (Sanchez-Catalan et al., 2014). Acetaldehyde is a highly reactive and short-lived metabolite of ethanol that reacts with biogenic amines like dopamine and forms condensation products like Salsolinol.

Studies reported that salsolinol may exert some of the effects of ethanol by activating μ opioid receptors on GABAergic neurons signaling onto dopaminergic neurons in the mesolimbic system. However, the mechanisms are complex, and it seems like salsolinol would reduce GABAergic activity while ethanol increases it, suggesting opposite responses on GABAergic receptor activity from ethanol and one of its metabolites, also causing a downstream opposite effect on dopamine release (Peana et al., 2017).

Finally, the direct role of acetate on GABAergic regulation has not been reported. However, acetate was reported to contribute to increased cerebral blood flow (Tanabe et al., 2019), increased neuronal excitability, and enhanced glutamatergic activity (Chapp et al., 2021), whereas ethanol boosts GABA-mediated inhibition. Accordingly, existing literature indicates that concrete experimental evidence is required to confirm the effects of ethanol's metabolites on the GABAergic system.

3. GABAergic mechanisms involved in AUD

GABA is the main inhibitory neurotransmitter in the brain. It exerts its function by binding to two types of receptors: $GABA_A$

and $GABA_B$. $GABA_A$ receptors are ionotropic chloride channels (Enna, 2007), while $GABA_B$ are metabotropic G-coupled protein receptors (GPCR) (Pinard et al., 2010). $GABA_B$ receptors mediate slow inhibitory transmission, while $GABA_A$ mediates fast inhibition. $GABA_A$ and $GABA_B$ have been extensively reviewed for their potential in pharmacotherapies (Sarasa et al., 2020) and link to AUD (Ghit et al., 2021; Holtyn and Weerts, 2022).

$GABA_A$ receptors are heteropentamers composed of various subunits such as α, β, γ, δ, ε, θ, π, and ρ (Figures 2A,B), which are found throughout the brain (Fritschy and Mohler, 1995), including regions involved in alcohol-related use such as the prefrontal cortex, thalamus, cerebellum, or the amygdala (Bowery et al., 1987). Ethanol acts as a positive allosteric modulator (PAM) of $GABA_A$ receptors, binding to several subunits, mostly α-subunits, thus explaining its sedative and neuromodulating properties (Ghit et al., 2021). Other PAMs include benzodiazepines and Z-drugs that promote sedation, anxiolysis, muscle relaxation, and anti-seizure properties.

$GABA_B$ receptors are the only metabotropic G protein-coupled receptors for GABA (Figure 2C) and can be found in presynaptic (auto-inhibitory) and postsynaptic membranes and distributed throughout the CNS and PNS. The two main subunits of the $GABA_B$ receptor are $GABA_BR1$ and $GABA_BR2$. For the $GABA_B$ receptors to be active and functional, these subunits need to interact to form a stable heterodimer. Importantly, orthosteric agonists and antagonists bind to $GABA_BR1$, while PAMs bind to the $GABA_BR2$ subunit. $GABA_B$ receptors are primarily found in the cerebellum, prefrontal cortex, and thalamus, in addition to the interpeduncular nucleus and the olfactory nucleus (Bowery et al., 1987). Alcohol is known to interact with the $GABA_B$ receptors in the brain, but the exact binding site and mechanism of action are not completely understood. $GABA_B$ receptor-binding drugs have anti-convulsant and analgesic properties (Terunuma, 2018) and are also found to reduce craving and

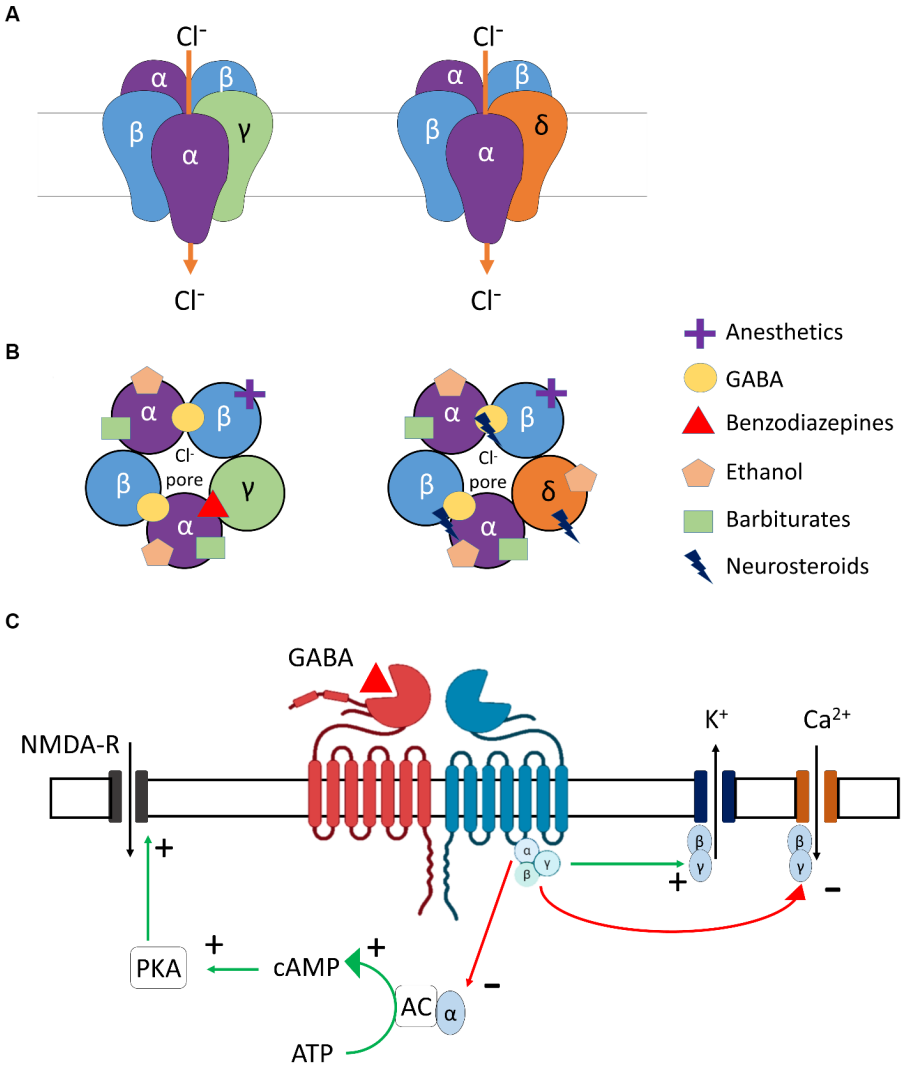

FIGURE 2
GABA receptor subtypes involved in modulation of ethanol. **(A)** Molecular structures of γ- and δ- subunit-containing $GABA_A$ receptors. **(B)** Ligand-specific binding sites of γ- and δ- subunit-containing $GABA_A$ receptors. **(C)** Molecular structure and downstream signaling of $GABA_B$ receptors. α, β, γ, δ, subunits of $GABA_A$ receptor; Cl-, Chloride ion; GABA, Gamma-aminobutyric acid; NMDA-R, N-Methyl-D-aspartic acid receptor; K^+, Potassium ion; Ca^{+2}, Calcium ion; PKA, Protein kinase A; cAMP, Cyclic Adenosine monophosphate; ATP, Adenosine triphosphate; AC, Adenylyl cyclase.

withdrawal symptoms in dependent individuals [for example, Baclofen (Logge et al., 2022)].

4. From alcohol use to alcohol use disorders – the GABAergic system

DSM-5 classifies substance-related disorders into substance-use disorders (SUD) and substance-induced disorders (intoxication, withdrawal, and other substance/medication-induced mental ailments). Clinically, SUDs occur in a range of severity based on a number of symptom criteria endorsed. Mild (2–3 symptoms), moderate (4–5), and severe (>5). The DSM-5 diagnostic criteria do not describe levels or types of alcohol use or alcohol use harms (American Psychological Association, 2013); however, for this review, we chose to include some of the most commonly used categories of this kind (e.g., binge alcohol use) for a better illustration of the AUD pathophysiology and the involvement of GABAergic system to align with clinical presentations of AUD and alcohol withdrawal. AUD encompasses various disorders characterized by different consumption patterns, impacting the brain and the GABAergic system. Alcohol consumption, including alcohol use not meeting the criteria for AUD, also impacts the GABAergic system. For example, minimal alcohol intake will enter the brain and target $GABA_A$ receptors, causing a cascade of regulatory events, potentially leading to behavioral changes. When consumption becomes chronic, or during binge drinking episodes, the impact of alcohol on the brain is even more profound, triggering activation/inhibition of other biological pathways (as described earlier in Figure 1). Table 1 below summarizes alcohol use at different levels, explains the different considerations given for men and women, and highlights the impact on the GABAergic system and symptoms related to the use of alcohol.

4.1. Occasional, moderate, and safe use of alcohol with low risk for AUD

The safe or moderate use of alcohol is considered with less than 2 drinks per day for men and 1 for women (0.02–0.04 g/dL blood alcohol concentration), where the risk for developing AUD remains low. Even with such use, the acute or low level of ethanol present in the system is enough to potentiate the action of GABA at $GABA_A$ receptors, inducing relaxation. Even in rats, acute ethanol administration induces a state of anxiolysis driven by the potentiation of the $GABA_A$ receptor in the basolateral amygdala, acting on multiple cell populations (Herman and Roberto, 2016). Low levels of ethanol already play a role in the expression and trafficking of $GABA_A$ receptors in the brain by rapidly downregulating $\alpha_4\beta_3\delta$-$GABA_A$ receptors in the hippocampus (Chandler et al., 2017). Expression of the $\alpha_1\beta_3\gamma_2$-$GABA_A$ receptors is also downregulated after several hours of consumption, followed by an upregulation of $\alpha_4\beta_3\gamma_2$ and $\alpha_2\beta_3\gamma_1$ after a couple of days. This demonstrates the broad and long-lasting kinetics of an acute consumption of ethanol, which is reversible, but the recovery timeline is dose-dependent (Holford, 1987).

During medium-risk drinking, i.e., drinking episodes of alcohol when the volume of alcohol is consumed in a short period but not binge drinking (not more than 5 drinks in 2 h for men, 4 in 2 h for women, and < 0.08 g/dL) (World Health Organization, 2000), ethanol levels can range from 5 to 30 mmol/L. This potentiates the $GABA_A$ receptors in the brain, decreasing excitatory glutamatergic neurotransmission and causing slight sedation, a feeling of relief, slight alteration of short-term memory, decreased attention, and potential mood changes (Liang and Olsen, 2014). Studies in rats have demonstrated that this dose level increases GABAergic firing rate and afferent-evoked synaptic response in the VTA, a central hub for dopaminergic projections in the brain, regulating motivation, cognition, reward valuation, and addiction. This impact on the VTA, potentially driven by changes in firing rates from the GABAergic system, contributes to increased alcohol intake (Tateno and Robinson, 2011).

Interestingly, preclinical studies using rats also demonstrated that reducing α_4-subunit expression via a viral-mediated RNA interfering with the α_4-protein synthesis in the NAc allowed for a reduction of self-administered ethanol. Similar results were observed when pharmacologically blocking the $GABA_A$ receptors in the paraventricular nucleus of the hypothalamus, further confirming the role of GABAergic potentiation in increasing alcohol intake and seeking behaviors (Li et al., 2011).

4.2. At-risk drinking patterns

Greater than the threshold set for safe and moderate use described above, consumption of alcohol is considered at risk (NIAAA, 2018). In this case, ethanol induces $GABA_A$ receptor activation in the VTA, NAc, hypothalamus, and hippocampus, causing an overall imbalance in excitation/inhibition, leaning toward increased inhibition. At a certain point, thought to be above 13 mmol/L (Liang and Olsen, 2014), the reward pathways of the mesolimbic system are directly and indirectly activated (as described in the previous section on *Impact of Ethanol on the Brain*), allowing dopamine release, which fosters the development of addictive properties of alcohol consumption.

4.3. Alcohol use disorder

AUD is considered when the drinking pattern is above established standards, either due to volume or frequency of intake. One tool used worldwide to identify AUD is the Alcohol Use Disorder Identification Tool (AUDIT), developed by WHO (Higgins-Biddle and Babor, 2018). While the classification of AUD has changed over the years and is country-dependent, most medical and addiction professionals frequently break AUD into two categories: binge and heavy drinking (Kranzler and Soyka, 2018).

Binge drinking is the acute consumption of large amounts of alcohol (for example, five or more drinks in less than 2 h for men and four or more for women, leading to >0.08 g/dL of blood alcohol concentration). Binge drinking leads to cognitive deficits, reduced inhibition, and reduced ability to control alcohol intake voluntarily, thereby increasing the chances of developing more frequent AUD in the future (Chmielewski et al., 2020). Risk factors for binge drinking include age, male sex, alcohol consumption at a young age, a patient's state of mental health, and genetic susceptibility (NIAAA, 2020).

Preclinical studies of psychological changes and alcohol consumption have determined that in young rats (postnatal days

TABLE 1 Alcohol consumption, symptoms, and the role of the GABAergic system.

Stage of alcohol use	Men	Women	Involvement of GABAergic system	Symptoms/Behavioral outcomes
Moderate use – low risk drinking	2 drinks/day or 28 g of ethanol/day*	1 drink/day or 14 g of ethanol/day*	Following acute ethanol ingestion, GABAA receptors are activated in basolateral amygdala and decreases glutamate action. Ethanol also downregulates extrasynaptic α4βδ–$GABA_A$Rs in the hippocampus (Liang and Olsen, 2014).	Anxiolysis, sedation accompanied by decreased attention, alterations in memory, mood changes, and lethargy.
Use above low-risk drinking	>2 drinks/day and <14 drinks/week	>1 drink/day and <7 drinks/week	At low concentrations (10 mmol/L), GABAA receptors are activated in VTA, NAc, hypothalamus and hippocampus, while at concentrations higher than 13 mmol/L activates the mesolimbic reward pathway and increases the DA levels.	Increased voluntary ethanol ingestion
Binge drinking	>5 drinks/2 h Or > 60 g of ethanol/occasion	>4 drinks/2 h Or > 40 g of ethanol/occasion	Compensatory downregulation of cortical GABA levels and $GABA_A$ receptors along with hyperexcitability (Marinkovic et al., 2022).	Insomnia, irritability, anxiety, autonomic hyperactivity and seizures
Heavy drinking	>5 drinks/day or > 15 drinks/week	>4 drinks/day or > 8 drinks/week	Heavy alcohol consumption causes increased internalization of α1 and α4 subunit-containing $GABA_A$ receptors on hippocampal pyramidal cells thereby decreasing the availability of post-synaptic $GABA_A$ receptors. Which in turn leads to increased alcohol consumption to attain the activation of desired GABA activity (Trudell et al., 2014).	Chronic downregulation of α1 and α4 subunit GABAA receptors may lead to increased alcohol tolerance, leading to dependence.
Dependence/ Alcoholism	Compulsive drinking with increased alcohol tolerance		GABAergic hypofunction following chronic alcohol consumption leads to reduced GABAergic (via $GABA_B$ receptors) inhibition of DA neurons in VTA leads to reward-associated alcoholism (Enoch, 2008).	Development of positive (pleasure) and negative (aversive – avoiding anxiety) reinforcement behaviors as the motivation to seek more alcohol.
Withdrawal (AWS)	Symptoms following the discontinuation or complete cessation of alcohol consumption		Chronic alcohol drinking increases GABA activity in comparison to glutamate (GABA > Glutamate). In the absence of alcohol (withdrawal), the GABA activity decreases but the increased glutamate (as compensation) levels remain about the same and leading Glutamate > GABA state.	Withdrawal causes hyperexcitability, elevated adrenergic system responses along with anxiety, insomnia and dysphoria.
Relapse	Spontaneous or delayed reoccurrence of alcohol drinking to avoid AWS or due to various internal or external stimuli		Hyperexcitability, seizures, and anxiety due to withdrawal-related GABA hypofunction can be the major reasons behind the relapse. Furthermore, reduced GABAergic and uninhibited DA transmission in NAc may lead to cue-induced/reward-based (craving) relapse (Heinz et al., 2009).	Relapse-related DA-reward "hijack" leads to the dysfunction of different domains of cognition.

A regular alcoholic drink = 10–14 g of ethanol. *on days when alcohol is consumed.

28–42), binge drinking induces a state of anxiety-like behavior and leads to alcohol dependence in adulthood (Pandey et al., 2015). Stress and withdrawal-induced anxiety are correlated to increased voluntary ethanol drinking in alcohol-preferring rats (Meyer et al., 2013), and chronic psychosocial stressed male mice showed increased voluntary ethanol drinking (Bahi, 2013). Human magnetic resonance spectroscopy studies have shown that cortical GABA levels are reduced in young adult binge drinkers (Marinkovic et al., 2022). Following acute high-dose ethanol administration in rats, thalamic α_4-$GABA_A$ receptor levels were regulated temporally, as a decrease was observed at 2 h followed by a delayed transient increase (Werner et al., 2016). Other studies using a transgenic dopaminergic D3 receptor knockout mouse model combined with an α6-$GABA_A$ receptor ligand (RO 15–4,513) also showed that increased GABAergic inhibition in the NAc contributes to reducing binge drinking, confirming the critical role of GABAergic neurotransmission in reducing alcohol intake (Leggio et al., 2019).

Heavy drinking is defined as drinking more than recommended during a week, leading to 0.1–0.2 g/dL of blood alcohol concentration, depending on the number of drinks. For a man, having more than 15 standard alcoholic drinks weekly is considered heavy drinking. For women, having more than 8 drinks a week meets the criteria for heavy drinking (NIAAA, 2018). Heavy drinking leads to increased neuronal atrophy and reduces white matter fiber integrity (Daviet et al., 2022), associated with increased risk for dependence, anxiety, depression, cognitive deficits, altered control over drinking habits, cardiovascular diseases, and other health risks.

Studies have shown that the behavioral changes are primarily due to the plastic changes of $GABA_A$ receptors that occur after chronic ethanol exposure, which include significantly reduced post-synaptic α_1 and increased α_4-containing $GABA_A$ receptors. The subunit composition of $GABA_A$ receptor subtypes is expected to determine their physiological properties and pharmacological profiles. An in-depth study of $GABA_A$-subunits using genetically engineered mice

has shown that the α_1 subunit involves sedation, anti-convulsant activity, anterograde amnesia functions, etc., while the α_4 subunit is involved in changes in mood and anxiety. Thus, these $GABA_A$ receptor subunit composition changes are a mechanism underlying the behavioral changes after chronic ethanol exposure, which leads to additional risks of developing dependence. Heavy drinking triggered by chronic stress and any induced anxiety is an additional risk factor for developing alcohol dependence, observed in animal models and humans (McCaul et al., 2017). Conversely, stopping or reducing alcohol consumption, in turn, aggravates stress or anxiety due to an overall imbalance in brain homeostasis (Schmidt et al., 2016).

4.4. Chronic/daily alcohol use leading to dependence

With chronic alcohol consumption comes an increased risk for reward-associated habitual alcohol abuse, pronounced craving behavior for alcohol, and inability to stop seeking alcohol. This is usually highly linked to the development of dependence, a severe form of AUD that occurs when a person develops tolerance to the effect of alcohol and, therefore, seeks further alcohol consumption to prevent experiencing withdrawal symptoms. Alcohol dependence is a serious condition that requires comprehensive treatment to address the physical, emotional, and behavioral aspects of AUD.

Postmortem studies found a loss of GABAergic markers in the human brains of adults with alcohol dependence, particularly in men (Behar et al., 1999; Dodd et al., 2006). Transcranial magnetic stimulation (TMS) studies also demonstrated that chronic alcohol dependence has some level of impact on $GABA_A$ and $GABA_B$ receptor function, which seems to vary from study to study (Mohammadi et al., 2006; Ziemann et al., 2015). Several studies found no effects on short-interval cortical inhibition or TMS-evoked N45 potential (Conte et al., 2008; Nardone et al., 2010; Mon et al., 2012; Naim-Feil et al., 2016), thought to index $GABA_A$ receptor function. However, other studies found a general decrease in GABA levels (Prisciandaro et al., 2019; Shyu et al., 2022), including in youth with alcohol dependence (Kaarre et al., 2018). Given the dynamic nature of alcohol's effects on GABA, the GABA levels depend on several states (e.g., recently detoxified or more prolonged abstinence) and traits (e.g., age). One report on long-interval cortical inhibition thought to index $GABA_B$ showed decreases in alcohol-dependent patients (Naim-Feil et al., 2016).

Multiple preclinical studies demonstrated that chronic ethanol consumption alters $GABA_A$ receptor plasticity, leading to ethanol dependence (Olsen and Liang, 2017). Other preclinical studies established that general $GABA_A$ receptor expression and function changes in cases of alcohol dependence, both synaptically and extra-synaptically, in brain regions highly involved in establishing dependence and symptom emergence (i.e., the cortex, hippocampus, and central amygdala). This translates into a general loss of phasic and tonic GABAergic inhibition, tolerance to ethanol, and cross-tolerance to benzodiazepines and other sedative-hypnotics acting on GABA receptors (Kumar et al., 2009; Olsen and Liang, 2017; Bohnsack et al., 2018).

With such alteration in overall GABAergic functioning, a drastic imbalance in excitation/inhibition develops across multiple brain regions [medial prefrontal cortex (Pleil et al., 2015)], amygdala circuit (Herman et al., 2016; Herman and Roberto, 2016; Hughes et al., 2019), intrahippocampal circuits (Liang et al., 2004), and VTA circuits (Arora et al., 2013) causing a decrease in inhibitory control in multiple neurotransmitter firing activity, leading to the emergence of various behavioral changes including cognitive deficits, seeking behavior, humor changes, and others (Morrow et al., 2020).

Chronic alcohol consumption in heavy drinking, dependence, and associated $GABA_A$ plasticity changes also lead to DA release changes in the reward neurocircuitry. During acute alcohol withdrawal, changes occur, such as upregulation of α_4-containing $GABA_A$ receptors and downregulation of α_1- and α_3-containing $GABA_A$ receptors (Liang and Olsen, 2014). $GABA_A$ receptor downregulation may contribute to anxiety and seizures of withdrawal. During withdrawal periods, rats show a significant decrease in DA and serotonin levels in the reward neurocircuitry commonly associated with dysphoria, depression, and anxiety disorders. These psychological changes may also contribute to ethanol-seeking behavior, again demonstrating the complexity of changes induced by chronic alcohol consumption.

5. Existing interventions

Existing therapeutic interventions for AUD and alcohol withdrawal have attempted to harness the various CNS systems on which alcohol acts to limit the harms associated with alcohol consumption. The existing therapeutic interventions have diverse efficacy levels, various side effects, and contraindications (Table 2). Several clinical trials have shown the efficacy of certain pharmacotherapies that are approved by regulatory agencies for treating AUD or withdrawal and that are used off-label (Carpenter et al., 2018; Sloan et al., 2020).

5.1. Non-GABAergic pharmacologic interventions

Disulfiram has been an FDA-approved drug used to treat AUD since 1951. It inhibits the acetaldehyde dehydrogenase enzyme involved in ethanol metabolism, leading to higher plasma concentrations of acetaldehyde, which induces unpleasant side effects if a patient consumes alcohol while taking this medication, preventing further drinking. Disulfiram-induced reactions can include hepatotoxicity and death, which is why disulfiram needs to be used with caution (Kranzler and Soyka, 2018; Stokes and Abdijadid, 2022). Nowadays, the most used pharmacotherapy is naltrexone (commercialized under the brand name Revia®), a competitive μ opioid receptor antagonist and a partial antagonist of the δ and κ opioid receptors (Liang and Olsen, 2014; Sloan et al., 2020; Singh and Saadabadi, 2023). It decreases craving by reducing the rewarding and euphoric effects of alcohol and is one of the few AUD pharmacotherapies approved by the FDA. It is generally well tolerated but has minor side effects (Singh and Saadabadi, 2023).

Acamprosate is an FDA-approved drug used in Europe and North America for alcohol craving and relapse prevention (Franck and Jayaram-Lindström, 2013; Kalk and Lingford-Hughes, 2014). Although its exact mechanisms are unknown, it decreases glutamate during alcohol withdrawal through NMDA receptor modulation and

TABLE 2 Existing pharmacological therapeutics to treat AUDs, their efficacy, and limitations.

Drug name	Indications	Mechanism of action (MoA)	Effects on AUDs	Adverse drug reactions/side effects	Contra indications	References
Acamprosate	AUD in Europe and North America (FDA approved)	Unknown. ↓ Glutamate during alcohol withdrawal via NMDA modulation. Potentiates $GABA_A$ receptors through $GABA_B$ receptor inhibition.	Decreases alcohol craving and prevents relapse. Reduce alcohol consumption and increases abstinence when combined with psychosocial support.	Suicidality, amnesia, anxiety, depression, somnolence, nausea, vomiting, abdominal pain, pruritis, and rashes.	Severe renal diseases and dose lowered in mild renal diseases.	Franck and Jayaram-Lindström (2013), Sloan et al. (2020)
Baclofen	AUD in France (Off label in other countries) Primary indication: Centrally acting muscle relaxant.	$GABA_B$ agonist ↑ K^+ and ↓Ca^{2+} influx in neurons. ↓ dopamine release.	Can reduces craving and withdrawal symptoms in dependent individuals. (Inconsistent findings).	Drowsiness, sedation, dizziness, headache, confusion, muscle stiffness, excessive perspiration, itching, abnormal muscle movements, numbness, and slurred speech.	Cardiac disease Respiratory disease Severe psychiatric disorders Liver or kidney disease (require adjusted dosing)	Garbutt (2019), Mason (2017), Rolland et al. (2020), Sloan et al. (2020)
Disulfiram	AUD (second-line treatment)	Irreversible inhibitor of acetaldehyde dehydrogenase.	Elevated levels of acetaldehyde lead to severe adverse reactions, limiting patient to consume further alcoholic beverages.	Optic neuritis, psychosis, hepatotoxicity, peripheral neuropathy Metallic aftertaste, dermatitis, moderate to severe drowsiness, hepatitis, neuropathy, headaches, and confusion.	Use of metronidazole, paraldehyde or alcohol-containing products Cardiac Disease Hepatic Disease Diabetes Pregnancy.	Kranzler and Soyka (2018), Sloan et al. (2020)
Nalmefene	Controlled drinking (Australia and Europe)	Antagonist of μ and δ opioid receptors Partial agonist at the κ receptor. ↓ Dopamine release in the nucleus accumbens.	It modulates dopaminergic NAc circuitry via kappa receptor activation to reduce dependence by decreasing the rewarding and craving effects of alcohol. It can help control alcohol consumption with psychosocial support.	Nausea, dizziness, insomnia, headache, vomiting, fatigue, and drowsiness.	It may elicit opioid withdrawal in patients taking opioids or recently suffering from opioid addiction.	López-Pelayo et al. (2020)
Naltrexone	AUD (first-line treatment and FDA-approved)	Competitive antagonist at the μ opioid receptor with mild antagonistic activity at the δ and κ opioid receptors.	Reduce cravings and feelings of euphoria associated with AUD. Reduces the chances of relapsing. Reduces opioidergic-dependent dopamine activity in the mesolimbic system to reduce the rewarding effects.	Hepatotoxicity, precipited withdrawal, depression and suicidality Somnolence, nausea, vomiting, anorexia, insomnia, headache, dizziness, gastrointestinal discomfort, including abdominal cramps and diarrhea.	Concurrent opioid use. Liver failure or liver disease Bleeding or coagulation disorder	Liang and Olsen (2014), Sloan et al. (2020)
Gabapentin	AUD (Off label) Primary indication: neuropathic pain, neuralgia, and seizure	GABA analog but unknown MOA. supposed main target: α2δ1 voltage-gated Ca^{2+} channel ↑ GABA concentrations in the brain.	Reduces cravings, decreases the risk of relapse to heavy drinking, and increases abstinence. More significant effects are seen when taken in combination with Naltrexone.	Anaphylaxis, suicidality Dizziness, somnolence, ataxia, dry mouth, weight gain, fatigue, nystagmus, and tremor.	Severe renal disease	Anton et al. (2020), Cai et al. (2012), Sloan et al. (2020)

(Continued)

TABLE 2 (Continued)

Drug name	Indications	Mechanism of action (MoA)	Effects on AUDs	Adverse drug reactions/side effects	Contra indications	References
Topiramate	AUD (Off label) Primary indication: Anti-convulsant	↑ $GABA_A$ receptor activity. ↓ Glutamate release via AMPA receptor. ↓ Dopamine release in the nucleus accumbens.	Reduces craving, reward, and the risk of relapse. Decreases withdrawal symptoms by mediating hyperexcitability in the brain, thereby increasing abstinence.	Nephrolithiasis, Hyperammonemia, suicidality, hyperthermia, metabolic acidosis, glaucoma Cognitive dysfunctions, Paresthesia, dysgeusia, anorexia, anorexia, weight loss, nervousness, dizziness, and somnolence.	Pregnancy	Burnette et al. (2022), Paparrigopoulos et al. (2011), Sloan et al. (2020), Wenzel et al. (2006)
Benzodiazepines	Withdrawal	Allosteric modulator of $GABA_A$ receptors ($\alpha 1/2/3/5\beta 1/3\gamma 2$)	Treats acute alcohol withdrawal symptoms. Prevents withdrawal-induced seizures.	Sedation, drowsiness, ataxia, and anterograde amnesia.	Current consumption of alcohol Renal or liver disease	Nelson et al. (2019)

indirectly potentiates $GABA_A$ receptors. Acamprosate is generally well tolerated (Kalk and Lingford-Hughes, 2014).

Nalmefene is another antagonist of the μ and δ opioid receptors but is a partial agonist at the κ receptor. It is currently approved for AUD indication in Australia and Europe. Nalmefene decreases dopamine release in the NAc and reduces alcohol dependence and consumption by decreasing the rewarding and craving effects of alcohol (Paille and Martini, 2014). It can help control alcohol intake and has shown better results in those benefiting from psychosocial support. It has mild side effects, which generally disappear with time (Paille and Martini, 2014; López-Pelayo et al., 2020).

5.2. GABAergic pharmacologic interventions

Baclofen is only approved for the treatment of alcohol withdrawal in France (Garbutt, 2019). Despite multiple trials supporting its efficacy in reducing the risk of relapse and increasing abstinence days (Agabio et al., 2023), its efficacy remains controversial, and systematic reviews consider the evidence of its efficacy insufficient (Jonas et al., 2014). It acts as an agonist at the $GABA_B$ receptor and decreases dopamine release in the mesolimbic system, which reduces craving and withdrawal symptoms in dependent individuals. Baclofen has multiple side effects, limiting its use (Romito et al., 2021).

Gabapentin is a GABA analog used as an anti-epileptic medication for over 30 years. Clinical trials have shown dose-dependent efficacy in reducing craving, reducing anxiety, and facilitating abstinence (Anton et al., 2020). However, some studies also raise concerns due to its sedating properties and documentation of extra-medical use of this medication (Modesto-Lowe et al., 2019; Weresch et al., 2021). It was also found that Gabapentin causes respiratory depression when used alone and increases the risk of opioid-related deaths when combined with opioids (Gomes et al., 2017). Despite being a GABA analog, its mechanism of action is still unclear and seems unrelated to GABAergic modulation. Its main target seems to be the $\alpha_2\delta$-subunit of the voltage-gated calcium channel. It also increases GABA concentrations in the brain (Cai et al., 2012).

Topiramate is not yet approved by the FDA for the treatment of AUD. Still, clinical trials have demonstrated reductions in craving and risk of relapse and increasing abstinence (Kranzler et al., 2014; Manhapra et al., 2019; Wetherill et al., 2021). It is an approved anti-convulsant for treating epilepsy and seems to act through $GABA_A$ receptor modulation (Fariba and Saadabadi, 2022). It also binds the AMPA receptor to decrease glutamate release and decreases dopamine release in the NAc. It has some side effects, including paresthesia, dysgeusia, anorexia, and cognitive impacts such as slowing mental and physical activity and trouble concentrating or attention (Wenzel et al., 2006).

Benzodiazepines (BZ) are allosteric modulators of the $GABA_A$ receptor that bind to the $\alpha_{1,\,2,\,3,\,5,}$ and γ subunits. They enhance the activity of GABA when binding at its receptor and are recommended in managing acute alcohol withdrawal (Nelson et al., 2019), but not for the treatment of AUD itself. They can lead to sedation, ataxia, anterograde amnesia, and have abuse potential (Engin, 2022). Alcohol delays the metabolism of BZ (Hoyumpa, 1984), prolonging its bioavailability, causing psychomotor impairment, and increasing the risk of overdosing of BZ. Studies showed that BZ also modulates part of ethanol's reinforcing and/or aversive properties. BZ and ethanol co-consumption is also known to amplify the effect of alcohol.

5.3. Psychotherapeutic interventions

In contrast to pharmacological interventions, Cognitive Behavioral Therapy (CBT) is a form of psychotherapy that involves challenging automatic thoughts, cognitive distortions, existing beliefs, and problematic behaviors (Chand et al., 2023). It is one of the most studied forms of treatment for SUD and has the most support from evidence-based studies. Adults with problematic drinking who received CBT showed decreased alcohol consumption, and newer variants of CBT, such as virtual reality-assisted CBT (Thaysen-Petersen et al., 2023), appear to be more successful than traditional methods (Carroll and Kiluk, 2017).

Motivational Enhancement Therapy (MET) is another psychosocial treatment that applies principles from motivational

psychology. MET is often the foundation of brief interventions for risky alcohol use, and indeed, protocols can be very short, requiring only a few sessions of client-centered interventions (Ceci et al., 2022). MET focuses on identifying a reason for a change in alcohol consumption, but outcomes vary substantially with commitment and readiness to change to have an impact (Hodgins et al., 2009).

However, existing therapeutic options have shown limitations. Some drugs, repurposed from other indications, show direct or indirect activity in the GABAergic system (Gabapentin, topiramate, and baclofen). The GABAergic system is a key player in the pathophysiology of AUD and alcohol withdrawal and is a desirable target for drug development (Liang and Olsen, 2014; Mirijello et al., 2015). Indeed, the previous sections showed how intertwined central pathways are in the context of ethanol consumption and how instrumental the GABAergic system is in modulating most of the effects, directly or indirectly. However, AUD is broad and can vary in expression in multiple ways (volume consumed, acute or chronic consumption, etc.). Therefore, the impact of ethanol on the GABAergic system may vary depending on the manifestation of AUD, and different interventions acting on different aspects of the GABAergic system may be required to elicit optimal outcomes in treating AUD or alcohol withdrawal. The following sections will present novel GABAergic interventions currently being investigated.

6. GABAergic interventions in preclinical models and their impact on alcohol-related symptoms: reconciling risk and benefits

6.1. $GABA_A$: involvement in AUD and therapeutic potential

Since ethanol facilitates the activity of GABA and has such a large effect on GABAergic receptor expression and function, it can be difficult to anticipate what impact a GABAergic drug would have on individuals with AUDs. Benzodiazepines (BZ), binding at the interface between $\alpha_{1\text{-}2\text{-}3\text{-}5}$ and γ subunits of the $GABA_A$ receptors, are known enhancers of phasic GABAergic inhibition across brain regions and induce internalization of synaptic $GABA_A$ receptors (Gallager et al., 1984; Tehrani and Barnes, 1997). Therefore, BZs promote the mechanisms leading to some ethanol-induced deficits in GABAergic inhibition. However, BZs have beneficial effects in the context of acute withdrawal symptoms as they act as a substitute for ethanol and can help individuals in withdrawal re-establish a new excitation/inhibition balance without alcohol (refer to Figure 1B).

In recent years, BZ-derivatives acting preferentially at selected α-subunits were developed and tested in preclinical models for their activity on ethanol self-administration and craving behaviors (Table 3). Activation of α_2/α_3-$GABA_A$ receptors by the HZ-166, XHe-II-053, YT-III-31, or YT-III-271 PAMs in ethanol discrimination studies augmented the reinforcing effects of ethanol via increasing the self-administration in rhesus monkeys (Berro et al., 2019). These findings are aligned with clinical evidence that demonstrated a positive association of both the GABRA2 and GABRA3 gene expression with an increased risk for developing alcoholism (Covault et al., 2004; Enoch, 2008; Soyka et al., 2008; Mallard et al., 2018). Similarly, potentiation of the α_5-$GABA_A$ receptor via QH-ii-066 administration was also shown to enhance the reinforcing effects of alcohol in non-human primates, while using an inverse agonist at the α_5-$GABA_A$ receptor (Xli-093) inhibited such reinforcement effects (Rüedi-Bettschen et al., 2013). Consistently, intra-hippocampal infusions of an α_5-$GABA_A$ receptor inverse agonist RY023 reduced ethanol-maintained responses in a dose-dependent manner, suggesting that the α_5-$GABA_A$ receptors in the hippocampus play an important role in regulating ethanol-seeking behaviors (June et al., 2001). This was further supported by studies using the partial α_5-$GABA_A$ receptor inverse agonist Ro 15–4,513, by the selective α_5_$GABA_A$ inverse agonist (α5IA-II) (Stephens et al., 2005) and by the use of the α_5-$GABA_A$ receptor knockout mice model showing reduced ethanol preference (Boehm II et al., 2004; Stephens et al., 2005).

However, the studies mentioned above all evaluated the impact of positive modulation of the α_x-$GABA_A$ receptor in the context of alcohol consumption or alcohol discrimination when the system is already sensitized to further GABAergic activity (Figure 1B – central panel). However, it remains unclear how such modulation would play in the context of withdrawal when the system is deficient in GABAergic regulation, which is, in turn, causing craving behaviors. Knowing the anti-craving effect of BZ (Nelson et al., 2019), one could expect that the α_2-, α_3- or α_5-PAMs can contribute to the anti-craving effect of BZ in a brain system during a withdrawal state and could further elicit beneficial effects without the side effects observed with benzodiazepines.

While BZ and derivatives bind and act at the interface between $\alpha_{1\text{-}2\text{-}3\text{-}5}$ and γ subunits, neurosteroids bind between α and β subunits of the $GABA_A$ receptors. Furthermore, such binding is greatly facilitated by the presence of the δ subunit in the pentamer (Gatta et al., 2022; Figure 2B). Neurosteroids are potent and effective neuromodulators synthesized from cholesterol in glial and neuronal cells of the central (CNS) and peripheral nervous systems (PNS). They act at extrasynaptic receptors, facilitating tonic inhibition (Chen et al., 2019; Belelli et al., 2022). With acute alcohol intake, the cerebral levels of allopregnanolone were found to be increased, whereas its levels were reduced during chronic alcohol consumption and withdrawal (Romeo et al., 1996). In addition, stimulation of neurosteroidogenesis by metyrapone was found to reduce cocaine intake in rats (Goeders and Guerin, 2008), and one could suppose a similar effect for alcohol intake.

Recent studies found that allopregnanolone has antidepressant properties for women with postpartum depression (Pinna et al., 2022), a disorder with reduced GABAergic function (Prevot and Sibille, 2021). Therefore, with their action of the GABAergic system, and their involvement in arousal, cognition, emotion, and motivation, neurosteroids may hold therapeutic potential in treating AUD (Zorumski et al., 2013; Gatta et al., 2022), and such effects are being investigated (Morrow et al., 2020; Mounier et al., 2021).

6.2. $GABA_B$: involvement in AUD and therapeutic potential

The involvement of $GABA_B$ receptors in the development of AUD is still unclear. However, studies in clinical populations (using Baclofen) and animals [experimental candidates listed in Table 4 (Maccioni and Colombo, 2019)] showed that $GABA_B$ receptor

TABLE 3 Role of $GABA_A$ receptor subunits in alcohol abuse-related effects (Berro et al., 2019).

Drug candidate	MoA	Outcomes of the treatment on AUDs symptoms	Reference
HZ-166	α2 and α3 $GABA_A$ PAM	Following the administration, the drug increased the alcohol-related lever pressing and significantly increased the ethanol self-administration (reinforcement). The effects are similar to the ethanol indicating the respective subunit's involvement in the dependence behavior responsible for prolonged ethanol intake.	Berro et al. (2019), Rüedi-Bettschen et al. (2013)
YT-III-31 & YT-III-271	Selective α3 $GABA_A$ PAM		
QH-ii-066	α5-$GABA_A$ receptor-preferring PAM		
L-838417	α1-sparing, functionally selective partial PAM of α2/3/5-$GABA_A$ receptors		
YT-III-271	Selective α3 $GABA_A$ PAM		
XHe-II-053	Selective α2 and α3 $GABA_A$ PAM		
XLi-093	α5 antagonist	Decreased ethanol discrimination and reinforcements.	Rüedi-Bettschen et al. (2013)
RY023	α5 inverse agonist	Intrahippocampal administration decreases ethanol-maintained responses in lever pressing task	June et al. (2001)
Ro 15–4,513	BZ reverse agonist and $\alpha_{4,6}$-agonist	Reduction of operant response for ethanol	Stephens et al. (2005)
α5IA-II	α5 inverse agonist	Decreased lever pressing in rats with alcohol dependence	Stephens et al. (2005)

TABLE 4 $GABA_B$-positive allosteric modulators under development for AUD.

Drug candidate	Outcomes of the treatment	Reference
GS39783	Attenuates (repeated dosing) and reduces (acute treatment) ethanol-induced hyper locomotion at (30 mg/kg; ip)	Kruse et al. (2012)
	Dose-dependently suppressed the acquisition of alcohol-drinking behavior. Also, reduced daily alcohol intake by 30–40%.	Orrù et al. (2005)
	Reduced alcohol intake in a dose-dependent manner.	Colombo et al. (2015)
	Reduced binge-like alcohol drinking	Linsenbardt and Boehm Ii (2014)
	Decreases self-administration of alcohol	Lorrai et al. (2019)
		Maccioni et al. (2017)
Rac-BHFF	Repeated dosing reduced alcohol-reinforcing properties. Also, prevented tolerance development.	Maccioni et al. (2015)
	7 consecutive dose administrations reduced daily alcohol intake in Sardinian alcohol-preferring rats.	Loi et al. (2013)
	At non-sedative doses, it reversed ethanol-induced plasticity and reduced ethanol drinking.	de Miguel et al. (2019)
ORM-27669	Pretreatment with ORM-27669 only reversed ethanol-induced neuroplasticity and attenuated ethanol drinking	de Miguel et al. (2019)
CGP7930	Dose-dependently suppressed the acquisition of alcohol-drinking behavior. Also, reduced daily alcohol intake by 30–40%.	Orrù et al. (2005), Maccioni et al. (2018)
ADX71441	Dose-dependent reduction of alcohol self-administration and suppressed stress-induced relapse.	Augier et al. (2017)
	Reduced alcohol drinking in intermittent and drink-in-the-dark (DID) models.	Hwa et al. (2014)
CMPPE	Dose-dependent reduction in self-administration and cue-induced reinstatement of alcohol seeking in alcohol-preferring rats.	MacCioni et al. (2009)
BHF177	Dose-dependently reduced alcohol self-administration.	MacCioni et al. (2009)
	Acute administration at non-sedative doses, it selectively reduced alcohol intoxication in binge-like drinking experiments.	Lorrai et al. (2022)
ASP8062	Reduced the alcohol self-administration but did not alter alcohol-related locomotion.	Haile et al. (2021)
KK-92A	Dose-related suppression in alcohol self-administration	Maccioni et al. (2022)

modulation was beneficial in AUD management. For instance, rats receiving baclofen showed reduced hyper-locomotion caused by acute alcohol administration (Besheer et al., 2004), and reduced anxiety-like behavior and tremors following chronic alcohol withdrawal (Knapp et al., 2007). Table 4 includes a list of $GABA_B$ PAMs such as CGP7930, GS39783, BHF177, Rac-BHFF, ADX71441, CMPPE, COR659, and

TABLE 5 GABA modulators in clinical trials for AUD and alcohol withdrawal treatment (Source: clinicaltrials.org).

Drug candidate and details of clinical trial	MoA	Indications	Current status	Reference
ASP8062 Sponsors: NIAAA & Astellas Pharma Inc. Trial No. NCT05096117	$GABA_B$-positive allosteric modulation	AUD, alcohol craving	Phase 2	Walzer et al. (2020)
Brexanolone Sponsors: Yale University, NIAAA & Sage Therapeutics Trial No. NCT05223829	$GABA_A$ targeting neurosteroid	Stress-induced alcohol use in men and women with PTSD	Phase 1	Patatanian and Nguyen (2022)
Propofol **Midazolam** Sponsor: Virginia Commonwealth University Trial No. NCT00871039	$GABA_A$-positive allosteric modulation $GABA_A$-positive allosteric modulation	Stress response and immune function in mechanically ventilated patients with AUD	Withdrawn due to logistical purposes in 2016	Marik (2004), Zaporowska-Stachowiak et al. (2019)
Baclofen Sponsor: Universitair Ziekenhuis Brussel Trial No. NCT03293017	$GABA_B$ agonist	Management of acute alcohol withdrawal – comparison with Diazepam	Phase 4	De Beaurepaire (2018), Dhaliwal et al. (2022)
Valproate **Lorazepam** Sponsor: CAMC Health System Trial No. NCT03235531	Inhibitor of GABA metabolism and GABA reuptake (so increases GABA levels) $GABA_A$-positive allosteric modulation	Ethanol withdrawal syndrome, comparison with BZ (Lorazepam)	Phase 4	Ghiasi et al. (2023), Johannessen and Johannessen (2003)
Disulfiram + Lorazepam Sponsor: University of New Mexico and NIAAA Trial No. NCT00721526	Irreversible inhibitor of acetaldehyde dehydrogenase. + $GABA_A$-positive allosteric modulation	Combination therapy for patients with alcohol dependence and anxiety disorder	Open label Phase 4 Completed	Bogenschutz et al. (2016)

ORM-27669 that were primarily studied in rodent models and were found to be beneficial in AUDs.

7. Novel therapeutic agents targeting the GABAergic system in clinical trials

7.1. Pharmacological interventions

With the increased characterization of the impact of alcohol on the GABAergic system and the increasing characterization of the link between GABAergic functions, receptor subtype, and symptom relief in the context of AUD, more clinical trials are being initiated to investigate how GABAergic modulation can contribute to better treatment of AUDs and alcohol withdrawal (Table 5). Interventions acting on $GABA_A$ receptors are investigated in multiple clinical trials. For example, DZ is already the standard of care for reducing withdrawal symptoms. Midazolam, another benzodiazepine, and propofol, a $GABA_A$ receptor agonist, were withdrawn from Phase 4 studies in 2016 due to logistical reasons. They were studied for their potential effect on stress response and immune functions in mechanically ventilated patients with AUDs.

Brexanolone, a $GABA_A$-targeting neurosteroid, is about to start recruiting for a Phase 1 study to demonstrate safety before assessing efficacy in participants with AUD and PTSD. Brexanolone is already approved for treating postpartum depression (Morrow et al., 2020).

Baclofen, a $GABA_B$ agonist, is currently under Phase 4 to assess its efficacy in managing acute alcohol withdrawal. As mentioned in Table 1, baclofen is already approved in France for reducing craving and withdrawal syndrome, but some literature suggests its efficacy for this indication is limited (Cooney et al., 2019). ASP8062, a $GABA_B$-PAM, is currently investigating the efficacy of 2 weeks of treatment in a Phase 2 study in participants with moderate AUD at reducing alcohol cravings. Preclinical studies in rats showed promising effects in reducing alcohol self-administration without side effects observed with baclofen (Haile et al., 2021), and phase 1 studies in humans confirmed the safety of ASP8062 (Ito et al., 2022).

The antiepileptic valproate also acts indirectly on the GABAergic system by blocking the metabolism of GABA and by blocking GABA reuptake, increasing GABA levels in the brain (Janmohamed et al., 2020). Clinical trials are ongoing to determine the efficacy of valproate treatment at reducing ethanol withdrawal, compared to benzodiazepines, here lorazepam. Lorazepam was also used in another open-label clinical trial completed in 2013 to assess the efficacy of a combination with disulfiram. Reports showed a significant reduction in anxiety, depression, and craving; such effects were observed 24 weeks after intervention (Bogenschutz et al., 2016).

7.2. Non-pharmacological interventions – rTMS

Repetitive transcranial magnetic stimulation, i.e., rTMS, is a noninvasive neurostimulation modality delivering focused magnetic field pulses to the cortex that modulate cortical activity. Treatment sessions are generally delivered daily over several weeks, which results in the induction of long-term changes in cortical excitability through neuroplasticity. This includes modulation of the implicated neurocircuits underlying alcohol use disorder and is under investigation as a potential treatment. Enduring changes in cortical activity (namely inhibition and excitation) resulting from rTMS have implications for enduring changes in GABA activity (Daskalakis et al., 2006). Over a decade ago, the first published clinical trial demonstrated efficacy in reducing cravings in adults with AUD over a sham-control condition (Mishra et al., 2010). Since then, the majority of trials have delivered rTMS over the left or right dorsolateral prefrontal cortex, with a recent meta-analysis showing a signal for reduced alcohol craving with rTMS treatment (Sorkhou et al., 2022), potentially driven by the impact of rTMS on GABAergic signaling. However, most RCTs have been small single-center trials, and given the substantial heterogeneity in parameters utilized across studies, the optimal protocol has not yet been determined.

Additionally, there is growing interest in using deep rTMS™ using coils (H Coils) that can induce a broader electrical field within the cortex. For example, a recent RCT using rTMS with an H7 Coil stimulating the bilateral medial prefrontal cortex and anterior cingulate cortex showed positive results in reducing craving and alcohol consumption in treatment-seeking patients with AUD (Harel et al., 2022). Moreover, another trial that utilized a coil that stimulates the bilateral lateral PFC and insula showed efficacy for nicotine dependence in a large, definitive, multi-site RCT that subsequently paved the way for FDA clearance for this indication (Zangen et al., 2021), demonstrating the first time FDA cleared indication for any substance use disorder. Taken together, further exploration of the therapeutic potential of rTMS for AUD is warranted. Given the well-described link between GABA dysfunction in AUD and rTMS effects on the GABAergic system, it will be important to explore whether biomarkers of GABAergic functions can serve as mediators or moderators of rTMS efficacy.

8. Conclusion

Alcohol use-related disorders are significant risk factors for other high mortality-causing diseases. Although the mechanisms are elusive, the GABAergic system's involvement seems critical in AUD development. Currently, GABAergic drugs are used in the second or third line of treatment of AUD and mitigation of alcohol withdrawal. Studies indicate that pharmacological modulation of GABA receptors may be a promising therapeutic option in achieving long-term abstinence by decreasing the daily alcohol intake and withdrawal effects. However, extensive research is needed in this line to uncover the pharmacological potential of the GABAergic system in managing alcohol use-related disorders.

Author contributions

RD and TP conceptualized the review. RD, CP-L, and TP wrote the review, collected sections, and contributions from other co-authors, and prepared the figures and tables. VT, MS, YN, PP, AR, KS, DV, DB, IB, NB, PG, EV, OM, ES, and LQ provided content and critical revision of review drafts. All authors approved the final version of the manuscript.

Acknowledgments

The authors thank the CAMH Discovery Fund for supporting the Cognitive Dysfunction in Addiction (CDiA) research program, to which all co-authors are contributors.

Conflict of interest

TP receives compensation for consulting work from Damona Pharmaceutical Inc., a biotech company developing GABAergic molecules for the treatment of cognitive dysfunctions in depression. ES is co-founder, CEO and CSO of Damona Pharmaceutical Inc. DB receives research support from CIHR, NIH, Brain Canada, and the Temerty Family through the CAMH Foundation. He received research support and in-kind equipment support for an investigator-initiated study from Brainsway Ltd. and has been the site principal investigator for three sponsor-initiated studies for Brainsway Ltd. DB also received in-kind equipment support from Magventure for 3 investigator-initiated studies. DB received medication supplies for an investigator-initiated trial from Indivior. DB has participated in one Scientific Advisory Board Meeting for Janssen and one meeting for Welcony Inc. DV holds the Labatt Family Professorship in Depression Biology, a University Named Professorship at the University of Toronto. She receives research support from CIHR, NIH, the Centre for Addiction and Mental Health (CAMH), University Hospital Network (UHN) and the Department of Psychiatry at the University of Toronto. DV declares no biomedical interests or conflicts.

The remaining authors declare that the research was conducted in the absence of any commercial or financial relationships that could be construed as a potential conflict of interest.

Publisher's note

References

Abrahao, K. P., Salinas, A. G., and Lovinger, D. M. (2017). Alcohol and the brain: neuronal molecular targets, synapses, and circuits. *Neuron* 96, 1223–1238. doi: 10.1016/j.neuron.2017.10.032

Addolorato, G., Leggio, L., Hopf, F. W., Diana, M., and Bonci, A. (2012). Novel therapeutic strategies for alcohol and drug addiction: focus on GABA, ion channels and transcranial magnetic stimulation. *Neuropsychopharmacology* 37, 163–177. doi: 10.1038/npp.2011.216

Agabio, R., Saulle, R., Rösner, S., and Minozzi, S. (2023). Baclofen for alcohol use disorder. *Cochrane Database Syst. Rev.* 2023:CD012557. doi: 10.1002/14651858.CD012557.pub3

American Psychological Association. (2013). *Diagnostic and statistical manual of mental disorders: DSM-5™, 5th Edn* Arlington, VA: American Psychiatric Publishing, Inc., 947.

Anton, R. F., Latham, P., Voronin, K., Book, S., Hoffman, M., Prisciandaro, J., et al. (2020). Efficacy of gabapentin for the treatment of alcohol use disorder in patients with alcohol withdrawal symptoms: A randomized clinical trial. *JAMA Intern. Med.* 180, 728–736. doi: 10.1001/jamainternmed.2020.0249

Arora, D. S., Nimitvilai, S., Teppen, T. L., McElvain, M. A., Sakharkar, A. J., You, C., et al. (2013). Hyposensitivity to gamma-aminobutyric acid in the ventral tegmental area during alcohol withdrawal: reversal by histone deacetylase inhibitors. *Neuropsychopharmacology* 38, 1674–1684. doi: 10.1038/npp.2013.65

Augier, E., Dulman, R. S., Damadzic, R., Pilling, A., Hamilton, J. P., and Heilig, M. (2017). The GABAB positive allosteric modulator ADX71441 attenuates alcohol self-administration and relapse to alcohol seeking in rats. *Neuropsychopharmacology* 42, 1789–1799. doi: 10.1038/npp.2017.53

Avegno, E. M., Lobell, T. D., Itoga, C. A., Baynes, B. B., Whitaker, A. M., Weera, M. M., et al. (2018). Central amygdala circuits mediate hyperalgesia in alcohol-dependent rats. *J. Neurosci.* 38, 7761–7773. doi: 10.1523/JNEUROSCI.0483-18.2018

Bahi, A. (2013). Increased anxiety, voluntary alcohol consumption and ethanol-induced place preference in mice following chronic psychosocial stress. *Stress* 16, 441–451. doi: 10.3109/10253890.2012.754419

Banerjee, N. (2014). Neurotransmitters in alcoholism: A review of neurobiological and genetic studies. *Indian J. Hum. Genet.* 20, 20–31. doi: 10.4103/0971-6866.132750

Barchiesi, R., Chanthongdee, K., Domi, E., Gobbo, F., Coppola, A., Asratian, A., et al. (2021). Stress-induced escalation of alcohol self-administration, anxiety-like behavior, and elevated amygdala Avp expression in a susceptible subpopulation of rats. *Addict. Biol.* 26:e13009. doi: 10.1111/adb.13009

Behar, K. L., Rothman, D. L., Petersen, K. F., Hooten, M., Delaney, R., Petroff, O. A., et al. (1999). Preliminary evidence of low cortical GABA levels in localized 1H-MR spectra of alcohol-dependent and hepatic encephalopathy patients. *Am. J. Psychiatr.* 156, 952–954. doi: 10.1176/ajp.156.6.952

Belelli, D., Peters, J. A., Phillips, G. D., and Lambert, J. J. (2022). The immediate and maintained effects of neurosteroids on GABAA receptors. *Curr. Opin. Endocrine Metab. Res.* 24:100333. doi: 10.1016/j.coemr.2022.100333

Berro, L. F., Ruedi-Bettschen, D., Cook, J. E., Golani, L. K., Li, G., Jahan, R., et al. (2019). GABA(A) receptor subtypes and the abuse-related effects of ethanol in rhesus monkeys: experiments with selective positive allosteric modulators. *Alcohol. Clin. Exp. Res.* 43, 791–802. doi: 10.1111/acer.14000

Besheer, J., Lepoutre, V., and Hodge, C. W. (2004). GABA B receptor agonists reduce operant ethanol self-administration and enhance ethanol sedation in C57BL/6J mice. *Psychopharmacology* 174, 358–366. doi: 10.1007/s00213-003-1769-3

Bobrova, N. P., and Covaltchuk, V. G. (1980). "The effect of ethanol and acetaldehyde on GABA transport systems and its synthesis in rat BRAIN synaptosomes" in *Synaptic constituents in health and disease*. eds. M. Brzin, D. Sket and H. Bachelard (Amsterdam: Elsevier), 109.

Boehm, S. L. II, Ponomarev, I., Jennings, A. W., Whiting, P. J., Rosahl, T. W., Blednov, Y. A., et al. (2004). γ-Aminobutyric acid A receptor subunit mutant mice: new perspectives on alcohol actions. *Biochem. Pharmacol.* 68, 1581–1602. doi: 10.1016/j.bcp.2004.07.023

Bogenschutz, M. P., Bhatt, S., Bohan, J., Foster, B., Romo, P., Wilcox, C. E., et al. (2016). Coadministration of disulfiram and lorazepam in the treatment of alcohol dependence and co-occurring anxiety disorder: an open-label pilot study. *Am. J. Drug Alcohol Abuse* 42, 490–499. doi: 10.3109/00952990.2016.1168430

Bohnsack, J. P., Hughes, B. A., O'Buckley, T. K., Edokpolor, K., Besheer, J., and Morrow, A. L. (2018). Histone deacetylases mediate GABAA receptor expression, physiology, and behavioral maladaptations in rat models of alcohol dependence. *Neuropsychopharmacology* 43, 1518–1529. doi: 10.1038/s41386-018-0034-8

Bowery, N. G., Hudson, A. L., and Price, G. W. (1987). GABAA and GABAB receptor site distribution in the rat central nervous system. *Neuroscience* 20, 365–383. doi: 10.1016/0306-4522(87)90098-4

Burnette, E. M., Nieto, S. J., Grodin, E. N., Meredith, L. R., Hurley, B., Miotto, K., et al. (2022). Novel agents for the pharmacological treatment of alcohol use disorder. *Drugs* 82, 251–274. doi: 10.1007/s40265-021-01670-3

Cai, K., Nanga, R. P., Lamprou, L., Schinstine, C., Elliott, M., Hariharan, H., et al. (2012). The impact of gabapentin administration on brain GABA and glutamate concentrations: a 7T ^{1}H-MRS study. *Neuropsychopharmacology* 37, 2764–2771. doi: 10.1038/npp.2012.142

Carpenter, J. E., LaPrad, D., Dayo, Y., DeGrote, S., and Williamson, K. (2018). An overview of pharmacotherapy options for alcohol use disorder. *Federal Practitioner* 35, 48–58.

Carroll, K. M., and Kiluk, B. D. (2017). Cognitive behavioral interventions for alcohol and drug use disorders: through the stage model and back again. *Psychol. Addict. Behav.* 31:847. doi: 10.1037/adb0000311

Carvalho, A. F., Heilig, M., Perez, A., Probst, C., and Rehm, J. (2019). Alcohol use disorders. *Lancet* 394, 781–792. doi: 10.1016/S0140-6736(19)31775-1

Castaldelli-Maia, J. M., and Bhugra, D. (2022). Analysis of global prevalence of mental and substance use disorders within countries: focus on sociodemographic characteristics and income levels. *Int. Rev. Psychiatry* 34, 6–15. doi: 10.1080/09540261.2022.2040450

Ceci, F. M., Francati, S., Ferraguti, G., Coriale, G., Ciccarelli, R., Minni, A., et al. (2022). Behavioral dysregulations by chronic alcohol abuse. Motivational enhancement therapy and cognitive behavioral therapy outcomes. *Riv. Psichiatr.* 57, 1–9. doi: 10.1708/3749.37321

Chand, S. P., Kuckel, D. P., and Huecker, M. R. (2023). "Cognitive Behavior Therapy," in *StatPearls [Internet]*. (Treasure Island (FL): StatPearls Publishing) Available at: https://www.ncbi.nlm.nih.gov/books/NBK470241/

Chandler, C. M., Overton, J. S., Rüedi-Bettschen, D., and Platt, D. M. (2017). "GABAA Receptor Subtype Mechanisms and the Abuse-Related Effects of Ethanol: Genetic and Pharmacological Evidence," in *The Neuropharmacology of Alcohol. Handbook of Experimental Pharmacology*, Eds. K. Grant and D. Lovinger (Springer, Cham). 248, doi: 10.1007/164_2017_80

Chandrasekar, R. (2013). Alcohol and NMDA receptor: current research and future direction. *Front. Mol. Neurosci.* 6:14. doi: 10.3389/fnmol.2013.00014

Chapp, A. D., Mermelstein, P. G., and Thomas, M. J. (2021). The ethanol metabolite acetic acid activates mouse nucleus accumbens shell medium spiny neurons. *J. Neurophysiol.* 125, 620–627. doi: 10.1152/jn.00659.2020

Chen, Z.-W., Bracamontes, J. R., Budelier, M. M., Germann, A. L., Shin, D. J., Kathiresan, K., et al. (2019). Multiple functional neurosteroid binding sites on GABAA receptors. *PLoS Biol.* 17:e3000157. doi: 10.1371/journal.pbio.3000157

Chiva-Blanch, G., and Badimon, L. J. N. (2019). Benefits and risks of moderate alcohol consumption on cardiovascular disease: current findings and controversies. *Nutrients* 12:108. doi: 10.3390/nu12010108

Chmielewski, W. X., Zink, N., Chmielewski, K. Y., Beste, C., and AK, S. (2020). How high-dose alcohol intoxication affects the interplay of automatic and controlled processes. *Addict. Biol.* 25:e12700. doi: 10.1111/adb.12700

Colasanti, A., Searle, G. E., Long, C. J., Hill, S. P., Reiley, R. R., Quelch, D., et al. (2012). Endogenous opioid release in the human brain reward system induced by acute amphetamine administration. *Biol. Psychiatry* 72, 371–377. doi: 10.1016/j.biopsych.2012.01.027

Colombo, G., Lobina, C., Maccioni, P., Carai, M. A. M., Lorrai, I., Zaru, A., et al. (2015). Anxiety-like behaviors at the end of the nocturnal period in sP rats with a "history" of unpredictable, limited access to alcohol. *Alcohol* 49, 707–712. doi: 10.1016/j.alcohol.2015.04.010

Conte, A., Attilia, M. L., Gilio, F., Iacovelli, E., Frasca, V., Marini Bettolo, C., et al. (2008). Acute and chronic effects of ethanol on cortical excitability. *Clin. Neurophysiol.* 119, 667–674. doi: 10.1016/j.clinph.2007.10.021

Cooney, G., Heydtmann, M., and Smith, I. D. (2019). Baclofen and the alcohol withdrawal syndrome-A short review. *Front. Psych.* 9:773. doi: 10.3389/fpsyt.2018.00773

Covault, J., Gelernter, J., Hesselbrock, V., Nellissery, M., and Kranzler, H. R. (2004). Allelic and haplotypic association of GABRA2 with alcohol dependence. American journal of medical genetics – neuropsychiatric. *Genetics* 129B, 104–109. doi: 10.1002/ajmg.b.30091

Daskalakis, Z. J., Möller, B., Christensen, B. K., Fitzgerald, P. B., Gunraj, C., and Chen, R. (2006). The effects of repetitive transcranial magnetic stimulation on cortical inhibition in healthy human subjects. *Exp. Brain Res.* 174, 403–412. doi: 10.1007/s00221-006-0472-0

Daviet, R., Aydogan, G., Jagannathan, K., Spilka, N., Koellinger, P. D., Koellinger, P. D., et al. (2022). Associations between alcohol consumption and gray and white matter volumes in the UK biobank. *Nat. Commun.* 13:1175. doi: 10.1038/s41467-022-28735-5

Davis, T. J., and de Fiebre, C. M. (2006). Alcohol's actions on neuronal nicotinic acetylcholine receptors. *Alcohol Res. Health* 29, 179–185.

De Beaurepaire, R. (2018). A review of the potential mechanisms of action of baclofen in alcohol use disorder. *Front. Psych.* 9, 1–12. doi: 10.3389/fpsyt.2018.00506

de Miguel, E., Vekovischeva, O., Kuokkanen, K., Vesajoki, M., Paasikoski, N., Kaskinoro, J., et al. (2019). GABAB receptor positive allosteric modulators with different efficacies affect neuroadaptation to and self-administration of alcohol and cocaine. *Addict. Biol.* 24, 1191–1203. doi: 10.1111/adb.12688

De Witte, P. (2004). Imbalance between neuroexcitatory and neuroinhibitory amino acids causes craving for ethanol. *Addict. Behav.* 29, 1325–1339. doi: 10.1016/j.addbeh.2004.06.020

Dhaliwal, J. S., Rosani, A., and Saadabadi, A. (2022). "Diazepam," in *StatPearls [internet]*. Treasure Island (FL): StatPearls Publishing. Available at: https://www.ncbi.nlm.nih.gov/books/NBK537022/

Dodd, P. R., Tracey Buckley, S., Eckert, A. L., Foley, P. F., and Innes, D. J. (2006). Genes and gene expression in the brains of human alcoholics. *Ann. NY Acad. Sci.* 1074, 104–115. doi: 10.1196/annals.1369.010

Engin, E. (2022). GABAA receptor subtypes and benzodiazepine use, misuse, and abuse. *Front. Psych.* 13:2931. doi: 10.3389/fpsyt.2022.1060949

Enna, S. J. (2007). The GABA receptors. Humana Press.

Enoch, M. A. (2008). The role of GABA(A) receptors in the development of alcoholism. *Pharmacol. Biochem. Behav.* 90, 95–104. doi: 10.1016/j.pbb.2008.03.007

Fariba, K. A., and Saadabadi, A. (2022). *Topiramate*. StatPearls: Tampa, FL.

Ferraguti, G., Pascale, E., and Lucarelli, M. (2015). Alcohol addiction: a molecular biology perspective. *Curr. Med. Chem.* 22, 670–684. doi: 10.2174/0929867321666141229103158

Foo, J. C., Vengeliene, V., Noori, H. R., Yamaguchi, I., Morita, K., Nakamura, T., et al. (2019). Drinking levels and profiles of alcohol addicted rats predict response to Nalmefene. *Front. Pharmacol.* 10:471. doi: 10.3389/fphar.2019.00471

Franck, J., and Jayaram-Lindström, N. (2013). Pharmacotherapy for alcohol dependence: status of current treatments. *Curr. Opin. Neurobiol.* 23, 692–699. doi: 10.1016/j.conb.2013.05.005

Fritschy, J. M., and Mohler, H. (1995). GABAA-receptor heterogeneity in the adult rat brain: differential regional and cellular distribution of seven major subunits. *J. Comp. Neurol.* 359, 154–194. doi: 10.1002/cne.903590111

Gallager, D., Lakoski, J., Gonsalves, S., and Rauch, S. J. N. (1984). Chronic benzodiazepine treatment decreases postsynaptic GABA sensitivity. *Nature* 308, 74–77.

Garbutt, J. C. (2019). Approval of baclofen for alcohol use disorders in France: A perspective from the United States. *Alcohol Alcohol.* 55:48. doi: 10.1093/alcalc/agz084

Gatta, E., Camussi, D., Auta, J., Guidotti, A., and Pandey, S. C. (2022). Neurosteroids (allopregnanolone) and alcohol use disorder: from mechanisms to potential pharmacotherapy. *Pharmacol. Ther.* 240:108299. doi: 10.1016/j.pharmthera.2022.108299

Ghiasi, N., Bhansali, R. K., and Marwaha, R. (2023). "Lorazepam" in *StatPearls [Internet]*, (Treasure Island (FL): StatPearls Publishing). Available at: https://www.ncbi.nlm.nih.gov/books/NBK532890/

Ghit, A., Assal, D., Al-Shami, A. S., and Hussein, D. E. E. (2021). GABA(A) receptors: structure, function, pharmacology, and related disorders. *J. Genet. Eng. Biotechnol.* 19:123. doi: 10.1186/s43141-021-00224-0

Gilman, J. M., Ramchandani, V. A., Davis, M. B., Bjork, J. M., and DWJJoN, H. (2008). Why we like to drink: a functional magnetic resonance imaging study of the rewarding and anxiolytic effects of alcohol. *J. Neurosci.* 28, 4583–4591. doi: 10.1523/JNEUROSCI.0086-08.2008

Gil-Mohapel, J., Bianco, C. D., Cesconetto, P. A., Zamoner, A., and Brocardo, P. S. (2019). "Chapter 51 – ethanol exposure during development, and brain oxidative stress" in *Neuroscience of alcohol*. ed. V. R. Preedy (Cambridge, MA: Academic Press), 493–503.

Giuliano, C., Peña-Oliver, Y., Goodlett, C. R., Cardinal, R. N., Robbins, T. W., Bullmore, E. T., et al. (2018). Evidence for a Long-lasting compulsive alcohol seeking phenotype in rats. *Neuropsychopharmacology* 43, 728–738. doi: 10.1038/npp.2017.105

Goeders, N. E., and Guerin, G. F. (2008). Effects of the combination of metyrapone and oxazepam on cocaine and food self-administration in rats. *Pharmacol. Biochem. Behav.* 91, 181–189. doi: 10.1016/j.pbb.2008.07.005

Gomes, T., Juurlink, D. N., Antoniou, T., Mamdani, M. M., Paterson, J. M., and van den Brink, W. (2017). Gabapentin, opioids, and the risk of opioid-related death: A population-based nested case-control study. *PLoS Med.* 14:e1002396. doi: 10.1371/journal.pmed.1002396

Grant, K. A., and Lovinger, D. M. (2018). *The neuropharmacology of alcohol*. New York: Springer.

Haile, C. N., Carper, B. A., Nolen, T. L., and Kosten, T. A. (2021). The GABA(B) receptor positive allosteric modulator ASP8062 reduces operant alcohol self-administration in male and female Sprague Dawley rats. *Psychopharmacology* 238, 2587–2600. doi: 10.1007/s00213-021-05881-0

Harel, M., Perini, I., Kämpe, R., Alyagon, U., Shalev, H., et al. (2022). Repetitive transcranial magnetic stimulation in alcohol dependence: A randomized, double-blind, sham-controlled proof-of-concept trial targeting the medial prefrontal and anterior cingulate cortices. *Biol. Psychiatry* 91, 1061–1069. doi: 10.1016/j.biopsych.2021.11.020

Heinz, A., Beck, A., Grüsser, S. M., Grace, A. A., and Wrase, J. (2009). Identifying the neural circuitry of alcohol craving and relapse vulnerability. *Addict. Biol.* 14, 108–118. doi: 10.1111/j.1369-1600.2008.00136.x

Herman, M. A., Contet, C., and Roberto, M. (2016). A functional switch in tonic GABA currents alters the output of central amygdala corticotropin releasing factor receptor-1 neurons following chronic ethanol exposure. *J. Neurosci.* 36, 10729–10741. doi: 10.1523/JNEUROSCI.1267-16.2016

Herman, M. A., and Roberto, M. (2016). Cell-type-specific tonic GABA signaling in the rat central amygdala is selectively altered by acute and chronic ethanol. *J. Neurosci.* 21, 72–86. doi: 10.1111/adb.12181

Higgins-Biddle, J. C., and Babor, T. F. (2018). A review of the alcohol use disorders identification test (AUDIT), AUDIT-C, and USAUDIT for screening in the United States: past issues and future directions. *Am. J. Drug Alcohol Abuse* 44, 578–586. doi: 10.1080/00952990.2018.1456545

Hodgins, D. C., Ching, L. E., and McEwen, J. (2009). Strength of commitment language in motivational interviewing and gambling outcomes. *Psychol. Addict. Behav.* 23, 122–130. doi: 10.1037/a0013010

Holford, N. H. (1987). Clinical pharmacokinetics of ethanol. *Clin. Pharmacokinet* 13, 273–292. doi: 10.2165/00003088-198713050-00001

Holtyn, A. F., and Weerts, E. M. (2022). GABA(B) receptors and alcohol use disorders: preclinical studies. *Curr. Top. Behav. Neurosci.* 52, 157–194. doi: 10.1007/7854_2020_178

Hoyumpa, A. M. Jr. (1984). Alcohol interactions with benzodiazepines and cocaine. *Adv. Alcohol Subst. Abuse* 3, 21–34. doi: 10.1300/J251v03n04_03

Hughes, B. A., Bohnsack, J. P., O'Buckley, T. K., Herman, M. A., and Morrow, A. L. (2019). Chronic ethanol exposure and withdrawal impair synaptic GABA(A) receptor-mediated neurotransmission in deep-layer prefrontal cortex. *Alcohol. Clin. Exp. Res.* 43, 822–832. doi: 10.1111/acer.14015

Hwa, L. S., Kalinichev, M., Haddouk, H., Poli, S., and Miczek, K. A. (2014). Reduction of excessive alcohol drinking by a novel GABAB receptor positive allosteric modulator ADX71441 in mice. *Psychopharmacology* 231, 333–343. doi: 10.1007/s00213-013-3245-z

Ito, M., Spence, A., Blauwet, M. B., Heo, N., Goldwater, R., Maruff, P., et al. (2022). A phase 1 study to assess potential interaction between ASP8062 and alcohol in healthy adult subjects. *J. Psychopharmacol.* 36, 756–767. doi: 10.1177/02698811211058967

Janmohamed, M., Brodie, M. J., and Kwan, P. (2020). Pharmacoresistance–epidemiology, mechanisms, and impact on epilepsy treatment. *Neuropharmacology* 168:107790. doi: 10.1016/j.neuropharm.2019.107790

Jesse, S., Bråthen, G., Ferrara, M., Keindl, M., Ben-Menachem, E., Tanasescum, R., et al. (2017). Alcohol withdrawal syndrome: mechanisms, manifestations, and management. *Acta Neurol. Scand.* 135, 4–16. doi: 10.1111/ane.12671

Johannessen, C. U., and Johannessen, S. I. (2003). Valproate: past, present, and future. *CNS Drug Rev.* 9, 199–216. doi: 10.1111/j.1527-3458.2003.tb00249.x

Jonas, D. E., Amick, H. R., Feltner, C., Bobashev, G., Thomas, K., Wines, R., et al. (2014). Pharmacotherapy for adults with alcohol use disorders in outpatient settings: A systematic review and meta-analysis. *JAMA* 311, 1889–1900. doi: 10.1001/jama.2014.3628

June, H. L., Harvey, S. C., Foster, K. L., McKay, P. F., Cummings, R., Garcia, M., et al. (2001). $GABA_A$receptors containing α5 subunits in the CA1 and CA3 hippocampal Fields regulate ethanol-motivated Behaviors: an extended ethanol reward circuitry. *J. Neurosci.* 21, 2166–2177. doi: 10.1523/JNEUROSCI.21-06-02166.2001

Kaarre, O., Kallioniemi, E., Könönen, M., Tolmunen, T., Kekkonen, V., Kivimäki, P., et al. (2018). Heavy alcohol use in adolescence is associated with altered cortical activity: a combined TMS-EEG study. *Addict. Biol.* 23, 268–280. doi: 10.1111/adb.12486

Kalk, N. J., and Lingford-Hughes, A. R. (2014). The clinical pharmacology of acamprosate. *Br. J. Clin. Pharmacol.* 77, 315–323. doi: 10.1111/bcp.12070

Kirkland, A. E., Browning, B. D., Green, R., Leggio, L., Meyerhoff, D. J., and Squeglia, L. M. (2022). Brain metabolite alterations related to alcohol use: a meta-analysis of proton magnetic resonance spectroscopy studies. *Mol. Psychiatry* 27, 3223–3236. doi: 10.1038/s41380-022-01594-8

Kisby, B. R., Farris, S. P., McManus, M. M., Varodayan, F. P., Roberto, M., Harris, R. A., et al. (2021). Alcohol dependence in rats is associated with global changes in gene expression in the central amygdala. *Brain Sci.* 11:1149. doi: 10.3390/brainsci11091149

Knapp, D. J., Overstreet, D. H., and Breese, G. R. (2007). Baclofen blocks expression and sensitization of anxiety-like behavior in an animal model of repeated stress and ethanol withdrawal. *Alcohol. Clin. Exp. Res.* 31, 582–595. doi: 10.1111/j.1530-0277.2007.00342.x

Koob, G. F., and Volkow, N. D. (2016). Neurobiology of addiction: a neurocircuitry analysis. *Lancet Psychiatry* 3, 760–773. doi: 10.1016/S2215-0366(16)00104-8

Kranzler, H. R., Covault, J., Feinn, R., Armeli, S., Tennen, H., Arias, A. J., et al. (2014). Topiramate treatment for heavy drinkers: moderation by a GRIK1 polymorphism. *Am. J. Psychiatry* 171, 445–452. doi: 10.1176/appi.ajp.2013.13081014

Kranzler, H. R., and Soyka, M. (2018). Diagnosis and pharmacotherapy of alcohol use disorder: a review. *JAMA* 320, 815–824. doi: 10.1001/jama.2018.11406

Kruse, L. C., Linsenbardt, D. N., and Boehm, S. L. (2012). Positive allosteric modulation of the GABA B receptor by GS39783 attenuates the locomotor stimulant actions of ethanol and potentiates the induction of locomotor sensitization. *Alcohol* 46, 455–462. doi: 10.1016/j.alcohol.2012.03.004

Kumar, S., Porcu, P., Werner, D. F., Matthews, D. B., Diaz-Granados, J. L., Helfand, R. S., et al. (2009). The role of GABAA receptors in the acute and chronic effects of ethanol: a decade of progress. *Psychopharmacology* 205, 529–564. doi: 10.1007/s00213-009-1562-z

Laniepce, A., Cabé, N., André, C., Bertran, F., Boudehent, C., Lahbairi, N., et al. (2020). The effect of alcohol withdrawal syndrome severity on sleep, brain and cognition. Brain. *Communications* 2:fcaa123. doi: 10.1093/braincomms/fcaa123

Larsson, S. C., Burgess, S., Mason, A. M., and Michaëlsson, K. (2020). Alcohol consumption and cardiovascular disease: A mendelian randomization study. *Circ. Genom. Precis. Med.* 13:e002814. doi: 10.1161/CIRCGEN.119.002814

Larsson, A., Edström, L., Svensson, L., Söderpalm, B., and Engel, J. A. (2005). Voluntary ethanol intake increases extracellular acetylcholine levels in the ventral tegmental area in the rat. *Alcohol Alcohol.* 40, 349–358. doi: 10.1093/alcalc/agh180

Leggio, G. M., Di Marco, R., Gulisano, W., D'Ascenzo, M., Torrisi, S. A., Geraci, F., et al. (2019). Dopaminergic-GABAergic interplay and alcohol binge drinking. *Pharmacol. Res.* 141, 384–391. doi: 10.1016/j.phrs.2019.01.022

Li, J., Bian, W., Dave, V., and Ye, J.-H. (2011). Blockade of GABAA receptors in the paraventricular nucleus of the hypothalamus attenuates voluntary ethanol intake and activates the hypothalamic–pituitary–adrenocortical axis. *Addict. Biol.* 16, 600–614. doi: 10.1111/j.1369-1600.2011.00344.x

Liang, J., Cagetti, E., Olsen, R. W., IJJoP, S., and Therapeutics, E. (2004). Altered pharmacology of synaptic and extrasynaptic GABAA receptors on CA1 hippocampal neurons is consistent with subunit changes in a model of alcohol withdrawal and dependence. *J. Pharmacol. Exp. Ther.* 310, 1234–1245. doi: 10.1124/jpet.104.067983

Liang, J., and Olsen, R. W. (2014). Alcohol use disorders and current pharmacological therapies: the role of GABA(A) receptors. *Acta Pharmacol. Sin.* 35, 981–993. doi: 10.1038/aps.2014.50

Linsenbardt, D. N., and Boehm Ii, S. L. (2014). Alterations in the rate of binge ethanol consumption: implications for preclinical studies in mice. *Addict. Biol.* 19, 812–825. doi: 10.1111/adb.12052

Littleton, J. (1998). Neurochemical mechanisms underlying alcohol withdrawal. *Alcohol. Health Res. World* 22, 13–24.

Logge, W. B., Morley, K. C., and Haber, P. S. (2022). GABA(B) receptors and alcohol use disorders: clinical studies. *Curr. Top. Behav. Neurosci.* 52, 195–212. doi: 10.1007/7854_2020_182

Loi, B., Maccioni, P., Lobina, C., Carai, M. A. M., Gessa, G. L., Thomas, A. W., et al. (2013). Reduction of alcohol intake by the positive allosteric modulator of the GABAB receptor, rac-BHFF, in alcohol-preferring rats. *Alcohol* 47, 69–73. doi: 10.1016/j.alcohol.2012.11.002

López-Pelayo, H., Zuluaga, P., Caballeria, E., Van den Brink, W., Mann, K., and Gual, A. (2020). Safety of nalmefene for the treatment of alcohol use disorder: an update. *Expert Opin. Drug Saf.* 19, 9–17. doi: 10.1080/14740338.2020.1707802

Lorrai, I., Contini, A., Gessa, G. L., Mugnaini, C., Corelli, F., Colombo, G., et al. (2019). Operant, oral alcohol self-administration: sex differences in Sardinian alcohol-preferring rats. *Alcohol* 79, 147–162. doi: 10.1016/j.alcohol.2019.04.003

Lorrai, I., Shankula, C., Gaytan, J. M., Kawamura, T., Maccioni, P., Mugnaini, C., et al. (2022). Reducing effect of the novel positive allosteric modulator of the GABA(B) receptor, COR659, on binge-like alcohol drinking in male mice and rats. *Psychopharmacology* 239, 201–213. doi: 10.1007/s00213-021-06022-3

Lovinger, D. M. (1997). Serotonin's role in alcohol's effects on the brain. *Alcohol Health Res. World* 21, 114–120.

Ma, H., and Zhu, G. (2014). The dopamine system and alcohol dependence. *Shanghai Arch. Psychiatry* 26, 61–68. doi: 10.3969/j.issn.1002-0829.2014.02.002

MacCioni, P., Carai, M. A. M., Kaupmann, K., Guery, S., Froestl, W., Leite-Morrism, K., et al. (2009). Reduction of alcohol's reinforcing and motivational properties by the positive allosteric modulator of the GABAB receptor, BHF177, in alcohol-preferring rats. *Alcohol. Clin. Exp. Res.* 33, 1749–1756. doi: 10.1111/j.1530-0277.2009.01012.x

Maccioni, P., and Colombo, G. (2019). Potential of GABA(B) receptor positive allosteric modulators in the treatment of alcohol use disorder. *CNS Drugs* 33, 107–123. doi: 10.1007/s40263-018-0596-3

Maccioni, P., Colombo, G., Lorrai, I., Zaru, A., Carai, M. A. M., Gessa, G. L., et al. (2017). Suppressing effect of COR659 on alcohol, sucrose, and chocolate self-administration in rats: involvement of the GABAB and cannabinoid CB1 receptors. *Psychopharmacology* 234, 2525–2543. doi: 10.1007/s00213-017-4644-3

Maccioni, P., Kaczanowska, K., McDonald, P., and Colombo, G. (2022). Development of partial tolerance to the suppressing effect of the positive allosteric modulator of the GABAB receptor, KK-92A, on alcohol self-Administration in Rats. *Alcohol Alcohol.* 57, 706–711. doi: 10.1093/alcalc/agac026

Maccioni, P., Lorrai, I., Contini, A., Leite-Morris, K., and Colombo, G. (2018). Microinjection of baclofen and CGP7930 into the ventral tegmental area suppresses alcohol self-administration in alcohol-preferring rats. *Neuropharmacology* 136, 146–158. doi: 10.1016/j.neuropharm.2017.10.012

Maccioni, P., Vargiolu, D., Thomas, A. W., Malherbe, P., Mugnaini, C., Corelli, F., et al. (2015). Inhibition of alcohol self-administration by positive allosteric modulators of the GABAB receptor in rats: lack of tolerance and potentiation of baclofen. *Psychopharmacology* 232, 1831–1841. doi: 10.1007/s00213-014-3815-8

Mallard, T. T., Ashenhurst, J. R., Harden, K. P., and Fromme, K. (2018). GABRA2, alcohol, and illicit drug use: an event-level model of genetic risk for polysubstance use. *J. Abnorm. Psychol.* 127, 190–201. doi: 10.1037/abn0000333

Manhapra, A., Chakraborty, A., and Arias, A. J. (2019). Topiramate pharmacotherapy for alcohol use disorder and other addictions: A narrative review. *J. Addict. Med.* 13, 7–22. doi: 10.1097/ADM.0000000000000443

Marik, P. E. (2004). Propofol: therapeutic indications and side-effects. *Curr. Pharm. Des.* 10, 3639–3649. doi: 10.2174/1381612043382846

Marinkovic, K., Alderson Myers, A. B., Arienzo, D., Sereno, M. I., and Mason, G. F. (2022). Cortical GABA levels are reduced in young adult binge drinkers: association with recent alcohol consumption and sex. *NeuroImage* 35:103091. doi: 10.1016/j.nicl.2022.103091

Mason, B. J. (2017). Emerging pharmacotherapies for alcohol use disorder. *Neuropharmacology* 122, 244–253. doi: 10.1016/j.neuropharm.2017.04.032

McCaul, M. E., Hutton, H. E., Stephens, M. A. C., Xu, X., and Wand, G. S. (2017). Anxiety, anxiety sensitivity, and perceived stress as predictors of recent drinking, alcohol craving, and social stress response in heavy drinkers. *Alcohol. Clin. Exp. Res.* 41, 836–845. doi: 10.1111/acer.13350

McCunn, P., Chen, X., Gimi, B., Green, A. I., and Khokhar, J. Y. (2022). Glutamine and GABA alterations in cingulate cortex may underlie alcohol drinking in a rat model of co-occurring alcohol use disorder and schizophrenia: an 1H-MRS study. *Schizophrenia* 8:67. doi: 10.1038/s41537-022-00272-6

Melis, M., Enrico, P., Peana, A. T., and Diana, M. (2007). Acetaldehyde mediates alcohol activation of the mesolimbic dopamine system. *Eur. J. Neurosci.* 26, 2824–2833. doi: 10.1111/j.1460-9568.2007.05887.x

Meyer, E. M., Long, V., Fanselow, M. S., and Spigelman, I. (2013). Stress increases voluntary alcohol intake, but does not alter established drinking habits in a rat model of posttraumatic stress disorder. *Alcohol. Clin. Exp. Res.* 37, 566–574. doi: 10.1111/acer.12012

Mira, R. G., Tapia-Rojas, C., Pérez, M. J., Jara, C., Vergara, E. H., et al. (2019). Alcohol impairs hippocampal function: from NMDA receptor synaptic transmission to mitochondrial function. *Drug Alcohol Depend.* 205:107628. doi: 10.1016/j.drugalcdep.2019.107628

Mirijello, A., Caputo, F., Vassallo, G., Rolland, B., Tarli, C., Gasbarrini, A., et al. (2015). GABAB agonists for the treatment of alcohol use disorder. *Curr. Pharm. Des.* 21, 3367–3372. doi: 10.2174/1381612821666150619091858

Mishra, B. R., Nizamie, S. H., Das, B., and Praharaj, S. K. (2010). Efficacy of repetitive transcranial magnetic stimulation in alcohol dependence: a sham-controlled study. *Addiction* 105, 49–55. doi: 10.1111/j.1360-0443.2009.02777.x

Mitchell, J. M., O'Neil, J. P., Janabi, M., Marks, S. M., Jagust, W. J., and Fields, H. L. (2012). Alcohol consumption induces endogenous opioid release in the human orbitofrontal cortex and nucleus accumbens. *Sci. Transl. Med.* 4:116ra6. doi: 10.1126/scitranslmed.3002902

Modesto-Lowe, V., Barron, G. C., Aronow, B., and Chaplin, M. (2019). Gabapentin for alcohol use disorder: A good option, or cause for concern? *Cleve. Clin. J. Med.* 86, 815–823. doi: 10.3949/ccjm.86a.18128

Mohammadi, B., Krampfl, K., Petri, S., Bogdanova, D., Kossev, A., Bufler, J., et al. (2006). Selective and nonselective benzodiazepine agonists have different effects on motor cortex excitability. *Muscle Nerve* 33, 778–784. doi: 10.1002/mus.20531

Mon, A., Durazzo, T. C., and Meyerhoff, D. J. (2012). Glutamate, GABA, and other cortical metabolite concentrations during early abstinence from alcohol and their associations with neurocognitive changes. *Drug Alcohol Depend.* 125, 27–36. doi: 10.1016/j.drugalcdep.2012.03.012

Morrow, A. L., Boero, G., and Porcu, P. (2020). A rationale for allopregnanolone treatment of alcohol use disorders: basic and clinical studies. *Alcohol. Clin. Exp. Res.* 44, 320–339. doi: 10.1111/acer.14253

Mounier, N. M., Wahdan, S. A., Gad, A. M., and Azab, S. S. (2021). Role of inflammatory, oxidative, and ER stress signaling in the neuroprotective effect of atorvastatin against doxorubicin-induced cognitive impairment in rats. *Naunyn Schmiedebergs Arch. Pharmacol.* 394, 1537–1551. doi: 10.1007/s00210-021-02081-7

Möykkynen, T., and Korpi, E. R. (2012). Acute effects of ethanol on glutamate receptors. *Basic Clin. Pharmacol. Toxicol.* 111, 4–13. doi: 10.1111/j.1742-7843.2012.00879.x

Naim-Feil, J., Bradshaw, J. L., Rogasch, N. C., Daskalakis, Z. J., Sheppard, D. M., Lubman, D. I., et al. (2016). Cortical inhibition within motor and frontal regions in alcohol dependence post-detoxification: A pilot TMS-EEG study. *World J. Biol. Psychiatry* 17, 547–556. doi: 10.3109/15622975.2015.1066512

Nardone, R., Bergmann, J., Kronbichler, M., Caleri, F., Lochner, P., Tezzon, F., et al. (2010). Altered motor cortex excitability to magnetic stimulation in alcohol withdrawal syndrome. *Alcohol. Clin. Exp. Res.* 34, 628–632. doi: 10.1111/j.1530-0277.2009.01131.x

Nelson, A. C., Kehoe, J., Sankoff, J., Mintzer, D., Taub, J., and Kaucher, K. A. (2019). Benzodiazepines vs barbiturates for alcohol withdrawal: analysis of 3 different treatment protocols. *Am. J. Emerg. Med.* 37, 733–736. doi: 10.1016/j.ajem.2019.01.002

Newman, R. K., Gallagher, M. A. S., and Gomez, A. E. (2023). "Alcohol withdrawal," in *StatPearls [Internet]*. Treasure Island (FL): StatPearls Publishing. Available at: https://www.ncbi.nlm.nih.gov/books/NBK441882/

NIAAA (2018). Drinking patterns and their definitions. *Alcohol Res.* 39, 17–18. Available at: https://arcr.niaaa.nih.gov/volume/39/1/drinking-patterns-and-their-definitions

NIAAA. (2020). *Understanding Alcohol Use Disorder*. Available at: https://www.niaaa.nih.gov/publications/brochures-and-fact-sheets/understanding-alcohol-use-disorder

Olsen, R. W., and Liang, J. (2017). Role of GABA(A) receptors in alcohol use disorders suggested by chronic intermittent ethanol (CIE) rodent model. *Mol. Brain* 10:45. doi: 10.1186/s13041-017-0325-8

Orrù, A., Lai, P., Lobina, C., Maccioni, P., Piras, P., et al. (2005). Reducing effect of the positive allosteric modulators of the GABA B receptor, CGP7930 and GS39783, on alcohol intake in alcohol-preferring rats. *Eur. J. Pharmacol.* 525, 105–111. doi: 10.1016/j.ejphar.2005.10.005

Paille, F., and Martini, H. (2014). Nalmefene: a new approach to the treatment of alcohol dependence. *Subst. Abus. Rehabil.* 5, 87–94. doi: 10.2147/SAR.S45666

Pandey, S. C., Sakharkar, A. J., Tang, L., and Zhang, H. (2015). Potential role of adolescent alcohol exposure-induced amygdaloid histone modifications in anxiety and alcohol intake during adulthood. *Neurobiol. Dis.* 82, 607–619. doi: 10.1016/j.nbd.2015.03.019

Paparrigopoulos, T., Tzavellas, E., Karaiskos, D., Kourlaba, G., and Liappas, I. (2011). Treatment of alcohol dependence with low-dose topiramate: an open-label controlled study. *BMC Psychiatry* 11:41. doi: 10.1186/1471-244X-11-41

Paradis, C., Butt, P., Shield, K., Poole, N., Wells, S., et al. (2022). *Update of Canada's low-risk alcohol drinking guidelines: Final report for public consultation*. Ottawa, ON: Canadian Centre on Substance Use and Addiction.

Patatanian, E., and Nguyen, D. R. (2022). Brexanolone: A novel drug for the treatment of postpartum depression. *J. Pharm. Pract.* 35, 431–436. doi: 10.1177/0897190020979627

Peana, A. T., Sánchez-Catalán, M. J., Hipólito, L., Rosas, M., Porru, S., et al. (2017). Mystic acetaldehyde: the never-ending story on alcoholism. *Front. Behav. Neurosci.* 11:81. doi: 10.3389/fnbeh.2017.00081

Pérez-Ramírez, Ú., López-Madrona, V. J., Pérez-Segura, A., Pallarés, V., Moreno, A., et al. (2022). Brain network allostasis after chronic alcohol drinking is characterized by functional dedifferentiation and narrowing. *J. Neurosci.* 42, 4401–4413. doi: 10.1523/JNEUROSCI.0389-21.2022

Pinard, A., Seddik, R., and Bettler, B. (2010). GABAB receptors: physiological functions and mechanisms of diversity. *Adv. Pharmacol.* 58, 231–255. doi: 10.1016/S1054-3589(10)58010-4

Pinna, G., Almeida, F. B., and Davis, J. M. (2022). Allopregnanolone in Postpartum Depression. *Front. Glob. Womens Health* 3:823616. doi: 10.3389/fgwh.2022.823616

Pleil, K. E., Lowery-Gionta, E. G., Crowley, N. A., Li, C., Marcinkiewcz, C. A., et al. (2015). Effects of chronic ethanol exposure on neuronal function in the prefrontal cortex and extended amygdala. *Neuropharmacology* 99, 735–749. doi: 10.1016/j.neuropharm.2015.06.017

Prevot, T., and Sibille, E. (2021). Altered GABA-mediated information processing and cognitive dysfunctions in depression and other brain disorders. *Mol. Psychiatry* 26, 151–167. doi: 10.1038/s41380-020-0727-3

Prisciandaro, J. J., Schacht, J. P., Prescot, A. P., Renshaw, P. F., Brown, T. R., and Anton, R. F. (2019). Brain glutamate, GABA, and glutamine levels and associations with recent drinking in treatment-Naïve individuals with alcohol use disorder versus light drinkers. *Alcohol* 43, 221–226. doi: 10.1111/acer.13931

Quertemont, E., Grant, K. A., Correa, M., Arizzi, M. N., Salamone, J. D., et al. (2005). The role of acetaldehyde in the central effects of ethanol. *Alcohol. Clin. Exp. Res.* 29, 221–234. doi: 10.1097/01.ALC.0000156185.39073.D2

Rehm, J., Gmel, G. E. Sr., Gmel, G., Hasan, O. S. M., Imtiaz, S., et al. (2017). The relationship between different dimensions of alcohol use and the burden of disease-an update. *Addiction* 112, 968–1001. doi: 10.1111/add.13757

Rolland, B., Simon, N., Franchitto, N., and Aubin, H. J. (2020). France Grants an approval to baclofen for alcohol dependence. *Alcohol Alcohol.* 55, 44–45. doi: 10.1093/alcalc/agz082

Romeo, E., Brancati, A., De Lorenzo, A., Fucci, P., Furnari, C., et al. (1996). Marked decrease of plasma neuroactive steroids during alcohol withdrawal. *Clin. Neuropharmacol.* 19, 366–369. doi: 10.1097/00002826-199619040-00011

Romito, J. W., Turner, E. R., Rosener, J. A., Coldiron, L., Udipi, A., et al. (2021). Baclofen therapeutics, toxicity, and withdrawal: a narrative review. *SAGE Open Med.* 9:205031212110221. doi: 10.1177/20503121211022197

Rüedi-Bettschen, D., Rowlett, J. K., Rallapalli, S., Clayton, T., Cook, J. M., and Platt, D. M. (2013). Modulation of α5 subunit-containing GABAA receptors alters alcohol drinking by rhesus monkeys. *Alcohol. Clin. Exp. Res.* 37, 624–634. doi: 10.1111/acer.12018

Sanchez-Catalan, M. J., Kaufling, J., Georges, F., Veinante, P., and Barrot, M. (2014). The antero-posterior heterogeneity of the ventral tegmental area. *Neuroscience* 282, 198–216. doi: 10.1016/j.neuroscience.2014.09.025

Sarasa, S. B., Mahendran, R., Muthusamy, G., Thankappan, B., Selta, D. R. F., and Angayarkanni, J. J. C. (2020). A brief review on the non-protein amino acid, gamma-amino butyric acid (GABA): its production and role in microbes. *Curr. Microbiol.* 77, 534–544. doi: 10.1007/s00284-019-01839-w

Saunders, J. B., Degenhardt, L., Reed, G. M., and Poznyak, V. (2019). Alcohol use disorders in ICD-11: past, present, and future. *Alcohol. Clin. Exp. Res.* 43, 1617–1631. doi: 10.1111/acer.14128

Savin, Z., Kivity, S., Yonath, H., and Yehuda, S. (2018). Smoking and the intestinal microbiome. *Arch. Microbiol.* 200, 677–684. doi: 10.1007/s00203-018-1506-2

Schmidt, K. J., Doshi, M. R., Holzhausen, J. M., Natavio, A., Cadiz, M., and Winegardner, J. E. (2016). Treatment of severe alcohol withdrawal. *Ann. Pharmacother.* 50, 389–401. doi: 10.1177/1060028016629161

Shyu, C., Chavez, S., Boileau, I., and Le Foll, B. (2022). Quantifying GABA in addiction: A review of proton magnetic resonance spectroscopy studies. *Brain Sci.* 12:918. doi: 10.3390/brainsci12070918

Singh, D., and Saadabadi, A. (2023). "Naltrexone," in *StatPearls [Internet]*. Treasure Island, FL: StatPearls Publishing. Available at: https://www.ncbi.nlm.nih.gov/books/NBK534811/

Sloan, M. E., Werner, R. B., Yarnell-Macgrory, S., and Petrakis, I. (2020). *Alcohol*, pp. 121–137: New York: Springer International Publishing

Solanki, N., Abijo, T., Galvao, C., Darius, P., Blum, K., and Gondré-Lewis, M. C. (2020). Administration of a putative pro-dopamine regulator, a neuronutrient, mitigates alcohol intake in alcohol-preferring rats. *Behav. Brain Res.* 385:112563. doi: 10.1016/j.bbr.2020.112563

Sorkhou, M., Stogios, N., Sayrafizadeh, N., Hahn, M. K., Agarwal, S. M., and George, T. P. (2022). Non-invasive neuromodulation of dorsolateral prefrontal cortex to reduce craving in alcohol use disorder: A meta-analysis. *Drug Alcohol Depend. Rep.* 4:100076. doi: 10.1016/j.dadr.2022.100076

Soyka, M., Preuss, U. W., Hesselbrock, V., Zill, P., Koller, G., and Bondy, B. (2008). GABA-A2 receptor subunit gene (GABRA2) polymorphisms and risk for alcohol dependence. *J. Psychiatr. Res.* 42, 184–191. doi: 10.1016/j.jpsychires.2006.11.006

Stephens, D. N., Pistovcakova, J., Worthing, L., Atack, J. R., and Dawson, G. R. (2005). Role of GABAA alpha5-containing receptors in ethanol reward: the effects of targeted gene deletion, and a selective inverse agonist. *Eur. J. Pharmacol.* 526, 240–250. doi: 10.1016/j.ejphar.2005.09.031

Stokes, M., and Abdijadid, S. (2022). *Disulfiram in StatPearls*. Treasure Island, FL: StatPearls Publishing Copyright.

Tanabe, J., Yamamoto, D. J., Sutton, B., Brown, M. S., Hoffman, P. L., et al. (2019). Effects of alcohol and acetate on cerebral blood flow: A pilot study. *Alcohol. Clin. Exp. Res.* 43, 2070–2078. doi: 10.1111/acer.14173

Tarren, J., Shariff, M., Holgate, J., and Bartlett, S. E. (2016). "Chapter 38 – effects of alcohol on nicotinic acetylcholine receptors and impact on addiction" in *Neuropathology of drug addictions and substance misuse*. ed. V. R. Preedy (San Diego: Academic Press), 411–419.

Tateno, T., and Robinson, H. P. C. (2011). The mechanism of ethanol action on midbrain dopaminergic neuron firing: a dynamic-clamp study of the role of IH and GABAergic synaptic integration. *J. Neurophysiol.* 106, 1901–1922. doi: 10.1152/jn.00162.2011

Tehrani, M. H., and Barnes, E. M. (1997). Sequestration of γ-aminobutyric acidA receptors on clathrin-coated vesicles during chronic benzodiazepine administration *in vivo*. *J. Pharmacol. Exp. Ther.* 283, 384–390.

Terunuma, M. (2018). Diversity of structure and function of GABA(B) receptors: a complexity of GABA(B)-mediated signaling. *Proc. Jpn. Acad. Ser. B Phys. Biol. Sci.* 94, 390–411. doi: 10.2183/pjab.94.026

Thaysen-Petersen, D., Hammerum, S. K., Vissing, A.-C., Arnfred, B. T., Nordahl, R., et al. (2023). Virtual reality-assisted cognitive behavioural therapy for outpatients with alcohol use disorder (CRAVR): a protocol for a randomised controlled trial. *BMJ Open* 13:e068658. doi: 10.1136/bmjopen-2022-068658

Tizabi, Y., Bai, L., Copeland, R. L., and Taylor, R. E. (2007). Combined effects of systemic alcohol and nicotine on dopamine release in the nucleus accumbens shell. *Alcohol Alcohol.* 42, 413–416. doi: 10.1093/alcalc/agm057

Trantham-Davidson, H., and Chandler, L. (2015). Alcohol-induced alterations in dopamine modulation of prefrontal activity. *Alcohol* 49, 773–779. doi: 10.1016/j.alcohol.2015.09.001

Trudell, J. R., Messing, R. O., Mayfield, J., and Harris, R. A. (2014). Alcohol dependence: molecular and behavioral evidence. *Trends Pharmacol. Sci.* 35, 317–323. doi: 10.1016/j.tips.2014.04.009

Turton, S., Myers, J. F. M., Mick, I., Colasanti, A., Venkataraman, A., et al. (2020). Blunted endogenous opioid release following an oral dexamphetamine challenge in abstinent alcohol-dependent individuals. *Mol. Psychiatry* 25, 1749–1758. doi: 10.1038/s41380-018-0107-4

Valenzuela, C. F. (1997). Alcohol and neurotransmitter interactions. *Alcohol Health Res. World* 21, 144–148.

Valenzuela, C. F., and Jotty, K. (2015). Mini-review: effects of ethanol on GABAA receptor-mediated neurotransmission in the cerebellar cortex—recent advances. *Cerebellum* 14, 438–446. doi: 10.1007/s12311-014-0639-3

Vengeliene, V., Bachteler, D., Danysz, W., and Spanagel, R. (2005). The role of the NMDA receptor in alcohol relapse: a pharmacological mapping study using the alcohol deprivation effect. *Neuropharmacology* 48, 822–829. doi: 10.1016/j.neuropharm.2005.01.002

Volkow, N. D., Wang, G.-J., Tomasi, D., and Baler, R. D. (2013). Unbalanced neuronal circuits in addiction. *Curr. Opin. Neurobiol.* 23, 639–648. doi: 10.1016/j.conb.2013.01.002

Walzer, M., Marek, G. J., Wu, R., Nagata, M., and Han, D. (2020). Single-and multiple-dose safety, tolerability, and pharmacokinetic profiles of ASP8062: results from 2 phase 1 studies. *Clin. Pharmacol. Drug Dev.* 9, 297–306. doi: 10.1002/cpdd.766

Wenzel, R. G., Schwarz, K., and Padiyara, R. S. (2006). Topiramate for migraine prevention. *Pharmacotherapy* 26, 375–387. doi: 10.1592/phco.26.3.375

Weresch, J., Kirkwood, J., and Korownyk, C. S. (2021). Gabapentin for alcohol use disorder. *Can. Fam. Physician* 67:269. doi: 10.46747/cfp.6704269

Werner, D. F., Porcu, P., Boyd, K. N., O'Buckley, T. K., Carter, J. M., et al. (2016). Ethanol-induced GABAA receptor alpha4 subunit plasticity involves phosphorylation and neuroactive steroids. *Mol. Cell. Neurosci.* 72, 1–8. doi: 10.1016/j.mcn.2016.01.002

Wetherill, R. R., and Fromme, K. (2016). Alcohol-induced blackouts: A review of recent clinical research with practical implications and recommendations for future studies. *Alcohol. Clin. Exp. Res.* 40, 922–935. doi: 10.1111/acer.13051

Wetherill, R. R., Spilka, N., Jagannathan, K., Morris, P., Romer, D., et al. (2021). Effects of topiramate on neural responses to alcohol cues in treatment-seeking individuals with alcohol use disorder: preliminary findings from a randomized, placebo-controlled trial. *Neuropsychopharmacology* 46, 1414–1420. doi: 10.1038/s41386-021-00968-w

WHO. (2021). *Global strategy to reduce harmful use of alcohol*. Geneva: WHO

WHO-ICD11. (2022). *International classification of diseases: Eleventh revision (ICD-11)*. Geneva: WHO

Wilson, D. F., and Matschinsky, F. M. (2020). Ethanol metabolism: the good, the bad, and the ugly. *Med. Hypotheses* 140:109638. doi: 10.1016/j.mehy.2020.109638

World Health Organization. (2000). *International guide for monitoring alcohol consumption and related harm*. Geneva: World Health Organization

Yang, W., Singla, R., Maheshwari, O., Fontaine, C. J., and Gil-Mohapel, J. (2022). Alcohol use disorder: neurobiology and Therapeutics. *Biomedicine* 10:1192. doi: 10.3390/biomedicines10051192

Zangen, A., Moshe, H., Martinez, D., Barnea-Ygael, N., Vapnik, T., et al. (2021). Repetitive transcranial magnetic stimulation for smoking cessation: a pivotal multicenter double-blind randomized controlled trial. *World Psychiatry* 20, 397–404. doi: 10.1002/wps.20905

Zaporowska-Stachowiak, I., Szymański, K., Oduah, M.-T., Stachowiak-Szymczak, K., Łuczak, J., and Sopata, M. (2019). Midazolam: safety of use in palliative care: A systematic critical review. *Biomed. Pharmacother.* 114:108838. doi: 10.1016/j.biopha.2019.108838

Zhao, J., Stockwell, T., Naimi, T., Churchill, S., Clay, J., and Sherk, A. (2023). Association between daily alcohol intake and risk of all-cause mortality: A systematic review and meta-analyses. *JAMA Netw. Open* 6:e236185. doi: 10.1001/jamanetworkopen.2023.6185

Ziemann, U., Reis, J., Schwenkreis, P., Rosanova, M., Strafella, A., et al. (2015). TMS and drugs revisited 2014. *Clin. Neurophysiol.* 126, 1847–1868. doi: 10.1016/j.clinph.2014.08.028

Zorumski, C. F., Paul, S. M., Izumi, Y., Covey, D. F., and Mennerick, S. (2013). Neurosteroids, stress and depression: potential therapeutic opportunities. *Neurosci. Biobehav. Rev.* 37, 109–122. doi: 10.1016/j.neubiorev.2012.10.005

Frontiers in
Neural Circuits

Explores the emergent properties of neural circuits - the brain's elementary modules

Part of the most cited neuroscience journal series, focuses on the anatomy, physiology, development and function of neural circuitry, exploring how plasticity shapes the architecture of the brain's elementary modules.

Discover the latest Research Topics

See more →

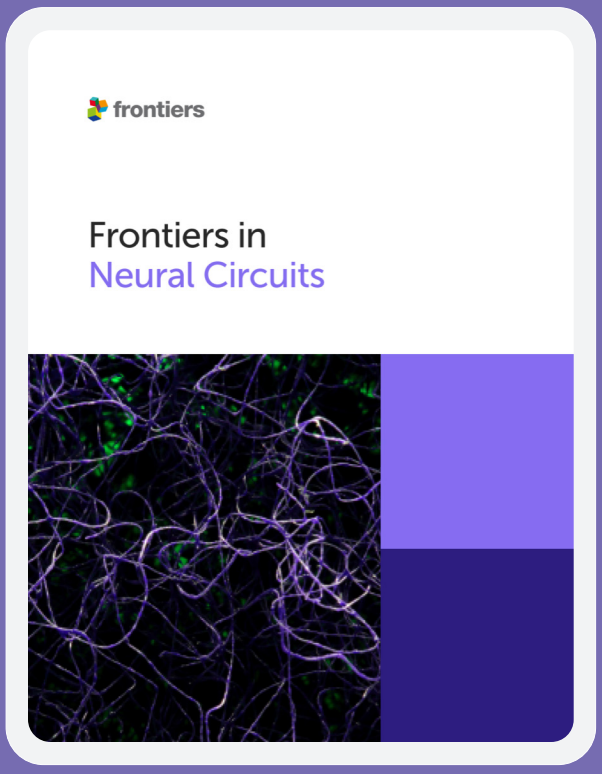

Frontiers

Avenue du Tribunal-Fédéral 34
1005 Lausanne, Switzerland
frontiersin.org

Contact us

+41 (0)21 510 17 00
frontiersin.org/about/contact